



<https://theses.gla.ac.uk/>

Theses Digitisation:

<https://www.gla.ac.uk/myglasgow/research/enlighten/theses/digitisation/>

This is a digitised version of the original print thesis.

Copyright and moral rights for this work are retained by the author

A copy can be downloaded for personal non-commercial research or study,
without prior permission or charge

This work cannot be reproduced or quoted extensively from without first
obtaining permission in writing from the author

The content must not be changed in any way or sold commercially in any
format or medium without the formal permission of the author

When referring to this work, full bibliographic details including the author,
title, awarding institution and date of the thesis must be given

Enlighten: Theses

<https://theses.gla.ac.uk/>
research-enlighten@glasgow.ac.uk

Neotectonics and Palaeoseismicity
in
North West Scotland

A Thesis submitted for the degree of
Doctor of Philosophy

by
Clark Henderson Fenton
B.Sc. University of Glasgow

Department of Geology & Applied Geology
University of Glasgow

August 1991

ProQuest Number: 11011411

All rights reserved

INFORMATION TO ALL USERS

The quality of this reproduction is dependent upon the quality of the copy submitted.

In the unlikely event that the author did not send a complete manuscript and there are missing pages, these will be noted. Also, if material had to be removed, a note will indicate the deletion.



ProQuest 11011411

Published by ProQuest LLC (2018). Copyright of the Dissertation is held by the Author.

All rights reserved.

This work is protected against unauthorized copying under Title 17, United States Code
Microform Edition © ProQuest LLC.

ProQuest LLC.
789 East Eisenhower Parkway
P.O. Box 1346
Ann Arbor, MI 48106 – 1346

Declaration

The material presented in this thesis summarises the results of four years of research carried out in the Department of Geology & Applied Geology, University of Glasgow and also the former Department of Applied Geology, University of Strathclyde. This study is based on my own independent research and any previously published or unpublished results of other researchers used in this thesis have been given full acknowledgement in the text.

Clark Fenton.

November 1991.

Abstract

Detailed field investigation has revealed a number of faults that display late Quaternary movement in the formerly glaciated Highlands of North West Scotland. These include NE-orientated reverse, WNW- to NW-orientated sinistral strike-slip and N- to NNW-orientated dextral strike-slip faults. In all cases movement has occurred along pre-existing basement faults. The faults offset late Quaternary morphological features, including drainage courses, and disrupt late- and post-glacial sediments. Electron Spin Resonance was used in an attempt to accurately age-date the fault movements. Although this proved unsuccessful, this study showed the limitations of using this technique in relation to fault dating studies. Fault movement was accompanied by coseismic ground deformation as shown by the density of seismically-triggered slope failures and seismite soft sediment deformation around the fault ground ruptures. The areal distribution of these deformation features and the dimensions of the associated fault ruptures indicate elevated levels of seismic activity, with events up to M_s 7.0. This is considerably greater than the levels of seismic activity experienced at present. Faulting was associated with a period of rapid isostatic uplift during and immediately following the decay of the last glacial episode, the Main Late Devensian, c.13,000 years BP. A short-lived glacial readvance, the Loch Lomond Stadial, lasting from c. 11,000 to 10,300 years BP, caused temporary redepression of the crust halting uplift and faulting prior the main period of fault activity post-10,300 years BP. Although the majority of fault movement occurred in the immediate post-glacial period, significant fault movement has occurred as recently as 2,400 years BP. Faulting resulted from the sudden release of glacial loading stresses and tectonic stresses stored during ice-sheet residence. Elevated pore fluid pressure is seen to be important in the timing and sustaining of fault movement outwith the immediate post-glacial period. Such elevated pore fluid pressure also allowed the reactivation of faults that were less favourably orientated with respect to the regional stress field.

This evidence for fault movement and seismic activity in the early part of the Holocene is compared with present day seismotectonic activity and used to predict the present day risk of ground rupture and damaging earthquake activity in the UK as a whole. It is proposed that present day crustal movements result from the actions of the NW European regional stress field, the effects of glacially-induced stresses now having decayed to insignificant levels.

Acknowledgements

This research project was funded by the Natural Environment Research Council, grant GT4/87/GS/107. NERC also provided additional funding for the extensive programme of fieldwork and the Electron Spin Resonance age-dating study.

The project was initiated by Colin Davenport at the Department of Applied Geology, University of Strathclyde. His interest and enthusiasm provided direction in the early stages. The unwelcome actions of higher authority consumed the 'old' Strathclyde Department in 1989. Research then moved to the new Department of Applied Geology & Geology at Glasgow University. To Iain Allison I am greatly indebted for assuming the role of supervisor and seeing the project through to its conclusion. Many thanks are also offered to Stuart Haszeldine, unofficial supervisor extraordinaire, for his unending interest in and enthusiasm for the world of Scottish neotectonics (Not many N-S linears though!). The remainder of the Strathclyde staff: Roger Anderton, Brian Bell, Alan Hall, Jeff Harris, Mike Russell and especially George Bowes, for his help in untangling many a mess on the computer system, are all thanked for their interest, support, good humour and just making Strathclyde a great place to belong to. Within the new Department Ben Doody, Peter Haughton, Graham Jardine, Bernard Leake, 'Old Norway' and Geoff Tanner are all thanked for providing stimulating discussion and encouragement.

*The technical staff of both Departments made many a task much easier during the course of this research. Their help and advice has been invaluable: Murdoch MacLeod, Dougie Turner and Jim Gallagher all kept a safe distance during mineral separations, John Gilleece and Peter 'Pigg' Wallace showed the utmost patience in making "all thae b*****d slides", Jim Kavanagh sorted many a problem with the Apple Macs, Pete Ainsworth ably piloted the Starship Enterprise (SEM!) and Kenny Roberts repaired the coring drills. Douglas MacLean deserves a special mention for the time and effort he spent transforming a large number of slides into the prints for this thesis. Roddy Morrison is thanked for providing the raw materials of post-grad. research and for managing to run the Department despite the warring factions. 'The Jannies': Eddie Alec and John provided good humour and anything else that could not be procured by normal means!*

The post-grad. fraternity of both Departments, both past and present, made my period of research a pleasure. Thanks for friendship and humour: Fawzi, Sherif, Kerr, Anne, Arshad, John (Le Cube), Russ, Pete, Scummy, Maggie, Ahmed, Ali, Lindsay, Amar, John, Wamid, Richard, Zaid, Garry, Kerim, Calum, Tim, Tom, Gordon, Rona,

Orla (who wanted a mention on her own),

Andy, Paul, Wobbly, Mohamed, Robbie, Morgan, Rachel, Susan and Derek. Pete Chung is especially thanked for his donkey work during the collection of samples for ESR age-dating.

Outwith the Department(s) many people have helped with this project, providing data, advice, accommodation or merely an encouraging word. The staff of the BGS Global Seismology Unit, especially Pete Marrow and Terry Turbitt, provided the data concerning instrumental seismicity in the

UK. Colin Ballantyne, Dougie Benn, Rob Duck, Patricia Lowe and Jill Tate of St. Andrews University taught the author about glacial geomorphology and provided much information on the Quaternary history of Scotland. Geoff Boulton (Edinburgh) and Doug Peacock (Heriot-Watt) provided stimulating discussion on all matters Quaternary. Martin Kralik (Vienna), Robert Maddock (Geoscience Ltd), David Sanderson (SURRC) and Rainer Grün (Cambridge) were all generous in their advice concerning age-dating of intrafault materials. To Rainer I am deeply indebted for his participation in the ESR age-dating study and braving the Scottish weather in October! Graham Eaton (BNF plc), Colin Ferguson (Dames & Moore), Paul Hancock (Bristol) and Graham Park (Keele) all provided information on faults both old and new. H.J. Melosh (Arizona) generously gave much information on rock avalanches from around the world. Svensk Kärnbränslehantering AB, the Swedish Nuclear Fuel & Waste Management Co., generously paid for a visit to the Lansjärv fault in Northern Sweden. Ann-Marie Hultqvist, Lars Ericsson and Roy Stanfors are thanked for their organisation and generous hospitality. Robert Lagerbäck (SGU) and Odleiv Olesen (NGU) are especially thanked for going out of their way to show me the other post-glacial faults of northern Fennoscandia. A special thank you to Robert and Anders for the memorable heli-field trip to the Pärvie fault. John Adams and Doug Grant (Canadian Geol. Surv.), Arch Johnston (Memphis), Robert Lagerbäck (SGU), Nils-Axel Mörner (Stockholm), Robert Muir Wood (BEQE) and Chris Talbot (Uppsala) have all provided stimulating discussion throughout the course of this research. Phil Ringrose (Heriot-Watt) more than most has been a constant source of information and enthusiasm throughout the past few years.

During the course of fieldwork many people have helped smooth the way. Nic & Jean Lancaster (Rattagan), Gerry Howkins (Craig), Neil Morrison (Torridon) and Donald & Aileen Cameron (Kinloch Hourn) have all been generous hosts. The SYHA and MBA have provided all other accommodation. Ian Bennett (Strathvaich), Donald Cameron (Kinloch Hourn), Robert Carr (Killilan), Carl Lawaetz (Cozac & East Benula), Jock Logie (Lochluichart), Richard Munro (Alladale), Christopher MacKenzie (Achnashellach), Norrie Matheson (Fannich), J. Meldrum (Scardroy), Richard Noble (Finlayson Hughes) and Roddy Sinclair (Braeroy) all allowed access onto the various estates, sometimes at delicate times of the year, as did the Forestry Commission and National Trust for Scotland. The local knowledge of stalkers, keepers and 'worthies' has proved invaluable in tracking down evidence of past earthquake activity; to all many thanks. To all those forestry and estate workers that have given lifts to a foot-weary palaeoseismologist I am eternally grateful. The 'Strath-on-Rock' Team and various members of EKMC all allowed release from the grind of research by means of more vertiginous pursuits.

Above all I would like to thank my Mother and Father for their support (both moral and financial) and encouragement throughout the period of this research. Without their help this work would not have been possible. Finally, to Fiona who made the quest for ancient Scottish earthquakes more bearable with her constant companionship and understanding, I am forever indebted.

Contents

		<i>Page No.</i>
Abstract		i
Acknowledgements		ii
Contents		iv
Chapter 1	Introduction.	1
1.1	Introduction	1
1.2	Long-Term Behaviour of 'Stable' Crustal Areas	1
1.3	Neotectonics - A Problem of Definition	2
1.4	Post-Glacial Faulting: Previous Research	3
1.5	Objectives of the Present Study	4
1.6	Format of the Thesis	7
1.7	References	8
1.8	Figure 1.1	14
Chapter 2	Late Quaternary Fault Activity in N.W. Scotland.	15
2.1	Abstract	15
2.2	Introduction	16
2.3	Tectonic History	16
2.4	'Recent' Fault Movements	17
2.5	Post-Glacial Faults (PGFs): Criteria for Recognition	19
2.6	Post-Glacial Faulting in N.W. Scotland	21
2.6.1	Coire Mor Fault	21
2.6.2	Strath Vaich Fault	24
2.6.3	Garbh Choire Mor Faults	26
2.6.4	Beinn Alligin Fault	28
2.6.5	Cuaig Fault	29
2.6.6	Loch Maree Fault	30
2.6.7	Bac an Eich Fault	33

2.6.8	Beinn Tharsuinn Fault	34
2.6.9	Loch Monar (Allt nan Uan) Fault	35
2.6.10	Coire Eoghainn Fault	35
2.6.11	Glen Elchaig (Strathconon) Fault	37
2.6.12	Glen Affric Faults	38
2.6.13	Gleann Lichd Fault	40
2.6.14	Glen Shiel Fault Swarm	41
2.6.15	Creag na Damh (Am Fas Allt) Fault	42
2.6.16	Sgurr a' Bhealaich Dheirg 'Faults'	42
2.6.17	Sgurr na Ciste Duibhe (Five Sisters) Fault	44
2.6.18	Arnisdale Faults	45
2.6.19	Coire Dho Fault	46
2.6.20	Kinloch Hourn Fault	47
2.6.21	Glen Gloy Fault	47
2.6.22	Other Reported Post-Glacial Faults	48
2.7	Palaeoseismicity	48
2.8	Discussion	51
2.9	Conclusions	53
2.10	Acknowledgements	54
2.11	References	55
2.12	Figure Captions	62
2.13	Figures	68
2.14	Table 2.1	106

Chapter 3 Glacio-Isostatic Faulting and Ground Deformation in the Area of Glen Roy and Glen Gloy, Scotland. 112

3.1	Abstract	112
3.2	Introduction	113
3.3	Glen Gloy Fault: Surface Expression and Morphotectonics	114
3.4	Recent Fault Movement and Ground Deformation	115
3.5	Age of Faulting	117
3.6	Slope Failures	118
3.7	Deformation Chronology	120
3.8	Magnitude Estimates	120

3.9	Rebound Tectonics	122
3.10	Conclusions	126
3.11	Acknowledgements	127
3.12	References	128
3.13	Figure Captions	132
3.14	Figures	135
3.15	Tables	144
3.16	Appendix: Modified Newmark Analysis	147
Chapter 4	UK Seismicity During the Holocene: A Comparison of Instrumental, Historical and Palaeoseismic Data From N.W. Scotland.	149
4.1	Abstract	149
4.2	Introduction	150
4.3	Plate Tectonic Setting of the UK	151
4.4	Seismotectonic Investigations	152
4.5	Seismic Risk Investigation	153
4.6	Seismicity Data Bases for the UK	154
4.7	Instrumental Seismicity: 1969-1988	155
4.7.1	Magnitude-Frequency Relationship	157
4.7.2	Tectonic Deformation	159
4.8	Historical Seismicity	163
4.8.1	Compilation and Standardisation of Historical Seismicity Data	163
4.8.2	Historical Seismicity: UK	165
4.8.3	Historical Seismicity UK: 1700-1990	165
4.9	Palaeoseismicity	168
4.9.1	Palaeoseismic Magnitude Calculations	169
4.9.2	Magnitude Errors	170
4.9.3	Paleoseismicity: North & West Scotland	172
4.10	Palaeoseismotectonics	174
4.11	Conclusions	177
4.12	Acknowledgements	178
4.13	References	179
4.14	Figure Captions	187
4.15	Figures	190

4.16	Tables	207
4.17	Appendix: Distribution of UK Instrumental Seismicity 1969-'88.	215
Chapter 5	Attempted Age-Dating of Late Quaternary Fault Movements in N.W.Scotland Using ESR and Intrafault Quartz Grain Morphology.	220
5.1	Abstract	220
5.2	Introduction	221
5.3	Electron Spin Resonance (ESR): An Introduction	222
5.3.1	Principles of ESR Age-Dating	222
5.3.2	ESR Spectra of Quartz and Resetting Mechanisms	224
5.3.3	Sample Collection and Preparation	225
5.3.4	Sample Irradiation	226
5.3.5	Results	227
5.3.6	Discussion	227
5.4	SEM Investigation of Surface Morphologies of Intrafault Quartz Grains	228
5.4.1	Group I Textures	229
5.4.2	Group II Textures	229
5.4.3	Group III Textures	230
5.4.4	Group IV Textures	230
5.4.5	Sample Collection and Preparation	231
5.4.6	Results	232
5.4.7	Discussion	232
5.5	Conclusions	234
5.6	Acknowledgements	236
5.7	References	237
5.8	Figure Captions	241
5.9	Figures	243
5.10	Tables	254
5.11	Appendix A: Location of ESR Sample Sites	256
5.12	Appendix B: Location of SEM Sample Sites	258

Chapter 6	The Effects of Ice-Cap Loading on Crustal Stress Patterns and the Consequences for the Generation of Seismicity in the Post-Glacial Environment.	260
6.1	Abstract	260
6.2	Introduction	261
6.3	Late Tertiary Tectonics	261
6.4	The Effects of Ice-cap Loading: General Considerations	263
6.4.1	The Effects of Ice-cap Loading: Wet Crust	264
6.5	Unloading: Ice-Melt Rebound and Deglaciation	
	Tectonics	267
6.6	Fault Reactivation	270
6.7	Late Devensian Ice Loading in Scotland	271
6.7.1	Late Quaternary Glacial History of Scotland	272
6.8	Regional Ice Loading and Stress System	
	Evolution in Scotland	272
6.9	Removal of Late Devensian Ice Cover	
	(Windermere Interstadial)	275
6.10	Reloading and Rebound Retardation	278
6.11	Post-glacial Fault Reactivation in Scotland	279
6.12	Refined Ice Loading Model	280
6.13	First Order Fault Movement Chronology	283
6.14	Discussion	287
6.15	Conclusions	291
6.16	Acknowledgements	292
6.17	References	293
6.18	Figure Captions	300
6.19	Figures	302
6.20	Table 6.1	313
Chapter 7	A Large Rock Avalanche Triggered by Late Quaternary Seismic Activity in North West Scotland.	314
7.1	Abstract	314
7.2	Introduction	315

7.3	Rock Avalanches	316
7.4	Beinn Alligin Slope Failure	318
7.4.1	Source Slope Failure Scar	318
7.4.2	Slope Failure Debris	319
7.5	Discussion	321
7.6	Conclusions	326
7.7	Acknowledgements	327
7.8	References	328
7.9	Figure Captions	333
7.10	Figures	335
Chapter 8	Conclusions and Recommendations For Further Research.	344
8.1	Introduction	344
8.2	General Comments	344
8.3	Quaternary Seismotectonics	345
8.4	Results of This Study	348
8.5	Present and Future Crustal Movements	349
8.6	Understanding Post-Glacial Fault Movements	350
8.7	Recommendations for Further Research	350
8.8	References	352
Appendix A	Seismically-Induced Slope Failures	I
Appendix B	Neotectonic Fracture Orientations	XLV

Chapter 1

Introduction

1.1 Introduction

This introduction provides an overview of the background to, and the objectives of this study. Earlier work on recent fault movements in Scotland is briefly discussed, fundamental terminology is defined and the scope of the present study is outlined.

1.2 Long-Term Behaviour of 'Stable' Crustal Areas

The long-term behaviour and stability of 'stable' crustal areas has recently become a major environmental concern with the ever increasing need for sites for the safe disposal of radioactive waste (radwaste) products. The plans for many proposed sites worldwide consider sub-surface installations situated in areas of crystalline bedrock. These sites will have to be capable of storing radwaste for periods of time in excess of 10^6 years. Therefore the behaviour of the crust over such extended periods of time is of prime importance in the siting and design of such sensitive underground engineering structures. The long-term stability of the crust is equally important to a wide variety of surface structures.

The safety of radwaste storage is dependent on the performance of the waste itself and engineered barriers - storage canisters and repository construction materials. Although this is an area of concern outwith the scope of this thesis, these factors themselves are dependent upon the hydrological, chemical and tectonic conditions of the rockmass within which the repository has been sited. It is vital that the rockmass provides a mechanically stable environment with low groundwater flow and a favourable chemical environment for the duration of waste storage.

Of the many investigations required to assess stability of the rockmass, the analysis of 'recent' fault movements is of prime importance. It is vital to evaluate if such fault movements are continuing and if not, under what conditions they are likely to be reactivated. The level of seismic activity associated with fault movement and its effect on ground stability is also of importance. The possibility of the creation of new fractures is probably the greatest concern with bodies involved in the disposal of radwaste (Dames & Moore 1990). The effect that fault movements have on the hydrological regime and chemical environment in the vicinity of the repository are also

factors of great importance. To understand the long-term behaviour of the crust it is important to carry out a thorough investigation into the most 'recent' tectonic history of the area and combined with present day data, such as stress measurements and seismic activity, attempt to make predictions for the future behaviour. Although not the main thrust of this thesis, the research herein goes a long way to fulfilling these requirements.

1.3 Neotectonics - A Problem of Definition

Understanding the long-term behaviour of the crust requires the investigation of the most 'recent' tectonic, or *neotectonic*, history of an area. This in itself provides a problem of definition. In the most general of terms neotectonics concerns the study of 'recent' geological structures and processes. However it is important to define exactly what is meant by the rather vague term 'recent'. Where exactly do we draw the line between 'old' and 'recent' structures and processes?

The term neotectonics was originally proposed by Obruchev in 1948 (Mescherikov 1968). Other authors subsequently used similar terms, for example "lebendige tektonik" (living tectonics) of Wegmann (1955), to describe recent and active structural processes. Several authors have used arbitrary temporal limits to define neotectonics as late Cenozoic crustal deformation (Fairbridge 1981; Vita-Finzi 1986; Bates & Jackson 1987; Summerfield 1987). In some cases this may be further constrained to the Quaternary period. However such arbitrary time limits are not entirely satisfactory for defining the neotectonic period; the processes may have been occurring for a much shorter (or even longer) period than that defined above. Hence the beginning of the neotectonic period is not a global fixed value, but is dependent on the geological characteristics of individual (tectonic) environments. A more useful definition is that of Blenkinsop (1986) who defined neotectonics as beginning with the onset of the contemporary stress field. This definition was echoed by Pavlides (1989) who stated that neotectonics is the study of young tectonic events which have occurred or are still occurring in a given region after its last significant tectonic reorganisation.

For the purposes of this study the latter two definitions are adopted, thereby defining neotectonics as the study of structures and tectonic processes that arise as a consequence of the contemporary stress field. With respect to the United Kingdom this is taken as the last c. 6 myr (Muir Wood 1989). However the effects of repeated glaciations during the Quaternary period have significantly altered the stress field in the latter part of the Quaternary, resulting in tectonic activity (Lundqvist & Lagerbäck

1976; Ringrose 1987; Lagerbäck 1990). So it can be argued that the present day stress system is a product of the Devensian glacial period acting in conjunction with the ambient regional tectonic stress field. Therefore, by definition, in this study the neotectonic period as far as the UK is concerned is considered to be the last 10,000 years i.e. the Holocene or post-glacial period.

1.4 Post-Glacial Faulting: Previous Research

Fault movement in an area considered to be tectonically stable was first reported from Finnish Lapland by Kujansuu (1964), but it was not until Lundqvist & Lagerbäck (1976) described the late- to post-glacial movements on the Pärvie Fault from northern Sweden that the thought that such movements could be more widespread was considered. The impetus of a search by SKB, the Swedish Nuclear Fuel and Waste Management Company, for a hard-rock site for a radwaste repository and the work of Nils-Axel Mörner of Stockholm University brought the phenomena of post-glacial fault movements in so-called 'stable' crustal areas to light internationally (Mörner 1978, 1981). The research carried out into post-glacial fault activity in Scandinavia far outweighs that carried out in the UK, and thus forms a strong background with which to compare the findings from Scotland.

The idea that the UK ceased to be tectonically active at the end of the Tertiary (c. 2 Ma) was, and in many cases still is, a widely held view within the geological community. The attitude that the Quaternary was merely a period of repeated glaciation that did no more than cover the 'interesting' rocks with a mantle of 'drift' has prevailed. It was the community of physical geographers that first discovered, albeit unknowingly, that the late Quaternary was not a time of absolute tectonic stability in the UK. However the increasingly interdisciplinary nature of earth science studies, in response to increased environmental concerns and awareness, is now sweeping aside the old prejudices that the Quaternary does not constitute 'real' geology!

In the UK the first description of Quaternary fault activity was from the upper Forth Valley where two dislocations in the "Main Buried Shoreline" were measured during shoreline levelling studies (Sissons 1972). Subsequent work along the west coast of Scotland reported further incidences of differential uplift and dislocations in the shoreline profiles (Gray 1974a, 1974b, 1978). This evidence began to suggest that post-glacial rebound was more complex than a uniform isostatic response of the crust to the removal of the Devensian ice cover. Despite the accumulating evidence for shoreline offsets (Cullingford 1977; Robinson 1977), the significance of such data

was not fully realised until Sissons & Cornish (1982) noted the offset of the late glacial lake shorelines in Glen Roy and put forward the theory of differential isostatic uplift using faults for stress release, giving rise to elevated levels of seismic activity. Elevated levels of seismicity during the immediate post-glacial period were also hinted at by Holmes (1984) and Ballantyne & Eckford (1984) from studies of rock slope failures. However the significance of these findings with respect to late Quaternary seismotectonic activity was slow to be realised (e.g. Sissons 1975). Firth (1986) presented evidence for differential redepression of the crust during the Loch Lomond Readvance, apparently confirming the behaviour of the crust with respect to ice loading/unloading as proposed by Sissons & Cornish (1982).

The first specific study of post-glacial fault activity in Scotland by Ringrose (1987) gave an insight into the degree of fault movement and seismic activity during the late- and post-glacial period. Using previously reported data and extensive new field evidence Ringrose (1987) showed that fault activity was spatially associated with regions of maximum post-glacial uplift.

However only recently has the subject of Quaternary tectonic activity raised substantial interest in the UK as the problem of disposal of radwaste increases (Dames & Moore 1990). The recent occurrence of 'large' seismic events have increased awareness of fault reactivation and seismic risk within the UK (Marrow & Walker 1988; Woodcock 1990). The nuclear industry is now actively searching for the site of a repository (Nirex 1989) and geological considerations, especially the risk of faulting and ground rupture, are of prime importance (G. Eaton pers. comm. 1990).

This study follows on from the work of Ringrose (1987) and expands the geographical coverage of neotectonic and palaeoseismic data in Scotland. Consideration is also given to the mechanisms of Quaternary tectonics in Scotland and the reactivation of faults in a glacio-isostatic environment in general. All significant published data to date relating to Quaternary tectonics in the UK, and also relevant data worldwide, are referenced and discussed in the relevant sections within this thesis.

1.5 Objectives of the Present Study

The original title of this research project was "*Engineering Geological Hazards: Neotectonics, Palaeoseismicity and Geotechnics in Scotland*". During the course of this research the emphasis has swung away from the engineering-geotechnical aspects

and concentration has been placed on the tectonics, seismology and seismic risk elements of an area of 'stable' crystalline crust that has undergone repeated glaciations and subsequent unloading. This focus has been due to interests of the author and the deficiencies in such fields in previous studies concerning post-glacial fault activity. The main research objectives therefore became the following:

- to map and quantify post-glacial fault movement in Scotland.
- to construct a chronology of fault movement for the late Quaternary.
- to calculate seismic activity from mapping of ground deformation features.
- to compare instrumental, historical, and palaeoseismic data to calculate present seismic risk.
- to assess the mechanisms leading to fault failure.
- to assess the risk of further movement and the creation of new fractures.

From 1988 to 1990 an extensive programme of fieldwork was carried out at a number of sites in North West Scotland (Figure 1.1). These field sites were identified from four principal sources:

- sites recommended for further study in Ringrose (1987).
- features of possible seismogenic origin mentioned in the literature.
- features identified from aerial photographs.
- areas suspected of showing seismotectonic features due to the orientation of faults with respect to the regional stress field.

Prior to the start of fieldwork a programme of background research was carried out. This included a literature search to identify and catalogue numerous ground deformation features that may have had a seismogenic origin. This involved the search of a diverse range of sources including geological maps and memoirs, geomorphological and geographical periodicals and texts, sand and gravel resource

reports (to locate soft sediment deformation sites) and engineering geological reports. In conjunction with this, information on morphotectonic features related to recent fault movements, particularly in 'stable' continental areas of post-glacial rebound, such as slope failures, fault ground rupture and soft-sediment liquefaction was collated to compare with features already described from Scotland. An extensive search of the aerial photographic archive at the Scottish Development Department (Aerial Photography Unit) also identified a number of possible sites for further field investigation. In addition studies were made of the present day stress measurements and seismic activity in order to make comparisons with historical and palaeoseismic data (Ambraseys 1988). The work of Ringrose (1987) gave a firm foundation on which to build this study and many of his data were used to direct the initial stages of research.

Fieldwork methodology and philosophy owes much to that of previous workers in the field of palaeoseismology, particularly those of the USGS (Allen 1975; Crone 1987). Fieldwork involved the mapping of various morphotectonic features (Doornkamp 1986) such as fault scarps and fault ground rupture features (Wallace 1977; Bucknam & Anderson 1979; Mayer 1984; Mohr 1986; Lubetkin & Clark 1988), the analysis of fracture faces and fault architecture (Hancock & Engelder 1989), the recognition and measurement of offset or disruption of Quaternary geomorphology and drainage patterns by fault movement (Allen 1975; Allen *et al.* 1984), excavation and logging of fault zones (Douglas 1980; Bell & Katzer 1990; Lagerbäck 1990) and mapping of seismically-induced ground deformation features such as liquefied sediments (Kuribayashi & Tatsuoka 1975; Sims 1975; Youd 1977; Obermeier *et al.* 1985; Allen 1986) and slope failures (Keefer 1984a, 1984b; Wilson & Keefer 1985; Harp *et al.* 1986; Jibson 1987).

Subsequent work comprised the study of fault gouge material with a view to age-dating, as accurately as possible, the movement of the fault offsets observed. This involved SEM investigation of quartz grain surface morphology (Kanaori *et al.* 1980; Kanaori 1983, 1985) and Electron Spin Resonance (ESR) age-dating of the intrafault quartz grains (Ikeya *et al.* 1982; Miki & Ikeya 1982; Ikeya & Miki 1985; Grün 1991).

Additionally studies were made of the seismicity in the immediate post-glacial period and that presently experienced in the UK. The mechanisms of post-glacial fault reactivation were also considered in both site-specific and general terms.

1.6 Format of the Thesis

This thesis comprises eight chapters, six of which (Chapters 2-7) detail the results and findings of this research. Each chapter is a self contained paper with its own abstract and reference list. The final chapter is a summary of the conclusions and views expressed in each of the preceding chapters. In this final chapter a list of recommended themes for further research is outlined. The content of the other chapters is as follows:

Chapter 2 presents the field evidence for post-glacial fault movement and palaeoseismic activity in Scotland. Criteria for the recognition of post-glacial fault activity are defined and the mechanisms of post-glacial faulting are briefly discussed.

Chapter 3 details the evidence for late- and post-glacial fault activity in the area of Glen Roy and Glen Gloy. Particular attention is paid to the detailed chronology of fault movement and the mechanisms of fault reactivation at this site.

Chapter 4 compares the seismicity of the UK, and in particular N.W. Scotland, throughout the Holocene period. The quality of the instrumental, historical and palaeoseismic records is assessed with respect to completeness and accuracy. Temporal changes in seismic activity are discussed in conjunction with the tectonic deformation during this time.

Chapter 5 gives the results of a programme of age-dating using ESR and SEM to ascertain the exact age of fault movement during the late- and post-glacial period.

Chapter 6 considers the effects of ice-cap loading on the generation of the crustal stress regime, both in general terms and more specifically in relation to the Late Devensian glacial periods in Scotland. The mechanisms of post-glacial fault reactivation are also considered.

Chapter 7 describes a large seismically-triggered rock avalanche on Beinn Alligin in Wester Ross, N.W. Scotland.

1.7 References

Allen, C.R. 1975. Geological criteria for evaluating seismicity. *Geol. Soc. Am. Bull.* 86, 1041-1057.

Allen, C.R., Gillespie, A.R., Yuan, H., Sieh, K.E., Buchun, Z. & Chengnan, Z. 1984. Red River and associated faults, Yunnan Province, China: Quaternary geology, slip rates and seismic hazard. *Geol. Soc. Am. Bull.* 95, 686-700.

Allen, J.R.L. 1986. Earthquake magnitude-frequency, epicentral distance, and soft-sediment deformation in sedimentary basins. *Sedimentary Geology* 46, 67-75.

Ambraseys, N.N. 1988. Engineering seismology. *Earthquake Engineering and Structural Dynamics* 17, 1-105.

Bates, R.L. & Jackson, J.A. (eds.) 1987. *Glossary of Geology*. American Geological Institute. 3rd Edition.

Ballantyne, C.K. & Eckford, J.D. 1984. Characteristics and evolution of two relict talus slopes in Scotland. *Scot. Geog. Mag.* 100, 20-33.

Bell, J.W. & Katzer, T. 1990. Timing of late Quaternary faulting in the 1954 Dixie Valley earthquake area, central Nevada. *Geology* 18, 622-625.

Blenkinsop, T.G. 1986. *in* P.L. Hancock & G.D. Williams (eds.) *Neotectonics* (conference report) *J. Geol. Soc. London*, 143, 325-326.

Bucknam, R.C. & Anderson, R.E. 1979. Estimation of scarp-slope ages from a scarp-height-slope-angle relationship. *Geology* 7, 11-14.

Crone, A.J. (ed.) 1987. Proceedings of conference XXXIX - Directions in palaeoseismology. USGS Open File Rpt. 87-673.

Cullingford, R.A. 1977. Late glacial raised shorelines and deglaciation in the Earn-Tay area. *in* J.M. Gray & J.J. Lowe (eds.) *Studies in the Scottish late-glacial environment.*, 15-32, Pergamon, Oxford.

Dames & Moore 1990. Report of a meeting on "*Fractures and fracture development*" DoE Report No. DOE/RW/90.014 Dames & Moore International Technical Report TR-D&M-17.

Doornkamp, J.C. 1986. Geomorphological approaches to the study of neotectonics. *J. Geol. Soc. London* 143, 335-342.

Douglas, L.A. 1980. The use of soils in estimating the time of last movement of faults. *Soil Science* 129, 345-3352.

Eaton, G. 1990. British Nuclear Fuels Plc., Hinton House, Risley, Cheshire, WA3 6AS

Fairbridge, R.W. 1981. The concept of neotectonics: an introduction. *Zeit. fur Geomorphology Suppl.* - BD 40, vii-xii.

Firth, C.R. 1986. Isostatic depression during the Loch Lomond Stadial: preliminary evidence from the Great Glen, Northern Scotland. *Quaternary Newsletter* 48, 1-9.

Gray, J.M. 1974a. The main rock platform of the Firth of Lorn, western Scotland. *Trans. Inst. Br. Geogr.* 61, 81-99.

Gray, J.M. 1974b. Lateglacial and postglacial shorelines in western Scotland. *Boreas* 3, 129-138.

Gray, J.M. 1978. Low-level shore platforms in the South-West Scottish Highlands: altitude, age and correlation. *Trans. Inst. Br. Geogr., New Series* 3, 151-164.

Grün, R. 1991. Some remarks on ESR dating of fault movements. *J. Geol. Soc. London* (*in press*).

Hancock, P.L. & Engelder, T. 1989. Neotectonic joints. *Geol. Soc. Am. Bull.* 101, 1197-1208.

Harp, E.L., Wilson, R.C., Keefer, D.K. & Wieczorek, G.F. 1986. Seismically induced landslides: current research by the US Geological Survey. *Geologia Applicata Idrogeologia* 21, 159-173.

Holmes, G. 1984. Rock-slope failure in parts of the Scottish Highlands. Unpubl. Ph.D. Thesis, University of Edinburgh.

Ikeya, M. & Miki, T. (eds.) 1985. ESR Dating and Dosimetry. IONICS, Tokyo, 538pp.

Ikeya, M., Miki, T. & Tanaka, K. 1982. Dating of a fault by electron spin resonance on intrafault materials. *Science* 215, 1392-1393.

Jibson, R.W. 1987. Summary of research on the effects of topographic amplification of earthquake shaking on slope stability. USGS Open File Rpt. 87-268.

Kanaori, Y. 1983. Fracturing mode analysis and relative age dating of faults by surface textures of quartz grains from fault gouges. *Engineering Geology* 19, 261-281.

Kanaori, Y. 1985. Surface textures of intrafault quartz grains as an indicator of fault movement. *CATENA* 12, 271-279.

Kanaori, Y., Miyakoshi, K., Kakuta, T. & Satake, Y. 1980. Dating fault activity by surface textures of quartz grains from fault gouges. *Engineering Geology* 16, 243-262.

Keefer, D.K. 1984a. Rock avalanches caused by earthquakes: source characteristics. *Science* 223, 1288-1289.

Keefer, D.K. 1984b. Landslides caused by earthquakes. *Geol. Soc. Am. Bull.* 95, 406-421.

Kujansuu, R. 1962. Nuorista sirroksta Lapissa (Recent faults in Lapland). *Geologi* 16, 30-36.

Kuribayashi, E. & Tatsuoka, F. 1975. Brief review of liquefaction during earthquakes in Japan. *Soils & Foundations* 15, 81-92.

- Lagerbäck, R. 1990.** Late Quaternary faulting and palaeoseismicity in northern Fennoscandia, with particular reference to the Lansjärv area, northern Sweden. *Geologiska Föreningens i Stockholm Förhandlingar* 112, 333-354.
- Lubetkin, L.K.C. & Clark, M.M. 1988.** Late Quaternary activity along the Lone Pine Fault, eastern California. *Geol. Soc. Am. Bull.* 100, 755-766.
- Lundqvist, J. & Lagerbäck, R. 1976.** The Pärve Fault: a late glacial fault in the Precambrian of Swedish Lapland. *Geologiska Föreningens i Stockholm Förhandlingar* 98, 45-54.
- Marrow, P.C. & Walker, A.B. 1988.** Lleyn earthquake of 1984 July 19: aftershock sequence and focal mechanism. *Geophysical Journal* 92, 487-493.
- Mayer, L. 1984.** Dating Quaternary fault scarps formed in alluvium using morphological parameters. *Quaternary Research* 22, 300-313.
- Mescherikov, Y.A. 1968.** Neotectonics. *in* R.W. Fairbridge (ed.) *Encyclopedia of Geomorphology*. Reinhold, New York.
- Miki, T. & Ikeya, M. 1982.** Physical basis of fault dating with ESR. *Naturwissenschaften* 69, 390-391.
- Mohr, P. 1986.** Possible late Pleistocene faulting in Iar (west) Connacht, Ireland. *Geol. Mag.* 123, 545-522.
- Mörner, N-A. 1978.** Faulting, fracturing, and seismicity as functions of glacio-isostasy in Fennoscandia. *Geology* 6, 41-45.
- Mörner, N-A. 1981.** Crustal movements and geodynamics in Fennoscandia. *Tectonophysics* 71, 241-251.
- Muir Wood, R. 1989.** Fifty million years of "passive margin" deformation in North West Europe. *in* S. Gregersen & P.W. Basham (eds.) *Earthquakes at North Atlantic Passive Margins: neotectonics and postglacial rebound.*, 7-36, Kluwer Academic Publishers, Dordrecht.

Nirex Ltd. 1989. Deep repository project: preliminary environmental and radiological assessment and preliminary safety report. Nirex Rpt. No. 71, 130pp.

Obermeier, S.F., Gohn, G.S., Weems, R.E., Gelinas, R.L. & Rubin, M. 1985. Geologic evidence for recurrent moderate to large earthquakes near Charleston, South Carolina. *Science* 227, 408-411.

Pavrides, S.B. 1989. Looking for a definition of neotectonics. *Terra Nova* 1, 233-235.

Ringrose, P.S. 1987. Fault activity and palaeoseismicity during Quaternary time in Scotland. Unpubl. Ph.D. Thesis, University of Strathclyde. 2 vols.

Robinson, M. 1977. Glacial limits, sealevel changes and vegetational development in part of Wester Ross. Unpubl. Ph. D. Thesis, University of Edinburgh.

Sims, J.D. 1975. Determining earthquake recurrence intervals from deformational structures in young lacustrine sediments. *Tectonophysics* 29, 141-152.

Sissons, J.B. 1972. Dislocation and non-uniform uplift of raised shorelines in the western part of the Forth Valley. *Trans. Inst. Br. Geogr.* 55, 145-159.

Sissons, J.B. 1975. A fossil rock glacier in Wester Ross. *Scott. J. Geol.* 11, 83-86.

Sissons, J.B. & Cornish, R. 1982. Rapid localised glacio-isostatic uplift at Glen Roy, Scotland. *Nature* 297, 213-214.

Summerfield, M.A. 1987. Neotectonics and landform genesis. *Progr. Phys. Geogr.* 11, 384-297.

Vita-Finzi, C. 1986. Recent earth movements, an introduction to neotectonics. Academic Press, London, 266pp.

Wallace, R.E. 1977. Profiles and ages of young fault scarps, north-central Nevada. *Geol. Soc. Am. Bull.* 88, 1267-1281.

Wegmann, E. 1955. Lebendige Tektonik, eine Übersicht. *Geol. Rdsch.* 43, 4-34.

Wilson, R.C. & Keefer, D.K. 1985. Predicting areal limits of earthquake-induced landsliding *in* J.I. Ziony (ed.) Evaluating earthquake hazards in the Los Angeles Region - an earth science perspective. USGS Professional Paper 1360, 317-345.

Woodcock, N. 1990. Ancient faults and modern earthquakes. *New Scientist* 127 No.1724, 38-41.

Youd, T.L. 1977. Discussion of brief review of liquefaction during earthquakes in Japan. *Soils & Foundations* 17, 82-85.

1.8 Figure 1.1

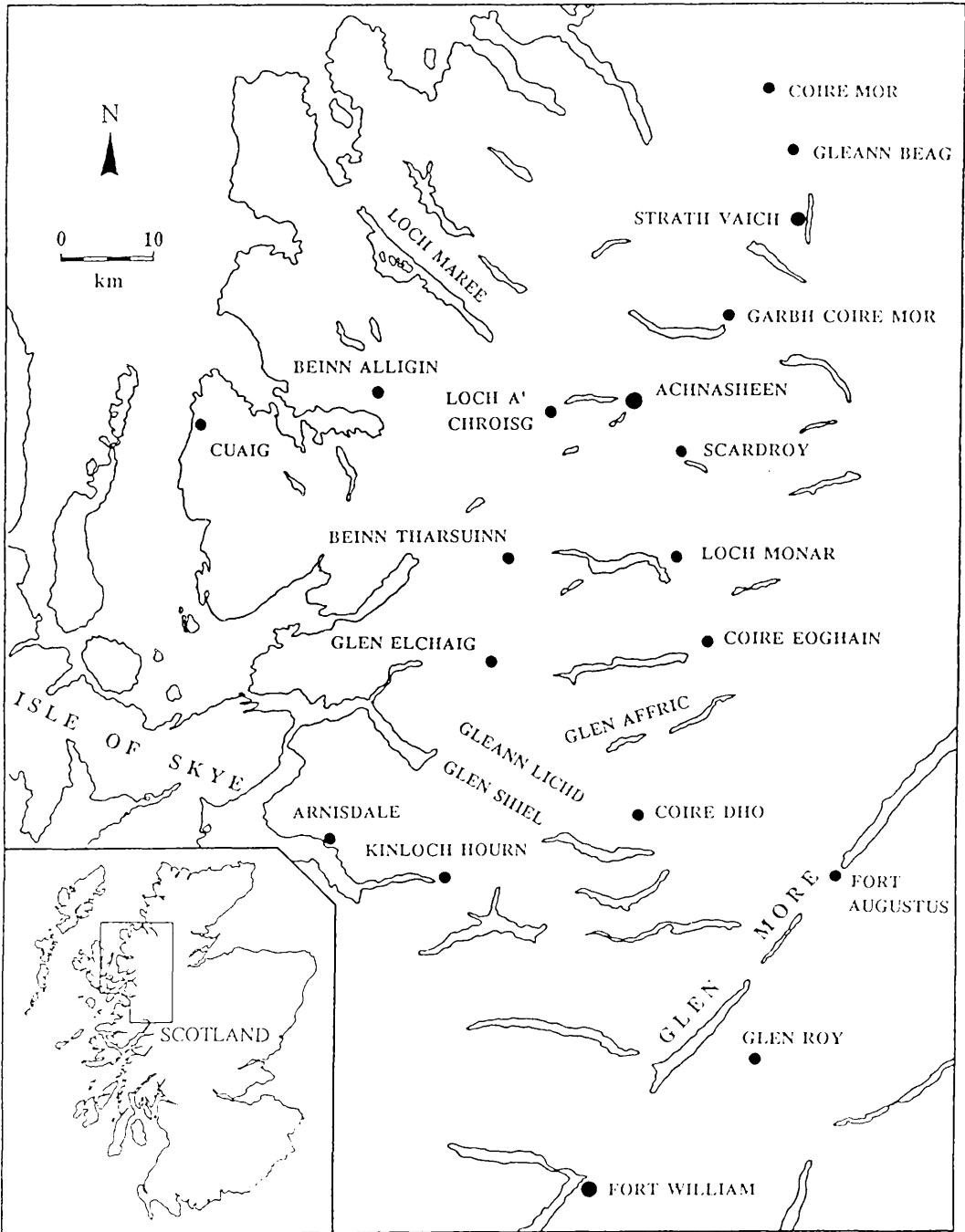


Figure 1.1 Location of principal field sites showing evidence of late Quaternary seismotectonic activity in N.W. Scotland. Inset shows location of the area of study.

Chapter 2

Late Quaternary Fault Activity in N.W. Scotland

Clark Fenton

Department of Geology and Applied Geology

University of Glasgow, Glasgow, G12 8QQ.

2.1 Abstract

Detailed field examination has revealed evidence for late Quaternary movement along a number of faults in North West Scotland. Fault movement has occurred along reactivated basement faults and displaces drainage courses and other late Quaternary geomorphological features. The pattern of faulting is consistent with the release of stress built up by a combination of glacial loading and tectonic compression. Faulting is associated with a period of rapid isostatic uplift and enhanced strain rate during and immediately following deglaciation. However, on certain faults, such critical levels of stress may have persisted well into the Holocene, allowing the continuation of fault movement outwith the immediate post-glacial period. The degree of fault offset and distributions of associated slope failures and soft-sediment deformation show that fault movement was accompanied by enhanced levels of seismic activity, with events as large as 7.0 M_S .

2.2 Introduction

The North West Highlands of Scotland is an area comprised almost entirely of Archaean and Proterozoic rocks of the Moine and Lewisian successions, effectively an area of Precambrian shield or craton. Such areas are characterised by general (tectonic) stability, and as such have been called 'Stable Continental Interiors' on account of their low seismicity levels (Johnston 1989). Indeed Scotland is presently an area of especially low seismic strain release [§ 4.3, p151]. Quaternary tectonics of the region have been dominated by glacio-isostatic depression and rebound in response to repeated glacial episodes during this time. However a number of recent reports detailing large surface fault offsets and evidence for anomalously large seismic events in such areas have called into question the concept, and use, of the highly relative term 'stable' (Adams 1989; Bäckblom & Stanfors 1989; Grant 1990; Lagerbäck 1990; Adams *et al.* 1991). In particular, workers in Scandinavia have shown that in formerly glaciated areas the glacio-isostatic rebound phase is tectonically a very active period (Kujansuu 1964; Talbot 1986; Lagerbäck 1988, 1990; Muir Wood 1989b; Olesen 1989). Recent studies in Scotland show that this enhanced level of tectonism and seismicity may last for longer than merely the immediate post-glacial period, depending on the local geological conditions and the stress history during the glacial period (Sissons & Cornish 1982; Ringrose 1987, 1989a, 1989b; Davenport *et al.* 1989; Ringrose *et al.* 1991). This paper outlines the evidence for post-glacial fault activity and palaeoseismicity in North West Scotland.

2.3 Tectonic History

Scotland is dissected by a large number of faults (Figure 2.1) that record a history of tectonism extending back to the Precambrian time. These faults have a number of dominant orientations that, under favourable stress conditions, have been subject to reactivation in a number of tectonic episodes. Caledonian orogenesis, Permo-Carboniferous rifting and Tertiary vulcanism are responsible for the dominant fault trends seen in the area. These are:

(i) NE to NNE Caledonian strike-slip faults, most common in the central and east northern Highlands. These are long faults that show offsets of the order of kilometres, e.g. Strathconon, Strathglass and Great Glen Faults.

(ii) WNW-trending faults. These may be of Caledonian age, however similar fault trends in the North Sea suggest they may be of Permo-Carboniferous age. Some show Tertiary reactivation (Johnston & Frost 1977).

(iii) E- & ENE-trending Permo-Carboniferous rift and wrench faults of the Midland Valley and possibly the southern Highlands.

(iv) NE-trending faults of Tertiary volcanic rifting developed in the Inner Hebrides and SW Scotland.

Less prominent faults are:

(v) E-W faults of uncertain origin in the SW Highlands. These form topographic features between Caledonian shear zones and possibly represent the axial traces of folds associated with Caledonian sinistral shear. They are known to cut Devonian rocks (Johnston & Frost 1977).

(vi) Radial and concentric fractures associated with Tertiary igneous centres. Auden (1954) noted radial fractures converging on and concentric fractures circling the Island of Eigg in the Inner Hebrides. Radial fractures were also noted around the Cairngorm granite complex.

The fault distribution of the NW Highlands (Figure 2.2) is dominated by the NE-trending the Caledonian age Strathconon, Strathglass, Helmsdale and Great Glen Faults. The largest 'fault' in the area is the Moine Thrust Zone that extends for over 200 km from Durness on the north coast to Sleat on the SW tip of Skye. This marks the front of the Caledonian Orogen in NW Scotland. There are also a number of NW-trending faults, most prominent of which is the Loch Maree Fault extending from the Rubha Reidh on the west coast to abut against the Strathconon Fault 70 km further inland. It is faults paralleling the Loch Maree trend and those with a more northerly or easterly trajectory that would be preferentially reactivated under the present NW-SE orientated regional stress field.

2.4 'Recent' Fault Movements

The last major tectonic movements in Scotland were during the Tertiary (Muir Wood 1989a) and involved displacement along a number of Caledonian faults and also the creation of a number of new NW- and N-trending faults (Battiau-Queney

1989). In the Highlands of Scotland this was essentially a period of differential block movement and uplift (Le Coeur 1988), as shown by the relative heights of the Hebridean Tertiary igneous centres (Muir Wood 1989a). Most fault movement was accommodated along offshore faults e.g. in the Moray Firth Basin. The regional stress field [§ 1.3, p2] was initiated at c. 6 Ma, i.e. the late Miocene (Muir Wood 1989a). This is the stress field that has been responsible for all subsequent tectonic movements i.e. Quaternary fault activity.

The study of faults in Scotland, and indeed the UK as a whole, has concentrated on the main periods of orogenesis such as the Caledonian and the Hercynian. Even the Tertiary did not raise much interest until the discovery of hydrocarbon plays on the continental shelf. For this reason much of the data concerning Tertiary tectonics has remained proprietary. However the continental shelf programme of the BGS has recently allowed the publication of some of this information in the form of the offshore geology maps. This has given an insight into the degree of fault movement and allowed a better understanding of the stress system acting at this time. The more detailed studies of the continental shelf programme have shown that some of this fault movement has continued into the Quaternary (Kirkton & Hitchen 1987). This has been shown on previous BGS surveys (Figure 2.3) but has never 'merited' comment (Evans *et al.* 1979).

The current need for the location of a nuclear waste repository in the UK has led an increase in fault activity evaluation studies (Dames & Moore 1990) and subsequently the recognition of a number of fault movements in the Quaternary period (G. Eaton pers. comm. 1990). Until now the reporting of Quaternary fault activity has been minimal. Several offsets of late- and post-glacial shorelines were reported by various members of the geographic community and tentatively attributed to offset by tectonic fractures (Sissons 1972; Gray 1974; Robinson 1977; Sissons & Cornish 1982; Firth 1986). The work of Ringrose (1987) was the first to address the phenomena of fault activity during the Quaternary period in the UK. This showed that there was enhanced levels of fault activity and seismicity in the immediate post-glacial period. This study extends the work of Ringrose (1987) by increasing the data base of Quaternary tectonic activity in both the number of faults and the geographical area covered.

2.5 Post-glacial Faults (PGFs): Criteria for Recognition

Examination of aerial photographs will show that Scotland is covered by a number of 'strong' linear features, not all of which are faults, and definitely not all of which are the result of recent fault activity. Therefore it is only by detailed fieldwork that it is possible to determine which linear features are in the first instance the result of fault activity and not the due to differential erosion, glacial plucking or merely due to the structure of the underlying bedrock.

A number of likely targets were first chosen from an aerial photographic survey using the criteria of Lagerbäck (1979) for identifying neotectonic features in the Norbotten region of Sweden. In this manner a data base of likely recent faults was compiled and acted as the focus for subsequent fieldwork.

The preservation of fault scarps is primarily dependent on climate and the material from which the scarp has been formed, with unconsolidated surficial materials such as colluvium, peat and alluvium only preserving scarps for a few thousand years at most, even in arid climates (Wallace 1977; Bucknam & Anderson 1979). Bedrock scarps are much less susceptible to denudation, and therefore have much better potential for preservation (Stewart & Hancock 1990). However by virtue of their similar morphology to fault scarps, glacially plucked scarps are often erroneously interpreted as being the result of fault activity, as seems to be the case with a number of so-called PGFs in southern Sweden (Mörner *et al.* 1989; SKB 1990). With this caveat in mind, care must be exercised in identifying PGFs in areas that have a poorly developed or non-existent late Quaternary stratigraphy, such as the N.W. Highlands of Scotland, with which to date the exact timing of fault movement. The following criteria for the identification of PGFs in such an area has been modified and expanded from that of Mohr (1986):

- (i) surface rupture/fault scarp must be continuous over a distance of at least 1 km with a marked morphological break, continuous surface disruption features or consistent offset of pre-existing morphological features.
- (ii) scarp faces must show no signs of glacial modification such as striations, evidence of glacial plucking or preferential erosion of pre-existing linear features by melt water.

- (iii) scarp or ground rupture must not be controlled by banding, bedding, or schistosity of the country rock, and therefore introduce the possibility that the scarp is the result of differential erosion.
- (iv) surface rupture must be seen to disturb and/or displace late Quaternary sediments or morphological features such as shorelines, glaciated surfaces, glacial geomorphology or periglacial and Holocene deposits.
- (v) scarps in superficial material must be shown to be the result of fault movement and not the result of differential compaction or drape over pre-existing (erosional) scarps.
- (vi) trenching across the scarp is necessary to ensure that the scarp is the result of fault activity, and if so to note the degree of modification by later erosional processes.

It must be noted that fault scarps produced by recent movement in areas undergoing post-glacial rebound, even when the locus of seismicity is shallow as with the Ungava earthquake in N.E. Canada, are not necessarily as prominent as the 'classic' PGF scarps described from northern Sweden (Lagerbäck 1988, 1990; Muir Wood 1989b; Adams *et al.* 1991). As a consequence many such scarps may neither be preserved nor recognised. Indeed the fact that the scarps are the result of *post-glacial* faulting removes some of the doubt that such scarps may pre-date the glacial period, as it is unlikely that such 'delicate' features would survive the effects of the severe erosion associated with the passage of 'active' glacial ice. The fact that the last glacial event in Scotland, the Loch Lomond Readvance (LLR), removes most of the evidence of former late Quaternary glacial episodes in the North West Highlands of Scotland shows that it was an extremely erosive event and would most likely have destroyed any pre-existing fault scarps. Thus, unless there is other evidence to refute the case, it is considered that all the true pristine fault scarps identified in this area are the result of fault activity post-dating the LLR.

The recognition of palaeoseismic activity, if any, associated with post-glacial fault activity uses the same criteria that have now become well established from worldwide studies into palaeoseismology (Allen 1975; Sims 1975; Crone 1987). This involves the recognition of seismite ground deformation features such as liquefaction of sediments, slope failures and other ground disruption features. The type, areal extent and distribution of these features allows estimates of the magnitude of the seismic events to be made using the statistical relationships defined from numerous

studies worldwide (Youd 1977; Bonilla *et al.* 1984; Keefer 1984a; Kuribayashi 1985; Khromovskikh 1989).

2.6 Post-glacial Faulting in N.W. Scotland

Most of the field sites are located in North West Scotland in the areas of Inverness-shire and Ross-shire (Figure 2.4). The morphotectonic features (Doornkamp 1986) of each fault are described in detail, as are the associated seismic deformation features. (NB. In the following sections strike azimuths are measured clockwise through 360° using the left hand rule.)

2.6.1 Coire Mor Fault

The Coire Mor fault (Figure 2.5) is a major basement fault trending NW-SE (between 126° and 154°) extending along the length of Coire Mor to the NW and SE onto the plateau of 'Monadh Dubh' above Gleann Beag in Easter Ross. At its SE end the fault terminates against the N-S trending Strath Vaich fault [§ 2.6.2, p24], itself part of the Strathconon Fault system (Figure 2.2). The fault has displaced Moine psammities and pelitic gneisses by 0.7-0.75 km in a dextral manner. This movement is probably of Caledonian age (c. 500-400 Ma). Only a 3.5 km section of the fault along the bottom of Coire Mor shows evidence for recent movement. The NW continuation of the fault is obscured by blanket peat.

From Loch a' Choire Mhoir [Grid Ref. NH307887] to the headwall of Coire Mor [NH330865] the fault has a pronounced surface trace clearly visible on air photographs and from the surrounding hills (Figure 2.6) as a remarkably straight linear feature crossing rugged, glaciated topography varying from 300 to 700 m above sea level. Linearity over such terrain is indicative of a vertical or sub-vertical fault plane. In cross-section the NW segment of the fault is seen to be a N-facing scarp up to 4 m in height (A, Figure 2.5). This forms an upstanding ridge of some 700 m in length before the fault gully on the uphill side of the ridge is in-filled with peat (B, Figure 2.5) and the fault is marked by a continuous rocky break in slope downhill from an almost flat area of blanket peat. The scarp height decreases, and eventually disappears to the SE until the fault trace again outcrops in Allt a' Choire Mhoir as 70°/320° fractures and an unconsolidated, open-network, splinter breccia. The fault trace is then exposed along a subsidiary watercourse [NH328876]. From this exposure a narrow depression runs uphill to join the exposed fault in a narrowing

gully in the crags of the corrie headwall before the fault is finally obscured below slope wash and extensive frost shattered debris on the plateau of 'Monadh Dubh'.

When bedrock is exposed the fault is marked by a zone of intense fracturing and brecciation. This is generally in the form of unconsolidated, fragmented rock. Fault gouge is found only at one site in the gully of the corrie headwall [NH331864]. This seems merely to be a formerly indurated epidote clay gouge, found at various points along the fault trace, that has been 'reworked' during the most recent fault movement. It is up to a maximum of 20 mm thick, and along with small rock fragments, fills 140° fractures. For the majority of the fault exposure such fractures (trending 126° to 154°) are open by up to 15 mm and spaced at c. 20 cm, decreasing to 2-3 cm in zones of most intense deformation.

The fault trace runs sub-parallel to the floor of Coire Mor and the main drainage course, Allt Choire Mhoir. However tributaries flow S to SW cross the fault, four of which show dextral offset of the order of tens of metres. Those that show no offset are generally very shallow and flow over recent surface deposits, namely peat and slope wash. The four displaced streams are deeply incised, by 2-3 m, into bedrock and exhibit dextral offset in the range of 30 to 100 m. The upper limit may be an over estimate due to the possibility of realignment of the upper stream course in this instance. If this is the case, the magnitude of the offset is reduced to between 30 m and 50 m, a seemingly more acceptable value for strike-slip displacement along a fault of this length. However, the blanket peat cover of the fault's NW extension down Strath Mulzie may be concealing a significant portion of the fault that may also have also undergone recent movement. In this instance 100 m movement would not be so implausible.

The morphology of the fault scarp, a north-facing scarp-ridge of up to 4 m in height, suggests downthrow of this order to the north. This corresponds to the evidence from the incision of the drainage courses across the fault. All displaced streams show enhanced incision on the SW (upthrown) side of the fault, a feature noted in other faulted drainage patterns as the watercourses attempt to re-equilibrate their profiles from the knickpoints created by the fault movement (Ringrose 1989a, 1989b).

The fault scarp itself is a relatively delicate feature, comprising a ridge of up to 4 m high and a few tens of metres in width at its maximum and composed of shattered and fractured Moine psammities and pelitic gneisses. It would not be expected that

such a feature would survive the last glaciation (Coire Mor contained 200-400 m thickness of ice during the LLR (Sissons 1977b)) and indeed the scarp face shows no evidence of glacial striations or other indicators for the passage of ice that are so abundant on the surrounding rock surfaces. From this it is clear that formation of the fault scarp was post-glacial in age i.e. post 10.3 kyr BP. Also the lack of appreciable frost shattering of the scarp shows that the fault scarp must have been formed well into the post-glacial period. The age of the offset of the drainage courses is uncertain. Fault movement obviously post-dates the formation of the local drainage patterns. However the age of the drainage courses is uncertain. At most they will be Pleistocene in age as it is thought unlikely that such features would have survived the effects of repeated glaciations. The fact that the fault scarp is in-filled with peat on its uphill side along part of its length shows that the movement must have ceased by the time of peat formation, c. 6-4 kyr BP (Birks 1977). In the absence of any more accurate dating (due to a lack of suitable material) this gives a reasonable constraint on the age of faulting. It is likely that the lateral displacement along the fault, of the order of 30 to 50 m, and possibly as great as 100 m, in a dextral sense occurred as a number of events. It has not been possible to establish the number, magnitude and timing of such movement increments. It is not thought that all this displacement occurred in the post-glacial period, but represents multiple movements during the Quaternary (Averaged over this time this magnitude of displacement would give a movement rate of 0.015-0.1 mm yr⁻¹). However the 4 m scarp is thought to be a post-glacial feature.

The surrounding area is one of a high plateau deeply dissected by glacially eroded glens that has left a number of slopes in a critically oversteepened state, resulting in a large number of large slope failures. In addition there are a number of slope failures that have occurred on what seem to be stable slope configurations: gentle slopes with low angle failure planes. This seems to suggest that these failures were the result of more than gravitational slope collapse. Holmes (1984), investigating rock slope failures throughout the Highlands using limit equilibrium analysis, proposed that such failures were the result of high 'cleft' water pressure. However such a mechanism would be more likely to cause gradual progressive failure and not the sudden collapse that is exhibited by the morphology of a number of these failures. The fact that failure has occurred as sudden events without further movement suggests that the failures were the result of a single destabilizing event. The slope failures all disturb glacial and periglacial deposits as well as bedrock suggesting that failure occurred sometime into the post-glacial period, by which time the high 'cleft' water pressure of Holmes (1984) would have decayed. This is not to say that previous high fracture fluid pressures could not have weakened the slopes prior to this time, just not

sufficiently to cause failure. The post-glacial age for the failure triggering and the suddenness of the failure styles suggests that the trigger was seismic activity associated with the movement along the Coire Mor fault. The morphologies of the slope failures also suggest that seismic activity was the trigger for these failures. The failure at the head of Alladale [NH358880] is similar to the 'jumbled castle' failure attributed to high magnitude seismic shaking (Eisbacher 1979). Failure has occurred along a low angle ($<25^\circ$) basal plane. Downslope displacement has resulted in disaggregation of the sliding block resulting in a number of unstable blocks and towers. Rockfall activity in Gleann Beag [NH327837] (Figure 2.7a) shows excess travel distance. The height of fall is insufficient to provide enough initial momentum to create a true rock avalanche, however long-duration seismic ground motion would be sufficient to keep the debris in motion along the shallow angle slope at the base of the source area. Other failures in the area (Figure 2.7b) are interpreted as 'sudden collapse slumps' that have occurred on otherwise stable slope configurations. These occur only in close proximity to the fault and are thought to be the result of violent, near-field seismic ground acceleration. Slope failures are the only 'seismite' deformation features observed in the area. Quaternary sediments comprise almost entirely of sandy tills that show no signs of having been affected by strong ground motions.

2.6.2 Strath Vaich Fault

The Strath Vaich fault (Figure 2.4) is a N-S trending splay from the NE-trending Strathconon-Glen Calvie fault system. This is a long-lived basement fault that is coincident with a steepening, to vertical, of the regional dip of the Moine country rock. The fault extends for 16 km, on a 345° to 360° trajectory, from the Strathconon Fault [NH692357] in the south to its 'junction' with the Coire Mor fault on 'Monadh Dubh' [NH3485] at the northern end. The relation between the two faults is obscured by extensive cover of peat and frost shattered debris. The fault seems to have been active during the Devonian, controlling the deposition of conglomerates resting on the Moine basement (R.S.Haszeldine pers. comm. 1989). A number of features along the fault length are indicative of some degree of recent movement.

Attention was first drawn to the area by the number of large slope failures in close proximity to the fault surface trace, suggesting that movement along the fault may have been responsible for seismic activity that in turn triggered the slope failures. Surface expression of recent fault movement is sporadic, occurring along a 5 km section of the fault on the eastern side of Loch Vaich. At its northern end the fault acts as the sidewall release fracture for a large slump failure on Cail Mor [NH344844].

This section of fault is probably not strictly part of the Strath Vaich fault, but a 'linking segment' between the Strath Vaich and Coire Mor faults. On the eastern side of Meall a' Chuaille [NH348823] a slight break in slope is highlighted by a line of relict debris flow scars over a distance of c. 800 m. This may represent a former spring line along the fault allowing the escape of overpressurised groundwater created by glacial loading and released during post-glacial fault movement [§ 6.9, p277]. Peat obscures the actual fault until it crosses Allt nam Fiadh [NH350812] as a series of N-S trending fractures. A subsidiary fracture set trends 120-300°. South of here the main fault is obscured by blanket peat before disappearing into Loch Vaich. However on the hillside to the east of the loch a number of fault zones are exposed in the beds of streams. These show shattering and open fracturing of the country rock along 350° to 010°. One particular example above Lubachlaggan [NH252788] continues southwards for 350 m as a 2 m high uphill (east) facing scarp. The scarp cuts obliquely across the strike of the Moine psammities and forms a prominent, upstanding feature, peat-filled on its uphill side. It may be more extensive than its present expression would suggest possibly due to the extensive cover of peat to the south and a slope failure to the north obscuring any possible extension of the feature in these directions. Assuming that the fault continues under the slope failure the scarp length would be up to 1000 m. If the spring lines on Meall a' Chuaille are considered to represent part of the active fault length then the surface rupture length is c. 6 km. South of Loch Vaich the fault is obscured by extensive glacial outwash deposits. When exposed (at NH350748 and NH361703) the fault shows no evidence for recent movement, being merely a zone of silicified breccia or indurated epidote clay.

Although the fault trace runs across the drainage courses on the eastern side of Loch Vaich it shows no evidence for drainage offset. However, where drainage courses cut across the fault scarp above Lubachlaggan there is a marked incision on the western side of the fault scarp. This agrees with the offset determined from scarp morphology and suggests downthrow to the east. The fact that the fault movement seems to have been accommodated along a number of small surface fractures seems to suggest reactivation of a complex fault structure. Indeed, cross sections constructed using the data on the BGS sheet 93 show the fault to have an upward bifurcating, flower structure. Morphology of the fault scarp suggests reactivation as a reverse fault.

Fault movement is of post-glacial origin, as the fault scarp, being composed of shattered Moine psammite, would not have withstood glacial erosion. Indeed the scarp face itself shows no evidence of glacial scouring. The fault scarp is partially infilled

with peat on its uphill side and disappears beneath peat to the south. Fault movement obviously pre-dates the formation of the peat. The spring-line debris flows on Meall a' Chuaille also affect only glacial debris and not the later formed peat. Thus the fault movement occurred sometime between 10.3 and 6 kyr BP. This probably occurred as a one-off 'pop-up' event associated with seismic activity that acted as the trigger for the widespread slope failures seen in the area.

There are a number of slope failures in the vicinity of the Strath Vaich fault. As with those adjacent to the Coire Mor fault they show morphological features that suggest sudden collapse where movement has occurred on what should have been stable slope configurations. An interesting feature of a number of the failures is the 'dry stane dyke' texture of the rock mass within the failed areas (Figure 2.8). The rock has been disaggregated along pre-existing discontinuities to form a loose jig-saw of sub-metric sized boulders. This is not confined to the basal and lateral movement zones within these slumped masses as is normally the case, but is present throughout the whole failed mass. It is tentatively suggested that this total disaggregation of the rock mass is due to seismic shaking.

2.6.3 Garbh Choire Mor Faults

Garbh Choire Mor [NH2567], at the eastern end of the Fannich Mountains, is the site of a rockfall avalanche (Figure 2.9a,b). Such slope failures are usually indicative of seismicity $\geq M_L$ 6.0 (Keefer 1984a,b). This is 9 km distant from the Strathconon Fault, close enough for a major seismic event along this fault to have caused such slope failure. However this segment of the fault shows no evidence for any significant movement in post-glacial times. The slope failure must have occurred after the disappearance of LLR ice as the debris rests on glacially scoured slabs in the corrie floor.

Investigations in the area of Garbh Choire Mor have revealed a roughly N-S trending fault that may be responsible for generating the seismic activity to trigger the slope failure. The south wall of the corrie is cut by a shallow vertical gully up to 2 m in width (Figure 2.9c). This is filled by unconsolidated sheared rock, cut by anastomosing 171° to 181° and 012° to 030° fractures, in a zone of intense shearing trending 172 - 352° and up to 1 m in width. This is a reactivated basement fault of probable Caledonian age; the gully walls are composed of silicified breccia. No sense of displacement can be determined from the limited exposure.

The central gully in the corrie backwall (Figure 2.9a), adjacent to the rock avalanche scar, exposes a 117-297° trending fault zone with continuous open or epidote-clay filled fractures trending 283° to 299° over an exposure of 40 m. Splays from these fractures trend 309° to 330°. Further up the gully the fault zone becomes a loose breccia in a matrix of soft gouge-like material.

Both faults seem candidates for recent movement due to the 'fresh' (open fractures containing unconsolidated breccia or soft gouge) nature of the fractures and unconsolidated state of the fractured rock. Neither has any indicators of movement direction nor do they show any considerable movement as judged from the surrounding morphologies. The amount of movement was probably of the order of a metre, merely reflecting differential rebound movement following the removal of LLR ice. Indeed ice removal could have either:

i) triggered movement along the N-S fracture causing seismicity that was responsible for the triggering of the rock avalanche, this (the unloading of $0.6 \times 10^6 \text{ m}^3$ of rock) in turn causing subsequent movement along the 297° fault zone.

ii) both faults triggered at the one time, both being responsible for the generation of seismicity.

iii) movement on one fault or the other disturbing crustal equilibrium causing multiple, contemporaneous seismicity giving a large input of cyclic seismic shaking leading to the destabilization of a possibly pre-weakened rock slope giving rise to what under 'normal' conditions would have been a rock fall, but the additional shaking energy promoting the failure into a rock avalanche (Eisbacher 1979) [§ 7, p324].

Whatever the case, the area was one experiencing a high degree of movement during the period following the removal of the last glacier ice. In front of the main debris lobe of the rockfall is an area of smoothed glaciated slabs that are cut by a number of fractures that displace the smoothed surface, showing quite clearly that the movement along these faults was post-glacial in age (Figure 2.9d). These fractures trend 70°/276°, with a subordinate set at 90°/234°, and consistently show down throw to the north, movement being of the order of 2-3 mm. Morphology of the fractures suggests that they are shallow features and represent the surface expression of localised differential relaxation, accommodated along a number of small surface fractures.

Individually the ground deformation features in the area of Garbh Choire Mor are not conclusive proof for palaeoseismic activity. However the recent fractures that cut the glacially-smoothed slabs in the corrie floor do suggest that the area was undergoing some degree of differential uplift, possibly associated with the release of seismic strain, during the post glacial period. Also the fact that the slope failure from the corrie backwall has progressed to become a rock avalanche with a fahrböschung (Hsü 1975) of 27° and an excess travel distance of 191 m suggests that the trigger was more than gravitational instability. The mechanism for rock avalanche triggering is most often seismic shaking with the action of long duration seismic ground motion giving rise to 'streaming' of the debris resulting in the excess travel distance observed (Eisbacher 1979). Rock avalanche behaviour is triggered by seismic activity $>M6.0$ (Keefer 1984a). The area surrounding Garbh Choire Mor has a number of large, deep-seated slump failures that may or may not have been triggered by seismic ground shaking. There are no deformation features observed within the sediments (sandy tills and peats) in the surrounding area. The rock avalanche has fallen onto glacially-scoured slabs within the limits of the LLR ice in the area and is in turn partially covered by peat. By inference the seismic activity must have occurred between 10.3 and 6 kyr BP.

2.6.4 Beinn Alligin Fault

The Beinn Alligin fault (Figure 2.10) follows a sinuous course trending N-S to NW-SE for a distance of 7 km from Coire Mhic Nobuil, through the peak of Sgurr Mhor on Beinn Alligin and northwards across an area of moorland. The fault cuts the massive sequence of arkoses and conglomerates that comprise the Applecross Formation of the Torridonian Supergroup. The fault is one of several NW-trending faults in the area.

At its southern end the fault is exposed as a zone of shearing, fracturing and brecciation where it crosses the Allt Mhic Nobuil [NG877587] and runs along the Allt Toll a' Mhadaidh. The uniform nature of the Applecross Formation precludes any estimate of the pre-Quaternary offset along the fault at these localities.

Attention was drawn to Beinn Alligin by the presence of a large rockfall avalanche deposit on the floor of the corrie of Toll a' Mhadaidh Mor [§ 7, p324]. This feature is similar to rock avalanches described from seismically active areas worldwide (Eisbacher 1979; Keefer 1984b). The source slope for the avalanche is bounded on its eastern side by a planar rock wall (Figure 2.11a) that is coincident with the mapped

trace of the Beinn Alligin fault. The fault zone was found to be exposed at the base of this wall over a distance of c. 1 km. A zone of open fracturing and soft fault gouge up to 0.5 m in width, trending 151° to 163° cuts through an older silicified and epidotised zone of crushed and sheared rock. The fault faces are vertical or dip steeply ($>80^{\circ}$) to the east and west. The gouge zone itself (Figure 2.11b,c) is exposed for a distance of over 200 m at the top of Eag Dubh na h-Eigheachd; lower down the avalanche scar it tends to be obscured by fallen blocks or is housed in a rubble and sand-filled gully up to 1.5 m wide trending $158-338^{\circ}$. The gouge is a composite zone grey-green gouge up to 3 cm wide in a wider zone of sheared rock fragments in a 'clay' matrix. At some exposures of the fault zone there is also a deep red gouge developed adjacent to a zone of older silicified sheared sandstone. Where the fault crosses the ridge crest the gouge zone is covered by aeolian sands (weathered from the bedrock) and further to the north it is obscured by frost shattered debris and slope wash deposits. The eastern sidewall of the failure scar above the fault zone exposures shows no evidence of kinematic indicators for the most recent fault movements. Within the gouge zone itself there is no sense of shear displayed. However, the topographic profiles of the slopes either side of 'Eag Dubh' suggest downthrow to the west with possible sinistral movement.

Fault movement is post-glacial as it is assumed that this was the trigger for the rockfall avalanche [§ 7, p324]. Since the rock avalanche deposit is covered by peat fault movement must have occurred in the period 10.3 kyr BP to 6-4 kyr BP. It is assumed that fault movement was a one-off event as the unstable sidewalls of the avalanche scar would have been subject to further failure had there been subsequent seismic activity of a substantial nature: this is not supported by the morphology of the avalanche debris [§ 7, p324].

2.6.5 Cuaig Fault

Robinson (1977) measuring late glacial shorelines in Applecross, Wester Ross noted a c. 1.7 m vertical dislocation in the shoreline north of Kalnakill [NG6955] (Figure 2.4). This also corresponds with a regional warping or dislocation of the higher glaciated rock platform in Applecross. Although the Applecross Peninsula is cut by a number of NW- and NE-trending faults, none correspond with the offset of the shorelines.

The area around Kalnakill is composed of Applecross Formation arkoses. These dip $<15^{\circ}$ to the west and south-west and are cut by numerous fractures trending

116-296° and 134-314°. Immediately to the north of Kalnakill on the coast at NG693355 is a wide zone of intense fracturing and crushing composed of sandstone breccia in 125-305° and 112-292° fracture zones. This can be followed inland for c. 100 m as a narrow linear depression before it becomes obscured beneath a thick cover of glacial drift. This zone of fracturing corresponds with the only exposures of rockhead along the surface of the raised shoreline platform and is coincident with the marked change in shoreline altitude observed by Robinson (1977). It may be that this area has been subject to uplift relative to the gravel-covered area of platform to the south. It is also important to note that this offset is only 1 km south of the Wester Ross Readvance limit, and may be due to differential isostatic rebound in response to this period of partial reloading. If this is the case then fault movement can be dated, at best, as being post-13.5 kyr BP and pre-formation of the peat now covering the platform.

The only deformation features in the area of the fault are large blocks of Torridonian sandstone, up to 4000 m³, that have slid down gently dipping bedding planes. This may or may not be a manifestation of seismic ground shaking.

2.6.6 Loch Maree Fault

The Loch Maree Fault is the largest NW-trending fault in NW Scotland (Figure 2.2). It is a major basement fault that extends for 70 km from Rubha Reidh in the NW to Scardroy in the SE, where it terminates against the Strathconon fault zone (Figure 2.12). The fault is a long-lived structure that has a history of movement dating back to the Precambrian (R.G. Park, pers. comm. 1988). The most notable feature along the fault is the displacement of the Moine Thrust Zone at Kinlochewe by c. 3 km in a dextral sense. (Earlier faults e.g. along Gleann Bianasdail [NH0165] are displaced by c. 5 km in a dextral sense and downthrown by c. 300 m to the north.) The amount of displacement decreases eastward to become only about 0.6 km (dextral) offset of the Lewisian inlier at Scardroy. A discordance in the hornblende rocks on either side of Loch Beannacharain suggest that the fault trace continues to the SE to abut against the Strathconon Fault zone.

The most recent movement along the fault, i.e. reactivation during the Quaternary, is confined to the eastern end of the fault where it outcrops at Scardroy in Strathconon (Figure 2.12). More tenuous evidence for Quaternary fault movement is found at the western end of Loch a' Chroisg where the fault trace runs along the Allt Glac an Sguitheir [NH0957] (A, Figure 2.12). Rupturing occurs along 120° to 150°

trending fractures that cut across all pre-existing fractures and breccia zones. Fractures dip steeply ($70^{\circ}+$) to the NE and SW and are spaced at decimetric intervals. This creates a loose jig-saw fit network of blocks with no development of fault gouge material. This may be the surface manifestation of small incremental movement along this section of the fault, possibly vertical in nature, causing fracturing of the rock using pre-existing joint and fracture patterns to create this block network texture.

Also of note is a terrace of glacial outwash (δ) material with a displaced sequence of gravel units immediately adjacent to this area of recent shattering. This may be the result of offset due to faulting or slump failure due to ground shaking.

More convincing evidence for recent fault movement is that displayed along the Scardroy Burn [NH2052] in Upper Strathconon (Figure 2.12) where the fault is exposed over a distance of 1.5 km before the trace disappears beneath a cover of peat to the WNW.

Several localities along the exposed fault contain zones of fault gouge, some with several generations of gouge. Development is almost continuous over a distance of 1 km. Gouge zones vary from simple, narrow zones containing one fault gouge generation to zones up to 40 cm thick containing as many as six units. Where gouge is absent the fault is marked by extensive open fracturing trending 127° to 140° . Offset along these fractures is seen to be of the order of 2.0 ± 0.5 cm along individual fractures in a sinistral manner. Some show evidence for a degree of downthrow to the NE. Fractures are vertical or dip steeply ($70-80^{\circ}$) to SW and, with the small degree of lateral movement observed, is suggestive of reverse movement along a steeply dipping basement fault.

Although exposed over a distance of 1 km, the gouge zone is best developed at two localities: NH206520 (Figure 2.13) and NH204523 (Figure 2.14). Both exposures show a composite gouge zone up to 0.4 m wide with up to six generations of gouge material. This in turn is found within a wider zone of silicified and epidotised, sheared and brecciated gneisses. Such a wide zone of gouge implies either a large amount of fault offset or a protracted period of recent fault movement. Evidence from the offset of rock surface morphology measured along fractures elsewhere along the fault trace does not support large amounts of movement. This wide zone may have been the result of a long history of 'shuffling' movements due to repeated differential isostatic uplift in response to the numerous glaciations during the Quaternary.

Much of the gouge zone contains reworked material, such as epidote, that obviously formed when the fault was at much greater depths within the crust. This has proved troublesome in attempting to age date the intrafault materials [§ 5, p220]. SEM analysis of the intrafault quartz grain surface morphologies suggests that the most recent grains were formed post-Pleistocene, although the spread of ages is from the Holocene to the end-Pliocene [§ 5, p220].

As stated above the gouge zone is a composite of several generations of fault gouge material. However at other localities the fault zone is represented by either a single generation of blue-grey gouge (Figure 2.15) or in a few cases, a khaki and blue-grey zone double gouge zone. The blue-grey gouge is universally present in fault exposures and normally forms a narrow zone, <2 cm wide, adjacent to the SW sidewall of the fault and is smeared out along this sidewall. It also frequently contains fragments of older material. This zone is assumed to be a product of the most recent major fault movement along this section of the fault by virtue of the fact that it cuts across all pre-existing gouge units and is preserved along the entire length of the surface rupture.

Where the fault and the Scardroy Burn diverge for a distance of c. 200 m, the fault trace is obscured by a thick cover of glacial drift and peat. There is no evidence for recent fault movement in the form of a scarp or any ground rupture. This does not preclude the formation of ground disruption due fault movement as this area has been subject to extensive erosion and slope wash activity that would have quickly removed evidence of a fault scarp in such soft material.

The age of fault movement can merely be constrained as being sometime between 10.3 and 6-4 kyr BP as the most recent fractures disturb glacially smoothed bedrock but do not seem to cause any disturbance of the overlying peat cover.

The area of Strathconon has an extensive cover of glacial and glacio-fluvial sediments containing an abundance of soft sediment deformation structures including slumping, micro-faulting and water escape structures. However these deformation features occur in a number of horizons and do not show any degree of lateral continuity, therefore they do not conform to the criteria of Sims (1975) for defining seismites. However a pocket of glacio-fluvial sands in the upper reaches of Strathconon, beside the River Meig [NH191503] show pseudo-nodule structures and the almost complete destruction of primary sedimentary structures (Figure 2.16). This complete liquefaction is suggestive of seismic shaking rather than water escape in

response to freeze-thaw or compaction. Also the fact that this pocket of sediment has been preserved in an eroded hollow in a ridge of Moinian bedrock marking a nick point in the river profile suggests that such a topographic 'high' would have caused the amplification of seismic shaking energy, thus causing greater deformation than in the immediate surrounding area leading to the complete liquefaction of the water saturated sedimentary sequence (Jibson 1987). The deformed sediments are overlain by undeformed peat, suggesting that seismic activity occurred in the period 10.3 to 6 kyr BP. This corresponds to the age of movement on the Loch Maree Fault at Scardroy.

2.6.7 Bac an Eich Fault

South of the 'active' segment of the Scardroy fault a 'zone of crush' trends 140-320° across the hill of Bac an Eich [NH2248] to abut against the Strathconon Fault in Gleann Chaorainn [NH2448], a distance of 5 km (Figure 2.12). This fault cuts Moine psammites and pelites and Lewisian intercalations. For a distance of 500 m along the Allt Coire Feola [NH2050] there is evidence for recent movement along this fault. This comprises a narrow zone of shattered and brecciated rock cutting through the pre-existing zone of silicified and sheared rock. Most of this zone of recent movement is composed of a loose network of splintered rock fragments. Striated fracture surfaces indicate lateral movement, however the direction of movement is ambiguous.

As the fault trace diverges from the watercourse it is exposed for a height of 50 m in the side wall of the gorge created by the river (Figure 2.17a). At the base of this zone the fault is marked by a number of discrete fractures that pass up into a progressively more fractured and brecciated zone (Figure 2.17b). The apparent offset of the rock surface morphology is sinistral, however this may be a manifestation of erosion of the fault zone, as the rock is no more than an indurated clay-like material.

The age of fault movement is also a problem. As the fault crosses Coire Feola [NH2149] it is obscured beneath a thick cover of glacial drift, peat and rockfall debris. There is no offset or disturbance of this material suggesting that fault movement predates, or was of insufficient magnitude to affect, these deposits. The fact that the most recent zone of movement is a loose, open breccia that has not been subject to preferential erosion by the Allt Coire Feola and shows no infilling by silt or other debris is suggestive of a recent, and possibly post-glacial, origin for this particular fault movement. The proximity to the Scardroy segment of the Loch Maree Fault makes it difficult to determine whether the deformation features observed in the immediate and surrounding area are due to movement on this or the Scardroy fault

segment. These deformation features have been arbitrarily attributed to movement along the Scardroy fault segment on account of the greater evidence for recent movement along this fault.

2.6.8 Beinn Tharsuinn Fault

Beinn Tharsuinn (Figure 2.20) stands in a remote tract of country at the western end of Loch Monar. The SE ridge of this mountain is cut by a 020-200° trending fault that shows evidence of late Quaternary movement. This is an area of high relief, with the surrounding hills affected by a large number of slope failures. Beinn Tharsuinn itself is also the site of a large translational sliding failure. It was this concentration of slope failures that first drew attention to this area with respect to Quaternary seismotectonics.

The Beinn Tharsuinn fault is exposed in a shallow gully that crosses the east ridge of the mountain at NH058428 (Figure 2.20). Further excavation revealed over 100 m of exposure before the fault trace was obscured by rockfall debris and peat to the north. The fault zone is a reactivated basement fault, accommodated within a zone of brecciated and silicified Moine psammite up to 4 m in width. The zone of most recent movement (Figure 2.21) dips 80°/006-014°. A zone of soft blue-grey gouge up to 25 mm wide is found adjacent to the fracture face. To the east the gouge is bounded by a zone of loose, non-cohesive sheared fragments in a pale grey gouge matrix approximately 0.5-0.75 m wide. This is in turn bounded by fractured psammite.

The gouge zone extends up into the overlying cover of sandy peat where there is alignment of psammite clasts parallel to the fault face. This evidence suggests that fault movement occurred after the deposition of the peat, with the western side of the fault being upthrown by 0.5 ± 0.1 m. The gouge zone lacks any features that would point toward any degree of lateral movement. To the south of the fault zone exposure the fault is marked by a subtle break in slope of 0.25-0.4 m that faces east, extending for a distance of c. 150 m. Extension of the fault to the south is obscured by frost shattered debris. The northward extension of the fault is marked by an area of spring lines and saturated ground.

As stated above the surrounding area is one of high relief with a large number of slope failures concentrated around the fault rupture while slopes of equal steepness and geometry outwith the immediate area have not suffered failure. The spatial association of slope failures with the surface rupture and the style of slope failures suggests that

they were triggered by seismic activity, either a single event or a number of events. The slope failures disturb both bedrock and post-glacial surficial materials showing that they are Holocene in age.

2.6.9 Loch Monar (Allt nan Uan) Fault

A WNW-ESE trending fault cuts the Moinian bedrock at the eastern end of Loch Monar [NH1940] and has a strong geomorphic expression over a distance of 3 km. The fault is exposed along the Allt nan Uan as a series of open and gouge-filled fractures trending 273° to 280°. This is paralleled by a number of continuous fractures that cut, but do not seem to displace, the glacially smoothed bedrock on the western slopes of Beinn na Muice [NH2040]. These fractures are similar to those on Sgurr a' Chaorainn in Coire Dho [§ 2.6.19, p46]. Although the fault zone has the appearance of being of recent origin, excavation across the fault along the shore of Loch Monar [NH191414] and where the fault crosses the Allt Coire na Faochaige [NH207410] has failed to show any offset or disturbance of the late Quaternary deposits (peats and sandy tills). However, the 'fresh' appearance of the fault and the spatial association with a large number of slope failures, including a remarkable slump failure on Sgurr na Ruaidhe [NH2942], similar to those described by Palvides & Tranos (1991) as being the result of seismic slope shaking, in the surrounding area provide at least circumstantial evidence to support the occurrence of post-glacial faulting and seismic activity in this area.

2.6.10 Coire Eoghainn Fault

The Coire Eoghainn fault (Figure 2.18) at the eastern end of Loch Mullardoch in Glen Cannich is an east-west trending basement fault cutting the complexly folded Moine psammites and pelites of the Glenfinnan Division over a distance of 5 km. This fault has a history of movement extending from Caledonian time: a microdiorite dyke of this age is intruded along part of the fault plane. The fault also acted as a zone of crustal weakness in Permo-Carboniferous time allowing the intrusion of a lamprophyre at A, Figure 2.18. The dominant movement over this time has been downthrow to the north with a smaller degree of sinistral movement. The fault zone is relatively narrow, being a zone of crushing and shearing up to 3.5 m in width. Exposed fault planes and the mapped fault trace show that the fault dips steeply, 75-80°, to the north. The fault is a marked topographical scarp running parallel to the floor of Glen Cannich for a distance of 3 km from Loch Sealbhanach (Figure 2.19a) in the east to the Allt Mullardoch in the west. It is essentially a straight feature crossing

topography from 200 to 600 m. Along the length of the fault there are a number of features that suggest late Quaternary movement. The fault zone itself is exposed continuously along the Allt Coire Eoghainn for a distance of 1.5 km. Within the zone of silicified fault crush rock is a set of discrete fractures, and often a single gouge-filled fracture (Figures 2.19b & 2.19c), trending 272° to 290° and dipping 58° to 80° to the north. The gouge zone is 20-27 mm wide and is smeared out along the fracture faces in a manner that is suggestive of lateral fault movement. Across the fault there is a mismatch of glacial drift cover (C, Figure 2.18) where the glacial deposits seem to run into the fault plane. There is no evidence of ice scouring or moulding of the scarp face as is the case with the surrounding rock outcrops. Thus the fault scarp must have been formed in post-glacial times and as such the mismatch of glacial deposits implies downthrow to the north. Towards the west the fault passes under a cover of peat at NH224323. The fault then reappears as it crosses the area of glacially scoured slabs at Creag Feusag [NH215324] as a peat-filled hollow. As there is no disturbance of peat stratigraphy fault movement must have occurred prior to the deposition of peat in the area i.e. 6 kyr BP.

The most striking feature is the diversion of the course of the Allt Coire Eoghainn and a number of other tributary streams in a sinistral sense. The amount of movement is 20-25 m. The streams are relatively shallow water courses cut into the hillside to the north of the fault. On the southern (downhill) side of the fault the watercourses are more deeply incised, as would be expected on the uplifted side of the fault [§ 2.6.1, p22]. As well as the offset of the streams there are a number of dry watercourses on the southern side of the fault. These are usually shallow features merely cut into the glacial drift and may have been the former courses of ephemeral streams found along the northern side of the fault and are now deflected along the line of the fault trace. The number of abandoned watercourses and the amount of displacement point toward the fault movement occurring as a number of increments. The amount of movement is too great to have occurred during the inter- of post-glacial period as this would give fault movement rates similar to plate margin environments. If the movement is assumed to have occurred throughout Quaternary time then the movement rate becomes 0.01 mm yr^{-1} .

Despite the extensive cover of late Quaternary sediments in the area of Glen Cannich no evidence of seismic soft sediment deformation was discovered; the majority of sediments are sandy tills and coarse outwash gravels overlain by a thick cover of peat. However the surrounding area is one of the greatest relief in the western Highlands and is affected by a large number of slope failures. Most of these are

attributed to the effects of slope creep as a result of oversteepening by glacial erosion, but a number have failed on slope configurations that should have been stable under normal conditions. In addition the morphologies of the failures suggests that failure was a one-off event and not the result of protracted slope weakening. These failures include sudden collapse slumps on An Riabhachan [NH1133 and NH1433] similar to the earthquake-induced slope failures described by Pavlides & Tranos (1991), and ridge crest foundering failures on Sgurr na Lapaich [NH1634] attributed to the topographic amplification of seismic shaking at a ridge crest mid or high point (Jibson 1987). All the failures involve periglacial slope material as well as bedrock and glacial deposits. The fact that the fissures of the backing areas of the failures are now filled in or covered with peat dates these failures to the period 10.3 to 6 kyr BP, most likely outwith the immediate post-glacial period as periglacial deposits are also affected by slope movement.

2.6.11 Glen Elchaig (Strathconon) Fault

The Strathconon Fault system is the largest of a number of NE-trending faults in NW Scotland, extending from Glenelg in the SW to Glen Calvie in the NE, a distance of 98 km (Figure 2.2). It has had a long and complex history of movement, most of which was accomplished during the Caledonian Orogeny. At Strathcroe [NG9421] at the head of Loch Duich it offsets the Morar-Glenfinnan Division boundary and the Sgurr Beag Slide by c. 10 km in a dextral manner. Numerous Permo-Carboniferous dykes have been intruded along the fault zone in Glen Elchaig. As with most large faults it is a wide (c. 2 km) zone of anastomosing fault planes.

Investigation along the majority of the fault length failed to find any evidence for recent fault movement, with the exception of two localities in Glen Elchaig (Figure 2.22a) and Invershiel (Figure 2.23) where the fault is exposed for short distances as narrow zones of soft gouge within a matrix of sheared and brecciated country rock. In Glen Elchaig the fault is exposed as a zone up to 10 m wide of intense shearing trending 061-241° cutting a granitic pegmatite, this in turn houses a dark blue-grey fault gouge orientated 78°/058°. The gouge zone averages 8.5 cm in width, reaching a maximum of 15 cm. It is composed of dark grey gouge with streaks of pale green granular gouge material that dominates towards the surface. Intercalation of these two generations of intrafault material has given rise to a number of shear textures that show the most recent movement has been reverse on a fault plane dipping steeply to the SE (Figure 2.22b).

At Invershiel a wide zone of fractures cuts the Rattagan adamellite. A single fracture trending $78^{\circ}/256^{\circ}$ contains a two-phase soft blue-grey gouge. This is tentatively correlated with the fault zone at Glen Elchaig. There is no independent, unequivocal evidence to suggest late Quaternary movement at either site other than the 'fresh' appearance of the fault zones. Both exposures are seen to contain a two-phase gouge zone and have the same general orientation; however, the intervening 7 km between the sites shows no evidence of late Quaternary reactivation except for the 'fresh' fracturing of bedrock along the Allt Coire Sgeilm [NH0026] above Glen Elchaig. The fact that the Strathconon Fault is a complex zone of many fault strands suggests that any movement would have been accommodated along a number of short fault segments rather than a continuous strand. If the fault is continuous, i.e. a surface rupture of c. 7 km, then the estimated magnitude of seismicity accompanying rupture would be 5.7-6.9 M_S [§ 2.14, p208] There are a number of slope failures in the immediate area, however none can be attributed to the effects of seismic ground shaking with any degree of confidence.

2.6.12 Glen Affric Faults

The area of Glen Affric has the greatest concentration of slope failures in the N.W. Highlands. This is believed to be a reflection of the high degree of seismic activity in the area during the post-glacial period. In an area of 68 km² there are at least seventeen major rock slope failures. These include deep-seated sudden collapse slump failures, ridge crest foundering, translational sliding on low angle detachments and incipient rock avalanches. All are indicative of seismic slope shaking (Keefer 1984a,b; Jibson 1987). Two faults in the immediate area display post-glacial movement.

(i) *An Sornach Fault*

Late Quaternary movement was first implied from this site by Holmes (1984) to explain a NW-trending linear feature cutting a late-glacial/early post-glacial slope failure on the southern slopes of An Sornach in Glen Affric (Figure 2.24a). This 'fault' linear is marked by a $123-303^{\circ}$ trending hollow and scarp running diagonally across an area of slump failure (Figure 2.24b). The hollow is up to 8 m wide and filled with boulder debris from the scarp faces on either side. On the uphill (NE) side of the hollow is a scarp face reaching 4-5 m high formed by fractures running parallel and sub-parallel to the hollow. These fracture faces show no evidence for fault movement. The downhill (SW) side of the hollow is an obsequent or uphill-facing scarp, increasing in height from <1 m to c. 10 m towards the NW (Figure 2.24c); this increase in scarp height corresponds to an increase in width of the hollow to c. 20 m.

As this 'fault' scarp approaches the headscarp area of the slope failure it decreases in height to 5 m. About 50 m short of the headscarp it again reduces in height to 1 m and also changes direction to a more northerly trend. Holmes (1984) claimed that this scarp extended outwith the area of failure and on this basis stated that the fault movement post-dated the slope failure. No evidence was found for the direct continuation of the scarp outwith the area of failure. There is a 330° to 340° trending downhill-facing break in slope that can be followed for c. 70 m across the hillside to the NW of the area of failure. However this faces in the opposite direction to the scarp as it traverses the slope failure and is also not a direct continuation of this feature, being offset to the north by approximately 6 m and following a different trajectory. The continuation of the scarp to the SE, reported by Holmes, also faces downhill. As the scarp intersects a number of 080-260° obsequent scarps it is itself 'offset', giving a rather saw-tooth trajectory. Although much of the evidence points to this not being a fault scarp, it is believed that this has formed as a result of fault activity. Fault movement at a depth below the ground surface has disturbed the overlying network of blocks (created by rebound fractures) and has induced slope failure and the development of a ragged scarp [§ 3.14, p138]. A similar feature, termed 'jostle-up', has been described by Talbot (1986) from northern Scandinavia.

(ii) *Sgurr na Lapaich Fault*

Holmes (1984) also described a large 'slope failure' (c. $7.5 \times 10^6 \text{ m}^3$) on Sgurr na Lapaich [NH152246] at the eastern end of Glen Affric (Figure 2.25a). For the volume of failure and the amount of downslope movement, c. 4 m, there is surprisingly little deformation of the 'failed' mass and there is no evidence of rotation or translation of any of the slope mass as a result of 'failure'. In addition, although appearing curved, the backing scarp is composed of a number of right-stepping scarps trending 70°/266° (Figure 2.25b). The step scarps trend 120-300°. All scarps cut periglacial debris and there is no evidence of glacial scouring or frost shattering of the scarp face, thus the scarp is definitely post-LLR. There is no dilation of the slope in the region of the 'headscarp' as would be expected from a slope failure of this magnitude and the scarp face shows multiple generations of slickensides. The lack of internal deformation within the 'failed' area and the total lack of dilation at the base of the slope suggests that this is more than a simple slumped slope. Indeed the systematic geometry of the 'headscarp', utilising pre-existing faults suggests that this is a 'pop-up' related to differential glacio-isostatic uplift. The ragged nature of the scarp as it uses pre-existing fractures is similar to such 'pop-ups' described from northern Sweden (Talbot 1986). Holmes (1984), using an infinite-equilibrium model, showed that the slope was stable even without considering the effects of asperities and rock

bridges. This suggests that movement must have been tectonic and not gravity induced. It is suggested that this feature is the result of block movement in response to differential isostatic uplift following the decay of the LLR ice. It should be noted that even if this is not a true fault movement, the sudden displacement of such a slope volume would itself have been the cause of a substantial seismic event (R. Muir Wood, pers. comm. 1991).

2.6.13 Gleann Lichd Fault

The fault running along the upper part of Gleann Lichd is one of several NW-trending basement faults that traverse the area of Kintail. A number of these faults show evidence for reactivation during the late Quaternary (Figure 2.26).

The Gleann Lichd fault extends from the northern spur of Meall a' Chara [NH021164] north westwards for 3.5 km along the floor of the glen to a point just to the south of the River Croe [NG984189]. There is also evidence to suggest that the fault extends further to the SE across Am Fraoch-Choire for a further 2 km. The fault is a long-lived basement fault that offsets the Moine outcrop by 100 m to 250 m in a dextral sense. The fault itself has been intruded by lower Devonian lamprophyres and felsites that cut earlier pegmatites. Along its entire length the fault has a strong geomorphic expression that points to reactivation during the post-glacial period. When exposed, the fault zone is seen to be a 'fresh' feature that comprises a thin zone of fault gouge in a wider zone of non-cohesive shattered breccia (Figure 2.27a). The fault is also spatially related to one of the largest post-glacial rock slope failures in the Scottish Highlands (Figure 26).

From [NG984188] where the fault crosses the River Croe to Glen Licht House [NH006173] the fault is exposed as a conspicuous SW-facing scarp up to 5 m in height. The fault scarp is obscured at two localities by recent debris flow activity and slope failure movements on the southern slopes of Beinn Fhada. Where the fault disappears under the slope failure there is a continuous line of springs issuing from the base of the failure. The fault reappears SE of Glenlicht House where it is exposed along the Allt Lapain [NH0117] as a wide zone of shearing with the open fracture planes orientated 136-316°. The fault also causes a 90° turn in the direction of drainage of the Allt Lapain at this point. The fault then continues to the SE over the shoulder of Meall a' Chara where it is exposed for a distance of c. 200 m along the course of the Allt Ruighe nam Freumhe. This exposure shows a thin pale grey gouge, 5-19 mm thick, in a zone of crushed and brecciated rock up to 1 m wide trending 114-294°

(Figure 2.27b). As the fault crosses the ridge crest it is marked by a conspicuous notch (Figure 2.27a). The morphology of this topographic offset is consistent with that of the fault scarp in Gleann Lichd i.e. downthrow to the SW. There are no indicators of lateral fault movement.

The age of fault movement can only be ascertained relative to the surrounding geomorphology. The fault scarp is a post-glacial feature; the scarp face shows no evidence for the passage of ice, and indeed no such feature would have survived the passage of the ice that was present in Gleann Lichd, as shown by the extensively moulded and smoothed topography. Neither is the scarp the product of post-glacial periglacial processes as there is an absence of rockfall debris below the scarp faces, nor are they due to the slope movement on the southern flanks of Beinn Fhada as the scarp extends well outside the area affected by slope movements and the sense of movement on the scarp is incompatible with that implied by slope movement. The slope failure on the southern flanks of Beinn Fhada is probably immediate post-glacial in age as shown by the amount of periglacial debris that has accumulated behind the obsequent scarps in the area of failure. As the slope failure cuts the fault scarp, movement along the fault must have been late-glacial or immediate post-glacial. Peat covers or is draped against the scarp face showing that it must have formed prior to 6-4 kyr BP. The fault does not disturb any post-glacial deposits present. However, ball and pillow liquefaction structures are found in glacial outwash sands, pointing to seismic activity during or after the deposition of these sediments (GL 1, Figure 2.26). The amount of fault movement has not been ascertained, but fault scarp morphology points to this as being of the order of 3-5 m with downthrow to the SW.

Due to the density of post-glacial fault activity in the immediate area and also the poor control on the exact age of the post-glacial fault movements it is impossible to attribute the seismically-induced slope failures in the immediate area to any particular fault movement.

2.6.14 Glen Shiel Fault Swarm

The area around Glen Shiel is presently one of the most seismically active areas in the UK with 21 events of 3.0 M_L or greater recorded over a twenty year period [§ 4.15, p195]. The area also shows evidence of being tectonically one of the most active areas during the post-glacial period.

The area of Glen Shiel in Kintail has some of the greatest relief in the western Highlands with 1000 m peaks rising from sea level in distances of under 4 km. The country rock, Moine pelites and psammities of the Morar Division, is cut by a number of NW to WNW trending faults, here collectively termed the Glen Shiel fault swarm (Figure 2.26). These parallel the Gleann Lichd and Kinloch Hourn Faults and display similar morphotectonic features that point to reactivation during post-glacial period. The faults of the Glen Shiel Swarm are all long-lived basement features that offset the Moine bedrock in a dextral manner by 100-200 m. In all cases recent movement has occurred along pre-existing faults of Caledonian age.

2.6.15 Creag na Damh (Am Fas Allt) Fault

The peak of Creag na Damh on the south side of Glen Shiel is cut by the obvious NW-SE gully of Am Fas Allt (Figure 2.28). This is the northern extension of a Caledonian fault that offsets the Sgurr Beag Slide by c. 100 m in a dextral manner. The strong geomorphic expression of this fault suggested that it may have been subject to late Quaternary reactivation. This was found not to be the case. However, evidence for late Quaternary movement was found along a 120-300° trending fault conjugate to the main Creag na Damh fault. This is parallel to the other post-glacial faults in Glen Shiel. This fault was noted to deflect drainage of Am Fas Allt [NG984117] and to offset the drainage in Am Fraoch-choire [NG995114] by c. 20 m in a sinistral sense. The fault is marked by a shallow linear depression running obliquely across the hillside of Sgurr a' Chuilin (Figure 2.28) at the base of which, adjacent to the main gully of Am Fas Allt, is an exposure of a gouge-bearing fault zone trending 121-301° [NG975123]. In addition the slopes of Sgurr a' Chuilin are cut by a number of open 120-300° fractures dipping 70-80° to the north. There is no development of a continuous fault scarp, however the deflection of shallow drainage features and the 'fresh' nature of the exposed fault zone seem to suggest that this fault was the locus of post-glacial movement.

2.6.16 Sgurr a' Bhealaich Dheirg 'Faults'

The area of Glen Shiel contains a number of large deep-seated slope failures (Figure 2.26), one of which occurs on the southern slopes of Sgurr a' Bhealaich Dheirg (Figure 2.29). While almost all slope failures in the area involve some degree of slumping and the development of obsequent scarps, this failure differs in that it is cut by two main obsequent scarps up to 7.2 m in height and over 400 m in length that seem to extend outwith the area of failure. In contrast with other obsequent or

uphill-facing scarps these scarps follow a straight course ($120\text{-}300^\circ$) for their entire length and are not concave upslope (Bovis 1982). The scarp faces are steep, dipping $60\text{-}80^\circ$ into the slope. The schistosity/banding of the Moine bedrock dips $50^\circ/070^\circ$ to $60^\circ/020^\circ$, thus the scarps are not the result of interlayer slip or toppling, frequently the cause of such features (deFreitas & Watters 1973; Bovis 1982). The fracture faces of the scarps show the development of quartz slickensides indicating that they are fault planes. All other minor scarps on the hillside are formed by fractures.

These two scarps seem to extend outwith the area of failure to the east and in this sense post-date the slope failure. However the cover of slope materials makes it difficult to determine the exact mode of slope failure and hence the exact extent of the failure area is difficult to define, therefore the relationship between the scarps and the slope failure is not too clear. From the limited exposure in the area there does not seem to be any planes to facilitate basal sliding and the only discontinuities in the rockmass affected by slope failure are banding/schistosity and fractures running sub-parallel to the scarps. In addition a poorly developed set of conjugate cross fractures run sub-parallel to the banding and $046\text{-}226^\circ$. Both fracture sets are vertical or dip steeply to the west. Failure seems to be essentially toppling in the lower section of failure as shown by the bulging toe of the failed area. Upslope from the two scarps the mode of failure has been slumping. The scarps mark the boundary between the two styles of failure. These scarps are also coincident with the extension of two faults exposed on the northwestern slopes of Saileag [NH0114]. These two faults are marked by a network of 'fresh' fractures and crushed, unconsolidated breccia. It is proposed that the twin scarps are 'pop-up' scarps related to differential glacio-isostatic uplift with the movement being accommodated along pre-existing faults. From the fault scarps, movement seems to have been essentially vertical, with downthrow to the north. The relationship between faulting and slope failure is not fully understood. However it seems as if faulting was the trigger for failure: fault movement at depth is amplified towards the surface by being accommodated along a number pre-existing fractures and rebound fractures created by the removal of ice cover from the area resulting in dilation of the slope by block movements, both rotational and translational [§ 3.4, p114]. This would account for the complex nature of the slope failure. It is considered that this was a one-off event as shown by the lack of subsequent movement even in the critically oversteepened region of the failure toe. The age of the failure, and hence the fault movement is most likely late glacial to immediate post-glacial as shown by the frost shattering of the scarps but the lack of glacial striae on any of the scarp faces or shattered blocks. The hollows behind the scarps have subsequently been partially infilled with peat. Again, as with the Sgurr na Lapaich failure in Glen Affric, the

volume of the slope failure would ensure that it was the trigger for significant seismic activity even if the scarps are not true fault scarps.

2.6.17 Sgurr na Ciste Dhuibe (Five Sisters) Fault

The Sgurr na Ciste Duibhe or Five Sisters fault is a reactivated basement fault of Caledonian age, trending NW-SE (between 310° and 320°) showing an active surface expression over a distance of 6 km (Figure 2.26). This is one of several faults dissecting the area on the northern side of Glen Shiel that show evidence of late Quaternary movement. The fault also acts as the backing joint/head scarp for a large slope failure on the southern flank of Sgurr na Ciste Duibhe (Figure 2.30). Recent movement along the fault seems primarily to be vertical in nature with a minor component of sinistral strike slip movement. The strike slip component along the fault is smaller than on faults of comparable size and age (e.g. Kinloch Hourn, Coire Mor) due to the density of faulting in the area, each fault accommodating some of the displacement across the area, and therefore there only being a small lateral displacement factor in each fault.

The fault trace traverses some of the greatest relief in the NW Highlands, running across 1000 m peaks and descending to sea level in a distance of under 4 km. The country rock is Moine psammities with minor tectonic slices of gneisses and marbles of Lewisian affinity along the Sgurr Beag Slide. Foliation generally dips steeply to the east at 50-80°.

Evidence for late Quaternary movement on the Sgurr na Ciste Dhuibe fault comprises a fault scarp of up to 5 m in height, trending 120-300° and facing SW that runs obliquely across the ridge of the 'Five Sisters' on the northern side of Glen Shiel (Figure 2.30), approximately 1000 m of topography. The fault displaces both bedrock and surficial deposits including glacial and periglacial deposits (Figure 2.31a). In addition the fault is seen to displace the ridge crest morphology by up to 15 m in a sinistral manner below the peak of Sgurr na Ciste Dhuibe [NG985150] (Figure 2.31b). The scarp shows no signs of glacial striations but is frost shattered in places (Figure 2.31c). At the eastern end of the fault it is obscured by present day slope movements and peat deposits, towards the west the fault disappears under a cover of hummocky moraine-like material that mantles the lower slopes of the Five Sisters Ridge. The fault has also acted as the backing plane for a number of slope failures on the southern slopes of the Five Sisters, the largest of which occurs on the southern slopes of Sgurr na Ciste Dhuibe itself (Figure 2.30). This is a complex failure

involving elements of toppling, rotation and rockfall activity. The failure is deep-seated, with the basal failure plane thought to exist at a depth of c. 100 m. The failed area is heavily fractured and has disaggregated in places to form mobile streams of rockfall debris. In addition to this deep-seated failure are two 'pseudo-rock avalanches' (not of large enough volume to develop into true rock avalanches) that have formed from the total collapse of toppling failures on the southern slopes of the Five Sisters. However these two failures seem to be much younger than either the fault or the Sgurr na Ciste Duibhe slope failure. These may have been the result of later seismic activity causing failure on previously weakened slopes. In addition to slope failure activity, palaeoseismic activity is recorded by liquefaction features preserved in glacio-fluvial outwash sands found along the floor of Glen Shiel (GS 1-6, Figure 2.26). These include ball and pillow, fault grading, injection and flame structures (Figure 2.32a,b). As these structures occur in the same horizon and are seen to be laterally continuous throughout the sedimentary cover they conform to the criteria of Sims (1975) for the description of seismites.

2.6.18 Arnisdale Faults

The area around Arnisdale on Loch Hourn (Figure 2.33) displays a number of prominent east-west linear features, clearly seen on aerial photographs. These are basement faults cutting north-south striking Moine psammities and pelites. Of these, that exposed along the Allt Rarsaidh is the most prominent and best exposed. This fault, along with that immediately to the south, shows the clearest evidence for recent movement. Glaciated topography is offset in a sinistral manner by 15 ± 2 m and 10 ± 1 m respectively along these fractures. Both these and the other two faults have well defined scarp faces that dip steeply ($80^\circ +$) to the north. Scarp faces show no evidence for the passage of ice and are inferred to be post-glacial in age. The hollows in front of the scarp faces are partly infilled with peat and slope wash deposits. The three southernmost faults can be traced for no more than 600 m, while the Allt Farsaidh fault has an active expression of 3.5 km. As well as sinistral offset there is a suggestion of downthrow to the north by c. 10 m. When exposed itself, the fault zone is composed of a 1-2 m wide zone of 087 - 267° open fractures sometimes containing an unconsolidated breccia. Fracture faces immediately adjacent to the main fault exhibit 'fresh' plumose markings that are suggestive of fracture propagation towards the east.

Although the faults are believed to have been reactivated during the post-glacial period, there is insufficient evidence to put a lower bound estimate on the age of this movement.

2.6.19 Coire Dho Fault

Coire Dho, west of Invermorriston in Inverness-shire (Figure 2.4), is the site of a former ice-dammed lake (Sissons 1977a) and as such was investigated to see if the lacustrine sediments preserved any deformation features that could have been due to seismic activity. The sediments show a variety of deformation styles, not all of which are unequivocal pointers to palaeoseismicity. However, a single deformation horizon (Figure 2.34a) is found to contain structures, including ball and pillow, flame, injection and fault grading structures, that are consistent with deformation due to seismic activity (Sims 1975). In addition to this deformation a large open fracture was discovered on the eastern flanks of Creag a' Chaorainn (Figure 2.34b). This trends NE-SW for a distance of 1.1 km and is exposed for a height of 485 m as a straight feature cutting the hillside, dipping at an angle of c. 45° to the northwest. Where this feature crosses the ridge crest it is marked by a distinct topographic notch. Surface expression of the fracture to the SW of this notch is obscured by extensive cover of frost shattered debris. The fault cuts across an area of glacially smoothed bedrock as a very marked linear feature, however no sense of movement can be determined, even from this extensive exposure. There is no evidence for any glacial erosion (such as plucking of the fracture edges) as would be expected if this feature had formed prior to or during glaciation. This apparent recent origin for this feature and the lack of demonstrable offset along the fracture suggests that this is a neotectonic fracture (Hancock & Engelder 1989), possibly created as a result of differential stress relief during glacial unloading. The limited and uniform nature of the 'movement' along this fracture precludes it being the result of slope movements; there is, however, a small rockfall from the cliffs on the western side of the fracture.

A late glacial age for the development of the fracture is supported by the soft sediment deformation as the seismically deformed horizon is overlain by undeformed horizons and ultimately a slumped horizon, the latter presumably associated with lake drainage. Thus, the seismicity responsible for the deformation features must have occurred prior to the disappearance of the ice in the lower part of the glen that dammed the lake, but after the glacial activity that was responsible for the development of the erosion in the upper part of the glen. Assuming that the development of the fracture and seismic activity were contemporaneous this dates the fracture development as being late-glacial. Further circumstantial evidence for the age of fracture development comes from Coire nan Clach [NH1412] on the southern flanks of Carn Gluasaid. Here a large volume rockfall has fallen onto and been transported a short distance glacier ice. Morphology of the debris points to this being the result of a single event. The

reasonably stable configuration of the discontinuities in the source slope area requires an additional force to trigger failure, and the topographic position, the nose of a ridge, of the source slope is consistent with the expected point of maximum topographic amplification of seismic energy (Jibson 1987). This suggests that slope failure was due to seismic activity during the Loch Lomond Readvance, possibly related to the creation of the neotectonic fracture in Coire Dho.

2.6.20 Kinloch Hourn Fault

The Kinloch Hourn Fault (Figure 2.35) was first described by Ringrose (1987, 1989) as displaying late Quaternary reactivation. Many of the criteria used by Ringrose (1987) to demonstrate and quantify late Quaternary movement along the fault have been adapted during this study and applied to other reactivated basement faults in NW Scotland. Further investigation of the fault zone structure in this study, both on a macro- and microscopic scale, has been used to determine the age and kinematics of fault movement during the late Quaternary and has identified a contemporaneous slope failure on the eastern slopes of Sgurr a' Mhaoraich.

From the offset of stream courses it is seen that there has been 160 m cumulative sinistral displacement along an active segment of 14 km sometime between 13 and 10.3 kyr BP (Ringrose 1987). Radiocarbon-dating has shown that movement has occurred as recently as 2.4 kyr BP (Ringrose 1987, 1989). Results of an age-dating programme to confirm these results are given elsewhere [§ 5, p220]. Movement along the Kinloch Hourn Fault is thought to have been associated with seismic events of 6.0 M_S and greater (Table 2.1).

2.6.21 Glen Gloy Fault

Quaternary fault activity was first described from the area of Glen Roy by Sissons & Cornish (1982) and subsequently quantified by Ringrose (1987, 1989) and Ringrose *et al.* (1991). These studies showed that there had been 0.5 m dextral offset along a 155° to 165° trending fault c. 10.3 kyr BP. Work carried out during this study, using slope failures to constrain the chronology of faulting/seismicity and also addressing the problem of style of faulting has refined the picture of post-glacial fault activity in the area and shed new light on the style of post-glacial fault reactivation. These findings are detailed elsewhere [§ 3, p112]. Fault surface rupture dimensions and the distribution of ground deformation features suggests that there have been at least three seismic events as large as 5.7-6.9 M_S (Table 2.1).

2.6.22 Other Reported Post-Glacial Faults

Several other incidences of PGF activity have been reported from western Scotland where detailed levelling has shown offset of late- and post-glacial shorelines and morphological features by up to 2.7 m (Gray 1974; Firth 1986; Ringrose 1987, 1989b) (Table 2.1). One isolated example has been reported from the western Forth valley (Sissons 1972). In addition there are offshore late Quaternary fault movements reported from the continental shelf around Scotland and northern England (Kirkton & Hitchen 1987; G. Eaton 1990). As well as the above corroborated incidences of PGF activity, there are several dubious claims for post-glacial seismotectonic activity that are discounted on account of the lack of substantiating evidence and the failure of the evidence to satisfy the criteria for identifying PGF activity (Bennett & Langridge 1990; Ballantyne *et al.* 1991).

Of the previously reported incidences of PGF activity that of Firth (1986) is of most interest. Detailed levelling of shorelines around the southwestern end of Loch Ness has shown that the weight of the LLR ice was sufficient to not only halt the rebound associated with the removal of the late Devensian ice cover, but also to cause redepression of the crust. This has great implications for the timing and mechanics of PGF activity in Scotland [§ 6, p260].

2.7 Palaeoseismicity

There are a number of features that indicate the PGF movement was associated with elevated levels of seismicity in comparison to those currently experienced in Scotland [§ 4, p149]. The most dramatic of these features are the concentrations of large slope failures found in close proximity to the fault ruptures (e.g. Figures 2.7, 2.8, 2.9 & 2.11a). Although slope failures occur under a vast number of conditions, there are a number of features that point to a seismic trigger being responsible for these failures.

The concentration of these failures around the surface fault ruptures, while other areas of similar slope geometry are lacking in such failures, initially suggests some connection between the two features. In addition, the slope failure types are the same as those described from numerous sites worldwide as being diagnostic of seismic slope shaking (Eisbacher 1979; Keefer 1984a,b, 1987; Jibson 1987; Pavlides & Tranos 1991). A large number of the sites of slope failure activity would also have been stable under normal gravitational conditions, and as such would have required

some triggering mechanism to initiate failure. Some of the more spectacular slope failures such as the rock avalanche on Beinn Alligin [§ 7, p314] and the ridge crest collapse failure on Carn na Con Dhu in Glen Affric would have required the additional energy of seismic slope shaking for failure to progress in the manner that it has (Keefer 1984a,b; Jibson 1987). However no flow slides or lateral spreading failures, similar to those described from northern Sweden (Lagerbäck 1990), have been recognised from the areas of PGF activity in Scotland. This is probably due to the lack of suitable surficial deposits and the steepness of the slopes as the lateral spreading slope failure in Sweden occur on slopes of $<10^\circ$.

The other indicator of large seismic events associated with PGF activity is seismite soft sediment deformation. Many deformation features have been found in the late Quaternary sediments of the Highlands of Scotland, many of which can be attributed to the effects of cryoturbation, glacio-tectonics or differential loading and water-escape. However there are a number of deformed sedimentary sequences that exhibit structures that are consistent with the effects of seismically-induced liquefaction. These deformational features conform to the criteria of Sims (1975) for describing seismite soft sediment deformation; that is, that the deformation is continuous over a wide area and confined to a discrete horizon or horizons. In addition, where the Quaternary sediment cover is extensive enough, the deformation features are seen to be zoned concentrically around surface fault rupture (Ringrose 1987, 1989a). This zoned nature of deformation intensity is interpreted as representing differing levels of intensity of seismic shaking i.e. they represent palaeo-iseismals. Seismite liquefaction is seen in fine grained lacustrine sediments and in medium to fine outwash sand sequences. The structures are similar to those described from other more (seismically) active areas (Seilacher 1969, 1984; Hempton & Dewey 1983; Scott & Price 1988) and those created experimentally by subjecting saturated sediment to shaking (Kuenen 1958). These include fault grading, ball and pillow structures, flaming and other injection/water escape structures (Figures 2.16, 2.32 & 2.34a). In most cases the deformation has been so great that there are no remaining primary sedimentary structures. These are similar to the seismites described from the Lansjärv area of northern Sweden (Lagerbäck 1990, 1991).

The degree of deformation and the distribution of the deformation features can be used to estimate the magnitude of the palaeoseismic activity that was responsible for the creation of these features. Using the empirical relationships developed between earthquake magnitude and slope failure type and slope failure distribution (Keefer 1984a,b, 1987) and between area affected by liquefaction and earthquake magnitude

(Youd 1977; Kuribayashi 1985), magnitude estimates have been assigned to the palaeoseismic events identified in Scotland (Table 2.1). It is seen that there is often considerable spread in the magnitude estimates and there is a marked discrepancy between the magnitude estimates obtained from the distribution of these deformation features and the magnitude estimates obtained from the fault surface rupture dimensions (Bonilla *et al.* 1984; Khromovskikh 1989). This can be interpreted in a number of ways. The difficulty in attributing slope failures to earthquake shaking may have led to an underestimation of the area affected by slope failure activity, and hence an underestimation in the magnitude of the palaeoseismic events. Indeed a number of slope failure types, namely rockfalls and soil slumps, which are usually the most common and widespread slope failures associated with seismic slope shaking, have been ignored in the assessment of slope failures due to the impossibility in determining the trigger for these failures as they are so widespread in a number of geological environments. Likewise, the distribution of seismicite sediment deformation may also be an underestimation, as the late Quaternary sedimentary record for the Highlands of Scotland is not particularly well developed, with much of the sediment comprising coarse gravels and tills that are not suitable for liquefaction. Therefore it is considered that the magnitude estimates obtained from the distribution of these deformation features be treated as minimum estimates for the seismic activity that accompanied the fault activity observed. In addition a caveat must be attached to the magnitude estimates obtained from the surface rupture dimensions of the faults. As a result of the poor stratigraphic control over the timing of fault movement it is not possible to determine whether the observed fault ruptures occurred as single events or were the result of several movement episodes. If the faults were the result of several movement episodes then the magnitude estimates obtained are overestimates. Hence the magnitude estimates from the dimensions of the surface ruptures in Table 2.1 must be considered to be maximum values for the seismicity associated with fault movement. However the evidence from post-glacial fault activity in Sweden, where there is better stratigraphic control over the timing of fault movement, suggests that post-glacial fault activity tends to occur as single events along the individual faults. Thus, for the magnitude estimates obtained from surface rupture dimensions in Table 2.1, the majority are considered to be truer representations of the seismicity associated with fault movement than the estimates obtained from the distribution of deformation features; that is, with the exception of the faults that show considerable lateral offset, where it is obvious that this amount of movement did not occur as a single rupture event and as such represent a number of seismic events. In such cases the magnitude estimate from the surface rupture length must be considered as an upper-bound estimate. Fault offset has only been used to determine the magnitude of associated seismic activity where it is clear

that this offset occurred as a single event. Using these considerations the magnitude estimates obtained show that post-glacial fault activity was associated with seismic activity up to 7.0 M_S , with numerous events of 5.5-6.5 M_S .

2.8 Discussion

All the faults described in this study cut and offset late- and post-glacial deposits and morphological features. The possibility that these scarps could have formed prior to and survived the late Devensian glacial episodes is ruled out on account of the highly erosive nature of the ice at this time that would not have allowed the survival of such delicate features. In most cases the fault movement occurred prior to the formation of the peat cover in the area c. 6 kyr BP (Birks 1977). However two faults, the Kinloch Hourn and Beinn Tharsuinn, are seen to cut and displace peats showing that fault movement was not confined to the immediate post-glacial period. In addition the lack of frost-shattering on many of the fault scarps shows that much of this fault movement was not immediately post-glacial when the climate would have been one of permafrost and periglacial activity. Those faults that show considerable lateral offset may have been active during previous ice-free periods, e.g. Pleistocene and Windermere Interstadials, as it is unlikely that such large movements occurred solely within the period 10.3-6 kyr BP. If the latter were the case the amount of offset would require unfeasibly large fault movement rates, similar to those for plate margin environments. When averaged over the entire Quaternary the observed lateral fault offsets give movement rates of 0.01-0.1 mm yr⁻¹. The height of post-glacial fault scarps and the degree of offset of post-glacial morphological features suggests that fault movement rates in the immediate post-glacial period were at least an order of magnitude greater than the average rate calculated for the Quaternary as a whole.

In all instances post-glacial fault movement has occurred on pre-existing faults with movement histories extending as far back as the Precambrian. There is no evidence for the creation of substantial new faults, although there may be new rupture sections, during this period of fault movement. The geometry of post-glacial faults can only be inferred from the surface expressions of the faults. In all faults observed to date the surface ruptures or scarps run discordantly across areas of considerable relief. This implies vertical or steeply dipping fault planes. This is reinforced by the geometry of the scarp faces which are commonly seen to dip at angles of 70-80°. Additional supporting evidence for steeply dipping fault planes is the narrow nature of the deformation zones associated with ground rupture. This is similar to the majority of post-glacial faults reported from Scandinavia (Lagerbäck 1990) and Canada (Adams

1989). If these faults were shallow dipping thrust flakes as proposed by Talbot (1986) it would be expected that the fault trajectories would be more topographically controlled and that the ground rupture zones would be much wider than those observed.

Several of the faults show considerable lateral offset, however the most common fault movement is vertical with normal or reverse sense. The majority of fault movement is that expected in a compressional tectonic environment. Post-glacial faults have a number of orientations (Figure 2.36) with the dominant direction being NW-SE. It is these faults that show sinistral strike-slip as well as vertical movement while faults orthogonal to this, i.e. NE-SW, show reverse movement. More northerly orientated faults such as those in Glen Gloy and on Lismore show dextral strike-slip movement. These fault movements are consistent with the WNW to NW orientated regional tectonic stress regime that has been active since c. 6 Ma (Muir Wood 1989a). This raises questions as to what is the cause of fault movement. The fact that the most spectacular faulting occurred during the immediate post-glacial period suggests that faulting was triggered by unloading of the crust. Johnston (1987) suggests that the imposition of an ice sheet suppresses seismicity in regions under tectonic compression. Muir Wood (1989b) proposes a similar mechanism for northern Scandinavia where glacial unloading and the creation of fluid overpressuring creates a unique stress regime that led to the triggering of the faults. A similar mechanism has been proposed for the post-glacial fault activity in Scotland [§ 6, p260]. In addition it is seen that the role of fluid overpressuring is important in perpetuating fault movement outwith the immediate post-glacial period [§ 6, p260]. However it should be noted that if fault movement was merely a result of glacial unloading it would be expected that, within the region of maximum rebound uplift, fault movement would have been extensional. Except for the offshore areas (Figure 2.3), there is no evidence of extensional fault movement in either Scotland or northern Scandinavia. Mohr (1986) claims that the "suspected" late Pleistocene fault activity in the west of Ireland is extensional. As the fault movement observed in Scotland occurs in the formerly glaciated region, hence the area of post-glacial doming, the fault movement is discordant with the theory that it was controlled by the effects of post-glacial isostatic rebound. Thus, fault activity must be controlled by the tectonic (compressive) stress regime, with the effects of post-glacial rebound merely acting as a mechanism to trigger fault movement in an already critically stressed crustal regime. Similarly the post-glacial fault activity in northern Scandinavia is seen to be located within the region of greatest post-glacial rebound but again the fault movement is reverse.

It is interesting to note that the fault activity in northern Sweden is an order of magnitude greater than that observed in Scotland. In Scotland the post-glacial faults are seen to be up to c. 10 km in length and are spaced at c. 10 km intervals with vertical throws of <10 m (Figure 2.36) while in northern Scandinavia the faults are up to 150 km in length, spaced at c. 100 km intervals and have vertical throws of up to 30 m (Figure 2.37) (Lagerbäck 1979, 1988, 1990; Bäckblom & Stanfors 1989; Muir Wood 1989b). This may be a reflection of the greater thickness of ice cover over northern Scandinavia during the late Devensian or may be related to the greater seismicity, and hence greater stress drop, associated with the movement along the Scandinavian faults. Also of interest is the absence of faults showing any degree of lateral movement in northern Scandinavia. However this may be merely due to the fact that only the largest faults have been discovered in this region due to the thickness of the surficial deposits that may mask smaller movements, similar to those observed in Scotland. Only after a thorough search for post-glacial faults in these regions has been carried out can a detailed comparison be carried out and only then will a consensus regarding the mechanisms of post-glacial faulting be reached.

2.9 Conclusions

A number of fault scarps and surface fault ruptures cutting late- and post-glacial deposits and morphological features indicate that the period immediately following disappearance of the late Devensian ice in Scotland was a period of enhanced tectonic activity. The average fault movement rate for the Quaternary was 0.01-0.1 mm yr⁻¹ while in the immediate post-glacial period this was at least an order of magnitude greater. Earthquakes associated with this fault activity triggered slope failures over wide areas surrounding the fault ruptures and caused liquefaction of water saturated sediments. The fact that faulting occurred close to deglaciation in the region of maximum post-glacial rebound suggests that crustal unloading was responsible for triggering this fault activity. However, the style of faulting, reverse and strike-slip, is inconsistent with that expected from crustal doming in response to glacio-isostatic rebound and that faulting continued outwith the immediate post-glacial period shows that faulting is essentially controlled by the regional (tectonically-generated) stress field with the effects of post-glacial rebound merely acting as a trigger mechanism for fault movement in an already critically stressed crust. The dimensions of the fault offsets and surface ruptures and the association of large areas of slope failure activity and seismic soft sediment deformation shows that fault movement was accompanied by large magnitude seismic activity, with numerous events of 5.5-6.5 M_s and possibly as large as 7.0 M_s .

The final question that needs to be addressed regarding post-glacial fault activity is concerned with whether there is present day movement along these faults. As stated previously, the area around Glen Shiel is still one of the most seismically active regions within the UK and several of the other locations of post-glacial activity have been subject to considerable swarms of seismic activity during both the period of instrumental recordings and of historical seismicity. However there have been no corroborated accounts of ground rupture during this time. With the present seismic activity in the UK it seems reasonable to assume that there is little or no risk of damaging seismic activity let alone from ground rupture. At present it seems that the present movement along faults in Scotland is negligible. A similar situation is observed in Sweden. However, in light of the recent fault rupture associated with a shallow earthquake in Ungava District, Quebec Province (Adams *et al.* 1991), a region considered to be tectonically stable but undergoing glacio-isostatic rebound, it may be wise to rethink our prejudices concerning seismic risk within the UK.

2.10 Acknowledgements

This work was carried out at the Department of Applied Geology, University of Strathclyde and at the Department of Geology & Applied Geology, University of Glasgow while in receipt of NERC studentship GT4/87/GS/107. F. McKenzie is thanked for help during field work. D. MacLean is thanked for the preparation of the photographic plates. J. Adams, I. Allison, G. Eaton, D.R. Grant, R.S. Haszeldine, R. Lagerbäck, R. Muir Wood, O. Olesen, R.G. Park, P.S. Ringrose and C. Talbot are all thanked for providing useful and stimulating discussion. SKB AB, R. Lagerbäck and O. Olesen are thanked for giving the author the opportunity to visit the PGFs of northern Scandinavia. The comments of I. Allison are much appreciated for clarifying an earlier version of this paper.

2.11 References

- Adams, J. 1989.** Postglacial faulting in eastern Canada: nature, origin and seismic hazard implications. *Tectonophysics* 163, 323-331.
- Adams, J., Wetmiller, R.J., Drysdale, J. & Hasegawa, H. 1991.** The first surface rupture from an earthquake in eastern North America. *in* Current Research, Part C, Geological Survey of Canada, Paper 91-1C, 9-15.
- Allen, C.R. 1975.** Geological criteria for evaluating seismicity. *Geol. Soc. Am. Bull.* 86, 1041-1057.
- Auden, J.B. 1954.** Drainage and fracture patterns in north west Scotland. *Geol. Mag.* 91, 327-351.
- Bäckblom, G. & Stanfors, R. (eds.) 1989.** Interdisciplinary study of post-glacial faulting in the Lansjärv area northern Sweden 1986-1988. SKB Technical Report 89-31.
- Ballantyne, C.K., Benn, D.I., Lowe, J.J. & Walker, M.J.C. 1991.** The Quaternary of the Isle of Skye: Field Guide. Quaternary Research Association, Cambridge, 172pp.
- Battiau-Queney, Y. 1989.** Constraints from deep crustal structure on the long term landform development of the British Isles and Eastern United States. *Geomorphology* 2, 53-70.
- Bennett, M. & Langridge, A.J. 1990.** A two stage rock slide in Gleann na Guiseran, Knoydart. *Scott. J. Geol.* 26, 53-56.
- Birks, H.J.B. 1977.** The Flandrian forest history of Scotland: a preliminary synthesis. *in* F.W. Shotton (ed.) *British Quaternary Studies: recent advances.* Clarendon Press, Oxford, 119-135.
- Bonilla, M.G., Mark, R.K. & Lienkaemper, J.J. 1984.** Statistical relations among earthquake magnitude, surface rupture length, and surface fault displacement. *Seis. Soc. Am. Bull.* 74, 2379-2411.

- Bovis, M.J. 1982.** Uphill-facing (antislope) scarps in the Coast Mountains, southwest British Columbia. *Geol. Soc. Am. Bull.* 93, 804-812.
- Bucknam, R.C. & Anderson, R.E. 1979.** Estimation of scarp-slope ages from a scarp-height-slope-angle relationship. *Geology* 7, 11-14.
- Crone, A.J. (ed.) 1987.** Proceedings of conference XXXIX - Directions in palaeoseismology. USGS Open File Rpt. 87-673.
- Dames & Moore 1990.** Report of a meeting on "Fractures and fracture development", DoE Report No. DOE/RW/90.014 1990. Dames & Moore International Technical Report TR-D&M-17.
- Davenport, C.A., Ringrose, P.S., Becker, A., Hancock, P. & Fenton, C. 1989.** Geological investigations of late and post-glacial earthquake activity in Scotland. *in* S. Gregerson & P.W. Basham (eds.) *Earthquakes at North Atlantic Passive Margins: Neotectonics and postglacial rebound.* 175-194. Kluwer Academic Publishers, Amsterdam.
- Doornkamp, J.C. 1986.** Geomorphological approaches to the study of neotectonics. *J. Geol. Soc. London* 143, 335-342.
- Eaton, G. 1990.** British Nuclear Fuels Plc., Hinton House, Risley, Cheshire, WA3 6AS.
- Eisbacher, G.H. 1979.** Cliff collapse and rock avalanches (stürztstroms) in the MacKenzie Mountains, northwestern Canada. *Can. Geotech. J.* 16, 309-334.
- Evans, D., Kenolty, N., Dobson, M.R. & Whittington, R.J. 1979.** The geology of the Malin Sea. *Rep. Inst. Geol. Sci.* 79/15, 43pp.
- Fenton, C.H. 1991.** Neotectonics and Palaeoseismicity in N.W. Scotland. Unpubl. Ph.D. Thesis, Univ. Glasgow.
- Firth, C.R. 1986.** Isostatic redepression during the Loch Lomond Stadial: preliminary evidence from the Great Glen, Northern Scotland. *Quaternary Newsletter* 48, 1-9.

- deFreitas, M.H. & Watters, R.J. 1973.** Some field examples of toppling failure. *Geotechnique* 23, 495-514.
- Grant, D.R. 1990.** Late Quaternary movement of Aspy Fault, Nova Scotia. *Can. J. Earth Sci.* 27, 984-987.
- Gray, J.M. 1974.** The main rock platform of the Firth of Lorn, western Scotland. *Trans. Inst. Br. Geogr.* 61, 81-99.
- Hancock, P.L. & Engelder, T. 1989.** Neotectonic joints. *Geol. Soc. Am. Bull.* 101, 1197-1208.
- Haszeldine, R.S. 1989.** Department of Geology & Applied Geology, University of Glasgow, G12 8QQ.
- Hempton, M.R. & Dewey, J.F. 1983.** Earthquake-induced deformational structures in young lacustrine sediments, East Anatolian Fault, southern Turkey. *Tectonophysics* 98, T7-14.
- Holmes, G. 1984.** Rock slope failure in parts of the Scottish Highlands. Unpubl. Ph.D. Thesis, University of Edinburgh.
- Hsü, K. 1975.** Catastrophic debris streams (sturtzstroms) generated by rockfalls. *Geol. Soc. Am. Bull.* 86, 129-140.
- Jibson, R.W. 1987.** Summary of research on the effects of topographic amplification of earthquake shaking on slope stability. USGS Open File Rpt. 87-268, 171pp.
- Johnston, A.C. 1987.** Suppression of earthquakes by large continental ice sheets. *Nature* 330, 467-469.
- Johnston, A.C. 1989.** The seismicity of "Stable Continental Interiors". *in* S. Gregerson & P.W. Basham (eds.) *Earthquakes at North Atlantic Passive Margins: Neotectonics and postglacial rebound*, 299-327. Kluwer Academic Publishers, Amsterdam.

- Johnston, M.R.W. & Frost, R.T.C. 1977.** Fault and lineament patterns in the southern Highlands of Scotland. *Geol. en Mijnbouw* 56, 287-294.
- Johnstone, G.S. & Mykura, W. 1989.** The Northern Highlands of Scotland (British Regional Geology). British Geological Survey, HMSO London, 219pp.
- Keefer, D.K. 1984a.** Landslides caused by earthquakes. *Geol. Soc. Am. Bull.* 95, 406-421.
- Keefer, D.K. 1984b.** Rock avalanches caused by earthquakes: source characteristics. *Science* 223, 1288-1289.
- Keefer, D.K. 1987.** Landslides as indicators of prehistoric earthquakes. *in* A.J. Crone (ed.) Proceedings of conference XXXIX - Directions in palaeoseismology. 178-180. USGS Open File Rpt. 87-673.
- Khromovskikh, V.S. 1989.** Determination of magnitudes of ancient earthquakes from dimensions of observed seismodislocations. *Tectonophysics* 166, 269-280.
- Kirkton, S.R. & Hitchen, K. 1987.** Timing and style of crustal extension north of the Scottish mainland. *in* M.P. Coward, J.F. Dewey & P.L. Hancock (eds.) Continental extensional tectonics. *Geol. Soc. Special Publ.* 28, 501-510.
- Kuenen, P.H. 1958.** Experiments in geology. *Trans. Geol. Soc. Glasgow* 23, 1-28.
- Kujansuu, R. 1964.** Nuorista siirroksista Lapissa (Recent faults in Lapland). *Geologi* 16, 30-36.
- Kuribayashi, E. 1985.** *in* Ambraseys, N.N. 1988. Engineering seismology. *Earthquake Engineering & Structural Dynamics* 17, 1-105.
- Lagerbäck, R. 1979.** Neotectonic structures in northern Sweden. *Geologiska Föreningens i Stockholm Förhandlingar* 100, 263-269.
- Lagerbäck, R. 1988.** Postglacial faulting and palaeoseismicity in the Lansjärv area, northern Sweden. SKB Technical Report 88-25.

Lagerbäck, R. 1990. Late Quaternary faulting and palaeoseismicity in northern Fennoscandia, with particular reference to the Lansjärv area, northern Sweden. *Föreningens i Stockholm Förhandlingar* 112, 333-354.

Lagerbäck, R. 1991. Seismically deformed sediments in the Lansjärv area, Northern Sweden. SKB Technical Report 91-17.

Le Coeur, C. 1988. Late Tertiary warping and erosion in western Scotland. *Geografiska Annaler* 70A, 361-367.

Mohr, P. 1986. Possible late Pleistocene faulting in Iar (west) Connacht, Ireland. *Geol. Mag.* 123, 545-552.

Mörner, N-A., Somi, E. & Zuchiewicz, W. 1989. Neotectonics and palaeoseismicity within the Stockholm intracontinental region in Sweden. *Tectonophysics* 163, 289-303.

Muir Wood, R. 1989a. Fifty million years of 'passive margin' deformation in North West Europe. *in* S. Gregerson & P.W. Basham (eds.) *Earthquakes at North Atlantic Passive Margins: Neotectonics and postglacial rebound*. 7-36. Kluwer Academic Publishers, Amsterdam.

Muir Wood, R. 1989b. Extraordinary deglaciation reverse faulting in Northern Fennoscandia. *in* S. Gregerson & P.W. Basham (eds.) *Earthquakes at North Atlantic Passive Margins: Neotectonics and postglacial rebound*. 141-173. Kluwer Academic Publishers, Amsterdam.

Olesen, O. 1989. The Stuoragurra fault, evidence of neotectonics in the Precambrian of Finmark, northern Norway. *Nor. Geol. Tidsskr.* 68, 107-118.

Park, R.G. 1988. Department of Geology, University of Keele, Keele, Staffordshire, ST5 5BG.

Pavlidis, S.B. & Tranos, M.D. 1991. Structural characteristics of two strong earthquakes in North Aegian (1932) and Agios Efstratios (1968). *J. Structural Geol.* 13, 205-214.

- Ringrose, P.S. 1987.** Fault activity and palaeoseismicity during Quaternary time in Scotland. Unpubl. Ph.D. Thesis (2 Volumes), University of Strathclyde.
- Ringrose, P.S. 1989a.** Palaeoseismic (?) liquefaction event in late Quaternary lake sediment at Glen Roy, Scotland. *Terra Nova* 1, 57-62.
- Ringrose, P.S. 1989b.** Recent fault movement and palaeoseismicity in western Scotland. *Tectonophysics* 163, 305-314.
- Ringrose, P.S., Hancock, P.L., Fenton, C. & Davenport, C.A. 1991.** Quaternary tectonic activity in Scotland. *in* A. Foster, M.G. Culshaw, J.C. Cripps, J.A. Little & C.F. Moon (eds.) *Quaternary Engineering Geology*, Geol. Soc. Eng. Geol. Special Publ. No.7, 679-686.
- Robinson, M. 1977.** Glacial limits, sea level changes and vegetational development in part of Wester Ross. Unpubl. Ph.D. Thesis, University of Edinburgh.
- Scott, B. & Price, S. 1988.** Earthquake-induced structures in young sediments. *Tectonophysics* 147, 165-170.
- Seilacher, A. 1969.** Fault-graded beds interpreted as seismites. *Sedimentology* 13, 155-159.
- Seilacher, A. 1984.** Sedimentary structures tentatively attributed to seismic events. *Marine Geology* 55, 1-12.
- Sims, J.D. 1975.** Determining earthquake recurrence intervals from deformational structures in young lacustrine sediments. *Tectonophysics* 29, 141-152.
- Sissons, J.B. 1972.** Dislocation and non-uniform uplift of raised shorelines in the western part of the Forth Valley. *Trans. Inst. British Geogr.* 55, 145-159.
- Sissons, J.B. 1977a.** Former ice-dammed lakes in Glen Moriston, Inverness-shire, and their significance in upland Britain. *Trans. Inst. Br. Geogr.*, NS2, 224-242.

Sissons, J.B. 1977b. The Loch Lomond Readvance in the Northern Mainland of Scotland. *in* J.M. Gray & J.J. Lowe (eds.) *Studies in the Scottish Lateglacial environment*. Pergamon, Oxford, 45-59.

Sissons, J.B. & Cornish, R. 1982. Rapid localized glacio-isostatic uplift at Glen Roy, Scotland. *Nature* 297, 213-214.

SKB. 1990. Gransking av Nils-Axel Mörners arbete avseende postglaciala strukturer på Äspö. SKB Arbetsrapport 90-18, 54pp.

Stewart, I.S. & Hancock, P.L. 1990. What is a fault scarp? *Episodes* 13, 256-263.

Talbot, C. 1986. A preliminary structural analysis of the pattern of post-glacial faults in Northern Sweden. SKB Technical Report 86-20.

Wallace, R.E. 1977. profiles and ages of young fault scarps, north-central Nevada. *Geol. Soc. Am. Bull.* 88, 1267-1281.

Youd, T.L. 1977. Discussion of Brief review of liquefaction during earthquakes in Japan. *Soils Found.* 17, 82-85.

2.12 Figure Captions

- Figure 2.1** Major faults in Scotland. NE trending faults of Caledonian age dominate. Major thrust faults of the NW margin of the Caledonian orogen are marked by unbroken lines.
- Figure 2.2** Major faults in North West Scotland. GGF: Great Glen Fault, HF: Helmsdale Fault, LMF: Loch Maree Fault, SCF: Strathconon Fault, SGF: Strathglass Fault [After Johnstone & Mykura 1989].
- Figure 2.3** (a) Sparker profile across Rathlin Sound, off the Antrim coast, Northern Ireland showing a fault cutting up into and displacing the Quaternary cover [From Evans *et al.* 1979]
(b) Detail of the fault from (a).
(c) Line drawing of the interpretation of (b). Mesozoic sediments are faulted against basalts. Drag structures in the overlying Quaternary sediments suggest normal movement.
- Figure 2.4** Location of sites of Quaternary fault activity in North West Scotland. Inset boxes represent the area covered by subsequent figures.
- Figure 2.5** Morphotectonic features along the surface exposure of the Coire Mor fault. Key also applies to Figures 2.10, 2.12, 2.18, 2.26, 2.33 & 2.35.
- Figure 2.6** Coire Mor fault scarp viewed from the slopes of Creag an Duine (Looking NE). Possible dextral offset of c. 100 m of drainage courses is marked by arrows.
- Figure 2.7** (a) A catastrophic rockfall on the north side of Gleann Beag. Largest boulders in centre are 20 m across (Looking NE).
(b) Slump type failure adjacent to the fault (marked by arrow) on the northern side of the upper reaches of Glen More. Slope height 300 m (Looking NNE).
- Figure 2.8** (a) Slump failure on Beinn a' Chaisteil on the eastern side of Loch Vaich adjacent to the Strath Vaich fault (marked the arrows).

(b) "Dry stane dyke" texture within the failed mass on Beinn a' Chaisteil. Attributed to strong earthquake shaking disaggregating the rockmass along pre-existing discontinuities (Looking S).

- Figure 2.9**
- (a) Garbh Choire Mor. Rock avalanche deposit (R) and suspected faults (F) are marked. The area of glaciated slabs cut by rebound fractures lies in front of the rock avalanche debris (Looking W).
 - (b) Detail of the avalanche debris in Garbh Choire Mor showing 'jig-saw fit' boulders and overthrusting (Looking N).
 - (c) Garbh Choire Mor rock avalanche debris viewed from the source slope. Possible late Quaternary fault is marked by arrow.
 - (d) Rebound fractures running left to right ($70^{\circ}/276^{\circ}$) cutting glaciated slabs in front of the rock avalanche debris. Lens cap 52 mm diameter (Looking S).

- Figure 2.10** Morphotectonic and palaeoseismic features adjacent to the Beinn Alligin fault. 1 and 2 are exposures of the fault zone detailed in Figure 2.11b and 2.11c respectively.

- Figure 2.11**
- (a) Rock avalanche source slope on Sgurr Mhor bounded on the right (east) side by the Beinn Alligin fault. Slope height 550 m (Looking N).
 - (b) Detail of the fault zone in the gully of 'Eag Dhuibh na h-Eigheachd' (1 in Figure 2.10). Lens cap 60 mm (Looking N).
 - (c) Detail of the fault zone at the top of the gully of 'Eag Dhuibh na h-Eigheachd' (2 in Figure 2.10). Most recent movement has occurred in the grey-green gouge. Vertical section looking north.

- Figure 2.12** Morphotectonic features along the surface expression of the Loch Maree Fault at Scardroy in Strathconon. Inset: the surface trace of the Loch Maree Fault with the two sites of late Quaternary reactivation at Scardroy and Loch Crann marked (A & B). Bac na Eich fault is also marked (C).

- Figure 2.13** (a) Fault zone exposure at NH206520. Several generations of fault gouge in a 40 cm wide zone. Shovel is 0.7 m long (Looking SE).
(b) Detail of the 40 cm wide composite gouge zone at NH206520. Numbers represent sample points (Correspond to positions of the sample tubes in Figure 2.13a).
- Figure 2.14** (a) Fault zone exposure with several generations of fault gouge at NH204523. Sample tubes are 25 mm diameter (Looking NW).
(b) Detail of the composite gouge zone at NH204523. Numbers represent sample points (Correspond to the position of the sample tubes in Figure 2.14a)..
- Figure 2.15** Exposure of the fault zone at NH205523 showing a single unit of gouge material. Sample tube diameter 25 mm (Looking S).
- Figure 2.16** Seismite liquefaction ball and pillow of pseudo-nodule structures in glacio-fluvial outwash sands in the upper part of Strathconon [NH191503] (Looking S).
- Figure 2.17** (a) The zone of most recent movement along the Bac na Eich fault. Arrow marks the location of the 'fresh' fractures detailed in Figure 2.17b. Rucsac at base of the fault zone is 0.7 m long (Looking SE).
(b) Detail of the most recent fracture offset adjacent to the Allt Coire Feola [NH2050]. Sense of movement is sinistral. Lens cap is 52 mm diameter.
- Figure 2.18** Morphotectonic features along the surface rupture of the Coire Eoghainn fault, Glen Cannich. A and B are field sketches of fault gouge exposures. C is a diagrammatic section across the fault. The block diagram shows the fault in relation to the basement geology.
- Figure 2.19** (a) Looking west along the incised gully that marks the Coire Eoghainn fault.
(b) & (c) Exposures of fault gouge along the Coire Eoghainn fault (Correspond to A and B in Figure 2.18). Trowel is 25 cm long.
- Figure 2.20** View of Beinn Tharsuinn from the east. Fault (F) and the area of slope failure (SF) are marked.

- Figure 2.21** (a) Excavated fault zone on the south east ridge of Beinn Tharsuinn. Note the peat down faulted against the Moine bedrock, rotated clasts within the peat and 'intrusion' of the peat by blue-grey fault gouge material. Shovel is 0.7 m long (Looking S).
(b) Detail of the fault zone excavated on Beinn Tharsuinn. Most recent movement has occurred within the blue-grey gouge zone.
- Figure 2.22** (a) Exposure of the zone of most recent movement along the Strathconon Fault in Glen Elchaig at NH008267. Trowel is 10 cm across (looking NE).
(b) Detail of the fault gouge from the fault zone in Glen Elchaig. Rotation of clasts show structures similar to δ -type porphyroclasts displaying sinistral shear (inset). Dots represent granular crushed material, white areas are dark grey gouge 'clays' containing rotated clasts.
- Figure 2.23** Exposure of a gouge-bearing segment of the Strathconon Fault system in a road cut at Invershiel (Looking SW).
- Figure 2.24** (a) Slope failure on An Sornach, Glen Affric. Slope height is 500 m (Looking WSW).
(b) An Sornach slope failure from the south. Note the prominent lineament running diagonally from top left to bottom right (NW-SE) across the area of failure and out into the surrounding slope.
(c) Looking SE down the uphill-facing 'fault scarp' as it crosses the An Sornach slope failure. Scarp decreases from c. 2 m to 1 m in height away from the camera until it dies out at the edge of the area of failure to be replaced by a downslope-facing scarp of c. 1 m height for c. 100 m to the SE.
- Figure 2.25** (a) 'Slope failure' on Sgurr na Lapaich, Glen Affric viewed from the NW. Note the 4 m scarp backing the failed area and the lack of deformation at the base of the slope. Scarp represents about 2% of the total slope height.
(b) Detail of the scarp on the ridge crest of Sgurr na Lapaich. Note that the curved scarp is in fact composed of a number of right-stepping linear elements (Looking W).

- Figure 2.26** Morphotectonic features along the faults in Gleann Lichd and Glen Shiel.
- Figure 2.27** (a) The Gleann Lichd fault in the upper part of the glen, marked by the course of the Allt Lapain in the foreground and the conspicuous notch and gully crossing the shoulder of Meall a' Chara. Exposure of the fault zone (Figure 27b) is marked by the arrow (looking E from Glenlichd House).
(b) Exposure of the most recent zone of movement at NH014167. Pencil is 10 cm long (Looking E).
- Figure 2.28** Creag na Damh, Glen Shiel. A late Caledonian fault runs up the main gully falling from the ridge crest. Late Quaternary movement is shown by the fault splay on the left, marked by arrows (View SE from the River Shiel).
- Figure 2.29** Pop-up scarps (up to 7 m high) on the southern slope of Sgurr a' Bhealaich Dheirg, Glen Shiel (Looking SE from Saileag).
- Figure 2.30** The Sgurr na Ciste Duibhe or Five Sisters fault, Glen Shiel. The fault runs from the skyline notch and is marked by the obvious lineament running diagonally across the slope, obscured in part by later slope movements. Near the summit the fault has acted as the backing plane for a large, complex slope failure (View NW from Glen Shiel).
- Figure 2.31** (a) The Five Sisters fault marked by a prominent lineament cutting glacial and periglacial debris. Viewed from the top of the skyline notch, looking WSW.
(b) The Five Sisters fault as it crosses the ridge crest, just below the summit of Sgurr na Ciste Duibhe [NG985150]. The scarp faces right (southwest), fronted by shattered debris. The ridge crest is offset by c. 15 m in a sinistral sense at this point resulting in the strange ridge crest hollow seen here.
(c) Looking NW back along the fault from the ridge crest offset to the skyline notch. The c. 5 m high scarp has crossed the ridge but still faces the same direction and displays the same amount of throw.

- Figure 2.32** Seismite liquefaction features in glacial outwash sediments in Glen Shiel.
(a) Ball and pillow or pseudonodule structures at NG950178 (GS1 on Figure 2.26). Card is 12 cm across.
(b) Injection and flame structures, fault grading and other water escape structures at NG956167 (GS5 on Figure 2.26). Card is 12 cm across.
- Figure 2.33** Morphotectonic features along the suspected post-glacial faults at Arnisdale. Inset: N-S section across the fault scarp.
- Figure 2.34** (a) Flame and injection structures confined to a single horizon in lacustrine sediments in Coire Dho [NH194138]. Lens cap 60 mm diameter.
(b) Neotectonic fracture on the northeast slopes of Creag a' Chaorainn, Coire Dho [NH1413]. The fracture cuts across glacially-smoothed rock outcrops. Slope height 540m.
- Figure 2.35** Morphotectonic features along the Kinloch Hourn Fault. A: Detail of fault gouge in peat lens. B: Seismite liquefaction adjacent to Dubh Lochain [After Ringrose 1987].
- Figure 2.36** Post-glacial faults in Scotland. Faults are shown with their sense of movement. Fault length is not to scale.
- Figure 2.37** Post-glacial faults in northern Scandinavia. Barbs on the downthrown sides. 1: Pärvie Fault, 2: Kåfjord Fault, 3: Stuoragurra Fault, 4: Skipskjølen Fault, 5: Fiskarhalvøya Faults, 6: Lainio Fault, 7: Merasjärvi Fault, 8: Lansjärv Fault, 9: Faults in Finnish Lapland. (Redrawn from Bäckblom & Stanfors 1989; Lagerbäck 1990).
- Table 2.1** Morphotectonic features and corresponding palaeoseismicity magnitude estimates for post-glacial faults in Scotland. Numbers correspond to Figure 2.36.

2.13 Figures

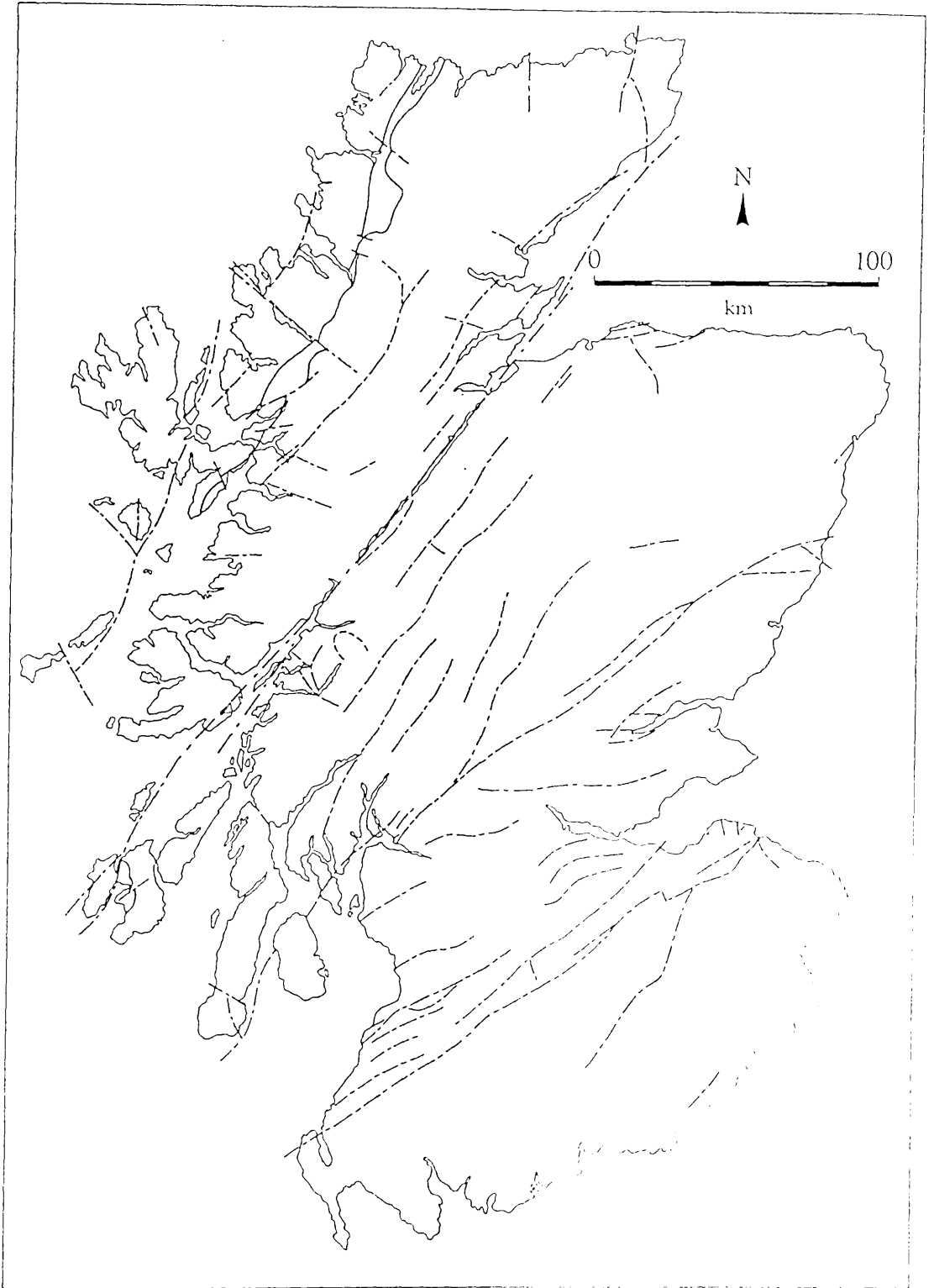


Figure 2.1

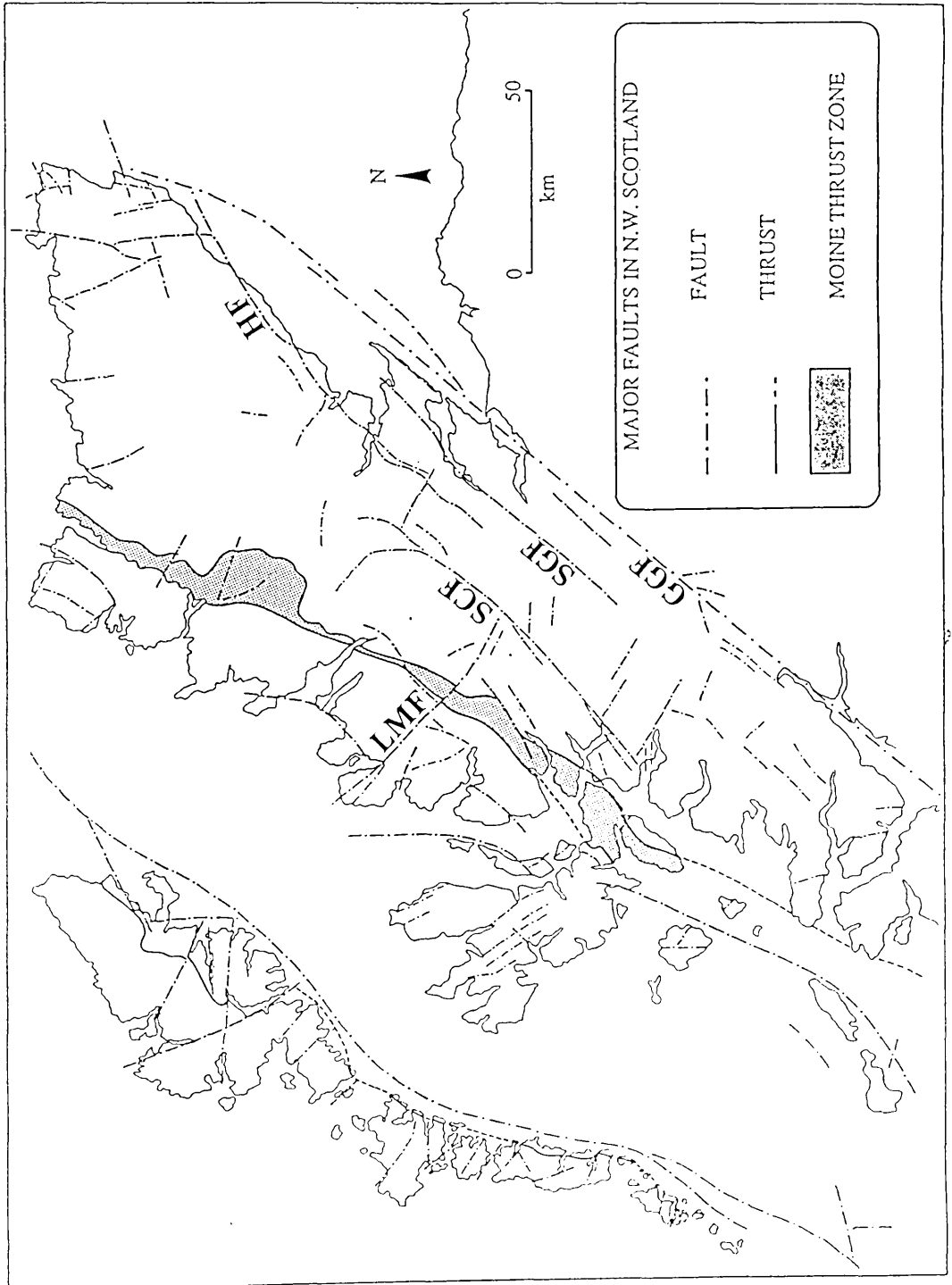


Figure 2.2

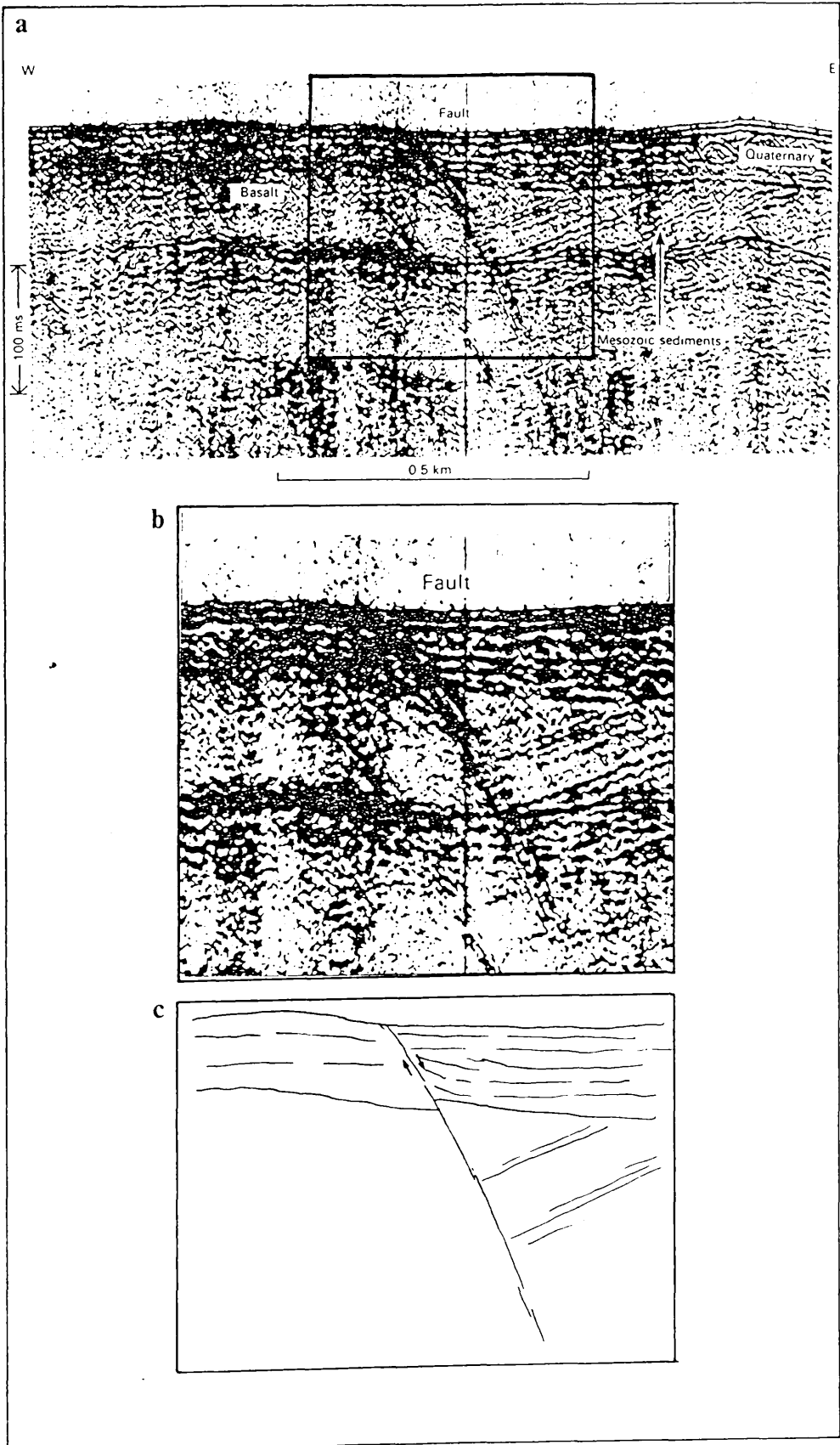


Figure 2.3

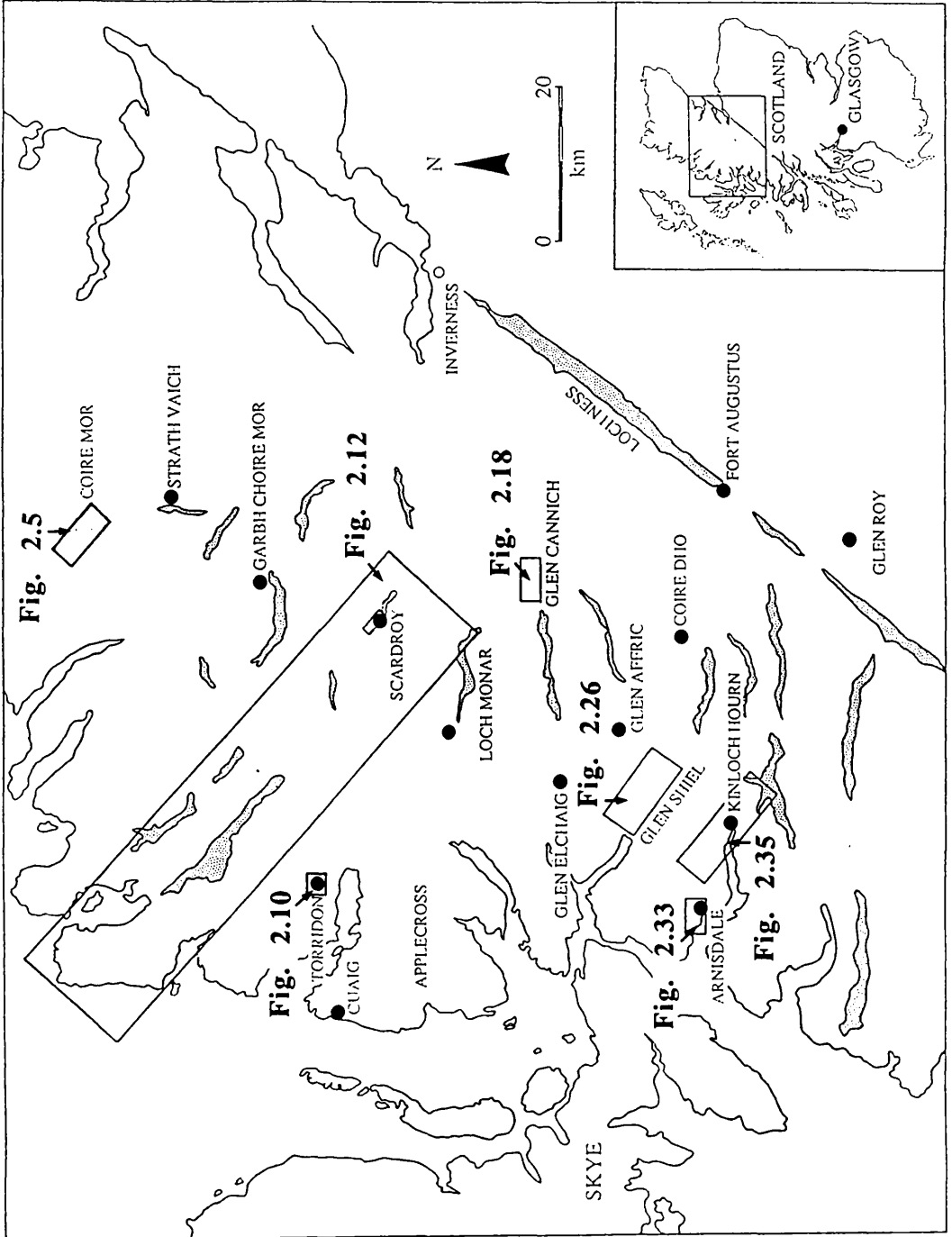


Figure 2.4

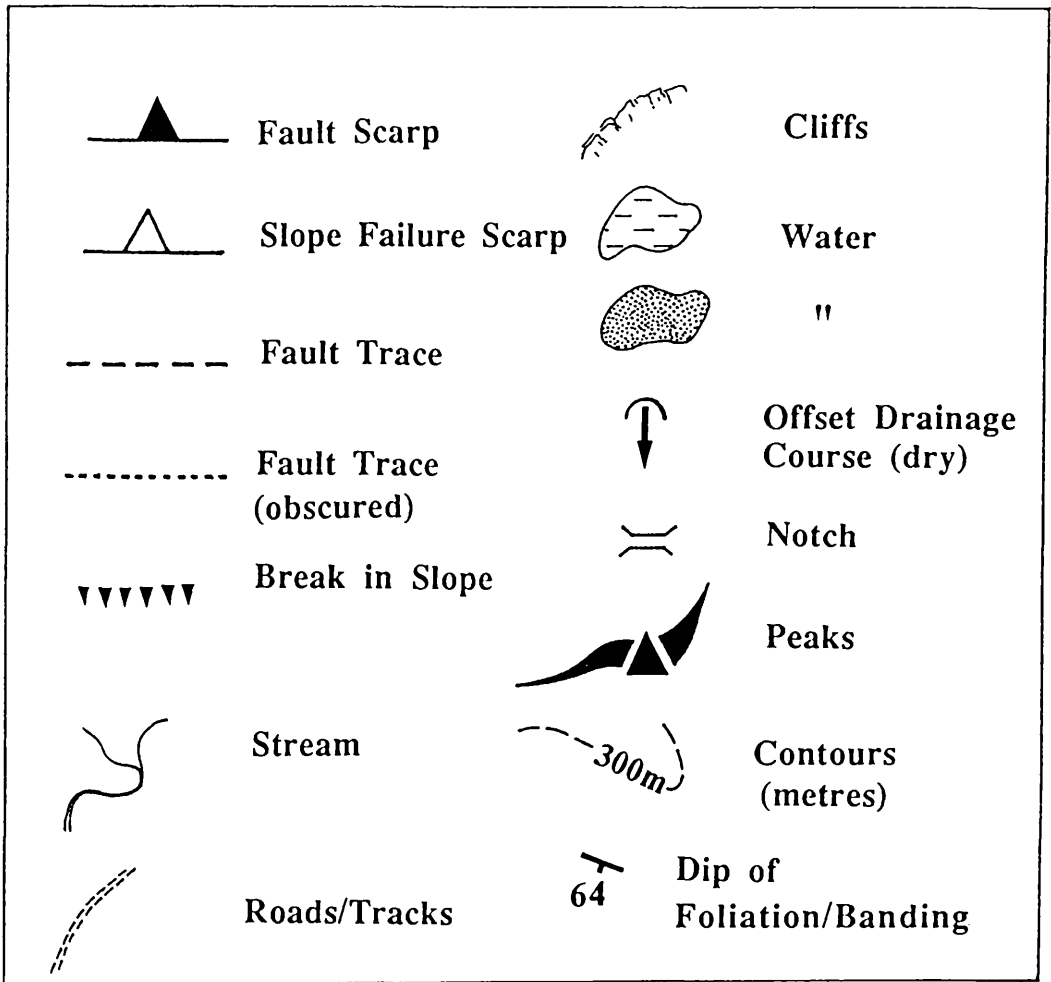


Figure 2.5 (Key)

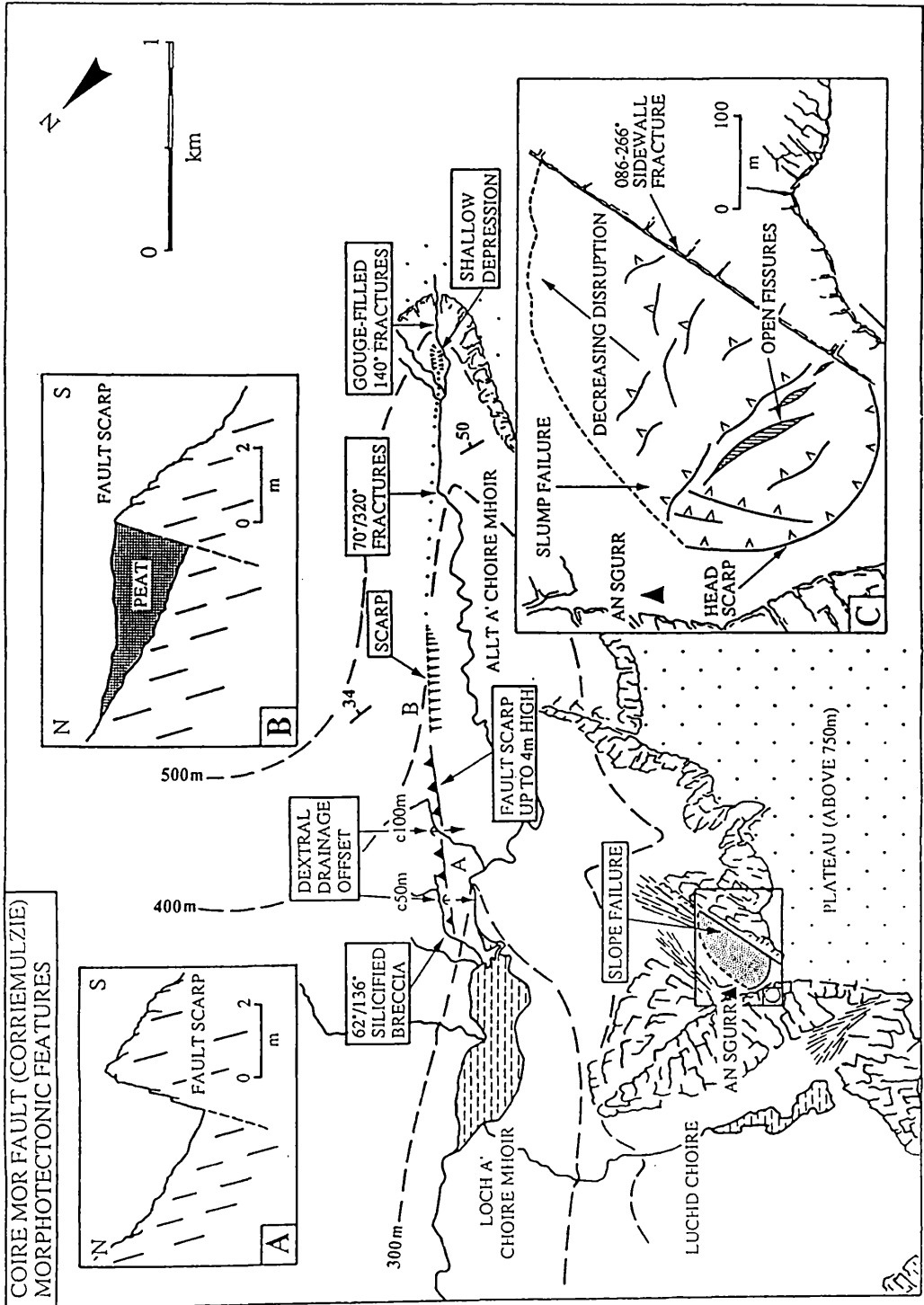


Figure 2.5



Figure 2.6



Figure 2.7a



Figure 2.7b



Figure 2.8a



Figure 2.8b



Figure 2.9a



Figure 2.9b



Figure 2.9c



Figure 2.9d

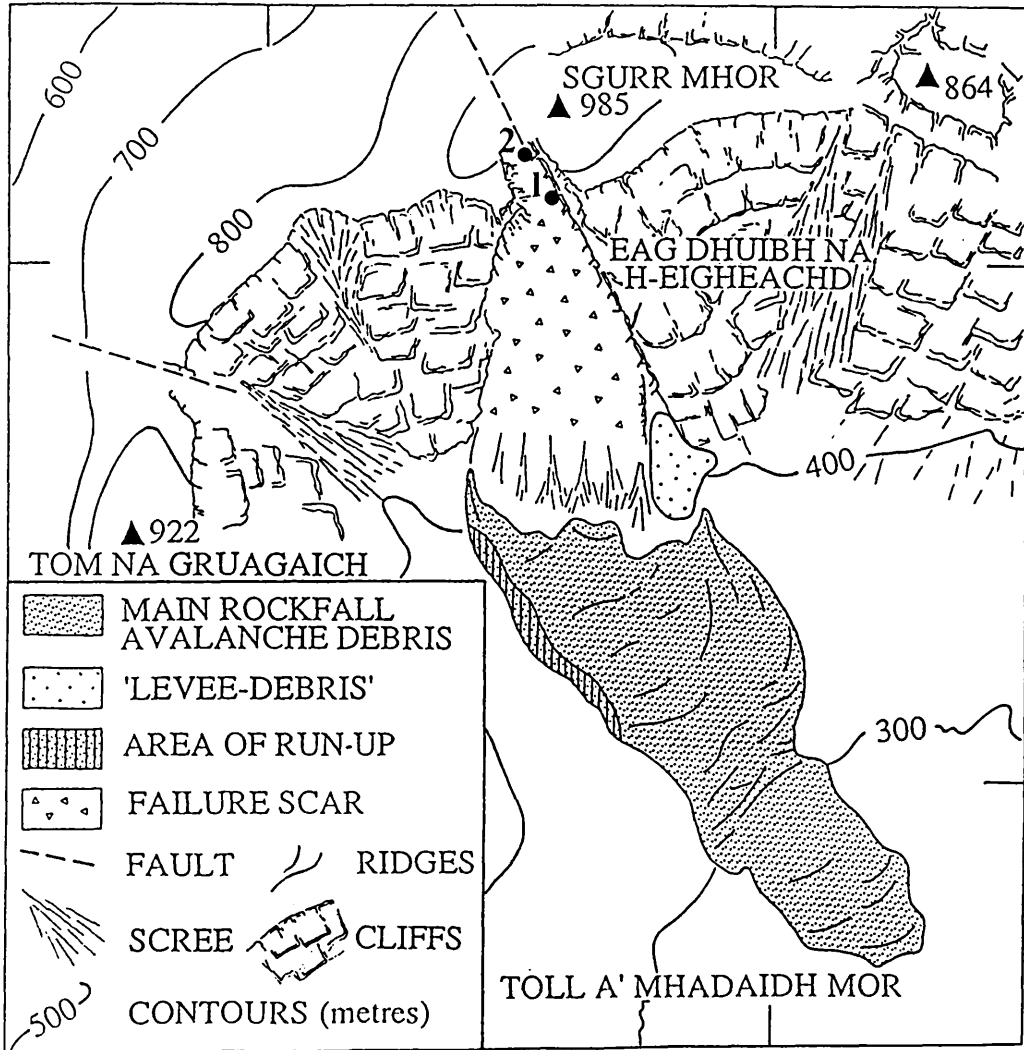


Figure 2.10

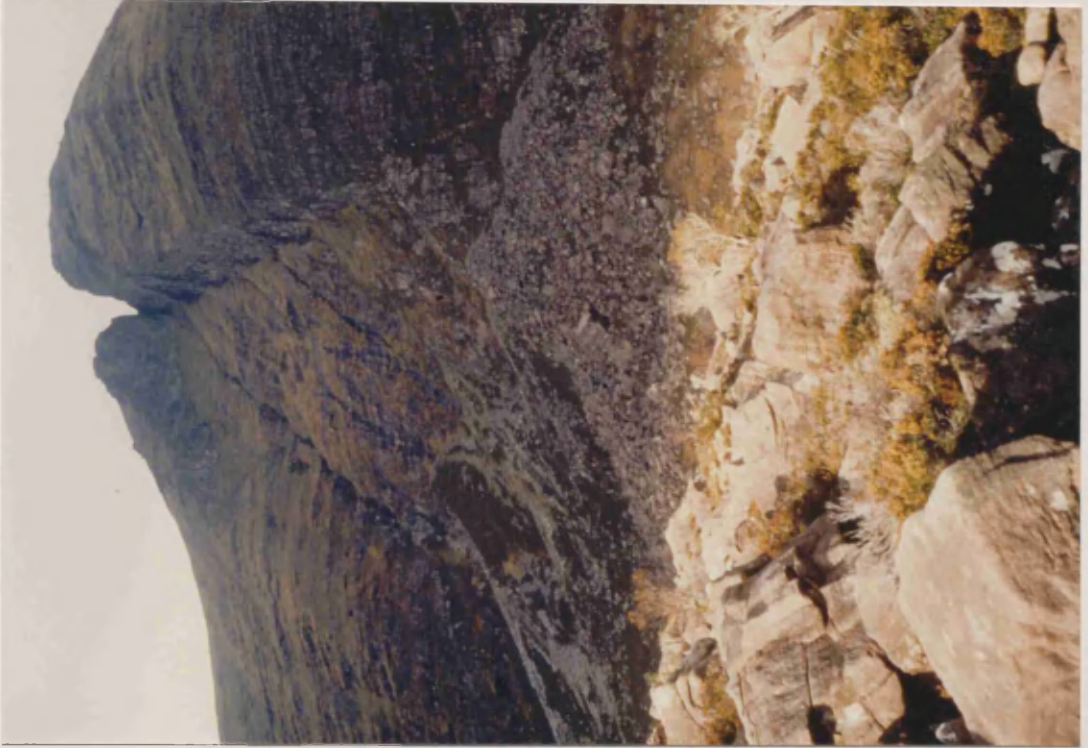


Figure 2.11a

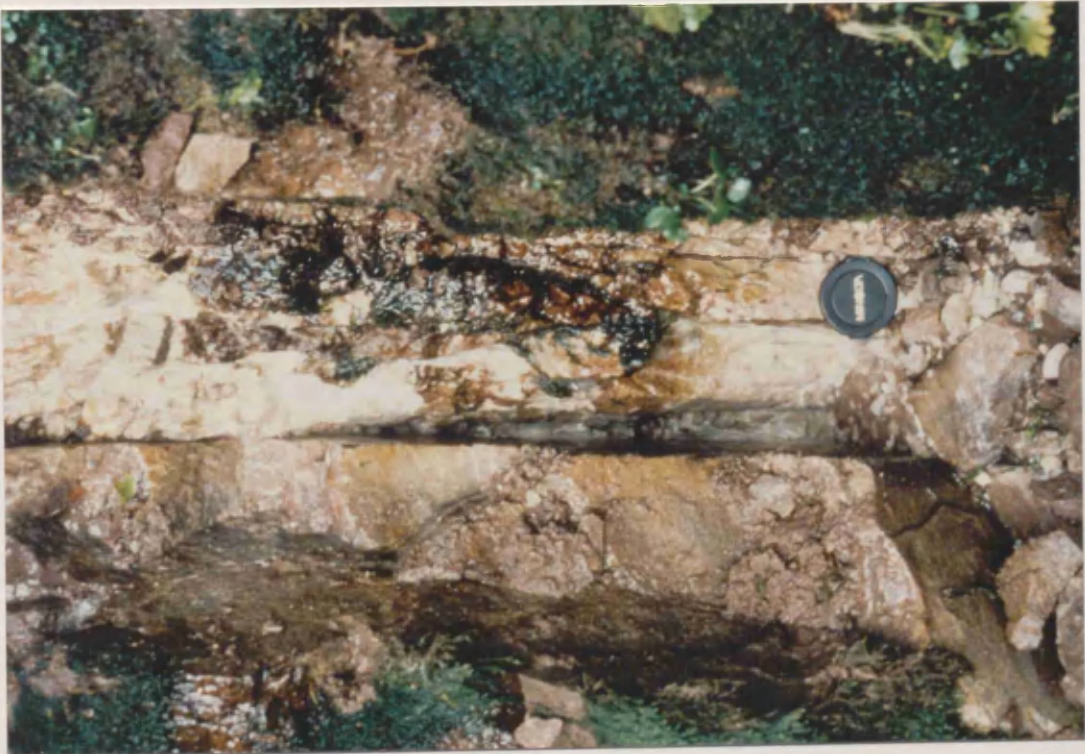


Figure 2.11b

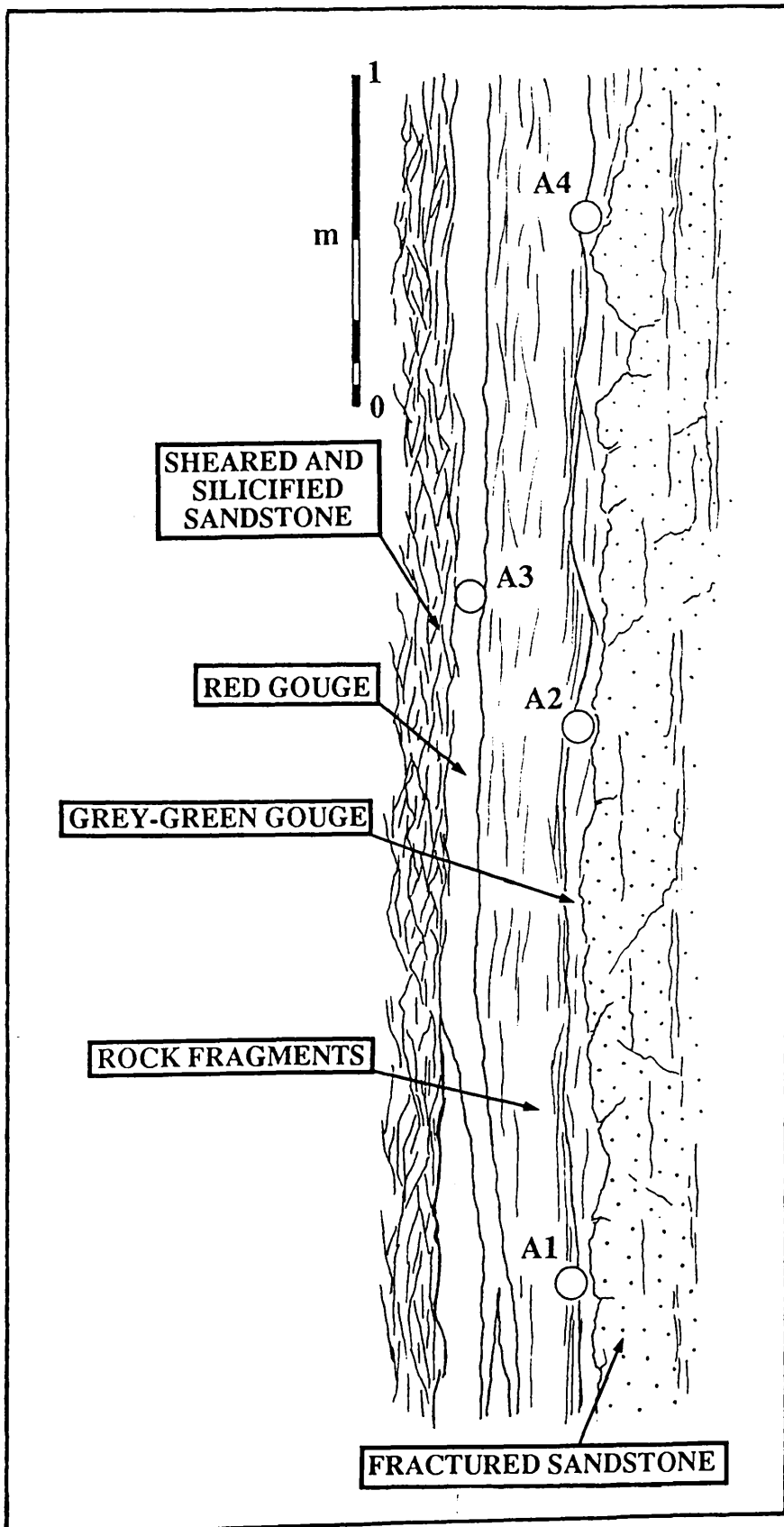


Figure 2.11c

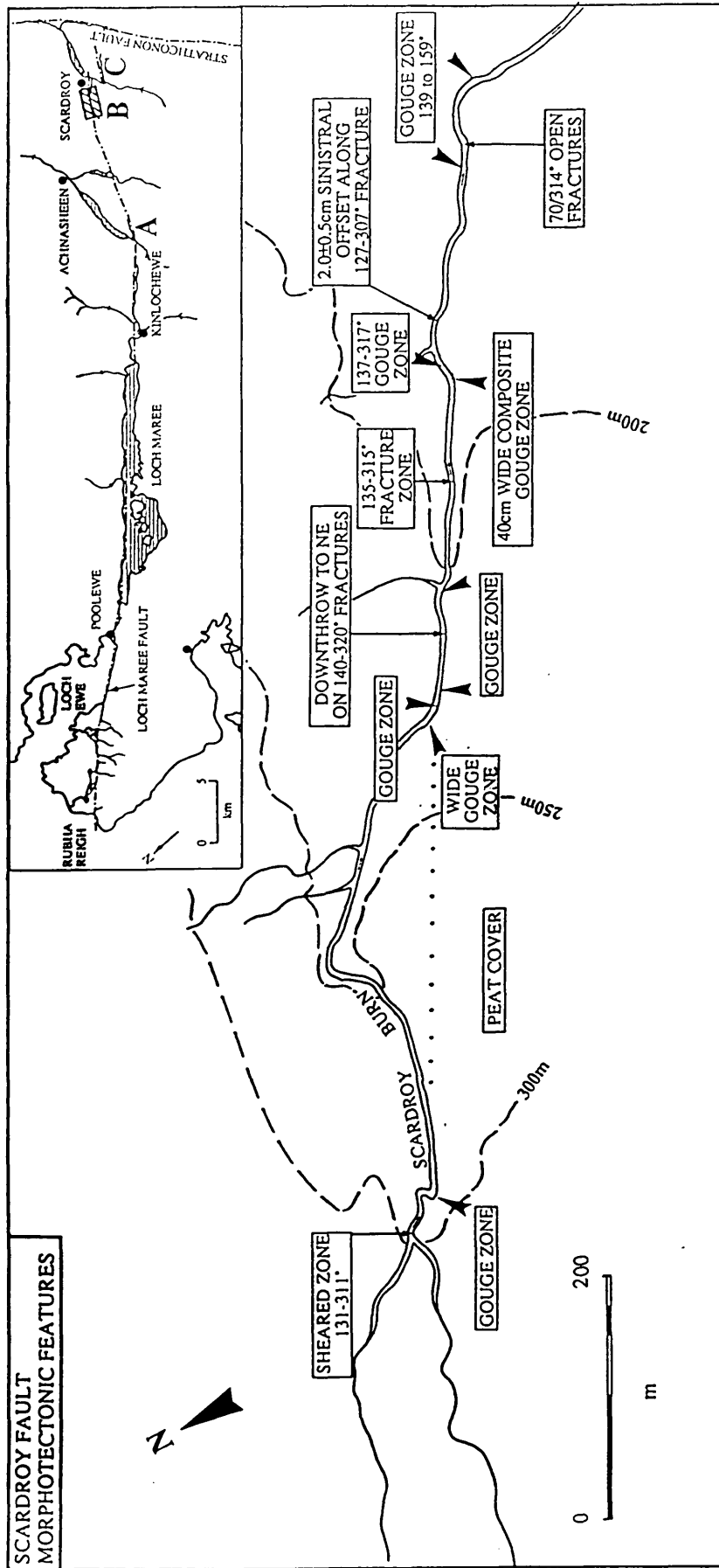


Figure 2.12



Figure 2.13a

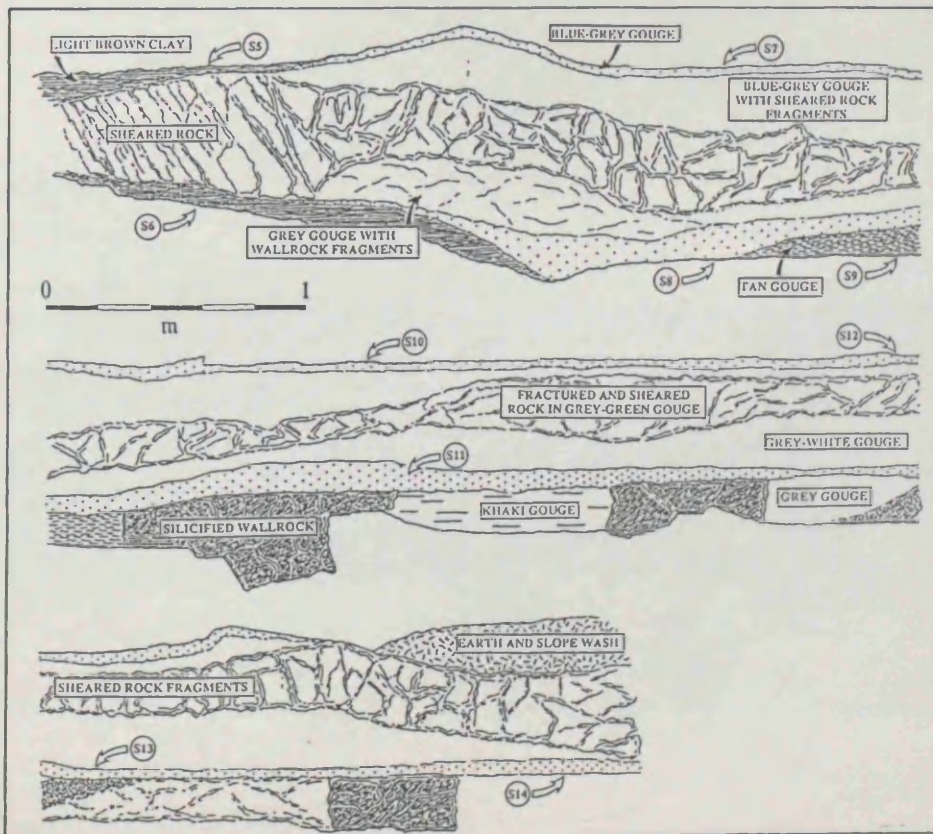


Figure 2.13b



Figure 2.14a

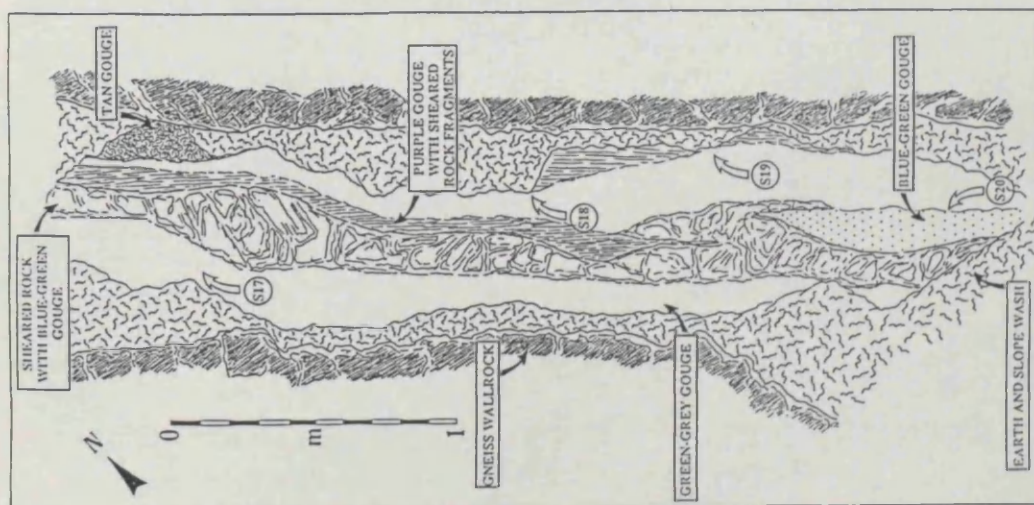


Figure 2.14b



Figure 2.15



Figure 2.16

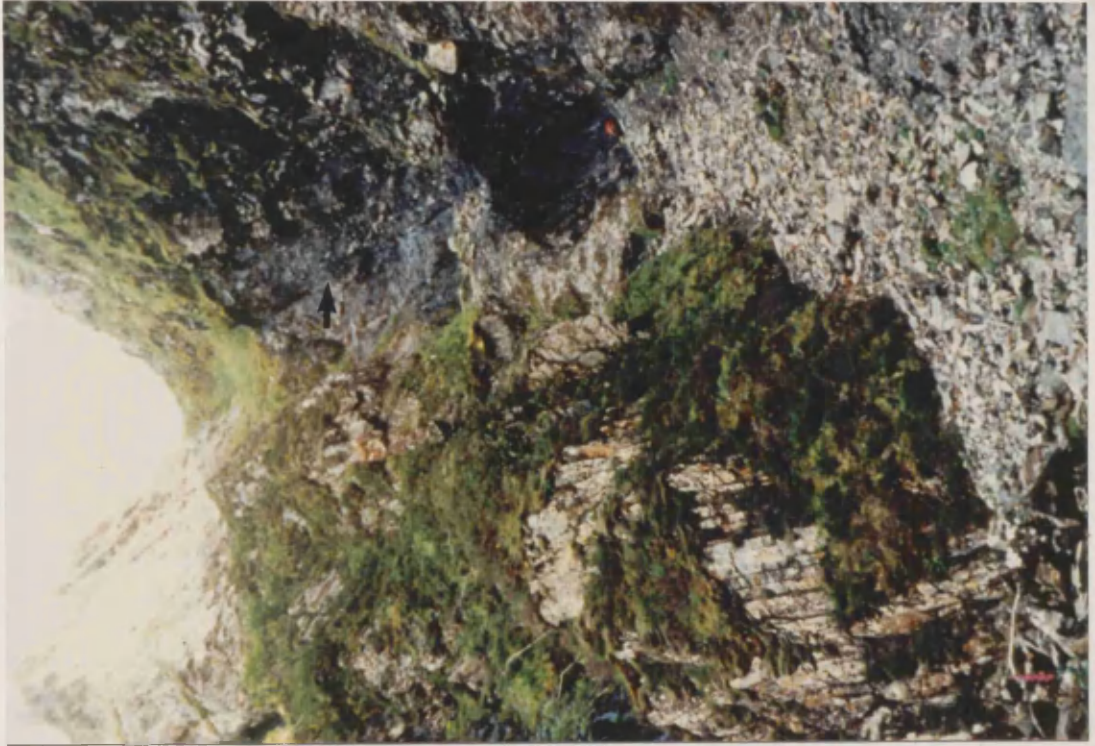


Figure 2.17a



Figure 2.17b

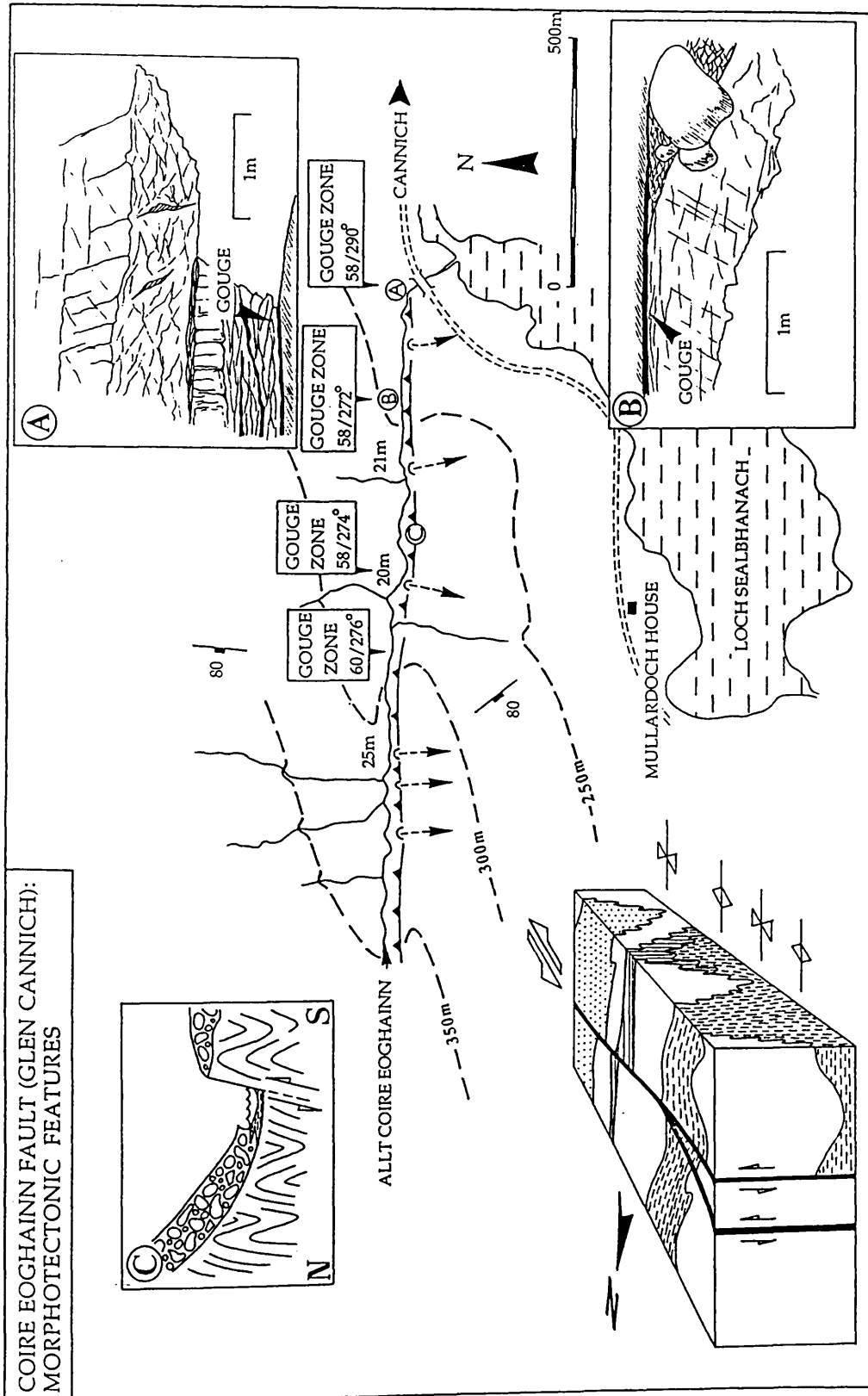


Figure 2.18



Figure 2.19a



Figure 2.19b



Figure 2.19c



Figure 2.20



Figure 2.21a

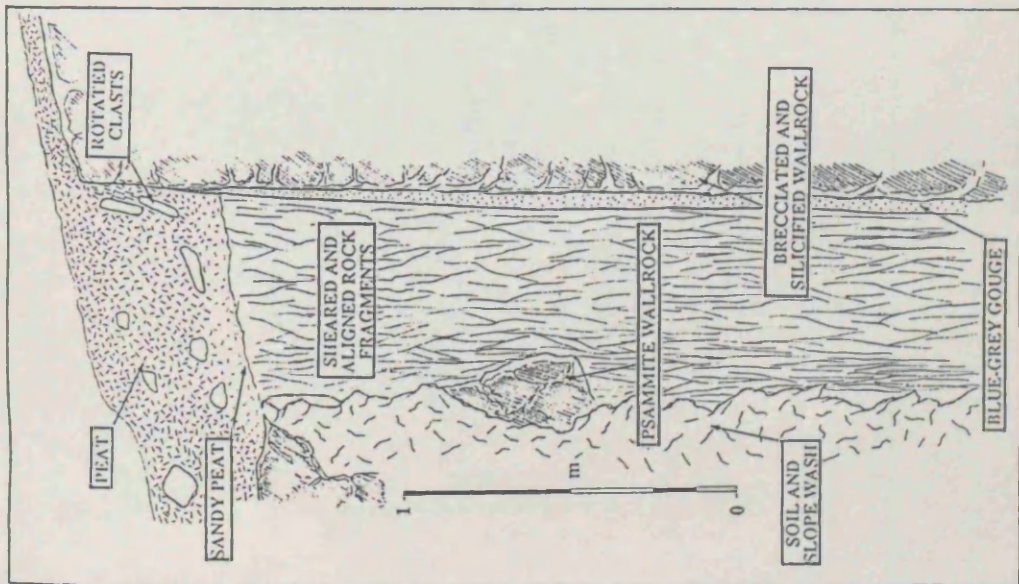


Figure 2.21b



Figure 2.22a

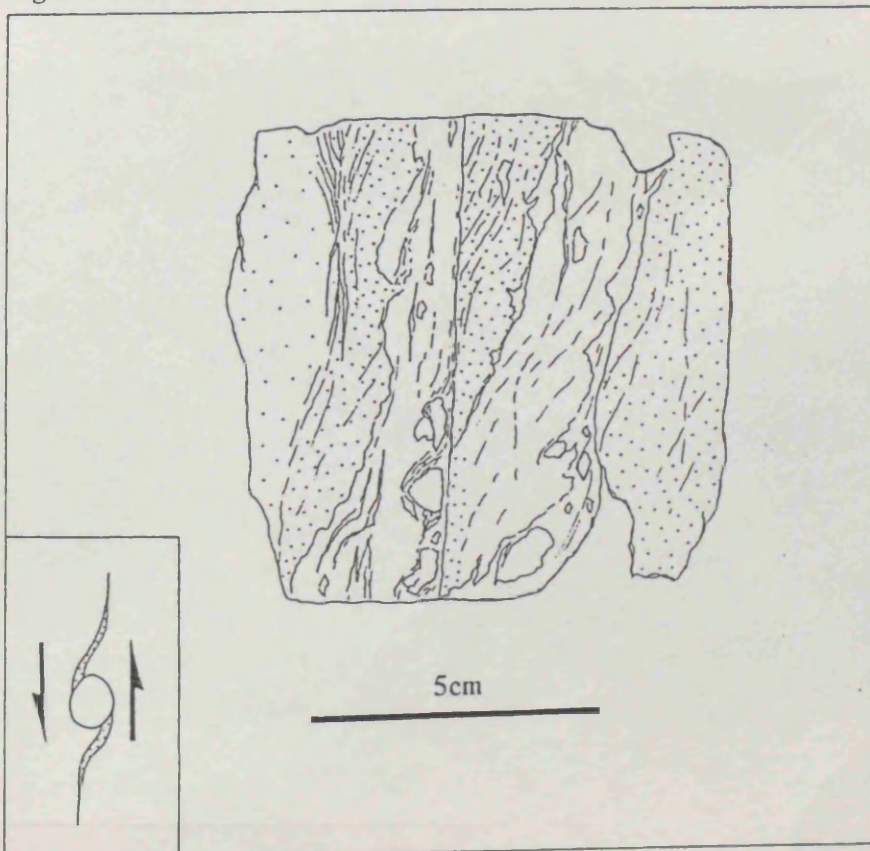


Figure 2.22b



Figure 2.23



Figure 2.24a



Figure 2.24b

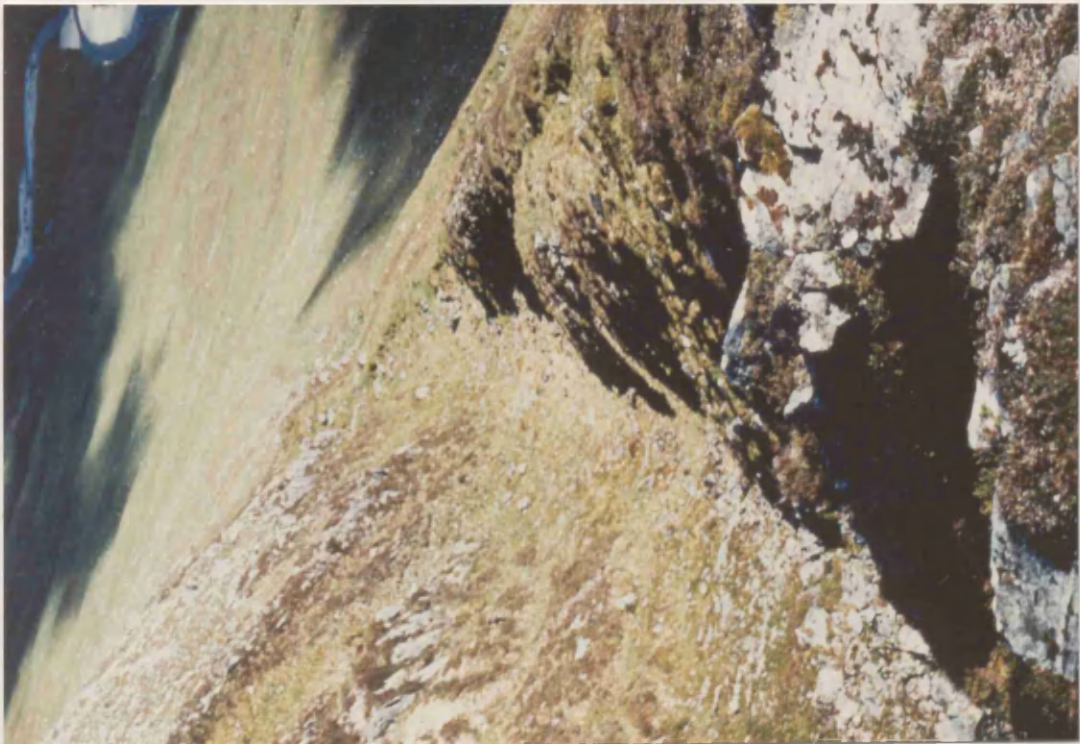


Figure 2.24c



Figure 2.25a



Figure 2.25b



Figure 2.27a



Figure 2.27b



Figure 2.28



Figure 2.29



Figure 2.30

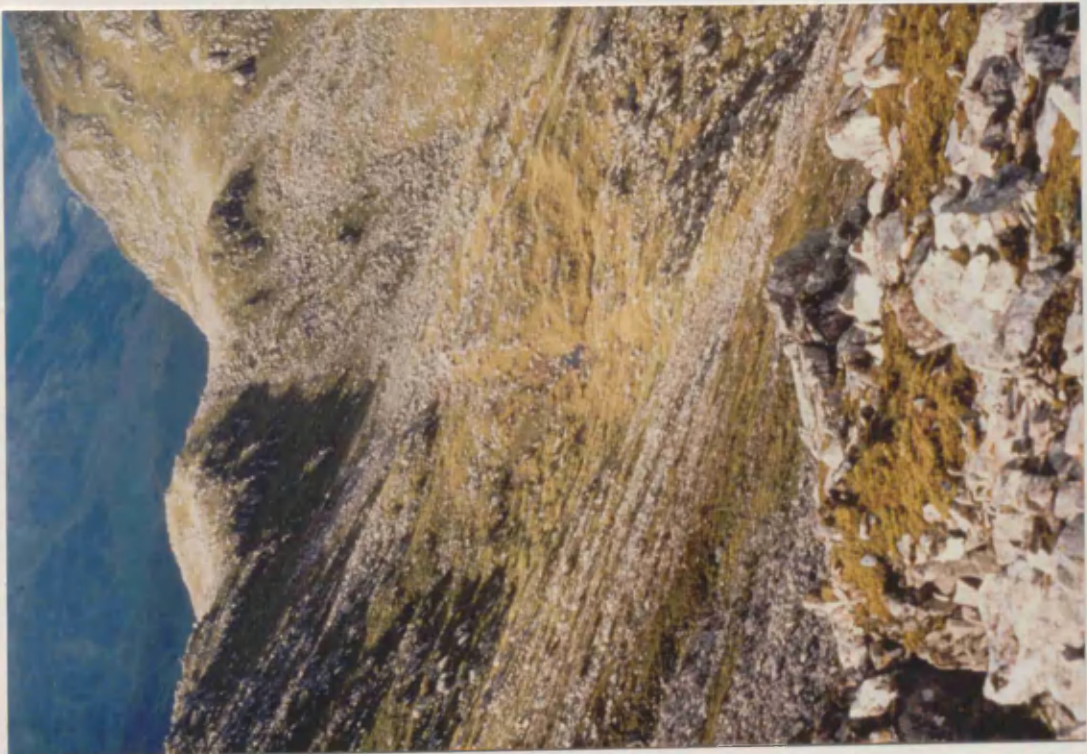


Figure 2.31a



Figure 2.31b

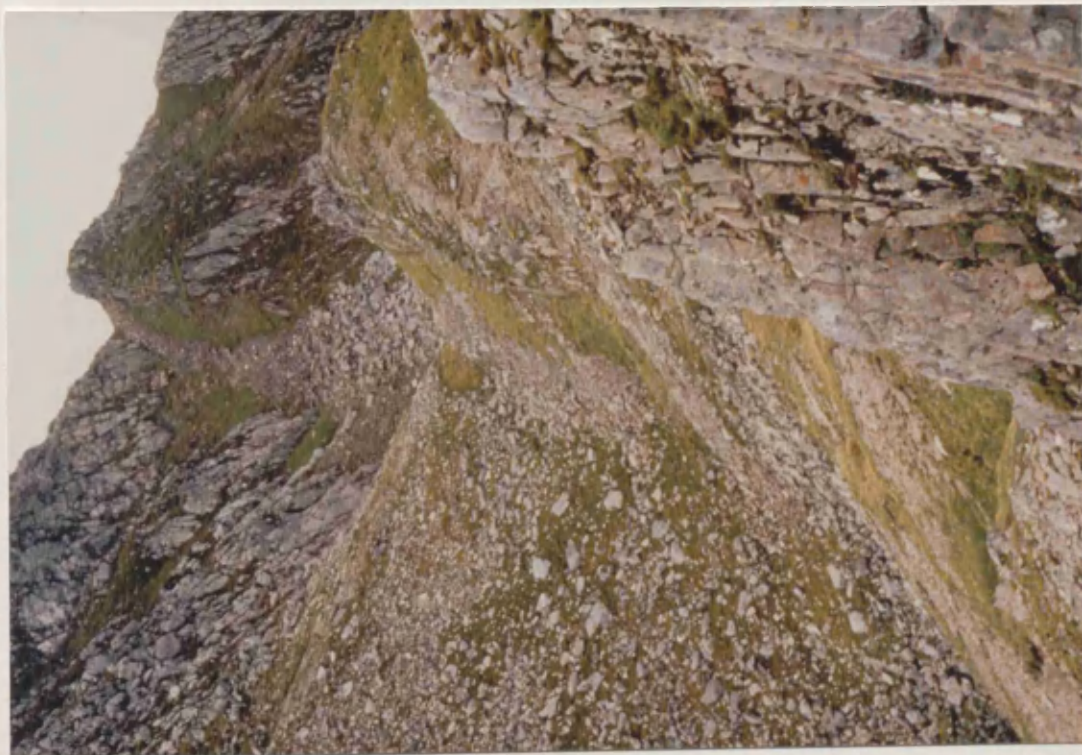


Figure 2.31c

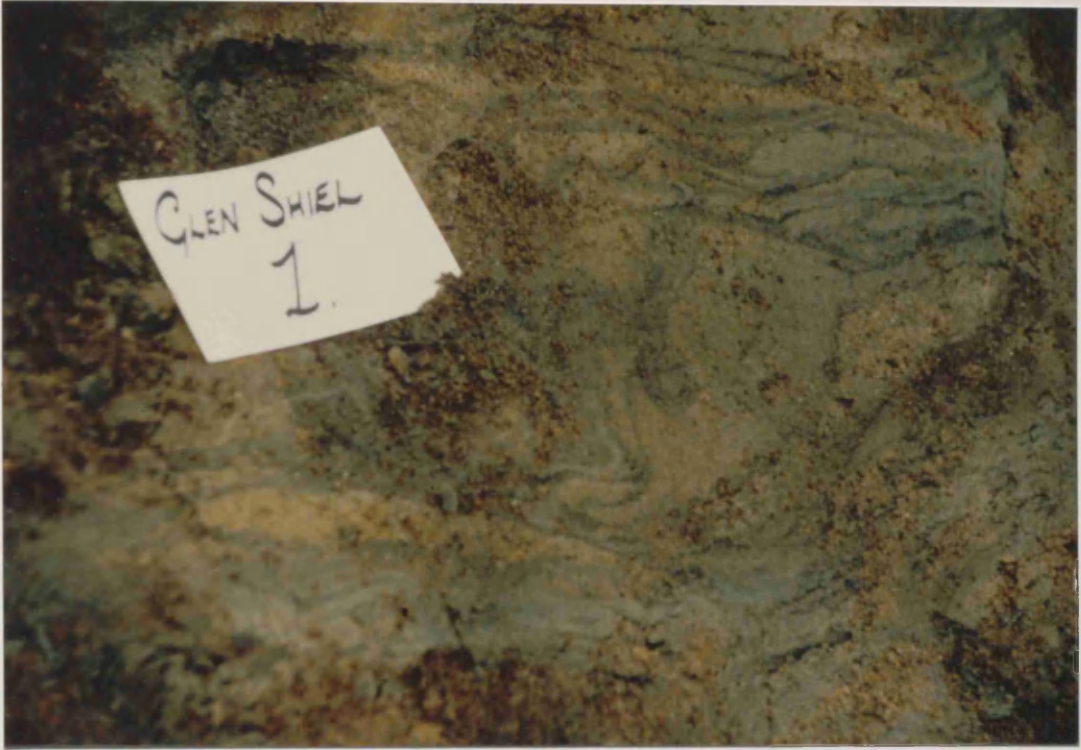


Figure 2.32a



Figure 2.32b

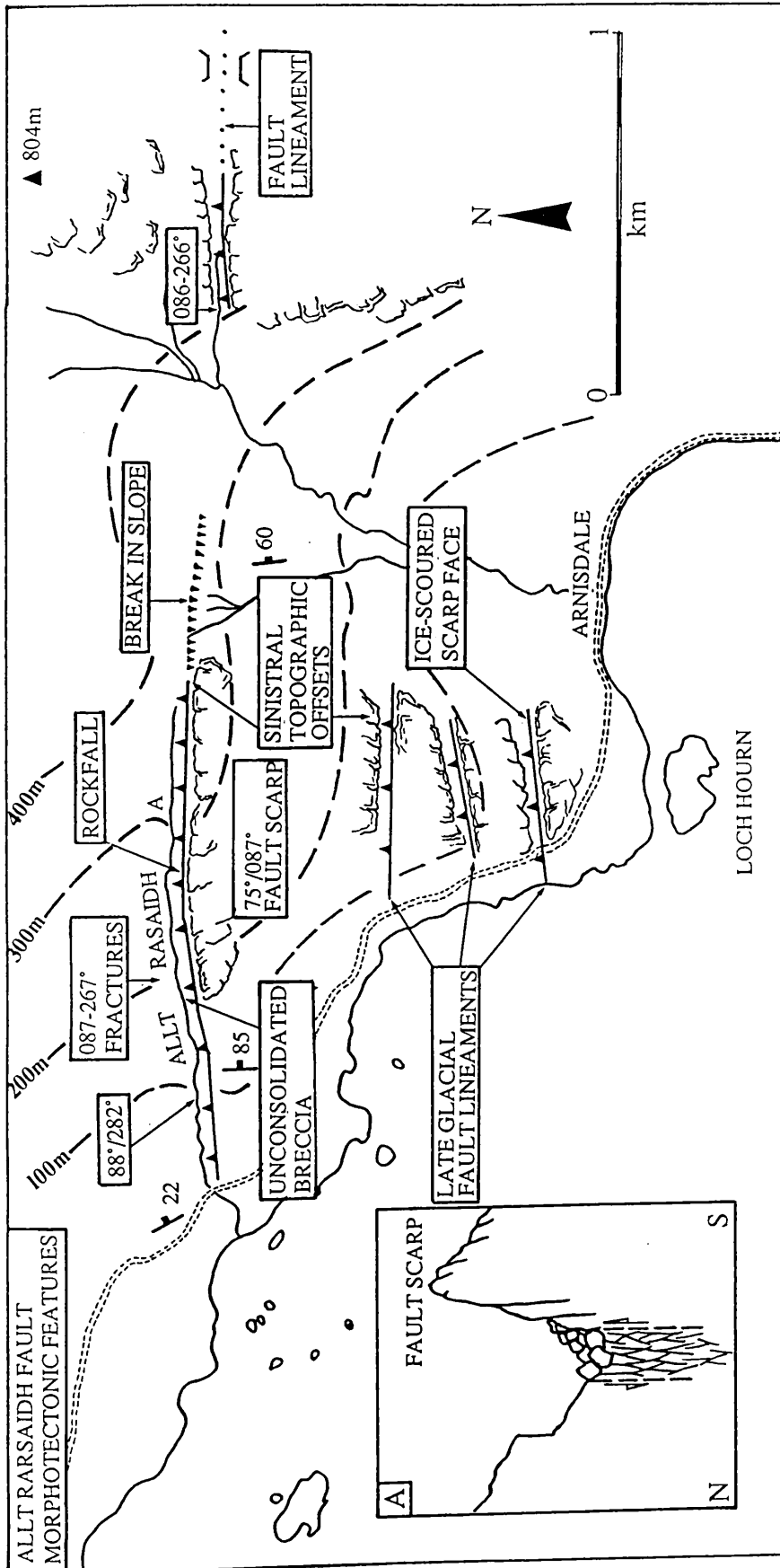


Figure 2.33



Figure 2.34a



Figure 2.34b

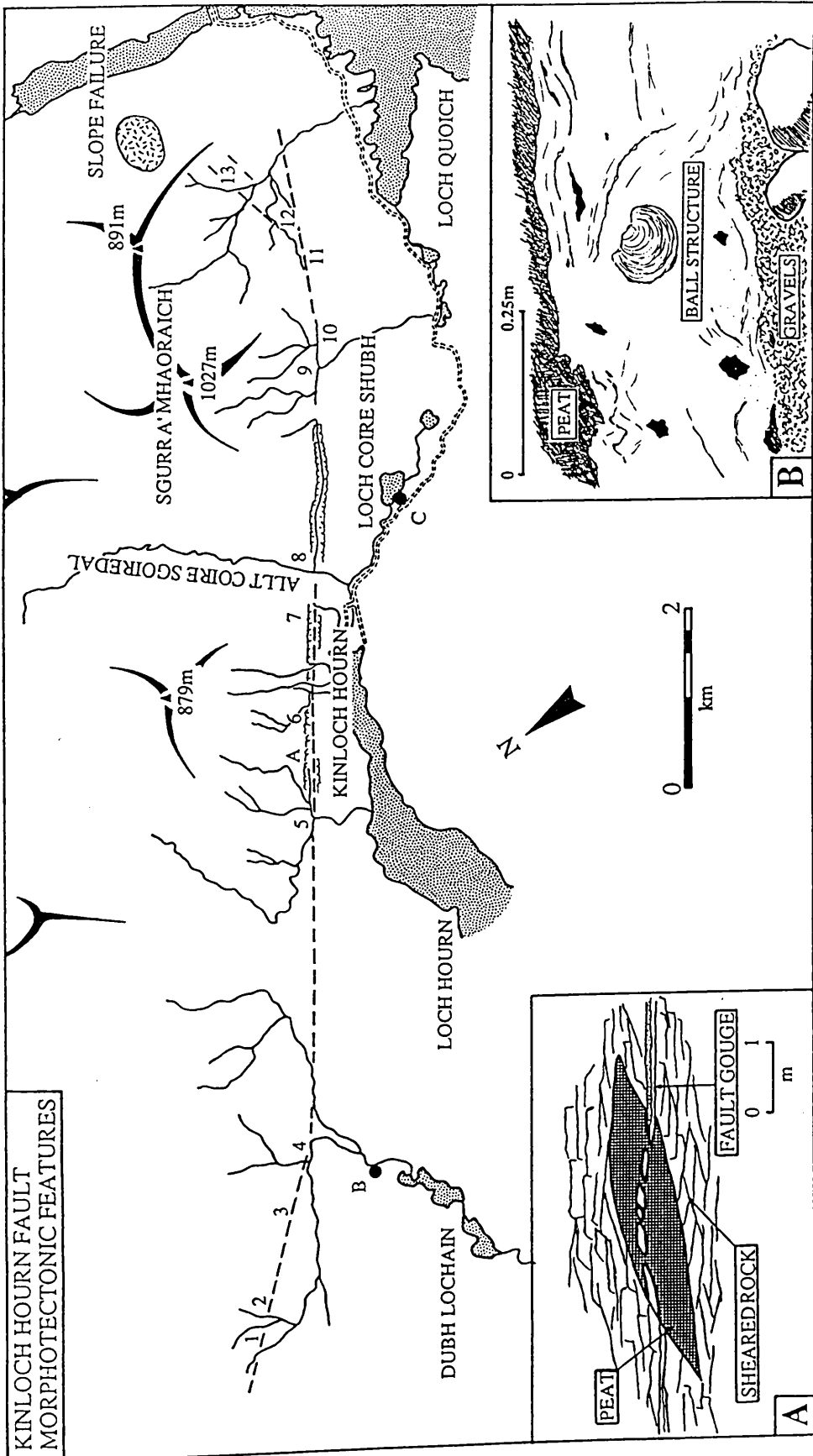
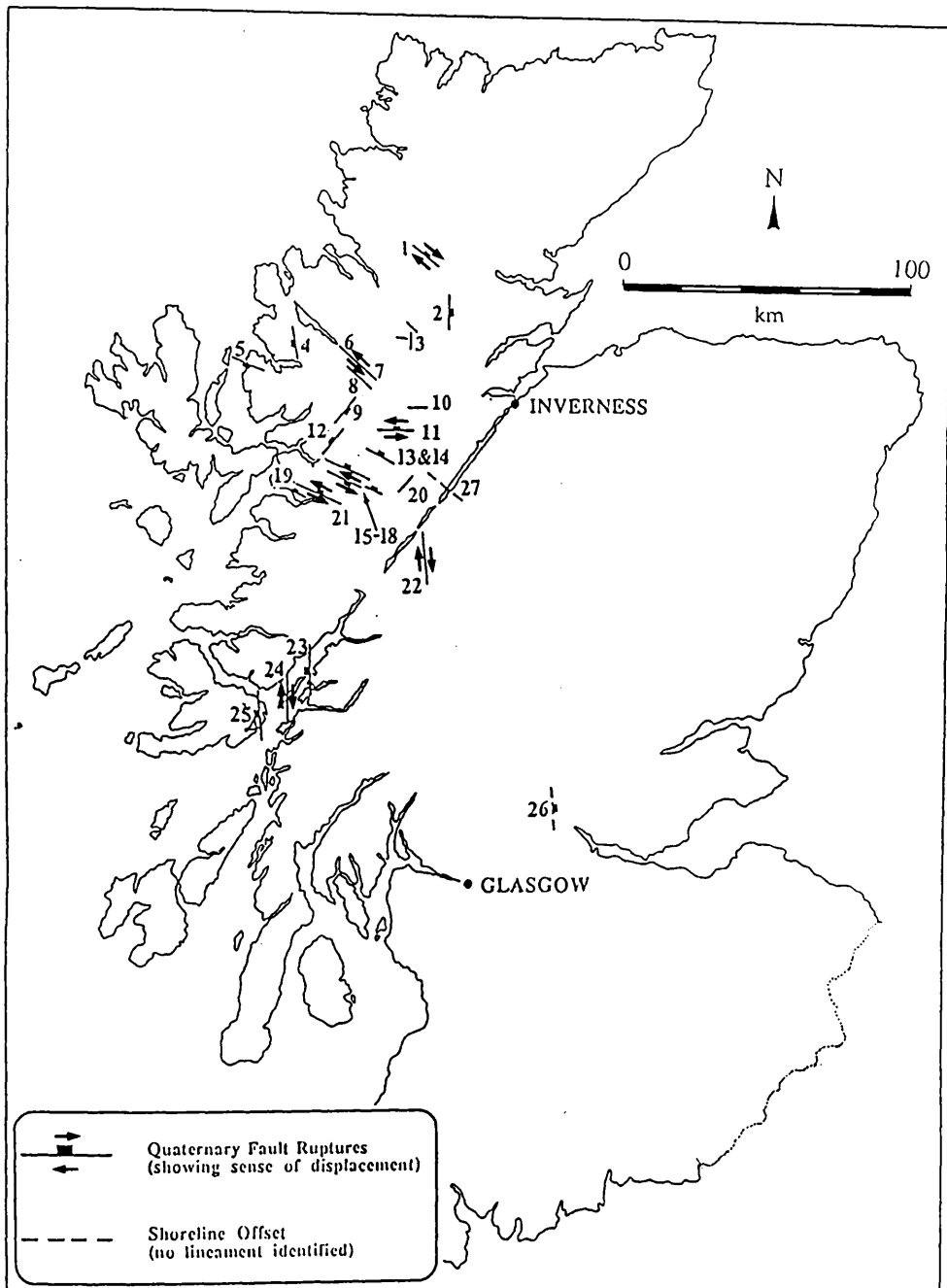


Figure 2.35



- | | | |
|--------------------------------|--------------------------------------|-------------------------------|
| 1. Coire Mor Fault | 10. Loch Monar Fault | 19. Arnisdale Faults |
| 2. Strath Vaich Fault | 11. Coire Eoghainn Fault | 20. Coire Dho Fault |
| 3. Garbh Choire Mor Faults | 12. Glen Elchaig (Strathconon Fault) | 21. Kinloch Houran Fault |
| 4. Beinn Alligin Fault | 13. An Sornach Fault | 22. Glen Gloy Fault |
| 5. Cuaig Fault | 14. Sgurr na Lapaich Fault | 23. Shuna Displacements |
| 6. Loch Crann (L. Marce Fault) | 15. Glcann Lichd Fault | 24. Lismore Displacements |
| 7. Scardroy (L. Marce Fault) | 16. Creag na Damh Fault | 25. Port Donain Displacements |
| 8. Bac an Eich Fault | 17. Sgurr a' Bhealaich Dheirg Fault | 26. Forth Valley Offsets |
| 9. Beinn Tharsuinn Fault | 18. Sgurr na Ciste Duibhe Fault | 27. Loch Ness Offsets |

Figure 2.36

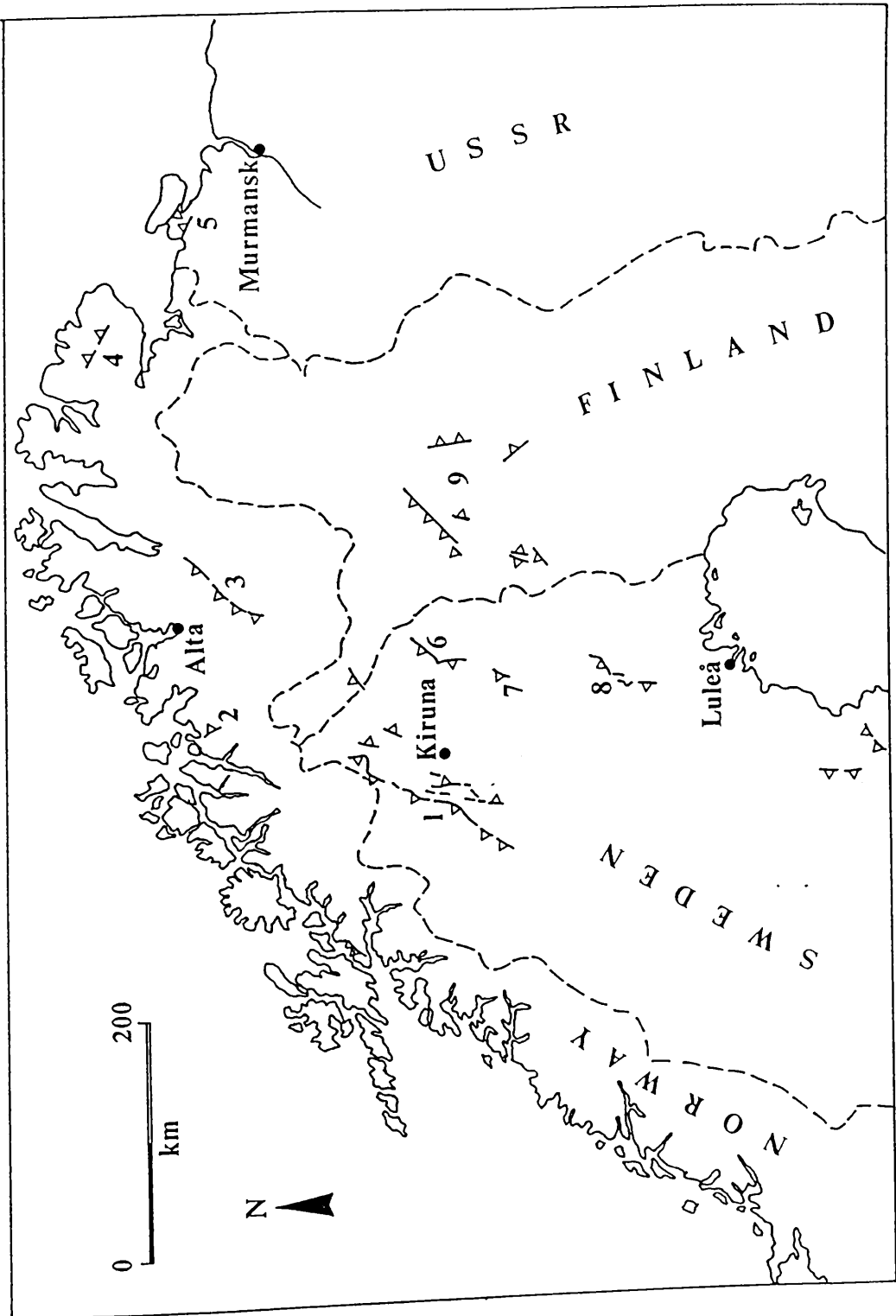


Figure 2.37

2.14

Table 2.1

Fault Location.	Orientation.	Approx. Age	Morphotectonic features.	Magnitude Estimates.(Refs.)
Coire Mor (1)	126 to 154°	10.3-6kyr BP.	3km "active" fault length.	6.0±0.4
			40±10m dextral offset.	5.5-6.6
			c.4m downthrow to N.	4.9
			Landslide area: 50km ² Max. distance to coherent slides: 7km. Max. distance to disrupted slides: 3.5km	5.4 4.6
Strath Vaich (2)	345 to 020°	10.3-6kyr BP.	6km "active" length.	6.4±0.4
			1.5±0.5m downthrow to E.	5.6-6.6
			Landslide area: 46km ²	4.9
			Max. distance to coherent slides: 3.5km. Max. distance to disrupted slides: 5km.	5.1 4.7
Garbh Choire Mor (3)	172-352° 283 to 299° 234 to 276°	10.3-6kyr BP.	Rock avalanche activity.	>6.0
Beinn Alligin (4)	156 to 159°	10.3-6kyr BP.	1.5km "active" length.	5.7±0.3
			Sinistral displacement with downthrow to W.	5.0-6.2
			Rock avalanche activity.	>6.0
			Landslide area:c.40km ² Max. distance to disrupted slides: 7km.	4.9 4.8

Table 2.1(cont.)

Cuaig (5)	112 to 125°	13-6kyr BP.	1.7m downthrow to S.	6.9-7.3	Bonilla <i>et al.</i> (1984)
Loch Crann (L.Maree Fault) (6)	130 to 160°	10.3-6kyr BP.	1.5km "active" length. Unknown vertical movement.	5.7±0.3 5.0-6.2	Khromovskikh (1989) Bonilla <i>et al.</i> (1984)
Scardroy (L.Maree Fault) (7)	120 to 140°	10.3-6kyr BP.	2km "active" length. c.1m sinistral displacement? 2km to liquefaction sites. Max. distance to coherent slides: 9km.	5.8±0.2 5.5-6.6 5.5 5.5	Khromovskikh (1989) Bonilla <i>et al.</i> (1984) Youd (1977) & Kurbayashi (1985) Keefer (1984a)
Bac an Eich (8)	140-320°	10.3-6kyr BP.	1km "active" length.	5.45±0.3 5.0-6.2	Khromovskikh (1989) Bonilla <i>et al.</i> (1984)
Beinn Tharsuinn (9)	019 to 024°	10.3-6kyr BP. post-6kyr BP.	c.1km "active" length. 0.5±0.1m vertical offset. Landslide area: 40km ² Max. distance to coherent slides: 5km. Max. distance to disrupted slides: 3km.	5.45±0.3 5.0-6.2 6.4-6.6 4.9 5.2 4.6	Khromovskikh (1989) Bonilla <i>et al.</i> (1984) " " Keefer (1984a) " " " "
Loch Monar (10)	273 to 280°	10.3-6kyr BP.	3km "active" length. Landslide area: 53km ² Max. distance to coherent slides: 8km Max. distance to disrupted slides: 7km	6.0±0.4 5.5-6.6 4.9 5.4 4.8	Khromovskikh (1989) Bonilla <i>et al.</i> (1984) Keefer (1984a) " " " "

Table 2.1(cont.)

Coire Eoghainn (11)	094 to 120°	10.3-6kyr BP.	3km "active" length.	6.0±0.4 5.5-6.6	Khromovskikh (1989) Bonilla <i>et al.</i> (1984)
			20-25m sinistral displacement. c.1-2m downthrow to N. Max. distance to coherent slides: 6km. Max. distance to disrupted slides: 8km.	5.4 4.9	Keefe (1984a) "
Glen Elchaig (12)	061 to 076°	10.3-6kyr BP.	7km "active" fault length.	6.5±0.4 5.7-6.7	Khromovskikh (1989) Bonilla <i>et al.</i> (1984)
An Sornach (13)	123 to 153°	10.3-6kyr BP.	1km "active" length.	5.45±0.3 5.0-6.2	Khromovskikh(1989) Bonilla <i>et al.</i> (1984)
			c.5m downthrow to N. Landslide area: 68km ²	5.0 5.3	Keefe (1984a) "
			Max. distance to coherent slides: 5km. Max. distance to disrupted slides: 7km.	4.8	"
Sgurr na Lapaich (14)	086-266°	10.3-6kyr BP.	1km "active" length.	5.45±0.3 5.0-6.2	Khromovskikh (1989) Bonilla <i>et al.</i> (1984)
			c.4m downthrow to the N. Landslide area: 68km ²	5.0 5.4	Keefe (1984a) "
			Max. distance to coherent slides: 8km. Max. distance to disrupted slides: 8km.	4.8	"

Table 2.1(cont.)

Gleann Lichd (15)	110 to 140°	10.3-6kyr BP.	5km "active" fault length.	6.3±0.4	Khromovskikh (1989)
			Approx. 2m downthrow to N. 1km to liquefaction site.	5.5-6.6	Bonilla <i>et al.</i> (1984)
			Landslide area: c.43km ² Max. distance to coherent slides: 2km. Max. distance to disrupted slides: 4km.	5.0-5.2	Youd (1977) & Kuribayashi (1985) Keefer (1984a) " "
Creag na Damh (16)	120-300°	10.3-6kyr BP.	2km "active" length.	5.8±0.2	Khromovskikh (1989)
			c.20m sinistral offset. Landslide area: 43km ² Max. distance to disrupted slide: 5km.	5.5-6.6	Bonilla <i>et al.</i> (1984) Keefer (1984a) "
				4.8 4.7	
Sgurr a' Bhealaich Dheirg (17)	124 to 135°	10.3-6kyr BP.	2km "active" length.	5.8±0.2	Khromovskikh (1989)
			Possible downthrow to N of c4m. Landslide area: 43km ² Max. distance to disrupted slides: 5km.	5.5-6.6	Bonilla <i>et al.</i> (1984) Keefer (1984a) "
				4.8 4.7	
Sgurr na Ciste Dhuibe (18)	115 to 140°	10.3-6kyr BP.	5km "active" length.	6.3±0.4	Khromovskikh (1989)
			Downthrow 4m to S. Sinistral displacement of c15m. 4km to liquefaction sites.	5.5-6.6	Bonilla <i>et al.</i> (1984) Youd (1977) & Kuribayashi (1985) Keefer (1984a) "
			Landslide area: 43km ² Max. distance to disrupted slides: 2km.	5.7-5.9	
				4.8 4.5	

Table 2.1(cont.)

Arnisdale (19)	085 to 117°	post 10.3kyr BP.	1.5km "active" length. 10±5m sinistral displacement. with c.4m downthrow to N.	5.7±0.3 5.0-6.2	Khromovskikh (1989) Bonilla <i>et al.</i> (1984)
	056-236°	post 10.3kyr BP.	1.1km "active" length. 5km to furthest liquefaction.	5.45±0.3 5.0-6.2 5.5-5.8	Khromovskikh (1989) Keefer (1984) Youd (1977) Kuribayashi (1985)
Kinloch Hourn (21)	115 to 140°	13-10kyr BP. post 2kyr BP.	14km "active" length. 160±40m sinistral displacement. 1.2km to liquefaction sites. 2km to coherent slide.	6.9±0.5 6.1-6.9 5.1-5.3 4.9	Khromovskikh (1989) Bonilla <i>et al.</i> (1984) Youd (1977) & Kuribayashi (1985) Keefer (1984a)
	155 to 165°	c.10.3kyr BP.	7km "active" length. 0.5m dextral displacement. 15km to furthest liquefaction. Landslide event areas: 21km ² 8km ² 39km ² Max. distance to coherent slides: 3km. Max. distance to disruptive slides: 3km.	6.5±0.4 5.7-6.7 5.7-6.9 6.3-6.5 4.6 4.3 4.8 5.1 4.6	Khromovskikh (1989) Bonilla <i>et al.</i> (1984) " Youd (1977) & Kuribayashi (1985) Keefer (1984a) " " " "
Glen Gloy (22)					

Table 2.1(cont.)

Shuna (23)	Approx. NNW	post 10.3kyr BP.	1.0m downthrow to W.	6.3-7.1	Bonilla <i>et al.</i> (1984)
Lismore (24)	020 to 030°	3-2kyr BP.	3km "active" length. 0.5m sinistral displacement.	6.0±0.4 5.2-6.5 5.7-6.9	Khromovskikh (1989) Bonilla <i>et al.</i> (1984) "
Mull (25)	350 to 355°	post 10.3kyr BP.	2km "active" length. 2.7±0.5m downthrow to W.	5.8±0.2 5.5-6.6	Khromovskikh (1989) Bonilla <i>et al.</i> (1984)
Forth Valley (26)	Approx. NNW	9.6-8.8kyr BP.	1.0m vertical displacement. 1.5m vertical displacement.	6.3-7.1 6.8-7.2	Bonilla <i>et al.</i> (1984) "

Chapter 3

Glacio-Isostatic Faulting and Associated Ground Deformation in the Area of Glen Roy and Glen Gloy, Scotland.

Clark Fenton

*Department of Geology and Applied Geology,
University of Glasgow, Glasgow, G12 8QQ*

3.1 Abstract

Detailed analysis of seismically-induced deformation features in the area of Glen Roy and Glen Gloy has shown that during and immediately following the disappearance of the Loch Lomond Readvance ice c. 10.3 kyr BP there were a number of large seismic events. Such seismic activity, up to $6.2 \pm 0.5 M_S$, in what is at present an area of very low seismic strain release, is attributed to the effects of differential isostatic recovery being accommodated along pre-existing faults. High porewater pressure, due to increased head as a result of both glacial lake impoundment and sub-glacial fluid recharge, is seen to be important in the generation of high crustal stress levels and also, to a degree, in controlling the timing and nature of the subsequent fault activity. A chronology of deformation events based on the lake levels has shown that the delicate interplay between glacial volume and the fluctuating lake levels gives rise to conditions of critical stress levels that are relieved by movement along favourably orientated faults.

3.2 Introduction

The Glen Roy - Glen Gloy area (Figure 3.1) has been the subject of a number of investigations concerning recent crustal movements and in this respect is probably the most studied area of Scotland (Sissons & Cornish 1982; Ringrose 1987, 1989; Ringrose *et al.* 1991).

Initial attention was drawn to the area after Sissons & Cornish (1982) reported vertical offsets of the c. 10.3 kyr. BP. shorelines of a former ice-dammed lake in Glen Roy (Figure 3.1). Detailed levelling showed that the shorelines were offset in a number of locations, with the most spectacular being a c. 3 m offset affecting the shorelines over a length of 2 km. This offset was considered to have occurred on a NE-trending 'fault' running up the hillside away from the point where the shorelines are dislocated. This was stated to have been a result of differential glacio-isostatic uplift and the resultant seismicity from the fault movement deemed responsible for the occurrence of large landslides in the immediate area.

Ringrose (1987, 1989) then provided further evidence for the (palaeo-) seismic activity associated with the crustal block movement. Mapping liquefied horizons within lacustrine sediments in Glens Roy and Gloy and the neighbouring Glen Spean (all were part of the same late-glacial lacustrine basin), Ringrose (1987, 1989) showed that the deformation was zoned in intensity in a concentric manner around a suspected fault rupture. The area of most intense sediment deformation was also coincident with a number of large slope failures (Figure 3.1). The concentric zonal nature of deformation intensity, and the confinement of such deformation to discrete horizons conforms to Sims (1975) criteria for earthquake-induced, soft-sediment deformation. The deformation structures observed are the same as those described as seismites (Seilacher 1984; Hempton & Dewey 1983; Scott & Price 1988).

As part of an on-going project investigating post-glacial crustal movements in Scotland (Fenton 1991 - initiated at the Department of Applied Geology, University of Strathclyde) the area of Glen Roy was again subject to rigorous investigation. Of primary importance was to obtain an accurate age for the seismic activity and fault movements identified by Ringrose (1987, 1989) in order to gain an insight into the likely mechanisms of glacio-isostatic reactivation of old basement faults. Initially a detailed investigation of the Glen Gloy fault was carried out to confirm the offset magnitudes reported by Ringrose (1987, 1989) and to collect fault gouge samples for age-dating. In addition to this the large number of slope failures in the area were

investigated to see if they could be attributed to seismic activity, and if so, used to construct a chronology of late-glacial tectonic movements in the area.

3.3 Glen Gloy Fault: Surface Expression and Morphotectonics.

The Glen Gloy fault is a NNW-trending basement fracture that cuts through Moine psammities in upper Glen Gloy. The SSE extension of this fault corresponds to the offset of the lake shorelines in Glen Roy. Details of the morphotectonic features (Doornkamp 1986) along the fault are shown on Figure 3.2.

The fault has a surface trace of c. 20 km, of which c. 7 km show an active expression. The fault zone itself is exposed along the Allt Neurlain [NN3092] in upper Glen Gloy, for a distance of over 1 km, as a series of gouge-filled fractures displacing bedrock morphology and drainage courses.

To the north the fault is obscured by an area of rotational slump slope failure (Figure 3.2, location 1). Following the fault trace south it is hidden by gravels along the River Gloy. The first exposures in the Allt Neurlain show a zone of sheared and brecciated Moine psammite cut by two 350°-trending fractures. These fractures offset a basic dyke of uncertain age by 39.0 ± 0.5 m in a sinistral manner (Figure 3.2, location 2). Further upstream displacements also occur along discrete, continuous fractures trending 340-350° that can be traced for more than 150 m. These fractures are generally open, 1-4 mm in width, sometimes containing a blue-grey fault gouge (Figure 3.2, locations 2,3 & 5). It was noted that these fractures offset the smoothed bedrock morphology along the stream bed by 0.30-0.45 m in a dextral sense (Figure 3.2, locations 3 & 5). The magnitude and sense of the dyke offset corresponds with the evidence from stream capture and dry water courses further upstream (Figure 3.2, location 4), and also the offset of a hillslope scarp (Figure 3.2, location 6) (Ringrose 1987, 1989).

Detail of the most recent zone of movement is shown in the inset of Figure 3.2 and in Figure 3.3a. Two N-S trending units of blue-grey fault gouge 20-25 mm in width are found in a zone of unconsolidated, sheared and fractured country rock (psammities and mica schists) which passes into a wider zone of silicified sheared country rock. Offset of rock surface morphology suggests 0.3-0.4 m dextral movement across the most recent fractures. XRD analysis of this fault gouge showed it to have the same mineralogical composition as the country rock (Figure 3.3b), showing it is a true fault gouge produced by mechanical grinding of the country rock

at the fracture faces, and not 'exotic' fracture infilling nor a product of hydrothermal alteration or weathering.

Both Ringrose (1987) and Sissons & Cornish (1982) have identified 'fault scarps' that have orientations that coincide with the point of shoreline dislocation in Glen Roy. Sissons & Cornish (1982) have identified a NNE-trending linear ridge (Figure 3.2, location 9) as being the fault rupture responsible for the offset of the shorelines. They argue that the morphology of the ridge suggests a reverse fault. However excavation across the ridge and examination of the fracture faces of the ridge clearly show that this is a tensional feature; fracture faces show concentric, plumose patterns and a trench fronting the ridge is an open fissure filled with frost-shattered debris (a thrust fault would be expected to have tight, slickensided fracture faces). This suggests that the ridge is due to down-slope movement. Indeed the orientation of the ridge (020-200°) is the same as cross joints and sidewall fractures in the area of slope failure.

Ringrose (1987) identified a NNW-trending, 2 m high, west-facing series of scarps as being the surface rupture of the fault displacing the shorelines (7, Fig.2). Examination of the scarp faces shows no slickensides and fracture patterns are those of plumose markings showing tensional failure. This scarp is a discontinuous feature that rapidly decreases in height northwards, away from the area of slope failure. It is also sub-parallel to a set of sidewall fractures in the area of slope failure. This scarp must also be rejected as a candidate for the surface expression of the fault responsible for the shoreline offset. It is proposed that although these are not true fault scarps, both are a result of fault movement (see below).

3.4 Recent Fault Movement and Ground Deformation

The most recent movement episodes along the Glen Gloy fault are manifested in a c. 40 m sinistral offset of drainage patterns and a c. 0.5 m dextral displacement of bedrock morphology (Ringrose 1987). It is assumed that the latter was the cause of the seismic activity resulting in the liquefaction of lacustrine sediments and slope failures in Glen Roy.

The drainage offsets occur on continuous 340° to 350° trending fractures. These fractures, usually two, sometimes three, in number, are continuous along the entire length of the fault exposure and cut across all other fracture orientations. These fractures are 'fresh' in appearance being non-cemented, open or containing a thin

infilling of soft fault gouge. These fractures are also noted to offset the smoothed bedrock morphology at several locations along the Allt Neurlain by c. 0.5 m in a dextral sense. Ringrose (1987) and Ringrose *et al.* (1991) claim that the fault can be followed from its exposure along the Allt Neurlain in Glen Gloy (Figure 3.2, location 6) across the hillside as a series of 'fault (?scarp) segments' to meet with the 'fault scarp' (Figure 3.2, location 7) identified in Glen Roy. There is no evidence to suggest that these are individual fault segments, especially in light of the evidence from late and post-glacial events in Fennoscandia (Talbot 1986; Bäckblom & Stanfors 1989) and more recent ground ruptures in Australia (Gordon & Lewis 1980) showing that surface fault rupture displays a complex, ragged pattern. In many cases the surface disturbances are not true fault scarps, but are due to block movements along pre-existing fractures. This can give rise to the paradox of tensional features in what may be essentially a zone of compressional or transpressional faulting (Figure 3.4). This is similar to the 'jostle up' features described by Talbot (1986). This effect of fault movement being accommodated near surface by dilational and rotational movement of fracture bounded blocks would be enhanced in the post glacial environment by the creation of surface-parallel rebound fractures created by unloading of the crust (Nichols 1980). This style of surface deformation would be expected to occur on a variety of scales. As the 'fault scarps' in the region of the shoreline offset in Glen Roy and also those scarps traversing the hillside between Glens Roy and Gloy do not show any evidence of being 'true' fault scarps, it is assumed that they are the result of dilational block movements accommodating near surface fault movement (Figure 3.4). This may also account for the large amount of movement (c. 3 m) shown by shoreline levelling in comparison to that displayed along the fault exposed along the Allt Neurlain (c. 0.5 m) i.e. fault movement may be amplified by such block displacements. This surface deformation would also account for the relatively wide zone of deformation marked by the scarps of Ringrose (1987, 1989) and Sissons & Cornish (1982) in comparison to the narrow fault zone exposed in the upper part of Glen Gloy.

If the scarps observed in Glen Roy are the result of dilational block movements and do not represent true fault movement as assumed this may have important implications on the interpretation of fault rupture history and the stress system acting at the time of fault rupture.

3.5 Age of faulting

It is clear that fault movement post-dates the formation of the shorelines. The levelling survey of Sissons & Cornish (1982) showed that gravel terraces formed shortly after drainage of the lake are unaffected by fault movement. Therefore fault movement must have occurred at some time between these two events. The formation of the lake shorelines is attributed to the growth stage of the Loch Lomond Readvance (LLR) ice (Peacock & Cornish 1989), with further modification occurring during lake level fall during the ice retreat stage of the LLR. Thus, fault movement must have occurred at some time between 11 and 10.3 kyr BP.

Sissons & Cornish (1982) stated that the fault movement was a consequence of glacio-isostatic recovery triggered by the drainage of the 260 m lake level, and therefore occurred at the beginning of the Holocene. This is at odds with the evidence from the deformation sequences in the lacustrine sediments detailed by Ringrose (1987) which shows the following sequence of events (Figure 3.5):

1. Deposition of lacustrine sediments
2. First Deformation Event: showing fault grading, ball and pillow and flame structures.
3. Unconformity
4. Further deposition of lacustrine sediment.
5. Unconformity.
6. Deposition of red sand and silt, locally with gravel and clay clasts.
7. Second Deformation Event: slumping.
8. Deposition of silt, sand and gravel.
9. Production of freeze-thaw structures: involutions and brittle faulting.

Of these Ringrose (1987) considered 1-4 to be related to the 260 m lake level and 6 and 7 to be related to the end of lake sedimentation, possibly post-dating it, and 8 with sub-aerial conditions following lake drainage. From this it is clear that the seismic event that caused liquefaction of the lacustrine sediments (2, above) occurred before the drainage of the 260 m lake in Glen Roy and the 355 m lake in Glen Gloy. The second deformation event is related to either a second seismic event or to lake drainage (Ringrose 1987, 1989). Since the first deformation event is almost unequivocally seismic in origin it seems more likely that the shoreline offset observed was associated with this event and not with the drainage of the lake. However the lacustrine basins of the Glen Roy area had an extremely fluctuating history during the period of the LLR

as shown by the numerous faint shorelines that can be seen along the flanks of the surrounding hillsides. This reflects the rapidly varying loads imposed on the crust not only by the fluctuating lake levels due to the complex interplay between water level and ice growth/decay, but also the varying pore pressures induced in the crust due to the rapidly changing head of water. These factors, in addition to a crust that had undergone compression without sufficient stress release (Johnston 1989) would lead to stress instabilities that fluctuating pore pressures would release, due to the 'jacking' open of fractures, resulting in periodic seismic events i.e. a form of hydroseismicity (Costatin *et al.* 1987). Thus the area of Glen Roy may have experienced more seismic activity than has been recorded in the lake sediments. As a consequence of this, it may be impossible to correlate deformation in the sediments with offset observed in the shorelines. However a programme of age-dating was embarked upon to tie down the timing of seismic activity and the age of faulting.

3.6 Slope Failures

A large number of slope failures occur in the area of the palaeo-epicentre in Glen Roy and Glen Gloy (Figure 3.1). It is suspected that these slope failures are also the result of seismic activity. Using a modified form of limit equilibrium and Newmark analyses [§ 3.16, p147] it is seen that these slopes would have been stable under conditions of gravitational loading alone (Hoek & Bray 1981; Wilson & Keefer 1985; Jibson 1987). Thus, it is invoked that seismic activity, acting in conjunction with elevated pore pressure levels, would have acted to destabilise the slopes causing the degree of slope failure seen at present.

Such retrospective analysis of such slope failures is rather unsatisfactory in the light of the number of unknown parameters e.g. porewater pressures, water table, intensity and duration of seismic shaking. Traditional limit equilibrium analysis fails to take into account dynamic loads such as seismic shaking (Hoek & Bray 1981). In addition, analysis of slopes under conditions of seismic loading (e.g. Hencher 1980; Crawford & Curran 1982; Ghosh & Haupt 1989) is usually predictive and site specific, using simplistic models of slope failure geometry and 'design' earthquakes. Using the inverse of such approaches for suspected seismic slope failures is not always ideal, as these methods usually fail to consider the effects of 'real' geology in causing amplification of seismic shaking (Jibson 1987) and also the effects of cyclic pore pressure in fractured and jointed rock masses. In addition the complexities of fracture geometries can lead to major complications in the mode of failure, thus the resultant failures do not fall into the standard geotechnical categorisation schemes, and

as such do not fit with the 'ideal' models of slope failure under seismic loading. A more fruitful approach is the comparison of the type of slope failures and the distribution of such failures with those noted from recorded (historical or instrumental) seismic activity (Keefer 1984).

Although slope failures occur under almost any geological conditions, there are certain types of failure and slope failure morphological features that are almost entirely attributed to the effects of seismic ground shaking (Eisbacher 1979; Keefer 1984). In addition the distribution of slope failures caused by seismic activity, like other seismically-induced deformation features, can be seen to be zoned concentrically around the epicentral zone (Keefer 1984). Thus in the analysis of suspected palaeoseismic slope failures it is more important to consider the failure type and the failure distribution rather than the geometry of rock slope stability.

The slope failures in the area of Glen Roy and Glen Gloy (Table 3.1) are seen to be proximal to or within the zone of maximum deformation as defined by the intensity of seismite liquefaction (Figure 3.1). In most cases the failures are deep-seated and show a combination of sliding and toppling failure. The bedrock is composed of moderate to steeply dipping schists and psammities with a regional strike to the NE or NNE. With the exception of the Glenfintaig failure (15, Figure 3.1 & Figure 3.6) there are no catastrophic failures. All show a finite degree of downslope movement, as predicted by Newmark (1965) for slopes under the influence of cyclic dynamic loads. The failure above Glenfintaig (Figure 3.6) is a catastrophic sliding failure with an area of c. 0.2 km² and up to 70 m in depth. Failure has occurred using slope parallel schistosity as basal sliding planes and sub-vertical backing and sidewall release joints. Some blocks have remained intact but the majority have been subject to extreme disaggregation. In the area of the toe of the failed mass there is abundant brittle folding and thrusting of planar blocks. This slide morphology is similar to that described by Eisbacher (1979) and Pavlides & Tranos (1991) from known seismically-induced slope failures. The remainder of the slope failures are dominantly sliding and slump failures with limited amounts of downslope displacement. These types of failure are geologically cosmopolitan and cannot be used as unequivocal evidence for a seismic trigger for their initiation. However when considered with the seismite deformation and the relative ages of the slope failure episodes with respect to the lake shorelines, a chronology of deformation can be constructed. In addition using the criteria developed by Keefer (1984) and Wilson & Keefer (1984) estimates of magnitude, ground acceleration and shaking intensity can be made.

3.7 Deformation Chronology

All landslides in the Glen Roy-Glen Gloy area are within or immediately peripheral to the area of greatest liquefaction (Figure 3.1). Sissons & Cornish (1982) stated that the landslides were a consequence of the seismic activity that occurred when the shorelines were offset by fault movement. However careful examination of the slope failures in the area shows that they display a range of age with respect to the lake shorelines (Table 3.1), thus not all the failures occurred during one seismic event. In fact a chronology of slope failures can be constructed to show that there were at least three episodes of slope failure (Figure 3.8). One population of failures pre-dates the 350 m shoreline, a smaller group post-dates the 350 m shoreline but pre-dates the 325 m shoreline. The final group post-dates all of the shorelines. Each group affects an area of 21 km², 8 km² and 39 km² respectively. Ringrose (1987) states that slope failure affected an area of 80 km². From the above arguments this is clearly in error. However, estimates for the area affected by slope failures must be considered to be minimum estimates due to the difficulty in recognising seismically-induced slope failures and also the difficulty in defining an accurate chronology of slope failure activity outside the immediate lacustrine basin where there are no shorelines to act as time markers. Thus no attempt has been made to link slope failures from outwith the immediate area of Glen Roy and Glen Gloy with the detailed chronology of slope failure that has been defined for the immediate epicentral area.

3.8 Magnitude Estimates

The magnitude of palaeoseismic events can be calculated from the relationships determined between the distribution of deformation features and earthquake magnitude for recorded seismic events. In such a manner the areal extent of liquefaction and slope failures, fault rupture length and offset can be used to give an estimate of palaeomagnitude (Kuribayashi & Tatsuoka 1975; Youd 1977; Bonilla *et al.* 1984; Keefer 1984; Kuribayashi 1985 *in* Ambraseys 1988; Khromovskikh 1989).

From the chronology of slope failures it is seen that there were possibly three seismic events. This remains speculative, but not altogether unlikely (see below). Assuming that each slope failure population is the result of seismic activity and using the data of Keefer (1984), the areas affected by slope failure can be used to estimate the magnitude of the seismic events responsible (Table 3.2). The magnitudes obtained, 4.6, 4.3 and 4.8, for the areas affected by slope failures are less than the threshold magnitudes generally accepted for causing the differing types of slope

failure (Keefer 1984). Indeed rock slumps and rock block slides, the predominant form of failure in the area, have threshold magnitudes of 5.0 (Keefer 1984). This discrepancy can be explained by the arbitrary extrapolation of the data set of Keefer (1984) for events $<5.2M$ in the relationship between magnitude and area affected by slope failure activity. However the number of slope failures in the immediate area agrees with the evidence that "earthquakes of $M < 5.5$ cause a few tens of landslides" (Keefer 1984). Establishing palaeomagnitude from the areal extent of slope failures must be treated with caution. Some types of failure, namely rockfalls and soil slumps and slides, are difficult to distinguish as being the result of seismic shaking. Also, as they are seen to occur over a much larger area than other more diagnostic seismic failures, many may not have been recognised in conjunction with the Glen Roy seismic events due to their almost ubiquitous presence under almost all geological conditions and the lack of a tightly constrained chronology outwith the immediate area of the former glacio-lacustrine basin. Due to these uncertainties it has not been possible to determine if slope failures outwith the immediate area of Glen Roy - Glen Gloy are related to any of the three episodes of slope failure identified. Thus the magnitude estimates for the areal extent of slope failures must be considered as minimum estimates.

The Modified Mercalli Intensity (MMI) scale uses slope failure criteria to define intensities greater than MMI VII. However it is seen that slope failures are generally triggered by seismic activity at least one intensity level less than that predicted by the MMI scale. Disrupted slides and falls occur at MMI as low as IV (usual threshold is seen to be VI) while coherent slides can occur at MMI V (usual threshold is VII). In addition modified Newmark analysis shows that coherent slides are triggered at critical acceleration levels (I_a) of 0.5 ms^{-1} while disrupted slides are triggered at $I_a = 0.15 \text{ ms}^{-1}$ and lateral spreads or liquefaction occurs at $I_a = 0.5 \text{ ms}^{-1}$ (Wilson & Keefer 1985; Jibson 1987). Critical acceleration needed to initiate failure at the maximal distances from the epicentral area is seen to be 0.05 g (Wilson & Keefer 1985).

Thus using the slope failures observed in the area of Glen Roy and Glen Gloy it is seen that the area must have been subject to seismic activity of $>5.0M$ with epicentral intensities of $>MMI V$, where the ground acceleration was at least 0.05 g (Peak acceleration values would probably have been an order of magnitude greater).

The area affected by liquefaction is primarily controlled by the distribution of potentially liquefiable (lacustrine) sediments. Hence again the magnitude estimates of

6.3-6.5 M_S must be considered to represent, at best, a minimum estimate of the seismic activity responsible.

The extent of the surface rupture in Glen Gloy and the amount of fault offset gives magnitude estimates of the order of 5.7-6.5 M_S . Using the length of the exposed fault rupture gives estimates of 5.0-6.2 M_S [§ 2.14, p110].

It can be seen that there is a wide spread of magnitude estimates, from 4.3 to 6.9, for the palaeoseismic activity in the area of Glen Roy. This represent two orders of magnitude difference with respect to seismic strain release. As stated above these values can only be used as first order estimates of the seismic activity. The uncertainties in the calculations using slope failures and liquefaction have already been outlined. The magnitude calculated from the active fault length and surface rupture must also be treated with care due to the difficulty in determining whether the observed dimensions are the result of a single event or have been due to a number of events. In conclusion it can be said is that there is evidence that the area has been subject to elevated levels of seismicity, with events as large as $6.2 \pm 0.5 M_S$. To determine the timing of the release of such seismic strain energy it is necessary to consider the build-up of stress in the late glacial environment. In addition, with the knowledge of the chronology of deformation events, it may be possible to relate seismic events to the fault offsets observed.

3.9 Rebound Tectonics

Post glacial faulting has been described from a number of localities in Canada and Fennoscandia (Adams 1989; Muir Wood 1989b; Grant 1990; Lagerbäck 1990). As with the faults described from Scotland (Ringrose 1987) [§ 2, p15 *et seq.*] all are in areas of presently low seismic strain release with no evidence of present day ground rupture. Fault movement is usually reverse or transcurrent, accommodated along pre-existing lines of crustal weakness. It has been shown that the high levels of stress required to trigger such seismogenic fault activity are the result of loading of the crust by large volumes of ice that act to prevent the release of tectonic stress and induce substantial loading stresses and elevate pore fluid pressures (Johnston 1987, 1989; Adams 1989; Muir Wood 1989b) [§ 6, p260 *et seq.*]. The stresses created during the Late Devensian glaciation in Scotland have been discussed in detail elsewhere [§ 6, p260 *et seq.*]. However in the area of Glen Roy and Glen Gloy there is the added complication of the effect of fluctuating lake levels and the resultant

changes in pore fluid pressure to consider. This is now discussed in more detail in an attempt to decipher the sequence of deformation events observed in the area.

The initial state of stress in the crust was one of a compressive regime with S_H orientated WNW to NW, the regional stress regime active since the late Miocene (Davenport *et al.* 1989; Muir Wood 1989a, 1990). For shallow crustal levels at least, σ_3 would have been vertical (A, Figure 3.9). This would create a situation of reverse faulting. During the late Devensian almost the whole of Scotland was subject to complete ice cover for the period 26-13 kyr BP. This imposed a vertical load of c. 180 bar (for a maximum ice thickness of 2 km) and would induce a corresponding increase in the value of S_V causing a switch in the principal stresses such that S_V becomes σ_2 , if not even σ_1 (B, Figure 3.9). As the pore fluid pressure equilibrated with respect to the increased head (recharge would have been driven by the full weight of the ice cover) this would be reduced to σ_3 . However upon deglaciation c. 13 kyr BP (C, Figure 3.9) the reduction in the ice load would have left the crust in a state of critical fluid overpressuring. Such high fluid pressure, accompanied by the effects of isostatic rebound, would have given rise to fault movement to accommodate differential uplift. Such fault movement would be expected to be associated with enhanced levels of seismicity. This could have been the trigger for the slope failures that pre-date the formation of the 350 m shorelines. Seismic activity would persist until the cumulative stress drop was sufficient to return the crust to stability or until the crust was again subject to the effects of ice loading during the Loch Lomond Stadial (D, Figure 3.9). This would cause redepression of the crust and the suppression of seismic strain release (Johnston 1987, 1989). As well as the effects of ice loading, the area of Glen Roy and Glen Gloy was subject to loading by the glacial lakes impounded behind the mass of ice that occupied Glen Spean at this time (Peacock & Cornish 1989). This would again increase the level of pore fluid pressure causing a reduction in the effective crustal stresses. During this period the loading stresses would not have been as great as during the Main Late Devensian glaciation, however they would be sufficient to prevent the release of seismic strain [§ 6, p260 *et seq.*]. As the ice grew and receded during the Loch Lomond Stadial, so the level of the ice dammed lakes rose and fell, as shown by the number of shorelines preserved along the hillsides of Glen Roy and particularly Glen Gloy. Such fluctuating lake levels (E, Figure 3.9) have been shown to be sufficient to cause seismicity in crust that is stressed closed to the point of failure (Costain *et al.* 1987). Even changes in the head as little as 0.1 m (1 bar) can be sufficient to trigger seismicity and small changes in the lake levels, of which there were many, would have been capable of causing seismicity. The sudden drops in lake level between the main shoreline levels would

have given rise to bursts of quite violent seismic activity. The population of slope failures that occurred between the formation of the 350 m and the 325 m shorelines could be the result of hydroseismicity, where crustal fluid overpressuring, due to the fall in lake levels, would promote failure on neighbouring faults. It is possible that each decrease in the lake levels, due to ice wastage in the dying stages of the Stadial, could have triggered seismic activity. The density difference between ice and water is thought to be insufficient to have caused differential loading. The final catastrophic drainage of the lake would have been the trigger for a sudden rapid burst of seismicity. This would have been the trigger for the slope failures that post-date all shorelines. Seismic activity would persist in the post glacial period for as long as the elevated levels of stress persisted, i.e. until the seismic stress drop returned the crust to the field of stability (F, Figure 3.9). Only further tectonic strain accumulation would cause further failure. As the tectonic strain rate in intraplate regions is very low (Anderson 1986) the present day seismic activity is exceedingly low in comparison with that experienced during and immediately after the last period of deglaciation.

The above discussion provides one plausible explanation for the slope failure activity observed in the area. However the problem of when the sediment deformation occurred still exists. The first deformation event is almost unequivocally seismic in origin, while the second event may be related to the effects of sudden drainage of the lake basin, although the area affected by the second sediment deformation event is almost coincident with the area of greatest deformation in the first event and is not universally present throughout the whole lake basin as would be expected if it had been due to the sudden drainage of the lake basin (Ringrose 1987, 1989). This also seems to suggest that the second deformation event may also be seismic in origin, although this is by no means unequivocal. Ringrose (1987) believed that the first deformation event was related to the 260 m lake level. However Peacock (in Peacock & Cornish 1989) doubted the correlation of this deformation event with the observed offset of the shorelines on the basis that sedimentation continued for some time after the first deformation event, therefore this could not be related to the shoreline offset which obviously occurred sometime after the drainage of the lake basin. On this evidence it was stated that it was more likely that the second (slumping) deformation event was correlated with the offset of the shorelines. The top of the first deformation event is marked by an unconformity (3, Figure 3.5). This may mark a major change in the level of the lake, possibly from 350 m to 325 m, therefore it is possible that this deformation event may have been the result of hydroseismic activity. The fact that there is a further unconformity after the renewed period of lake sedimentation above the first deformation event may represent the second major drop in the lake level from

325 m to 260 m. This would also be a time of hydroseismic activity, as shown by the slope failures triggered at this time. However the lack of seismic liquefaction does not necessarily refute this hypothesis; it may be the case that the sediments did not have enough water content to become liquefied by the seismic shaking or that the seismic activity was not great enough ($M < 5.0$) to cause liquefaction. From the sedimentological evidence (Figure 3.5) it is clear that the second deformation event was related to the drainage of the lake basin, and it does seem more likely, as Peacock (in Peacock & Cornish 1989) suggests, that this event is related to the offset of the shorelines. Thus the first sediment deformation event must have occurred some time prior to lake drainage, possibly as the result of hydroseismic activity, while the second deformation event is seen to be related to the rapid final drainage of the lake basin and is possibly the result of isostatic rebound induced seismicity.

As with other Scottish and Fennoscandian post-glacial faults, the most recent movement along the Glen Gloy fault would probably have been a single event (Muir Wood 1989b; Lagerbäck 1990) [§ 2, p15]. The earlier c. 40 m sinistral offset of drainage features noted along the Allt Neurlain (Figure 3.2) must have occurred prior to the Loch Lomond Stadial, as this would have been the result of several movement episodes. This movement is consistent with the NW-orientated neotectonic stress field acting on a NNW-trending fault (Ringrose *et al.* 1991). However the most recent 0.5 m dextral movement along the fault exposed along the Allt Neurlain obviously represents a different stress system. Ringrose *et al.* (1991) state that this movement may have been the result of a rotation of the stress field through c. 70°, to a NE-SW direction, due to the presence of a mass of ice to the west in the region of the Great Glen. As previously stated it is not thought that the density difference between ice and the water occupying Glens Roy and Gloy would have been sufficient to have caused any substantial effects on the local stress system. This change in the stress system could be attributed to the effects of high fluid pressures acting at seismogenic depths acting to cause swapping of the principal stresses. It is noted that aftershock sequences in 'wet' faults can give focal plane mechanisms that suggest an entirely different stress regime to that of the main shock event (M.D. Zoback, pers. comm. 1991). This could be the case in the area of Glen Roy where previous sinistral movement along the fault allowing stress release could have caused swapping of the principal stresses or the degree of fluid overpressuring was so great that it caused a complete change in the local stress system from the regional NW-orientated compressive stress field to one where σ_1 was orientated NE-SW. Whatever the reason it is obvious that there was a marked change in the stress system in the period immediately following deglaciation of the area. The fault movement represented by the

offset of the shorelines is tentatively correlated with the 0.5 m dextral offset along the Allt Neurlain in Glen Gloy. The apparently differing styles of fault movement i.e. reverse and strike slip movement respectively is explained by the ground deformation expected from a 'blind' fault (Figure 3.4). This fault movement is clearly post-shoreline formation. This means that this fault movement would have occurred sometime between the 260 m shoreline and the formation of the gravel terraces formed shortly after the drainage of the lake. From this evidence it seems that this most marked episode of fault movement was the result of differential isostatic uplift caused by the unloading of the crust due to the rapid drainage of the lake basin and decay of Loch Lomond Stadial ice. This is also seen to be the period of most intense tectonic activity in other areas undergoing deglaciation (Mörner 1981). This would be a much greater degree of unloading than those experienced during the successive drops in the lake levels throughout the Stadial. This and the exceedingly sudden nature of the unloading - the drainage of the lake was a catastrophic jökulhlaup (Sissons 1979) - would have created a burst of rapid seismic activity that is now manifested as the large number of slope failures and seismite liquefaction seen in the area. The lack of diagnostic seismite structures in the second sediment deformation event may be due to the fact that this does indeed represent deformation associated with the sudden drop in pressure due to rapid lake drainage giving rise to slumping and de-watering. This would then have been followed immediately by seismic activity and faulting due to differential isostatic rebound. This may not have caused seismite deformation due to the sediments having been previously de-watered during lake drainage. However the almost coincident distribution of first and second deformation event structures does tend to suggest that both are due to seismic activity.

3.10 Conclusions

The deformation features observed in the area of Glen Roy and Glen Gloy show that there were at least three main episodes of enhanced seismic activity during and immediately after the Loch Lomond Stadial as a result of crustal loading by a combination of ice cover and lake impoundment. The first and second (and possibly a number of unrecorded) episodes of seismic activity were probably the result of fluctuating levels in the lake levels due to the decay of the ice dam in Glen Spean. This is analogous to present day hydroseismicity. The final episode of seismic activity was in response to the final unloading of the crust due to catastrophic lake drainage and ice decay at the end of the Loch Lomond Stadial. The exact relationships between sediment deformation and fault movement is by no means established, however the sediment deformation events can be constrained temporally fit with the first and final

seismic episodes. The cause of the second sediment deformation event is still to be conclusively established. A reappraisal of the stratigraphy established by Ringrose (1987) in conjunction with a programme of absolute age dating, possibly using thermoluminescence, would allow better control on the timing, and hence the origin, of these events. Despite these shortcomings, it is seen that the late- and immediate post-glacial environment in the Glen Roy area was tectonically very active, with seismic events up to two and possibly three orders of magnitude greater than those of the present day.

3.11 Acknowledgements

This research was carried out at the Department of Applied Geology, University of Strathclyde and at the Department of Geology & Applied Geology, University of Glasgow while in receipt of NERC studentship GT4/87/GS/107. F. McKenzie is thanked for help during fieldwork. R. Lagerbäck, R. Muir Wood, J.D. Peacock, P.S. Ringrose and M.D. Zoback provided useful discussion. D. MacLean prepared the photographic plates. The comments of I. Allison greatly improved an earlier draft of this paper.

3.12 References

Adams, J. 1989. Postglacial faulting in eastern Canada: nature, origin and seismic hazard implications. *Tectonophysics* 163, 323-331.

Ambraseys, N.N. 1988. Engineering seismology. *Earthquake Engineering & Structural Dynamics* 17, 1-105.

Anderson, J.G. 1986. Seismic strain rates in central and eastern United States. *Bull. Seism. Soc. Am.* 76, 273-290.

Bäckblom, G. & Stanfors, R. 1989. Interdisciplinary study of post-glacial faulting in the Lansjärv area Northern Sweden 1986-1988. SKB Technical Report 89-31.

Bonilla, M.G., Mark, R.K. & Lienkaemper, J.J. 1984. Statistical relations among earthquake magnitude, surface rupture length and surface fault displacement. *Bull. Seism. Soc. Am.* 74, 2379-2411.

Costain, J.K., Bollinger, G.A. & Speer, J.A. 1987. Hydroseismicity- a hypothesis for the role of water in the generation of intraplate seismicity. *Geology* 15, 618-621.

Crawford, A.M. & Curran, J.H. 1982. The influence of rate- and displacement- dependent shear resistance on the response of rock slopes to seismic loads. *Int. J. Rock Mech. Min. Sci. & Geomech.* 19, 1-8.

Doornkamp, J.C. 1986. Geomorphological approaches to the study of neotectonics. *J. geol. soc. London* 143, 335-342.

Eisbacher, G.H. 1979. Cliff collapse and rock avalanches (stürztstroms) in the Mackenzie Mountains, northwestern Canada. *Can. Geotech. J.* 16, 309-334.

Fenton, C.H. 1991. Neotectonics and palaeoseismicity in N.W. Scotland. Unpubl. Ph.D. Thesis, University of Glasgow.

Ghosh, A. & Haupt, W. 1989. Computation of the seismic stability of rock wedges. *Rock Mech. & Rock Eng.* 22, 109-125.

- Grant, D.R. 1990.** Late Quaternary movement of Aspy Fault, Nova Scotia. *Can. J. Earth Sci.* 27, 984-987.
- Gordon, F.R. & Lewis, J.D. 1980.** The Meckering and Calingiri earthquakes, October 1968 and March 1970. *Geol. Surv. W. Aust. Bull.* 126.
- Hempton, M.R. & Dewey, J.F. 1983.** Earthquake-induced deformational structures in young lacustrine sediments, East Anatolian Fault, southern Turkey. *Tectonophysics* 98, T7-T14.
- Hencher, S.R. 1980.** Friction parameters for the design of rock slopes to withstand earthquake loading. *in* Design of dams to resist earthquakes. ICE, London, 65-73.
- Hoek, E. & Bray, J.W. 1981.** Rock slope engineering. IMM London. (3rd. Edition), 358pp.
- Jibson, R.W. 1987.** Summary of research on the effects of topographic amplification of earthquake shaking on slope stability. USGS Open File Rpt. 87-268, 171pp.
- Johnston, A.C. 1987.** Suppression of earthquakes by large continental ice sheets. *Nature* 303, 467-469.
- Johnston, A.C. 1989.** The effect of large ice sheets on earthquake genesis. *in* Earthquakes at North-Atlantic Passive Margins: Neotectonics and post-glacial rebound. S.Gregerson & P.Basham (eds.). Kluwer Academic Publishers, Dortrecht , p581-599.
- Keefer, D.K. 1984.** Landslides caused by earthquakes. *Geol. Soc. Am. Bull.* 95, 406-421.
- Khromovskikh, V.S. 1989.** Determination of magnitudes of ancient earthquakes from observed seismodislocations. *Tectonophysics* 166, 269-280.
- Kuribayashi, E. & Tatsuoka, F. 1975.** Brief review of liquefaction during earthquakes in Japan. *Soils & Foundations* 15, 82-92.

- Lagerbäck, R. 1990.** Late Quaternary faulting and palaeoseismicity in northern Fennoscandia, with particular reference to the Lansjärv area, northern Sweden. *Föringens i Stockholm Förhandlingar* 112, 333-354.
- Mörner, N-A. 1981.** Crustal movements and geodynamics in Fennoscandia. *Tectonophysics* 71, 241-251.
- Muir Wood, R. 1989a.** Fifty million years of 'passive margin' deformation in North West Europe. *in* S. Gregerson & P.W. Basham (eds.) *Earthquakes at North Atlantic Passive Margins: Neotectonics and postglacial rebound*. 7-36. Kluwer Academic Publishers, Amsterdam.
- Muir Wood, R. 1989b.** Extraordinary deglaciation reverse faulting in Northern Fennoscandia. *in* S. Gregerson & P.W. Basham (eds.) *Earthquakes at North Atlantic Passive Margins: Neotectonics and postglacial rebound*. 141-173. Kluwer Academic Publishers, Amsterdam.
- Muir Wood, R. 1990.** The current tectonic regime in the United Kingdom and its NW European context (its bearing on the performance assessment of radioactive waste disposal sites). *in* Report of a meeting on "Fractures and fracture development". DOE Report No. DOE/RW/90.014. Dames & Moore International Technical Report TR-D&M-17.
- Newmark, N.M. 1965.** Effects of earthquakes on dams and embankments. *Geotechnique* 15, 139-160.
- Nichols Jr, T.C. 1980.** Rebound, its nature and effect on engineering works. *Q.J.eng. Geol. London* 13, 133-152.
- Pavrides, S.B. & Tranos, M.D. 1991.** Structural characteristics of two strong earthquakes in the North Aegian (1932) and Agios Efstratios (1968). *J. Structural Geol.* 13, 205-214.
- Peacock, J.D. & Cornish, R. 1989.** *Glen Roy Area- Field Guide*. Quaternary Research Association, Cambridge.
- Ringrose, P.S. 1987.** Fault activity and palaeoseismicity during Quaternary time in Scotland. Unpubl. Ph.D. Thesis (2 vols.), University of Strathclyde.

Ringrose, P.S. 1989. Palaeoseismic (?) liquefaction event in late Quaternary lake sediment at Glen Roy, Scotland. *Terra Nova* 1, 57-62.

Ringrose, P.S., Hancock, P., Fenton, C. & Davenport, C.A. 1991. Quaternary tectonic activity in Scotland. *in* A. Foster, M.G. Culshaw, J.C. Cripps, J.A. Little & C.F. Moon (eds.) *Quaternary Engineering Geology*, Geol. Soc. Engineering Geol. Special Publ. No.7, 679-686.

Scott, B. & Price, S. 1988. Earthquake-induced structures in young sediments. *Tectonophysics* 147, 165-170.

Seilacher, A. 1984. Sedimentary structures tentatively attributed to seismic events. *Marine Geology* 55, 1-12.

Sims, J.D. 1975. Determining earthquake recurrence intervals from deformational structures in young lacustrine sediments. *Tectonophysics* 29, 141-152.

Sissons, J.B. 1979. Catastrophic lake drainage in Glen Spean and the Great Glen, Scotland. *J. Geol. Soc. London* 136, 215-224.

Sissons, J.B. & Cornish, R. 1982. Rapid localized glacio-isostatic uplift at Glen Roy, Scotland. *Nature* 297, 213-214.

Talbot, C. 1986. A preliminary structural analysis of the pattern of post-glacial faults in Northern Sweden. SKB Technical Report 86-20.

Wilson, R.C. & Keefer, D.K. 1985. Predicting the areal limits of earthquake-induced landsliding. *in* J.I. Ziony (ed.) *Evaluating earthquake hazards in the Los Angeles Region - An earth science perspective*. USGS Pro. Paper 1360, 317-245.

Youd, T.L. 1977. Discussion of Brief review of liquefaction during earthquakes in Japan. *Soils & Foundations* 17, 82-85.

Zoback, M.D. 1991. Department of Geophysics, Stanford University, Stanford, California, 94305, USA. *Present Address*: Geophysikalisches Institut, Universität Karlsruhe, D-7500 Karlsruhe 21, FRG.

3.13 Figure Captions

Figure 3.1 Seismic deformation features in the upper part of Glen Roy and Glen Gloy, Lochaber. Slope failures are marked by heavy stipple (Numbers correspond to Table 3.1). The heavy dashed line marks the area of most intense seismic liquefaction [after Ringrose 1987]. Lighter dashed line marks some of the palaeo-shorelines. Star marks the point of shoreline dislocation reported by Sissons & Cornish (1982). Inset: location of the Glen Roy area.

Figure 3.2 Morphotectonic features along the Allt Neurlain (Glen Gloy) fault [After Ringrose 1987].

1. Slump-type slope failure, cut by the 355 m shoreline. Headscarp defined by a NE trending fracture lineament.
2. Basic dyke of uncertain age offset by c. 40 m in a sinistral manner along a vertical N-S trending, gouge-filled fracture. Fracture is continuous for over 150 m.
3. Exposure of fault zone (inset) shows two 20-25 mm wide zones of blue-grey fault gouge in a wider zone of unconsolidated crushed and sheared rock fragments. Offset of outcrop morphology and previous fractures shows a few decimetres of dextral offset along N-S trending fractures.
4. Stream capture and dry water courses suggest left-lateral offset of drainage in the order of tens of metres. This corresponds to the offset of the dyke at 2.
5. Two metre wide zone of brecciation and anastomosing shear planes is cut by two discrete, continuous fractures trending 340-350° over distances of several hundreds of metres. One fracture contains a thin (<3 mm) gouge. Offset of lithological features and other fractures is approximately 0.30-0.45 m. in a dextral manner.
6. Scarp on hillside is offset by a few tens of metres in a sinistral manner.

7. NNW-NW trending scarp feature ('fault scarp' of Ringrose (1987)). Possibly related to the older Brunachan slope failure (lighter stipple) as it quickly reduces from a 2 m-high west facing scarp to disappear as it is traced north out of the area of failure into the adjacent area of incipient failure and ground dilation.

8. Area of incipient slope failure. Dilation along 070-250° fractures forms open fissures up to 1 m wide and up to 40 m long.

9. 020-200° downslope-facing scarp (general orientation 80°/022°) up to 4 m high, fronted by a 2 m high ridge. It extends to the NE as a line of sink-hollows, dying out before the Brunachan failure headscarp. The SW projection corresponds with the measured offset of the lake shorelines. However no indicators of fault movement are found along the fault scarp face. Indeed, concentric, tensional stress release fracture patterns suggest that this is a tensional feature related to the slope failure and rather than due to fault movement.

10. Brunachan slope failure ; a complex failure involving elements of sliding and toppling. Shows several ages of movement (see Table 3.1)

Inset: Exposure of the Glen Gloy fault showing two northerly trending fault gouge units in a zone of crushed and sheared rock. Fault gouge consists of a blue-grey clay-like material, up to 25 mm in width, found in a zone of unconsolidated lath-shaped fragments of country rock. Numbered spots indicate ESR samples [§ 5, p220].

Figure 3.3 (a) Exposure of the fault zone (3, Figure 3.2) containing fault gouge adjacent to the Allt Neurlain, Glen Gloy. Hammer shaft is 40 cm long (Looking N).

(b) X-ray diffraction spectra for fault gouge and country rock showing that they have essentially the same composition. Q: quartz; F: feldspar; c: 'clays'; Ch: chlorite; K: kaolinite; Mu: muscovite.

- Figure 3.4** Schematic block diagram showing the development of surface deformation features due to movement on a non-visible (Die-out up) fault strand.
- Figure 3.5** Hypothetical log of depositional and deformation features in the Glen Roy and Glen Gloy lacustrine basin sediments.
2. First deformation event: fault grading, ball and pillow and flame structures.
 3. Unconformity.
 4. Deposition of lacustrine rhythmite silts.
 5. Unconformity.
 6. Deposition of red sand and silts. Local sands and gravels.
 7. Second deformation event: slumping of lacustrine rhythmites.
 8. Deposition of silt, sand and gravels.
 9. Freeze-thaw involutions and brittle faulting.
- Figure 3.6** Catastrophic disrupted sliding failure above Glenfintaig, Glen Gloy (Looking E from Glenfintaig Farm).
- Figure 3.7** (a) Brunachan slope failure, upper Glen Roy. A large complex failure that shows several episodes of movement (Looking W).
- (b) Braeroy slope failure. A large slump failure that shows two periods of movement. Earlier movement cuts 350 m shoreline but is cut by the 325 m shoreline. Most recent movement cuts the 325 m shoreline (Looking E from the Brunachan failure).
- Figure 3.8** Age of slope failures with respect to the lake shorelines.
- Figure 3.9** Diagrammatic representation of the late Quaternary loading of the crust in the area of Glen Roy and Glen Gloy. All sections orientated NW-SE.
- Table 3.1** Slope failures in the area of Glen Roy and Glen Gloy.
- Table 3.2** Magnitude estimates from the morphotectonic features observed in the areas of Glen Roy and Glen Gloy.

3.14 Figures

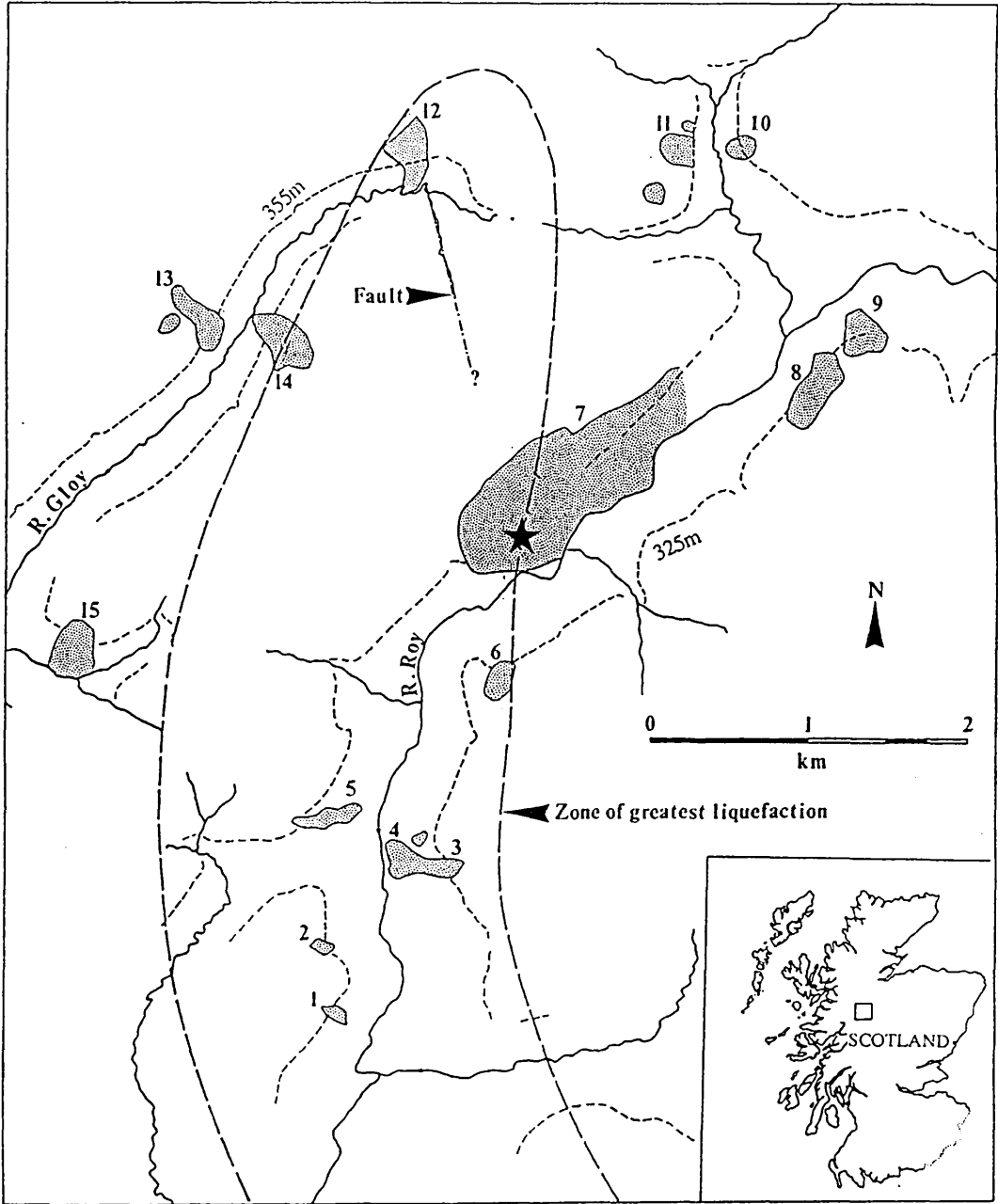


Figure 3.1

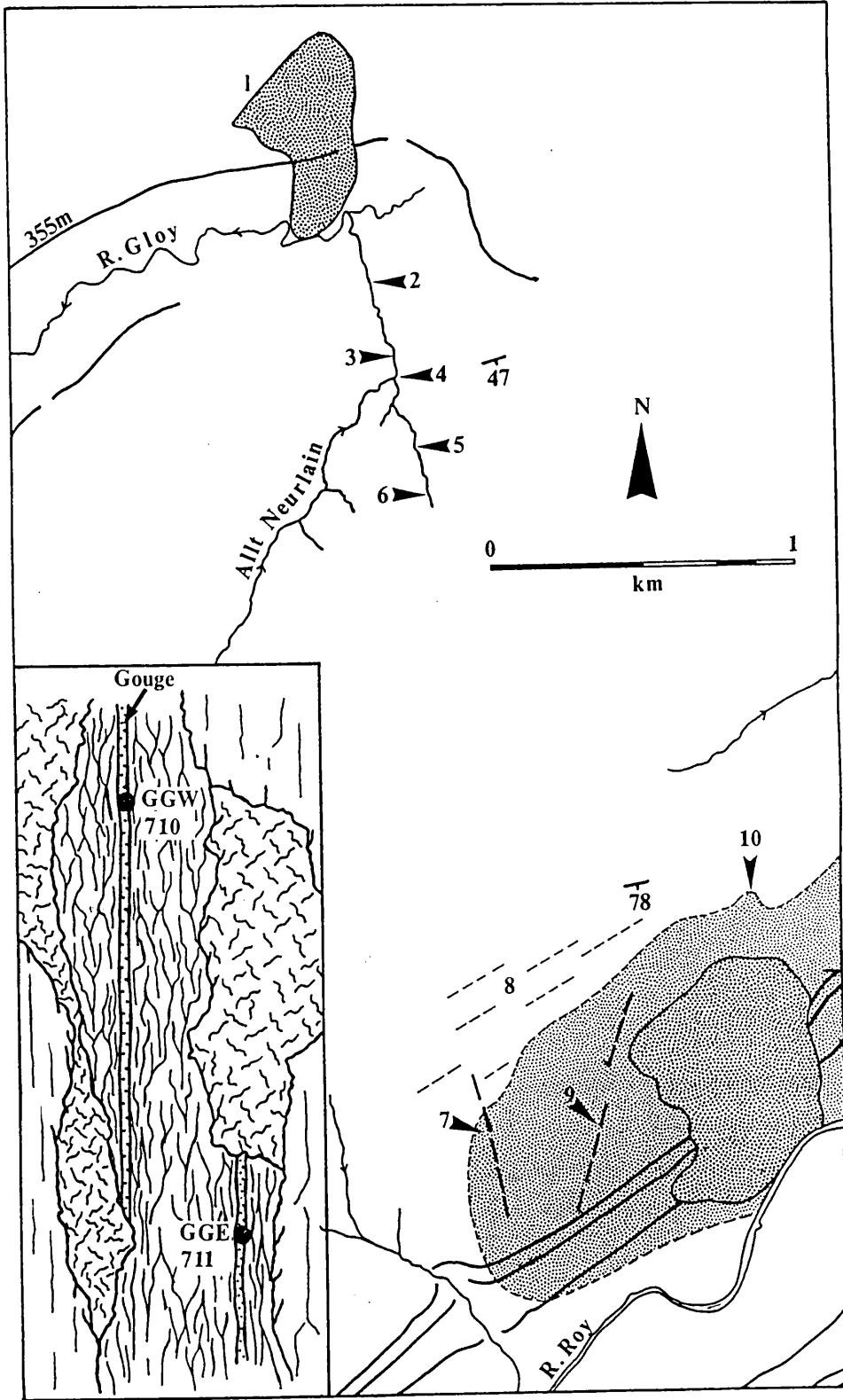


Figure 3.2



Figure 3.3a

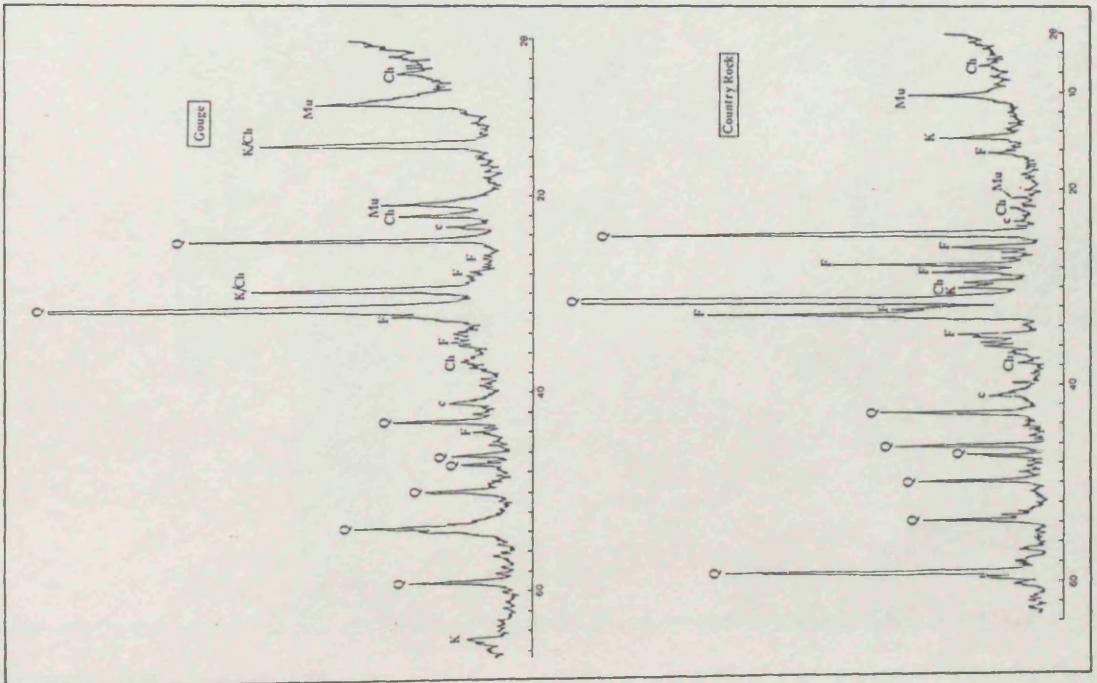


Figure 3.3b

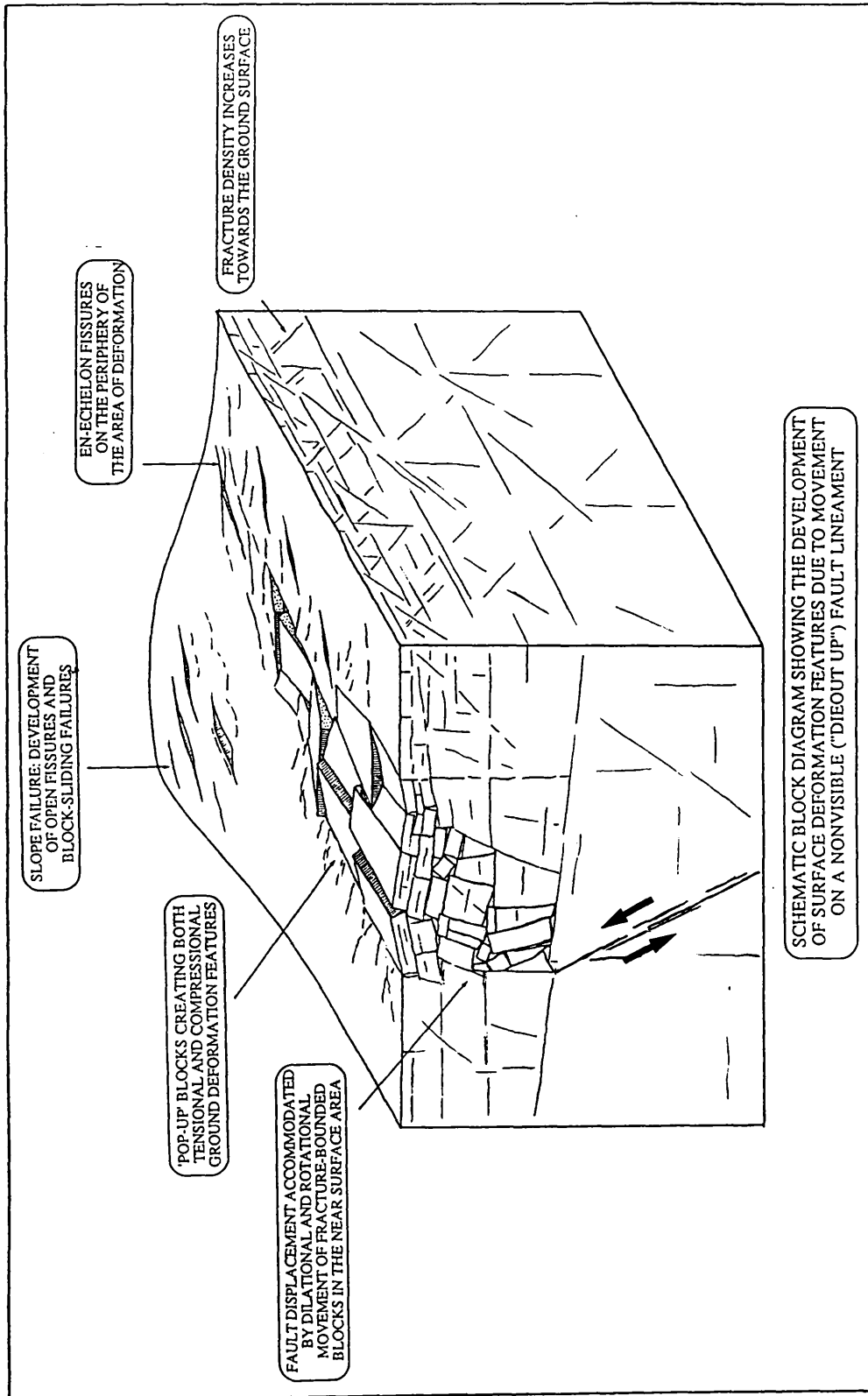


Figure 3.4

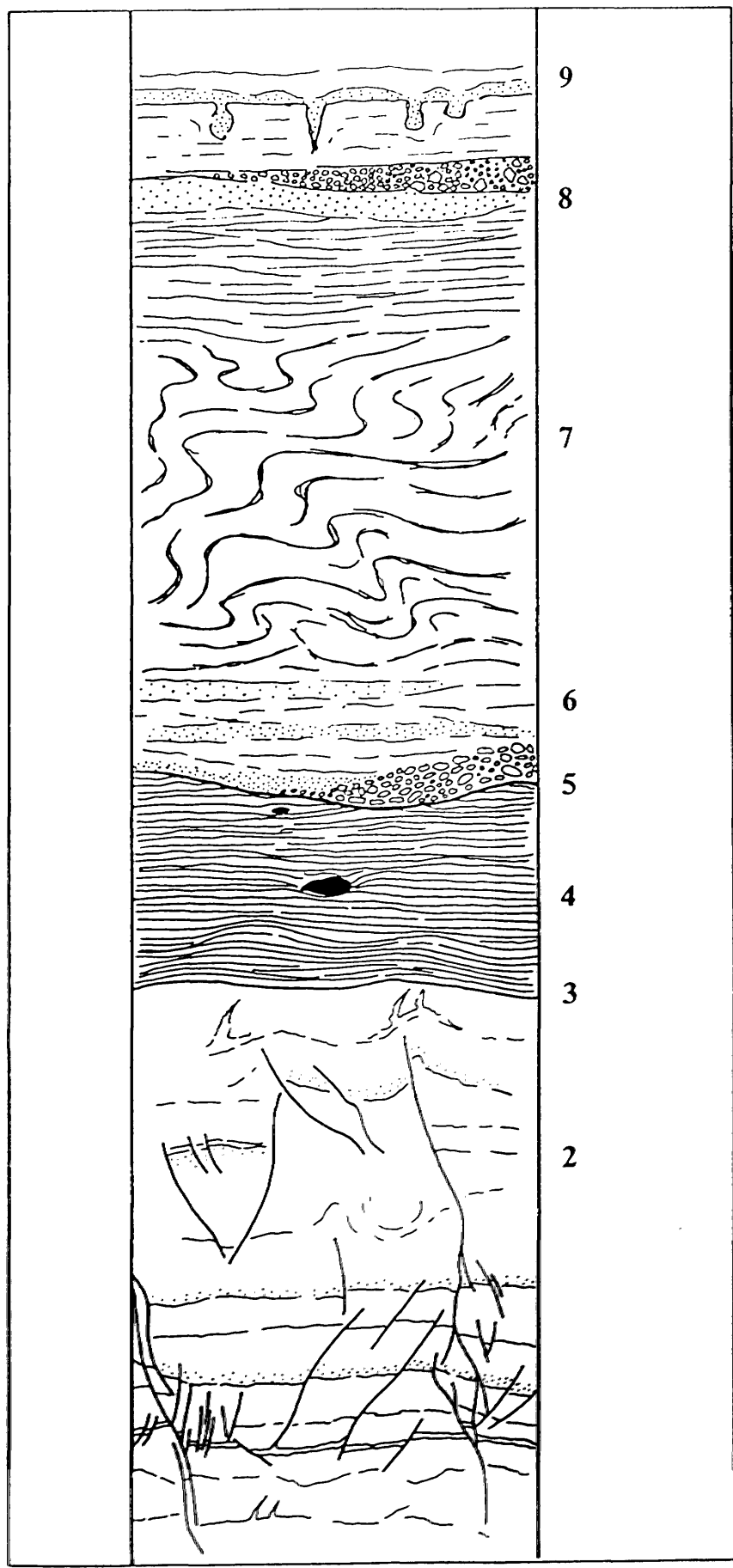


Figure 3.5



Figure 3.6



Figure 3.7a



Figure 3.7b

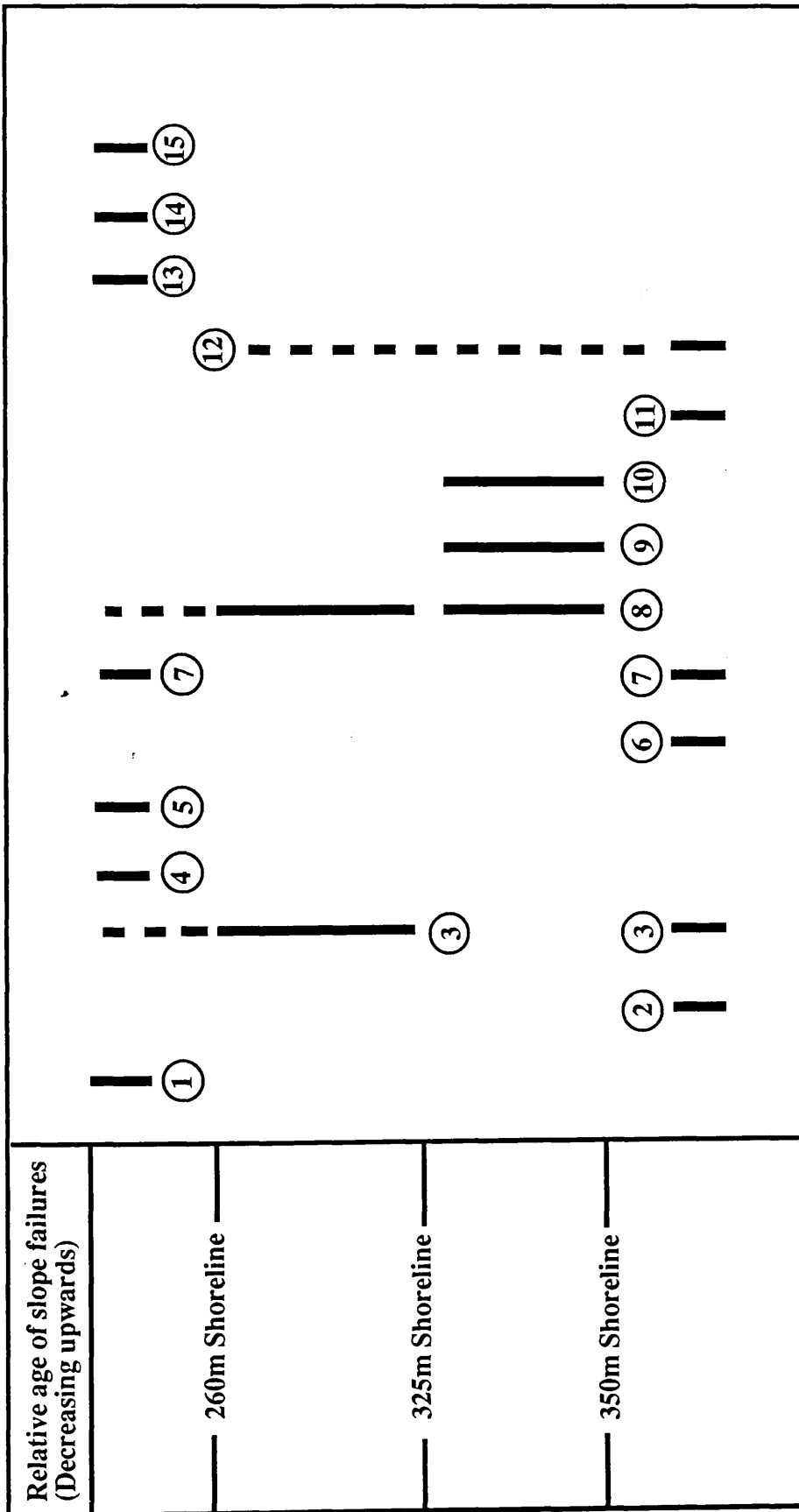


Figure 3.8

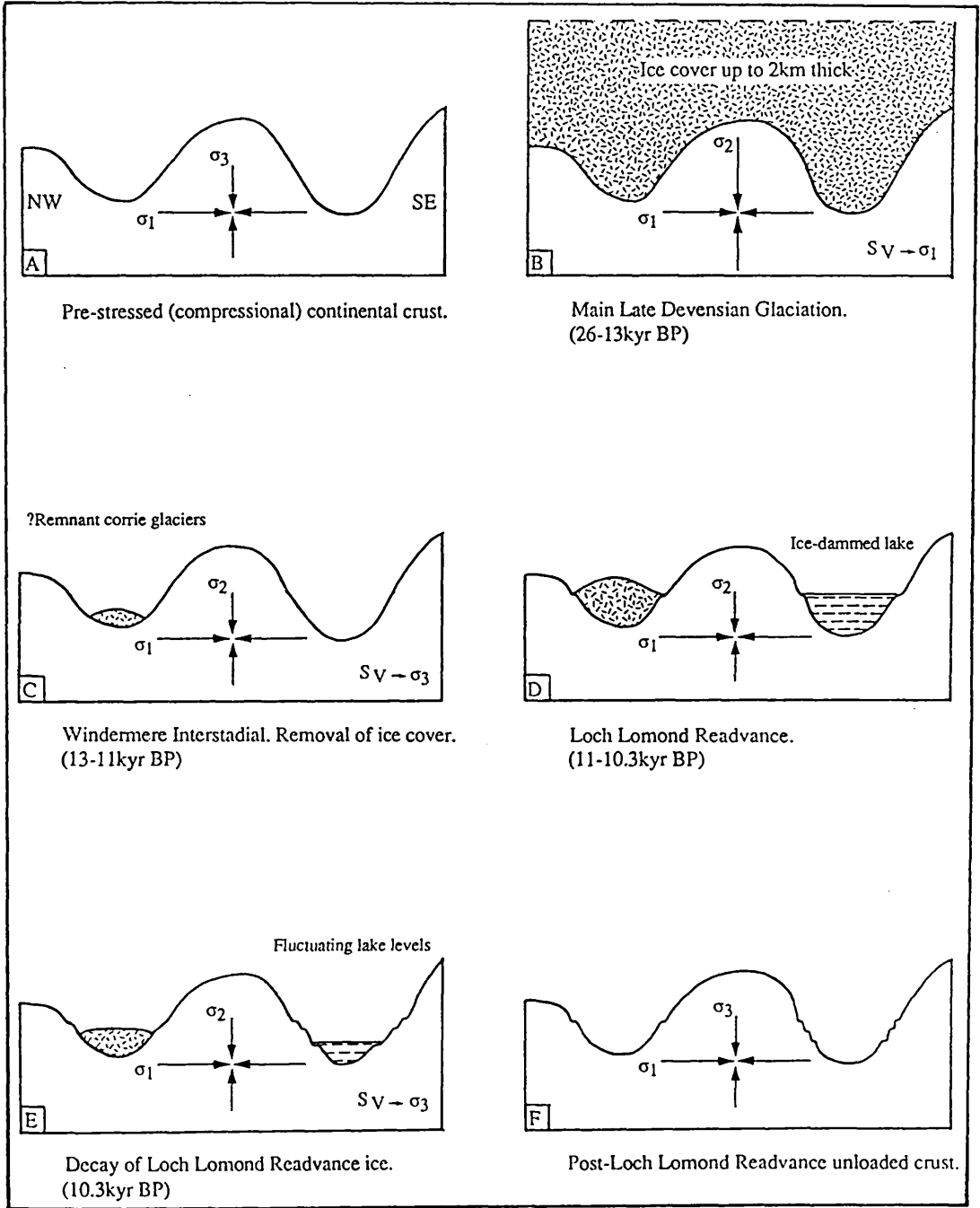


Figure 3.9

3.15 Tables

Table 3.1

LOCATION	TYPE OF FAILURE	RELATIVE AGE
1. Cranachan [NN293849]	Rotational slump.	Disturbs 325m & 260m shorelines.
2. Coire Mheallmain [NN292855]	Slump.	Cut by 350m shoreline.
3. Bohaskey Upper [NN305864]	Rotational slump.	Older failure cut by all shorelines. More recent failure cuts 350m & 325m shorelines (does not reach the 260m shoreline).
4. Bohaskey Lower [NN302867]	Simple slump.	Disrupts 260m shoreline.
5. Achavady [NN293869]	Toppling failure, development of obsequent scarps.	Disturbs all shorelines.
6. Braigh Bac [NN310883]	Rotational slump.	Cut by the 350m shoreline.
7. Bhrunachain [NN3190]	Complex failure involving toppling, rockfall and sliding.	Older toppling failure cut by all shorelines. Later failure destroys all shorelines.

Table 3.1(cont.)

8.	Braeroy [NN343914]	Rotational slump.	Older failure destroys 350m shoreline but is cut by the 325m shoreline. More recent failure cuts both the 350m & 325m shorelines but does not reach the 260m shoreline.
9.	Sgurr an Fithich [NN346917]	Deep seated slump.	Destroys the 350m shoreline but incised by the 325m shoreline.
10.	Glen Turret [NN327935]	Shallow rotational slumping.	Cuts 350m and is cut by the 325m shoreline.
11.	Glen Turret [NN334935]	Shallow slump.	Cut by the 350m shoreline.
12.	Carn a' Bhruic [NN300935]	Slump.	Cut by the 355m shoreline.
13.	Leitir Fhionnlaich [NN280917]	Rotational slump.	Cuts the 355m shoreline.
14.	Coire na Fail [NN288917]	Sliding failure, some rotation.	Cuts the 355m shoreline.
15.	Glenfintaig [NN267886]	(?Catastrophic) Disruptive sliding failure.	Cuts all shorelines.

Table 3.2

Morphotectonic Feature	Reference	Magnitude Estimate
7km 'active' fault trace.	Khromovskhikh (1989)	6.5±0.4
	Bonilla <i>et al.</i> (1984)	5.7 - 6.7
1km surface rupture.	Khromovskhikh (1989)	5.45±0.30
	Bonilla <i>et al.</i> (1984)	5.0 - 6.2
0.5m dextral displacement.	Bonilla <i>et al.</i> (1984)	5.7 - 6.9
Areal extent of slope failures:	Keefer (1984)	4.6
		4.3
		4.8
Max. distance to coherent slides.	Keefer(1984)	5.4
Max. distance to disrupted slides.	Keefer (1984)	4.6
Max. distance to liquefaction.	Kuribayashi (1985)/Youd (1977)	6.3 - 6.5

3.16 Appendix: Modified Newmark Analysis

Slope stability is normally assessed under static conditions where failure will only occur when the gravitational load (L) acting on the slope exceeds the shear resistance (R_{max}) of the slope mass (m). Slope stability is defined by the Factor of Safety (FS)

$$FS = \frac{R_{max}}{L} \quad (1)$$

where failure will occur when $FS \leq 1$.

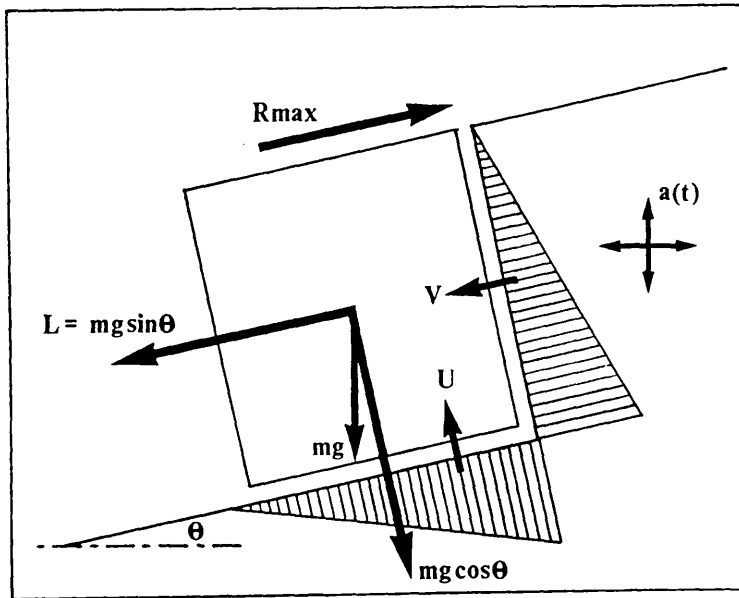


Figure A. Definitions of the forces acting on a slope subject to earthquake shaking.

In dynamic situations the propagation of seismic waves through the rock mass creates an additional load, $a(t)$. This load fluctuates with time and acts with L to produce a total downslope load of $[L + a(t)]$. When the total downslope load exceeds R_{max} irreversible displacement of the slope mass occurs. This will occur at a critical acceleration, A_c , where

$$m A_c = R_{max} - L \quad (2)$$

or

$$A_c = (FS - 1) g \sin\theta \quad (3)$$

where θ is the inclination of the failure plane and g is the acceleration due to gravity. A_c is the minimum ground acceleration required to overcome R_{max} . As the shear

strength of the slope decreases as failure progresses and the ground acceleration during earthquake shaking varies considerably this form of analysis tends to underestimate the amount of failure (Wilson & Keefer 1985).

Limit equilibrium analysis (Hoek & Bray 1981) considers a block of mass m resting on a slope θ° subject to cleft water pressure V in a downslope direction and U acting to lift the block. The condition of limiting equilibrium exists when

$$m g \sin\theta + V = cA + (m g \cos\theta - U) \tan \phi \quad (4)$$

where A is the area of the failure surface, c is the cohesion of the material and ϕ is the effective friction angle of the material. Thus in this situation the Factor of Safety becomes

$$FS = \frac{cA + (m g \cos\theta - U) \tan \phi}{L + V} \quad (5)$$

Values for c and ϕ are normally measured in situ, however for such a retrospective analysis tabulated values are used for the various lithologies: $25^\circ < \phi < 35^\circ$ and $2 \times 10^4 \text{ kPa} < c < 4 \times 10^4 \text{ kPa}$ for quartzites and psammities (Hoek & Bray 1981).

When considering slope failures suspected of having been triggered by seismic activity a 'worst-case' scenario has been assumed where the cohesion and effective friction angles are considered to be at a minimum and the fluid pressures within the rock mass are at a maximum. This will give the minimum value of FS for the various slope geometries. Thus if the value of FS is greater than unity under such unstable slope conditions failure must require an additional driving mechanism such as seismic slope shaking. The levels of A_c required to initiate failure can then be estimated from equation (3). For the slope failures in the area of Glen Roy and Glen Gloy, using values of $\phi = 25^\circ$, $c = 2 \times 10^4 \text{ kPa}$ and $U = V = 18 \text{ MPa}$ the values of FS obtained lie in the range 0.83 to 1.6. This shows that under the most unfavourable conditions the majority of the slopes that have failed would have been stable. Thus the effects of seismic shaking are required to promote failure. Using equation (3) the critical ground acceleration required to cause failure lies in the range 0.1 - 0.4g (0.9 - 3.9 ms^{-1}). This agrees with the measured values required to trigger such failure (Wilson & Keefer 1985; Jibson 1987), the measured values required to cause liquefaction (Kuribayashi & Tatsuoka 1975) and the values of ground acceleration calculated from the distribution of seismite deformation in the area (Ringrose 1987).

Chapter 4

UK Seismicity During the Holocene: A Comparison of Instrumental, Historical and Palaeoseismic Data From N.W.Scotland

Clark Fenton

*Department of Geology and Applied Geology,
University of Glasgow, Glasgow G12 8QQ.*

4.1 Abstract

Comparison of seismicity from instrumental and historical catalogues with that revealed by palaeoseismic investigations shows that the area of the United Kingdom and, in particular, North West Scotland, was subject to greater levels of seismic moment release during the early part of the Holocene, c. 10 kyr BP., than those currently experienced. This was the product of the effects of glacial loading from the late Devensian ice sheets, that covered the northern part of the UK, acting to store tectonic stresses and induce considerable loading stresses of their own over a period of c. 16 kyr. Temporal changes in the instrumental record and in the detail of the historical record are explained by decreasing thresholds of detection due to respectively, improved instrumentation and an increase in the geographic spread of the population. Fault plane solutions for a number of recorded events are compared with focal planes assigned to the palaeoseismic events. This seems to suggest a marked change in the crustal stress regime from the early Holocene to present. However, when viewed in light of the known fault chronology, the known late Quaternary neotectonic stress field and the mechanisms of glacial tectonic reactivation of faults, it is seen that this earlier period of enhanced seismic activity is purely the result of enhanced stress levels created by ice loading. The mode of stress release is controlled by the orientation of pre-existing crustal weaknesses.

4.2 Introduction

For the most part seismic activity is spatially non-random. More than 90% of the world's earthquake activity occurs along the margins of lithospheric plates (Figure 4.1). If the seismicity of Mesozoic-Cenozoic orogens is also taken into consideration, less than 1% of the total global seismic moment (M_0), the release of seismic strain, occurs in the region of plate interiors. Yet these so called 'stable continental interiors'(SCIs) (Johnston 1989) are not only subject to micro-seismic activity but also to infrequent, large seismic events. The frequency or return period of these large earthquakes may be so great that few, if any, will have been experienced during historical time. The energy released, and hence the damage caused, by these rare earthquakes is much more significant than the multitude of smaller events that occur annually in such regions. The seismicity of such regions has included some of the world's most devastating earthquakes in terms of losses of human life and property. The generally strong and intact nature of continental interior crust results in it being more efficient in the transfer of seismic energy than more active areas that are dissected by a number of faults, causing compartmentalisation of the crust with respect to the transfer of seismic strain release. This is shown by the size of the areas affected by large intraplate earthquakes in comparison to events of similar size at plate margin localities. The build-up and release of strain in SCIs is a product of the transfer of far field stresses from plate margins. This creates a broadly uniform stress field over large regions which, when concentrated, by perhaps some sub-crustal flow mechanism (Zoback *et al.* 1985.), and acting on pre-existing crustal weaknesses gives rise to the generation of intraplate seismicity. The periodicity of such seismic activity is still open to question, however the recurrence interval is definitely greater than that for plate margins (Johnston & Kanter 1990). Therefore it is important when investigating the seismic risk in such regions not only to consider the instrumental and historical records, but also to use the 'recent' geological record to look for evidence of such rare seismic events. This involves the searching sedimentary sequences for deformation features that can be attributed to the effects of seismic shaking (Sims 1975; Seilacher 1984; Obermeier *et al.* 1985; Allen 1986; Amick & Gelinas 1991). This is the discipline of *Palaeoseismicity*, the search for evidence of earthquake activity outside the realms of the historical record. Only by such an investigation will the seismic record be extended sufficiently to allow an accurate estimation of the seismic risk in the area under consideration.

4.3 Plate Tectonic Setting of the UK

The United Kingdom is situated on the northwestern margin of continental Europe, proximal to the north Atlantic passive margin. This is part of the European 'stable continental interior' (Johnston 1989). It is presently an area of low, but not altogether insignificant seismicity. The regional stress field acting in the area of the UK is orientated $N144^{\circ}\pm 26^{\circ}$ (Brereton & Müller 1991). This is within 17° of the calculated vectors of absolute plate velocity field for the Eurasian plate (Figure 4.2). The present stress field is seen to be a product of far field stresses from the Mid-Atlantic ridge push and convergence of North Africa and Eurasia (Muir Wood 1989a; Zoback *et al.* 1989). The stress field is essentially uniform over the entire area of northwestern Europe with the exception of minor perturbations around the rift structures of the Rhine Graben, the Central North Sea and off the western coast of Norway (Illies & Greiner 1978; Illies *et al.* 1981). Indeed from shallow stress measurements and focal plane mechanisms the direction of S_H in Scotland seems to be more WNW (Davenport *et al.* 1989). From geological evidence it is seen that the present stress system has been active since the late Miocene, c. 6 Ma. (Muir Wood 1989a, 1990), with only transient perturbations due to the effects of Late Devensian glacial loading [§ 6, p260]. In addition to the effects of far field stresses from plate boundary forces, the area of the UK is also subject to residual isostatic uplift due to the Late Devensian glaciations. This has had a strong influence on the seismotectonics of the northern part of the UK during the period of the late Quaternary [§ 2, p15; § 6, p260].

The northern part of the UK suffered an number of glacial episodes during the Quaternary in common with other high latitude areas of northwestern Europe. The most recent glacial episode, the Main Late Devensian Glaciation and the subsequent Loch Lomond Readvance, subjected the crust to a period of c. 16 kyr of loading. Deglaciation was extremely rapid in comparison to ice build-up. The relaxation due to the removal of the ice load resulted in a period of extensive post-glacial faulting (Ringrose 1987, 1989a, 1989b; Davenport *et al.* 1989; Ringrose *et al.* 1991) [§ 2, p15]. Attendant with this fault movement is evidence for enhanced levels of seismicity compared with that currently experienced in the UK. This fault activity and resultant seismicity has been attributed to the sudden release of the stresses created by glaciation and the tectonic stress 'stored' during the residence of the ice cover acting on the ambient stress field, resulting in the creation of a critical stress levels promoting crustal failure [§ 6, p260].

A comparison of the seismicity from instrumental, historical and palaeoseismic catalogues will show how the seismotectonic regime in the UK has evolved in the last 10 kyr of the Holocene era.

4.4 Seismotectonic Investigations

As stated above investigations into the seismicity/seismic risk of a region fall into three broad fields:

(i) *Instrumental seismicity*: consideration of the recorded seismicity allows a detailed insight into the earthquake mechanics of seismic activity in an area and can also reveal the response of the geology of the area when under dynamic seismic strains. Information concerning ground acceleration, shaking intensity and duration, focal depth and mechanism, seismic wave dispersal and amplification can all be obtained from instrumental records. The frequency of 'background' seismicity and hence energy release can also be calculated for the period of the instrumental record.

(ii) *Historical seismicity*: a historical perspective is needed to understand the long-term seismicity of a region. Information from a multitude of diverse sources (newspapers, parish records, diaries, personal correspondence etc.) is often collated to form seismicity catalogues. Gathering of such information, to ensure as complete as possible record for the ensuing data base, is a labour intensive activity. Such non-instrumental macroseismic data needs to be subject to rigorous critical appraisal to evaluate the quality of the information gathered and to standardise the information with respect to the instrumental record.

(iii) *Palaeoseismicity*: this is the identification and study of prehistoric earthquakes by the use of detailed microstratigraphic relationships along faults, fault scarp and terrace morphotectonics, and seismically-induced ground deformation features including 'seismite' soft sediment deformation, slope failures and rock block displacements. This increases the temporal cover of the seismic record to such an extent that it should be possible to compensate any irregularities in the record as may be displayed in historical and instrumental records. Any method by which it is possible to increase the temporal coverage of the seismic record will allow a clearer picture of the evolution of the seismotectonic regime of the area under consideration, thereby increasing the confidence in predictions for the future.

4.5 Seismic Risk Investigation

It is desirable to quantify the risk posed by seismic activity for any one crustal region in order to mitigate the effects of damaging earthquakes. The interdisciplinary field of engineering seismology has as its goal the *minimisation* of earthquake risk. This is achieved by providing the data required for proper seismic risk management criteria for the safe location of sensitive structures and the basic earthquake design ground motions and deformation that structures that such installations must survive (Ambraseys 1988). An evaluation of seismic hazard has the ultimate aim of producing a frequency-magnitude relationship of the form:

$$\log N_c = a - bM \quad (1)$$

as described by Gutenberg & Richter (1944) where N_c is the number of events greater than magnitude M occurring in a given time period, and a and b are constants. Constant a depends on the size of the area and length of time for which seismicity is recorded and is an overall measure of the seismicity of the area. The b -value varies with source region, focal depth, type of earthquake process, stress level and, in some cases, time. This is usually in the range 0.5-1.5, commonly observed to be close to unity (Kanamori & Anderson 1975). Such a relationship is only valid over the period for which the data has been gathered. If this comprises merely instrumental data, i.e. the period post-1904 for California or post-1967 in the case of the UK (Figure 4.3), this will generally be too short a time scale to produce a true picture of the seismic activity of a region, especially in intracontinental areas where the return period of large scale, damaging earthquakes can be an order, if not several orders, of magnitude greater than the time period over which instrumental recordings have been made. Thus, the present distribution of seismicity may not be a true reflection of the seismic distribution over a longer time period. For instance if we look at the distribution of present day instrumental seismicity (Figure 4.1) it seems that intraplate areas are almost aseismic. However such areas have been the locus of some of the world's most damaging earthquakes (Johnston 1989).

A historical perspective is therefore required to understand fully the longer term seismicity of a region. This requires a labour-intensive search of a disparate source of reference works to accumulate a data base, which then needs careful critical analysis in order to standardize the data, assign magnitude and/or intensity values, to prevent duplication of events and also to ensure relative completeness of the resulting catalogue

of seismicity. Such a historical catalogue of seismicity must be calibrated with respect to the observations of seismicity of the current instrumental period.

Earthquake size is usually expressed as magnitude or seismic moment. Several magnitude scales exist, so it is important to be consistent in the magnitude scale adopted when comparing seismicity. Magnitude can be assigned to historical data by using the radii of the isoseismal defining macroseismic phenomena, providing that there is sufficient reportage of the 'felt' effects of the events (Ambraseys 1988). Mislocation and inconsistencies in reporting of historical macroseismic data (Musson *et al.* 1984; Musson 1989, 1990a) are the main sources of error with macroseismic data from historical events. As stated above historical macroseismic information comes from many disparate sources. With regard to seismicity in the UK this provides coverage for the last 700 years (Ambraseys 1985a, 1985b, 1988; Ambraseys & Jackson 1985). This allows an insight into the seismicity not 'seen' by the instrumental record.

4.6 Seismicity Data Bases for the UK

Seismic activity is presently recorded by the British Geological Survey's Global Seismology Unit and published as annual catalogues (usually with a two year time lag to date of publication). Seismicity is also recorded at specific sites by concerned parties using high resolution, three component recorders to give very precise location of microseismic activity (W. Aspinall, pers. comm. 1991). However this data is usually proprietary and is therefore not available for use in this study. The majority of the data for the instrumental record used in this study is taken from BGS publications (Burton & Neilson 1980; Turbitt 1984, 1985, 1986, 1987, 1988, 1989, 1990). Additional information concerning fault plane solutions and the physical basis for the seismicity observed is taken from a number of sources (e.g. Marrow & Walker 1988).

Historical seismicity for the UK is recorded in a number of diverse publications. However as this study does not attempt, as its main aim, to analyse the quality of the historical record, information concerning historical seismicity is taken from a number of catalogues that were considered of sufficient quality to be used comparatively with the instrumental record (Davison 1924; Dollar 1951; Musson 1990b). The information from these sources is compared qualitatively with other historical seismicity studies (Ambraseys 1985a, 1985b; Ambraseys & Jackson 1985).

Palaeoseismic data has been collated from an extensive programme of field work in Scotland, particularly in the North West Highlands (Ringrose 1987) (Table 4.1). The gathering of palaeoseismic data followed a method (Figure 4.4) evolved from previous workers (Allen 1975; Doornkamp 1986; Crone 1987; Bäckblom & Stanfors 1989) to suit the investigation of the Highlands of Scotland for evidence of late Quaternary fault reactivation. The observed deformation features and magnitude of fault offsets has been compared with similar features noted from present day seismic events and on this basis have been assigned magnitudes (with appropriate error bounds).

There is an obvious disparity in the completeness of the various data sets. In addition the quality of the data sets decreases markedly, with the errors in the magnitude assignments increasing with age. To overcome the problems of changing threshold magnitudes in the detection limits of each data set, comparisons of the seismicity in each data set were eventually carried out using cumulative frequencies and moment release i.e. the amount of energy (in dyne cm) released by the seismicity. This has the advantage of making the shortfall in the number of small events negligible in comparison with the less frequent, but more easily recorded larger events that dominate the moment release distributions.

4.7 Instrumental Seismicity:1969-1988

A cursory glance at the annual distribution of epicentres (Figure 4.5) shows that seismicity is concentrated as swarms of several events at an number of centres that remain sporadically active over the period of recorded seismicity [§ 4.17b, p215]. This is set against a background of more diffuse seismicity of transient swarms, coalfield events and broad regional "patches" of seismicity. This rather random distribution of seismicity is common in plate interior regions, however when we look at the distribution of larger ($>3.0 M_L$) events in Scotland (Figure 4.6) it is seen that all the events cluster in two localities, around Ben Nevis and in the area of Kintail in Inverness-shire. Other minor clusters are seen at Ullapool and in the Ochil Hills. These are also the locations of transient swarms of microseismic activity throughout the duration of the instrumental record [§ 4.17b, p215]. As yet there is no objective view of the distribution of seismicity in space and time for the UK region, however this will hopefully be countered by improved instrumentation and detailed studies of the more significant events recorded on the BGS/DIAS seismograph network (Marrow & Walker 1988). The quality of the present data base allows the observation of some

elementary seismological relationships, however predictions concerning the details of the UK seismotectonic regime can only be considered as first order approximations.

BGS seismicity catalogues use Richter local magnitude (M_L), as defined by Richter (1935), as a measure of earthquake size. This takes the form:

$$M_L = \log_{10}(A/A_0) \quad (2)$$

where A is the deflection (centre to peak in μm) registered by an earthquake on a Wood-Anderson seismograph and A_0 is the deflection registered by a "standard" magnitude zero earthquake at the same source distance. Originally this was intended to be an approximate quantification of earthquake size with the attenuation term, A_0 , strictly only applying to California. However this formula and attenuation factor are in worldwide use. Errors in using this formula are claimed by BGS to be $<0.4 M_L$ (Turbitt 1989). Since this relationship is applied to UK seismicity, it is therefore not unreasonable to use the moment-magnitude relationship defined by Thatcher & Hanks (1973) also defined empirically for southern Californian earthquakes, such that:

$$\log_{10}M_0 = 1.5M_S + 16.0 \quad (3)$$

or

$$\log_{10}M_0 = 1.5M_W + 16.1 \quad (4)$$

where M_W is Moment Magnitude (Hanks & Kanamori 1979) and M_S is surface wave magnitude. M_S and M_L are related by a formula of the form:

$$M_S = \alpha M_L + \beta \quad (5)$$

where α and β are constants depending on the physical constraints of the source region. Bungum *et al.* (1991) defined the relationship for the region of the Norwegian continental shelf as being $M_S = 0.85M_L + 0.6$. Over the range $0 < M < 6$, this makes the two magnitude scales broadly coincident, and correspond exactly at $M=4.0$. This is in agreement with the findings of Kanamori (1983) and Scheidegger (1985). As the instrumental catalogues for the UK use Richter Local Magnitude (M_L) equation (3) is used in preference for this study. The inherent assumptions in determining M_L (see above) make the use of equation (3) as relevant as any other (P. Marrow, pers. comm. 1990) and the errors involved in the assumption that $M_S = M_L$ become negligible. Strictly this relationship is only valid for $3.0 < M_L < 6.0$. However it is also used to determine M_0 for $\leq 3.0 M_L$ events. The correctness of this procedure for lower

magnitude events is not of great concern due to the small contribution that such events make to the calculated value of M_0 compared to that of the rarer large events. Thus using this relationship we can calculate the annual seismic moment release rate for the UK knowing the magnitude frequency distributions given in the annual catalogues of seismicity. This gives a clearer picture of the energy released each year due to seismicity and can allow us to make predictions concerning the state of tectonic stress in the continental crust of the UK. It also gives a standardised base with which to compare present seismicity with that in other crustal regions and also with the historical and palaeoseismic records for the same region, to allow an insight into how tectonic stresses are changing with time.

4.7.1 Magnitude-Frequency Relationship

Instrumental data for the period 1969-'88 is plotted as a $\log_{10}(\text{Frequency})$ -Magnitude (Figure 4.7a). It can be seen that there is a broad inverse relationship between frequency and magnitude. There is considerable scatter in the data at the higher magnitudes. This is an inherent factor when dealing with such a small sample population. There is also a distinct drop in the number of events below $1.0 M_L$. This reflects the detection threshold for the UK seismometer network. This data set was also plotted as $\log_{10}(\text{Cumulative Frequency})$ -Magnitude (Figure 4.7b). This is essentially a log-log plot and should show a linear, inverse relationship as predicted by the Gutenberg-Richter equation (1). However it is noted that there is a drop-off in the linearity of the histogram plot at $\leq 1.0 M_L$ and a marked truncation of the data at $\geq 5.4 M_L$. The best fit line through the data set (Figure 4.8b) shows that there is a marked decrease $\geq 4.7 M_L$. As previously stated the former is due to the detection threshold for the UK seismometer network while the drop-off at higher magnitudes is a reflection of the short time span over which the catalogue of instrumental data has been compiled i.e. the time span of recorded seismicity is too short to fully represent the activity at these higher magnitudes. For the cumulative frequency plot (Figure 4.8b) the relationship is defined by the line with the equation $y = 3.9370 - 0.66509x$. This gives Gutenberg-Richter constants of $a=3.9$ and $b=0.67$. The aftershock sequence of the 1984 Lleyn earthquake ($5.4 M_L$) gave values of $a=2.73$ and $b=0.66$ (Marrow & Walker 1988). Events from the adjacent North Sea tectonic province give values in the range $2.8 < a < 4.5$ and $1.12 < b < 1.2$ (Havskov *et al.* 1989). The relatively low b-values for the UK events point to higher stress drops associated with earthquake rupture in an area of relatively strong crust. This is almost definitely the case for the Lleyn event where the hypocentral depth (18 km) and an audible aftershock sequence require a larger stress drop.

The fall-off of the $\log_{10}(\text{Cumulative Frequency})$ -Magnitude plot at $\geq 4.7 M_L$ shows that the catalogue is incomplete over this time span (1969-'88) for events of this magnitude. The sudden cut off at $5.4 M_L$ shows that the return period for events $\geq 5.4 M_L$ is greater than twenty years. To obtain a true picture of the frequency distribution of the higher magnitude events in the UK it is necessary to extend the seismicity record back to historical times.

Seismic moment (M_0) is considered a more accurate measure of earthquake size in that it does not suffer from the problems of saturation of other magnitude scales and, as it is a measure of the energy released during a seismic event, is a more useful parameter with which to compare seismicity from a number of areas or from diverse sources. Seismic moment for instrumental data from the UK is calculated using equation (3) as defined by Thatcher & Hanks (1973). When the total moment release for the period of instrumental seismicity in the UK is calculated it is seen that the small number of large events dominate (Figure 4.9b). The Lleyn event of 1984 ($5.4 M_L$) alone contributes 40% to the total moment release for the twenty year period! Thus it is seen that the contribution of the smaller magnitude events to the moment release is negligible when compared to these rare large events. This is of use when evaluating historical seismicity, as it will only be the larger events that will be recorded by macroseismic means. Therefore if it can be shown that the historical record is complete for events over some arbitrary magnitude, say $4.0 M_L$ for the UK, then if we consider the seismic activity in terms of moment release it is possible to obtain a true picture of the longer term seismic activity in a region. The choice of a threshold magnitude c. $4.0 M_L$ is probably just on the bounds of safety as far as seismic risk studies are concerned as smaller events do not usually pose a risk, unless they occur at exceptionally shallow depths or in areas of poorly engineered structures.

From the catalogued seismic events of the last twenty years we can observe a number of features:

- (1) from 1969 to 1988 a total of 3774 seismic events have been recorded, an average of 189 events per year, including 'coalfield events'.
- (2) from 1979 to 1988 there have been 2942 events, an average of 294 events per year. This apparent increase in frequency of events is a result of increased detection sensitivity of the BGS seismometer network, especially in the range $< 2.0 M_L$, and not due to an increase in seismic strain release. Frequency-magnitude plots for the periods of recorded seismicity pre- and post- 1979 (the time of increased coverage by the UK

seismometer network- Figure 4.3) show a fall-off from linearity $<1.0 M_L$ and $<0.5 M_L$ respectively, showing the increased detection limits for the UK seismometer network over this period (Figure 4.10).

(3) Seismic moment release rate was calculated for the periods 1969-1988, 1969-1978 and 1979-1988 to see if the deficiency in earlier detection limits has any effect on the calculated values of M_0 . Using equation (3) the following values for seismic moment release (M_0) were obtained:

1969 - 1988:	3.15×10^{24} dyne cm	i.e. 1.5×10^{23} dyne cm yr. ⁻¹
1979 - 1988:	1.66×10^{24} dyne cm	i.e. 1.66×10^{23} dyne cm yr. ⁻¹
1969 - 1978:	1.49×10^{24} dyne cm	i.e. 1.49×10^{23} dyne cm yr. ⁻¹

Each time period has a similar total moment release. When averaged over each time interval there is little difference in the annual moment release rate.

(4) The largest recorded onshore event, $5.4 M_L$ at Lley in 1984 gave an energy release of $M_0 = 1.26 \times 10^{24}$ dyne cm i.e. about eight times the annual seismic moment release for the UK.

(5) The calculated seismic moment release rate would only predict a $6.0 M_L$ event every 54 years, assuming no intervening stress release.

(6) The calculated annual seismic moment release rate is $<0.1\%$ of the global total (2.6×10^{26} dyne cm yr.⁻¹) (Johnston 1989) for 'stable continental interiors', and a mere $2.4 \times 10^{-4}\%$ of the total global seismic moment release (The annual M_0 for the UK is 0.04% of that for the 1989 $7.1 M_L$ Loma Prieta earthquake!).

4.7.2 Tectonic Deformation

M_0 is taken to be a measure of crustal deformation and can be related to the slip rate (\dot{s}) along individual faults, or the strain rate ($\dot{\epsilon}$) over a more diffuse area by the equations:

$$\dot{M}_0 = \mu A \dot{s} \quad (6)$$

and

$$\dot{M}_0 = \mu V \dot{\epsilon} \quad (7)$$

where μ is the rigidity modulus of the crustal material (c. 3×10^{11} dyne cm^{-2}), A is the area of the fault plane accommodating the slip, s , and V is the volume of the crustal zone undergoing deformation.

An estimate of the crustal deformation in the UK can be obtained from the relative uplift of Scotland and Northern England compared to the sinking of Southern England. Shennan (1989) has shown that the differential uplift to be of the order of 2.5 ± 1.5 mm yr^{-1} at present. This uplift is, in part, due to the final stages of post-glacial uplift although there may be a strong tectonic factor involved as well (Mörner 1981). If the northern and southern areas of the UK are treated as individual blocks moving relative to each other, with the movement being accommodated along an axis of zero relative uplift, this axis can be treated as a fault. The contour of zero relative uplift runs NE from North Wales through Liverpool to Teeside, a distance of c. 130 km (Shennan 1989 - figure 9). Knowing the relative movement either side of this axis and the dimensions of the axis itself, equation (6) can be used to calculate M_0 and therefore give an estimate of the tectonic moment release rate. The greatest errors in this calculation come from the dimensions of the 'fault plane'. The depth of the seismogenic zone in the UK is poorly constrained. The depth error on even the best located events is ± 2 km (P. Marrow, pers. comm. 1988). Aftershocks of the 1984 Lleyen Peninsula event were located at 19-24 km (Marrow & Walker 1988). Plotting data from BGS seismicity catalogues shows that the majority of events occur in the upper 15 km of the crust (Figures 4.11 & 4.12). Thus taking a depth of 15 km and a length of 130 km the area of the fault plane becomes 1950 km^2 or $1.95 \times 10^{13} \text{ cm}^2$. Thus using equation (6) and the following values

$$\begin{aligned}\dot{s} &= 0.25 \pm 0.15 \text{ cm yr}^{-1} \\ A &= 1.95 \times 10^{13} \text{ cm}^2 \\ \mu &= 3 \times 10^{11} \text{ dyne cm}^{-2}\end{aligned}$$

a value of $1.46 \times 10^{24} \pm 8.8 \times 10^{23}$ dyne cm yr^{-1} is obtained. This is significantly larger than the value obtained by Main & Burton (1984) on account of using a greater value for the depth of the seismogenic zone and also a larger value for the relative uplift. Reading (1991) using a similar procedure, but with an axis length of 100 km, calculated a value of $9 \times 10^{23} \pm 3 \times 10^{23}$ dyne cm yr^{-1} .

Comparing the tectonic moment with the seismic moment shows that only c. 10% of the tectonic activity in the UK occurs seismically. Thus the majority of crustal movement must occur by some aseismic mechanism. This would agree with the

hypothesis that present day uplift is a result of post-glacial rebound, as many long term rebound mechanisms invoke some form of ductile flow of lower or sub-crustal material into the former centre of ice loading with stress transfer into the the upper brittle crust only causing a minor amount of seismic activity in comparison to the total tectonic moment release (Muir Wood 1989b).

As yet there is scant direct tectonic evidence for UK seismicity. Fault plane solutions and accurate locations of aftershock sequences are rare. The best constrained fault plane solutions to date are shown in Figure 4.13. The individual solutions are consistent with a compressive intraplate stress regime. Averaging these as a 'knitting wool' diagram constrains the area within which the maximum horizontal stress (S_H) can lie (Teague *et al.* 1986). This suggests compression in a NW-SE direction ($160 \pm 15^\circ$), in agreement with the results from other stress measurements (Brereton & Müller 1991). Despite this apparent uniformity of the orientation of S_H over the UK there is a suggestion from the fault plane solutions that there is a systematic variation in the stress field. The nodal planes of the events seem to rotate clockwise with increasing latitude. However this remains a speculative observation as the number of observations is not great enough to have any statistical significance. Further data would be required to test the validity of this hypothesis. However shallow stress measurements in Scotland are suggestive of a more WNW-orientated S_H direction (Davenport *et al.* 1989). Regardless of speculation the fault plane solutions agree with the observed stress field for the remainder of NW Europe, showing S_H to be horizontal and orientated approximately NW-SE (Zoback *et al.* 1989).

The Carlisle and Lleyn events are the only two events with sufficient quality of data to allow a detailed insight into the mechanics of UK seismicity (King 1980; Marrow & Roberts 1985; Marrow & Walker 1988). Aftershocks of the Lleyn event define a thick planar zone 1.8 km wide, 4 km long and at a depth of 19-24 km, dipping steeply to the NNE. The zone trends 292° and corresponds to a nodal plane of the main shock focal plane mechanism (dextral strike slip). The Carlisle aftershock sequence defines a planar zone c. 10 km in length at a depth of 4-8 km, trending 236° and dipping steeply to the SW. This also corresponds to one of the main shock (dextral strike slip) nodal planes. The aftershock sequences are thought to define the area of slip during the main shock events. This gives a fault area of 40 km^2 for the Carlisle event and 20 km^2 (volume of 36 km^3) for the Lleyn event. Calculating the seismic moment release from equation (3) and substituting it into equation (6) a value for the slip involved in each event can be calculated from $s = M_0/\mu A$. This gives

values of 1.3 cm for the Carlisle event and 21 cm for the Lley event. The stress drop for such fault movement can be calculated from the formula:

$$\Delta\sigma = 7M_0/16r^3 \quad (8)$$

(Burton & Marrow 1989) where $\Delta\sigma$ is the stress drop and the fault area, $A = \Pi r^2$ i.e. the assumption is that the area of slip on the faults is circular. This gives a value of stress drop of 1.5 bar for Carlisle and 26 bar for Lley. These values are clearly far too small for seismicity of this magnitude, as if this was the case the UK would experience far more earthquakes of this magnitude than it does at present. The small stress drop involved meaning that it would require less strain build-up to trigger seismic activity, hence reducing the return period for events of this magnitude. Macroscopic data from Lley and the calculated b-value for the instrumental period in the UK also suggest that UK seismicity is associated with a larger stress drop. Thus there must be some error in the use of equation (8) to define the stress drop involved in these events or, as is more likely, there is a gross error in the calculation of the fault area involved in the earthquake process due to the location errors for the aftershock sequence.

King (1980) assumed that a stress drop of 30 bar was suitable for the UK. Seismic events are commonly associated with values of $\Delta\sigma$ of 10-100 bar (Kanamori 1978). Main & Burton (1984) proposed a value of 76 bar for intraplate regions. Using the distribution of extreme values over a six year interval of the instrumental record they showed that that ω , the maximum expected magnitude was $5.46 m_b$, where $M_s = 1.93m_b - 4.8$, i.e. $\omega = 5.7 M_s$ or using the equation of Bungum *et al.* (1991) $6.0 M_L$. Using the equation:

$$M_{0\omega} = 10^{A+Bm} \quad (9)$$

with the constants $A=15.7$ and $B=1.5$, the calculated $M_{0\omega}$ was c. 2×10^{24} dyne cm. This was then modelled as movement on a circular fault using the equation of Kanamori & Anderson (1975):

$$M_{0\omega} = C\Delta\sigma_{\max}(l_{\max})^3 \quad (10)$$

where C is a dimensionless constant dependent on the type of fault and l_{\max} is the greatest fault dimension. This gives a fault area of c. 350 km^2 for $\Delta\sigma = 76$ bar. Substituting the above values into equation (6) and using 1.6×10^{23} dyne cm yr⁻¹, a

value of $\dot{s} = 0.15 \text{ cm yr}^{-1}$ is obtained for the typical annual fault movement in the UK. Main & Burton (1984) calculated a value of 0.2 mm yr^{-1} due to using a much smaller moment release rate.

Using the same procedure for the Carlisle event, with $A=16.1$ to correspond to $\Delta\sigma=30 \text{ bar}$ and a moment release rate of $2.2 \times 10^{22} \text{ dyne cm yr}^{-1}$ for an event of $5.0 m_b$ gave a fault area of 1200 km^2 and a slip rate of 0.06 mm yr^{-1} . This gives a fault plane an order of magnitude larger than previously observed. Main & Burton (1984) state that a more realistic picture may be that this represents movement on several fault planes of the order of tens of km^2 , moving at rates of 0.1 mm yr^{-1} as calculated previously. If this was the case it would explain the diffuse distribution of epicentres in earthquake swarms in the UK (e.g. Lleyn aftershock sequence) and also the absence of catastrophic events.

4.8 Historical Seismicity

Before historical seismicity can be used to augment the instrumental record with any degree of confidence, it is important to appraise the accuracy of the data in terms of epicentral locations and magnitude assessments. Location of historical epicentres is complicated by factors such as depth, size of felt area, aftershock activity, local geology and topography, and location of the epicentre in relation to centres of population and areas of sea. In many cases the errors of location are large (Musson 1989) and in these situations where there is some uncertainty as to the exact location of the epicentres it is preferable to assign these events to an epicentral area. In some cases the integrity of the macroseismic information may be suspect (Musson 1990a) and lead to over-estimation of the earthquake size. Scarcity of macroseismic reports, most common in areas of sparse population, such as the Highlands of Scotland, will lead to underestimation of earthquake size. In such areas this may even lead to non-reportage of events.

4.8.1 Compilation and Standardisation of Historical Seismicity Data

There are two main sources of historical seismicity data: Primary sources including newspapers, journals, correspondence, monastic chronicles, estate accounts etc., and secondary sources that comprise early seismicity catalogues.

This present study will make use of the latter source, as it is regarded that these are reasonably complete with regard to larger events. Incompleteness of these records

due to the lack of smaller events recorded is considered to be a negligible factor, especially when comparing the various seismic records in terms of seismic moment, as larger events make a much larger contribution to the annual M_0 value than the multitude of smaller events. As with instrumental seismicity, historical data suffer from the effect of changing thresholds of detection due to factors such as spread of population centres, depopulation (in the case of the Scottish Highlands), increasing literacy and completeness of recording.

A number of catalogues of pre-instrumental seismicity have been compiled for the UK (Davison 1924; Dollar 1951; Musson 1990b). Each catalogue treats the data in a different manner, using a variety of magnitude and/or intensity scales. It is therefore important to standardize these data sets with respect to the parameters that are used to quantify the present day seismicity. As historical data from literary sources comprise the observations of the effects of seismicity of macroseismic data, this needs to be converted into a uniform intensity scale such as Modified Mercalli (MMI) or MSK. Early intensity scales e.g. that of Davison (1924) (Table 4.1) must also be standardised with respect to either MMI or MSK to make the data compatible with that of the instrumental era. Once this has been accomplished the revised intensity values can then be mapped out allowing intensity zones and isoseismals to be assigned to each historical event. The size of the isoseismals can then be used to estimate the magnitude of the event (Mallard 1986; Ambraseys 1988). The magnitude scale used must relate to the high frequency, near field effects of the earthquake. Thus M_w , M_s and M_L are of most use. Conversion of the magnitude values into seismic moment further eases the comparison with the instrumental record.

The location of the epicentres of historical events provides a particular problem. At best it may only be possible to locate an epicentral area (Musson 1989). In an area of moderate to low seismicity, such as the UK, where earthquakes will have small source dimensions, it will be, at best, optimistic to correlate seismic activity with movement along large surface faults (Ambraseys 1988). The greatest location errors are involved in events that occur in sparsely populated areas or occur offshore. The location of epicentres must therefore be qualified in depth and in areal extent. Only with exceptionally good control can they be assigned to individual faults. Many studies of historical seismicity erroneously locate events due to the elongation of isoseismals around a particular fault. This assumes an ideal, homogeneous, linear source. The effects of local geology on amplification of shaking intensities must be considered when evaluating macroseismic data.

The density of population can affect the quality of the macroseismic data. A similar event may seem to give higher shaking intensities in an urban environment due to the effects of seismic shaking on poorly maintained building stock and a 'panic factor' amongst the population that may lead to gross exaggerations of the reported effects of the event, while in a rural setting the small population may preclude the event being felt at all.

The majority of the problems of historical macroseismic data can be overcome by rigorous critical examination of the data and reappraisal of second-hand information.

4.8.2 Historical Seismicity: UK

Macroseismic coverage for the UK extends for c. 700yr. (Mallard 1986; Ambraseys 1988; Muir Wood 1990), although the quality of the data declines markedly prior to 1800 (Lilwall 1976). Previous appraisal of the historical seismicity for the UK (Ambraseys 1985a,b; Ambraseys & Jackson 1985) has shown that since 1247 AD of c. 2000 recorded events there have been no events >5.5 and epicentral intensities have exceeded MSK VII, but not MSK VIII for only four events. The occurrence of damaging events of epicentral intensity VII-VIII for the UK was stated as being $1.2 \times 10^{-4} \text{ yr}^{-1} 10^{-4} \text{ km}^{-2}$ i.e. very low indeed. Using the equation $\log_{10} M_0 = 17.4 + M$ for small seismic events Ambraseys & Jackson (1985) calculated a seismic moment release rate for the UK of $0.9 \times 10^{21} \text{ dyne cm yr}^{-1}$ for the UK between 1247 AD and 1984. For the period 1900 to 1984 they calculated a value of $1.0 \times 10^{21} \text{ dyne cm yr}^{-1}$. For the UK including the immediate offshore regions values of $1.3 \times 10^{21} \text{ dyne cm yr}^{-1}$ and $3.2 \times 10^{21} \text{ dyne cm yr}^{-1}$ were calculated for the same time periods respectively. The factor of three increase in the short term record for the UK and offshore area is attributed to the incomplete nature of the seismicity record for the North Sea prior to 1700.

4.8.3 Historical Seismicity UK: 1700-1990.

This present study makes use of the catalogue of Musson (1990b) that extends for 290 yr BP. and catalogues events of $4.0 M_L$ and greater. The lack of events $<4.0 M_L$ is considered insignificant in terms of seismic moment release (see Figure 4.9a) and therefore the catalogue is considered as complete as possible for the time period concerned.

The data is plotted as $\log_{10}(\text{Frequency})$ -Magnitude (Figure 4.14a). As with the instrumental data there is considerable scatter in the data, but again there is a crude inverse relationship between frequency and magnitude. This is seen more clearly by plotting the data as $\log_{10}(\text{Cumulative Frequency})$ -Magnitude (Figure 4.14b). As this is a log-log plot it should show an inverse linear Gutenberg-Richter relationship. However there is a noted drop-off at higher magnitudes ($\geq 5.2 M_L$). The best fit line through the data set (Figure 4.8a) shows that there is a similar pattern to that observed in the instrumental record with a fall-off from the ideal line at lower magnitudes, $\leq 4.4 M_L$, and at higher magnitudes, $\geq 5.2 M_L$. The lower bound represents the detection threshold for the pre-instrumental period, while the upper bound shows that the 290 year period is of insufficient length to fully represent events of these magnitudes. The cut off at $5.6 M_L$ shows that the return period for events of this magnitude is greater than than 290 years or that the crust in the UK is incapable of generating seismicity of this magnitude.

The cumulative frequency plot (Figure 4.8a) defines a line $y = 6.1588 - 0.96985x$. This give Gutenberg-Richter constants of $a=6.2$ and $b=0.97$. The b -value is c. 33% greater than that for the instrumental period. This possibly points to a lower stress drop associated with this period of seismicity. However it should be noted that this b -value has been calculated from a restricted data set (4.0 - $5.6 M_L$) and the correlation coefficient for the best fit line is significantly lower than that for the instrumental data set (Figure 4.8). Thus this higher value may be a manifestation of an incomplete data set. There is no independent geological evidence to suggest that there has been a change in the seismic stress drop in the last 300 years.

Seismic moment for this period is calculated using equation (3). This gives a total moment release of 2.69×10^{25} dyne cm, or a release rate of 9.3×10^{22} dyne cm yr⁻¹. This differs only slightly from the value obtained by Reading (1991) using the relationship $\log_{10} M_0 = A + Bm$, where $A=9.0$ and $B=1.5$. The value for the moment release rate is two orders of magnitude greater than that calculated by Ambraseys & Jackson (1985). This is probably due to the catalogue of Musson (1990b) including offshore events in the area 10°W to 5°E and 49°N and 62°N . However when this result is compared to that of Ambraseys and Jackson (1985) for the UK and offshore area it is still two orders of magnitude greater. This can probably be explained in terms of the relative completeness of the catalogues used. The catalogue of Musson (1990b) extends for only 290 years, approximately the limit of good quality data for the whole of the UK, while Ambraseys & Jackson (1985) use a catalogue extending for 737 years, and therefore will have a much less complete

picture of the seismic activity over the earlier part of this period. Although it is likely that both catalogues do represent a true distribution of events in the higher magnitude ranges (as these events would have been expected to have been felt over a much larger area), as the catalogues extend back in time a reduction in the population and the lack of written chronicles in certain parts of the country would have made it possible to miss a number of intermediate sized events, especially if these were at relatively shallow hypocentral depths and therefore subject to greater attenuation. This is a problem that will increase with the increasing age range of the catalogue. Even over the relatively short time span of Musson's catalogue Reading (1991) has shown that there is a marked increase in the frequency of occurrence of events of all magnitudes. This represents an increasing awareness of earth science over this time period. Thus the problem of detection thresholds is seen to increase with age. This creates a far greater problem than in the instrumental record as in the pre-instrumental period it is possible that a significant number of moderate events are not being recorded, hence giving an anomalously low value for the moment release rate.

Comparison with the instrumental record shows that the moment release rate for the historical period is about 60% of that calculated from present day seismicity. From the macroseismic reports of historical seismicity there is no evidence to suggest that there is any change in the pattern of seismic strain release in the UK between the two data sets. Of important note is the lack of historical seismicity in the Highlands of Scotland in comparison to the present day seismic activity. Historical seismicity data for the Highlands of Scotland seems to be a function of the distribution of population centres at that time. The majority of the activity is seen to be proximal to towns such as Inverness, Fort William and Oban. It is possible that a large number of events located at present day seismic centres such as Kintail and Ullapool were not recorded due to either the sparse nature of the population distribution, much of which was illiterate and had an oral tradition subsequently destroyed during the 'Highland Clearances' and disruption of the Clan system from the late 1700s to the late 1800s (Prebble 1963). Also many events may have gone unnoticed due to the tendency to explain many geological 'events' in terms of folk lore and superstition (Smith 1953).

Whatever the cause, there is a marked deficiency in the historical record when compared to the instrumental period. Assuming a present day moment release rate of 1.6×10^{23} dyne cm yr⁻¹ had acted for the previous 290 years, the total moment release over this period would have been of the order of 4.64×10^{25} dyne cm. However there is no macroseismic evidence to suggest a lower rate of seismic activity in the previous two centuries. To the contrary the historical record has accounts of ground disruption

far greater than anything reported accompanying present day seismicity. In Scotland there are three reports of ground deformation associated with historical seismic events:

- 23/10/1839. The Comrie earthquake (I_D VIII, Davison's Intensity: see Figure 14) caused fissures in the ground up to 180 m long at Amulree, 16 km north of Comrie.
- 30/4/1921. Sand and gravel embankments were caused to collapse due to an event of I_D IV.
- 16/8/1934. At Dornoch the ground was fissured and disturbed at several locations by an event of I_D VI.

Further evidence for widespread earthquake damage is given in the reports of the Colchester earthquake of 1884 ($4.7 M_L$), the contender for Britain's only 'catastrophic event' (Musson 1990a). Another possible ground rupture accompanying a seismic event was reported from Barrow-in-Furness in the last century (Muir Wood 1990). There are no reports of ground rupture associated with seismic activity in the instrumental record. Thus it is concluded that the apparent shortfall in the seismic activity in the historical record is a manifestation of the incomplete nature of the record and certainly does not seem to point to an increasing rate of seismic moment release in the UK at present.

4.9 Palaeoseismicity

Palaeoseismicity is the study of the age, frequency and size of prehistoric earthquakes (Crone 1987). This allows an expanded view of the behaviour of seismicity from the rather limited view provided by instrumental and historical seismicity. This involves the detailed examination of fault zone stratigraphy, mapping of deformation features such as soft sediment liquefaction, slope failures and various forms of ground rupture attributed to the action of seismic ground shaking. The crux of palaeoseismic investigations is the reliable and consistent age control for the identified seismic events. Most palaeoseismic studies are limited to the Quaternary era on account of the relatively good stratigraphic control on events during this time. Naturally, the errors in age estimation increase with age, therefore it is usually not of use to extend studies beyond this rather arbitrary temporal limit. This longer term study of the frequency of seismic activity will show any differences in the long and

short term behaviour of faults and seismicity, whether activity is regular, occurs as clustered events or shows some long term temporal variation.

Palaeoseismic data for the UK is sparse. The present data base is mainly the result of two specific studies into post-glacial fault activity in the Highlands of Scotland (Ringrose 1987; Fenton 1991). This has involved the mapping of faults displaying late Quaternary offset and the mapping of deformation features shown to be due to seismic activity attendant with such fault activity (Figure 4.15). The present data set is biased towards the Western Highlands. However, as this is thought to have been tectonically the most active area in mainland UK in the last 10 kyr, it is considered that the present data set is considered to be representative of the seismic strain release in the the UK as a whole at this time.

To date more than twenty incidences of post-glacial fault activity have been identified from Scotland. A number of fault scarps, considered to be post-glacial in origin, have been described from the west of Ireland (Mohr 1986). These have yet to be conclusively confirmed as being late Quaternary in age (B.E. Leake, pers.comm. 1990), and are therefore not considered in this study.

The data concerning post-glacial fault movements and seismicity in Scotland consist of information on fault offset, rupture length, areal extent of seismic liquefaction features, distribution of seismically-induced slope failures, approximate or absolute age of fault movement and fault orientation (Table 4.2).

4.9.1 Palaeoseismic Magnitude Calculations

From comparison with data sets of present day seismic deformation features and the empirical and statistical relationships defined between fault dimensions and distribution of deformation features and magnitudes (usually M_S) each palaeoseismic event was assigned a magnitude value, with where possible appropriate error bounds. The methods of magnitude assignation to palaeoseismic events is discussed below.

(i) Fault Offsets

Magnitude was assigned on the basis of fault rupture length and the amount of offset. Where possible the amount of offset in individual events was discerned and if this was not possible the seismic moment release rate was calculated from the cumulative offset using equation (6). The statistical relationships between fault dimensions and instrumental M_S values defined by Bonilla *et al.* (1984) allowed the additional parameter of type of fault movement to be used in discerning palaeomagnitudes while

the relationship defined by Khromovskikh (1989) only considers the physical fault parameters in the equation:

$$M = (5.45 \pm 0.28) + (1.25 \pm 0.19) \log_{10} L \quad (11)$$

where L is the surface rupture length in kilometres.

(ii) Liquefaction

Liquefaction has received more research than any other earthquake-induced deformation feature, hence the statistical relationships between earthquake magnitude and the area affected by liquefaction have become very sophisticated, and usually site specific for the areas of study. Two relationships were chosen to represent upper and lower bound estimates for palaeomagnitude attributable to the distribution of liquefaction. These are based on worldwide data sets and do not suffer from the failings of relationships defined from site specific studies. These are the equation defined by Youd (1977):

$$\log_{10} R = 0.88M - 4.4 \quad (12)$$

where R is the distance from the earthquake epicentre to the point of furthest liquefaction. The other equation is that of Kuribayashi (in Ambraseys 1988):

$$\log_{10} R = 0.74M - 3.4 \quad (13)$$

It should be noted that liquefaction does not occur at magnitudes $< 5.0M$ (Kuribayashi & Tatsuoka 1975; Keefer 1984b).

(iii) Slope Failures

Slope failures are the most ubiquitous deformation features associated with seismic activity. Keefer (1984a,b) showed empirical relationships between the area affected by slope failures and the maximum distance from the epicentre to differing types of slope failure for earthquakes of differing magnitude (Figure 4.16). It is also seen that there are threshold magnitudes below which no slope failure is involved.

4.9.2 Magnitude Errors

The assignment of palaeomagnitudes by the analysis of ground deformation, by its very nature, contains large errors. Individual fault movement increments can be

difficult, if not impossible, to distinguish. Therefore, in many cases the observed offsets are considered to have occurred as single events despite the lack of evidence to prove this. This is assumed unless there is reason to believe that this is not the case, for example in the case of the large lateral offset along the Kinloch Hourn Fault where individual movement increments cannot be discerned but it is obvious that >100 m lateral movement could not have occurred as a single event. Likewise rupture length for individual palaeoseismic events can be impossible to discern. Thus the rupture lengths quoted are assumed to have been created during a single event. If more than one fault movement episode is observed it is assumed that each movement increment ruptured the same length of fault segment. From the known geometries of fault ruptures surface rupture length will only give a rather conservative estimate of the true size of the fault segment involved in a particular event (Sibson 1989). Magnitudes assigned from fault offset parameters are given in surface wave magnitudes and the spread of values is due to the statistical uncertainties discussed by Bonilla *et al.* (1984) and Khromovskikh (1989). Palaeomagnitudes assigned from the distribution of ground deformation features are considered to be lower bound estimates for the following reasons:

(i) the difficulty in attributing slope failures to seismicity, let alone to any particular seismic event, has meant that the areal extent of slope failures definitely caused by seismic activity is probably an underestimation of the degree of deformation as many ambiguous slope failures of uncertain origin tend to be ignored. This is particularly the case for rockfalls, the most common type of failure occurring during seismic shaking (Keefer 1984), usually over very large areas in comparison to other types of failure. Unfortunately rockfalls also occur in many other geological environments, especially during periods of periglaciation, and therefore it is impossible to discern unequivocally the cause of their occurrence. They have therefore been universally ignored in this study.

(ii) seismically-induced liquefaction occurs in very specific environments and materials. Its occurrence is dependent on grain size, water content and a number of other factors, and is therefore not universally present with seismic activity. In addition the Quaternary deposits of Scotland are not prone to liquefaction; there are only rare pockets of sediments that have the potential to become liquefied under seismic ground acceleration. Also lacustrine sediments, needed to satisfy the conditions of seismic liquefaction proposed by Sims (1975), are extremely rare. Thus the distribution of liquefiable sediment rather than the size of the earthquake may control the distribution of the deformation features noted.

In order to standardise the palaeoseismic record it is necessary to convert palaeomagnitudes into seismic moment using equation (3). In addition it is possible to estimate seismic moment from equation (6) when sufficient fault dimension data are known. This allows the two methods of moment calculation to be compared.

4.9.3 Palaeoseismicity: North & West Scotland.

Merely by inspection, the seismic activity in the immediate post glacial period was substantially greater than that presently experienced in the UK (Table 4.2). The largest events in the instrumental and historical periods are 5.4 M_L and 5.6 M_L respectively. The palaeoseismic record shows numerous events that exceed this magnitude, a significant number being as large as 6.0-7.0 M_S . At present moment release rates for the UK, the largest palaeoseismic events represent almost 2×10^3 yrs. of seismic strain accumulation.

The incomplete nature of the palaeoseismic record makes the construction of a magnitude-frequency relationship meaningless. However it is noted that the majority of the events are found in the range 5.6-6.4 M_S with decreasing frequency at lower and higher magnitudes. The nature of the methods used to assign magnitudes to palaeoseismic events means that the smallest event likely to be unequivocally distinguished will be in the region of 5.0 M_S (The landslide relationships cover events as small as 4.0 M_S , however this is merely a reflection on the handling of the data set, and does not reflect an accurate representation of the distribution of slope failures at such small magnitudes).

To gauge as accurate as possible a picture of the seismic activity at this time the palaeomagnitudes were converted into seismic moment release using equation (3). This gave a value for the total moment release for the palaeoseismic catalogue of $1.53 \times 10^{27} \pm 1.2 \times 10^{27}$ dyne cm. If this is averaged out over the time interval over which the fault activity is thought to have occurred i.e. 10.3-6 kyr BP. (4.3 kyr) the average moment release rate becomes $3.6 (\pm 2.8) \times 10^{23}$ dyne cm yr⁻¹. This is up to four times the present rate of seismic strain release in the UK. However if the total moment release is averaged over a shorter time span, for example 2 kyr, as would be a more realistic picture of post glacial fault activity, the average moment release rate becomes $7.65 (\pm 6.0) \times 10^{23}$ dyne cm yr⁻¹, up to eight times the present seismic moment release rate. Reading (1991) using the same data set calculated the moment release rate for this period to be in the range $5.6 \times 10^{22} - 5.6 \times 10^{23}$ dyne cm yr⁻¹.

To check the validity of the above moment release values for the post glacial palaeoseismic period, moment release was calculated using equation (6) for those faults where both the fault rupture area and the cumulative offset is known. This was calculated for shallow focus events, $d \leq 5$ km, as it is thought that the majority of rebound faulting occurs at this depth [§ 6, p260] and also for the full depth of the seismogenic zone in the UK, $d \leq 15$ km. These values were chosen to give minimum and maximum bound estimates for this calculation. This calculation gave values of 4.2×10^{27} dyne cm and 1.3×10^{28} dyne cm respectively. Even if all fault movement was accommodated in the upper 5 km of the crust, the moment release value is 35% greater than that calculated from the sum of the seismic events. The apparent difference between the two estimates of moment release could be explained by a number of hypotheses:

(i) One or both calculations are in error. This is not disputed as the errors in magnitude assignment are compounded when these palaeomagnitudes are then converted into values for M_0 using equation (3). However the difference in the two estimates of M_0 is greater than the sum of the errors from the original magnitude calculations.

(ii) Many palaeoseismic events have not been recorded. Again this is not in dispute due to the known incompleteness in the palaeoseismic record. It is possible that a number of large events c. 6.0 M_S have not been identified from the area already investigated due to their effects having been masked by later or larger events on the same faults. It is also possible that if the seismic events have a shallow focal depth that they will be attenuated to such a degree that the deformation will only be of local extent, giving anomalously low magnitude estimates.

(iii) All of the area of rupture noted may not have been involved in seismic slip. There may have been a significant degree of aseismic slip due to the effects of transient high fluid pressure levels thought to have been present at this time acting to lubricate the fault planes (Muir Wood 1989b) [§ 6, p260].

Whatever the reason for the difference between the two calculated values of total M_0 it is clear that the level of seismic activity was significantly greater than that experienced at present. Despite the limitations of a quantitative analysis of palaeoseismic data it is clear that the seismotectonic regime in the Highlands of Scotland has undergone significant change in the last 10 kyr. Moment release rate has decreased significantly and the crustal depth of seismic rupture has also shown substantial change - no instrumental events are known to have resulted in ground

rupture, although a few historical events have been documented with associated ground disruption, although not necessarily of fault rupture [§ 4.8.3, p168], whereas the majority of the palaeoseismic record is based on evidence of surface fault rupture.

4.10 Palaeoseismotectonics

Field data concerning fault geometry and offset were used to create fault plane solutions for individual palaeoseismic events using the *FOCL* code at Edinburgh University (Reading 1991). The data were graded according to completeness in defining the fault plane: if two parameters were missing then the fault plane solution was not able to be drawn. If one parameter was missing then it was inferred from the nature of neighbouring faults that were completely defined. Those faults that were completely defined are represented by the larger symbol in Figure 4.17. Only the completely defined solutions (1, 11, 18 & 19 in Figure 4.17) were plotted as a composite plot to define the P and T axes (S_H and S_h directions respectively). The composite plot defines the direction of S_H as lying $045^\circ \pm 10^\circ$. This is markedly different from the present direction of maximum horizontal stress as defined by both focal plane solutions (Figure 4.13) and borehole breakouts (Zoback *et al.* 1989; Brereton & Müller 1991). The regional stress system is thought to have been active since the late Miocene and there is no geological evidence to suggest that there has been any significant rotation of the stress field since that time (Muir Wood 1989a, 1990). The apparent rotation of the stress regime in the early part of the Holocene could be the result of a number of factors:

- (i) The fault pattern observed is the result of radial strain recovery following deglaciation (Adams 1989).
- (ii) The faults were not subject to the same stress regime.
- (iii) The assumptions in assigning fault plane solutions are flawed.
- (iv) The stress regime has altered with time.
- (v) The faults were not reactivated at the same time.

If fault reactivation represented a radial pattern of strain recovery it would be expected that fault movement would be parallel or sub-parallel to the former ice front margins and that the type of fault movement would be compressional adjacent to the

ice margins and extensional in the region of the predicted forebulge (Adams 1989). This is seen not to be the case in Scotland where many of the faults are perpendicular to the ice front and display strike slip movement for extended periods of time (Ringrose 1987; 1989b; Davenport *et al.* 1989) [§ 2, p15]. Thus it is considered that the late Quaternary fault reactivation seen in Scotland is not the result of radial strain recovery due to deglaciation.

That the faults were not subject to the same stress regime has been shown to be an invalid argument [§ 6, p260]. It is known that late Quaternary fault reactivation was the result of a NW-SE regional tectonic stress field enhanced by the effects of late Devensian glacial loading. Although there were local perturbations in the stress field due to the effects of differential ice thickness and basal ice melt fluid recharge, there was no regional rotation of the principal stress directions. It is also thought that the stress field was broadly uniform across the whole of northern Scotland at this time.

The fault plane solutions assigned to the palaeoseismic data set were ranked according to the quality of the data and as a consequence only four were used to construct the composite plot (Figure 4.17). Each of these has assumed that the fault planes were vertical. From fault scarps and surface exposures of the fault zones themselves this is not the case, although the fault planes dip steeply, $>80^\circ$. This error is insufficient to explain the inconsistencies in the resultant plot with respect to the known direction of the stress system at this time. However it should be noted that the four fault plane solutions represent four faults where the data is for cumulative offset that possibly occurred over a protracted period of time. Therefore it is considered from this, and evidence of age-dating studies on other late Quaternary faults in Scotland (Ringrose 1987, 1989b) [§ 2, p15; § 6, p260], that fault movement was not contemporaneous, but occurred over an extended period of time and was not confined to the immediate post glacial period. Thus these focal plane mechanisms are not a true reflection of post-glacial seismotectonic activity, but are a cumulative estimate of displacement over an unknown period of time.

It should also be noted that the effects of glacio-isostatic rebound in triggering fault activity decays rapidly with time, so that from an initial state of rapid relief of vertical glacial-induced stresses where faults of various orientations can be reactivated as 'pop-ups', the stress system becomes one where tectonic stresses begin to dominate such that only the most ideally orientated faults will be reactivated [§ 6.13, p283]. The stress drop from an early burst of seismic activity will quickly remove the greater effects of glacially-induced stresses. This, in conjunction with the effects of falling

crustal fluid pressure causing greater friction across fault planes, will cause subsequent events to require a larger stress build-up to trigger seismic activity, hence increasing the return period for the generation of large, damaging earthquakes. This would explain the rapid burst of seismicity in the period 10.3-6 kyr BP. followed by decreasing activity throughout the Holocene to the present day levels as the effects of glacio-isostasy become negligible in comparison to the contribution from the ambient tectonic stress field. From studies of uplift rates in Fennoscandia it is seen that the rate of glacio-isostatic uplift peaks during and immediately after deglaciation and then decreases exponentially until it is replaced by a linear tectonic uplift c. 6 kyr BP. (Mörner 1981). A similar pattern is seen from shoreline uplift in the UK (Haggart 1989; Shennan 1989). Thus it is seen that the Holocene stress system is dynamic, decreasing in magnitude from 10 kyr BP to present and may not have been subject to significant rotation as suggested by palaeoseismic fault plane solutions. This may merely be the result of stress relief being accommodated along pre-existing faults, this in turn controls the type of fault movement therefore the fault plane solutions are a reflection of the ease of reactivation and not a true reflection of the stress system orientation at this time.

Using a similar procedure to that used for present day uplift data, the tectonic moment can be calculated for the post glacial period using the available data for shoreline uplift rates. For the period 9.6-6.5 kyr BP the maximum uplift was c. 10 m at a rate of 3.2 mm yr^{-1} (Ringrose 1987). In light of the data from Fennoscandia and that for subsequent periods in the post-glacial in Scotland (see below) this seems to be a very conservative estimate. Mörner (1981) shows that uplift at this time would be c. 10 cm yr^{-1} . This in turn seems rather high, especially in light of the current tectonic uplift rates in the Himalaya. The true value of uplift in the UK in the immediate post-glacial period is more likely to be of the order of c. 10 mm yr^{-1} . Using equation (6) and an axis area similar to that used for the calculation of the present tectonic moment, i.e. $1.95 \times 10^{13} \text{ cm}^2$, this gives a value for the tectonic moment in the period 9.6-6.5 kyr BP of $1.7 \times 10^{24} \text{ dyne cm yr}^{-1}$. Using the uplift rates of Mörner (1981) this increases to $5.3 \times 10^{25} \text{ dyne cm yr}^{-1}$. This would mean that only c. 38% of the tectonic strain at this time was released seismically (only 1.2% using the uplift rate of Mörner 1981). This is greater than the percentage of tectonic moment presently released by seismicity. However if the figure calculated from the uplift rates from Fennoscandia is thought to be correct such a small release of seismic strain agrees with the models of ductile lower and sub crustal flow in response to glacio-isostatic rebound (Muir Wood 1989b). For the subsequent periods where the uplift rates have been calculated, the calculated tectonic moment release rates are:

6.5-4.0 kyr BP	$\dot{s} = 5.2 \text{ mm yr}^{-1}$	$M_O = 3 \times 10^{24} \text{ dyne cm yr}^{-1}$
4.0-2.5 kyr BP	$\dot{s} = 4.0 \text{ mm yr}^{-1}$	$M_O = 2.3 \times 10^{24} \text{ dyne cm yr}^{-1}$

This shows that as recently as 2 kyr BP the UK was subject to twice the present rate of tectonic moment release rate. This is reflected by the movement along the Kinloch Hourn Fault that has occurred since 2400 ± 50 yr BP (Ringrose 1989b). Total uplift of the Main Late Glacial Shoreline of c. 48.5 m since 10 kyr BP gives a total tectonic moment for the Holocene of 2.84×10^{28} dyne cm. Over this period less than 10% of this strain has been released seismically.

4.11 Conclusions

Present day seismic activity in the UK is seen to be low in comparison to that of plate margin environments, however it is not entirely insignificant. Historical data show that the seismotectonic province of the UK and the surrounding continental shelf is capable of generating moderately sized earthquakes that may cause ground rupture and extensive damage to poorly engineered structures. Palaeoseismic investigations have revealed that during the early part of the Holocene the UK suffered enhanced seismic activity due to the effects of post glacial isostatic rebound, with events as large as $7.0 M_S$ as opposed to $5.4 M_L$ and $5.6 M_L$ for the largest instrumental and historical events respectively. There has been a reduction in both the seismic moment release rate and the total tectonic moment rate, as revealed by decreasing uplift rates (from c. 10 mm yr^{-1} 10 kyr BP to c. 2.5 mm yr^{-1} at present), during the last 10 kyr to reach the present levels. This is due to the decreasing influence of post glacial isostatic rebound as glacially-induced stresses decrease with time and become subordinate to the ambient tectonic stresses.

It has been demonstrated that palaeoseismic investigations, even in an area with a poorly developed Quaternary stratigraphy such as Northern Scotland, can provide a valuable extension to the short-term window of seismic activity provided by instrumental and historical seismic data, contrary to previously held beliefs as to the use of such studies in the investigation of seismicity (Mallard 1986). This allows an important insight into the temporal variations of seismic behaviour that are not seen in the shorter term records. Such a long term view of the seismotectonics of a region allows more confidence to be placed on forecasts and risk assessment studies.

From the largest earthquakes known to have occurred in the region surrounding the North Sea (the North West Europe seismotectonic province) (Table 4.3) it is seen

that the seismic risk for the region is far from insignificant. If the North Sea is undergoing a renewed period of extension as proposed by Thorne & Watts (1989), then the associated increased tectonic strain rates will lead to an increase in the frequency of damaging seismicity. In the absence of this occurrence the greatest risk posed to the UK from seismic activity is from a shallow focus event in the region of 5.0 M_L occurring adjacent to a population centre. Nor is the risk of ground deformation/rupture negligible: this has grave implications for the nuclear fuels industry which is particularly concerned with this occurrence (Dames & Moore 1990).

In the context of North Sea seismotectonics the greatest risk is posed by offshore events triggering a failure similar to the Storregga slide (Dawson *et al.* 1988). This caused a tsunami wave that affected the whole of the North Sea coast. The profusion of offshore installations in the North Sea would make this a disaster in terms of human life and also financially for the countries whose economies depend on the production of oil.

Future refinement of the understanding of the seismotectonic regime of the UK and N.W. Europe relies on the collation of seismic data from a number of sources. Seismology and geodesy will allow an accurate picture of the short term behaviour of seismic activity. Particularly microseismic networks and increased computation of fault plane solutions will allow a better understanding of earthquake rupture processes and the faults currently accommodating strain in an otherwise tectonically 'quiet' region. Palaeoseismology will remove the dependency on the short term record allowing a better insight in to the long term behaviour of seemingly erratic 'passive' margin seismotectonics.

4.12 Acknowledgements

This work was carried out at the Department of Applied Geology, University of Strathclyde and the Department of Geology & Applied Geology, University of Glasgow while in receipt of NERC studentship GT4/87/GS/107. The staff of the BGS Global Seismology Unit, especially P. Marrow, R. Musson and T. Turbitt, are thanked for providing data and advice. W. Aspinall is thanked for useful discussion concerning microseismicity. J.J. Doody enlightened the author with some basic concepts of seismology. A. Reading is especially thanked for the assignment of focal plane mechanisms to the palaeoseismic data. The comments of I. Allison greatly improved an earlier version of this manuscript.

4.13 References

- Adams, J. 1989.** Postglacial faulting in eastern Canada: nature, origin and seismic hazard implications. *Tectonophysics* 163, 323-331.
- Allen, C.R. 1975.** Geological criteria for evaluating seismicity. *Geol. Soc. Am. Bull.* 86, 1041-1057.
- Allen, J.R.L. 1986.** Earthquake magnitude-frequency, epicentral distance, and soft-sediment deformation in sedimentary basins. *Sedimentary Geology* 46, 67-75.
- Ambraseys, N.N. 1985a.** Magnitude assessment of northwestern European Earthquakes. *Earthquake Engineering & Structural Dynamics* 13, 307-320.
- Ambraseys, N.N. 1985b.** Intensity attenuation and magnitude-intensity relationships for northwest European earthquakes. *Earthquake Engineering & Structural Dynamics* 13, 733-778.
- Ambraseys, N.N. 1988.** Engineering Seismology. *Earthquake Engineering & Structural Dynamics* 17, 1-105.
- Ambraseys, N.N. & Jackson, J.A. 1985.** Long-term seismicity of Britain. *in Earthquake engineering in Britain.* 49-66, Thomas Telford, London.
- Amick, D. & Gelinis, R. 1991.** The search for evidence of large prehistoric earthquakes along the Atlantic seaboard. *Science* 251, 655-658.
- Aspinall, W. 1991.** Sunbury-on-Thames.
- Bäckblom, G. & Stanfors, R. (eds.) 1989.** Interdisciplinary study of post-glacial faulting in the Lansjärv area northern Sweden 1986-1988. SKB Technical Report 89-31.
- Bonilla, M.G., Mark, R.K. & Lienkaemper, J.J. 1984.** Statistical relations among earthquake magnitude, surface rupture length and surface fault displacement. *Bull. Seism. Soc. Am.* 74, 2379-2411.

Brereton, R. & Müller, B. 1991. The European stress map. Royal Society Discussion Meeting *on Origin and Distribution of Tectonic Stress in the Lithosphere*, London, April 1991.

Bungum, H., Alsaker, A., Kvamme, L.B. & Hansen, R.A. 1991. Seismicity and seismotectonics of Norway and nearby continental shelf areas. *J. Geophys. Res.* 96B, 2249-2265.

Burton, P.W. & Marrow, P.C. 1989. Seismic hazard and earthquake source parameters in the North Sea. *in* S. Gregerson & P.W. Basham (eds.). 1989. *Earthquakes at North Atlantic Passive Margins: Neotectonics and postglacial rebound.* 633-664. Kluwer Academic Publishers, Amsterdam.

Burton, P.W. & Neilson, G. 1979. Earthquake swarms in Scotland. *Forth Naturalist & Historian* 4, 3-26.

Burton, P.W. & Neilson, G. 1980. Annual catalogues of British earthquakes recorded on LOWNET (1967-1978). *Seismic Bull. No. 7*, Inst. Geol. Sciences, London.

Crone, A.J. (ed.) 1987. Proceedings of conference XXXIX - Directions in palaeoseismology. USGS Open File Report 87-673. 463pp.

Dames & Moore 1990. Report of a meeting on "Fractures and fracture development". DOE Report No. DOE/RW/90.014. Dames & Moore International Technical Report TR-D&M-17.

Davenport, C.A., Ringrose, P.S., Becker, A., Hancock, P. & Fenton, C. 1989. Geological investigation of late and post glacial earthquake activity in Scotland. *in* S. Gregerson & P.W. Basham (eds.). 1989. *Earthquakes at North Atlantic Passive Margins: Neotectonics and postglacial rebound.* 175-194. Kluwer Academic Publishers, Amsterdam.

Davison, C. 1924. A history of British earthquakes. Cambridge University Press.

Dawson, A.G., Long, D. & Smith, D.E. 1988. The Storregga slides; evidence from eastern Scotland for possible tsunami. *Marine Geology* 82,

Dollar, A.J.J. 1951. A catalogue of Scottish earthquakes, 1916-1949. *Trans. Geol. Soc. Glasgow* 21, 283-361.

Doornkamp, J.C. 1986. Geomorphological approaches to the study of neotectonics. *J. Geol. Soc. London.* 143, 335-342.

Fenton, C.H. 1991. Neotectonics and palaeoseismicity in North West Scotland. Unpubl. Ph.D. Thesis, University of Glasgow.

Gutenberg, B. & Richter, C.F. 1944. Frequency of earthquakes in California. *Bull. Seism. Soc. Am.* 34, 185-188.

Haggart, B.A. 1989. Variations in the pattern and rate of isostatic uplift indicated by comparisons of Holocene sea-level curves from Scotland. *J. Quaternary Sci.* 4, 67-76.

Hanks, T.C. & Kanamori, H. 1979. A moment magnitude scale. *J. Geophys. Res.* 84B, 2348-2350.

Havskov, J., Lindholm, C.D. & Hansen, R.A. 1989. Temporal variations in North Sea seismicity. *in* S. Gregerson & P.W. Basham (eds.). 1989. Earthquakes at North Atlantic Passive Margins: Neotectonics and postglacial rebound. 413-427. Kluwer Academic Publishers, Amsterdam.

Illies, J.H. & Greiner, G. 1978. Rheingraben and Alpine system. *Bull. Geol. Soc. Am.* 89, 770-782.

Illies, J.H., Baumann, H. & Hoeffers, B. 1981. Stress patterns and strain release in the Alpine foreland. *Tectonophysics* 71, 157-172.

Johnston, A.C. 1989. The seismicity of "Stable Continental Interiors". *in* S. Gregerson & P.W. Basham (eds.) Earthquakes at North Atlantic Passive Margins: Neotectonics and postglacial rebound. 299-327. Kluwer Academic Publishers, Amsterdam.

Johnston, A.C. & Kanter, L.R. 1990. Earthquakes in stable continental crust. *Scientific American* 262,42-49.

- Kanamori, H. 1978.** Quantification of earthquakes. *Nature* 271, 411-414.
- Kanamori, H. 1983.** Magnitude scale and quantification of earthquakes. *Tectonophysics* 93, 185-199.
- Kanamori, H. & Anderson, D.L. 1975.** Theoretical basis of some empirical relations in seismology. *Bull. Seism. Soc. Am.* 65, 1073-1095.
- Keefer, D.K. 1984a.** Landslides caused by earthquakes. *Bull. Geol. Soc. Am.* 95, 406-421.
- Keefer, D.K. 1984b.** Rock avalanches caused by earthquakes: source characteristics. *Science* 223, 1288-1289.
- Khromovskikh, V.S. 1989.** Determination of magnitudes of ancient earthquakes from dimensions of observed seismodislocations. *Tectonophysics* 166, 269-280.
- King, G. 1980.** A fault plane solution for the Carlisle earthquake, 26 December 1979. *Nature* 286, 142-143.
- Kuribayashi, E. & Tatsuoka, F. 1975.** Brief review of liquefaction during earthquakes in Japan. *Soils & Foundations* 15, 81-92.
- Leake, B.E. 1990.** Department of Geology & Applied Geology, University of Glasgow, Glasgow G12 8QQ.
- Lilwall, R.C. 1976.** Seismicity and seismic hazard in Britain. *Seism. Bull. Inst. Geol. Sci.* No.4.
- Main, I.G. & Burton, P.W. 1984.** Physical links between crustal deformation, seismic moment and seismic hazard for regions of varying seismicity. *Geophys. J. R. astr. Soc.* 79, 469-488.
- Mallard, D.J. 1986.** The investigation of historical earthquakes and their role in seismic hazard evaluation for the UK. IAEA Specialist Meeting on Ground Motion and Anti-seismic evaluation of Nuclear Power Plants, March 1986, Moscow.

- Marrow, P.C. & Roberts, G. 1985.** Focal mechanisms of aftershocks of the 1979 Carlisle earthquake: a re-interpretation. *Geophys. J. R. astr. Soc.* 83, 797-803.
- Marrow, P.C. & Walker, A.B. 1988.** Lleyn earthquake of 1984 July 19: aftershock sequence and focal mechanism. *Geophysical J.* 92, 487-493.
- Mohr, P. 1986.** Possible Late Pleistocene faulting in Iar (west) Connacht, Ireland. *Geol. Mag.* 123, 545-552.
- Mörner, N-A. 1981.** Crustal movements and geodynamics in Fennoscandia. *Tectonophysics* 71, 241-251.
- Muir Wood, R. 1989a.** Fifty million years of 'passive margin' deformation in North West Europe. *in* S. Gregerson & P.W. Basham (eds.) *Earthquakes at North Atlantic Passive Margins: Neotectonics and postglacial rebound.* 7-36. Kluwer Academic Publishers, Amsterdam.
- Muir Wood, R. 1989b.** Extraordinary deglaciation reverse faulting in Northern Fennoscandia. *in* S. Gregerson & P.W. Basham (eds.) *Earthquakes at North Atlantic Passive Margins: Neotectonics and postglacial rebound.* 141-173. Kluwer Academic Publishers, Amsterdam.
- Muir Wood, R. 1990.** The current tectonic regime in the United Kingdom and its NW European context (its bearing on the performance assessment of radioactive waste disposal sites). *in* Report of a meeting on "Fractures and fracture development". DOE Report No. DOE/RW/90.014. Dames & Moore International Technical Report TR-D&M-17.
- Musson, R.M.W. 1989.** Accuracy of historical earthquake locations in Britain. *Geol. Mag.* 126, 685-689.
- Musson, R.M.W. 1990a.** The Colchester forgeries: faking photographic evidence of earthquake damage. *Terra Nova* 2, 661-663.
- Musson, R.M.W. 1990b.** A provisional catalogue of UK earthquakes greater than 4 M_L, 1700-1990. Seismology Rpt. No. WL/90/28. British Geological Survey.

Musson, R.M.W., Neilson, G. & Burton, P.W. 1984. Macroseismic reports on historical British earthquakes III: Central and Western Scotland. British Geological Survey Global Seismology Unit Report No. 209.

Neilson, G., Musson, R.M.W. & Burton, P.W. 1984. The "London" earthquake of 1580, April 6. *Engineering Geology* 20, 113-141.

Obermeier, S.F., Gohn, G.S., Weems, R.E., Gelinas, R.L. & Rubin, M. 1985. Geologic evidence for recurrent moderate to large earthquakes near Charleston, South Carolina. *Science* 227, 408-411.

Papastamatiou, D. 1978. Contributions of early instrumental seismic recordings to engineering analysis. *in* Instrumentation for ground vibration and earthquakes, 119-124. Inst. Civil Engineers, London.

Prebble, J. 1963. The Highland Clearances. Penguin, London. 336pp.

Press, F. & Siever, R. 1982. Earth. 3rd Edition. W.H. Freeman & Co., San Francisco. 613pp.

Reading, A. 1991. UK seismotectonics and crustal stress - early Holocene to present day. Unpubl. B.Sc. Dissertation, University of Edinburgh (Dept. of Geophysics).

Richter, C.F. 1935. An instrumental earthquake magnitude scale. *Bull. Seism. Soc. Am.* 25, 1-32.

Ritsema, A.R. 1981. On the assessment of seismic risk in the North Sea area. Koninklijk Nederlands Meteorologisch Instituut Report, 19pp.

Ringrose, P.S. 1987. Fault activity and palaeoseismicity during Quaternary time in Scotland. Unpubl. Ph.D. Thesis (2 Volumes), University of Strathclyde.

Ringrose, P.S. 1989a. Palaeoseismic (?) liquefaction event in late Quaternary lake sediment at Glen Roy, Scotland. *Terra Nova* 1, 57-62.

Ringrose, P.S. 1989b. Recent fault movement and palaeoseismicity in western Scotland. *Tectonophysics* 163, 305-314.

- Ringrose, P.S., Hancock, P.L., Fenton, C. & Davenport, C.A. 1991.** Quaternary tectonic activity in Scotland. Quaternary Engineering Geology. Special Publication No.7.
- Scheidegger, A.E. 1985.** Recent research on the physical aspects of earthquakes. *Earth Sci. Rev.* 22, 173-229.
- Seilacher, A. 1984.** Sedimentary structures tentatively attributed to seismic events. *Marine Geology* 55, 1-12.
- Shennan, I. 1989.** Holocene crustal movements and sea-level changes in Great Britain. *J.Quaternary Sci.* 4, 77-89.
- Sibson, R.H. 1989.** Earthquake faulting as a structural process. *J. Structural Geology* 11, 1-14.
- Sims, J.D. 1975.** Determining earthquake recurrence intervals from deformational structures in young lacustrine sediments. *Tectonophysics* 29, 141-152.
- Smith, G.I. 1953.** Folk tales of the Highlands. Thomas Nelson & Sons Ltd. London.
- Teague, A.G., Bollinger, G.A. & Johnston, A.C. 1986.** Focal mechanism analysis of eastern Tennessee earthquakes (1981-1983). *Bull. Seism. Soc. Am.* 76, 95-109.
- Thatcher, W. & Hanks, T.C. 1973.** Source parameters of southern Californian earthquakes. *J. Geophysical Res.* 78B, 8547-8575.
- Thorne, J.A. & Watts, A.B. 1989.** Quantitative analysis of North Sea subsidence. *Am. Assoc. Petroleum Geol. Bull.* 73, 88-116.
- Turbitt, T.(ed.) 1984.** Catalogue of British Earthquakes recorded by the BGS Seismograph Network 1979, 1980, 1981. British Geological Seismology Global Seismology Report No. 210.

Turbitt, T.(ed.) 1985. Catalogue of British Earthquakes recorded by the BGS Seismograph Network 1982, 1983, 1984. British Geological Survey Global Seismology Report No. 260.

Turbitt, T. (ed.) 1987. Bulletin of British Earthquakes 1985. British Geological Survey Global Seismology Report No. 303.

Turbitt, T. (ed.) 1988. Bulletin of British Earthquakes 1986. British Geological Survey Technical Report No. WL/88/11.

Turbitt, T. (ed.) 1989. Bulletin of British Earthquakes 1987. British Geological Survey Technical Report No. WL/89/9.

Turbitt, T. (ed.) 1990. Bulletin of British Earthquakes 1988. British Geological Survey Technical Report No. WL/90/3.

Youd, T.L. 1977. Discussion of Brief review of liquefaction during earthquakes in Japan. *Soils & Foundations* 17, 82-85.

Zoback, M.D., Prescott, W.H. Kreuger, S.W. 1985. Evidence for lower crustal ductile strain localization in southern New York. *Nature* 317, 705-707.

Zoback, M.L., Zoback, M.D., Adams, J., Assumpcao, M., Bell, S., Bergman, E.A., Blumling, P., Brereton, N.R., Denham, D., Ding, J., Fuchs, K., Gay, N., Gregerson, S., Gupta, H.K., Gvishiani, A., Jacob, K., Klein, R., Knoll, P., Magee, M., Mercier, J.L., Muller, B.C., Paquin, C., Rajendran, K., Stephansson, O., Suarez, G., Suter, M., Udias, A., Xu, Z.H. & Zhizhin, M. 1989. Global patterns of tectonic stress. *Nature* 341, 291-298.

4.14 Figure Captions

- Figure 4.1** Earthquake epicentres (c. 30,000) recorded 1961-'67 by the US Coast & Geodetic Survey. The majority of events occur along plate margins, with <1% occurring in intraplate areas [Redrawn from Press & Siever 1982].
- Figure 4.2** Histograms comparing (a) the angular difference between the observed directions of S_{Hmax} and the computed absolute plate velocity field for Western Europe, and (b) the angular difference between the observed directions of S_{Hmax} and the computed vectors for Africa-Eurasia convergence. Black ornament represents data from continental Europe and the striped ornament data from the UK. [Redrawn from Zoback *et al.* 1989].
- Figure 4.3** A brief history of the recording of seismic activity in the UK with particular reference to Scotland.
- Figure 4.4** Flow diagram outlining the basic procedure used for palaeoseismic investigations in the Highlands of Scotland. NB. Most arrows are reversible!
- Figure 4.5** Earthquake activity recorded by BGS seismometer network 1985-1988. Symbols sizes are proportional to magnitude of the events. Activity seems diffuse, but swarms are observed to occur at a number of localities throughout the period of instrumental seismicity [From Turbitt 1987, 1988, 1989, 1990].
- Figure 4.6** Locations of seismic events $\geq 3.0 M_L$ recorded in Scotland 1969-'90 (43 events) by the BGS seismometer network. U: Ullapool, LM: Loch Maree, K: Kintail, BN: Ben Nevis.
- Figure 4.7** Frequency histograms for seismicity recorded in the UK on the BGS seismometer network 1969-'88. (a) $\text{Log}_{10}(\text{Frequency})$ -Magnitude plot. (b) $\text{Log}_{10}(\text{Cumulative Frequency})$ -Magnitude plot.

- Figure 4.8** Cumulative-frequency relationships for (a) historical seismicity $\geq 4.0 M_L$, 1700-1990, and (b) instrumental seismicity 1969-1988. Straight line fits to the data sets give Gutenberg-Richter parameters **a** and **b**. The departure of both data sets at low magnitudes is due to the detection thresholds and the fall-off of the data at high magnitudes is due to insufficient time to record such events that will have a return period greater than the period over which recording has been made.
- Figure 4.9** (a) Moment release (in dyne cm) in relation to earthquake magnitude (M_L) based on the equation of Thatcher & Hanks (1973). The contribution of large earthquakes is significantly greater than that for smaller events. (b) Total moment release for the instrumental record for the UK. It is seen that the contribution of events $\leq 3.0 M_L$ is negligible in comparison to larger events. A few large events dominate the moment release rate for the UK.
- Figure 4.10** Frequency-Magnitude (a) and $\log_{10}(\text{Frequency})$ -Magnitude (b) plots for the UK instrumental seismicity period showing the increase in detection limits corresponding to the increase in seismometer coverage in the late seventies and early eighties. There is a marked fall-off at $\leq 1.0 M_L$ in the recorded events prior to 1979 and at $\leq 0.5 M_L$ for the data recorded after 1979.
- Figure 4.11** Magnitude-depth plot for UK instrumental seismicity 1969-'88. No depth-magnitude relationship is observed, however the almost all events are seen to occur in the upper 15 km, with the majority of hypocentral depths being ≤ 10 km. A few events are recorded at 15-24 km.
- Figure 4.12** Magnitude-depth plots for instrumental seismicity at three centres (Located on Figure 4.6) of recurrent activity in the N.W. Highlands. It is seen that activity is almost entirely confined to the upper 10 km.

- Figure 4.13** Lower hemisphere fault plane solutions (dilatational quadrants shaded) for five instrumentally recorded UK seismic events. Inset shows a composite for all five events defining the orientation of the P(M) and T(m) axes defining the directions of maximum and minimum horizontal stress [Redrawn from Marrow & Walker 1988].
- Figure 4.14** Frequency histograms for UK historical seismicity 1700-1990. (a) $\log_{10}(\text{Frequency})$ -Magnitude plot and (b) $\log_{10}(\text{Cumulative Frequency})$ -Magnitude plot.
- Figure 4.15** Post glacial faults in Scotland. Faults are represented diagrammatically in their geographical locations.
- Figure 4.16** Graphs relating earthquake magnitude and areal distribution of slope failures [Redrawn from Keefer 1984a]. Lines mark the approximate upper bound enclosing all data.
- Figure 4.17** Lower hemisphere fault plane solutions (dilatational quadrants shaded) for seventeen palaeoseismic events. The larger spheres denote the fully defined fault plane solutions. Inset shows a composite plot created from the four fully defined fault plane solutions. P(M) and T(m) axes are defined. (Numbers correspond to the faults in Figure 4.15) [Redrawn from Reading 1991].
- Table 4.1** A comparison of the macroseismic criteria from historical catalogues with the Modified Mercalli scale [Redrawn from Burton & Neilson 1979].
- Table 4.2** Palaeoseismic data from the field studies of Fenton (1991) and Ringrose (1987).
- Table 4.3** Indicators of large earthquakes in the North Sea region [From Burton & Marrow 1989].

4.15 Figures

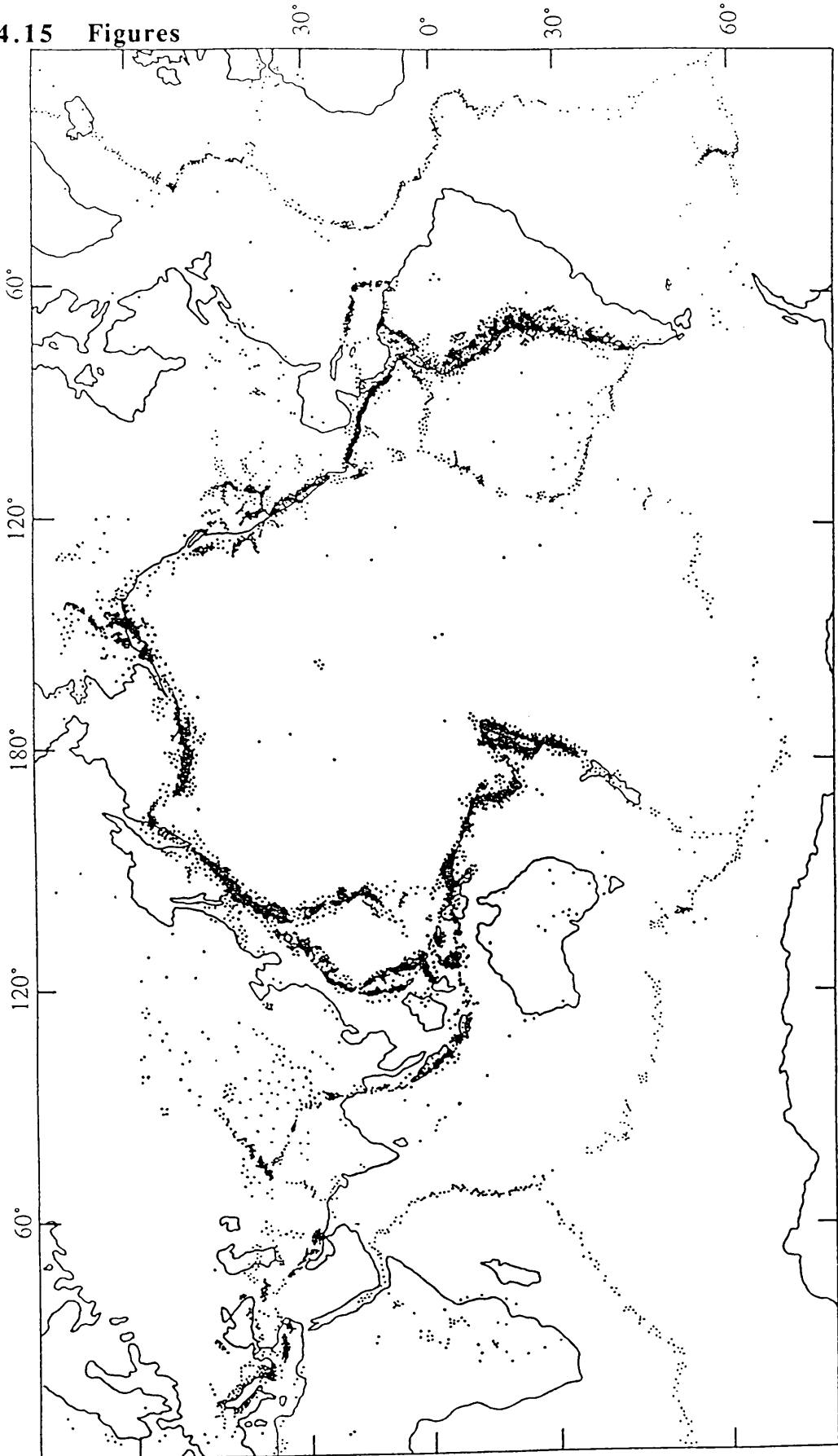


Figure 4.1

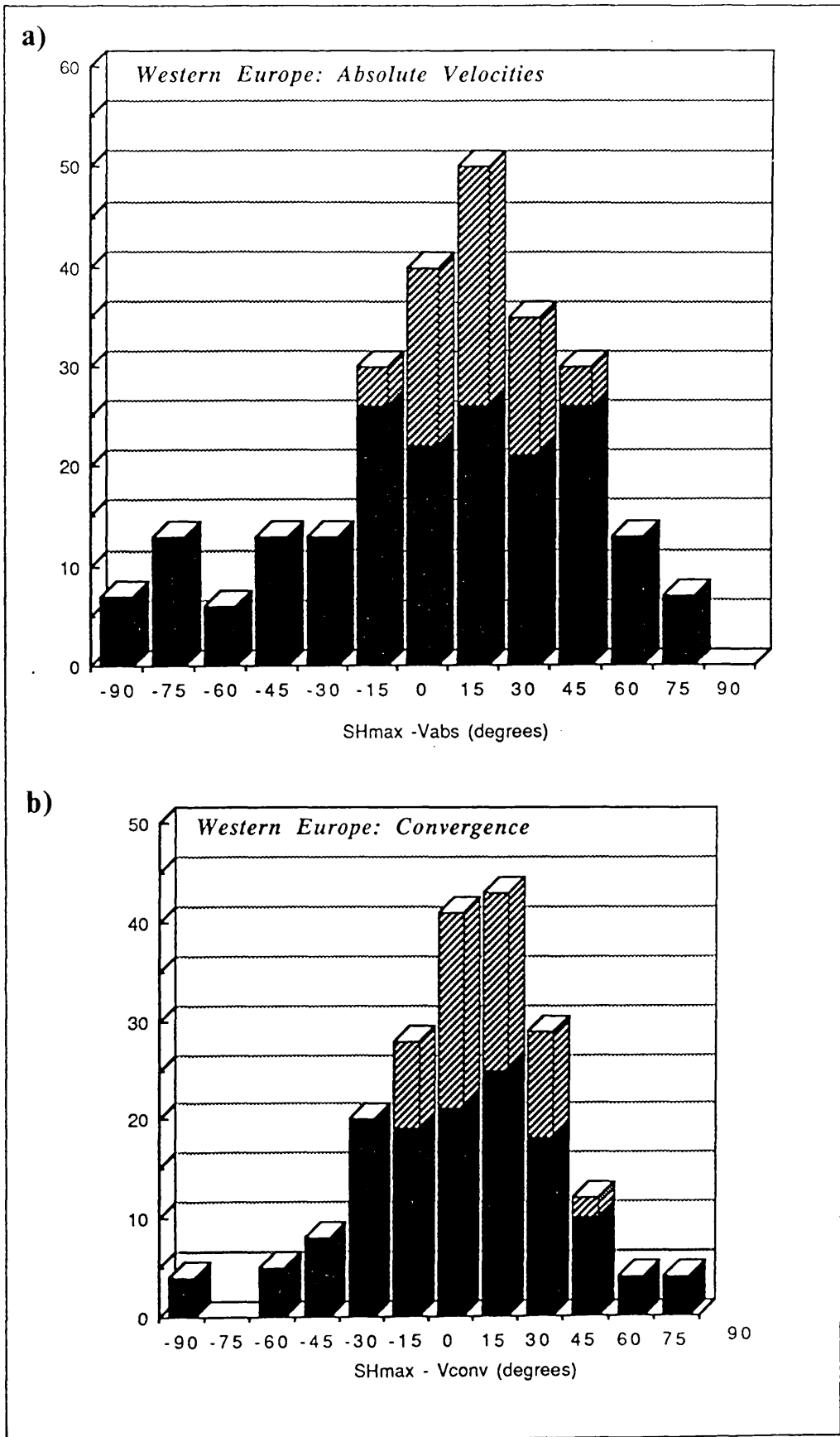


Figure 4.2

History of the Recording of Scottish Seismicity

- 1789-'97:** Comrie activity documented by Rev. Taylor of Ochertyre.
- 1791-1826:** Rev. Gilfillan recorded seismic events in the area of Comrie.
- 1839:** The British Association for the Advancement of Science set up a committee to register the earthquakes of Scotland and Ireland. Reports were confined to Comrie for the period 1841-1844.
- 1840:** The first three pendulum seismometers designed by Professor Forbes were set up in the Comrie district.
- 1841:** Further seismometers, making an array of eleven, set up in the area around Comrie. Two instruments were also installed at Kinlochmoidart, Argyll.
- 1844:** MacFarlane & Drummond record the activity in the Comrie area. As well as building crude pendulum seismometers he also devised an early ten point intensity scale.
- 1876:** A decrease in the swarm activity and corresponding decrease in interest caused the lapse of the Comrie Committee.
- 1896:** Davison and Milne of BAAS, Seismological Investigations Committee instigate the first World seismograph network. Seismographs installed at Paisley (1898), Edinburgh (1901), Eskdalemuir (1907) and Aberdeen (1926).
- 1924:** Davison's "A history of British Earthquakes" is published covering the period 974 to 1924.
- 1951:** Dollar continuing the work of Davison publishes "Catalogue of Scottish Earthquakes of 1916-1949" in Trans. Geol. Soc. Glasgow.
- early 1960s:** Large seismometer network installed at Eskdalemuir by UKAEA.
- 1967:** Installation of the Lowland Seismometer Network (LOWNET) by the IGS began. Fully operational by 1969.
- 1974:** First (accidental) recording of a local swarm of seismic activity (on the BIRPS LISPB network) at Kintail allowing the construction of a fault plane solution.
- 1978-'81:** LOWNET supplemented by a further 12 seismograph stations.
- 1984:** Temporary network installed to monitor the aftershocks of the Lleyn Peninsula event (5.4M_L). Similar network was installed around Longtown in 1979-1981.
- 1988:** Network of 100 seismograph stations operated by BGS, Leeds University and DIAS.

Figure 4.3

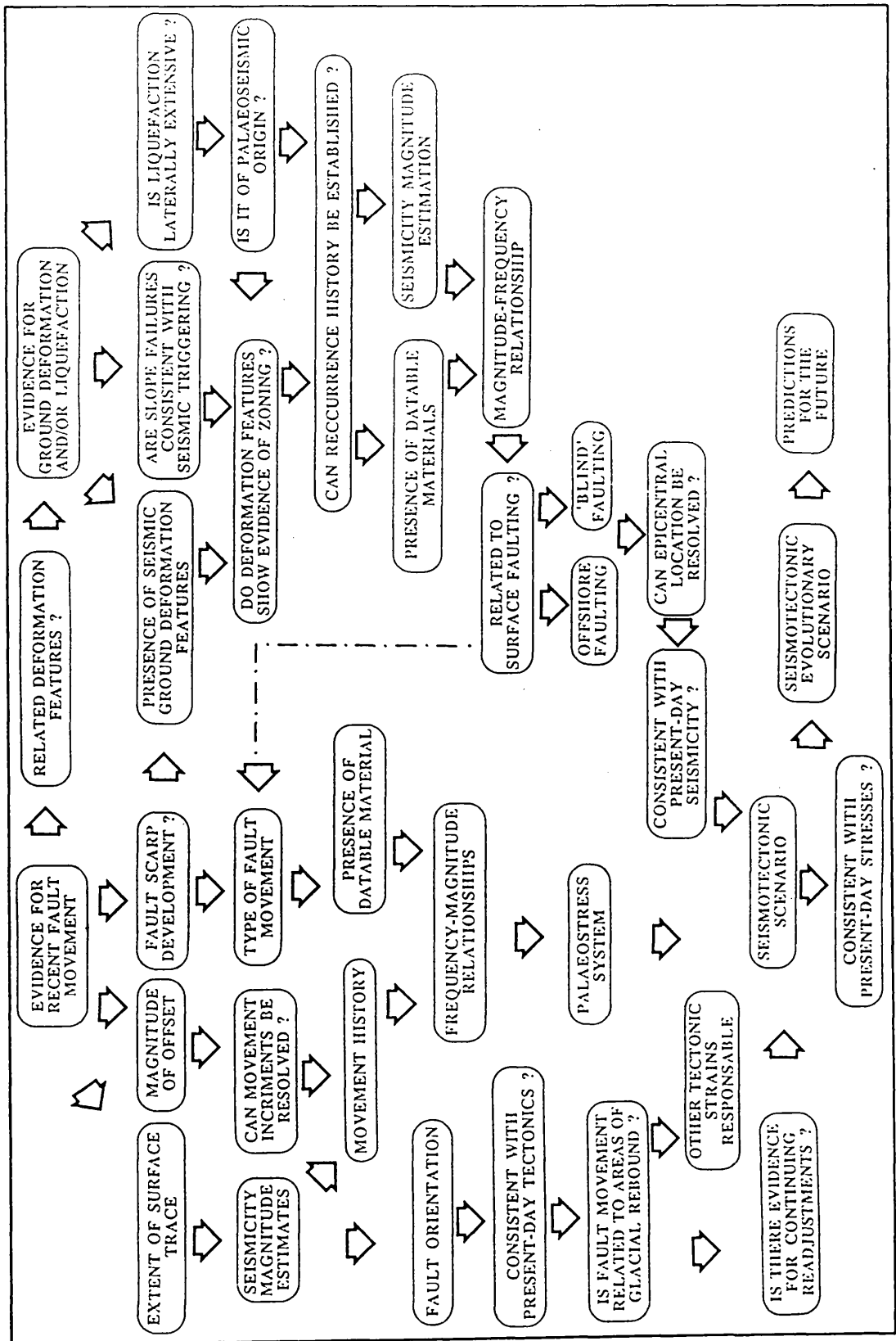


Figure 4.4

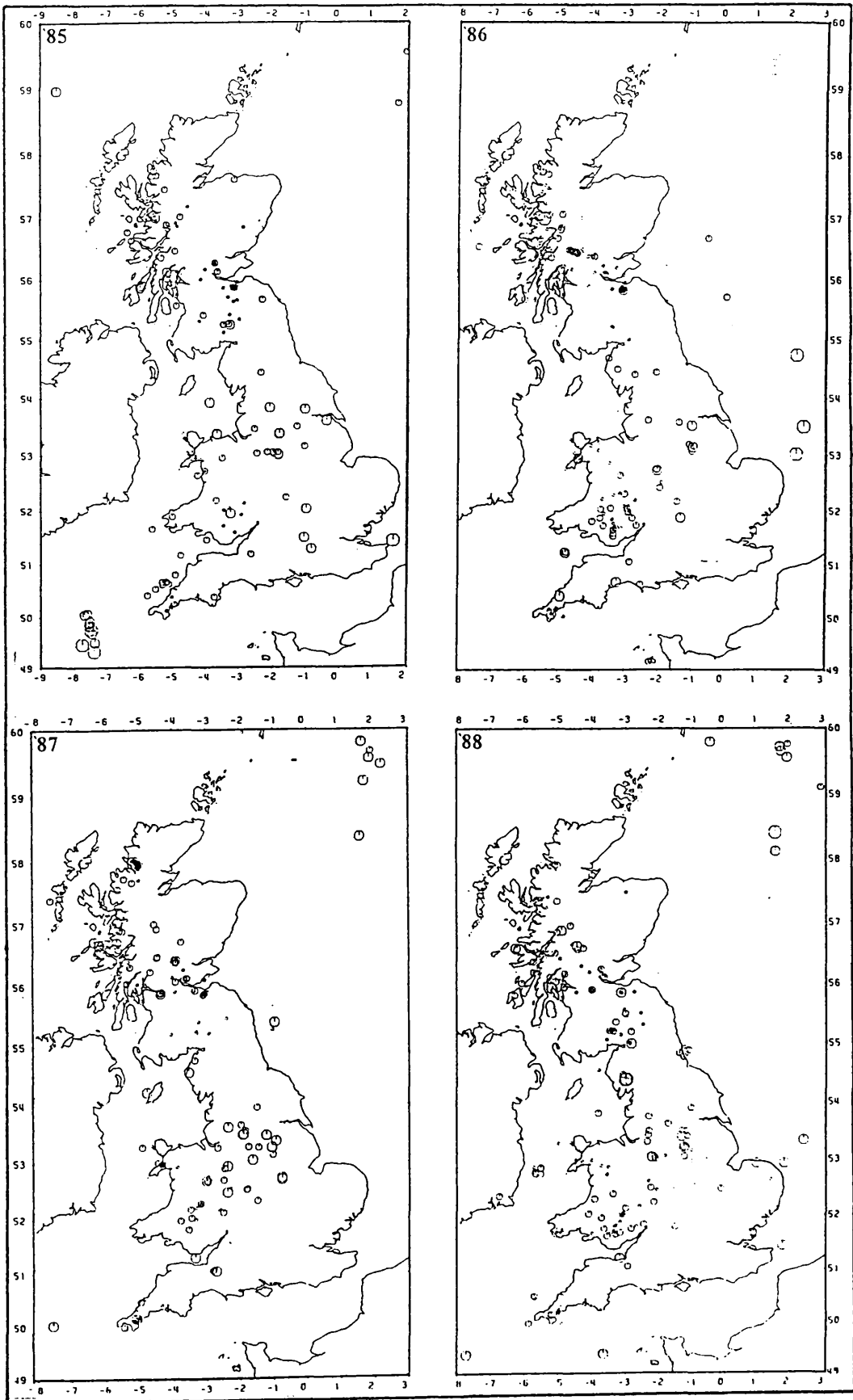


Figure 4.5

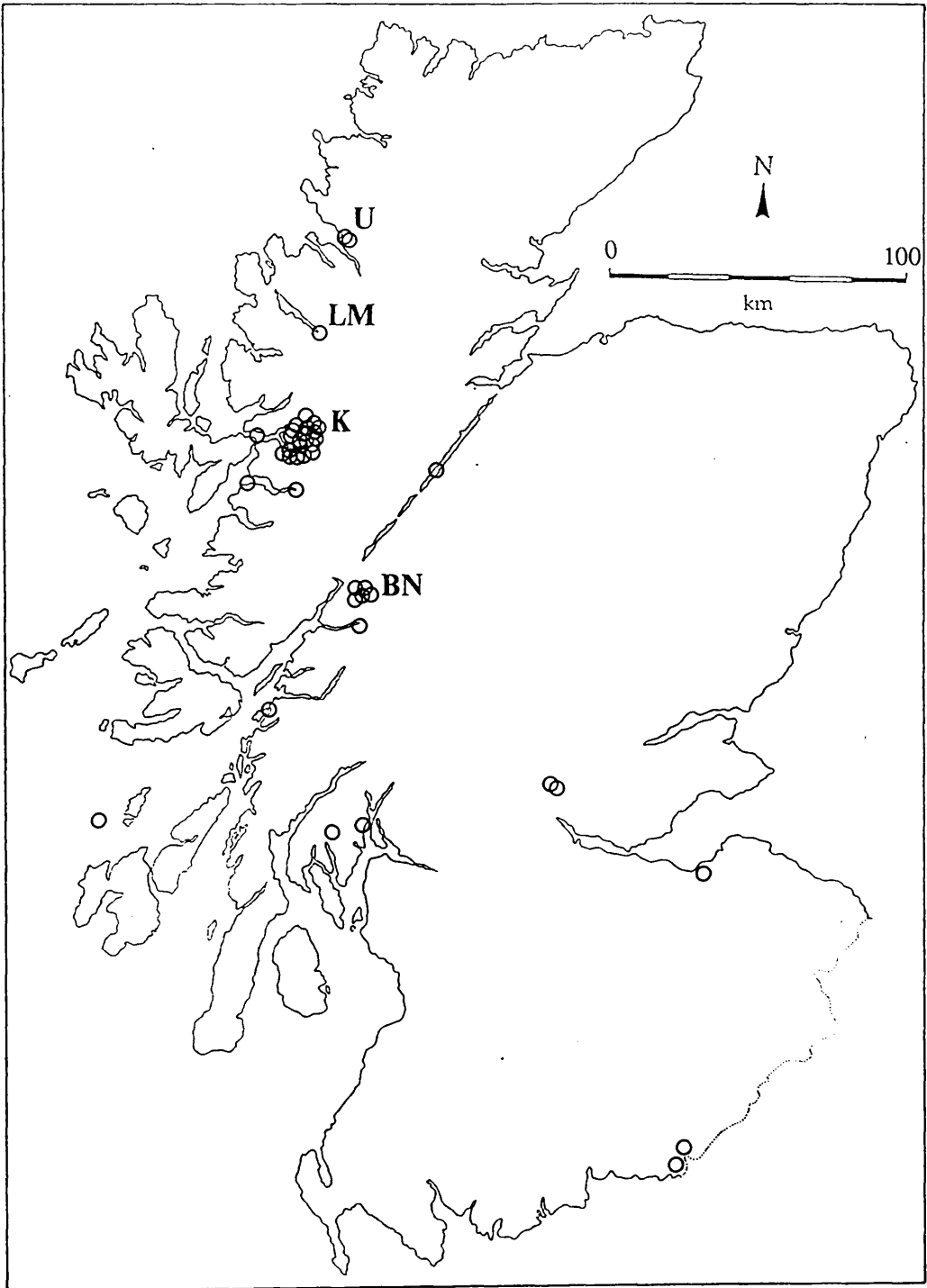


Figure 4.6

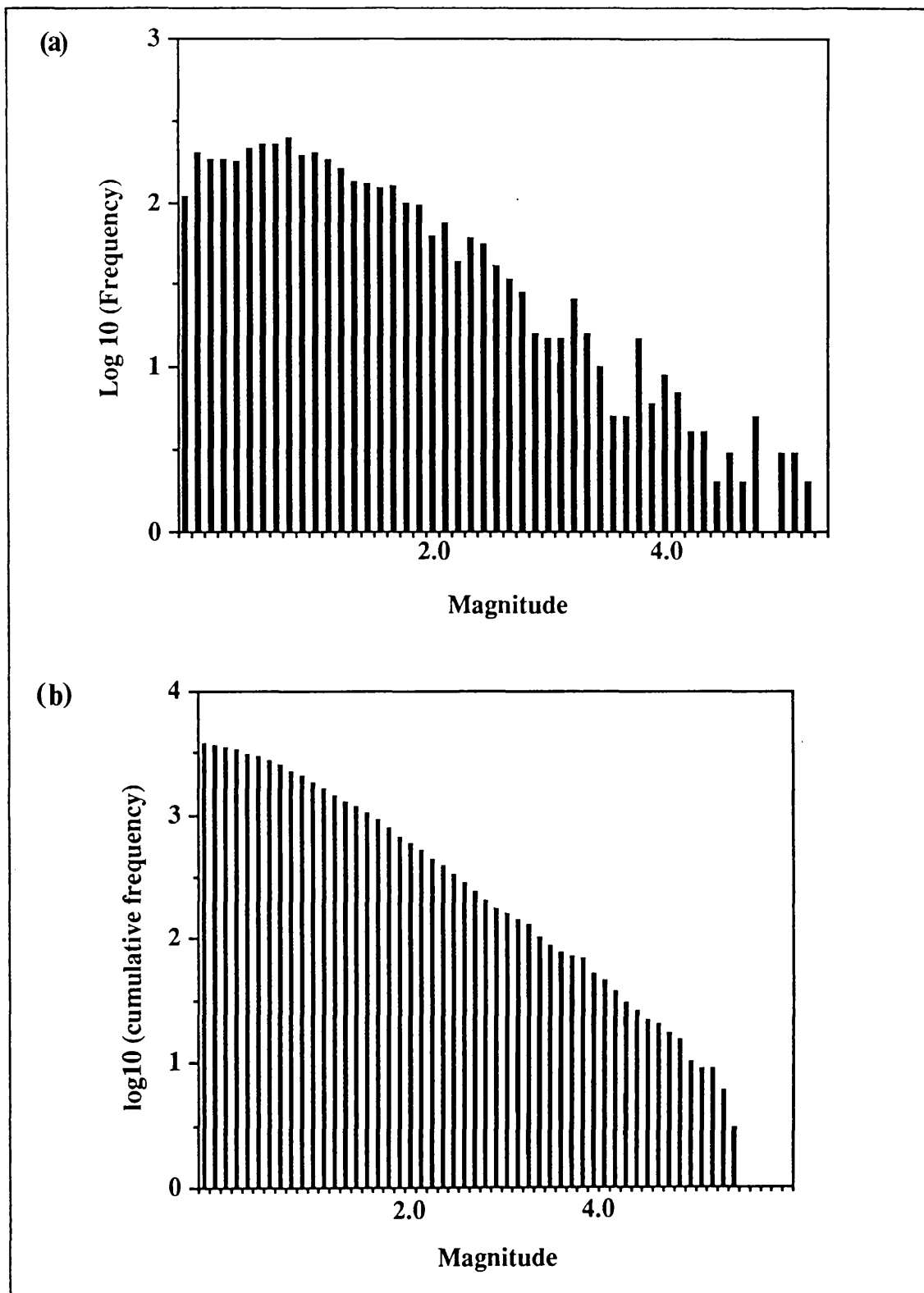


Figure 4.7

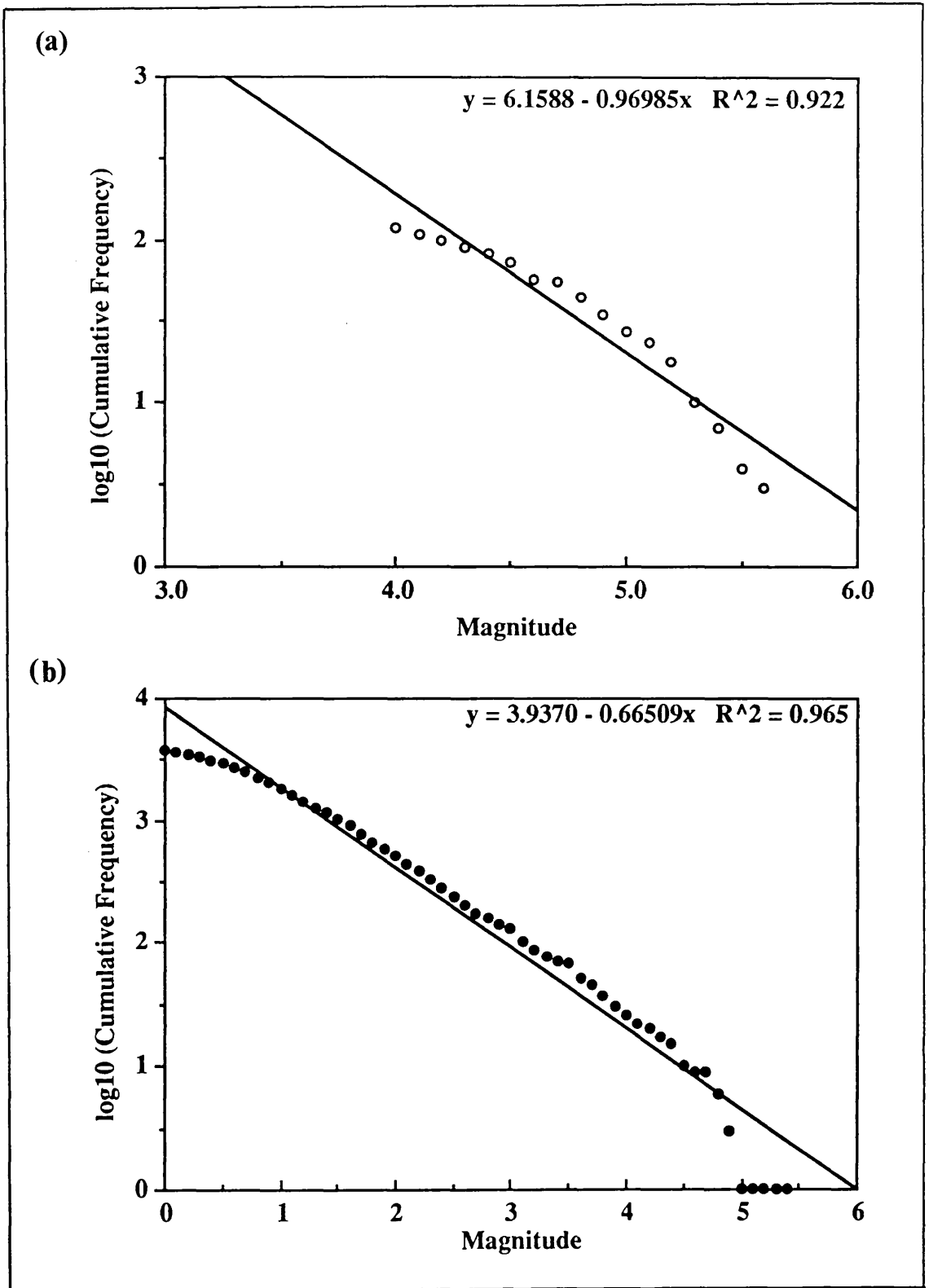


Figure 4.8

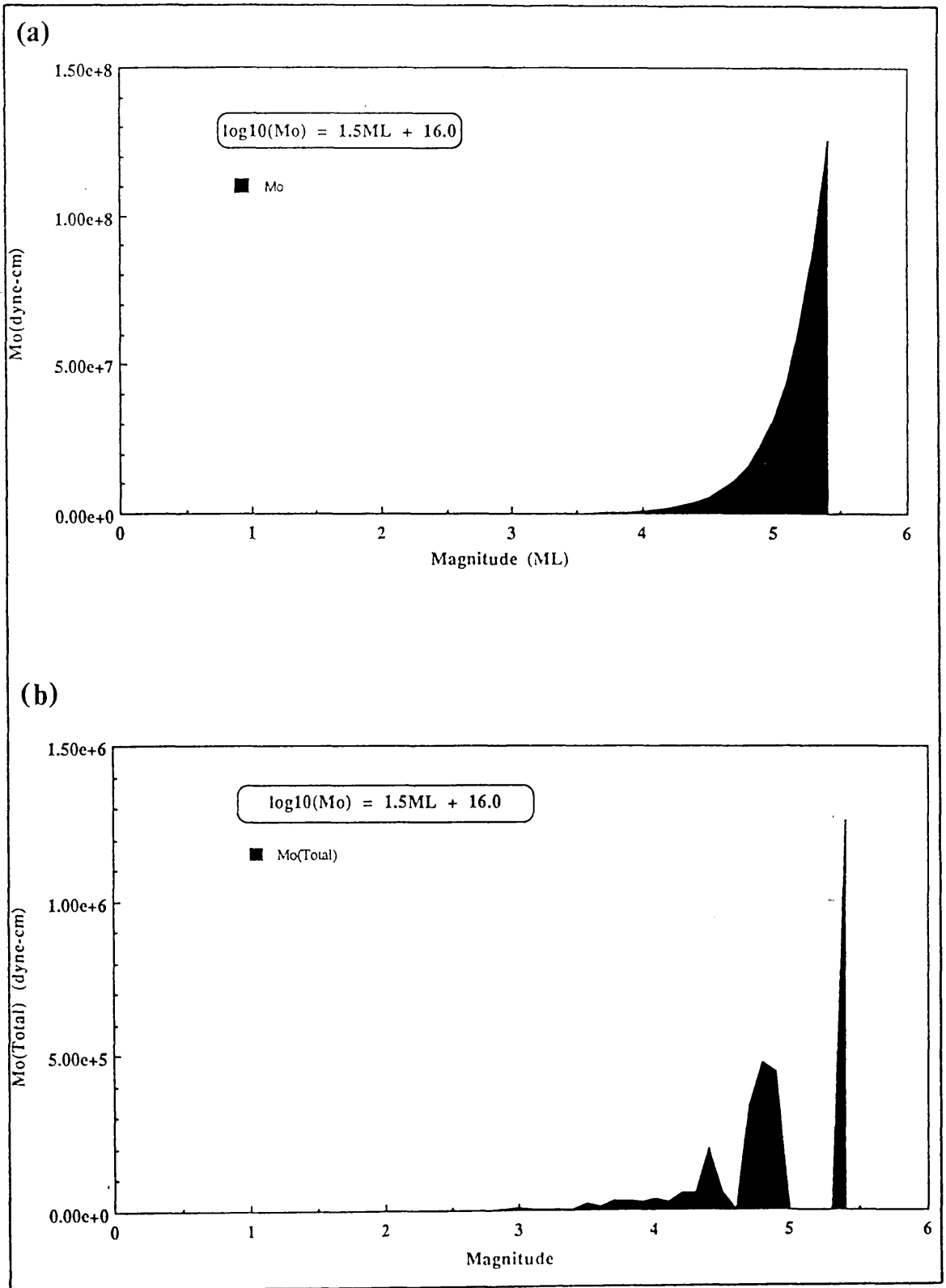


Figure 4.9

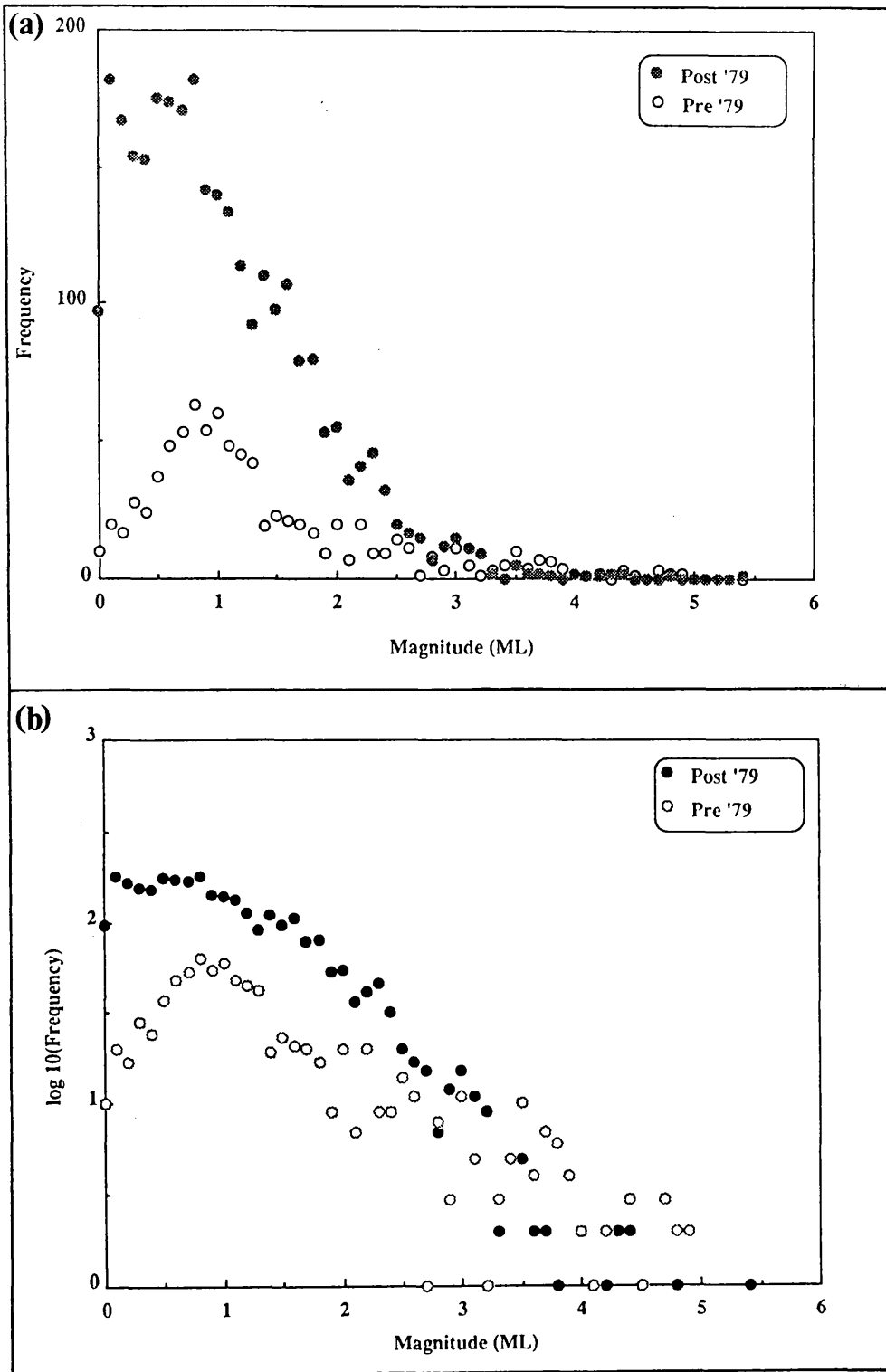


Figure 4.10

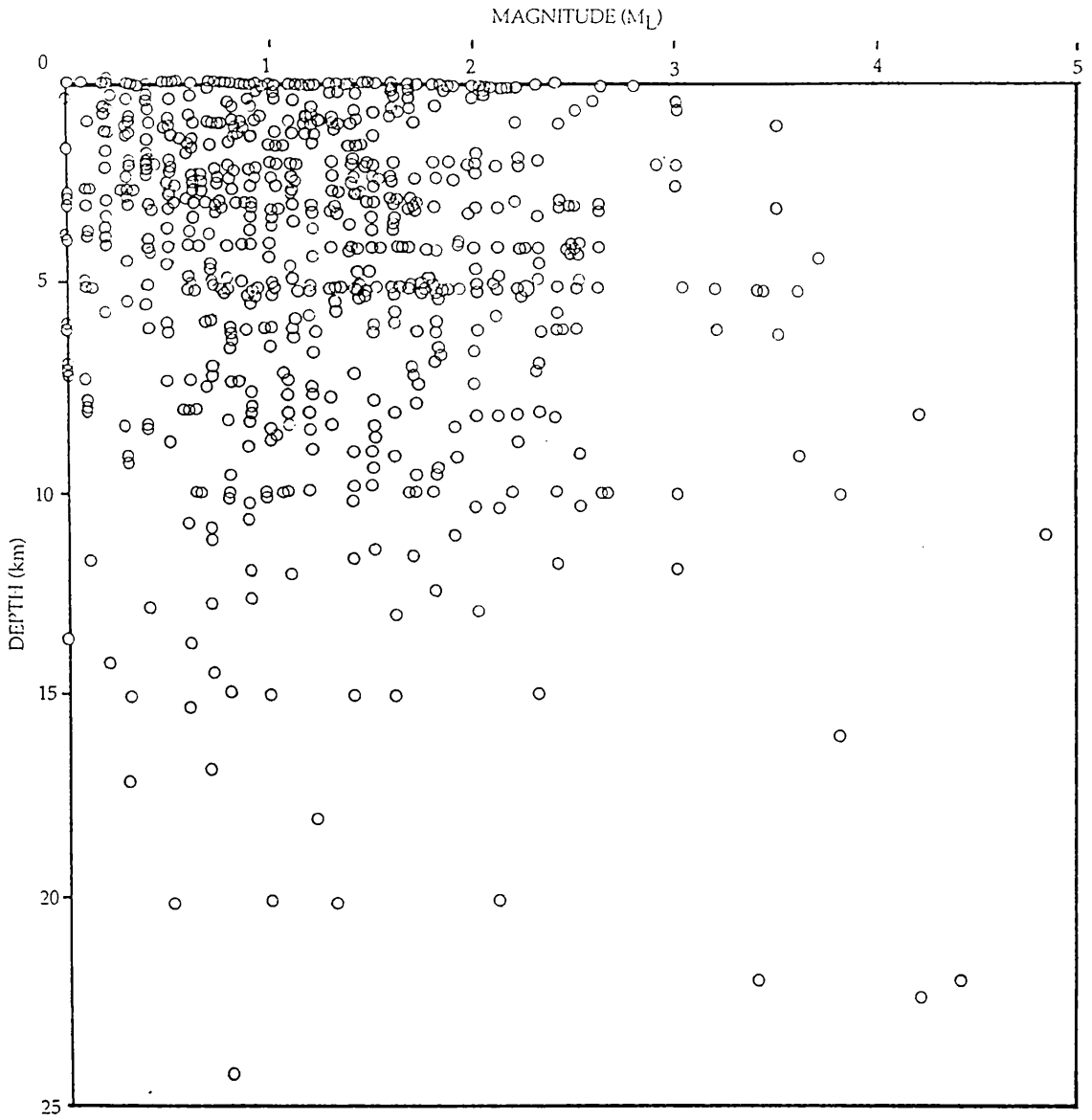


Figure 4.11

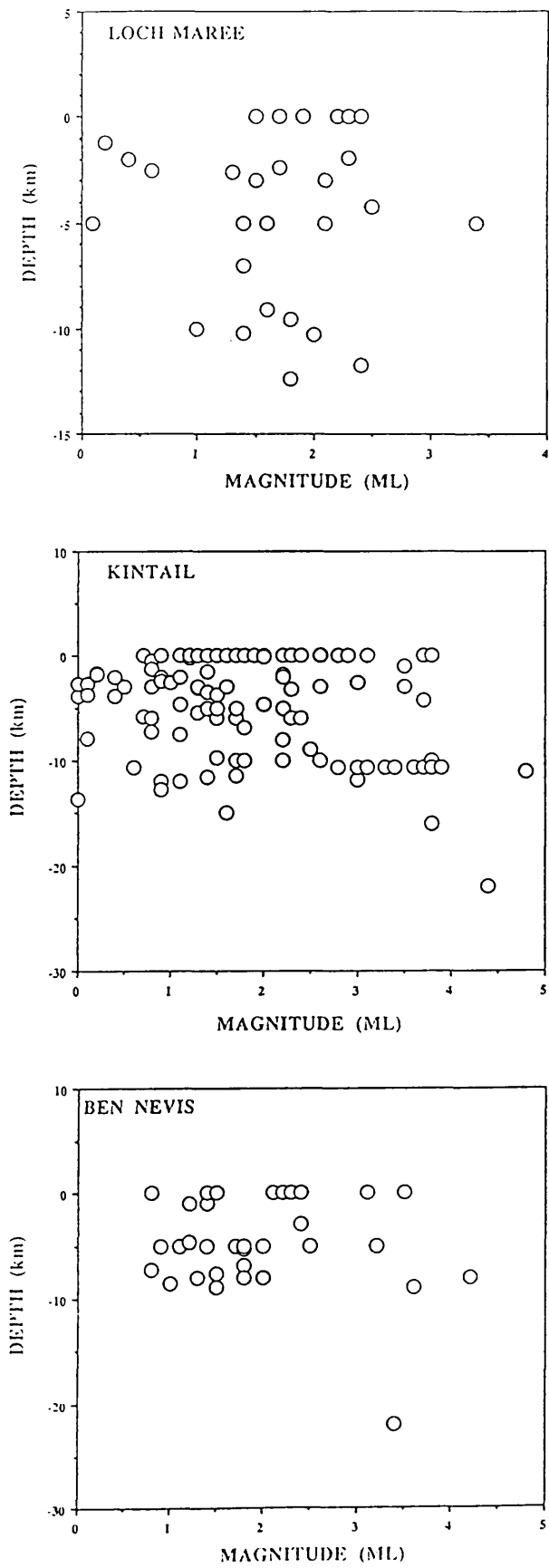


Figure 4.12

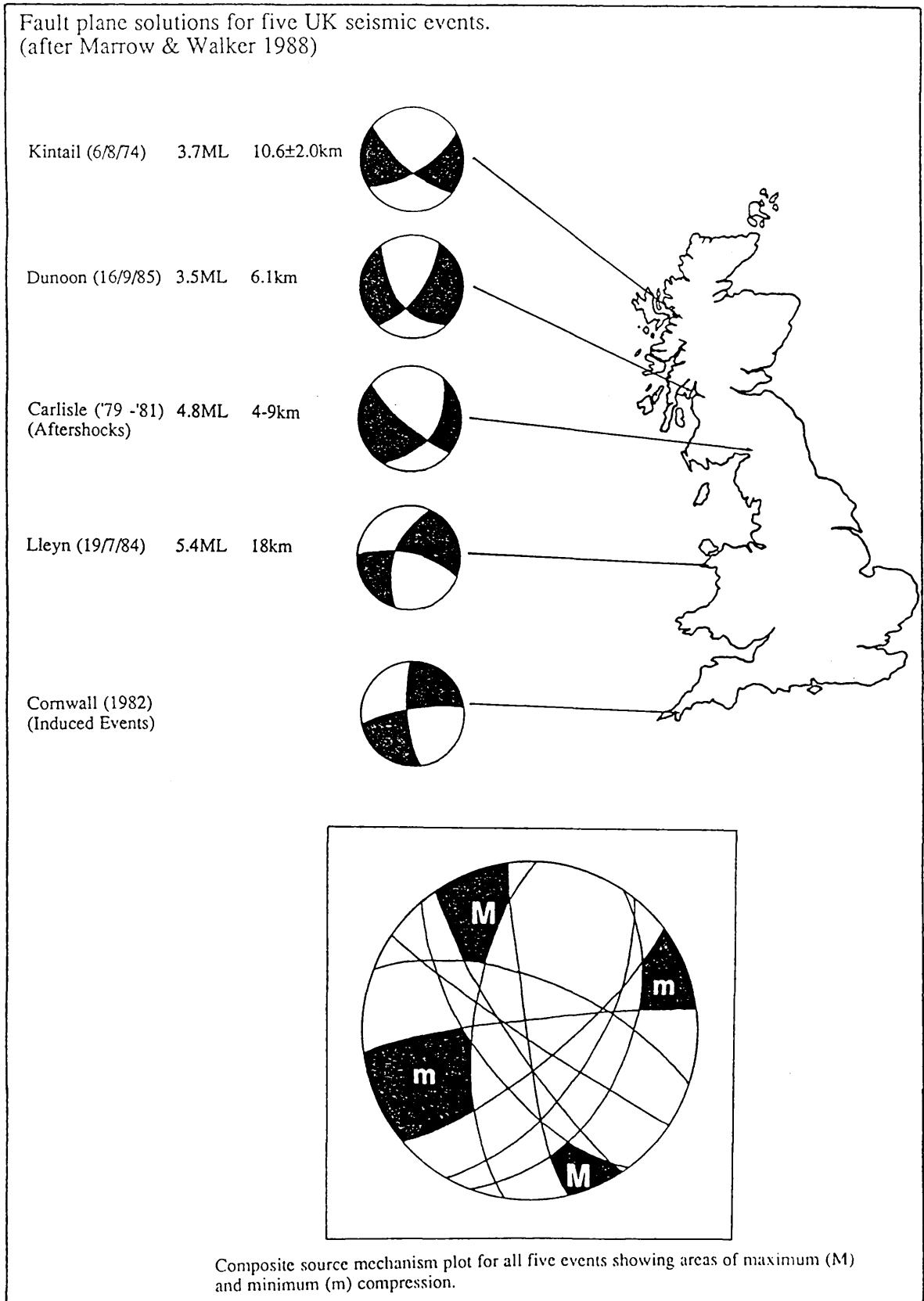


Figure 4.13

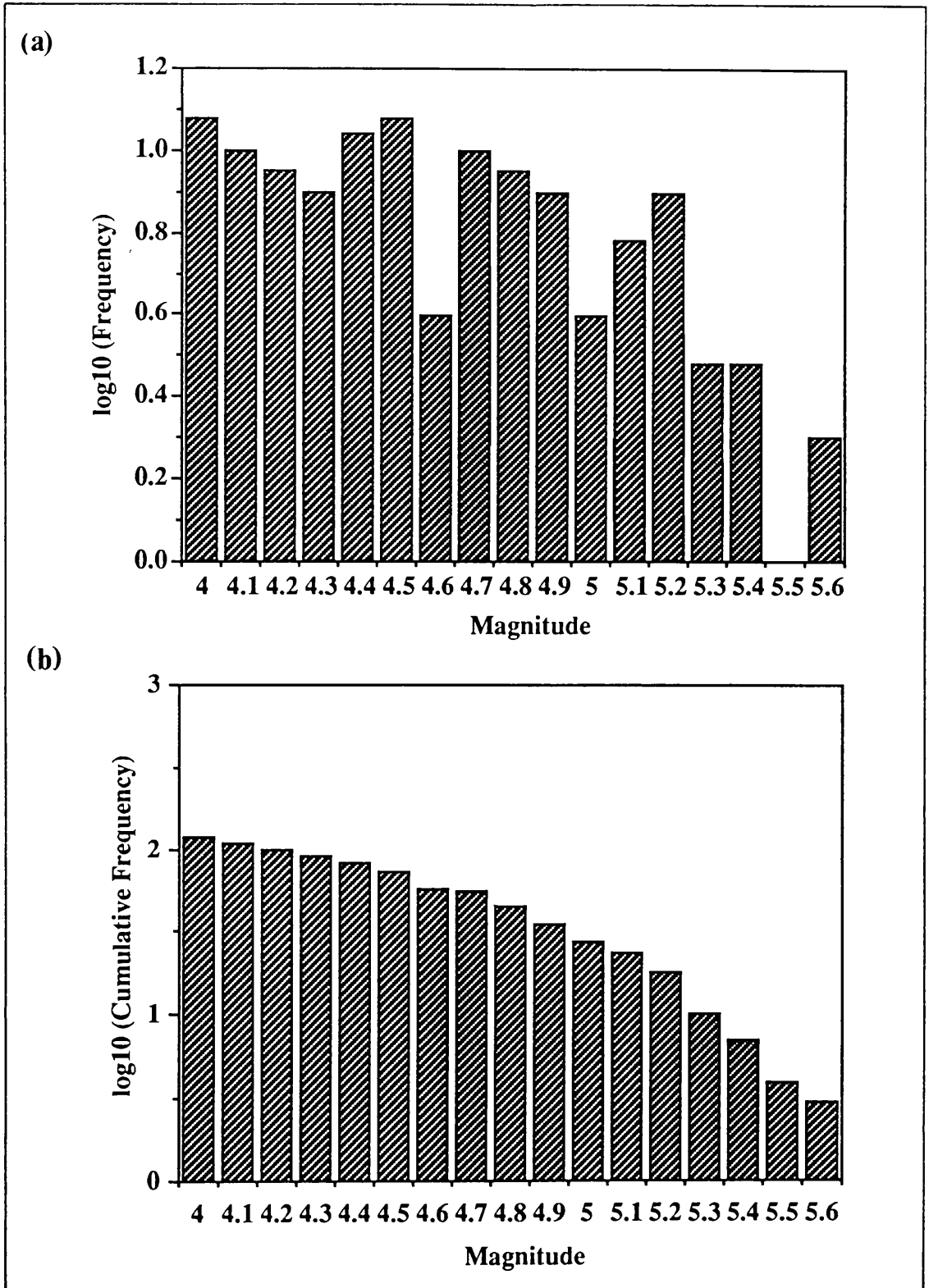
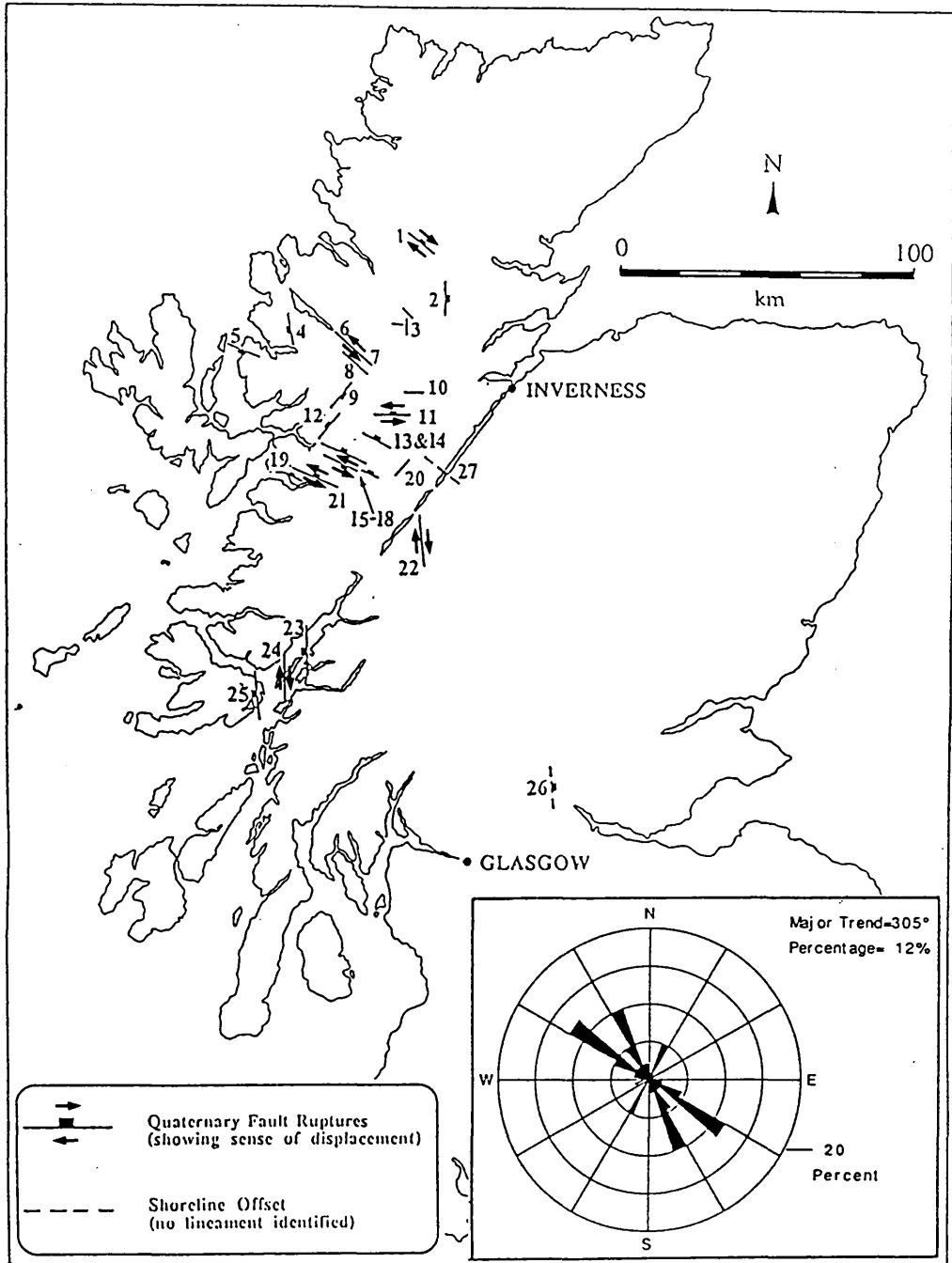
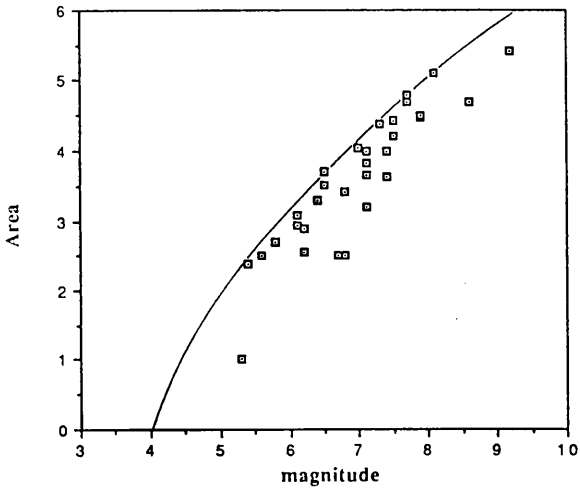


Figure 4.14

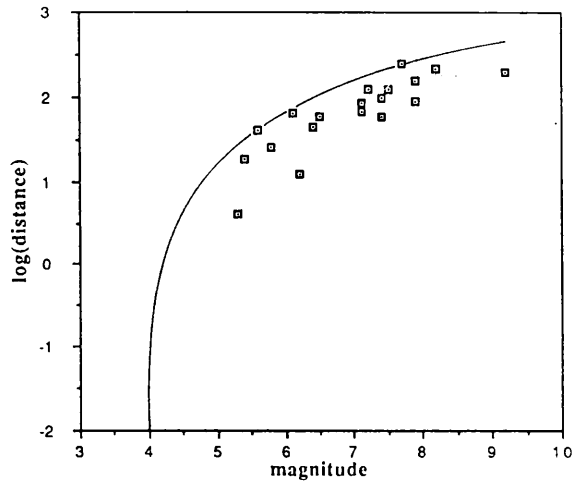


- | | | |
|--------------------------------|--------------------------------------|-------------------------------|
| 1. Coire Mor Fault | 10. Loch Monar Fault | 19. Arnisdale Faults |
| 2. Strath Vaich Fault | 11. Coire Eoghainn Fault | 20. Coire Dho Fault |
| 3. Garbh Choire Mor Faults | 12. Glen Elchaig (Strathconon Fault) | 21. Kinloch Houran Fault |
| 4. Beinn Alligin Fault | 13. An Sornach Fault | 22. Glen Gloy Fault |
| 5. Cuaig Fault | 14. Sgurr na Lapaich Fault | 23. Shuna Displacements |
| 6. Loch Crann (L. Marce Fault) | 15. Gleann Lichd Fault | 24. Lismore Displacements |
| 7. Scardroy (L. Marce Fault) | 16. Creag na Damh Fault | 25. Port Donain Displacements |
| 8. Bac an Eich Fault | 17. Sgurr a' Bhealaich Dheirg Fault | 26. Forth Valley Offsets |
| 9. Beinn Tharsuinn Fault | 18. Sgurr na Ciste Duibhe Fault | 27. Loch Ness Offsets |

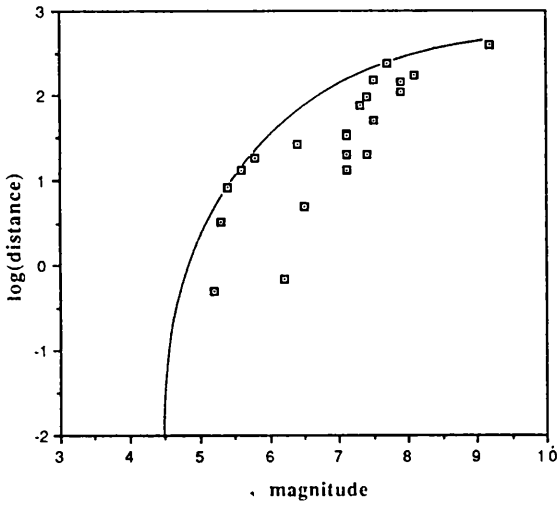
Figure 4.15



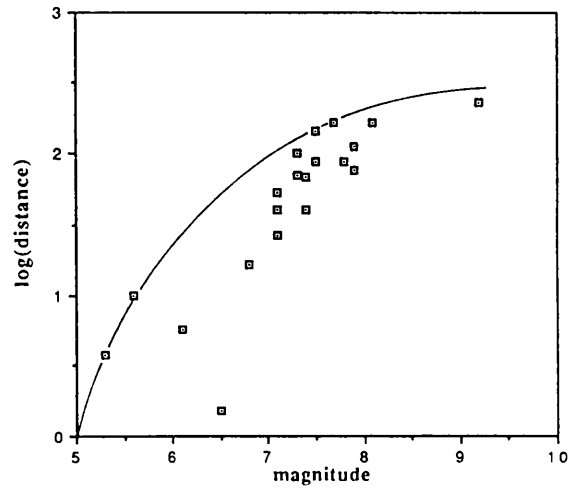
Plot of earthquake magnitude against the maximum area affected by slope failures. [Data from Keefer (1984)]



Plot of earthquake magnitude against the maximum distance of disrupted slides and falls from the fault rupture zone [Data from Keefer (1984)].



Plot of earthquake magnitude against the maximum distance of coherent slides and falls from the fault rupture zone [Data from Keefer (1984)].



Plot of earthquake magnitude against the maximum distance of lateral spreading and flow slides from the fault rupture zone [Data from Keefer (1984)].

Figure 4.16

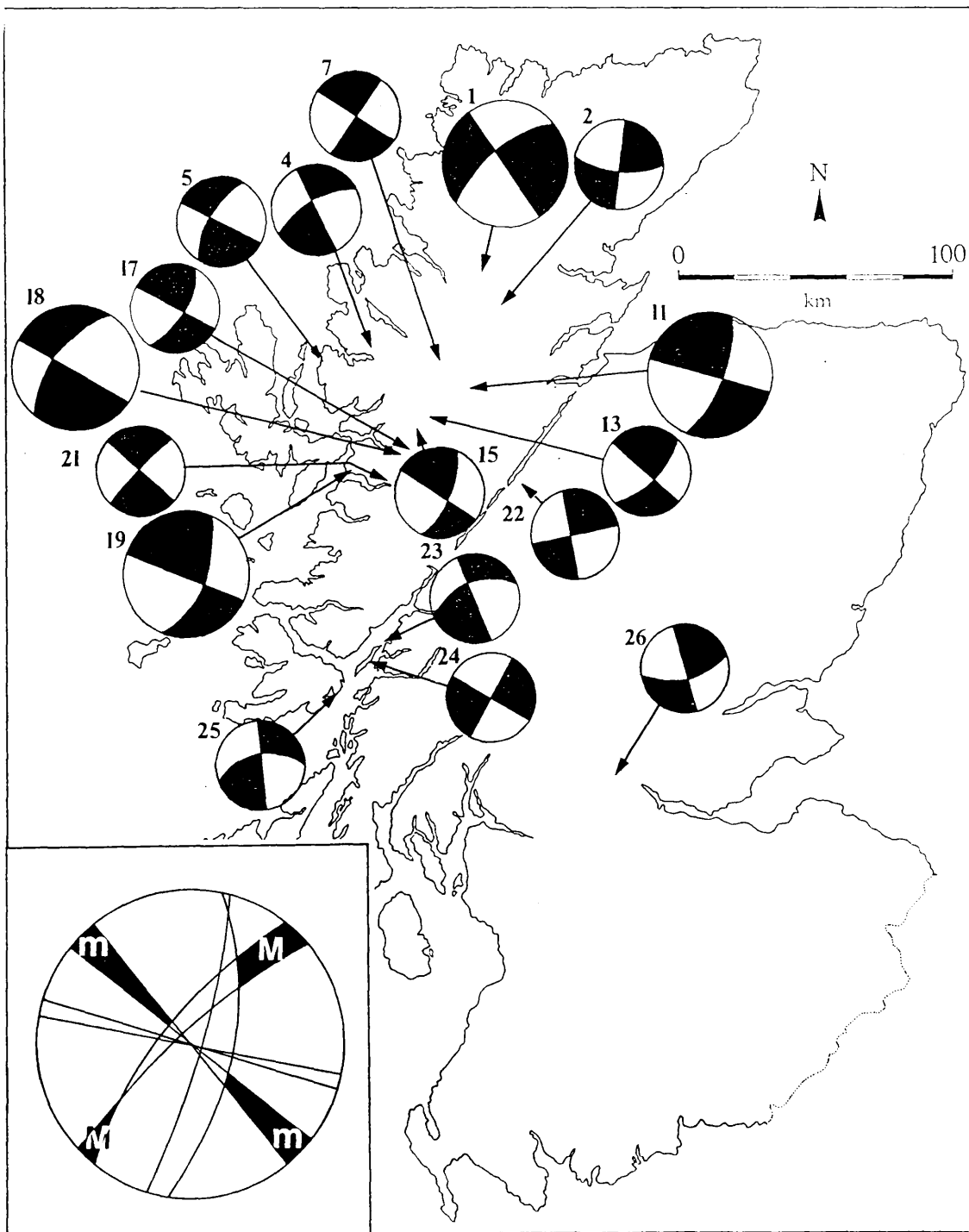


Figure 4.17

4.16 Tables

Earthquake Intensity on Davison's (1924) scale and the closest corresponding values on the Modified Mercalli Scale			
Perceptible Definition	Davison's Intensity (ID)	Closest Modified Mercalli Intensity (MMI)	
Recorded only by instruments.	I	I	
Felt only by a few persons lying down and sensitive to weak tremors.	II	II	
Felt by ordinary persons at rest; not strong enough to disturb loose objects.	III	III	
Windows, doors, fire-irons, etc., made to rattle.	IV	III 1/2	
The observer's seat perceptibly raised or moved.	V	IV	
Chandeliers, pictures, etc., made to swing.	VI	V	
Ornaments, vases, etc., overturned.	VII	V 1/2	
Chimneys thrown down and cracks made in the walls of some, but not all of the houses in one place.	VIII	VI	
Chimneys thrown down and cracks made in the walls of about half of the houses in one place.	IX	VII	

Table 4.1

Table 4.2

Fault Location.	Orientation.	Approx. Age	Morphotectonic features.	Magnitude Estimates.(Refs.)
Coire Mor (1)	126 to 154°	10.3-6kyr BP.	3km "active" fault length. 40±10m dextral offset. c.4m downthrow to N. Landslide area: 50km ² Max. distance to coherent slides: 7km. Max. distance to disrupted slides: 3.5km	6.0±0.4 5.5-6.6 4.9 5.4 4.6 Khromovskikh (1989) Bonilla <i>et al.</i> (1984) Keefe (1984a) " "
Strath Vaich (2)	345 to 020°	10.3-6kyr BP.	6km "active" length. 1.5±0.5m downthrow to E. Landslide area: 46km ² Max. distance to coherent slides: 3.5km. Max. distance to disrupted slides: 5km.	6.4±0.4 5.6-6.6 4.9 5.1 4.7 Khromovskikh (1989) Bonilla <i>et al.</i> (1984) Keefe (1984a) " "
Garbh Choire Mor (3)	172-352° 283 to 299° 234 to 276°	10.3-6kyr BP.	Rock avalanche activity.	>6.0 Keefe (1984a, b)
Beinn Alligin (4)	156 to 159°	10.3-6kyr BP.	1.5km "active" length. Sinistral displacement with downthrow to W. Rock avalanche activity. Landslide area:c.40km ² Max. distance to disrupted slides: 7km.	5.7±0.3 5.0-6.2 >6.0 4.9 4.8 Khromovskikh (1989) Bonilla <i>et al.</i> (1984) Keefe (1984a, b) Keefe (1984a)

Table 4.2(cont.)

Cuaig (5)	112 to 125°	13-6kyr BP.	1.7m downthrow to S.	6.9-7.3	Bonilla <i>et al.</i> (1984)
Loch Crann (L.Maree Fault) (6)	130 to 160°	10.3-6kyr BP.	1.5km "active" length. Unknown vertical movement.	5.7±0.3 5.0-6.2	Khromovskikh (1989) Bonilla <i>et al.</i> (1984)
Scardroy (L.Maree Fault) (7)	120 to 140°	10.3-6kyr BP.	2km "active" length. c.1m sinistral displacement? 2km to liquefaction sites. Max. distance to coherent slides: 9km.	5.8±0.2 5.5-6.6 5.5 5.5	Khromovskikh (1989) Bonilla <i>et al.</i> (1984) Youd (1977) & Kuribayashi (1985) Keefer (1984a)
Bac an Eich (8)	140-320°	10.3-6kyr BP.	1km "active" length.	5.45±0.3 5.0-6.2	Khromovskikh (1989) Bonilla <i>et al.</i> (1984)
Beinn Tharsuinn (9)	019 to 024°	10.3-6kyr BP. post-6kyr BP.	c.1km "active" length. 0.5±0.1m vertical offset. Landslide area: 40km ² Max. distance to coherent slides: 5km. Max. distance to disrupted slides: 3km.	5.45±0.3 5.0-6.2 6.4-6.6 4.9 5.2 4.6	Khromovskikh (1989) Bonilla <i>et al.</i> (1984) " Keefer (1984a) " "
Loch Monar (10)	273 to 280°	10.3-6kyr BP.	3km "active" length. Landslide area: 53km ² Max. distance to coherent slides: 8km Max. distance to disrupted slides: 7km	6.0±0.4 5.5-6.6 4.9 5.4 4.8	Khromovskikh (1989) Bonilla <i>et al.</i> (1984) Keefer (1984a) " "

Table 4.2(cont.)

Coire Eoghainn (11)	094 to 120°	10.3-6kyr BP.	3km "active" length. 20-25m sinistral displacement. c.1-2m downthrow to N. Max. distance to coherent slides: 6km. Max. distance to disrupted slides: 8km.	6.0±0.4 5.5-6.6	Khromovskikh (1989) Bonilla <i>et al.</i> (1984)
				5.4 4.9	Keefe (1984a) "
Glen Elchaig (12)	061 to 076°	10.3-6kyr BP.	7km "active" fault length.	6.5±0.4 5.7-6.7	Khromovskikh (1989) Bonilla <i>et al.</i> (1984)
An Sornach (13)	123 to 153°	10.3-6kyr BP.	1km "active" length. c.5m downthrow to N. Landslide area: 68km ² Max. distance to coherent slides: 5km. Max. distance to disrupted slides: 7km.	5.45±0.3 5.0-6.2	Khromovskikh(1989) Bonilla <i>et al.</i> (1984)
				5.0 5.3	Keefe (1984a) "
					4.8
Sgurr na Lapaich (14)	086-266°	10.3-6kyr BP.	1km "active" length. c.4m downthrow to the N. Landslide area: 68km ² Max. distance to coherent slides: 8km. Max. distance to disrupted slides: 8km.	5.45±0.3 5.0-6.2	Khromovskikh (1989) Bonilla <i>et al.</i> (1984)
				5.0 5.4	Keefe (1984a) "
					4.8

Table 4.2(cont.)

Gleann Lichd (15)	110 to 140°	10.3-6kyr BP.	5km "active" fault length.	6.3±0.4 5.5-6.6	Khromovskikh (1989) Bonilla <i>et al.</i> (1984)
			Approx. 2m downthrow to N. 1km to liquefaction site.	5.0-5.2	Youd (1977) & Kuribayashi (1985)
			Landslide area: c.43km ² Max. distance to coherent slides: 2km. Max. distance to disrupted slides: 4km.	4.8 4.9 4.7	Keefe (1984a) " "
Creag na Damh (16)	120-300°	10.3-6kyr BP.	2km "active" length.	5.8±0.2 5.5-6.6	Khromovskikh (1989) Bonilla <i>et al.</i> (1984)
			c.20m sinistral offset.	4.8	Keefe (1984a)
			Landslide area: 43km ² Max. distance to disrupted slide: 5km.	4.7	"
Sgurr a' Bhealaich Dheirg (17)	124 to 135°	10.3-6kyr BP.	2km "active" length.	5.8±0.2 5.5-6.6	Khromovskikh (1989) Bonilla <i>et al.</i> (1984)
			Possible downthrow to N of c4m.	4.8	Keefe (1984a)
			Landslide area: 43km ² Max. distance to disrupted slides: 5km.	4.7	"
Sgurr na Ciste Dhuibe (18)	115 to 140°	10.3-6kyr BP.	5km "active" length.	6.3±0.4 5.5-6.6	Khromovskikh (1989) Bonilla <i>et al.</i> (1984)
			Downthrow 4m to S.	5.7-5.9	Youd (1977) & Kuribayashi (1985)
			Sinistral displacement of c15m. 4km to liquefaction sites.	4.8 4.5	Keefe (1984a) " "
		Landslide area: 43km ² Max. distance to disrupted slides: 2km.			

Table 4.2(cont.)

Arnisdale (19)	085 to 117°	post 10.3kyr BP.	1.5km "active" length. 10±5m sinistral displacement. with c.4m downthrow to N.	5.7±0.3 5.0-6.2	Khromovskikh (1989) Bonilla <i>et al.</i> (1984)
Coire Dho (20)	056-236°	post 10.3kyr BP.	1.1km "active" length. 5km to furthest liquefaction.	5.45±0.3 5.0-6.2 5.5-5.8	Khromovskikh (1989) Keefer (1984) Youd (1977) Kuribayashi (1985)
Kinloch Hourn (21)	115 to 140°	13-10kyr BP. post 2kyr BP.	14km "active" length. 160±40m sinistral displacement. 1.2km to liquefaction sites. 2km to coherent slide.	6.9±0.5 6.1-6.9 5.1-5.3 4.9	Khromovskikh (1989) Bonilla <i>et al.</i> (1984) Youd (1977) & Kuribayashi (1985) Keefer (1984a)
Glen Gloy (22)	155 to 165°	c.10.3kyr BP.	7km "active" length. 0.5m dextral displacement. 15km to furthest liquefaction. Landslide event areas: 21km ² 8km ² 39km ² Max. distance to coherent slides: 3km. Max. distance to disruptive slides: 3km.	6.5±0.4 5.7-6.7 5.7-6.9 6.3-6.5 4.6 4.3 4.8 5.1 4.6	Khromovskikh (1989) Bonilla <i>et al.</i> (1984) " Youd (1977) & Kuribayashi (1985) Keefer (1984a) " " " "

Table 4.2(cont.)

Shuna (23)	Approx. NNW	post 10.3kyr BP.	1.0m downthrow to W.	6.3-7.1	Bonilla <i>et al.</i> (1984)
Lismore (24)	020 to 030°	3-2kyr BP.	3km "active" length. 0.5m sinistral displacement.	6.0±0.4 5.2-6.5 5.7-6.9	Khromovskikh (1989) Bonilla <i>et al.</i> (1984) "
Mull (25)	350 to 355°	post 10.3kyr BP.	2km "active" length. 2.7±0.5m downthrow to W.	5.8±0.2 5.5-6.6	Khromovskikh (1989) Bonilla <i>et al.</i> (1984)
Forth Valley (26)	Approx. NNW	9.6-8.8kyr BP.	1.0m vertical displacement. 1.5m vertical displacement.	6.3-7.1 6.8-7.2	Bonilla <i>et al.</i> (1984) "

Evidence of Large Earthquake	Magnitude	Reference
1. Largest Instrumental Recording: Oslofjord 1904.	6.4	Papastamatiou 1978
2. English Channel Event 1580.	6.2-6.9	Neilson <i>et al.</i> 1984
3. Cumulative strain release analysis of historical catalogue 1900-79.	6.44	Ritsema 1981
4. Gumbell III extreme value analysis of historical seismicity 1900-'79, using two year extremes.	6.9±2.9	Burton & Neilson 1989
5. Forecast of 10kyr earthquake	6.8±1.8	Burton & Neilson 1989
6. Palaeoseismology (Scotland)	6.5-7.0	Fenton 1991; Ringrose 1987
7. Palaeoseismology (Sweden): Pärve Fault	7.9	Muir Wood 1989b
8. Storregga slide event	>7.0	Dawson <i>et al.</i> 1988

Table 4.3

4.17 Appendix:

Distribution of UK Instrumental Seismicity 1969-'88.

The first seismometers in Europe were installed at Comrie in 1840 and by 1841 a total of 11 crude inverted pendulum instruments constituted the first microseismic array (Figure 4.3). However seismic events have been recorded in the UK since 1967, initially on the LOWNET/Eskdalemuir seismometer network and, more recently, on a more extensive nationwide network of 97 stations, both operated by the British Geological Survey (BGS). This information is catalogued (Burton & Neilson 1980; Turbitt 1984, 1985, 1987, 1988, 1989 & 1990) giving details of magnitude, time, location, depth, occasionally MSK intensity and, more recently, phase data for recorded events. Only rarely (usually for larger events) are isoseismal maps and fault plane solutions produced (e.g. Marrow & Walker 1988). Despite the lack of the latter information, maps of annual seismicity distributions give an insight into the present short-term seismotectonic regime in the UK. And in some cases such microseismic activity can be used to define active fault lineaments if of sufficient recording quality (Dames & Moore 1990) although this process is not without its problems (Ambraseys 1988).

A cursory glance at the annual distribution of epicentres shows that seismicity is concentrated as swarms of several events at an number of centres that remain sporadically active over the period of recorded seismicity. This is set against a background of more diffuse seismicity of transient swarms, coalfield events and broad regional "patches" of seismicity. In more detail the following patterns of seismicity emerge (The emphasis is on Scotland and the more significant events from elsewhere. Coalfield events, when discerned, are universally ignored):

i) **1969.** A series of events up to 1.7 M_L , all ≤ 5 km depth in the area of the Ochils. Several events recorded in the area of Loch Lomond reaching 2.0 M_L . Lochgilphead had two events of 2.0 & 2.4 M_L at depths of c. 10 km. The largest recorded event was 3.5 M_L in the area of Anglesey.

ii) **1970.** Activity continued in the Ochils with three shallow events up to 2.0 M_L . Other notable events were 3.5 M_L at Anglesey and an event of 4.8 M_B in the area of Kirby Stephen at a depth of c. 15 km.

iii) **1971.** Continuing activity in the Ochils with 4 events up to 1.4 M_L . Glen Almond area was the locus of a series of 21 events up to 2.6 M_L , all in the upper 5 km. Three events were recorded off Scarba and also in the area of Armadale.

iv) **1972.** Activity in Glen Almond reduced in both frequency and magnitude with 4 events only reaching 1.6 M_L . The locus of the Ochils events moved to the area of Dunblane with events up to 2.6 M_L . The Highland Border region was subject to several shallow, weak events in the area from Loch Lomond to Ben Ledi. Weak events were recorded in the area of Killin, Raasay and Luing. Events of most note were 3.6 M_L at a depth of c. 5 km near Lochgilphead and an event of 2.2 M_L at 22 km(?) in the area of Fort William. Elsewhere an event of 4.0 M_B was located at a depth of c. 6 km near Todmorden in Yorkshire.

v) **1973.** Glen Almond and the Ochils both had several minor events. The area of Penrith was the locus of 2 events of 3.9 & 4.9 M_L . A 3.5 M_B event at c. 5 km depth was recorded in the area of Mansfield.

vi) **1974.** The area of Kintail was subject to a swarm of 21 events up to 4.4 M_L , of which 14 were greater than 3.0 M_L . The area of the Ochils, Glen Almond and Lochgilphead were all subject to a number of weak, shallow events. Other events of interest were a 3.0 M_L event near Langholm, a 3.5 M_L at c. 15 km depth in North Wales, 2 events of 3.7 & 4.1 M_L near Newport and another South Wales event of 3.0 M_B .

vii) **1975.** Kintail continued to be the locus of intense activity with events up to 4.8 M_L , 4 of which exceeded 3.0 M_L . The Ochils, Glen Almond and the area of the Highland Boundary continued to have a number of weak events. A series of 12 events up to 4.2 M_L were located in the region of Ben Nevis while activity on the Great Glen Fault was centred around Invergarry. Other areas of note were Arran with an event of 2.5 M_L , a 4.0 M_L event off Colonsay, a 3.8 M_L in South Wales, 3.5 M_L near Hereford and 2 events of 2.2 M_L and 3.4 M_B near Stoke-on-Trent.

viii) **1976.** While activity in Kintail dropped to one event, Invergarry and Ben Nevis continued to be the locus of shallow events up to 2.0 & 3.1 M_L respectively. Activity also increased in the area of the Ochils with a number of small shallow events. An event of 2.5 M_L was recorded off Islay. Stoke was again the locus of 2 events of 2.5 & 3.0 M_B . The largest event of the year, 4.5 M_L , was recorded near Widnes at c. 2 km depth (?).

ix) **1977.** The area of the Ochils showed a continued increase in activity with events up to 2.6 M_L . Activity around Ben Nevis and on the Great Glen Fault reduced to the level of that at Kintail, i.e. 2 events in the range 2-2.5 M_L . Solitary events were recorded at Strathconon, Loch Fyne and Lochgilphead of 2.4, 2.1 & 1.5 M_L respectively. The largest onshore event was 3.5 M_L near Nottingham (N.Sea events reached 5.6 M_L)

x) **1978.** Activity at Kintail increased with 26 events up to 3.8 M_L , of which 4 were $\geq 3.0 M_L$. When resolved focal depth was of the order of c. 10 km or less. Activity in the areas of the Ochils and the Great Glen Fault showed a marked decrease in both frequency and magnitude. Glen Almond was again the locus of a small swarm of shallow, weak events. Kinlochewe and Oban became the sites of small swarms with events up to 3.4 and 2.3 M_L respectively. Other notable events were 2.9 M_B near Selby and 2.7 M_L at Anglesey.

xi) **1979.** Continued but reduced activity in Kintail with 4 events up to 2.9 M_L . The Ochil Hills were subject to a swarm of 27 events up to 3.2 M_L and MSK intensity 5. Oban and Lochgilphead were the sites of minor activity. The Torridon area suffered 2 events of 2.0 M_L and 2.2 M_L while other events were recorded off Jura, Armadale and at Kingairloch. Mansfield was again the locus of a small swarm of events up to magnitude 3.1 and intensity 4. The most significant seismic activity of the year was in the area around Longtown near Carlisle with a swarm of activity associated with a main shock of 4.8 M_L , intensity 6.

xii) **1980.** There was an increase in the amount of activity in the area of Longtown with 56 events up to 4.1 M_L (Intensity 5). Activity in the Ochils continued where there were 24 events of up to 3.0 M_L . Kintail, Lochgilphead and the Knoydart area showed continuing activity while activity resumed on the Great Glen at Ardgour and in the Moray Firth with events recorded at 2.0 M_L . Central Perthshire, around Ben Lawers, was subject to a number of small events. In the south the Stoke/Talke area was subject to a number of deep events, three of which were greater than 3.0 M_L . South Wales was the locus of a small swarm of events up to 2.4 M_L and one event of 3.0 M_L was recorded in North Wales.

xiii) **1981.** The swarm of deeper events in the Stoke area continued with a maximum of 3.1 M_L . Activity around the Ochils and Longtown declined in both magnitude and frequency, while that in the Kintail and Cowal-Lochgilphead areas remained comparable to previous years. Elsewhere in Scotland Oban, Lochaber and

Islay suffered minor events. The Great Glen area, Central Perthshire and Knoydart all had minor bursts of activity. The most intense activity of the year was recorded around Constantine in Cornwall where there was a massive swarm of 167 events up to 3.5 M_L , intensity 5 at depths of 5-10 km. Solitary events of 2.7 M_L were recorded in North Wales and near Nottingham.

xiv) **1982.** The Ochils, Cowal, Perthshire, Knoydart and Kintail were the locus of several small events. Lochaber and Cannich each suffered minor events. Activity in Cornwall dropped off to almost nothing. A single event of 3.0 M_L was recorded near Basingstoke.

xv) **1983.** Minor bursts of activity continued in Perthshire, Knoydart, Cowal (up to 2.4 M_L) and in the Ochils. Dumfries was the centre of a swarm of 9 events up to 2.3 M_L and intensity 3+. Lochaber, Loch Maree and the Great Glen at Strontian had events of 2.4, 2.0 and 2.0 M_L respectively. The Sound of Jura had 2 shallow events of 2.1 and 2.3 M_L . North Wales, Cornwall and Cumbria all suffered swarms of minor events. One event of 2.2 M_L near Harrogate was located at a depth of 28.9 km!

xvi) **1984.** The areas of the Ochils, Lochaber, Cowal, the Great Glen, Dumfries, Cornwall and Cumbria showed almost identical activity to the previous year. Kintail had 3 small events at shallow levels while the area of Knoydart had a shallow swarm of events up to magnitude 2.2. Loch Maree also showed an increase in activity with a series of 5 events up to 2.4 M_L . The most significant seismic activity of the year was on the Lleyn Peninsula in North Wales where there were 49 events culminating in an event of 5.4 M_L , intensity 6, the largest recorded event in onshore UK. Of this series of events 4 were greater than 3.5 M_L and 12 were greater than intensity 4+. This activity was recorded as having a source depth of 15-25 km. Two deep events of 3.0 M_L and 3.2 M_L were recorded in the areas of Selby and Accrington respectively.

xvii) **1985.** Aftershocks to 2.3 M_L continued on the Lleyn Peninsula. The Dumfries area, the Great Glen, Lochaber, the Ochils and Cumbria also continued to be the locus of activity. Kintail and Loch Maree were subject to several small shallow events. Two shallow events of 2.0 and 2.4 M_L were recorded near Jura. Activity increased in Knoydart and Cowal with events of 3.7 M_L , intensity 4 and 3.5 M_L , intensity 5. Elsewhere there was a shallow swarm of 13 events around the Scilly Isles up to 3.6 M_L .

xviii) **1986.** Aftershocks continued in the area of the Lley Peninsula with 34 events up to 2.7 M_L . Minor activity continued at Dumfries, Cumbria, the Ochils, the Great Glen, Lochaber and Kintail. There was a slight decrease in the amount of activity in the area of Loch Maree and also at Constantine in Cornwall (21 events up to 2.9 M_L). Cowal suffered 8 minor aftershock events. The Knoydart-Mallaig area was subject to 17 events up to 3.0 M_L , intensity 3+. Comrie was the site of renewed activity with 11 small events. Crianlarich was also the locus of a swarm of 34 minor events up to 1.9 M_L . Several minor events were also recorded around Torrion. The most significant seismicity of the year was found around Oban where there were 11 events up to 4.2 M_L , intensity 5. Also of note was an event of 2.9 M_L recorded at a depth of 23.5 km near Oxford.

xix) **1987.** Minor activity continued around Dumfries, Comrie, the Great Glen, Knoydart and Kintail, while Loch Maree, Torrion, Lochaber, Crianlarich and the Ochils showed a reduction in the frequency of seismicity. The Cowal area had 11 minor aftershock events while only one was recorded near Oban. 24 events up to 3.0 M_L , intensity 4+, were recorded in the area around Ullapool and a swarm of 14 events up to 2.6 M_L , intensity 3+, were recorded in the Mull/Ardnamurchan area. The Renfrew area was subject to 12 events up to 2.4 M_L , intensity 4+. Aftershock activity at Lley continued to decrease while Cornwall showed a slight increase.

xx) **1988.** Minor activity continued along the Great Glen, in the areas of Firth of Lorne and at Fort William, and also at Renfrew, Kintail, Oban, NW. Mull and the Ochils. Minor activity was also recorded near Ullapool, Loch Carron, Cumbernauld and Greenock. The Cowal area had 7 shallow events up to 2.7 M_L and Rannoch Moor had 4 events up to 2.6 M_L . Johnstonbridge in Dumfries & Galloway suffered 15 shallow events up to 1.8 M_L . Further diffuse activity in the Borders region was of minor significance. Longtown still showed activity with several events up to 2.4 M_L . The largest event of the year, a 3.2 M_L and 3.0 M_L double event at Ambleside in Cumbria occurred at 15 km with an intensity of 4+. Lley aftershocks continued with 23 events up to 2.1 M_L . Diffuse activity also continued around Constantine in Cornwall and in South Wales. Other small swarms were recorded in the southern Irish Sea and near Hay-on-Wye (16 events up to 1.4 M_L). Other significant events were 2.7 M_L at Bridgewater in Somerset and 2.7 M_L in the Scilly Isles.

Chapter 5

Attempted Age-Dating of Late Quaternary Fault Movements in N.W.Scotland using ESR and Intrafault Quartz Grain Morphology

Clark Fenton

*Department of Geology and Applied Geology,
University of Glasgow, Glasgow, G12 8QQ.*

5.1 Abstract

A programme of age-dating was carried out in order to constrain the timing of late Quaternary fault activity in relation to the removal of the last (Late Devensian) ice cover in N.W. Scotland. Due to the recency of the fault movements and the lack of a well developed and dated Quaternary stratigraphy in the area an attempt was made to apply the technique of Electron Spin Resonance (ESR) age-dating to intrafault quartz grains, assumed to have formed at the time of faulting due to mechanical grinding of the country rock within the fault zone itself. A parallel study using the grain surface morphology of intrafault quartz to estimate the age of fault movement was also carried out. The results of the ESR study showed that sampling of surface fault exposures did not yield material that had been reset during the most recent fault movement, and as such gave saturated ESR signals. The investigation of the surface morphologies of the intrafault quartz grains gave a crude indication of the recency of fault movement, but on their own these results are somewhat equivocal and require to be corroborated by independent dating means. Recommendations for the collection of samples for ESR study and samples for surface morphology studies are made.

5.2 Introduction

It is of importance to elucidate the last movement along faults to calculate the recurrence interval for such movements. This is especially important in respect to the siting of large engineering structures, particularly those of a sensitive nature such as nuclear power installations and radioactive waste repositories. It is often difficult to find evidence for recent fault movements (Bonilla & Lienkaemper 1990) and more difficult to obtain unambiguous age estimates for the timing of such movements due to the lack of material within fault zones that can be age-dated with the accuracy required of the seismic risk assessment studies.

As a consequence of fault movement the crushing and grinding of the fault side walls at shallow crustal levels produces a fine grained aggregate of the wallrock called fault gouge. This is composed of mechanically ground and fractured mineral fragments. Most minerals will break along their planes of cleavage and therefore are not very resistant to such mechanical abrasion. However quartz, which does not possess cleavage planes, is more resistant to crushing, breaking along conchoidal fracture faces, and is therefore usually the dominant mineral found in fault gouge. Thus by its almost universal occurrence in fault gouge quartz provides a possible medium for recording the history of fault movement.

Extensive fieldwork in N.W. Scotland has revealed the presence of a number of post-glacial faults (Figure 5.1) that show varying degrees of movement, offsetting late Quaternary landforms and drainage courses. Associated with this fault activity are extensive ground deformation features, namely liquefaction of sediments and large-scale slope failures (Ringrose 1987; 1989a, 1989b; Davenport *et al.* 1989; Ringrose *et al.* 1991) [§ 2, p15]. With the exception of ^{14}C dating of peat incorporated within the fault zone of the Kinloch Hourn Fault no absolute age dates for the movement along the faults have been obtained (Ringrose 1987, 1989b). The lack of a well developed Quaternary stratigraphy in N.W. Scotland precluded the use of more conventional age-dating techniques. Hence a new method of dating the gouge found within the fault zones was sought. ESR (Electron Spin Resonance) seemed to be ideal for the purpose in that it had already been widely used to date intrafault quartz grains from a number of locations, mostly in Japan (Ikeya & Miki 1985), and was accurate within the time span under consideration i.e. c. 10 kyr BP. Assuming that intrafault quartz grains are the product of mechanical grinding of the fault side walls, a parallel study was carried out using SEM (Scanning Electron Microscopy) to investigate the corrosion of the

conchoidal faces with time since faulting in an attempt to obtain a qualitative estimate of the time since the creation of the intrafault grains.

5.3 Electron Spin Resonance (ESR): An Introduction

ESR has been used to date a number of materials in the field of geology including quartz (flint, intrafault grains), carbonates (corals, speleothems, travertines), apatite and gypsum (Ikeya 1986; Grün 1989). ESR, although a relatively new arrival in the world of age-dating, has been the subject of several reviews which detail the advances in the various applications of the technique (Hennig & Grün 1983; Ikeya 1986; Grün 1989). The majority of fault dating studies using ESR have been carried out by workers in Japan (Ikeya & Miki 1985), however there are some notable exceptions (Schwarcz *et al.* 1987; Buhay *et al.* 1988). As far as is known this is the first such study carried out in the U.K.

5.3.1 Principles of ESR Age-Dating

ESR dating is based on the direct measurement of the number of (natural) radiation-induced paramagnetic electrons trapped in crystal structure defects. Radiogenic elements (eg. U, Th, K) generate 'free' electrons that accumulate in minerals over geological time. The ESR-age is calculated by dividing the total amount of accumulated radiation dose by the annual dose:

$$\text{ESR Age} = \frac{\text{Accumulated Dose}}{\text{Annual Dose}} \quad (1)$$

ESR spectroscopy is used to detect paramagnetic centres and radicals. These species can be formed in naturally occurring minerals by ionizing radiation which excites electrons from their valence band energy levels to higher energy levels called the conduction band. The electrons return to the valence band after a period of diffusion. However some of the electrons are trapped at natural charge deficit sites and form paramagnetic centres. The number of electrons trapped at a given centre, and hence the intensity (height of the spectrum) of the ESR signal, is proportional to the radioactive dose rate (strength of the radioactive field) and the time of exposure to this radiation of the sample, ie.

$$\text{Accumulated Dose} = \int_0^T \text{Dose Rate (t) dt.} \quad (2)$$

The sample records the radioactive dose from the environment (from up to 30 cm radius (Grün 1989)) and from cosmic rays. Such natural radiation results from the decay of isotopes of U- and Th- decay chains. ^{40}K , Rb and ^{14}C are also responsible for minor emissions.

Accumulated dose (AD) is the radiation dose that the sample has accumulated since formation or the last 'zeroing' event. AD is determined by the additive dose method; a number of aliquots of sample are irradiated stepwise with increasing doses of γ -radiation (from a ^{60}Co source) which causes an increase in intensity of particular ESR signals ie. creates more paramagnetic species.

If ESR signal intensity (spectrum peak height) is plotted against γ -dose and extrapolated to zero intensity we get a value for AD (Figure 5.2). The dose rate (D), given as averaged dose rate per year in units of Gray (Gy/yr), not necessarily constant over time, is calculated from chemical analysis of radiogenic elements (U, Th & K) in the sample. Radioactive field strength irradiating the sample is dependent on the concentration and distribution of radioactive elements in the sample and its immediate environment and also on cosmic rays. Various physical and chemical effects have to be taken into consideration when calculating D (Grün 1989). ESR age-dating requires the evaluation of the following parameters:

- (a) External γ -dose: measured on site using a portable gamma-spectrometer.
- (b) Cosmic dose rate: measured using gamma spectrometer or calculated from attenuation diagrams (Grün 1989, appendix A).
- (c) Radioactive elements: concentration in the sample is determined by Atomic Absorption, fission track or delayed neutron activation.
- (d) Isotopic ratios: often assumed or calculated iteratively.
- (e) Attenuation of radioactive particles: dependent on sample size.
- (f) Water content: accounted for if in situ external γ -dose determination is carried out.
- (g) Density: calculated from mineralogical tables.

The lower limit of the dating range is determined by the sensitivity of the ESR detection equipment used, and the upper limit by the lifetime of the electrons in the traps. For quartz from fault gouges the dating 'window' is from 1 kyr to 1-2 myr, approximately the duration of the Quaternary era.

5.3.2 ESR Spectra of Quartz and Resetting Mechanisms

ESR spectra of quartz are complicated (Figure 5.3A) and normally display up to five different paramagnetic centres. Some centres such as Ge, E' (oxygen vacancy centre) and OHC (oxygen hole centre) require recording at room temperature while Al and Ti centres have to be recorded at temperatures around 100 K. The basic assumption of ESR age dating is that samples do not contain paramagnetic centres at $t=0$. If samples previously contained paramagnetic centres some mechanism at $t=0$ must destroy these centres and reset the sample. At least four different zeroing mechanisms can be applied to the dating of quartz. The first is the formation of the mineral itself. The Ge centre is bleached by (7-8 hours of) sunlight and therefore is of no value to fault dating studies. Heating can also cause zeroing; Al and E' centres anneal at 200°C while Ge and OHC centres anneal at over 300°C (Fukuchi *et al.* 1985).

Quartz is most often used for ESR dating of faults. Miki & Ikeya (1982) report only partial resetting upon hydrostatic pressure, as do Sato *et al.* (1985). Grinding experiments (Ariyama 1985; Ito & Sawada 1985) show that E' and Ge centres are only totally reset when displacement is ≥ 500 mm and the pressure (overburden, tectonic etc) on the fault plane is ≥ 20 bar. Buhay *et al.* (1988) and also Schwarcz *et al.* (1987) show that the OHC centre is the most sensitive to pressure, with AD decreasing as pressure increases, followed by the Al, then the Ti centre. However the Ge centre intensity increases with pressure. There is a noted decrease in AD with increasing pressure for decreasing grain size to a minimum (plateau) value for grains below 80 μm .

Numerous fault-dating studies using ESR have shown the results obtained are consistent with geological evidence (Ikeya *et al.* 1982; Miki & Ikeya 1982; Kanaori *et al.* 1985; Toyokura *et al.* 1985; Zhuo-ran *et al.* 1985). Kosaka & Sawada (1985) show the importance of sampling individual laminations in a gouge zone where each laminations may represent a separate movement episode. Fukuchi (1989) shows that ESR signal intensity increases towards the fault boundary. Ito & Sawada (1985) show that to gain reliable ages samples must be collected from gouge zones of < 2 cm

thickness, flanked by wallrock and at the time of displacement were at depths of >70 m for strike-slip faults, >20 m for reverse faults, >100 m for normal faults (ie. subject to >20 bar) to ensure that the material has been totally reset by fault movement. Fukuchi (1991) suggests depths of >250 m. Ariyama (1985) shows that displacement should be at least 50 cm.

The differing stress sensitivities of the various ESR centres can be used as an indicator of complete resetting during fault movement i.e. the age estimates from each centre will only agree if resetting has been complete. If this is not the case the Ti centre will give an older age estimate than the Al centre, which in turn will be older than the OHC centre. Age estimates for the various grain sizes will only conform if the pressure during fault movement was sufficient to cause complete resetting. If for the smallest grain sizes the ADs of the various centres diverge and no age plateau can be determined for the OHC centre, then the sample was most probably not zeroed and no age estimate can be made. The minimum age for the smallest grains will give last movement of the fault. A further complication may be that not all samples contain OHC, E' and Ti centres.

Since faults are normally very disturbed geological environments the measurement of γ -dose rate in situ is desirable. β -irradiation can be calculated, by neutron activation, prior to quartz separation. It is also necessary to calculate the ADs for a range of grain sizes.

5.3.3 Sample Collection and Preparation

There seem to be as many sample preparation methods as there are published papers on ESR age-dating of intrafault quartz grains. This is probably due to the differing mineralogical compositions of fault gouge from faults cutting a wide variety of rock types. General considerations are that intense light and severe crushing should be avoided to preserve certain centres from being reset during sample preparation. The ultimate aim is to obtain a pure quartz sample from the heterogeneous fault gouge.

Samples were collected from various faults in NW Scotland (Figure 5.1; details of sample sites are given in Appendix A) that have been shown to have, or are suspected to have, undergone late Quaternary displacement (Ringrose 1987, 1989a, 1989b; Davenport *et al.* 1989; Ringrose *et al.* 1991) [§ 2, p15]. Samples were extracted from surface exposures of the faults; remote locations (and the financial constraints of a NERC studentship) prevented the collection of samples from

drill core. γ -dose rate and cosmic ray activity were recorded in situ using a portable γ -spectrometer (see Grün & Fenton 1990a); this required the drilling or excavation of a ≥ 30 cm deep hole in the fault zone to accommodate the spectrometer detector. Samples were immediately sealed in plastic bags and then wrapped in black polythene to avoid excessive exposure to strong light. Prior to sample preparation a representative fraction of each sample was taken for delayed neutron activation to discover the β -activity of each site. X-ray diffraction (XRD) was used to determine the composition of each sample (Table 5.1), thus making it easier to decide which reagents to use for quartz separation. Fault gouges were prepared in the following manner.

Samples of the soft clay-like gouges, about 500 cm³ in volume, were wet sieved through a series of mesh sizes (500-63 μ m) to give a number of size fractions. Each size fraction was then left in 10% HCl for 24 hours to remove carbonates. Following washing in de-ionised water each sample was put in 35% H₂SiF₆ for 30 hours to dissolve feldspar. The residue was again washed in de-ionised water and put in 50% HBF₄ at 30°C for 48 hours to remove mica. Those samples with an abundance of mica were first 'rolled' in cellophane film to remove the bulk of such grains prior to treatment with fluoboric acid. After further washing and air drying the samples were passed through a Franz isodynamic magnetic separator at a current of 2 amps to remove a dominantly quartz non-magnetic fraction. If the remaining fraction was noted to contain significant amounts of pyrite further treatment with concentrated HNO₃ at 50°C was carried out for 24 hours. Treatment with 10% HF for 2 hours then removed the surface 20 μ m of the grains that had been subject to α -radiation damage. A final washing with de-ionised water in a sonic bath for 30 minutes removed any traces of acid residues and any other particles adhering to the grain surfaces. Finally any remaining non-quartz grains were removed by hand-picking under a binocular microscope.

Each fault gouge site was now represented by five quartz grain size fractions: 355-250 μ m; 250-180 μ m; 180-125 μ m; 125-63 μ m; <63 μ m.

5.3.4 Sample Irradiation

Ten aliquots (40,100 or 200 \pm 0.1 mg depending on sample abundance) of each sample size fraction were weighed out and put in 2 mm thick glass vials for irradiation. This was carried out using a ⁶⁰Co γ -radiation source with an output of 0.5 kRad min⁻¹. The samples were irradiated for 0, 1, 2, 4, 8, 16, 32, 55, 80 and 100

minutes receiving equivalent doses of 0, 0.5, 1, 2, 4, 8, 16, 27.5, 40 and 50 kRad. [0, 5.7, 11.4, 22.8, 45.5, 91, 182, 313, 455 and 569 Gy].

5.3.5 Results

In situ dose rate and neutron activation analysis on the bulk gouge samples suggested that the maximum AD during the Holocene is less than 200 Gy (Grün & Fenton 1990b). ESR spectra were measured at room temperature and at c. 95 K. The samples did not contain OHC and Ge centres. The concentration of the Ti centre could not be quantified. All samples measured either yielded much higher ADs than were expected or, as was the case in many samples, were saturated i.e. additional radiation did not cause any further significant increase in the spectra intensity (Figure 5.3). This makes it impossible to obtain a value for AD as the extrapolated line on the dose-spectra intensity plot (see Figure 5.2) does not intercept the x-axis, but runs parallel to it.

5.3.6 Discussion

Possible explanations of the observed results are:

- (i) ESR does not work as an age-dating technique.
- (ii) Faulting is much older than first supposed.
- (iii) Pressure in the fault was not great enough to reset the ESR signal as fault movement has occurred on old faults and the most recent movement has been lubricated by old fault gouge.
- (iv) Pressure in the fault was not sufficient at the position from where the samples were collected (surface outcrops) to effect the ESR system.

A number of studies show that ESR age-dating is accurate when compared with other age-dating techniques (e.g. Ikeya & Ohmura 1983) and where independent geological control on the age of fault movement is present. Therefore hypothesis (i) that ESR does not work is rejected. Likewise hypothesis (ii) is rejected as there is abundant geological evidence to support the late Quaternary movement along the faults under consideration (Ringrose 1987, 1989a, 1989; Ringrose *et al.* 1991) [§ 2, p15]. That the fault gouges may be formed due to significantly older fault movements and

therefore acted as lubricating surfaces during the most recent movements, thus reducing the pressure on the fault surfaces to such an extent that it was not great enough to reset the ESR system is possible as most of the faults have had a long history of reactivation and several do show that there is reworking of older gouge materials [e.g. § 2.6.6, p30]. However examination of the gouges using SEM [§ 5.4] shows that many of the quartz grains display 'fresh' (conchoidal) fracture faces showing that there must have been sufficient pressure on the faults to have caused fracturing of intrafault grains. Evidence from deformation features spatially related to the faults and 'roughly' contemporaneous with the fault movement show that it was seismogenic in nature, therefore there must have been considerable stress acting across the fault zones at this time that was released by frictional slip and not by lubricated sliding. Thus statement (iii) is also rejected. Samples were collected from surface outcrops and therefore do not conform to the sampling recommendations of Ito & Sawada (1985) and in this respect may not have been fully reset due to insufficient pressure during the most recent fault movement. This is in agreement with the findings of the SEM study of quartz grain morphology where it is seen that the samples have more than one type of grain surface morphology, indicating a spread of 'ages' within each sample, pointing to the fact that surface samples were not fully reset during the most recent fault movements.

5.4 SEM Investigation of Surface Morphologies of Intrafault Quartz Grains

Intrafault quartz grains are found to have a surface texture peculiar to each fault. Complexities notwithstanding, the observed textures can be divided into ten differing types, which in turn can be classified into four groups based on the classification of Kanaori *et al.* (1980). This is an ordered series of increasing complexity from simple conchoidal faces to undulose faces and cavities.

When the grains are formed due to the mechanical degradation of the fault sidewalls they fracture to form smoothed or stepped conchoidal facets. In the time since the last faulting event these grains are subject to the effects of the prevailing groundwater geochemical regime. This results in progressive corrosion of the conchoidal facets with time, resulting in increasing complexity of grain surface morphology. The dissolution of quartz is controlled by the geochemical environment of the gouge. This is a function of temperature, groundwater geochemistry, and chemical composition and permeability of the fault gouge itself. As the solubility of quartz alters little under conditions of $\text{pH} < 9$, low temperature and pressure, the rate of

grain surface corrosion is similar in most near surface environments with the exception of areas of alkaline soils and geothermal zones. The rate of quartz dissolution in near surface environments has been shown to be on the scale of geological time (Kanaori *et al.* 1980), thus comparison of surface morphologies gives a useful estimate of the time of fault movement. By comparison with dates obtained from more conventional dating methods the observed textures have been correlated with absolute age dates (Kanaori 1983; Kanaori *et al.* 1985; Kanaori *et al.* 1986) (Figure 5.4).

The surface texture classification is as follows:

5.4.1 Group I Textures

The surface features of grains belonging to this group have irregular shapes. Edges have sharp apices and are characterised by simple and smooth faces. Minute holes of 1-3 μm may be present on some surfaces. The group contains two texture types:

Subconchoidal Texture (Ia) shows smooth surfaces with slightly blunted peaks. Minute holes of 1-3 μm diameter may appear on part of the smooth surfaces. Steps are 1-3 μm wide and have slightly blunted edges (Figure 5.5a,b).

Orange-peel Texture (Ic) has generally smooth, though slightly undulose surfaces. Edges and peaks are rounded with characteristic 'bite marks'. Small holes of less than 1 μm diameter occasionally form as clusters on the surfaces (Figure 5.5c)

An intermediate texture between the subconchoidal and orange-peel textures, the Ib (Figure 5.5d) texture shows the corrosion of the steps seen in Ia, but not to the extent of the 'bite marks' of the Ic texture.

5.4.2 Group II Textures

Grains in this group show small angular shapes with remnant sections of smooth faces. Faces have small undulations or small irregular holes (Figure 5.5e). Two texture types are represented:

Fish-scale Texture has surfaces of small v-shaped facets of approximately the same size and forming a line in a particular direction. These facets and undulations are about 3-5 μm in size.

Moss-like Texture shows hemispherical or moss-like aggregations with undefined edges. Undulations are of the order of 3-5 μm in height.

5.4.3 Group III Textures

Grains have well defined round shapes with considerably undulated surfaces. Undulation is of the order of 5-10 μm (Figure 5.5f). There are three texture types:

Moth-eaten Texture shows random development of complicated winding holes on the surface of the grains.

Stalactitic Textures comprises columnar protrusions with round points divided by incised valleys. Columns are 3-5 μm high, reaching a maximum of 10 μm .

Stalactitic and moth-eaten textures are only superficially different and, since the degree of undulation is nearly the same, are considered to belong to the same group.

Moss-like Texture is more uneven than that of Group II as no smooth surface remains. Undulation is of the order of 5-10 μm in height.

5.4.4 Group IV Textures

Grains are completely rounded and show well developed, interconnecting cavities that are remarkably large and deep. Cavities extend 50-100 μm into the grain. Two texture type are represented:

Pot-hole Texture shows hemispherical holes and deeper cylindrical holes. The holes overlap to produce a complex marginal line. The holes are 5-10 μm in diameter and 10-50 μm deep, although some reach c. 100 μm .

Coral-like Texture has continuous cavities irregularly developed on the grain surface. Cavities occupy the majority of the surface.

Comparing these textures with those of sedimentary quartz grains shows that the texture seen in Groups III and IV are considered to be unique to intrafault grains (Krinsley & Doorncamp 1973).

5.4.5 Sample Collection and Preparation

Samples were collected from three faults that had been shown to have exhibited late Quaternary movement. These corresponded with some of the sample sites used in the ESR study (see Appendix B). Two further faults in the area of Glen Shiel (Figure 5.1) suspected of having been active during the late Quaternary were also sampled. Samples were collected from shallow excavations of surface fault outcrops. Where there were multiple generations of fault gouge care was taken to sample each individual unit separately and avoid contamination.

Samples were prepared in a similar manner to those used in the ESR study. The mineralogy of the samples were determined by XRD (Table 5.2) in order to determine the method of sample preparation. About 200 cm³ of the fault gouge was disaggregated in de-ionised water. This was then stirred and the upper portion poured off several times until only the coarser grains remained. The residue was then immersed in 10% HCl for 24 hours to remove any carbonate minerals. The residue was then washed and wet sieved through No.60 and No.200 Tyler sieves to collect grains in the size range 250-64 µm. The grains were then cleaned in an ultrasonic bath with distilled water for 30 minutes to remove any particles adhering to the grain surfaces. The grains were then air dried and passed through a Franz isodynamic magnetic separator to collect the non-magnetic fraction. Finally using a binocular microscope, the remaining non-quartz grains were removed by hand picking.

A random sample from each prepared sample was placed on SEM stubs using double-sided adhesive tape. Each sample was represented by 40 to 100 individual quartz grains. The samples were then gold coated and examined using a Scanning Electron Microscope (SEM) with an energy-dispersive x-ray detector (EDAX). The EDAX system was used to ensure that the grains studied were quartz and not feldspar or any other mineral material.

5.4.6 Results

The grain surface morphologies noted in each sample are summarised as histograms in Figures 5.6, 5.7 and 5.8. These show frequency and percentage frequency of morphology type for each gouge sample.

The samples from the Loch Maree Fault at Scardroy (Figure 5.6a,b) show a dominance of 1c textures with the exception of sample CF27, which has a dominance of Ib textures. All samples contain traces of grains with Group II textures and there is an absence of 'older' textures. Only CF27 contains grains showing Ia textures.

The samples from the Beinn Tharsuinn and Kinloch Hourn Faults (Figure 5.7) show a dominance of Ic and Ib textures respectively. Both contain some Group II and Ia grains. The sample from Kinloch Hourn was noted to contain rare Group III grains.

The samples from Gleann Lichd (Figure 5.8) did not show dominance of any particular textural group with a spread of morphologies being present from Ia through to Group III.

The sample from the Glen Shiel (Figure 5.8) showed a dominance of Group II grain surfaces, but with a spread of surface types from Ib through to Group III.

None of the gouge samples examined contained Group IV grain surface morphologies and none had a dominance of 'fresh' Ia or conchoidal surfaces.

5.4.7 Discussion

The results from this study agreed with the findings of Kanaori *et al.* (1980) that the grain surface morphologies from an individual fault are unique and are dominated by one particular grain surface group, even where the fault cuts various rock types. The grain surface morphologies were plotted against approximate age of formation as determined by Kanaori (1983) and Kanaori *et al.* (1985) (Figure 5.9). This showed that using intrafault quartz grain surface morphologies gave an older age than that expected from the geological field evidence for the last movement of the faults [§ 2, p15]. This discrepancy could be due to number of factors:

- (i) The field evidence for the last movement of the faults is wrong or has been misinterpreted.
- (ii) Grain surface morphology cannot be used as an indicator of the time since last fault movement.
- (iii) Last fault movement did not effect the surface morphology of the intrafault material.

The field evidence for the late Quaternary movement of the faults in question is considerable and wide ranging (Ringrose 1987, 1989a, 1989b; Davenport *et al.* 1989; Ringrose *et al.* 1991) [§ 2, p15]. This includes the relative dating of the fault movement with respect to Quaternary deposits and landforms, and 'absolute' ^{14}C dates (Ringrose 1987) that clearly show that the last movement along these faults was post-glacial ie. occurred in the last 10 kyr. Thus hypothesis (i) is rejected. Hypothesis (ii) is also rejected on the evidence of the extensive work previously carried out using intrafault quartz grains to date the last movement that has been confirmed by independent dating techniques and other geological evidence.

That the last fault movement did not effect the gouge materials to such an extent as not to have significantly altered the surface morphologies of the intrafault quartz grains has been hinted at in the discussion of the ESR results where the observed results are attributed to insufficient pressure on the fault at the depth of sample collection. This may also have been the case with the observed grain surface morphologies being a result of previous fault movement episodes that have not been erased in the most recent fault movement. This could be due to either lubrication of the fault by pre-existing gouge material, with movement and fracturing being accommodated by the smaller interstitial grains, and the high amount of fluid thought to have been present in the faults at the time of movement [§ 6, p260] or the fact that the pressure acting on the fault planes at such shallow levels may have been insufficient to cause fracturing of the quartz grains. That the gouges have not been totally reset by the most recent episode of fault movement is shown by the almost total lack of Ia grain surface morphologies. Most of the samples do contain at least some Ia grains, but these are usually subordinate to the other 'minority' textures displayed. If the gouges had been reset by late Quaternary movement it would also be expected that there would be some conchoidal faces remaining, especially in the case of the Kinloch Hourn Fault where it has been shown to have moved as recently as 2.5 kyr BP (Ringrose 1989b). The fact that there has been only partial or no 'resetting' of the

gouges during the last fault movement is shown by the spread of morphologies exhibited by all the samples. This is particularly evident in the case of the samples taken from the Gleann Lichd fault where the field evidence points strongly to the gouge present in the most recent zone of movement having been created from the reworking of an older fault rock.

Despite the failure of the quartz textures to confirm post-glacial movement along the faults the results (Figure 5.9) still point to late Quaternary reactivation (<1.0 Ma, some showing <0.1 Ma) of the faults under investigation.

The difference in the dominant textural type displayed by sample CF27 from the other samples collected from Scardroy (CF25, 26 & 31) shows the importance of collecting from individual gouge zones and not from the fault zone as a whole. Reliable criteria for determining which particular gouge zone has been the subject of most recent fault movement are yet to be established (Grün 1991).

The fact that the samples do not seem to have been 'reset' by the most recent fault movement suggests that to obtain realistic results using SEM investigation of intrafault quartz grains may require the use of the same criteria as proposed for the collection of samples for ESR age dating; that is, samples collected from a depth that had experienced sufficient pressure in the fault zone to have caused fracturing of the pre-existing grains in the case of fault zone reactivation. If, as was previously suggested, movement along the faults has been lubricated by the presence of a pre-existing gouge and that the smaller grains accommodate movement (like ball bearings?) it will be necessary to investigate the smallest size fraction separated from the gouge material i.e. < 64 μm . This would prove to be unfeasibly problematic in sample preparation. Thus, it must be recommended that in the collection of samples for SEM investigation of intrafault quartz with a view to dating the time since formation workers use the criteria developed for the collection of samples for ESR age-dating if it is hoped to elucidate the time since the *last* movement along the fault under investigation.

5.5 Conclusions

Despite the failure of this study in its primary objective to give 'absolute' dates for the movement of post-glacial fault movement in N.W. Scotland, it has provided important information in the fields of ESR and intrafault quartz grain morphological dating of recent fault movements. The recommendations for the collection of samples

for ESR age-dating of Ito & Sawada (1985) and Kosaka & Sawada (1985) have been confirmed and expanded upon. The results of the SEM investigation of intrafault quartz grains shows that these criteria also require to be used in the collection of such samples if the grain morphologies are to be used as an indicator of the time since the last faulting episode. The intrafault quartz grain morphologies do however point to late Quaternary reactivation of these faults, although they do not record the most recent (post-glacial) fault movement observed. With this in mind it can be recommended that the use of quartz grain surface morphologies be used as a first order estimate of the time since last fault movement. For this technique to be of more widespread use it must be confirmed by an independent age-dating technique or unequivocal geological evidence.

ESR, in contrast to other physical dating techniques, has the potential to date the last movement of a fault. Despite the poorly understood resetting mechanisms of the ESR signal in intrafault quartz, it does not seem to be dependent on secondary processes such as hydrothermal activity. This is of particular importance in the dating of fault movement triggered by the isostatic response of the crust due to the decay of ice sheets, as is the case in Scotland where fault movements have occurred under 'cold' conditions. In order to establish the reliability of ESR age-dating it is necessary to demonstrate that the signal is completely reset at least under optimal conditions.

A problem inherent with both techniques in this study is the recognition of gouges that represent the most recent fault movement episode. In the complex mechanics of a reactivated fault zone, simple cross-cutting relationships may not be enough to establish which gouge represents the last movement of the fault. The development of reliable criteria to recognise the gouge produced or affected by the last fault movement is needed to overcome this problem. In the absence of such criteria systematic sampling of the fault zone is required. This may prove impossible if it requires drill-cored samples to obtain material that will satisfy the criteria of samples that are likely to have been reset during the most recent fault activity.

Once these uncertainties have been removed ESR age-dating, coupled with parallel studies on the morphologies of the intrafault quartz grains, will provide us with a very powerful method of establishing the timing of fault recurrence, enhancing our understanding of the palaeoseismic record and ultimately leading to a more accurate seismotectonic understanding of the area under consideration.

5.6 Acknowledgements

This research was carried out at the Department of Geology & Applied Geology, University of Glasgow and at the Sub-department of Quaternary Research, University of Cambridge while in receipt of NERC studentship GT4/87/GS/107. NERC also provided additional funding for the ESR age-dating programme. Rainer Grün is especially thanked for his participation and enthusiasm for this project. Irradiation of samples was carried out at Imperial College Nuclear Chemical Plant, ESR measurements and delayed neutron activation analysis at Royal Holloway & Bedford New College. SEM analysis was carried out at the Department of Metallurgy, University of Strathclyde and at the Department of Geology & Applied Geology, University of Glasgow. P.Chung is thanked for his help during sample collection. D. Turner and M. MacLeod are thanked for their time and patience during sample preparation. R. Sinclair (Braeroy), D. Cameron (Kinloch Hourn), R. Carr (Killilan), J. Meldrum (Scardroy) and C. MacKenzie (Achnashellach) are all thanked for allowing access onto the various estates during the stalking season. D. MacLean is thanked for preparing the photographic plates.

5.7 References

- Ariyama, T. 1985.** Conditions of resetting the ESR clock during faulting. *in* M. Ikeya & T. Miki(eds.). ESR dating and dosimetry, IONICS, Tokyo, 249-256.
- Bonilla, M.G. & Lienkaemper, J.J. 1990.** Visibility of fault strands in exploratory trenches and the timing of rupture events. *Geology* 18, 153-156.
- Buhay, W.M., Schwarcz, H.P. & Grün, R. 1988.** ESR dating of fault gouge: the effect of grain size. *Quaternary Sci. Rev.* 7, 515-522.
- Davenport, C.A., Ringrose, P.S., Becker, A., Hancock, P. & Fenton, C. 1989.** Geological investigation of late and post glacial earthquake activity in Scotland. *in* S. Gregerson & P.W. Basham (eds.) Earthquakes at North Atlantic Passive Margins: Neotectonics and postglacial rebound, 175-194. Kluwer Academic Publishers, Amsterdam.
- Fenton, C.H. 1991.** Neotectonics and Palaeoseismicity in N.W. Scotland. Unpubl. Ph.D. Thesis, University of Glasgow.
- Fukuchi, T. 1989.** Increase of radiation sensitivity of ESR centres by faulting and criteria of fault dates. *Earth and Planetary Science Letters* 94, 109-122.
- Fukuchi, T. 1991.** ESR studies for absolute dating of fault movements. *J. Geol. Soc. London* (in press).
- Fukuchi, T., Imai, N. & Shimokawa, K. 1985.** Dating of the fault movement by various ESR signals in quartz- Cases of the faults in the South Fossa Magna, Japan. *in* M. Ikeya & T. Miki (eds.). ESR dating and dosimetry, IONICS, Tokyo, 211-217.
- Grün, R. 1989.** Electron spin resonance (ESR) dating. *Quaternary International* 1, 65-109.
- Grün, R. 1991.** Some remarks on ESR dating of fault movements. *J. Geol. Soc. London* (*in press*).

Grün, R. & Fenton, C. 1990a. Internal dose rates of quartz grains separated from fault gouge. *Ancient TL* 8, 26-28.

Grün, R. & Fenton, C. 1990b. An ESR study of fault gouge from Holocene fault systems in Scotland. 6th International Specialist Seminar on Thermoluminescence & Electron Spin Resonance Dating. 2-6 July 1990, Clermont-Ferrand, France. Abstract 129.

Hennig, G.J. & Grün, R. 1983. ESR dating in Quaternary geology. *Quaternary Sci. Rev.* 2, 157-238.

Ikeya, M. 1986. Electron spin resonance. *in* M.R. Zimmerman & J.L. Angel (eds.) *Dating and age determination of biological materials*. Croom Helm, London. 59-125.

Ikeya, M. & Miki, T.(eds). 1985. ESR dating and dosimetry, IONICS, Tokyo, 538pp.

Ikeya, M., Miki, T. & Tanaka, K. 1982. Dating of a fault by electron spin resonance on intrafault materials. *Science* 215, 1392-1393.

Ikeya, M. & Ohmura, K. 1983. Comparison of ESR ages of corals from marine terraces with ^{14}C and $^{230}\text{Th}/^{234}\text{U}$ ages. *Earth & Planetary Science Letters* 65, 34-38.

Ito, T. & Sawada, S. 1985. Reliable criteria for selection of sampling points for ESR fault dating. *in* M. Ikeya & T. Miki (eds.). ESR dating and dosimetry, IONICS, Tokyo, 229-237.

Kanaori, Y. 1983. Fracturing mode analysis and relative dating of faults by surface textures of quartz grains from fault gouges. *Engineering Geology*. 19, 261-281.

Kanaori, Y., Miyakoshi, K., Kakuta, T. & Satake, Y. 1980. Dating fault activity by surface textures of quartz grains from fault gouges. *Engineering Geology* 16, 243-262.

Kanaori, Y., Tanaka, K. & Miyakoshi, K. 1985. Further studies on the use of quartz grains from fault gouges to establish the age of faulting. *Engineering Geology* 21, 175-194.

Kanaori, Y., Miyakoshi, K., Tanaka, K. and Satake, Y. 1986. Dating fault activity by use of intrafault quartz grains: perspectives for earthquake-proof designs in potentially unstable areas. *Geologia Applicata Idrogeologia* 21, 3-16

Krinsley, D.H. & Doornkamp, J.C. 1973. Atlas of quartz sand surface textures. Cambridge University Press, 91pp.

Kosaka, K. & Sawada, S. 1985. Fault gouge analysis and ESR dating of the Tsurukawa Fault, west of Tokyo: the significance of minute sampling. *in* M. Ikeya & T. Miki (eds.). ESR dating and dosimetry, IONICS, Tokyo, 257-266.

Miki, T. & Ikeya, M. 1982. Physical basis of fault dating with ESR. *Naturwissenschaften* 69, 390-391.

Ringrose, P.S. 1987. Fault activity and palaeoseismicity during Quaternary time in Scotland. Unpubl. Ph.D. Thesis (2 Volumes), University of Strathclyde.

Ringrose, P.S. 1989a. Palaeoseismic (?) liquefaction event in late Quaternary lake sediment at Glen Roy, Scotland. *Terra Nova* 1, 57-62.

Ringrose, P.S. 1989b. Recent fault movement and palaeoseismicity in western Scotland. *Tectonophysics* 163, 305-314.

Ringrose, P.S., Hancock, P.L., Fenton, C. & Davenport, C.A. 1991. Quaternary tectonic activity in Scotland. *in* A. Foster, M.G. Culshaw, J.C. Cripps, J.A. Little & C.F. Moon (eds.). Quaternary Engineering Geology, Geol. Soc. Engineering Geology Special Publication No.7, 679-686.

Sato, T., Suito, K. & Ichikawa, Y. 1985. Characteristics of ESR and TL signals on quartz from fault regions. *in* M. Ikeya & T. Miki (eds.). ESR dating and dosimetry, IONICS, Tokyo, 267-273.

Schwarcz, H.P., Buhay, W.M. & Grün, R. 1987. Electron Spin Resonance (ESR) dating of fault gouge. *in* A.J. Crone (ed.) Proceedings of Conference XXXIX - Directions in palaeoseismology. USGS Open File Report 87-673, 50-64.

Toyokura, I., Sakuramoto, Y., Ohmura, K., Iwasaki, E. & Ishiguchi, M. 1985. Determination of the age of fault movement - the Rokko Fault. *in* M. Ikeya & T. Miki (eds.). ESR dating and dosimetry, IONICS, Tokyo, 219-288.

Zhuo-ran, L., Mei-er, Y., Qi-chen, F. & Ikeya, M. 1985. ESR dating of the age of fault movement at San-Jiang fault zone in west China. *in* M. Ikeya & T. Miki (eds.). ESR dating and dosimetry, IONICS, Tokyo, 205-210.

5.8 Figure Captions

- Figure 5.1** Location of gouge-bearing late Quaternary faults in North West Scotland.
- Figure 5.2** Determination of the Accumulated Dose (AD). Irradiation from a calibrated source enhances the ESR intensity. Extrapolation to zero ESR intensity gives the AD as the intersection of the γ -dose axis. The value of AD obtained is dependent on the method of extrapolation (Linear line fit shown). 'Saturated' sample represented by the broken line parallel to the x-axis. In this case further irradiation dose not cause an increase in ESR intensity.
- Figure 5.3** ESR spectra for a saturated sample (725c). The solid lines represent the spectra of the natural sample, the dotted line the sample after being irradiated with +569 Gy.
(A) ESR spectrum at room temperature.
(B) ESR spectrum (E' centre) at room temperature.
(C) ESR spectrum at c. 95 K.
- Figure 5.4** Fault gouge quartz grain morphologies and their approximate ages as determined by ESR (after Kanaori 1983 and Kanaori *et al.* 1985).
- Figure 5.5** SEM photographs of fault gouge quartz grain surface morphologies.
- (a) Subconchoidal texture (Ia): almost pristine conchoidal fracture face. Note the radial fracture steps [Sample CF38].
- (b) Subconchoidal (Ia) face cutting faces showing Group Ic (right) and Group II (left) textures [Sample CF 34/35].
- (c) Orange-peel texture (Ic): undulose surface with small 'bite marks' on the fracture steps and slight pitting of the surface between steps [Sample CF36/37].

(d) Group Ib texture: note the slight blunting of the crests of the fracture steps [Sample CF34/35].

(e) Fish scale texture (II): surface composed of small v-shaped facets [Sample CF32/33].

(f) Moth-eaten texture (III): random development of holes [Sample CF 38].

Figure 5.6 Histograms of the surface texture groups of fault gouge from the Scardroy segment of the Loch Maree Fault.

Figure 5.7 Histograms of the surface texture groups of fault gouge from the Beinn Tharsuinn and Kinloch Hourn Faults.

Figure 5.8 Histograms of surface texture groups of 'reworked' fault gouge from the Gleann Lichd and Am Fas Allt Faults.

Figure 5.9 Approximate age of fault movement from examination of surface textures of intrafault quartz grains. Solid line represents dominant surface morphology, dotted line shows other surface types present.

Table 5.1 ESR fault gouge sample locations and mineralogy as determined by XRD.

Table 5.2 SEM fault gouge sample locations and mineralogy as determined by XRD.

5.9 Figures

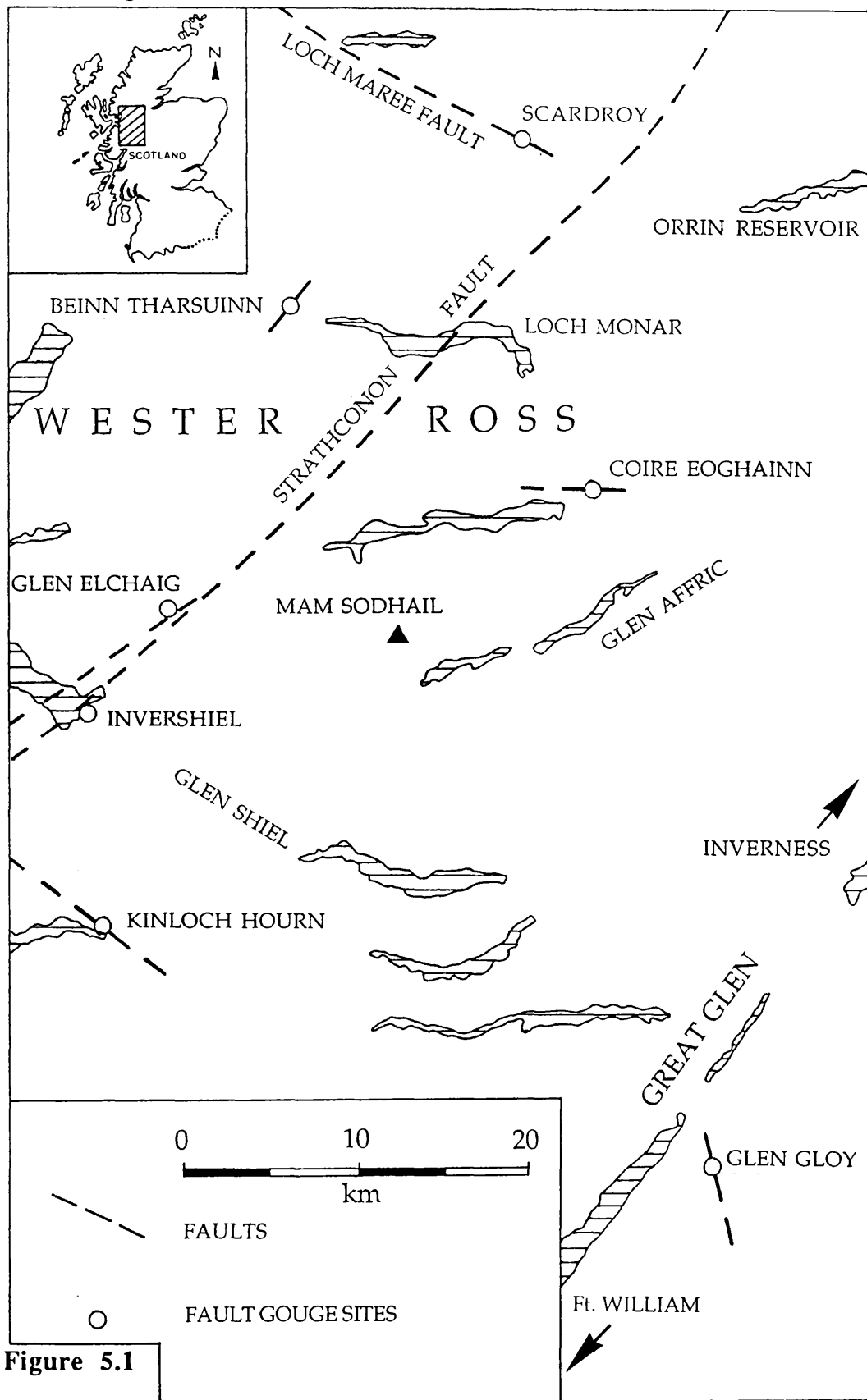


Figure 5.1

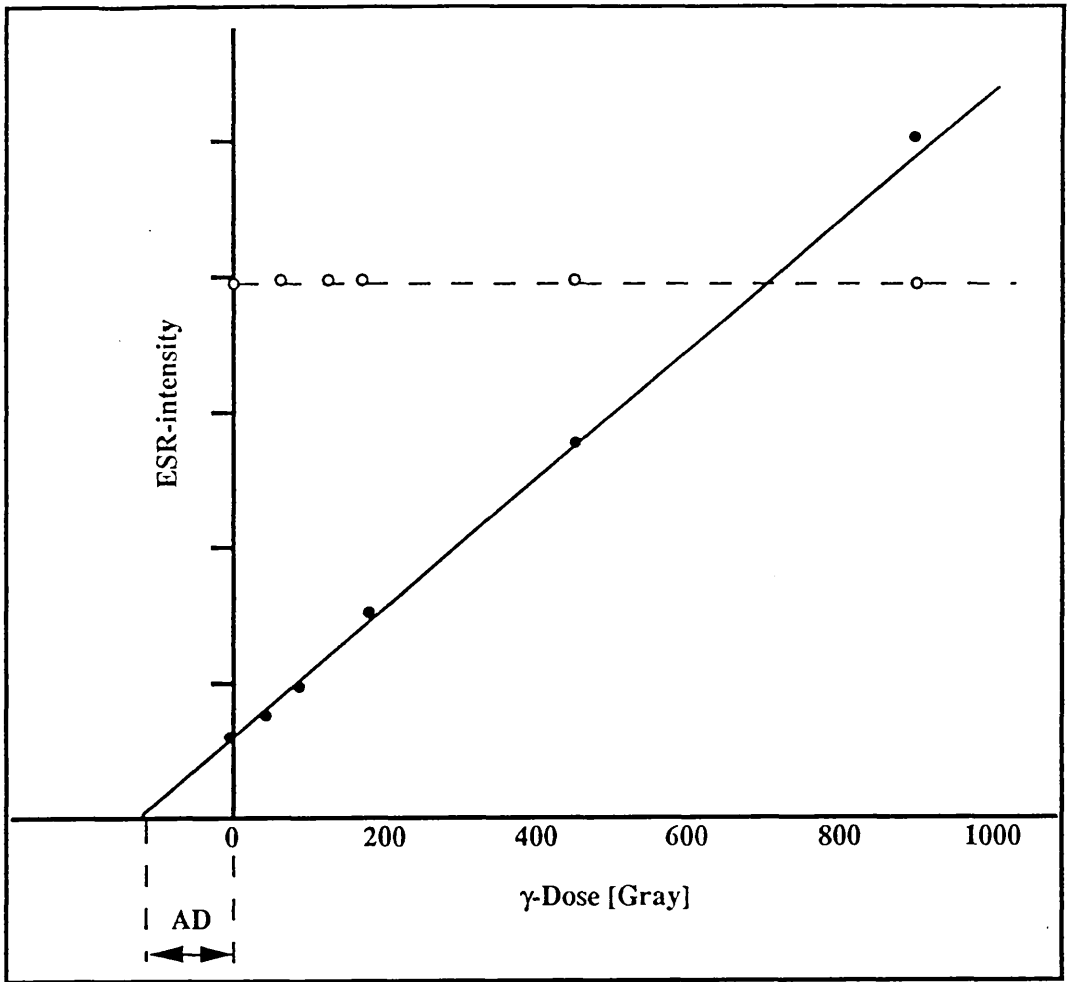


Figure 5.2

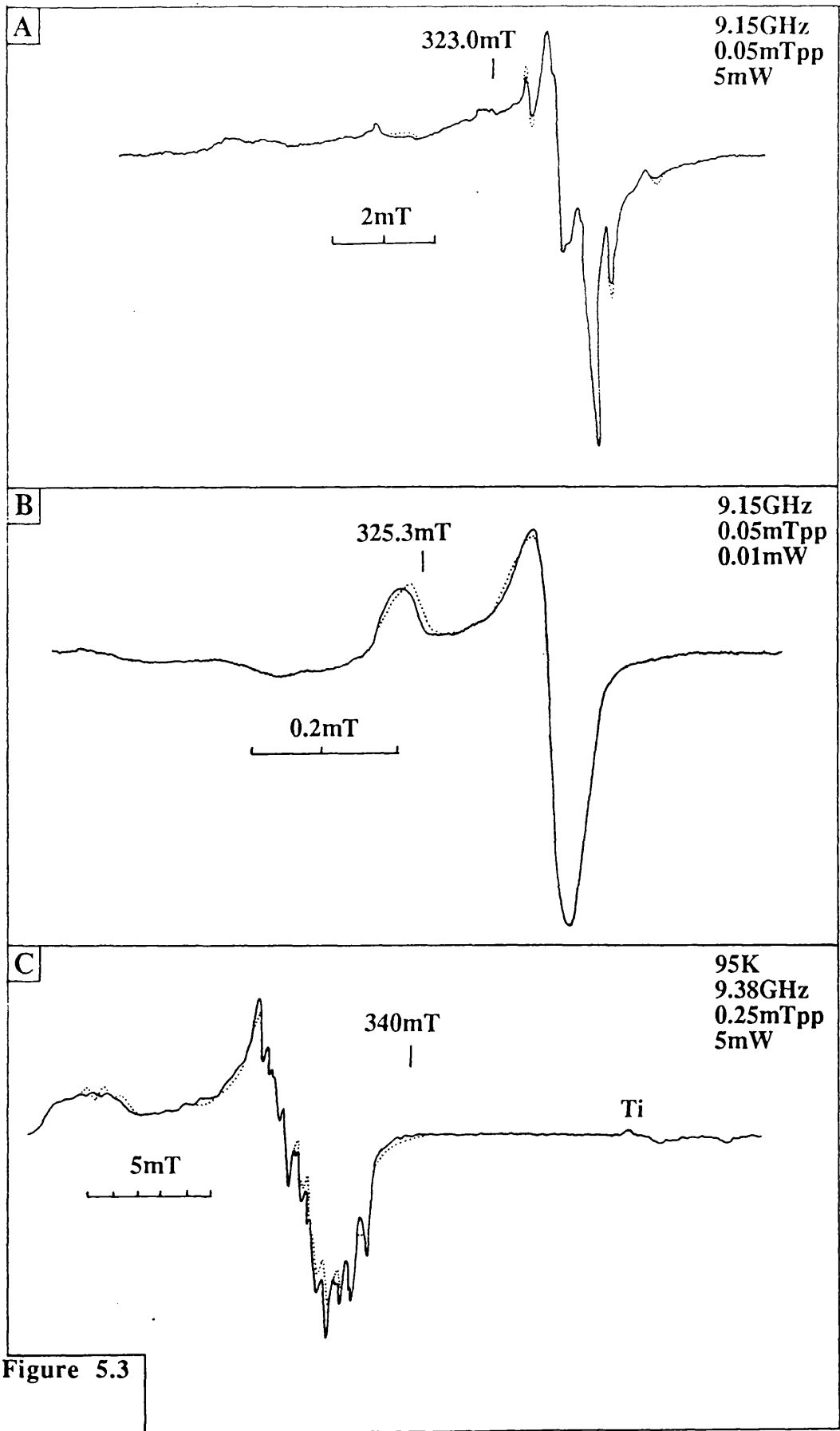


Figure 5.3

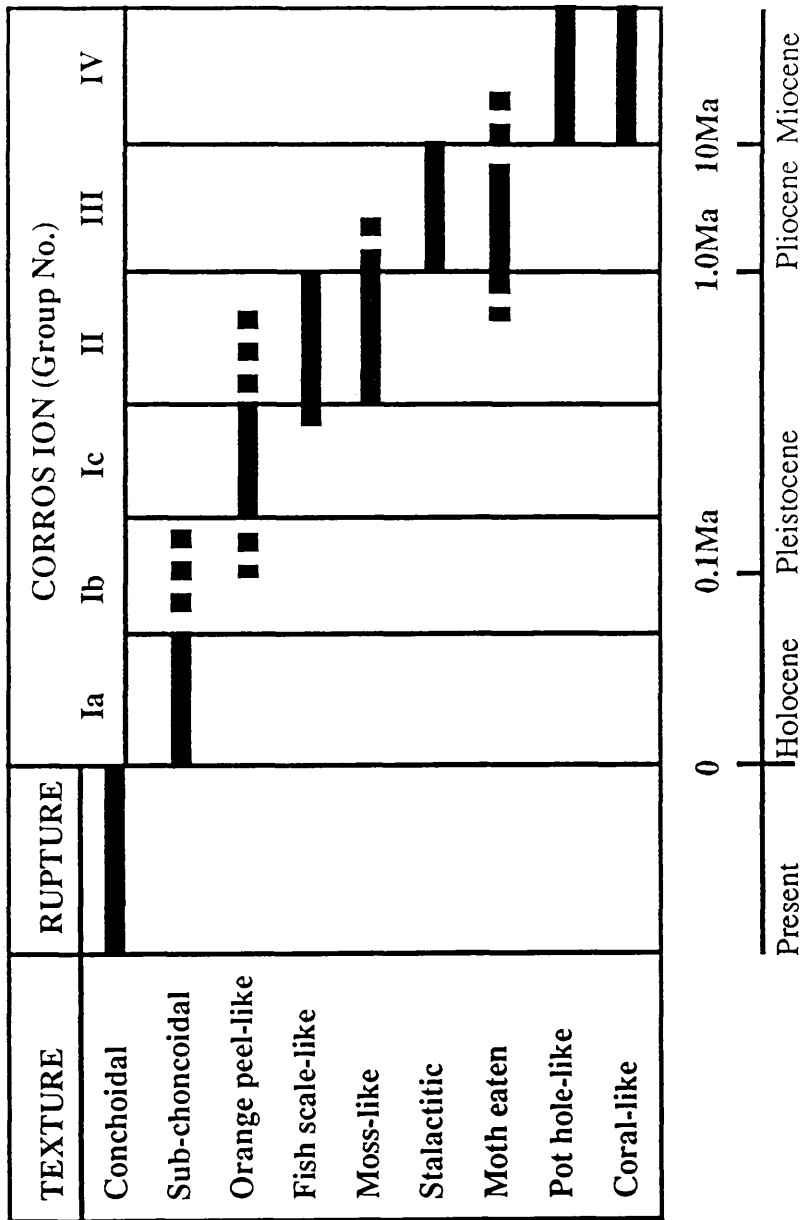
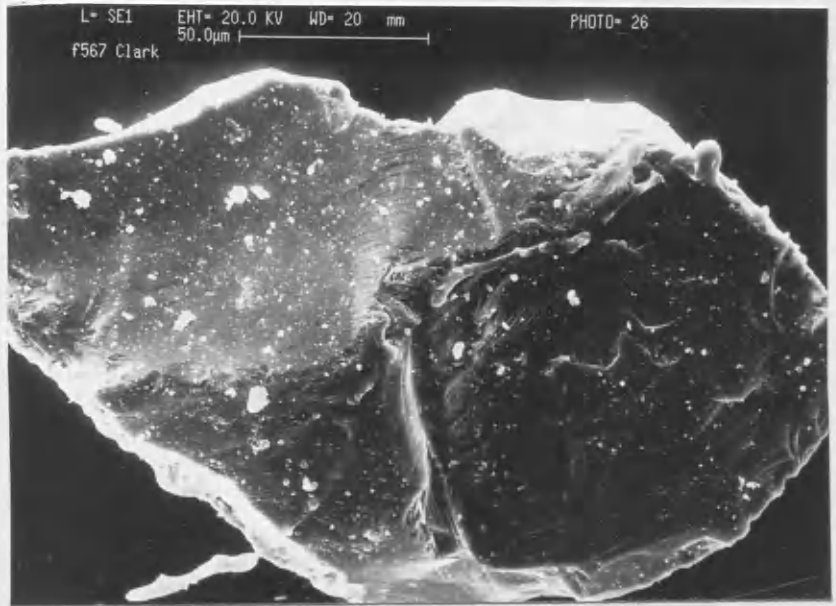


Figure 5.4

(a)



(b)



(c)

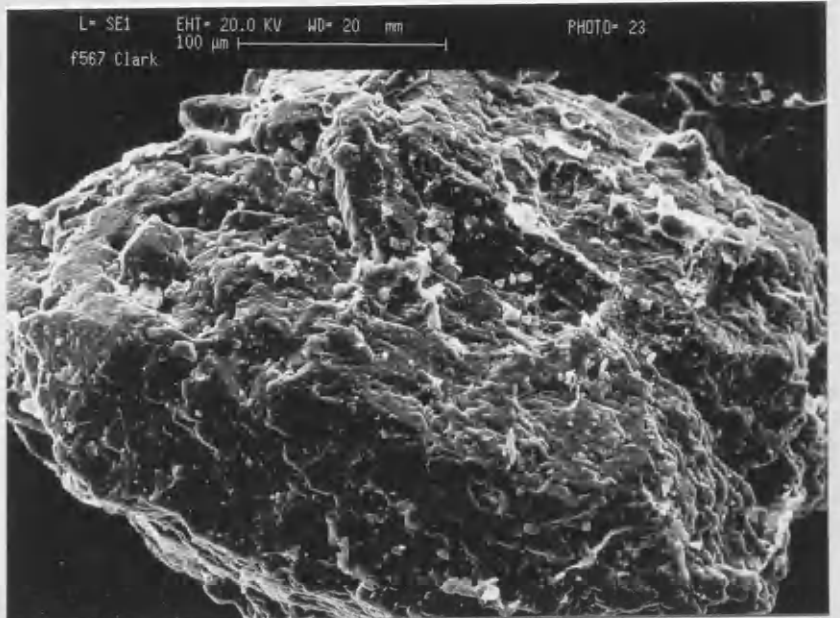


Figure 5.5

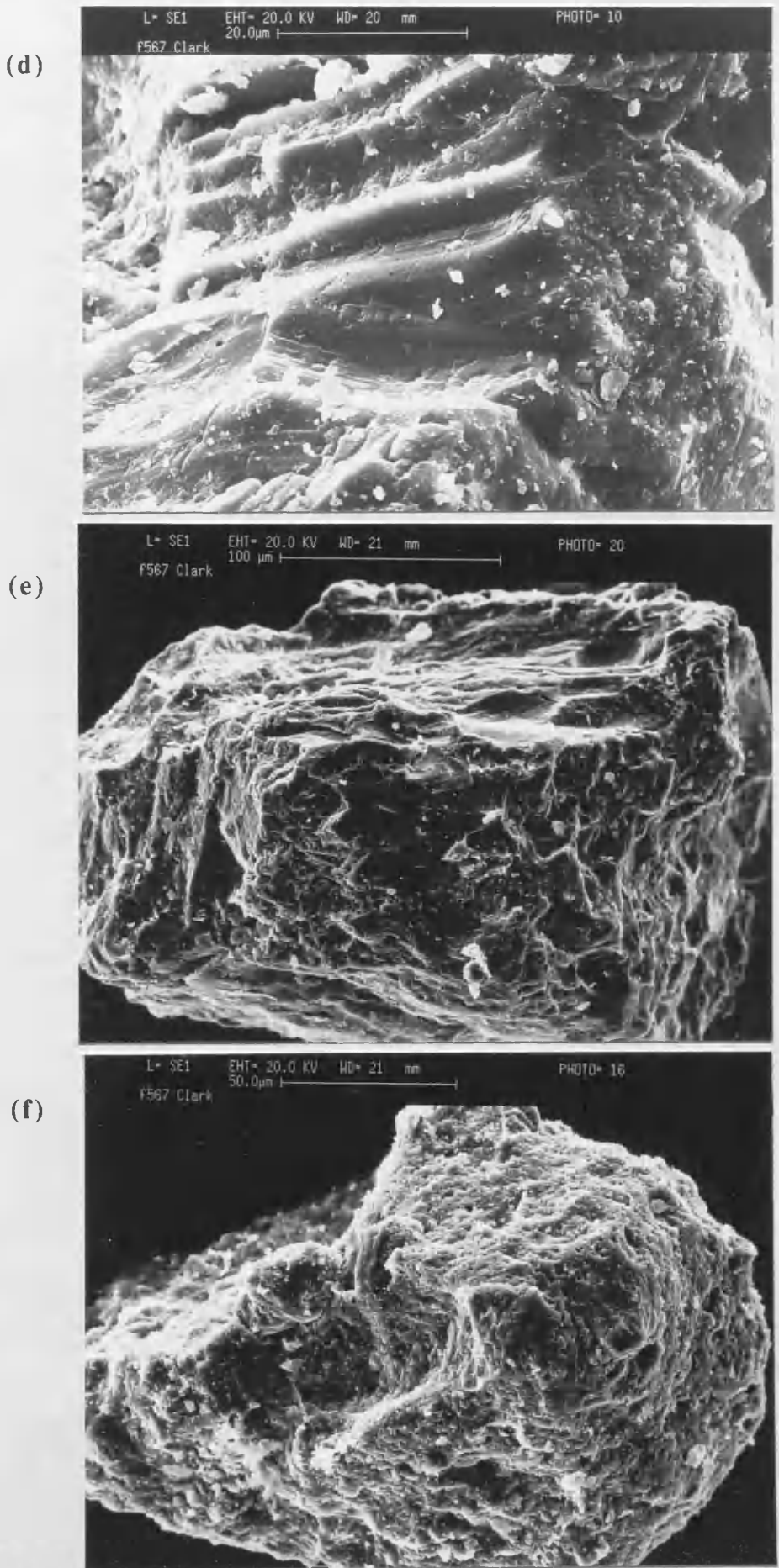
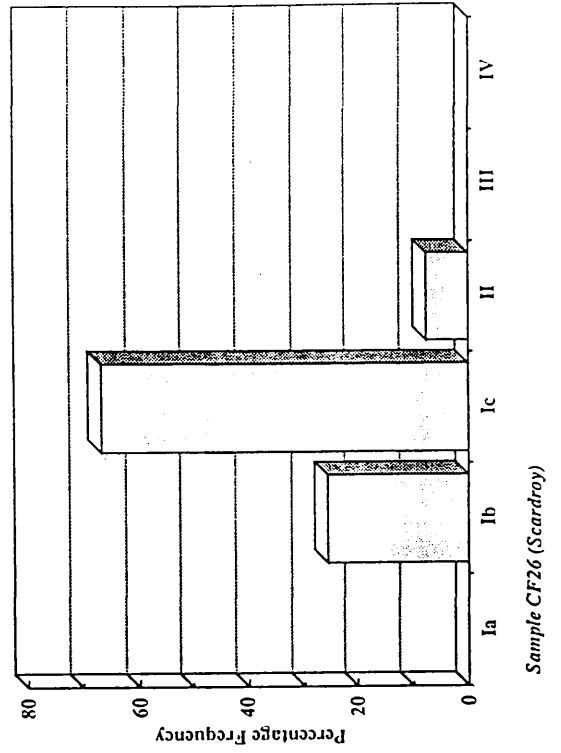
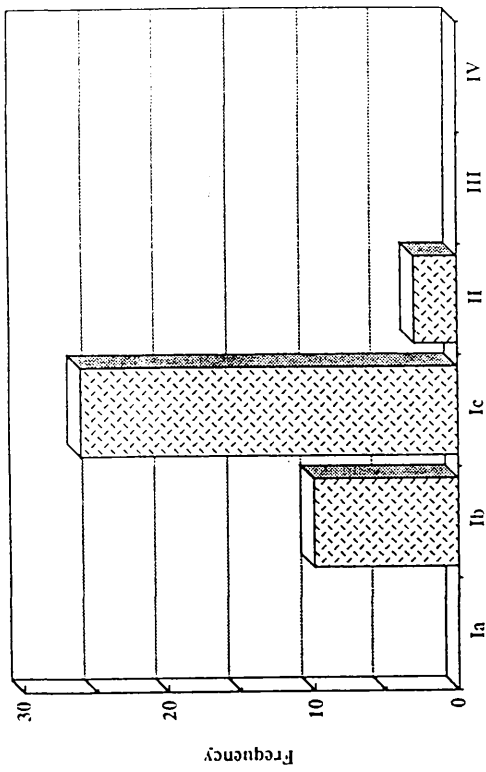
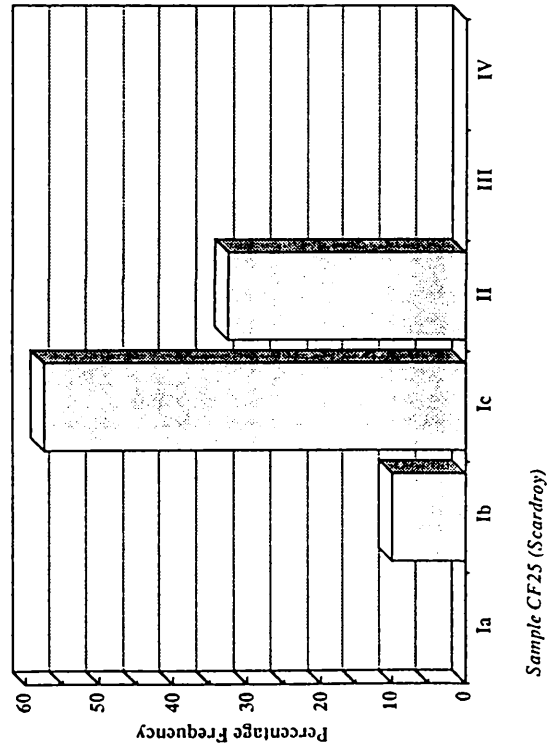
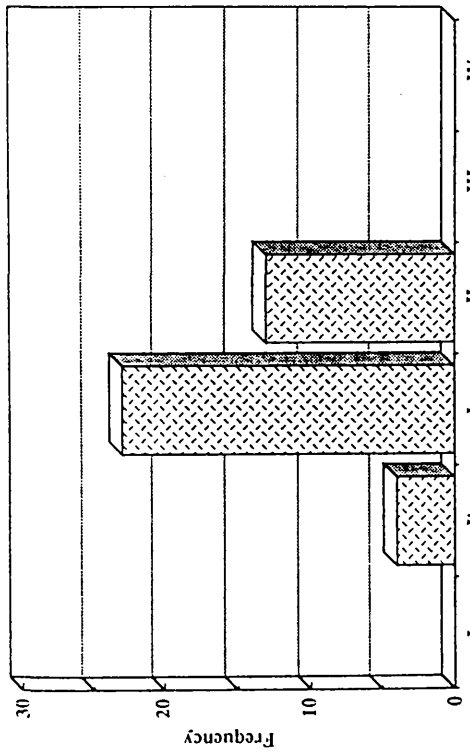


Figure 5.5



Sample CF26 (Scardroy)



Sample CF25 (Scardroy)

Figure 5.6

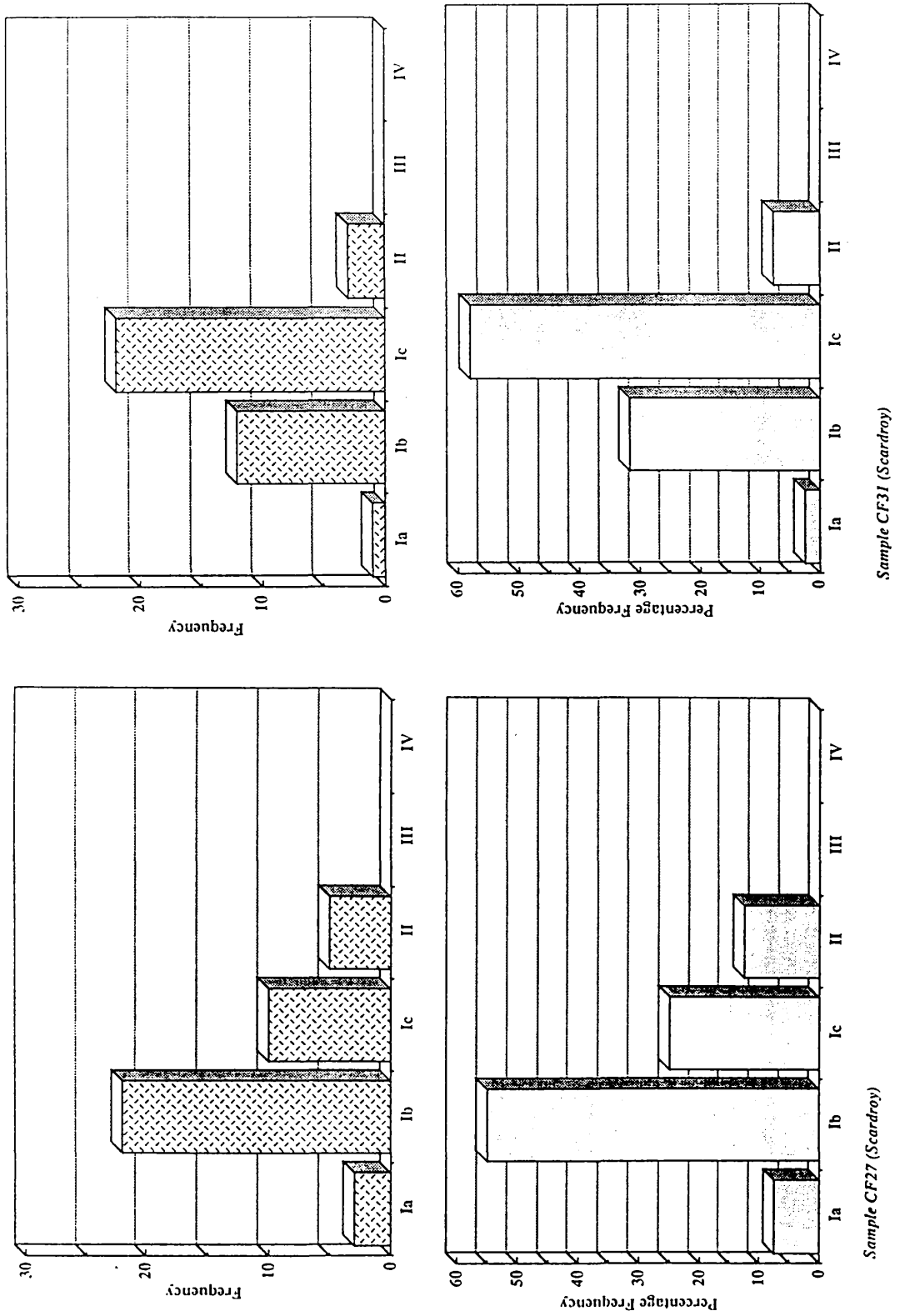
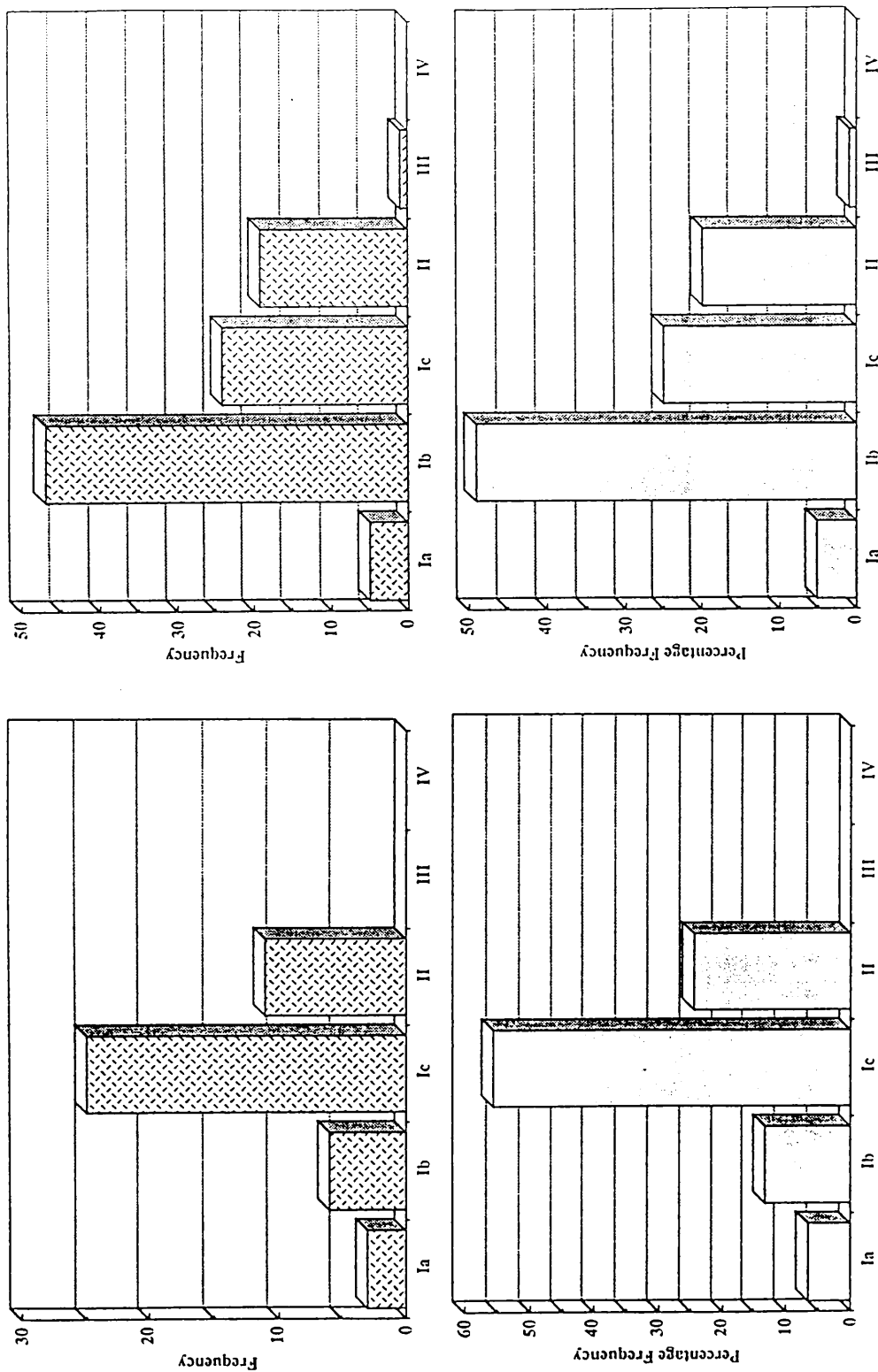


Figure 5.6



Sample 34/35 (Kinloch Fourn)

Sample CF32/33 (Beinn Tharsuinn)

Figure 5.7

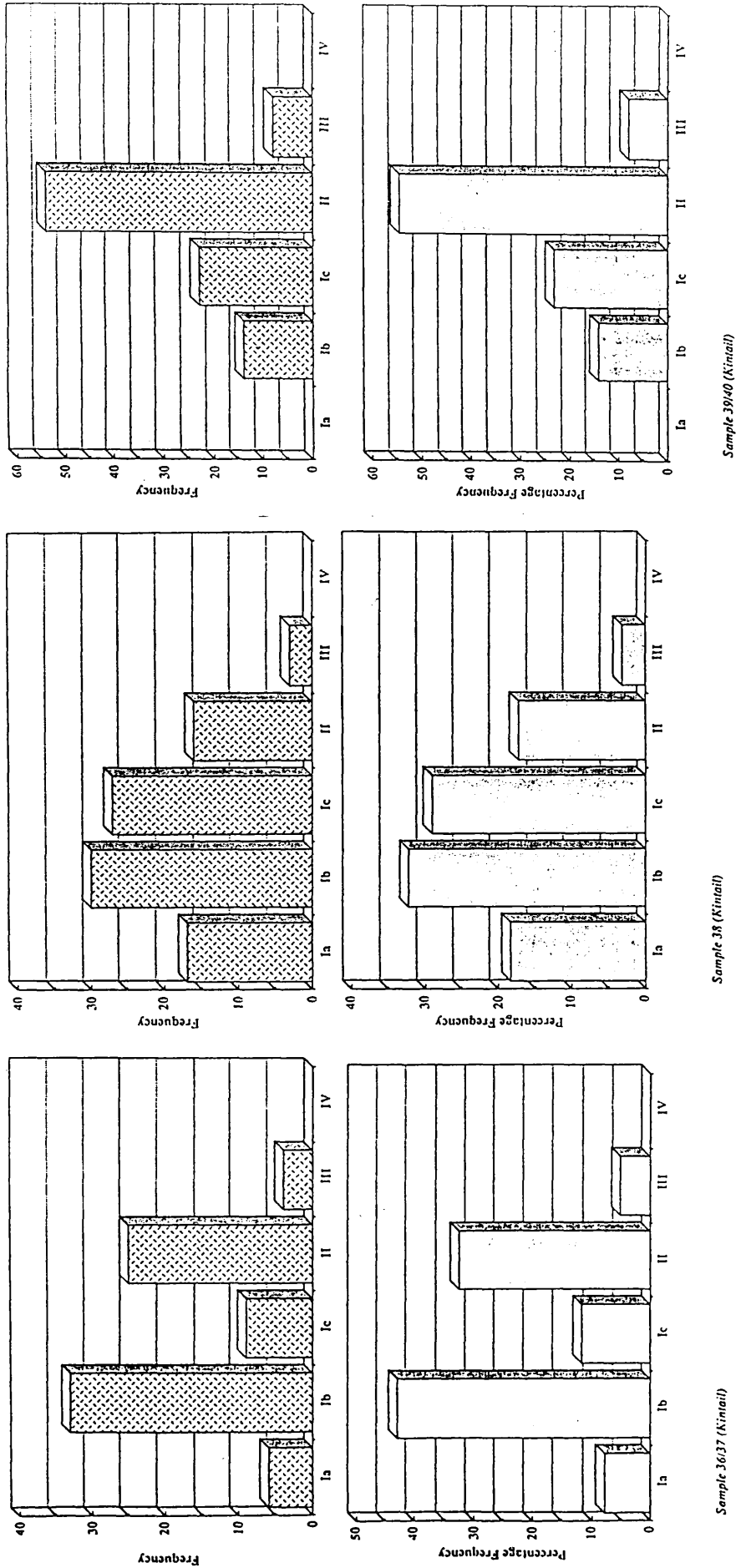


Figure 5.8

5.10 Tables

Table 5.1

Locality	Sample No.	Mineralogy
Glen Gloy	(GGW) 710	Qtz >> Feld > Mica > Ep > Kaol > Chl > Py.
Glen Gloy	(GGE) 711	Qtz >> Kaol > Feld > Mica > Chl > Ep > Ill > Py.
Kinloch Hourn	(KH) 712	Qtz >> Mu > Kaol > Feld.
Glen Elchaig	(GE) 713	Qtz >> Mu > Feld > Kaol > Chl.
Scardroy	(S1 NE) 714	Qtz > Kaol >> Ill > Feld.
Scardroy	(S1 SW) 715	Qtz >> Ill > Kaol > Feld > Mu.
Scardroy	(S2) 716	Qtz >> Ill > Cal > Kaol > Feld.
Scardroy	(S3) 717	Qtz >> Kaol > Ill > Mu > Feld.
Scardroy	(S4) 718	Qtz >> Feld > Kaol > Ill.
Scardroy	(S5a) 719	Qtz >> Ill > Kaol > Feld.
Scardroy	(S5b) 720	Qtz >> Clay > Cal > Mica > Feld.
Scardroy	(S5c) 721	Qtz >> Cal > Ill > Kaol > Feld.
Scardroy	(S5d) 722	Qtz >> Cal > Kaol > Mica > Feld > Ill.
Invershiel	(ISA) 723	Qtz >> Mu >> Chl >> Feld > Kaol.
Invershiel	(ISb) 724	Qtz >> Chl > Kaol >> Mu > Feld.
Glen Cannich	(GC) 725	Qtz >> Mu > Feld > Kaol > Chl > Feld > Ill.
Beinn Tharsuinn	(BT) 726	Qtz >> Chl, Kaol > Mu > Feld.

Table 5.2

Locality	Sample No.	Mineralogy
Scardroy	CF25	Qtz >> Kaol > Feld > Cal > Mica > Ill.
Scardroy	CF26	Qtz >> Kaol > Ill > Feld.
Scardroy	CF27	Qtz >> Kaol > Feld > Ill > Mica.
Scardroy	CF31	Qtz >> Kaol > Feld > Ill > Kaol.
Beinn Tharsuinn	CF32/33	Qtz >> Chl > Mu > Feld > Kaol.
Kinloch Hourn	KH34/35	Qtz >> Kaol > Mu > Chl > Feld.
Gleann Lichd	CF36/37	Qtz >> Mu > Kaol > Feld > Chl > Ep.
Gleann Lichd	CF38	Qtz >> Feld > Cal > Kaol > Ep.
Glen Shiel	CF39/40	Qtz >> Mu > Feld > Hae > Kaol.

5.11 Appendix A: Location of ESR Sample Sites

Glen Gloy

This is a NNW-trending basement fault of probable Caledonian age that shows evidence for reactivation over a length of c. 7 km from the head of Glen Gloy across the intervening hills and into the neighbouring Glen Roy. Several exposures along Allt Neurlain in Glen Gloy contain a soft grey-green fault gouge. Samples GGW and GGE were collected from the best exposed site [NN304927] where two fault gouge zones are exposed trending almost N-S. The gouges are up to 2.5 cm in width and are found within a wide zone of shattered country rock of psammites and mica schists.

Kinloch Hourn

The WNW-trending Caledonian age Kinloch Hourn Fault shows late Quaternary reactivation over a distance of c. 15 km. The fault zone is exposed above Kinloch itself [NG946076] as a wide zone of shattered psammites containing a 2.0 cm wide zone of blue-grey fault gouge. Sample KH was taken from a depth of c. 0.5 m.

Glen Elchaig

A sample was collected from a 058-138° trending segment of the Strathconon Fault system to the SW of Loch na Leitreach [NH009267]. A 4.5 cm wide zone of mixed pale and dark grey gouge is found in a wide zone of shattered pegmatite. Sample GE was collected from a depth of 2.0 m below the ground surface.

Scardroy

A number of samples were collected at several localities along the eastern section of the WNW-trending Loch Maree Fault where it is exposed along the Scardroy Burn in upper Strathconon.

Samples S1NE and S1SW were collected from a 0.4 m wide composite zone [NH206520] of gouge and shattered rock containing several generations of gouge material. The samples correspond to the blue-grey gouges that bound either side of the zone. Samples were collected from the surface.

Sample S2 [NH205522] was collected from a narrow zone of 'two-tone' khaki-pale grey gouge from a depth of 1.7 m below the ground surface.

Sample S3 [NH204522] was collected from a 3.0 cm wide vertical grey-green gouge zone at a depth of c. 0.5 m below the ground surface.

Sample S4 [NH204522] was collected from a narrow zone of grey-green gouge 10 m further upstream from S3.

Samples S5a-d [NH204523] were collected from a wide complex fault zone containing several generations of fault gouge. Two samples were taken, from the top and bottom, of the two most recent gouge zones, at depths of 2.5 and 4.0 m below the ground surface.

All localities at Scardroy cut a variety of Moine psammities, pelites and 'Lewisianoid' granulites and amphibolites.

Invershiel

Two samples ISa and ISb, one from the top and one from the bottom of a 78/076° trending fault cutting a late Caledonian adamellite intrusion exposed in a road cut [NG938198]. This comprised a 3.0 cm wide zone of pale grey-green gouge in a tight fracture that has been exposed due to the creation of the road cut. Samples were collected from the surface (a depth of c. 10 m prior to the formation of the road cut). This is part of the Strathconon Fault system.

Glen Cannich

A single sample GC was collected from the Coire Eoghainn Fault [NH235323]. The fault zone comprises an 18 mm wide unit of blue-grey gouge in a tight E-W trending fracture. Sample was collected from a surface exposure.

Beinn Tharsuinn

A single sample was taken of the blue-grey gouge found in a wide zone of shattered and sheared rock trending NNE on the east ridge of Beinn Tharsuinn in the West Monar Forest [NHG057429]. Sample was collected from a depth of 4 m below the ground surface.

5.12 Appendix B: Location of SEM Sample Sites.

Scardroy

A number of gouge samples were collected from the 160-340° trending Loch Maree Fault where it is exposed along the Scardroy Burn in upper Strathconon. The fault cuts a sequence of intensely folded Moine granulites and gneisses with 'Lewisianoid' intercalations. The samples were all collected from a wide fault zone exposure [NH206520] that contains several generations of fault gouge.

CF25*¹ is taken from the north-eastern gouge blue-grey gouge zone that bounds the edge of the fault zone that shows most recent movement.

CF26 is a pale grey gouge found adjacent to CF25.

CF27*² is taken from the south-western blue-grey gouge zone that bounds the opposite side of the fault zone from CF25. Sample taken approx. 5 m WNW of CF25 and CF26.

CF31 is the khaki-coloured gouge zone found between the two blue-grey gouge units (CF25 and CF27).

*¹,*²: These samples respectively correspond to ESR samples S1NE and S1SW.

Beinn Tharsuinn

A single sample was taken from within the 2.5 cm wide gouge zone the 020-200° trending fault zone that cuts across the eastern ridge of Beinn Tharsuinn [NH058448].

CF32/33 is a blue-grey fault gouge. Corresponds to ESR sample BT.

Kinloch Hourn

A single sample was collected from the 132-312° Kinloch Hourn Fault above Kinloch Hourn itself [NG946076] as the fault cuts a sequence of Moine psammites and pelites.

CF34/35 is a blue-grey fault gouge from a 2.0 cm zone. This corresponds to ESR sample KH.

Gleann Lichd

Two samples were collected from a 136-316° trending zone of crushed and brecciated rock cutting migmatised Moine granulites and pegmatites along the Gleann Lichd fault. This is an old lineament of probable Caledonian age that shows evidence for late Quaternary reactivation in the upper part of Gleann Lichd. Fault gouge is poorly developed and consists of 'reworked' fault breccia that has been subject to haematite staining epidote mineralisation.

CF36/37 is a red-green mixture of soft clays found in a 134-314° trending fracture zone [NH011169].

CF38 is a deep red coloured clay-like material found within 114-294° shear planes in a zone up to 0.5 cm wide.

Glen Shiel

A single sample was collected from a 120-300° trending fault zone along Am Fas Allt [NG975123].

CF39/40 is a red coloured gouge found in a zone up to 1.5 cm wide within a zone of indurated red fault crush rock.

Chapter 6

The Effects of Ice-cap Loading on Crustal Stress Patterns and the Consequences for the Generation of Seismicity in the Post-Glacial Environment.

Clark Fenton

Department of Geology & Applied Geology,
University of Glasgow, Glasgow G12 8QQ.

"It is worth reminding ourselves of the unusual history of earth rheology where very persuasive arguments have been made for some particular model only to find, within a few years, the argument inverted to favour the opposing model."

(Walcott 1980).

6.1 Abstract

A number of post-glacial faults and related seismic deformation features have been identified in North West Scotland. These have been the result of the unique stress system that arose from the interaction between the regional stress system of Western Europe, active since the late Miocene (8-6 Ma), and the loading stresses induced by repeated glaciations during the Quaternary period. Although much of the early Quaternary history of the Scottish Highlands has been destroyed by later glacial events, there is a good chronology for the latter part of the period, allowing a detailed insight into the subtle interactions between the build-up of tectonic stress and ice-cap loading stresses, giving rise to a period of enhanced seismotectonic activity at the beginning of the Holocene (10 kyr BP). Deglaciation allowed the release of the stress that had accumulated over the duration of the glacial residence. The nature and areal extent of the fault movements, the associated seismic deformation features and the timing of fault movement shows that sub-glacial fluid recharge plays an important control on the generation of seismogenic fault movement. The activity observed from Scotland is consistent with that observed from other areas subject to 'deglaciation tectonics'.

6.2 Introduction

The belief that during the Quaternary period Britain has been in a state of tectonic quiescence has been shown to be false (Ringrose 1987, 1989a, 1989b; Davenport *et al.* 1989; Ringrose *et al.* 1991) [§ 2, p15]. A number of faults have been demonstrated to have been active during the late Quaternary (Figure 6.1) and to have been associated with a period of enhanced seismic activity. This fault activity occurred after the disappearance of the last ice sheet of the Main Late Devensian Glaciation (26-13 kyr BP). Like other areas that have undergone post-glacial fault movement such as Fennoscandia, fault movement has occurred along pre-existing faults and has not created any substantial new fault breakages [§ 2.8, p51]. The relationship between fault movement and post-glacial rebound is universal. The orientation of fault reactivation and the style of fault movement is in sympathy with the regional stress field. This paper addresses the problem of the generation of a stress system in the post-glacial environment that allowed the reactivation of ancient faults and gave rise to enhanced levels of seismicity with particular reference to Scotland.

To understand the role of ice-cap loading and deglaciation in the triggering of fault movements it is important to consider the state of the crustal stress regime prior to glaciation as well as to have an appreciation for the effects of the long term ice loading and subsequent sudden relaxation of the imposed load.

6.3 Late Tertiary Tectonics

The late Tertiary-Quaternary tectonics of NW Europe are most readily revealed from offshore regions where the fault movements for this period are most extensively recorded. As most data for the NW European Continental shelf remains proprietary, due to the economic importance of the Tertiary tectonic structures, studies into late Tertiary tectonics involve a fair degree of interpolation. Nevertheless the data are sufficient to allow the broad scale, regional tectonic patterns to be appreciated.

For the previous 50 myr the north-western edge of the Europe had been a 'passive' continental margin, albeit of atypical nature (Muir Wood 1989a, 1990). During this period there were four main phases of deformation concentrated in zones that have extended northwestwards, connecting the Mediterranean and the North Atlantic plate boundaries.

These periods of deformation are as follows:

(i) a broad zone of dextral shear, along faults that were associated with the opening of the Atlantic, persisting from mid to late Eocene (Figure 6.2a) (Muir Wood 1989a).

(ii) the early Oligocene (Figure 6.2b) saw a narrow zone of deformation connecting the basins of the Rhine Graben to the inversion structures around the UK, possibly passing through Scotland. This resulted from the change in plate motions in the North Atlantic (Muir Wood 1989a).

(iii) in the late Oligocene (Figure 6.2c) a change in the style of deformation gave rise to the opening of a number of deep sedimentary basins along the west coast of the UK (Muir Wood 1989a).

(iv) the late Miocene (Figure 6.2d) saw the initiation of a period of inversion and uplift in the region of the UK, shown by the NE-SW trending folds found in the late Oligocene sedimentary basins off the west coast of Scotland. At this time the eroded remnants of the Hebridean volcanic centres were also probably subject to further renewed uplift. The relative elevations of the various centres, e.g. Blackstones and Lundy lie about 1000 m lower than their counterparts on Mull, Skye, Rum and St. Kilda, bears testimony to the deformation during this period. The amount of deformation increases to the NW and therefore cannot be attributed to Alpine Foreland compression alone. Stress transmitted from the mid-Atlantic spreading ridge around Iceland must also have played an important part in the tectonic regime at that time (Muir Wood 1989a).

It is clearly seen that the margin of NW Europe has suffered considerable deformation over the period of the last 50 myr. During this time the major transcurrent faults show several kilometres of post-Palaeocene movement and certain reverse faults have moved by more than 500 m. At times the amount of fault slip may have been as high as 1 mm yr^{-1} , possibly giving elevated levels of seismicity equivalent to those experienced in China in the present day (Muir Wood 1989a).

Over this period the positive (compressive) horizontal stress (S_H) direction in NW Europe has rotated from NW-SE to NE-SW between 60 Ma and 35 Ma, and then returned to NW-SE around 10 Ma. This late Tertiary tectonic pattern has continued to control the present day seismotectonics of NW Europe. The Rhine Graben, formed in the late Oligocene, continues to transfer Alpine deformation to the North Sea (Illies &

Greiner 1978; Illies *et al.* 1981) and the late Miocene inversion structures continue to be the locus of seismicity in the UK (Muir Wood 1989a). Within the UK at present the direction of S_H , from borehole breakouts (Whittaker *et al.* 1989), focal plane mechanisms (Marrow & Walker 1988) and shallow triaxial strain cell measurements (Davenport *et al.* 1989), is seen to be approximately NW-SE, corresponding to the stress system for the rest of NW Europe. This agrees with the absolute plate velocity field for the area (Zoback *et al.* 1989) showing that this is dominantly a tectonically driven stress system. However shallow stress measurements and fault plane solutions suggest a more WNW-orientated direction for S_H in Scotland.

Thus, following the definition of Blenkinsop (1986) that the neotectonic regime begins with the onset of the contemporary stress field, as far as the UK and Western Europe are concerned this can be taken as the last 8-6 myr, i.e. the time since the inception of the late Miocene "sub-plate boundary" (Muir Wood 1989a, 1990). However since that time there have been subtle changes to the local stress field induced by ice-cap loading during the repeated glaciations of the Quaternary. Although not causing any major change to the orientation of the tectonic stress field in terms of direction of dominant horizontal stress directions, the role of ice-cap loading is important in the triggering of fault movement and the generation of elevated levels of seismicity during the immediate post-glacial period. The effects of such crustal loading are discussed below with examples from Scotland.

6.4 The Effects of Ice-cap Loading: General Considerations

Consider a fault of any orientation subject to crustal stresses, such that the principal stresses $\sigma_1 > \sigma_2 > \sigma_3$ are mutually perpendicular (Figure 6.3a). If one stress is assumed to be the vertical overburden pressure and another principal stress is constrained to lie in the plane of the fault the scenario is simplified to a two-dimensional case. These principal stresses can be resolved into in-plane shear stress (τ) and normal stresses (σ_n) acting on the fault plane (Figure 6.3b) such that

$$\sigma_n = \frac{\sigma_1 + \sigma_3}{2} - \frac{\sigma_1 - \sigma_3}{2} \cdot \cos 2\theta \quad (1)$$

and

$$\tau = \frac{\sigma_1 - \sigma_3}{2} \cdot \sin 2\theta \quad (2)$$

where θ is the angle between the fault plane and the minimum principal stress.

Since the fault under consideration is of arbitrary orientation equations (1) and (2) can be simplified to:

$$\sigma_n \propto a\sigma_1 + b\sigma_3 \quad (3)$$

and

$$\tau \propto c(\sigma_1 - \sigma_3) \quad (4)$$

with a, b and c all constants. An increase in τ will promote failure of the fault, while an increase in σ_n will promote fault stability.

Now consider the simple cases of two crustal stress regimes, one compressional, one tensional, both subject to an increase in vertical stress (S_V) due to ice loading (Figure 6.4). It is seen that in crustal compression (Figure 6.4a) an increase in the value of S_V' , the effective vertical stress, causes a reduction in τ while σ_n is increased, thereby stabilizing the fault. In crustal tension (Figure 6.4b) the additional load causes an increase in the magnitude of σ_1 which in turn causes an increase in τ and also an increase in σ_n , thereby creating a situation that may cause destabilization of the fault, but at the same time may cause no difference to the deviatoric stress ($S_D' = [\sigma_1 - \sigma_3]$) value, thus maintaining a situation of stability. A similar ambiguous situation is created in strike-slip environments. It has been shown that the imposition of large ice sheets on continental crust subject to compression suppresses the occurrence of earthquakes (Johnston 1987, 1989). As well as reducing the deviatoric stress (S_D') acting within the crust, the induced load also increases the effective normal stress (σ_n) acting on potentially seismogenic fault planes, moving the faults away from failure. However this rather simplistic view only holds for a 'dry' crust where there are no effects due to resident crustal fluids and fluids introduced from basal melting of the ice sheet.

6.4.1 The Effects of Ice-cap Loading: Wet Crust

Water is known to exist at the base of ice sheets (Zotikov 1986) and indeed many of the erosional features attributed to glacial systems are a result of the action of basal fluid. The presence of sub-glacial water requires the temperature of the ice to rise above its pressure melting point. The presence of stagnant hollows beneath a mobile ice-sheet enhances basal ice melt (Muir Wood 1989b). Such sub-glacial water will

penetrate the underlying crust (Figure 6.5a) through open fractures, raising the hydrostatic pressure by the full weight of the ice-cap. This in turn will encourage further basal melting creating a dynamic hydrological regime.

The penetration of sub-glacial fluid into fractured crust will be a time-dependent diffusion process. Analogous studies from reservoir impoundment (Costain *et al.* 1987) suggest that, in crustal volumes with fracture permeability, increases in head of water (ice thickness in this case) can be transmitted to depths of 10-20 km. The timing of crustal fluid diffusion beneath a volume of ice is unknown, however if it follows the behaviour observed from reservoir-induced seismicity, this may occur over a relatively short time period, with crustal fluid pore pressures equilibrating with respect to the increased head in a matter of a few months to a few years. If fluid flow within the crust is channelled along a number of dominant fractures this may greatly increase the flow rate (Roeloffs 1988). Whatever the rate of sub-glacial fluid flow into fractured crust, over the time period of ice-cap residence pore fluid pressure will have time to equilibrate at depth with respect to the increased head, and indeed may be subject to subtle changes due to shorter time scale changes as the ice grows and recedes. Whatever the result, basal ice melt and the penetration of such fluid into the underlying fractured crust will have an important control on the generation of the glacial and post-glacial stress regime.

The imposition of a significant thickness of ice will have differing effects at different crustal depths due to changes in rheology and depth of penetration of sub-glacial melt water. Near surface, where the crust is essentially brittle, it is expected that there would be little or no horizontal deformation over the period of ice loading. However there may be vertical movement in the form of differential compressibility of adjacent rock types and the closing of open fractures. The effective vertical stress (S_V') acting on the crust would be increased by the full weight of the ice load (S_{VI}) where:

$$S_{VI} = \rho_I g h \quad (5)$$

with $\rho_I = 0.9 \text{ Mg m}^{-3}$, $g = 9.81 \text{ ms}^{-2}$ and $h =$ thickness of the ice cover.

In the presence of increased fluid pressure driven by the weight of the ice load, the increase in the effective vertical stress will be counteracted by a corresponding increase in fluid pressure (P_f) where:

$$P_f = \rho_I g h \quad (6)$$

The resultant vertical stress acting on the crust due to ice loading will be the product of the vertical lithostatic stress (S_V) and the weight of the ice load (S_{VI}), minus the effects of the increase in pore fluid pressure (P_f) i.e.

$$S_V' = S_V + S_{VI} - P_f \quad (7)$$

Which, from 5 and 6, simplifies to become:

$$S_V' = S_V \quad (8)$$

Thus, there will be no net increase in the effective vertical stress acting on the crust at depths where the crustal fluid pressure has equilibrated with respect to increased hydrostatic head.

The imposed ice load will also cause an increase in the effective horizontal stress (S_H') acting on the crust. Dependent on whether lateral constraint or isotropic boundary conditions are assumed the relative increase in S_H' due to the weight of the ice load (S_{HI}) will be:

$$S_{HI} = 0.3 \text{ to } 1.0 (S_{VI}) \quad (9)$$

However, since the time scale of ice loading is relatively short (in a geotectonic sense) and little or no horizontal deformation is expected, the lateral constraint conditions, (assuming no horizontal deformation) seem to be more appropriate, where:

$$S_{HI} = (\nu / 1-\nu) S_{VI} \quad (10)$$

where $\nu = 0.25$, Poisson's Ratio, gives a relative increase in S_H' equivalent to $0.33S_{VI}$. The presence of increased hydraulic pressure will reduce this by the value of P_f . Thus the resultant horizontal stress becomes:

$$S_H' = S_H + 0.33S_{VI} - P_f \quad (11)$$

which, from 5 and 6, can be simplified to:

$$S_H' = S_H - 0.66S_{VI} \quad (12)$$

This decrease in the value of effective horizontal stress will in turn cause a reduction in the value of the deviatoric stress such that:

$$S_D' = [(S_H - 0.66S_{VI}) - S_V] \quad (13)$$

i.e. a reduction in S_D' equivalent to $0.66S_{VI}$, thereby removing critically stressed crust from failure.

In the absence of sub-glacial fluid penetration into the shallow crust there would be an increase in the values of S_H' and S_V' equivalent to $0.33S_{VI}$ and S_{VI} respectively. This would also cause a reduction in the deviatoric stress promoting crustal stability. This latter case would pertain at mid-crustal depths below the reach of sub-glacial fluid recharge.

Towards the base of the brittle crustal regime there would be a similar increase in stress to that found in 'dry' mid-crustal levels. However with longer periods of ice residence there may be flow of underlying ductile material away from the centre of ice loading giving a decrease in σ_1 for flow parallel to S_H' and a corresponding decrease in σ_2 for flow parallel to the direction of S_H' (Muir Wood 1989b). If fluid flow does penetrate to lower crustal levels as proposed by Costain *et al.* (1987) this may have an effect on the depth of the brittle ductile transition zone (Strehlau 1990) and, consequently, greatly affect the build-up of stress during the period of ice loading and the subsequent release of seismicity as such stress is relieved during the immediate post-glacial period.

Johnston (1989) modelled the crustal stresses beneath ice sheets using both elastic and visco-elastic response crustal models with differing boundary conditions and pore pressure regimes. From this he was able to show that in compressive environments containing weak faults optimally orientated for reactivation at or near their failure threshold, the imposition of an ice cap load removed the crust from failure.

6.5 Unloading: Ice-Melt Rebound and Deglaciation Tectonics

Seismic activity can be triggered by stress changes of a few tens of bars (c. 1.0 MPa). In cases where the deviatoric stress is very near to or at the failure threshold, a few bars may be sufficient to promote instability and the triggering of seismic activity. This is shown where activities such as mining (Yerkes 1983), reservoir impoundment

(Costain *et al.* 1987; Roeloffs 1988) and fluid extraction (Segal 1989) are sufficient to cause failure in critically stressed crust. Therefore it is expected that deglaciation, with the potential to remove a load equivalent to hundreds of bars (c. 10 MPa), should trigger seismic activity.

Naturally, the build-up of stress during the glacial period controls the amount of stress release during deglaciation. The rate of deglaciation is usually significantly faster than that for ice growth, therefore the time period for relaxation of the ice load is considerably shorter than that for load accumulation. For example, in Scotland the rate of the ice melt of the Main Late Devensian glaciation was c. 8 times that for ice accumulation, while in Fennoscandia the rate of deglaciation of the last ice sheet was c. 14 times that for ice growth.

The immediate effect of removal of the ice cover will be the release and redistribution of the stresses imparted in the rock mass due to both the weight of the ice load and due to tectonic forces that were built up over the time of ice residence. As with crustal loading, unloading will have differing effects at different crustal levels.

At shallow crustal depths where there was formerly basal ice melting, the declining lithostatic pressure is exceeded by hydrostatic pressure. This fluid overpressuring leads to a situation where S_V' is reduced not only due to the response of the crust as the load is removed, but also by the effect of fluid pressure, P_f , such that the effective vertical stress becomes:

$$S_V' = S_V - P_f \quad (14)$$

This fluid overpressuring cannot be sustained in the shallow crust and must be released by either flow to the surface or by movement along fractures. Although deglaciation marks a period of climate amelioration, the immediate post-glacial time would be one of a climate severe enough for the development of permafrost (Ballantyne 1984; Sutherland 1984). This would possibly create an impermeable layer, of the order of a few tens of metres thick, that could prevent the release of fluid overpressuring by retarding flow to the surface. The entrapment of excess fluid pressure in near-surface environments could lead to critical build-up of pressure and to sudden release of episodic fluid 'outbursts' causing dilational disruption of the near-surface fractured rock mass (Talbot 1986; Muir Wood 1989b) (Figure 6.5b). The depth (h) to which fluid pressure (P_f) exceeds lithostatic pressure (P_L) is controlled primarily by the thickness of the former ice cover (h_I), such that:

$$P_f = \rho_I g h_I = P_L = \rho_L g h \quad (15)$$

i.e.

$$h = \rho_I h_I / \rho_L \quad (16)$$

If we consider $\rho_L = 2.7 \text{ Mgm}^{-3}$ and $\rho_I = 0.9 \text{ Mgm}^{-3}$ this is simplified to:

$$h = 0.33 h_I \quad (17)$$

Thus, to depths equivalent to a third of the former ice thickness, fluid escaping along sub-horizontal fractures will be capable of 'lifting' the overlying rock mass (Talbot 1990).

Below the depth to which fluid overpressuring exists there will be a decrease in S_V' equivalent to the stress imparted by the ice load. The reduction in S_V' is normally accomplished 'elastically' (Carlsson & Olsson 1982) while the reduction in S_H' due to ice wastage falls by only 0.25 of the increase due to ice loading due to the slow visco-elastic response of the crust. In the case where the crust was at or near failure this will increase the deviatoric stress, having the effect of putting the rock mass into the field of failure. This net increase in the value of deviatoric stress will be compounded by the increase in S_H' due to the long-term tectonic strain rate of the area. Such a rise in S_H' due to long-term rock-creep during the residence of the ice cover would not be relieved during the short term of deglaciation.

Towards the base of the brittle crust the removal of the ice load would also cause an increase the deviatoric stress according to the same mechanisms acting at mid-crustal (dry) levels. This would be enhanced by increases in σ_1 and σ_2 due to stress transfer from flow of ductile lower and sub-crustal material into the former centre of ice loading.

Crustal uplift due to isostatic rebound has been shown to begin during deglaciation and reach a maximum immediately prior to the final disappearance of the ice cover (Mörner 1978), possibly reflecting the increasing rate of ice wastage as deglaciation progresses (Muir Wood 1989b). The stresses created during ice loading and subsequent deglaciation are capable of causing failure in critically stressed regions, but are rarely capable of dictating the mode of failure (Quinlan 1984; Stein *et al.* 1989). The high stress levels imparted by glacial loading need not be released immediately

upon deglaciation in an elastic manner, but are more likely to be released in 'bursts' of activity in the period following ice wastage, decreasing in frequency and magnitude as time progresses, indicating a more visco-elastic response by the crust. The presence of high stress levels due to former ice loading are shown by anomalously high stress measurements in Sweden (Carlsson & Olsson 1982) and in Scotland (Knill 1972). Visco-elastic behaviour will particularly affect horizontal stress levels due to lateral constraints preventing deformation over the short time of unloading. Vertical stresses will equilibrate more readily to the state of ice removal due to the presence of a free surface (i.e. the ground surface) allowing a more elastic-like response to the removal of the ice. Indeed such rebound is most marked when the time period of load removal is short in comparison to the relaxation time for the material. The rate of relaxation decreases away from newly created free (ground) surface (Nichols 1980). If rebound is merely an elastic response to the removal of an external load it would seem that recovery should be instantaneous and involve little or no permanent deformation, that is unless relaxation creates large stress concentrations within the crust (Nichols 1980). The instantaneous *and* time-dependent aspects of rebound show that geological materials behave in a visco-elastic manner when subject to unloading. Rebound in an ideal visco-elastic material occurs in response to past loading and is also influenced by the stress at the time of unloading as well as the geometry of the body undergoing relaxation. The visco-elastic response of the crust is shown by the development of deformation features such as extensional sheeting fractures sub-parallel to, and increasing in density towards, the ground surface in crystalline rock masses and the long periods of post-glacial uplift exhibited by a succession of raised shorelines in areas such as Scandinavia and Scotland. Unloading, as seen above, causes changes in the local stress field that can bring the rock mass into failure. The state of stress at shallow depths is such that it is unlikely to cause shear failure of the rock mass except along pre-existing fractures (Nichols 1980). Failure along pre-existing discontinuities will occur when the stress ratio ($k = \sigma_1/\sigma_3$) exceeds a critical value. The development of near-surface fractures as a response to visco-elastic rebound will create an increase in permeability allowing the movement of overpressurised fluids that may in turn cause further disruption to the rock mass.

6.6 Fault Reactivation

As stated previously, fault instability is created by an increase in the value of τ due to an accumulation of strain or by a decrease in σ_n or an increase in P_f causing a reduction in the effective normal stress acting on the fault plane.

The ease of reactivation of pre-existing faults is dependent on their orientation with respect to the prevailing stress field. For cohesionless faults the conditions for reactivation are :

$$\tau = \tau_0 + \mu_s(\sigma_n - P_f) \quad (18)$$

(Sibson 1985) where μ_s = static coefficient of friction ($0.6 < \mu_s < 0.85$) and τ_0 , the cohesion strength of the fault, is zero. The optimal orientation, θr^* , for fault reactivation with respect to that of the prevailing stress field lies close to the original angle of the fault to the stress field when it first formed, i.e. the angle predicted by *Andersonian* fault behaviour. However, if the orientation of the fault with respect to the stress field deviates significantly from this value, the stress ratio (k) needed to promote failure along the fault will increase substantially, to such a degree that it will exceed that required for the formation of a new fault (Sibson 1990). In this case reactivation will only occur under conditions of elevated pore pressure, P_f , such that $\sigma_3' = (\sigma_3 - P_f) \rightarrow 0$. Thus for unfavourably orientated faults reactivation will only occur if $\sigma_3' < 0$ or $P_f > \sigma_3$. In the absence of elevated fluid pressure faults become frictionally locked as the angle of reactivation approaches twice that for the optimum orientation for reshear in the prevailing stress system (Sibson 1985, 1990). From the previous statements it can be seen that conditions of fluid overpressuring in the post-glacial period are capable of reactivating unfavourably as well as optimally orientated faults.

6.7 Late Devensian Ice Loading in Scotland.

The role of late Devensian glacial episodes in the evolution of the late Quaternary stress regime and genesis of tectonic and seismic activity in Scotland is now investigated. From ground deformation and fault offsets known to have occurred at this time (Sissons & Cornish 1982; Ringrose 1987, 1989a, 1989b; Davenport *et al.* 1989; Ringrose *et al.* 1991) [§ 2, p15] and knowing the tectonic setting at the time of glacial inception (Muir Wood 1989a, 1990), the formulation of a relationship between magnitude of stress build-up and resultant crustal deformation will give a first order understanding of the deformation expected in areas undergoing deglaciation, thereby providing a useful predictive tool for the long term study of seismotectonic modelling associated with engineering and environmental projects such as nuclear waste repositories.

6.7.1 Late Quaternary Glacial History of Scotland

The most recent glacial episode in Scotland, the Main Late Devensian glaciation of the Dimlington Stade, destroyed almost all evidence of previous Quaternary glaciations in the area, hence there is only an accurate record for the last 26 kyr. Evidence for the timing of ice sheet initiation, growth and culmination is absent from Scotland. However, evidence from ocean cores (Ruddiman *et al.* 1980) indicates that the last period of major mid-latitude ice sheet build-up occurred c. 75 kyr. BP. Ice cover in Scotland is proposed at this time but is not proven (Ballantyne & Sutherland 1987). Whatever the status of early Devensian ice cover in Scotland speleothem evidence suggests that large areas of Scotland were without ice cover from c. 35 to c. 26 kyr. BP (Atkinson *et al.* 1986).

The main late Devensian glaciation (Figure 6.6) began c. 26 kyr BP, reaching a maximum c. 18 kyr BP. This was followed by a period of complete, or almost complete, deglaciation, the Windermere Interstadial, around 13-11 kyr BP. Climate deterioration then allowed the formation of a further glacial episode, the Loch Lomond Readvance (LLR) 11-10.3 kyr BP. This is the best expressed glacial event in Scotland and was predominantly a period of valley glaciation, responsible for shaping the majority of landforms seen today. There is also evidence of smaller readvance episodes during the late Quaternary (Robinson & Ballantyne 1979; Sissons & Dawson 1981; Ballantyne & Sutherland 1987), but these are short-lived and of limited extent and importance when we consider the regional events during this time. Nevertheless they may be of importance if there is a need to explain some local deviations in stress generation and tectonic style from those predicted from the regional study.

In terms of crustal loading almost the whole of Scotland was subject to c. 13 kyr of glacial loading followed by a short period of relaxation before partial reloading during the LLR. In areas such as Glen Roy and Coire Dho this pattern of cyclic loading on a regional scale was further complicated by the fluctuating levels of glacially-dammed lakes inducing more localised stresses [§ 3.9, p122]. Other local fluctuations may have resulted from the localized ice readvances that are proposed for areas of Wester Ross.

6.8 Regional Ice Loading and Stress System Evolution in Scotland

The state of crustal loading due to mid-latitude glaciations pre-dating the Main Late Devensian episode remains a matter of speculation as to the size and duration of

these events. It is possible that there was a period of c. 40 kyr. of glacial loading of unknown magnitude prior to the Late Devensian. Due to the obvious uncertainties concerning the magnitude of this earlier loading event, it will not be considered.

The pattern of glaciation and deglaciation during the latter part of the Devensian gives rise to the following stress history:

During the Main Late Devensian Glaciation the whole of Scotland was under complete ice cover. This glacial episode lasted for c. 13 kyr reaching a maximum c. 18 kyr BP. The degree of ice cover fluctuation during this event is unknown. However it has been subject to modelling studies (e.g. Boulton *et al.* 1985) which, although overestimating the degree of ice cover (C.K. Ballantyne & C.J. Tate pers. comms. 1989), give a useful working estimate for ice loading studies. The model of Gordon (1979) closely agrees with the field evidence (Ballantyne & Sutherland 1987) for the lateral extent of ice cover and is used here to estimate the ice loading stresses over Scotland during the Late Devensian glaciation.

The Ice Maximum Model (Figure 6.6) gives an idea of the ice cover during the late Devensian glacial maximum at c. 18 kyr BP. The ice sheet is seen to be parabola-shaped and up to 2 km thick. The vertical stress induced by 2 km of ice (with density 0.9 Mgcm^{-3}) would be 180 bar (18 MPa). Thickness variations over the area of interest of this study give rise to vertical loads in the range of 117 -180 bar (12-18 MPa).

The model shows a central zone of basal freezing flanked by areas of basal melt, to the east and to the west, corresponding to areas of glacial scouring. This has important implications when modelling the glacially-induced stresses:

(i) *Central area of basal freezing*: In this area the weight of ice cover imposes a load of 180 bar. As the crust was subject to compression this gives rise to a reduction in the deviatoric stress promoting crustal stability. Basal freezing insulates the crust from fluid recharge that would otherwise destabilize the crust by reducing σ_n on faults (Johnston 1987). Therefore S_V' increases by 180 bar. The increase in S_H' due to ice loading is $0.33(S_V')$ i.e. an increase of 60 bar. The reduction in the deviatoric stress is equivalent to $[(\sigma_1 + 60) - (\sigma_3 + 180)]$ i.e. a reduction of 120 bar (12 MPa), promoting crustal stability.

The ability of the crust to support high deviatoric stress for extended periods of time is shown by the occurrence of earthquakes and high horizontal stress measured in boreholes. Long term relaxation mechanisms (e.g. creep) will tend to reduce this stress, however the time scale of glacial loading is usually insufficient to allow this to occur.

(ii) *Lateral areas of basal melting*: In these areas the effects of ice loading are complicated by having to account for pore pressure effects induced by fluid recharge at the base of the ice sheet. In these areas the ice sheet still imposes a load proportional to the thickness of the ice, increasing S_V' . However this effect is offset by the increase in pore fluid pressure. The diffusion of sub-glacial water into the fractured crust is a time dependent process that will eventually lead to the hydrostatic pressure being raised by the full weight of the ice sheet leading to no net increase in S_V' . S_H' is increased by $0.33(S_V I)$, but reduced by the hydrostatic pressure. For a 2 km thickness of ice cover this would lead to a reduction in S_H' of 120 bar. This scenario also reduces the deviatoric stress to $[(\sigma_1 - 120) - \sigma_3]$ i.e. a reduction of 120 bar (12 MPa), moving the crust away from failure.

In both cases, where there is crustal fluid recharge and crustal fluid insulation at the base of the ice sheet, the imposed load acts to move the crust away from failure. This is in agreement with the findings of Johnston (1989).

The action of the ice mass acting to close fractures in the upper crust, thus preventing fluid recharge is not feasible as the ice load was not imposed as an instantaneous event, but in a gradual manner, therefore allowing the crustal fluid pressure to increase at a similar rate, albeit with a slight time lag, due to the time-dependent nature of crustal hydraulic conductivity, to the increasing ice load .

The effects of fluid pressure in reducing both S_V' and S_H' would extend to depths of c. 5 km (Muir Wood 1989b) and possibly even deeper (Costain *et al.* 1987; Sibson 1990). Below this level it is only the imposed load that controls the changes in the stress levels. At such depths an imposed load of 2 km of ice would, as above, give a reduction in the deviatoric stress equivalent to 120 bar.

Beneath the base of the brittle crust there will be flow of the underlying ductile material away from the centre of loading causing a reduction in S_H' and S_h' . To what degree this occurred in Scotland during the last glaciation is unknown. However such

lower crustal flow would only have a minor effect in relation to the loading stresses over such a short time period.

Over the duration of ice loading there would have been a gradual increase in S_H' due to tectonic strain build-up. For a stable continental interior region with a strain rate of 10^{-11} s^{-1} to 10^{-12} s^{-1} (Anderson 1986), this would yield an increase in S_H' of <0.05 bar for the period of loading. Even using the strain rate for active continental interiors (10^{-9} to 10^{-10}) gives an increase of <5 bar. However although not being the dominant control in the build-up of stress at this time, this order of magnitude increase may be sufficient to bring the underlying crust close to failure. The latter 'high' strain rate is not inconceivable for the UK at this time, as it is unlikely that the elevated strain rates of the Tertiary ceased suddenly 2 myr BP and may have persisted for some time during the Quaternary period. In any case the increase in S_H' due to the tectonic strain rate is insignificant in comparison to the changes induced by ice loading no matter how large the tectonic strain rate for the time period (26-13 kyr. BP) under consideration.

Thus for the duration of the Main Late Devensian glaciation there is a general increase in S_V' relative to S_H' irrespective of the hydrological conditions. This will tend to promote crustal stability in areas subject to compression. In some instances the degree of loading may be such that the stress ratio becomes $S_V' \rightarrow S_H'$. This is very important when considering the mechanisms of stress release during unloading and therefore has great bearing on the understanding of post-glacial fault movements.

6.9 Removal of the Late Devensian Ice Cover (Windermere Interstadial)

Following the Main Late Devensian Glaciation was a period of climate amelioration, the Windermere Interstadial, when the ice was completely removed from the Scottish Highlands (some small corrie glaciers may have remained). This lasted for a period of c. 2 kyr before the onset of the next glacial event, the Loch Lomond Readvance. From the glacial maximum at c. 18 kyr BP there probably was a slight relaxation in the load imposed on the Highlands until c. 14 kyr BP when melting of the ice-cap began, culminating in a 2 kyr period when no vertical stress was imposed on the crust from an external source. The rate of unloading, assuming a constant rate of ice melt over this period of time, would be in the order of 0.18 bar yr^{-1} , although this may have been an order of magnitude greater as ice wastage reached its end (Muir Wood 1989b). This is c. 8 times that of the rate of loading, again assuming a constant rate of ice growth, from glacial inception to the glacial maximum.

As with ice loading, two cases have to be considered, one where the crust was insulated from fluid recharge during ice cover and one where fluid pressure within the crust has been elevated by the full weight of the ice cover.

(i) *Insulated (dry) crust*: At the glacial maximum S_V' was determined by the weight of the ice cap. This effective vertical stress falls 'elastically' to zero at the earth's surface upon deglaciation. The lateral stress field created during loading should remain provided that the strength of the rock mass is not exceeded. Adjustment of S_H' due to the decrease in S_V' amounts to about 0.25 of the increase induced by glacial loading (Carlsson & Olsson 1982). However actual behaviour of the crust should be more visco-elastic and there will still be a proportion of the ice-induced stresses remaining in the crust following deglaciation. The reduction of S_H' as a consequence of ice wastage is shown to be not entirely elastic by the development of large 'sheeting' fractures sub-parallel to the ground surface in areas such as Glen Etive and Glen Roy [§ 3.4, p116].

Immediately on deglaciation the crust is left in a state of being overstressed. S_V' of 180 bar in excess of lithostatic pressure is removed relatively quickly by the 'elastic' response of the crust. The data of Mörner (1978, 1981) show that the rate of uplift associated with deglaciation and rebound peaks immediately prior to the end of deglaciation, therefore the imposed vertical stress seems to decay in harmony with the ice cover. Thus upon deglaciation the S_V' element of glacial loading will have been removed leaving the S_H' element of glacial loading c. 75% of its maximum. This leaves the crust with a high potential for failure with S_H' greatly increased with respect to S_V' , thereby increasing the deviatoric stress (S_D') and bringing the crust close to, if not into, criticality. In view of the rapid rate of post-glacial crustal uplift and the flexural rigidity of the crust it is expected that uplift irregularities should be accommodated by bedrock discontinuities. Movement of such a nature would lead to seismogenic dislocation occurring contemporaneously with deglaciation.

The stress ratios, as well as the orientation of the principal stresses at the time of deglaciation has great bearing on the type of fault movement taking place at this time, and on the orientation of the faults that are capable of being reactivated (Sibson 1990).

Prior to glaciation this was an area of crustal compression with $S_H' = \sigma_1$, $S_h' = \sigma_2$ and $S_V' = \sigma_3$ where $\sigma_1 > \sigma_2 > \sigma_3$. During glaciation the increased vertical load would promote S_V' to equal σ_2 if not even σ_1 if the loading stresses are great enough. The removal of the ice cover would return S_H' to σ_1 status while the visco-elastic

response of the crust would retain S_V' as σ_2 for some time. This latter stress system would promote strike-slip faulting until the level of excess vertical stress was reduced. The vertical stress induced by glacial loading may, under some circumstances, remain for longer periods of time than are predicted, providing that it does not exceed the rock strength, e.g. at Cruachan where S_V' is 3-4 times that expected for the amount of overburden (Knill 1972), therefore preserving such a strike slip environment for extended periods of time. This could explain the large Quaternary lateral offsets observed along the Kinloch Hourn [§ 2.6.20, p47], Coire Mor [§ 2.6.1, p21] and Coire Eoghainn faults [§ 2.6.10, p35] (Ringrose 1987,1989b; Ringrose *et al.* 1989). Also at this time compressional features such as pop-ups and thrust faults would develop perpendicular to S_H' . The time dependent reduction in S_V' would eventually lead to the establishment of the stress system as it was prior to glaciation, albeit with elevated σ_1 . The initial stress release, via strike-slip faulting, would have created a more stable crustal stress regime, therefore the stress release with this secondary stress system would be much less, and thus marked by much less spectacular faulting of reverse nature, as represented by small pop-ups and observed metre-sized block fault offsets [§ 2, p15].

(ii) *Wet crust*: The sub-glacial hydraulic pressure in the superficial crust would exceed the lithostatic pressure gradient leading to fluid overpressuring. This would give rise to dilational movements along fractures, especially those created by rebound. Such fractures, lying sub-parallel to the free surface created by the removal of the ice cover, would allow the communication of fluids with the surface. However if the period of deglaciation was accompanied by conditions of permafrost, as is usually the case, then this fluid would be sealed below an impermeable surface layer. This would lead, when the pressure was sufficient, to episodic fluid outburst, possibly leading to dilational disruption of the near surface rock mass, a phenomenon described from both Sweden and Scotland (Talbot 1986) [§ 3, p112].

Assuming a permeable crust, the depth to which fluid pressure exceeds lithostatic pressure is dependent on the thickness of the former ice cover. For an average crustal density of 2.7 Mgm^{-3} , following the removal of 2 km of ice cover fluid overpressuring will extend to 0.66 km. At greater depths fluid overpressuring may become trapped (Muir Wood 1989b). This will reduce S_V' significantly (by 180 bars) and therefore increase the deviatoric stress to exceed the rock strength leading ultimately to failure in the area of fluid penetration.

At mid-crustal levels, below the level of fluid overpressuring, the removal of the ice and corresponding fall in the value of S_V' will give rise to a comparative rise in the value of S_H' . S_H' will also be raised by about 5 bar due to the accumulation of tectonic strain during the period of ice loading. This accounts for <3% of the total stress change induced by deglaciation. If any rock creep has occurred during the time of ice loading it will not be able to be restored during the period of deglaciation, thus becoming a "locked-in stress" (Stephansson *et al.* 1991) and therefore will also cause an increase in S_H' . If the deviatoric stress in the pre-glacial regime was equal to the strength of the fractured rock then the post-glacial stress alterations raise the deviatoric stress to exceed the fracture strength and thereby promote failure. At the base of the brittle crust the underlying ductile material will flow radially towards the former centre of ice loading, also the area of greatest uplift, increasing all horizontal compressive stresses in the area.

6.10 Reloading and Rebound Retardation

Following this period of deglaciation the crust was subject to partial reloading during the LLR. This glacial episode was characterised by much less extensive ice cover than the Main Late Devensian. It is modelled here using the Half ice maximum width model (Figure 6.6) of Gordon (1979). The areal extent of ice cover was much smaller and therefore did not have such an influence on the generation of the crustal stress regime as that of the previous glacial event. However it did play a major role in the retardation of rebound associated with the Main Late Devensian glaciation, a fact noted from the shoreline leveling studies of Firth (1986).

Again when considering the effects of glacial loading and unloading we have to consider the effects on both 'dry' crust insulated from basal ice melt fluid recharge and 'wet' crust where the weight of ice increases the fluid pressure in the underlying crust.

(i) *Basal freezing*: The weight of the ice during the LLR was considerably less than that of the Main Devensian glaciation and therefore does not have such a drastic effect on the stress in the underlying crust. An ice thickness of 0.5-1.0 km gives an increase in S_V' of 45-90 bars (4.5-9 MPa). Assuming lateral boundary conditions this would give an increase in S_H' of 15-30 bars (1.5-3 MPa). This would lower the deviatoric stress by 30-60 bars.

(ii) *Basal Ice Melt*: In the presence of elevated crustal fluid pressures driven by the weight of the overlying ice there would be no net change in S_V' as the increase in P_f negates that due to S_{VI} . S_H' would be lowered by $0.66S_{VI}$, a reduction of 30-60 bars. This would lower the deviatoric stress by 30-60 bars.

Both situations would be sufficient to promote stability in critically stressed crust. The extremely short duration of the readvance (11-10.3 kyr BP) makes the contribution due to the build-up of tectonic strain almost negligible.

The loading during the LLR may be further complicated by unrelieved stresses and fluid overpressuring from the late Devensian glacial episode. The readvance glaciation could also cause redepression of the crust and halt isostatic rebound. Evidence from shorelines at the southern end of Loch Ness (Firth 1986) shows this to be the case. Such reloading of the crust would also prevent the release of overpressurised fluids that had not been released following the decay of the Main Late Devensian Glaciation.

6.11 Post-glacial Fault Reactivation in Scotland

A number of faults in Scotland (Figure 6.1) have been shown to be active during the late Quaternary following the decay of the Devensian ice cover. These are almost all faults cutting metamorphic basement rocks and have had long histories of movement, sometimes as far back as Precambrian time. Thus, the late Quaternary was a time of fault reactivation and, as far as is known, there was no creation of significant surface ruptures during this time [§ 2.8, p51]. The orientation of the faults are quite diverse (Figure 6.1) and, as is expected in a compressional stress regime, the offsets are reverse, strike-slip or a combination of both. Despite intensive age-dating studies (Ringrose 1987) [§ 5, p220] the chronology of fault movements are poorly constrained and, at best, are dated relative to Quaternary deposits and geomorphology cut by the the faults. The majority of fault movement occurred following the disappearance of the ice cover c. 10.3 kyr BP and prior to the formation of the blanket peat cover in the Scottish Highlands c. 6 kyr BP (Birks 1977). There are some notable exceptions that show continued fault movement in more recent time (Ringrose 1989b) [§ 2.6.8, p34].

In an attempt to understand the history of fault movements following deglaciation it is necessary to consider the stresses and degree of fluid overpressuring generated during ice cap residence and try to synthesize how they would be relieved

during the phase of isostatic rebound following deglaciation. This requires some modification and refinement of the stress evolution situation considered above.

6.12 Refined Ice Loading Model

Prior to ice loading the crust is in compression, with $S_H' > S_V'$ such that S_D' is close to or at the failure threshold for the crustal material. Assuming that fluid pressure is hydrostatic in a fractured crust of density 2.7 Mgm^{-3} fluid density of 1.1 Mgm^{-3} to account for slightly saline ground waters [Sibson (1990) states $\rho_f/\rho_r \approx 0.4$]. If the stresses at a seismogenic depth of 5 km, subject to the imposition of 2 km thick ice cover, are considered the following stress history can be constructed:

(i) *Pre-ice loading.*

$$P_f = \rho_f g h = 539 \text{ bar}$$

$$S_V' = S_V - P_f = \rho_r g h - 539 = 785 \text{ bar}$$

$$S_H' = S_H - P_f = 3140 \text{ bar} *$$

* calculated from the relationship $(\sigma_1 - P_f)/(\sigma_3 - P_f) = \{ \sqrt{(\mu_s^2 + 1) + \mu_s} \}^2$ used by Johnston (1989) and assuming relatively strong faults ($\mu_s = 0.75$).

This gives a stress ratio, k' , of 4 and deviatoric stress value of 2356 bar. Using the criteria of Sibson (1985, 1990) this would only allow the reactivation of favourably orientated faults i.e. thrust faults dipping at $22-32^\circ$ and strike-slip movement on faults at $22-32^\circ$ to σ_1 .

(ii) *Early ice loading: fluid pressure hydrostatic.*

$$P_f = 539 \text{ bar}$$

$$S_{VI} = \rho_I g h = 176 \text{ bar}$$

$$S_V' = S_V + S_{VI} - P_f = 961 \text{ bar}$$

$$S_H' = S_H + 0.33 S_{VI} - P_f = 3199 \text{ bar}$$

This causes a decrease in k' to 3.3 and S_D' to 2238 bar. This removes the crust from failure and promotes stability (independent of the value of μ_s).

(iii) *Ice sheet loading: equilibrated fluid pressure.*

$$P_f = 539 + \rho_I gh = 715 \text{ bar}$$

$$S_V' = S_V + S_{VI} - P_f = 785 \text{ bar}$$

$$S_H' = S_H + 0.33S_{VI} - P_f = 3023 \text{ bar}$$

This raises k' to 3.85 while S_D' remains 2238 bar. This does not effect the stability of the crust, but the increase in k' will allow more faults of slightly unfavourable orientation to be potentially reactivable during unloading.

(iv) *Removal of half ice load: elastic removal of vertical stress.*

$$P_f = 715 \text{ bar}$$

$$S_V' = S_V + 0.5S_{VI} - P_f = 697 \text{ bar}$$

$$S_H' = 3023 \text{ bar}$$

This raises k' to 4.34 and S_D' to 2332 bar bringing the crust close to but not quite into failure. If S_H' also falls elastically on removal of the *half ice load* the value of k' becomes 4.3 and S_D' becomes 2296 bar.

(v) *Removal of ice load: elastic removal of S_{VI} , remaining fluid overpressuring.*

$$P_f = 715 \text{ bar}$$

$$S_V' = S_V - P_f = 609 \text{ bar}$$

$$S_H' = S_H + 0.33S_{VI} - P_f = 3023 \text{ bar}$$

This corresponds to the early post-glacial phase when S_H' has not had time to equilibrate with respect to the removal of the ice load. This creates a situation where k' is raised to 4.95 and S_D' to 2418 bar. The crust is placed into the field of failure by this increase in S_D' and the fact that k' is also increases allows faults of less favourable orientations (up to an angle of $\theta r^* \pm 0.5\theta r^*$ to σ_1) to be reactivated.

(vi) *Removal of ice load: elastic removal of all glacial stresses, remaining fluid overpressuring.*

$$P_f = 715 \text{ bar}$$

$$S_V' = 609 \text{ bar}$$

$$S_H' = 2964 \text{ bar}$$

In this case k' becomes 4.87 and S_D' 2356 bar. This also puts the crust into the field of failure and the value of k' allows less favourably orientated faults to be reactivated in this stress field. This is the same case as in (v).

(vii) *Loch Lomond Readvance Glaciation.*

There are far more unknowns when attempting to model the stress build-up during the LLR. For instance, to what degree were the stresses, particularly the amount of fluid overpressuring, relieved during the Windermere Interstadial. With this in mind the following scenarios are considered. Again stresses are calculated at a depth of 5 km this time with an ice overburden of 1 km thickness.

(a) *LLR reloading: remaining fluid overpressuring.*

$$S_{VI} = 88 \text{ bar}$$

$$P_f = 715 \text{ bar}$$

$$S_V' = S_V + S_{VI} - P_f = 697 \text{ bar}$$

$$S_H' = S_H - P_f = 2964 \text{ bar}$$

This situation gives values of 4.2 and 2268 bar for k' and S_D' respectively. This would be the case during early ice loading, creating stability within the crust as S_D' is moved away from failure. As S_H' equilibrates relative to the ice load, increasing to 2993 bar, S_D' becomes 2296 bar and k' equals 4.3 preserving the conditions of crustal stability.

However if it is assumed that fluid over-pressuring as a result of Devensian glaciation has been released the stresses evolve to become the following:

(b) *LLR reloading with hydrostatic fluid pressure.*

$$P_f = 539 \text{ bar}$$

$$S_V' = S_V + S_{VI} - P_f = 873 \text{ bar}$$

$$S_H' = S_H - P_f = 3140 \text{ bar}$$

In this case S_D' becomes 2268 bar and $k' = 3.6$. This promotes crustal stability on faults of all orientation. As the horizontal stress equilibrates with respect to the ice load S_H' becomes 3169 bar. This causes a slight increase in S_D' to 2296 bar while k' remains 3.6. This will preserve crustal stability.

(c) *LLR reloading with increased fluid pressure.*

Assuming basal ice melt, this will cause the following changes in the stress system:

$$P_f = 627 \text{ bar}$$

$$S_V' = S_V + S_{VI} - P_f = 785 \text{ bar}$$

$$S_H' = S_H + 0.33S_{VI} - P_f = 3081 \text{ bar}$$

This creates a situation of fault stability with S_D' of 2296 bar and k' of 3.9.

(d) *Decay of LLR ice: fluid overpressuring.*

$$P_f = 627 \text{ bar}$$

$$S_V' = 697 \text{ bar}$$

$$S_H' = 3081 \text{ bar}$$

This gives rise to the situation where S_D' is raised to 2384 bar and $k' = 4.4$ putting the crust into failure. This will allow faults orientated $\theta \pm 10^\circ$ to σ_1 to be reactivated. Even when S_H' equilibrates to the removal of the ice load the degree of fluid overpressuring maintains a situation of failure with S_D' of 2356 bar and k' of 4.4.

From this model of the temporal changes of stress (Figure 6.7) it can be seen that the yield strength of pre-existing fractures is exceeded in the immediate post-glacial periods when the relief of ice loading stresses coupled with the remaining fluid overpressuring raises the deviatoric stress, S_D' above S_{DCRIT} leading to failure. The corresponding increase in the value of the effective stress, k' , allows the reactivation of more unfavourably orientated faults. From this a rough chronology of fault movement can be calculated from the orientation and type of fault movements found in the Highlands of Scotland.

6.13 First Order Fault Movement Chronology

As stated above, the degree of fluid overpressuring can have an important control on the orientation of the faults subject to reactivation. Immediately upon deglaciation in areas of 'wet crust', fluid overpressuring, in conjunction with the effects of removal of the ice load, will lead to a dramatic reduction in S_V' relative to the reduction in S_H' . In areas of crustal compression this will cause a marked increase in the effective stress ratio ($k' = \sigma_1/\sigma_3$) and in the deviatoric stress, having the result

that the crust is put into failure or near failure conditions. The increased stress ratio will allow the reactivation of unfavourably orientated faults (in the absence of more favourably orientated faults) (Sibson 1990). The orientation of faults reactivated in the late Quaternary in Scotland (Figure 6.1) shows a large degree of variation, from those almost parallel to and others perpendicular to the WNW to NW trending regional stress field. This can be explained in terms of decreasing influence of fluid overpressuring with time during the post-glacial period.

From Figure 6.7. it is seen that immediately on deglaciation (e and g) that k' and S_D' are at a maximum. As S_D' exceeds S_{DCRIT} this puts the crust into the field of failure. With $k' \sim 5.0$, this will allow faults orientated at $\theta_r^* \pm 12^\circ$ to σ_1 to be reactivated. In a compressive stress regime reverse and strike slip faults will be reactivated at high angles (up to 44°) to the direction of S_H' . The possibility of movement along less favourably orientated faults will only arise in the absence of faults more favourably orientated with respect to the stress field or if these faults are weaker (due to recent movement) than neighbouring more favourably orientated faults.

The period immediately on deglaciation would be one of considerable stress relief in a vertical manner, due to the massive decrease in S_V' . The visco-elastic response of the upper part of the crust will lead to the development of rebound fractures parallel and sub-parallel to the newly created free (ground) surface. Spatial heterogeneity in the pattern of rebound (controlled by local ice thickness variations, geology etc.) will give rise to differential uplift. The heterogeneity in the degree of uplift will be accommodated along pre-existing lines of weakness. This will give rise to an environment of differential block uplift and the creation of 'pop-up' features. This in turn will give rise to shallow seismic activity. Occurring in the immediate post-glacial period, the time of most rapid isostatic uplift, this will be an instantaneous, 'elastic' response of the brittle crust to the disappearance of S_{VI} , with there being little control by the regional stress field on the orientation of the fractures reactivated during this period of movement. This episode would account for some of the more anomalously orientated reactivated fault orientations observed.

As a consequence of this period of 'chaotic' fault movement there would be an increase in the fracture permeability of the upper part of the crust. The stress drop due to seismic activity would lead to an increase in fluid overpressuring. Coupled with the increase in fracture permeability, this would lead to the upward expulsion of crustal fluids. This would cause a reduction in the value of P_f , in turn causing an increase in the effective crustal stresses present (see equations 7 & 11). Provided that the seismic

stress drop was not too great [Commonly 10-100 bar (Kanamori 1978)] the crust will remain in the field of failure. However, as a consequence of the reduction in P_f , there will be a corresponding decrease in the capability of the stress system to reactivate less favourably orientated faults. As the value of P_f decreases, the value of k' required to cause reactivation exceeds the strength of the rock. This would lead to the creation of new faults. This is neither observed in Scotland nor in Fennoscandia. The reactivation of less favourably orientated faults will only occur as long as $P_f > \sigma_3$ i.e. a $\sigma_3 < 0$. With the removal of the ice load, at shallow crustal levels, σ_3 will be vertical, thus leading to the situation predicted by Talbot (1990) where the shallow crust may be 'lifted' by the excess P_f . As stated previously, this will be a fairly transient situation in the immediate post-glacial period, effectively dissipated by its own creation as it disrupts the fractured crust. This is a possible mechanism to explain the unique large movements along Swedish post-glacial faults. The massive expulsion of water associated with such fault movement is shown by palaeo-spring lines along the Strath Vaich fault [§ 2.6.2, p25].

Following the initial period of 'chaotic' fault reactivation there would only be movement along the most favourably orientated faults, hence the dominance of NW-SE orientated fault reactivation, sub-parallel to the direction of the neotectonic stress field, during the Holocene in Scotland (Figure 6.1). Stress measurements in Scotland (Knill 1972) and Sweden (Carlsson & Olsson 1982) show that the high vertical stresses induced by glacial loading are not always dissipated on deglaciation and can be stored in crystalline rock for considerable lengths of time. The preservation of high levels of vertical stress would maintain an environment of strike-slip faulting for some time following deglaciation. In the absence of high values of S_V' faulting would be of reverse nature, with the strike of reactivated faults being aligned perpendicular to S_H' . This is consistent with the field evidence from Scotland (Ringrose 1987, 1989b) [§ 2, p15]. The action of the flow of lower crustal material back into the former centre of ice-loading will transfer stress into the upper crust maintaining enhanced levels of S_H' for some time after deglaciation. This may explain the swarms of seismicity around Rannoch Moor, the former centre for ice dispersal during the LLR [§ 4.17, p215]. Delayed rebound, due to the failure of crustal depression to equilibrate with the glacial maximum, can also lead to the preservation of high crustal stresses, and as a consequence prolonged fault activity (Koteff & Larsen 1989).

The best evidence for the time-dependent behaviour of the crust in Scotland to the effects of glacial loading is from raised shorelines. The most widely accepted pattern of isostatic recovery for Scotland was one of an elliptical dome of uplift centred

on the Rannoch Moor ice centre (Sissons 1983). Subsequent more detailed work has called into question this rather simplistic representation. Gray (1985) put forward evidence to suggest that the centre of uplift moved c. 30 km to the east during the Holocene. Ringrose (1987) suggests c. 70 km movement of the uplift centre to the southeast between 10.5 and 2.5 kyr BP. Plotting data for the main Post-glacial shoreline Ringrose (1987) showed there to be a bulge in the isobase distribution in the area of Morven, Mull and Jura. More recently Haggart (1989) comparing sea-level curves from the Firth of Forth, Strathearn, and the Solway and Moray Firths showed there to be marked differences in the relative rates of isostatic uplift throughout the Holocene. These data coupled with the evidence for dislocation of shorelines (Sissons 1972; Gray 1974; Sissons & Cornish 1982; Ballantyne & Sutherland 1987; Ringrose 1987, 1989b) suggests that isostatic recovery of the crust following deglaciation is complicated by non-uniform uplift utilising pre-existing lines of weakness to accommodate this movement. The bulge in the isobase distribution noted by Ringrose (1987) corresponds with faulted offsets on the Island of Mull. Present day crustal movements in the British Isles is seen to be a broad regional pattern of decaying uplift in Scotland and linear subsidence in southern and eastern England (Shennan 1989). Despite subtle local deviations, the patterns of vertical crustal movements in Scotland are seen to be in response to the decay of the last ice sheet. The data of Shennan (1989) show that there is an exponential decrease in the rate of uplift until c. 5 kyr BP. when a more linear (?tectonic) uplift took over. This is similar to the pattern of uplift observed in Fennoscandia (Mörner 1978). Thus it seems that by c. 5 kyr BP. the majority of the influence of the late Quaternary ice loading had decayed to be replaced by a tectonic element. Evidence from Canada shows decreasing uplift in the post-glacial period (Andrews 1970). Early, high rates of uplift could have masked slower tectonic movements that are not revealed until the amount of isostatic uplift decreases to allow the tectonic elements to become the dominant factor in crustal deleveling. It is tentatively suggested that present day movements and seismicity in Scotland owe more to tectonism than to the isostatic response of the crust to the last glacial period.

With regard to a chronology of fault movement during the post-glacial (Holocene) period the above considerations have to be compared with the evidence from dating studies (Ringrose 1987, 1989b) [§ 5, p220]. Geological evidence and 'absolute' age dating of fault movements in Scotland broadly agree with the statements made above: the majority of fault movement occurred during the period 10.3-6 kyr BP with only a limited amount of reactivation during the period from 6 kyr BP to the present day. The movement observed in these periods is consistent with the early

'chaotic' activity and a later prolonged period of movement on ideally orientated faults respectively.

An important observation is the apparent lack of fault activity in the eastern Highlands. Studies have shown there to be a dearth of post-glacial surface fault activity in this area. Despite this there is evidence for palaeoseismic activity (Davenport & Ringrose 1987; Ringrose 1987). The lack of surface faulting is thought to be a result of the differing regimes of ice cover between the eastern and western Highlands at this time. The more rounded, rolling topography of the eastern Highlands is testimony to a more passive ice erosive regime at this time; a contrast to the rugged ice-gouged topography of the western seaboard. This more passive erosive regime is attributed to the ice cover in the east being frozen to the underlying ground surface. With the ice freezing at its base this would prevent the creation of a sub-glacial fluid reservoir and as a consequence there would be no great changes in the crustal fluid pressure regime during glaciation. Thus, during deglaciation the crust would not be left in a state of being overpressurised with respect to P_f , and as a result not be subject to the disruption of the upper crust observed in the western Highlands. The movements that gave rise to the palaeoseismic deformation features observed must have occurred at depth and not affected the surface, or they may not have been recognised; this is though unlikely as they would be more prominent in such gentle topography and therefore be easily recognisable. Deglaciation in the east would only allow surface disruption on the order of localised block movements (as shown by the topography-parallel sheeting fractures in areas such as the Cairngorm Mountains) as predicted by more conventional rebound failure theory (Nichols 1980).

6.14 Discussion

So far what has been established is a simplistic, empirical model for the build-up of stress in an environment undergoing glaciation and subsequent unloading. It gives a useful, if imprecise, means for the prediction of crustal behaviour in the post-glacial period. If the preceding arguments are modified to account for more realistic situations a number of complications and assumptions must become involved. The following are the main uncertainties in the preceding arguments:

(i) Assumption of crust/fluid densities can lead to errors in the calculation of the depth to which fluid overpressuring can occur by up to 10%.

(ii) The degree of build-up of fluid overpressure cannot be accurately predicted. The mechanics of fluid flow through fractured crust, especially at depth, is a relatively poorly understood subject. Preliminary studies, however, do allow a first order understanding of the magnitude of fluid movements in fractured crystalline crust (Black 1987).

(iii) As stated previously this model is merely a first order prediction and the degree of stress build-up, stress release and strain rate for the time period under consideration are unknown and the figures quoted are limited by the amount of information available for this period.

(iv) Local complications arise due to several factors such as topographically-induced stress accumulations (Ling 1947), differential ice build-up and decay, stress partitioning within the crust, and reorganisation of the stress field in response to seismic stress drop.

(v) Specific to the study of the stress evolution in the area of N.W. Scotland are the uncertainties of whether all the fluid pressure created during the Devensian glacial episode was released during the Windermere Interstadial or whether it survived and was not released until the final unloading following the Loch Lomond Readvance. Local variations in ice accumulation and decay, and their significance in the generation of an unstable crustal stress regime are also uncertain.

Many other uncertainties have been mentioned in the specific sections within the preceding arguments. Despite these, the stress generated from the preceding models does agree with and explain the geological observations for the timing and style of fault movement during the Holocene in Scotland.

Previous attempts at unravelling the stress systems associated with the reactivation of faults in Scotland during the late Quaternary (Ringrose *et al.* 1991) seem overly complex in light of studies into fault scarp morphology on present day ground rupture movements in Australia (Gordon & Lewis 1980). These show that single fault displacement events do not create linear scarp profiles, but 'ragged' trajectories as ground rupture utilises pre-existing fracture orientations. This is also the case in rebound-induced fault movements in both Fennoscandia and Scotland (Lagerbäck 1990) [§ 3, p112]. Therefore care must be exercised when relating fault ground rupture orientation to the neotectonic stress field. Fortunately in Scotland most faults do not show the complexity of that exhibited in Glen Roy (Ringrose *et al.* 1991)

and therefore do not seem to offer any problems in interpretation of the co-existing stress field.

Most studies concerning the effects of ice loading consider the lithosphere as a whole and are primarily investigations of the physical properties of the mantle (e.g. Peltier & Andrews 1976), so therefore do not give much insight into the generation of stress in the upper brittle regime of the lithosphere. Despite inadequacies in this respect, such approaches do give a regional perspective of the behaviour of the crust in response to external loads. In such studies the lithosphere is modelled as a thin (visco) elastic sheet of infinite length subject to an external load. This results in flexure of the sheet giving rise to bending or "fiber stresses". This effect is greatest for loads of a width that is greater than the thickness of the lithosphere. Such "fiber stresses" reach a maximum for loads c. 4.4 times the flexural parameter of the lithosphere (commonly 55-100 km) i.e. load widths of c. 500 km. The maximum horizontal stresses created are c. 6 times the load pressure. Such bending stresses will become negligible compared to the load pressure when then the load width is >50 or <0.5 times the lithospheric parameter (Bott 1982).

On a regional scale ice-cap loading induces bending stresses of the order of 100 bar (10 MPa) (Quinlan 1984; Stein *et al.* 1989). Peltier & Andrews (1976) show that ice-cap melting involved the redistribution of mass in the planetary interior. This is accomplished partly elastically, i.e. there is an instantaneous response to changes in the ice load, and partly in an anelastic manner, occurring by mass transfer of sub-lithospheric plastic material. Such flow gradients acting on the base of the brittle part of the lithosphere will allow the transfer of stress into the upper brittle part of the lithosphere giving rise to longer lived glacially induced stresses than those associated with the elastic response of the crust.

Stein *et al.* (1989), in an attempt to resolve the cause of seismicity at 'passive margins', modelled the stresses due to glacial loading as flexure of an elastic plate. The stresses created are seen to be trivial in comparison to those created by sediment loading (Table 6.1). Evidence from earthquake source parameters does not point to the largest earthquakes being correlated with the areas of greatest sediment accumulation. However the limited data base on passive margin earthquakes does point to the largest earthquakes being in the areas that have been formerly glaciated. Thus glacial loading stresses, although seemingly small in comparison, must in some way control the locus of large passive margin seismic events. The work of Quinlan (1984) emphasises that glacially-induced stresses although being capable of triggering earthquake faulting, are

not of sufficient magnitude to dictate the mode of failure, and therefore need to be considered in conjunction with the (usually poorly understood) ambient stress field. The behaviour of the crust responds to the whole stress system that is active at any particular time, and is not controlled by any single mechanism, unless it can be shown that that particular mechanism dominates. The deglaciation model of Stein *et al.* (1989) predicts several hundred metres of rebound in response to the removal of 1 km thickness of ice. This agrees with the shoreline evidence from Fennoscandia (Mörner 1981). However the model fails to heed the advice of Quinlan (1984) in that it considers only the stresses due to the removal of the ice-load giving rise to a situation where the area of former ice cover is in extension while the area immediately outside this is in compression. From the styles of post-glacial faulting observed in Fennoscandia and Scotland this is clearly not the case. The model fails to account for the effects of the regional tectonic stress field. Adams (1989), describing the causes of post-glacial faulting in Canada, does consider both the regional stress field along with that created by glacial unloading and shows that the resultant stress field has the ability to trigger reverse faulting in the upper c. 500 m of the brittle crust. He states that the glacially-induced flexural stresses (of c. 20 MPa) may dominate the contemporary horizontal stress in the upper 300-1000 m of the brittle crust, and therefore may even dominate the regional stresses in this part of the crust. The brittle, fractured nature of the upper 500 m of the crust suggests that such stress is at least partly relieved and not stored elastically as would be the case at depth. Deeper, stored stress may be released suddenly, during or following deglaciation, by seismic activity. The small throw of the faults and parallelism of the fault orientations to the ice margins in eastern Canada point to fault movement being in response to transient stresses in the fractured upper 500 m. A much different response to deglaciation than that noted in Scotland and Fennoscandia where movement on individual faults is of the order of metres and even tens of metres. Bostrom (1984) considered the effects of crustal extension during the residence of an ice load. This was accomplished by the flow of asthenospheric material out of the centre of loading giving rise to tensional stresses. Deglaciation causes movement in the opposite direction and creates compressional stresses. Such asthenospheric flow is deemed responsible for the dissipation of isostatic stresses, prior to the yield strength of the quasi-plastic crust being reached, and as such may account for the lack of the expected spectacular post-glacial faulting in eastern Canada. However the recent report of a 15 m post-glacial throw on the Aspy Fault in Nova Scotia suggests that the lack of such faulting in eastern Canada may be due to the lack of an active search to find such features (Grant 1990; D.R. Grant pers. comm. 1991).

From this, and previous studies into glacial loading, it is clear that such work falls into two distinct groups. Either the work is concerned with 'whole lithosphere' studies and ignores, for the most part, the geological evidence for local perturbations in the proposed model, or the opposite where the investigation is of more localised scope attempting to explain a number of features in light of response of the crust to glacial loading/unloading. This paper has attempted to bring both approaches together in the study of one particular area (Scotland) where there is good geological evidence for the behaviour of the crust during the post-glacial period and to relate this to the known theory of crustal behaviour in the presence of external loads. A number of uncertainties still exist and a paper of this nature raises more questions than it answers. However it is hoped that this will stimulate further thought into the mechanisms of glacial tectonics and encourage subsequent work in this field.

6.15 Conclusions

Modelling the stresses required to cause reactivation of faults during the Holocene post-glacial period shows the importance of the creation of a regime of crustal fluid overpressuring to account for the observed fault movements. The modelled stresses are not absolute values, but give a relative, order of magnitude estimate of the tectonic regime pertaining to Scotland at that time. The model shows that in the immediate post-glacial period the sudden release of the vertical stress due to the ice load creates a situation of 'chaotic' fault activity, with the orientation of fault reactivation being only loosely controlled by the regional stress field. As the crustal stress levels are reduced by a combination of seismic stress drop and the decreasing influence of fluid overpressuring, a second phase of fault movement, utilising only the most favourably orientated faults, is initiated. With horizontal stress levels enhanced by stress transfer from the flow of sub-crustal material back into the former area of ice loading and localised preservation of high levels of vertical stress this period is characterised by strike-slip and reverse fault movement. From evidence of shoreline uplift the influence of the isostatic response of the crust to deglaciation decays by about 5 kyr BP and is replaced by a uniform tectonic stress field. Hence the present crustal movements and seismicity are thought to be the result of the North West European regional stress regime (Figure 6.8).

6.16 Acknowledgements

This work was carried out at the Department of Applied Geology, University of Strathclyde and the Department of Geology & Applied Geology, University of Glasgow while in receipt of NERC studentship GT4/87/GS/107. Many useful discussions were held with I. Allison, C.K. Ballantyne, D. Grant, R.S. Haszeldine, R. Muir Wood, P.S. Ringrose, M.D. Sullivan & C.J. Tate. The comments of I. Allison clarified an earlier draft of this paper.

6.17 References

- Adams, J. 1989.** Postglacial faulting in eastern Canada: nature, origin and seismic hazard implications. *Tectonophysics* 163, 323-331.
- Anderson, J.G. 1986.** Seismic strain rates in the central and eastern United States. *Bull. Seis. Soc. Am.* 76, 273-290.
- Andrews, J.T. 1970.** Present and postglacial rates of uplift for glaciated northern and eastern North America derived from postglacial uplift curves. *Can J. Earth Sci.* 7, 703-715.
- Atkinson, T.C., Lawson, T.J., Smart, P.L., Harman, R.S. & Hess, J.W. 1986.** New data on speleothem deposition and palaeoclimate in Britain over the last forty thousand years. *J. Quaternary Sci.* 1, 67-72.
- Ballantyne, C.K. 1984.** The late Devensian periglaciation of upland Scotland. *Quaternary Sci. Rev.* 3, 313-343.
- Ballantyne, C.K. & Sutherland, D.G. 1987.** *Wester Ross Field Guide.* Quaternary Research Association, Cambridge.
- Birks, H.J.B. 1977.** The Flandrian forest history of Scotland: a preliminary synthesis. *in* F.W. Shotton (ed.) *British Quaternary Studies: recent advances.* Clarendon Press, Oxford, 119-135.
- Black, J.H. 1987.** Flow and flow mechanisms in crystalline rock. *in* J.C. Goff & B.P.J. Williams (eds.) *Fluid flow in sedimentary basins and aquifers.* Geol. Soc. Special Publ. No. 34, 185-200.
- Blenkinsop, T.G. 1986.** *in* P.L. Hancock & G.D. Williams (eds.). *Neotectonics* (Conference report). *J. Geol. Soc. London* 143, 325-326.
- Bostrom, R.C. 1984.** Crustal extension under ice loads. *Modern Geology* 8, 249-259.
- Bott, M.H.P. 1982.** *The Interior of the Earth: its structure, constitution and evolution.* Edward Arnold Publishers, London, 403pp.

- Boulton, G.S., Smith, G.D., Jones, A.S. & Newsome, J. 1985.** Glacial geology and glaciology of the last mid-latitude ice sheets. *J. Geol. Soc. London* 142, 447-474.
- Carlsson, A. & Olsson, T. 1982.** High rock stresses as a consequence of glaciation. *Nature* 298, 739-342.
- Costain, J.K., Bollinger, G.A. & Speer, J.A. 1987.** Hydroseismicity - A hypothesis for the role of water in the generation of intraplate seismicity. *Geology* 15, 618-621.
- Davenport, C.A. & Ringrose, P.S. 1987.** Deformation of Scottish Quaternary sediment sequences by strong earthquake motions. *in* M.E. Jones & R.M.F. Peston, (eds.) *Deformation of Sediments and Sedimentary Rocks*, Geol. Soc. Special Publication No. 29, 299-314.
- Davenport, C.A., Ringrose, P.S., Becker, A., Hancock, P. & Fenton, C. 1989.** Geological investigation of late and post glacial earthquake activity in Scotland. *in* S. Gregerson & P.W. Basham (eds.) *Earthquakes at North Atlantic Passive Margins: Neotectonics and postglacial rebound*. 175-194. Kluwer Academic Publishers, Amsterdam.
- Fenton, C.H. 1991.** Neotectonics and palaeoseismicity in N.W. Scotland. Unpubl. Ph.D. Thesis, University of Glasgow.
- Firth, C.R. 1986.** Isostatic depression during the Loch Lomond Stadial: Preliminary evidence from the Great Glen, Northern Scotland. *Quaternary Newsletter* 48, 1-9.
- Gordon, F.R. & Lewis, J.D. 1980.** The Meckering and Calingiri earthquakes, October 1968 and March 1970. *Geol. Surv. W. Aust. Bull.* 126.
- Gordon, J.E. 1979.** Reconstructed Pleistocene ice-sheet temperatures and glacial erosion in Northern Scotland. *J. Glaciology* 22, 331-344.
- Grant, D.R. 1990.** Late Quaternary movement of Aspy Fault, Nova Scotia. *Can J. Earth Sci.* 27, 984-987.

Gray, J.M. 1974. The main rock platform of the Firth of Lorn, western Scotland. *Trans. Inst. British Geogr.* 61, 81-99.

Gray, J.M. 1985. Glacio-isostatic shoreline development in Scotland: an overview. Occasional Paper No. 24. Department of Geography & Earth Science, Queen Mary College, University of London. 61pp.

Haggart, B.A. 1989. Variations in the pattern and rate of isostatic uplift indicated by a comparison of Holocene sea-level curves from Scotland. *J. Quaternary Sci.* 4, 67-76.

Illies, J.H. & Greiner, G. 1978. Rheingraben and Alpine system. *Bull. Geol. Soc. Am.* 89, 770-782.

Illies, J.H., Baumann, H. & Hoeffers, B. 1981. Stress patterns and strain release in the Alpine foreland. *Tectonophysics* 71, 157-172.

Johnston, A.C. 1987. Suppression of earthquakes by large continental ice sheets. *Nature* 303, 467-469.

Johnston, A.C. 1989. The effects of large ice sheets on earthquake genesis. *in* S. Gregerson & P.W. Basham (eds.) *Earthquakes at North Atlantic Passive Margins: Neotectonics and postglacial rebound.* 581-599. Kluwer Academic Publishers, Amsterdam.

Kanamori, H. 1978. Quantification of earthquakes. *Nature* 271, 411-414.

Knill, J.L. 1972. The engineering geology of the Cruachan underground power station. *Engineering Geology* 6, 289-312.

Koteff, C. & Larsen, F.D. 1989. Postglacial uplift in Western New England: Geologic evidence for delayed rebound. *in* S. Gregerson & P.W. Basham (eds.) *Earthquakes at North Atlantic Passive Margins: Neotectonics and postglacial rebound.* 105-123. Kluwer Academic Publishers, Amsterdam.

Lagerbäck, R. 1990. Late Quaternary faulting and palaeoseismicity in northern Fennoscandia, with particular reference to the Lansjärv area, northern Sweden. *Geologiska Föreningens i Stockholm Förhandlingar* 112, 333-354.

Ling, C.B. 1947. On the stresses in a notched plate under tension. *J. Math. Physics*, 26, 284-289.

Marrow, P.C. & Walker, A.B. 1988. Lleyn earthquake of 1984 July 19: aftershock sequence and focal mechanism. *Geophysical J.* 92, 487-493.

Mörner, N-A. 1978. Faulting, fracturing and seismicity as functions of glacio-isostasy in Fennoscandia. *Geology* 6, 41-54.

Mörner, N-A. 1981. Crustal movements and geodynamics in Fennoscandia. *Tectonophysics* 71, 241-251.

Muir Wood, R. 1989a. Fifty million years of 'passive margin' deformation in North West Europe. *in* S. Gregerson & P.W. Basham (eds.) *Earthquakes at North Atlantic Passive Margins: Neotectonics and postglacial rebound*. 7-36. Kluwer Academic Publishers, Amsterdam.

Muir Wood, R. 1989b. Extraordinary deglaciation reverse faulting in Northern Fennoscandia. *in* S. Gregerson & P.W. Basham (eds.) *Earthquakes at North Atlantic Passive Margins: Neotectonics and postglacial rebound*. 141-173. Kluwer Academic Publishers, Amsterdam.

Muir Wood, R. 1990. The current tectonic regime in the United Kingdom and its NW European context (its bearing on the performance assessment of radioactive waste disposal sites). *in* Report of a meeting on "Fractures and fracture development". DOE Report No. DOE/RW/90.014. Dames & Moore International Technical Report TR-D&M-17.

Nichols, T.C. 1980. Rebound, its nature and effect on engineering works. *Q. J. eng. Geol.* 13, 133-152.

Peltier, W.R. & Andrews, J.T. 1976. Glacial-Isostatic adjustment - I. The forward problem. *Geophys. J. R. soc.* 46, 605-646.

Quinlan, G. 1984. Postglacial rebound and the focal mechanisms of eastern Canadian earthquakes. *Can. J. Earth Sci.* 21, 1018-1023.

- Ringrose, P.S. 1987.** Fault activity and palaeoseismicity during Quaternary time in Scotland. Unpubl. Ph.D. Thesis (2 Volumes), University of Strathclyde.
- Ringrose, P.S. 1989a.** Palaeoseismic (?) liquefaction event in late Quaternary lake sediment at Glen Roy, Scotland. *Terra Nova* 1, 57-62.
- Ringrose, P.S. 1989b.** Recent fault movement and palaeoseismicity in western Scotland. *Tectonophysics* 163, 305-314.
- Ringrose, P.S., Hancock, P.L., Fenton, C. & Davenport, C.A. 1991.** Quaternary tectonic activity in Scotland. *in* A. Forster, M.G. Culshaw, J.C. Cripps, J.A. Little & C.F. Moon (eds.) *Quaternary Engineering Geology*, Geol. Soc. Engineering Geol. Special Publ. No.7, 679-686.
- Robinson, M. & Ballantyne, C.K. 1979.** Evidence for a glacial readvance pre-dating the Loch Lomond Advance in Wester Ross. *Scott. J. Geol.* 15, 271-277.
- Roeloffs, E.A. 1988.** Fault stability changes induced beneath a reservoir with cyclic variations in water level. *J. Geophys. Res. B* 93, 2107-2124.
- Ruddiman, W.F., McIntyre, A., Niebler-Hunt, V. & Durazzi, J.T. 1980.** Oceanic evidence for the mechanism of rapid Northern Hemisphere glaciation. *Quaternary Res.* 13, 33-64.
- Shennan, I. 1989.** Holocene crustal movements and sea-level changes in Great Britain. *J. Quaternary Sci.* 4, 77-89.
- Sibson, R.H. 1985.** A note on fault reactivation. *J. Structural Geology* 7, 751-754.
- Sibson, R.H. 1990.** Conditions for fault-valve behaviour. *in* R.J. Knipe & E.H. Rutter (eds.) *Deformation Mechanisms, Rheology and Tectonics*, Geol. Soc. London Special Publ. No. 54, 15-28.
- Sissons, J.B. 1972.** Dislocation and non-uniform uplift of raised shorelines in the western part of the Forth Valley. *Trans. Inst. British Geogr.* 55, 145-159.

- Sissons, J.B. 1983.** Shorelines and isostasy in Scotland. *in* D.E. Smith & A.G. Dawson (eds.) *Shorelines and Isostasy*, Academic Press. 209-225.
- Sissons, J.B. & Cornish, R. 1982.** Rapid localized glacio-isostatic uplift at Glen Roy, Scotland. *Nature* 297, 213-214.
- Sissons, J.B. & Dawson, A.G. 1981.** Former sea-levels and ice limits in part of Wester Ross, northwest Scotland. *Proc. Geol. Assoc.* 92, 115-124.
- Segall, P. 1989.** Earthquakes triggered by fluid extraction. *Geology* 17, 942-946.
- Strehlau, J. 1990.** Seismicity and deformation on continental shear zones. *Terra Abstracts* 2, 22.
- Stein, S., Cloetingh, S., Sleep, N.H. & Wortel, R. 1989.** Passive margin earthquakes, stresses and rheology. *in* S. Gregerson & P.W. Basham (eds.) *Earthquakes at North Atlantic Passive Margins: Neotectonics and postglacial rebound*. 231-259. Kluwer Academic Publishers, Amsterdam.
- Stephansson, O., Ljunngren, C. & Jing, L. 1991.** Stress measurements and tectonic implications for Fennoscandia. *Tectonophysics* 189, 317-322.
- Sutherland, D.G. 1984.** The Quaternary deposits and landforms of Scotland and neighbouring shelves: a review. *Quaternary Sci. Rev.* 3, 157-254.
- Talbot, C. 1986.** A preliminary structural analysis of the pattern of postglacial faults in Northern Sweden. SKB Technical Report 86-20.
- Talbot, C.J. 1990.** Problems posed to a bedrock radwaste repository by gently dipping fracture zones. *Geologiska Föreningens i Stockholm Förhandlingar* 112, 355-359.
- Tate, C.J. 1989.** Department of Geography & Geology, The University, St. Andrews, Fife KY16 9AL.
- Walcott, R.I. 1980.** Rheological models and observational data of glacio-isostatic rebound. *in* N-A. Mörner (ed.) *Earth Rheology, Isostasy and Eustasy.*, 3-10. John Wiley & Sons, New York.

Whittaker, A., Brereton, N.R., Evans, C.J. & Long, R.E. 1989. Seismotectonics and crustal stress in Great Britain. *in* S. Gregerson & P.W. Basham (eds.) Earthquakes at North Atlantic Passive Margins: Neotectonics and postglacial rebound. 393-411. Kluwer Academic Publishers, Amsterdam.

Yerkes, R.F., Ellsworth, W.L. & Tinsley, J.C. 1983. Triggered reverse fault and earthquake due to crustal loading, northwest Transverse Ranges, California. *Geology* 11, 287-291.

Zoback, M.L., Zoback, M.D., Adams, J., Assumpcao, M., Bell, S., Bergman, E.A., Blumling, P., Brereton, N.R., Denham, D., Ding, J., Fuchs, K., Gay, N., Gregerson, S., Gupta, H.K., Gvishiani, A., Jacob, K., Klein, R., Knoll, P., Magee, M., Mercier, J.L., Muller, B.C., Paquin, C., Rajendran, K., Stephansson, O., Suarez, G., Suter, M., Udias, A., Xu, Z.H. & Zhizhin, M. 1989. Global patterns of tectonic stress. *Nature* 341, 291-298.

Zotikov, I.A., 1986. The thermophysics of glaciers. D. Riedel Publishing Co., Dordrecht.

6.18 Figure Captions

- Figure 6.1** Faults in Scotland showing Quaternary reactivation. Sense of displacement indicated. Regional stress field for NW Europe (direction of S_H) shown by the black arrows. NB. S_H in Scotland orientated more WNW shown by the white arrows. Inset: rose diagram of fault orientations.
- Figure 6.2 (Key)** Key to symbols used in Figures 6.2 and 6.9
- Figure 6.2** "Sub-plate boundary" zones of deformation in N.W. Europe during the Tertiary. After Muir Wood (1989a). Dashed line represents the margin of the continental shelf.
- (a) Mid-Late Eocene (c. 45-40 Ma).
 - (b) Early Oligocene (35 Ma).
 - (c) Late Oligocene (30-25 Ma).
 - (d) Late Miocene (6 Ma).
- Figure 6.3** Schematic representation of the stresses acting on a fault plane where σ_2 parallel to the fault plane.
- Figure 6.4** Diagrammatic comparison of the effects of ice loading on faults in compressive and tensional stress regimes.
- Figure 6.5a** The effects of ice cap loading on brittle crust under compression.
- Figure 6.5b** The effects of rebound following deglaciation on brittle crust in a compressive stress regime.
- Figure 6.6** Distribution of ice in N.W. Scotland during the Main Late Devensian and Loch Lomond Readvance glaciations. Compiled from various sources of field data. Modelled cross sections of ice thickness from Gordon (1979).

Figure 6.7 Diagrammatic representation of stress build-up and subsequent release during late Quaternary glacial and interglacial periods.

- a. Start of Main Late Devensian Glaciation at c. 26 kyr BP.
- b. Ice load maximum in the absence of equilibrated fluid pressure.
- c. Main Late Devensian Glacial Maximum c. 18 kyr BP.
- d. Start of ice decay c. 14 kyr BP.
- e. Disappearance of Devensian ice c. 13 kyr BP.
- f. Start of Loch Lomond Readvance c. 11 kyr BP.
- g. Decay of Loch Lomond Readvance ice c. 10.3 kyr BP.

Dotted line denotes the uncertainty in stress decay during the Windermere Interstadial period.

Figure 6.8 Holocene deformation zones in North Western Europe. Key as for Figure 6.2.

Table 6.1 Sources of stresses acting at 'passive' continental margins [after Stein *et al.* (1989)].

6.19 Figures

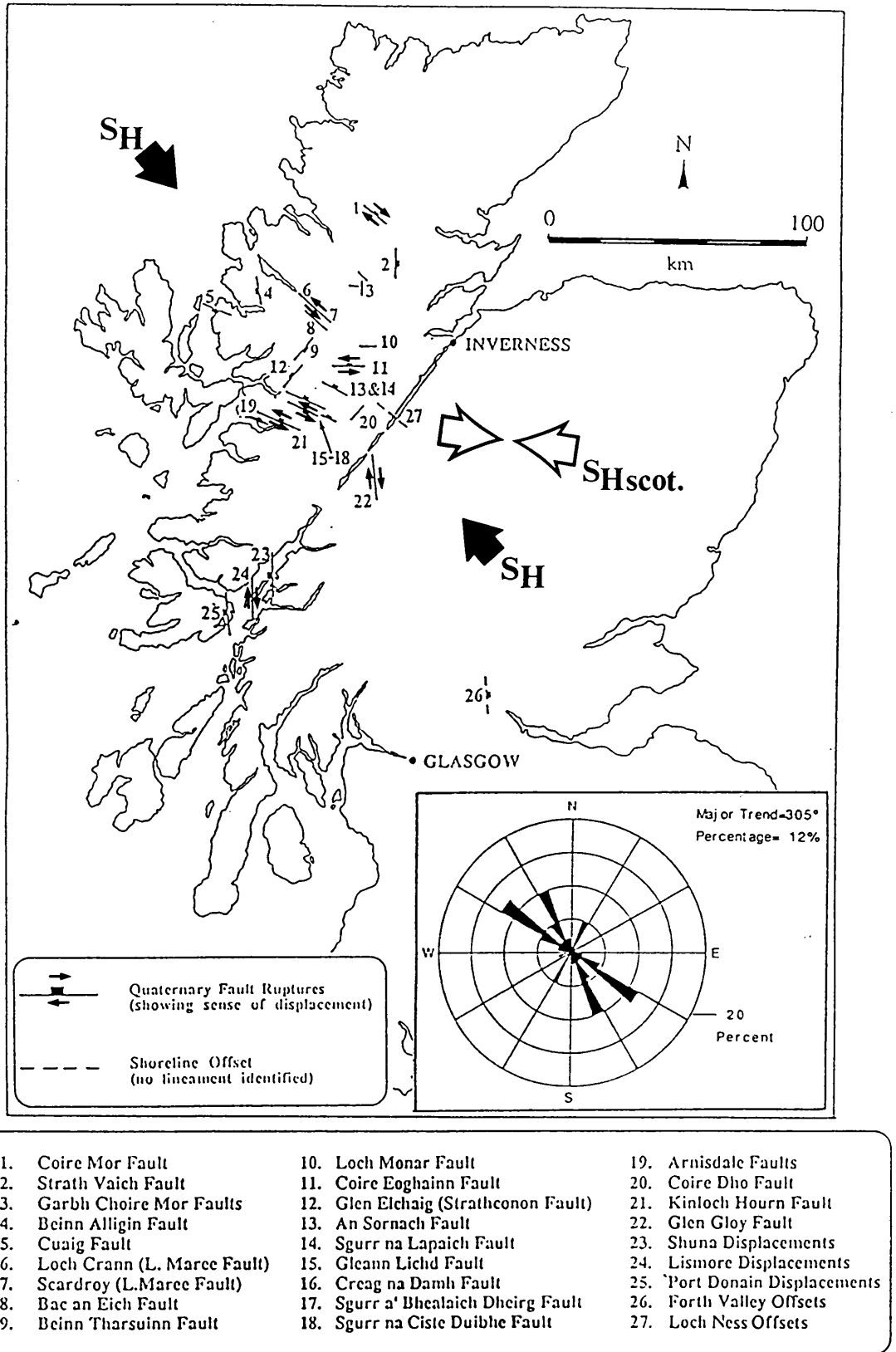


Figure 6.1

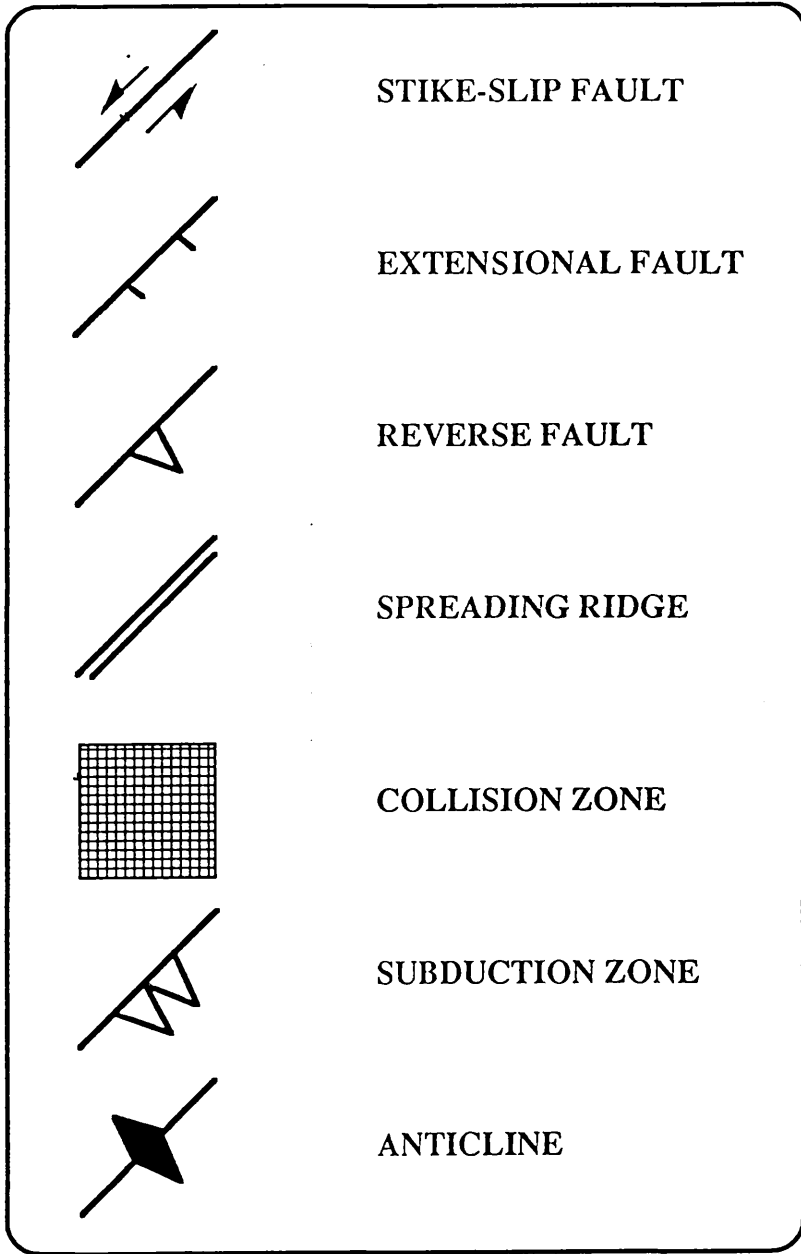


Figure 6.2 (Key)

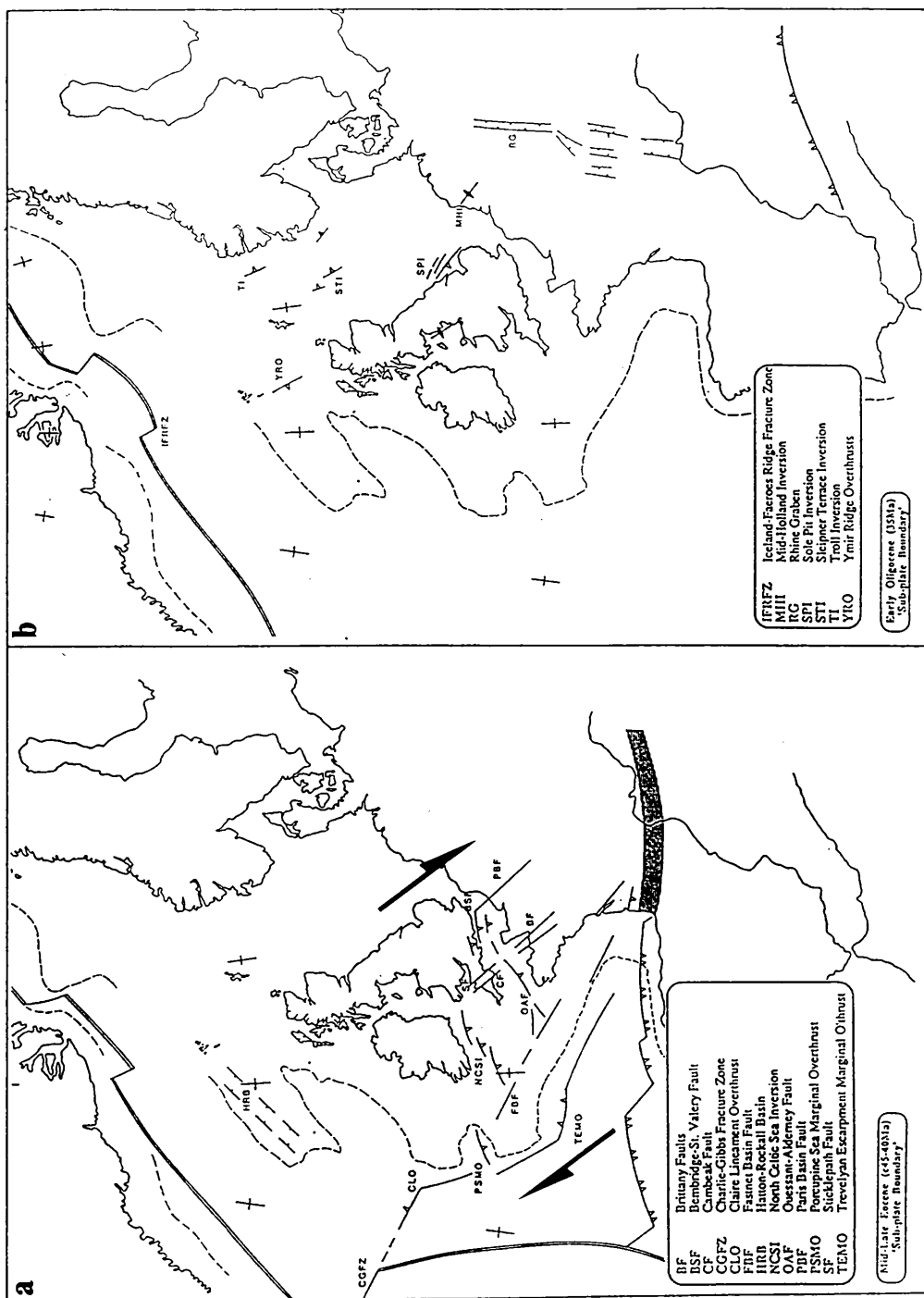


Figure 6.2

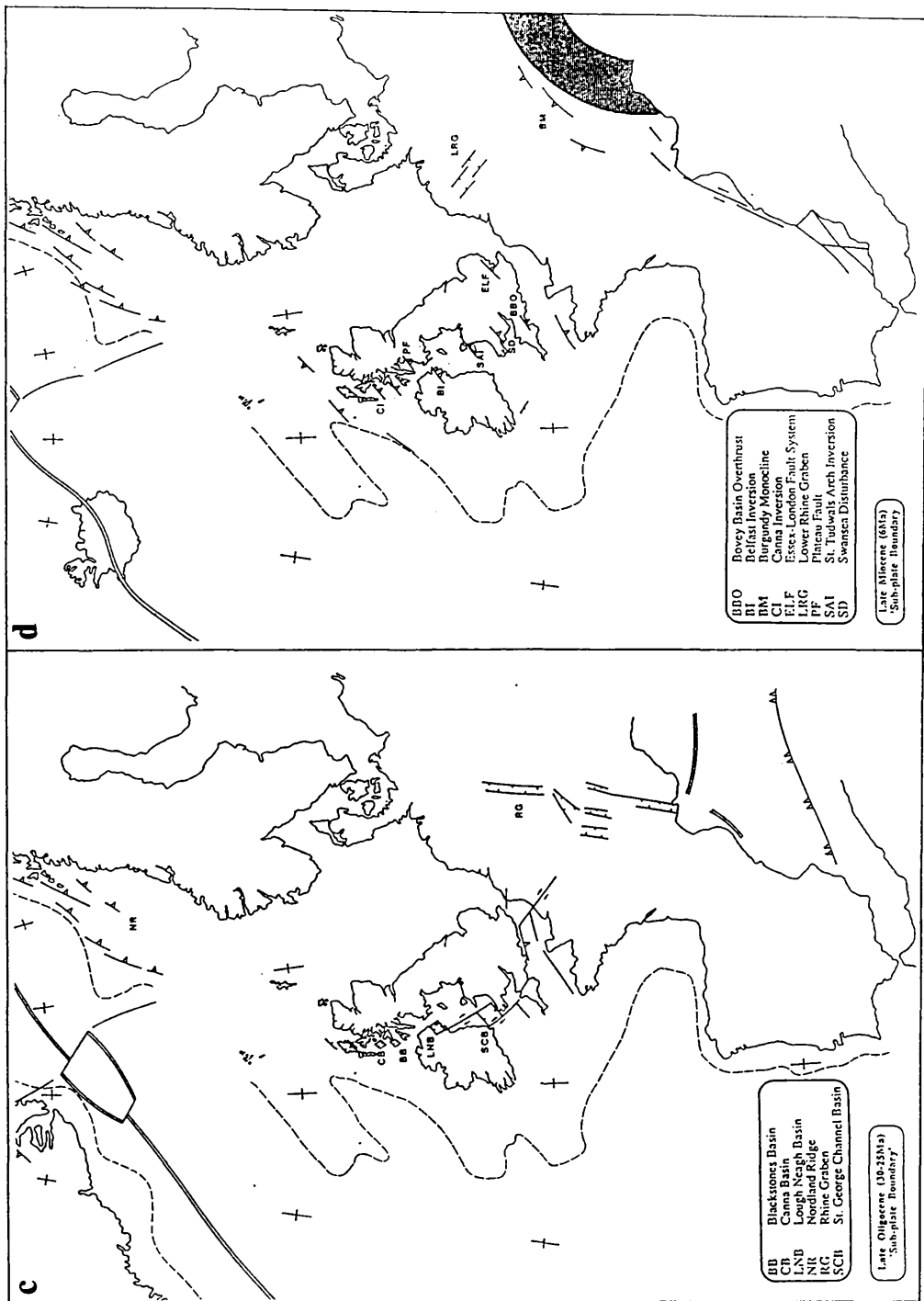


Figure 6.2

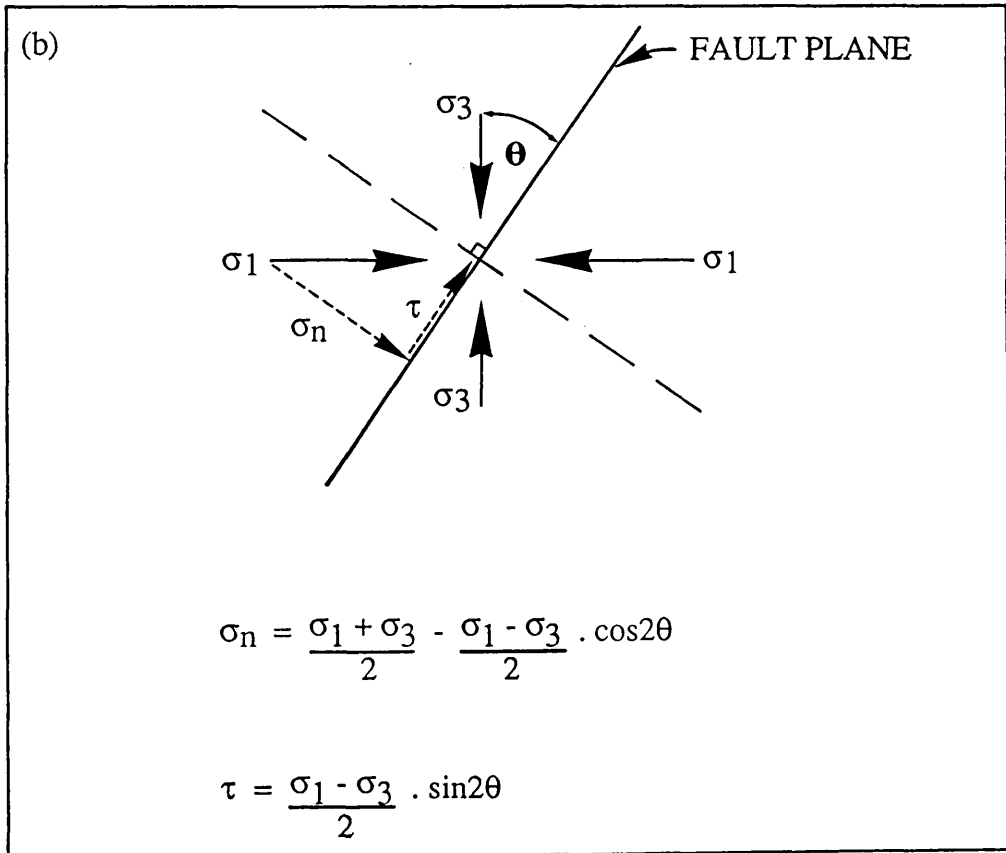
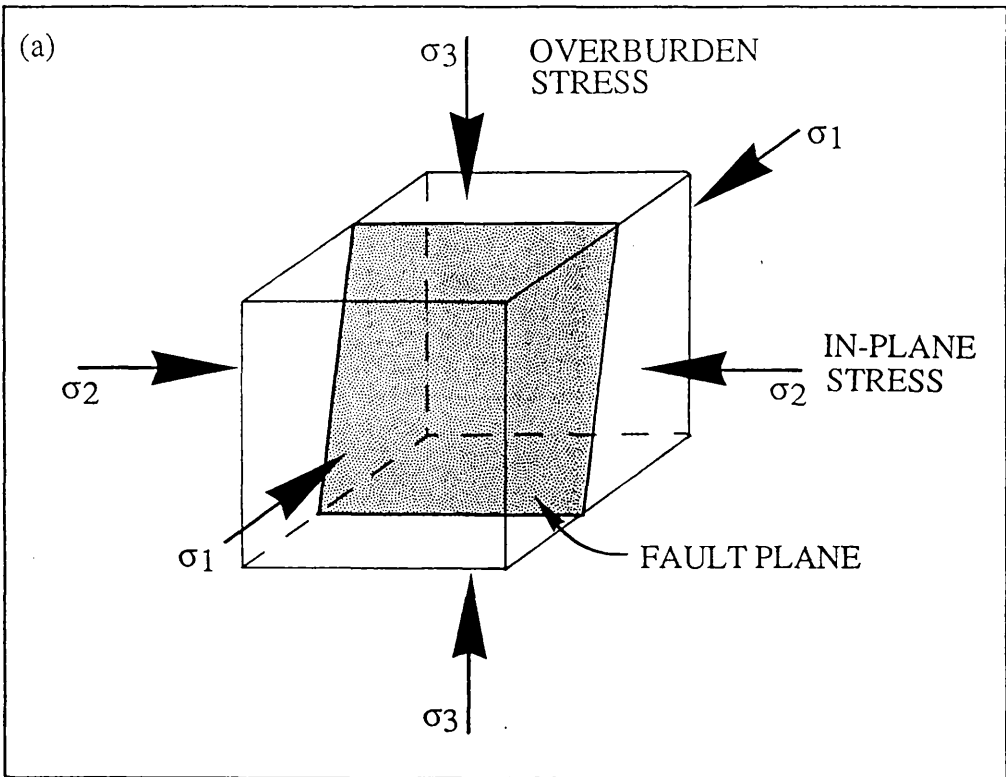


Figure 6.3

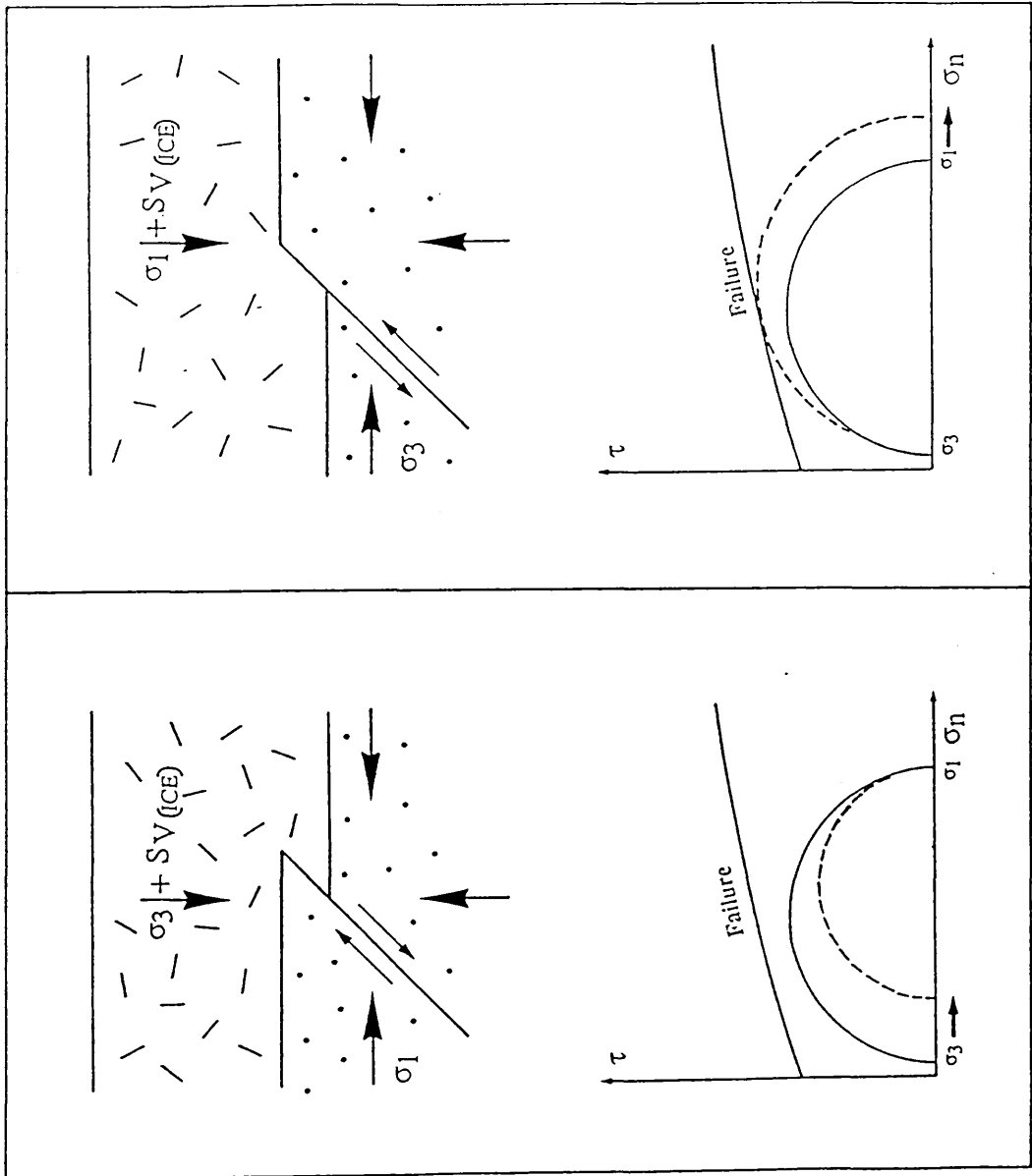


Figure 6.4

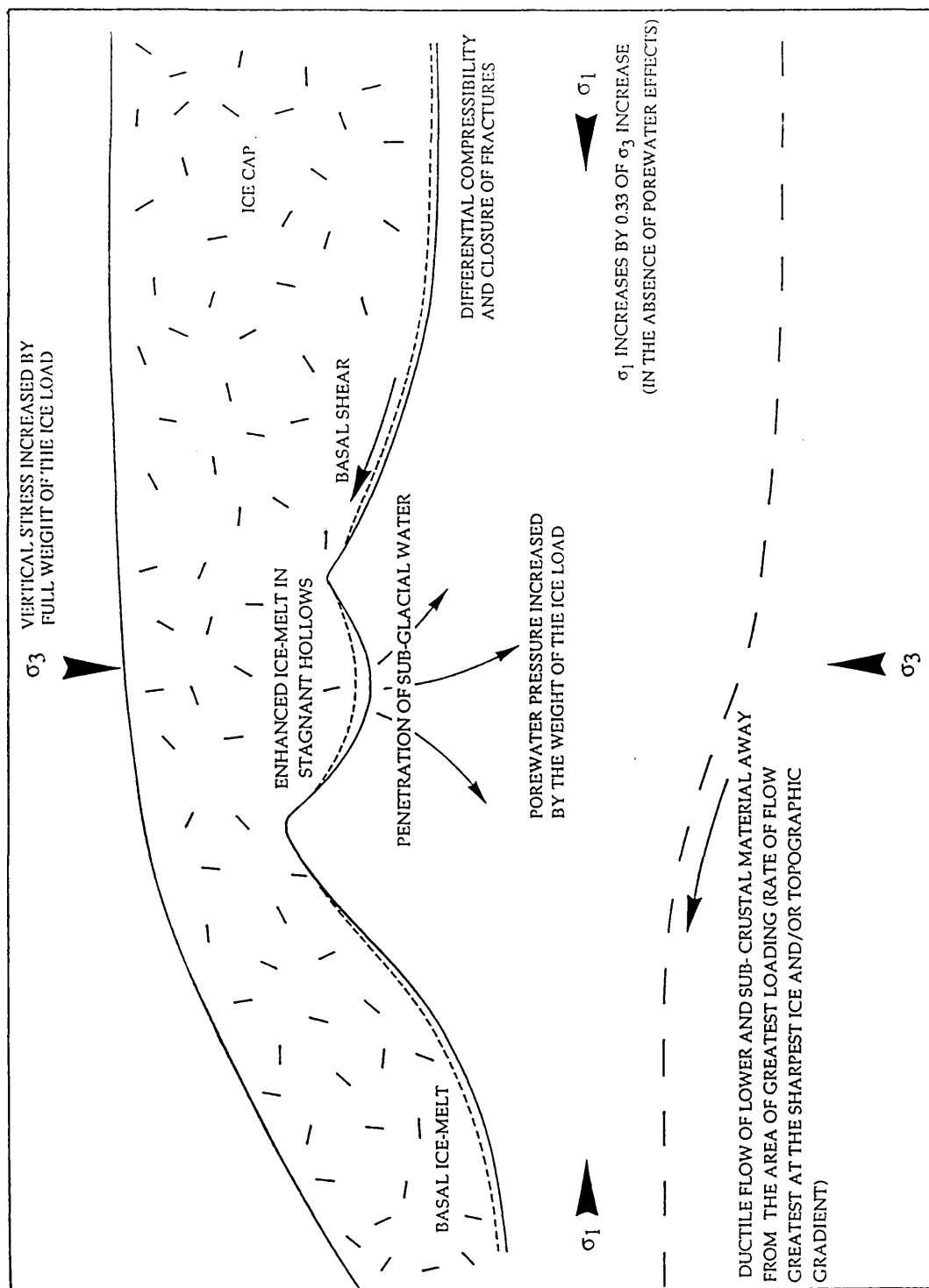


Figure 6.5a

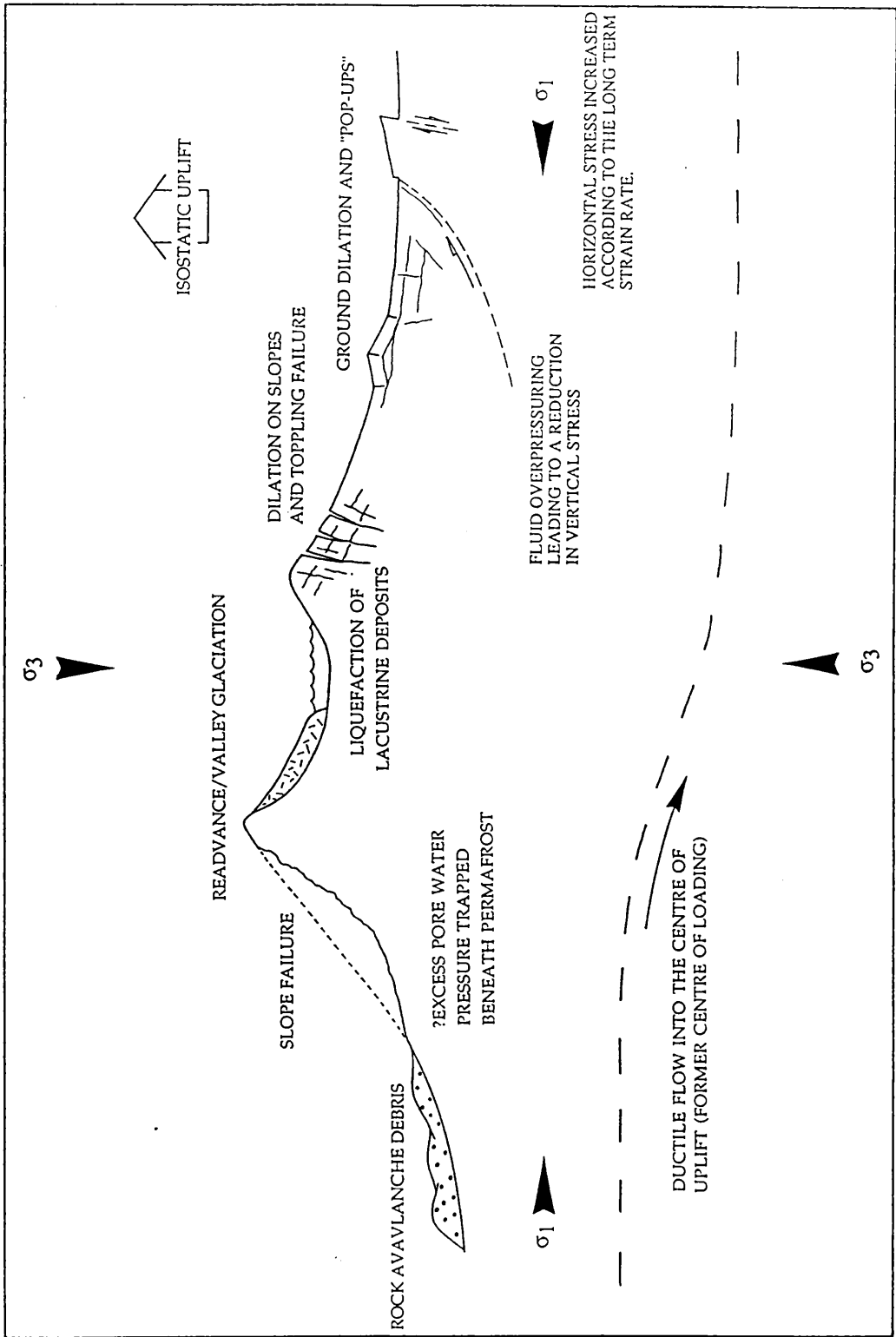


Figure 6.5b

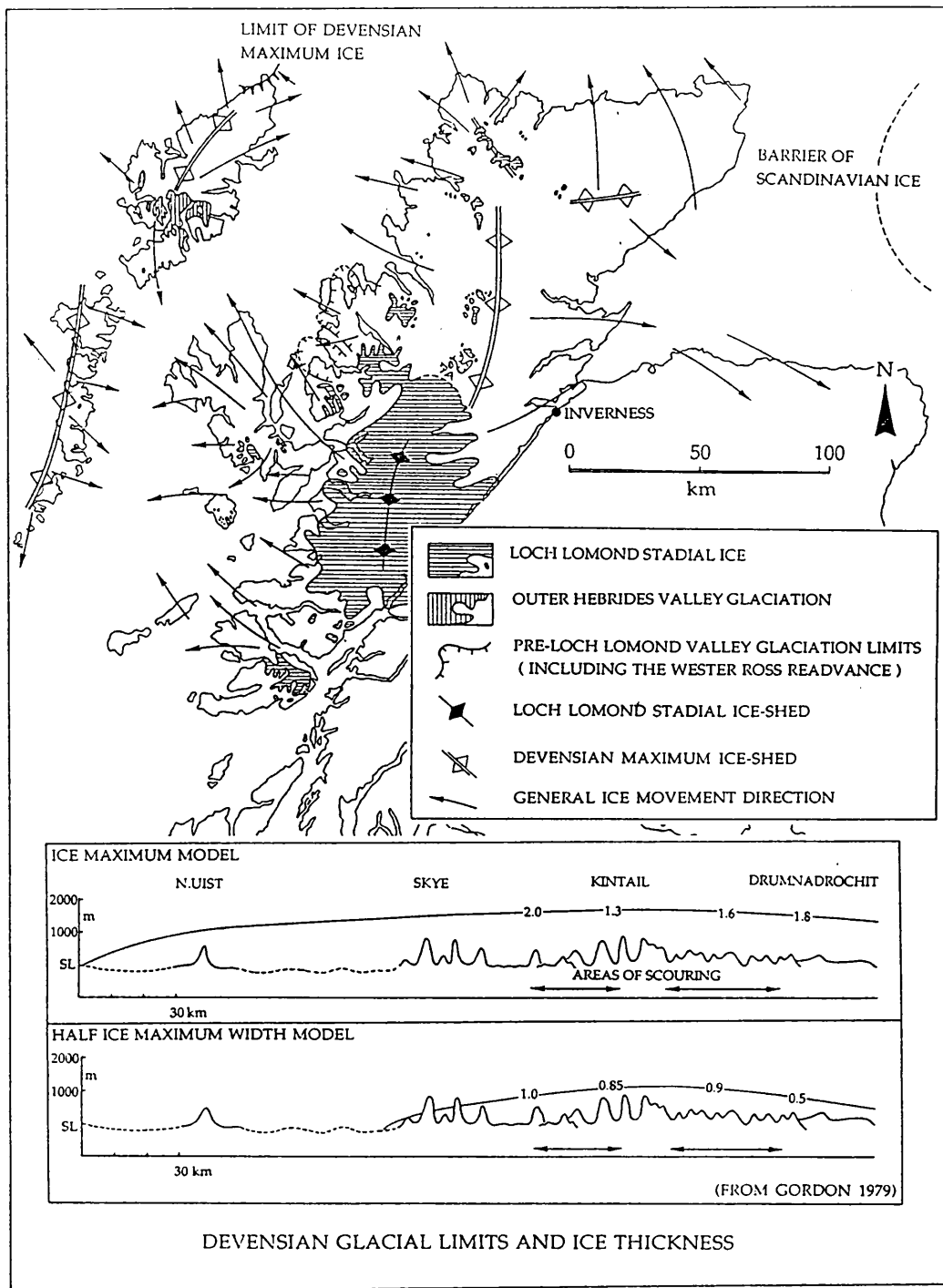


Figure 6.6

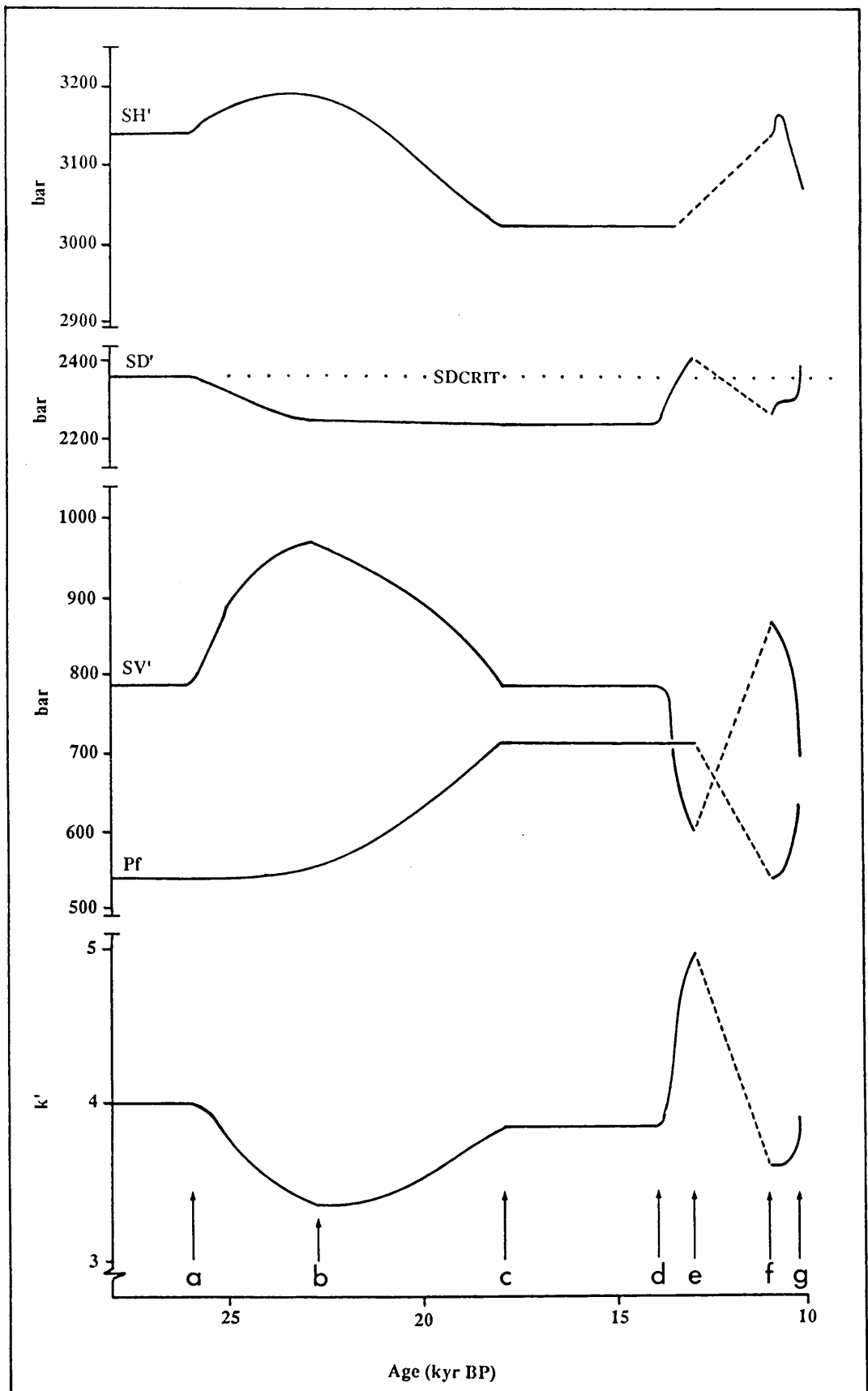


Figure 6.7

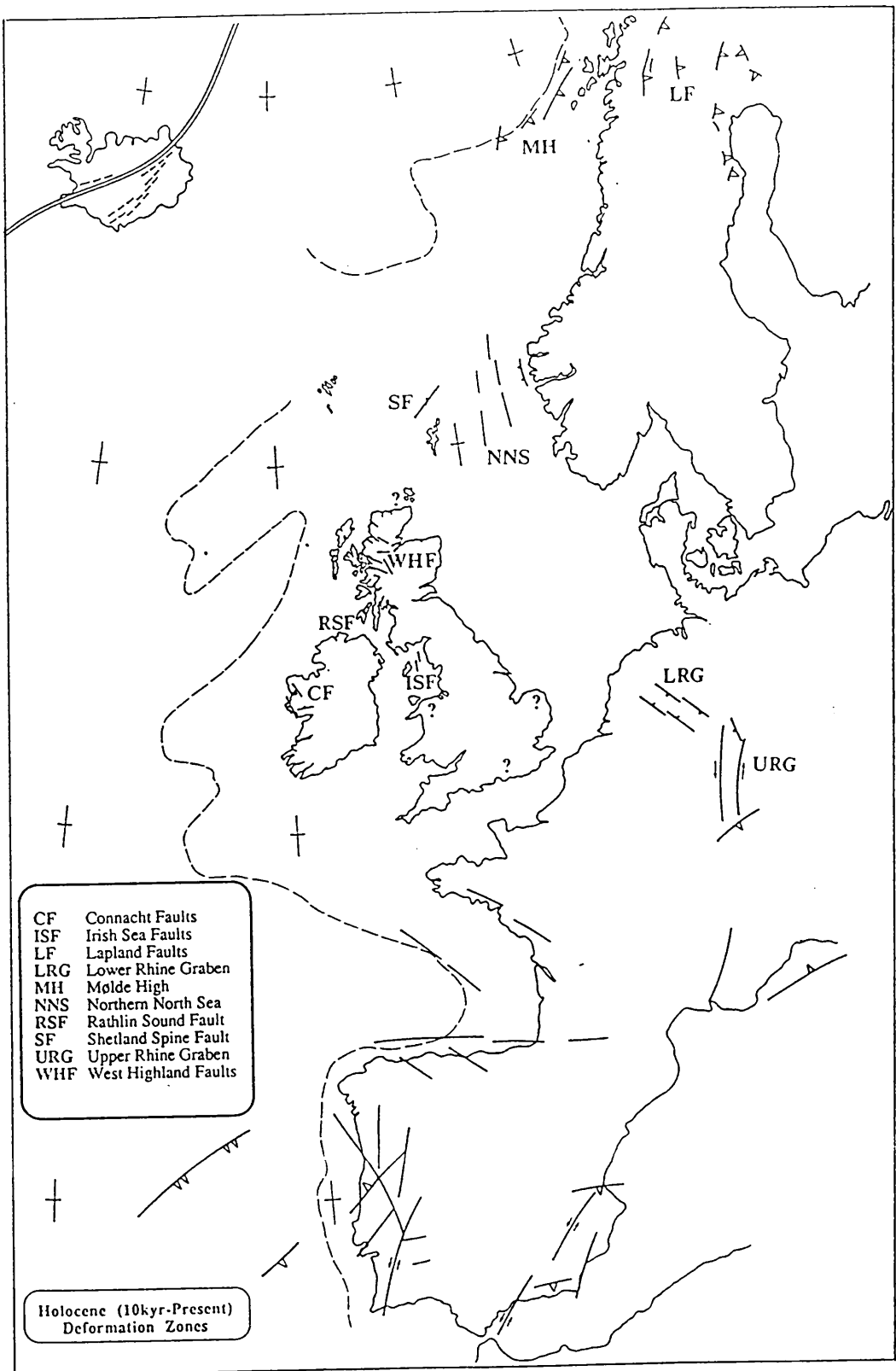


Figure 6.8

6.20 Table 6.1

POSSIBLE STRESS SOURCES AT PASSIVE MARGINS						
Type	Magnitude	Direction	Spatial Variation	Depth Variation	Location	
Deglaciation flexure.	10MPa.	Essentially margin normal.	Continent - extension. Ocean - compression.	Reverses.	Deglaciated Margins.	
Continental margin spreading.	10MPa.	Essentially margin normal.	Continent - extension. Oceanic - compression.	Monotonic.	All margins.	
Ridge push/ basal drag.	10MPa.	Variable, but often essentially margin normal.	Compression.	Monotonic.	All margins.	
Sediment flexure.	100MPa.	Essentially margin normal.	Continental - extension. Ocean - compression.	Reverses.	All margins.	

Chapter 7

A Large Rock Avalanche Triggered by Late Quaternary Seismic Activity in North West Scotland

Clark Fenton

*Department of Geology and Applied Geology,
University of Glasgow, Lillybank Gardens, Glasgow G12 8QQ*

7.1 Abstract

A large-volume debris lobe beneath Sgurr Mhor, Beinn Alligin, in Wester Ross has previously been described as resulting from a landslide falling onto decaying glacier ice and being further transported downslope in the form of a rock glacier. During the course of investigation into post-glacial fault movement and seismic activity in NW Scotland the landslide was subject to reappraisal. Detailed examination of the debris lobe geometry and morphology, the geometry of the failure scar and the NNW-trending fault that defines the eastern margin of the scar show features that are consistent with the debris lobe being the result of a rock avalanche, thus removing the need to invoke corrie glacier ice to provide 'excess' downslope travel distance. The proximity of a late Quaternary active fault suggests that the trigger for slope failure was seismic activity due to the release of stored stresses built up during the last glacial period.

7.2 Introduction

The mountain massif of Beinn Alligin stands on the north side of Upper Loch Torridon in Wester Ross (Figure 7.1). This is one of the many Torridonian sandstone peaks that stand proud of the Lewisian gneiss basement in the N.W. Highlands. At the foot of the highest peak, Sgurr Mhor (985 m), in the south-facing corrie of Toll a' Mhadaidh Mor, is a 1.2 km long debris lobe composed of sandstone blocks ranging from sub-metric to tens of metres in diameter (Figure 7.2). This is the result of a huge slope failure from the 500 m high corrie backwall immediately below the summit of Sgurr Mhor, leaving a large, roughly triangular-shaped scar appropriately called Eag Dhuibh na h-Eigheachd (The Black Cleft of the Shouting) (Figure 7.3).

Beinn Alligin is composed entirely of sandstones, siltstones and pebble conglomerates of the Applecross Formation, part of the Torridonian Supergroup. The strata are essentially flat lying, dipping gently, 10-15°, to the west and south-west. The individual beds weather out to form the characteristic stepped profile of the Torridonian hills. West of the summit of Sgurr Mhor basic dykes of undetermined (?Tertiary) age trend NW and NNW. Two major faults following a similar trend to the dykes cut across the ridge of Beinn Alligin. One fault runs approximately NW-SE just to the SW of the summit of Tom na Gruagaich (922 m) and defines the crags in the north-facing corrie that lies to the west of the main ridge. The other fault follows a slightly sinuous course with a general NW-SE trend and passes just to the west of the summit cairn of Sgurr Mhor and defines the prominent eastern wall of the failure scar (Figure 7.3). This has been shown to have been active during the late Quaternary [§ 2.6.4, p28].

Sissons (1975) describes the debris lobe as being the result of a large landslide but states that the morphology and 'excess' travel distance of the debris was the result of further transport of the debris in the form of a rock glacier. Whalley (1976) in discussion of Sissons (1975) agrees that the source of the debris was the result of a rockslide which was "probably a 'one-shot' event". While not totally dismissing the rock glacier hypothesis he proposes an alternative view that the debris lobe was the result of a landslide that had attained an excess travel distance by riding on a cushion of trapped compressed air (Shreve 1968) or by a mechanical flowing mechanism (Hsü 1975). In response Sissons (1976) argues strongly against the air-launch mechanism necessary for the air layer lubrication hypothesis but put forward no evidence to counter the mechanical flow theory. Ballantyne (in Ballantyne & Sutherland 1987) proposes a rock fall/avalanche origin for the debris but states that the excess travel

distance of the debris was due to transport by glacial ice, not a rock glacier. However there are a number of inconsistencies in the glacial transport theories for the Beinn Alligin debris lobe, not least being that the debris runs uphill against the lower slopes of Tom na Gruagaich (Figures 7.1 & 7.9) on the opposite side of the corrie from the source slope. In this paper a seismically-triggered rock avalanche origin is proposed to explain the 'excess' travel distance of the Beinn Alligin debris lobe. Although seismicity has previously been attributed to triggering a number of slope failures in the Highlands of Scotland (Ballantyne & Eckford 1984; Ringrose 1989) this is the first description of an earthquake-triggered rock avalanche in this region.

7.3 Rock Avalanches

Rock avalanches or *sturtzstroms* (Hsü 1975) are large volume slope failures that exhibit high degrees of mobility resulting in 'anomalously' large travel distances. They are up to $2 \times 10^{10} \text{ m}^3$ of essentially dry material that can reach speeds of 100 ms^{-1} and travel up to 15 km from source. Rock avalanche deposits are sheet-like, tongue or fan shaped lobes up to 15 km long, hundreds of metres to 16 km across and tens of metres deep. The surface of the deposits have hummocky relief with lateral and longitudinal ridges. The debris itself is clast supported and displays imbrication, brittle folding and basal scouring and inverse grading. Relict stratigraphy can be preserved. Individual blocks are up to tens of metres across and are usually randomly orientated.

Rock avalanches result from the catastrophic disintegration of large volume source blocks, possibly involving some form of power law flow, i.e. upward decreasing shear stress causing intense shearing at the base of the failed mass (Yarnold & Lombard 1989). From a study of worldwide occurrences Keefer (1984b) placed arbitrary conditions of a minimum source slope of 25° and slope height of 150 m for the generation of rock avalanches (Figure 7.4). Whitehouse (1983) states that a massive elastic source rock that failed along discontinuities as well as bedding planes is needed as a rock avalanche source.

The phenomenon of rock avalanches has been well documented from many localities worldwide (Heim 1932; Bock 1977; Coates 1977; Voight & Pariseau 1978; Eisbacher 1979; Whitehouse 1981, 1983; Whitehouse & Griffith 1983; Dawson *et al.* 1986; Hewitt 1988). Many rock avalanches are the result of seismic slope shaking by high magnitude events (Hadley 1978; Keefer 1984a,b; Kobayashi 1985; Evans *et al.* 1987; Jibson 1987) while others are the result of other means of slope weakening such as high rainfall, undercutting and even nuclear explosions (Melosh 1990).

Despite the wealth of descriptive evidence, including eye-witness accounts, the mechanisms of transport of large volume, long run-out landslides are poorly understood.

The transport mechanisms of large, dry rock avalanches have been the subject of considerable controversy. The observed long run-out distances (L) relative to the fall height (H) are much greater than can be explained by conventional sliding or grain flow mechanisms. As the majority of rock types have coefficients of friction ≥ 0.6 (Jaeger & Cook 1979), this predicts sliding movement on slopes of $\geq 30^\circ$ ($H/L \geq 0.58$). This behaviour is confined to low volume rockfalls. As the volume of the failure mass increases in rock avalanches the coefficient of friction can become as low as 0.1. It is seen that there is a linear correlation between H/L and volume (Scheidegger 1973; Hsü 1975; Ashida & Egashira 1986) (Figure 7.5). There have been numerous hypotheses put forward to explain the mobility of these deposits. These include air fluidization (Kent 1966), air layer lubrication (Shreve 1968), movement over a molten basal layer (Erismann 1979), grain flow with dust reduced friction (Hsü 1975), mechanical fluidization (Davies 1982), movement on a low density layer of active particles (Campbell 1989), shear-generated particle turbulence (Ashida & Egashira 1986) and acoustic fluidization (Melosh 1979; 1990). Other proposed mechanisms include the presence of varying amounts of water in an undersaturated rock mass (Habib 1975; Goguel 1978; Johnston 1978; Voight & Faust 1982). However the presence of long run-out rock avalanches on the Moon (Howard 1973) and on Mars (Lucchitta 1978; McEwen 1989) precluded the universal adoption of a fluid-based or gravity-driven mechanism for the exceptional travel distance of these slope failures. As these spectacular slope failures are found in such diverse environments it is more probable that there are a number of mechanisms that act either together or in isolation to give rise to the excess travel distances exhibited by these deposits. Part of the problem is the apparently contradictory behaviour of various failures. For example the Little Tahoma 'slide' on Mount Rainier, Washington State, passed over a 1.5 m thermograph station leaving it intact (Crandall & Fahnestock 1965) while the Elm sturzstrom gouged out a water pipe buried to a depth of 1 m (Hsü 1978).

One of the most notable features of rock avalanches is their ability to run uphill for considerable distances. Evans (1989) showed that the height of run-up can be as great as one third of the fall height (The Avalanche Lake failure in the MacKenzie Mountains of Canada fell from a 1220 m high, 31° slope and ran up 640 m on a 44° slope on the opposite side of the valley; a horizontal distance of 3.5 km). In addition many rock avalanches show marked changes in trajectory downslope as they are

affected by topographic obstacles. This results in the majority of the rockfall debris coming to rest close to the source slope while a thinner, more mobile sheet may continue further downslope by virtue of momentum transfer (Eisbacher 1979). This behaviour in rock avalanches is almost universal with the debris lobes showing a marked downslope decrease in thickness. McEwen (1989) explained this behaviour by treating 'dry' rock avalanches as having Bingham rheology and assuming uniform steady flow conditions such that the yield strength, K , of the material is given by the expression

$$K = \rho g D \sin \beta \quad (1)$$

where ρ is the density of the flow, g is the acceleration due to gravity (9.81 ms^{-2}), D is the deposit thickness and β is the angle of the slope. As uniform flow is never achieved in nature, this expression gives an underestimation of K . The yield strength for dry rock avalanches is 10^4 Pa while it is 10^3 - 10^2 Pa for water saturated debris flows. This is manifested in the thinner nature of wet debris flows as opposed to dry flows. Two possible mechanisms that would explain the thinning of rock avalanche debris away from the source slope are (1) that K decreases with distance, possibly due to the continued break-up of the debris during movement and (2) that the main body of the flow does not thin to the critical thickness maintaining a high value of K that acts to resist movement.

7.4 Beinn Alligin Slope Failure

7.4.1 Source Slope Failure Scar

The failure source is a 500 m high area roughly triangular in shape (Figure 7.3), bounded on its eastern side by a 151° to 163° trending fault showing evidence for late Quaternary reactivation [§ 2.6.4, p28]. The area of failure lacks the stepped topography that is characteristic of weathered Torridonian sandstone. This has been replaced by a basal failure plane, dipping 30 - $60^\circ/070$ - 110° , that daylight to the west and bounds the other lateral margin of the failure area. The basal failure plane also daylights at the base of the slope, but is intercepted by a vertical backing failure scarp at the head of the failure area (Figure 7.6). The basal failure plane shows large wavelength corrugations running parallel to the slope fall-line, hence the variation in the orientation of the plane (Figure 7.7). The vertical headscarp area is seen to be composed from a number of fracture orientations, with a fracture spacing of c. 10 m, forming a vertical cliff up to 150 m high. Lichen growth on the scarp face, and the

lack of fresh debris at the base of the scarp face shows that this is essentially a relict feature. The basal failure area is cut by a number of fractures that are sub-parallel to the fault bounding the eastern margin of the area of failure. Fracture density decreases markedly away from the fault. In addition there is a steep fracture set perpendicular to the fault orientation. All these fractures, in addition to the near-horizontal bedding planes, act to break the rock mass into blocks of c. 10 m across. The volume of the rock removed from the failure scar is c. $4.5 \times 10^6 \text{ m}^3$. The lichen cover on the scarp faces and the partial vegetation cover (in a peat soil) shows that this is a relict feature and not subject to episodic rockfall.

7.4.2 Slope Failure Debris

The slope failure debris forms a well defined tongue-shaped lobe (Figure 7.2) that reaches a maximum length of 1200 m, with the distal margin of the failure debris being 1300 m away from the base of the source slope (mid-point to mid-point distance is c. 920 m). It now rests on a 6° slope. The debris is composed dominantly of angular to sub-angular boulders of Torridonian Sandstone up to 7 m across with the average clast size being c. 3 m (Figure 7.8). The debris displays a crude coarsening upwards 'stratigraphy' with large angular blocks resting on smaller more rounded blocks that may only reach about 1-2 m across. This is similar to the "roller-bearing" morphology described from sturzstroms in the Canadian Cordillera (Eisbacher 1979). Many of the surface blocks have 'jig-saw fit' morphologies, i.e. they have been shattered but remain as intact units, whilst others show evidence of brittle folding and thrusting, especially in the region of the ridge fronts. Much of the volume of the deposit, possibly 35-40% in places, is void space. Volume of the debris is estimated as $4.1 \times 10^6 \text{ m}^3$. This compares with volume calculated from the dimensions of the source slope area. Both estimates are considerably greater than those of Whalley (1976). There are little or no fine materials present. The debris lobe is divided into two distinct sections (separated by a marked transverse hollow at a change in the thickness of the deposit): an upper section that reaches 430 m in width and in many places exceeds 20 m in thickness and a lower section that only attains 250 m in width and is seldom thicker than c. 5 m. The upper section is characterised by smaller clast sizes, with the largest blocks being 2 x 2 x 1 m. Clast size is seen to increase downslope to reach a maximum at the hollow separating the upper and lower sections. The lower section is composed of small blocks, up to 3 m across, that show slightly more abrasion than the remainder of the debris that is present on the surface of the debris lobe. The margins of the lobe are generally well defined (Figure 7.2), with the large blocky nature of the rockfall debris making it conspicuous against the sandy till

material upon which it rests. In plan (Figure 7.1) the debris lobe is seen to have an almost straight western margin where the deposit thickness reaches 10 m, while the eastern margin and the snout of the deposit are much thinner and less well defined being composed of a number of coalescing lobes usually no greater than one boulder thick. The western margin is topographically controlled by the lower slopes of Tom na Gruagaich, and for a distance of c. 600 m the debris is noted to have run uphill by at least 25 m (Figure 7.9).

The surface of the debris is marked by a number of ridges and hollows, the majority of which are transverse and concave up slope (Figure 7.10). These features are best developed in the upper section of the debris lobe. The ridges are up to 7 m high and are steeper on their downslope faces where they are fronted by hollows up to 4 m wide. Over much of the surface of the debris lobe the larger blocks that seem to ride on a cushion of smaller more abraded boulders are seen to be horizontal. However on the ridge fronts they dip steeply forwards, and in some cases are even vertical or overturned. This is particularly so at the large ridge that fronts the upper section of the debris lobe (Figure 7.8). This particular ridge is fronted by a 20 m wide hollow. In the upper section of the debris are a number of poorly defined longitudinal ridges parallel to the assumed direction of transport of the debris lobe. The western margin of the uppermost section of the debris is defined by an arcuate ridge of debris up to 10 m in height (Figure 7.10) that merges with the vegetation-covered debris at the base of the source slope. Although the main debris lobe seems to be separated from the vegetation-covered debris banked up at the base of the source slope careful examination shows the two to be continuous, merely separated by a 20 m wide depression.

An interesting feature is the presence of a secondary debris lobe resting on the slope immediately above the the main debris mass (Figure 7.3). This seems to be separate from the main debris lobe in that it rests on the source slope, close to the angle of repose, and is not in the fall-line from the source slope. The clast size and angularity of the debris is similar to that of the main mass, however it does not show the same crude upward fining stratigraphy seen in the main debris lobe. The lichen cover is similar to that of the main debris mass so the two deposits are assumed to be of the same relative age.

The lack of fresh boulders and impact marks on the vegetation-covered debris at the base of the source slope indicates that this is a fossil feature and has not accumulated by periodic rockfall activity continuing to the present day.

The whole debris lobe rests on sandy tills that are assumed to have been deposited by Loch Lomond Stadial glaciers (Sissons 1975). In turn the debris has a thin partial covering of peat. This serves to date the age of the deposit as being somewhere between 10.3 and 6 kyr BP (Formation of peat occurred 6-4 kyr BP (Birks 1977)). The cover and size of the lichen on the majority of the boulders show that the debris lobe is a relict feature that has not undergone any recent movement or modification.

The rock avalanche deposit below Beinn Alligin has fallen from a source slope of 500 m and has moved down slope for 1300 m away from the base of the source slope. This gives an angle of reach or *fahrböschung* of 19.1° and an equivalent coefficient of friction of 0.346 (Figures 7.5 & 7.11). If a rock mass slides down slope the distance of travel (L) and the fall height (H) are related by Coulomb's law of sliding friction

$$H = L \tan \theta \quad (2)$$

where $\tan \theta$ is the coefficient of friction, commonly assumed to be 0.6. From above it is seen that the Beinn Alligin slope failure gives a coefficient of friction half of that expected. The H/L index is the most widely used to describe the mobility of rock avalanches. Scheidegger (1973) showed that there is a log-linear relationship between avalanche volume and the equivalent coefficient of friction (Figure 7.5). Hsü (1975) used the excess travel distance (L_e) to describe the mobility of rock avalanches where

$$L_e = L - H/\tan 32^\circ \quad (3)$$

Using this formula the excess travel distance for the Beinn Alligin slope failure is 793 m. There is no doubt that the Beinn Alligin failure has travelled a great deal further than it would have under the influence of gravity alone. However controversy arises concerning the cause of this excess travel distance. A rock avalanche mechanism is proposed for the reasons detailed below.

7.5 Discussion

As stated previously there a number of features in the Beinn Alligin debris lobe that are inconsistent with a rock glacier/glacier transport hypothesis for the explanation of the 'excess' travel distance. Most important is the fact that the debris lobe quite clearly runs uphill over a distance of c. 600 m where it climbs the lower slopes of Tom na Gruagaich by at least 25 m. This is not observed in rock glaciers (Dyke

1990). Assuming the conservation of momentum (Evans 1989) the run-up can be used to calculate the velocity of the avalanche:

$$v^2 = 2gh \quad (4)$$

which for a run-up of 25 m gives a velocity of 22 ms^{-1} . Whitehouse (1983) used the following expression to calculate the velocity of rock avalanches:

$$v = 4\sqrt{h} \quad (5)$$

which gives a velocity of 20 ms^{-1} . Thus the velocity of the avalanche as it ran up the lower slopes of Tom na Gruagaich must have been at least $75 \pm 3 \text{ km/h}$ to produce the amount of run-up observed. From the height of fall from the source slope the maximum velocity of failure would have been 99 ms^{-1} or 356 km/h .

The debris lobe is noted to thin markedly downslope (Figure 7.11). This is a feature noted in all rockfalls and rock avalanches, especially the fact that the majority of the debris rests proximal to the base of the source slope while only a thin sheet-like lobe extends from the front of the main mass to travel the 'excess' distance (McSaveney 1978; Skermer 1985). The majority of rock glaciers are seen to thicken dramatically downslope and terminate in steep-fronted ridges that lie at or near to the angle of repose for the material that constitutes the debris. The Beinn Alligin debris lobe thins out at its eastern and terminal margins and is fronted by a number of individual boulders that constitute a spray fan, a feature diagnostic of rock avalanches.

The degree of size sorting i.e. the upward coarsening of the debris lobe with large angular boulders riding on a lower layer of smaller more rounded clasts is more in keeping with a rock avalanche origin (Eisbacher 1979). It is hard to envisage this sorting being created or preserved within or on a glacier. Also the preservation of 'jig-saw fit' boulders would be extremely unlikely by glacial transport of the debris.

The ridges and hollows also give an insight into the transport direction of the debris. It is seen that the ridges radiate outwards from the source slope (Figures 7.1 & 7.10) with the fall line vector directed towards the area of run-up. This causes thickening of the deposit in this direction while on the unconfined eastern margin the debris thins out to form a number of coalescing lobes. The front of the upper section of the debris is a steep fronted ridge where the normally horizontal boulders begin to dip steeply towards the front of the lobe. This may be due to some form of

'caterpillaring' action as the debris on the surface begins to over-run the lower debris that begins to lose momentum to the action of friction (Melosh 1990). The thinner frontal lobe is considered to have continued to have moved downslope by way of momentum transfer from the rear of the avalanche deposit to the front (Heim 1932; Eisbacher 1979; Davies 1982; Skermer 1985). If this is the case then the ridges represent pulses of motion, as would be the case if the failure progressed as a number of discrete failures occurring concurrently as the slope fails from the base upwards, with each following failure ploughing into the rear of the preceding failure, to create a highly mobile avalanche by virtue of momentum transfer. Movement would cease when the slope had failed completely and there was no further material to perpetuate the motion. As the debris ran into the lower slopes of Tom na Gruagaich it would lose momentum due to the work done to counteract gravity and the remaining momentum would be transferred to a thinner sheet with a lower yield strength (see equation 1, p318). It should be noted that there is a 37° change in the average motion vector of the trajectory of the upper and lower sections of the debris. This is due to deflection of the debris from the lower slopes of Tom na Gruagaich which it hits at an oblique angle. The debris is reflected off this obstacle, but the loss of momentum only allows a smaller portion of the debris to continue downslope. This sharp change in the movement direction due to topographic constraints is typical of highly mobile "streaming" rock avalanches (Eisbacher 1979). The similarity in the angle of incidence and the angle of reflection (Figure 7.12a) shows that the debris must have moved as a highly mobile 'fluidised' body and not as a slow moving plastic mass.

Slope failures of the size and nature of that on Beinn Alligin are rare, especially in Scotland, and indeed even where they have been reported previously (Ballantyne 1989b), the term rock avalanche has been applied rather loosely to include what are no more than large volume rockfalls (Holmes 1984).

The majority of historical rock avalanches have been triggered by high magnitude seismic activity (Whitehouse 1981; Keefer 1984a,b). Indeed more than eighty major rock avalanches were triggered by the 1964 M 8.5 Alaska earthquake (McSaveney 1978). Although there is no direct evidence, the presence of a fault showing late Quaternary reactivation in the area of the failure source slope suggests that fault movement and the resultant seismic activity acted as the trigger for the slope failure. The age of the fault movement and the age of the debris lobe are constrained to within the same time period i.e. 10.3 to 6 kyr BP [§ 2.6.4, p28]. The presence of a number of other large rock slope failures in the immediate area of Beinn Alligin (e.g. on Baosbheinn 7 km to the north and on Liathach 6 km to the southeast) also suggest

that a large seismic event was the trigger for slope failure initiation (Ballantyne 1986a). Therefore by inference the trigger for the slope failure is thought to be seismic activity associated with movement along the late Quaternary (post-10.3 kyr BP) fault that marks the eastern limit of the failure area. The fault has moved with downthrow to the west and possibly a small degree of sinistral strike slip motion [§ 2.6.4, p29]. Fault movement was due to differential isostatic uplift at the end of the last glacial episode in the Northern Highlands c. 10.3 kyr BP. The incidence of seismic activity may also be necessary to initiate the avalanche motion that allows the 'excess' travel distance of the failed rock mass. The seismic activity was thought to have been $5.7 \pm 0.3 M_s$ [§ 2.14, p106]. Most rock avalanches are triggered by seismic activity $>M 6.0$ (Keefer 1984a). Seismic activity would also input energy into the failed mass possibly creating the 'streaming' behaviour noted from other seismically-triggered rock avalanches that is thought responsible for the exceptional run-out distances achieved by these failures (McSaveney 1978; Eisbacher 1979; Evans *et al.* 1987). In this case the added input of seismic shaking energy not only acts to trigger the failure but also shakes the failed material causing dilation and fluidization of the debris mass to perpetuate downslope motion. A possible scenario for Beinn Alligin is detailed below.

Fault movement and seismic shaking act to disrupt the integrity of the slope. Deformation initiates as slow frictional sliding along pre-existing discontinuities. Seismic shaking and resultant dynamic pore fluid pressure effects act to put discontinuities under conditions of cyclic dilatant strain. This induces the shearing of asperities, leading to detachment of the rockmass. Down slope movement progresses from initial sliding to a combination of rolling, bounding and sliding as the rockmass disintegrates along pre-existing discontinuities. A decrease in particle size results in a reduction in the yield strength of the material, thus failure becomes self propelling (McEwen 1989). Disaggregation of the rockmass will be particularly well developed in the basal zone of the failed mass as mechanical abrasion causes a reduction in grain size and rounding of the blocks resulting in the creation of a basal layer of 'roller bearings' (Eisbacher 1979). This layer, by virtue of the clast size and geometry, would become a highly active mobile layer capable of carrying the overlying debris (Campbell 1989). The added energy input of seismic shaking would also give the debris mass greater energy than would have been the case if the failure had occurred under gravity alone. Seismic shaking also acts to dilate the debris by vibration thus fluidizing the debris mass (Davies 1982). Down slope movement of the mass will transfer the potential energy inherent in the rockmass and also the seismic shaking energy into kinetic energy giving rise to a highly mobile slope failure resulting in an

enhanced distance of travel. However, this alone will not explain the excess travel distance observed if the rockmass slides down slope losing much of its momentum to friction in the process. Additional mechanisms need to be invoked to account for the 793 m excess travel distance. The debris can attain a high velocity by virtue of the height of fall, however when this reaches the relatively flat ground at the base of the source slope the forward momentum of the mass will cause shear at the base of the debris. This in turn will cause vibrational dilation and reduction in particle size, having the double effect of reducing friction and lowering the yield strength of the material. The presence of even small amounts of fluid would lower the friction further. The water table would probably have been intercepted by such a deep-seated failure. If the avalanche had fallen onto remnant snow or ice (as would probably have been present immediately following the Loch Lomond Stadial, the time when the failure occurred) it would have incorporated this into the debris mass to lower the effective friction of the mass. As stated above it is thought that failure initiated at the base of the slope and progressed upwards with waves of debris streaming down the source slope ploughing into the back of the preceding debris. These pulses of flow or compression-rarefaction would be perpetuated downslope as shown by the preservation of the ridges and hollows perpendicular to the direction of travel of the avalanche. The transfer of momentum from the rear of the debris mass to the front is shown by the forward thrusting of blocks and the impact shattering and creation of 'jig-saw fit' boulders. Motion down the shallow slope at the base of the source slope would be perpetuated for as long as the momentum of the debris was sufficient to overcome the effects of friction. As stated above, friction would be lowered by the presence of minor amounts of fluid and by 'streaming' of the debris: crushing and grinding at the base of the debris mass would lower the yield strength of the material and also create more rounded clasts upon which the overlying more angular debris would ride. Undulations in the failure plane would cause these basal "roller-bearings" to bounce and bound rather than roll, thus reducing further the effects of friction and conserving energy. By the time that the debris mass hits the corrie floor it would be a highly mobile sheet of disaggregated angular boulders riding on a highly active layer of more rounded clasts. The fall line of the source slope meant that it ran straight into the lower slopes of Tom na Gruagaich (Figure 7.12) where the work done against gravity and friction as the front of the debris mass climbed upslope meant that the majority of the debris mass came to an abrupt halt. However momentum transfer from the rear of the debris mass was passed onto a thinner sheet of smaller, more rounded clasts that was deflected off the lower slopes of Tom na Gruagaich and continued downslope for a further c. 600 m down a slope of c. 6°. The smaller clast size of the frontal part of the debris lobe meant that it had a smaller yield strength and therefore needed less momentum to travel

further than would have the thicker part of the debris. Motion stopped when the debris thins to a critical thickness that can no longer maintain sufficient velocity to overcome the effects of friction (McEwen 1989). In addition to 'internal' mechanisms the effects of long duration seismic shaking can aid the long distance transport of rock avalanches. Severe ground motion can act to shake the debris when in motion, causing further dilation and fluidization of the debris aiding conservation of energy by overcoming the effects of frictional sliding and rolling. The inverse grading observed within this and other rock avalanches may be attributed to long-duration shaking, either as a result of avalanche motion or by seismic activity (Davies 1982). The debris that has been left on the source slope (Figure 7.3), thought by Sissons (1975) to have been merely debris that was not incorporated in the rock glacier, may owe its presence to a number of hypotheses. One is that it may have been part of the original rock avalanche but has become detached from the main debris mass as a 'swash' or 'levee' deposit (D.I. Benn, pers. comm. 1989) as it rode up and over an undulation in the basal failure plane, where due to its smaller mass it did not have sufficient momentum to progress further downslope. An alternative explanation is that it is a later failure, possibly due to aftershock activity associated with the trigger for the main slope failure, and due to its small size and possible shorter duration of shaking it did not develop into a proper rock avalanche.

7.6 Conclusions

The debris lobe beneath the peak of Sgurr Mhor on Beinn Alligin has been interpreted as a rock avalanche, removing the need to invoke remnant Loch Lomond Stadial ice in a south facing corrie. The trigger for the avalanche was seismic activity (c. M 6.0) associated with post-glacial movement on the fault that defines the eastern side of the failure area. The initial fall of the debris acted to disaggregate the rock mass and also provide sufficient momentum for the rockfall to progress into a rock avalanche by a process of mechanical fluidization. The presence of fluids and the effects of long duration seismic shaking may also have further added to the fluidization of the debris resulting in the 'excess' travel distance observed. The ultimate reach of this, and any other, rock avalanche is a reflection of the efficiency of momentum transfer from the thicker rear section of the debris to the thinner frontal sheet of debris that displays the 'excess' travel distance.

7.7 Acknowledgements

This research was carried out at the Department of Applied Geology, University of Strathclyde and latterly at the Department of Geology and Applied Geology, University of Glasgow while in receipt of NERC studentship GT4/87/GS/107. Useful discussion was had with I. Allison, C.K. Ballantyne, D.I. Benn, G.S. Boulton, R.S. Haszeldine, R. Muir Wood and P.S. Ringrose. F. McKenzie is thanked for help during fieldwork. D. MacLean prepared photographic plates. I. Allison's comments greatly improved an earlier draft of this paper.

7.8 References

Ashida, K. & Egashira, S. 1986. Running-out processes associated with the Ontake Landslide. *J. Nat. Disaster Sci.* 8, 63-79.

Ballantyne, C.K. 1986a. Protalus rampart development and the limits of former glaciers in the vicinity of Baosbheinn, Wester Ross. *Scott. J. Geol.* 22,13-25.

Ballantyne, C.K. 1986b. Landslides and slope failures in Scotland: a review. *Scot. Geog. Mag.* 102, 134-150.

Ballantyne C.K. & Eckford, J.D. 1984. Characteristics and evolution of two relict talus slopes in Scotland. *Scot. Geog. Mag.* 100, 20-33.

Ballantyne, C.K. & Sutherland, D.G.(eds.) 1987. Wester Ross Field Guide. Quaternary Research Association, Cambridge, 184pp.

Benn, D.I. 1989. Department of Geography & Geology, University of St. Andrews, St. Andrews, Fife, KY16 9ST.

Birks, H.J.B. 1977. The Flandrian forest history of Scotland: a preliminary synthesis. *in* F.W. Shotton (ed.) *British Quaternary Studies: Recent Advances.* Clarendon Press, Cambridge, 119-135.

Bock, C.G. 1977. Martinez Mountain rock avalanche, *in* D.R. Coates (ed) *Reviews in Engineering Geology Vol.III., Geol. Soc. Am.,* 155-168.

Campbell, C.S. 1989. Self-lubrication for long run-out landslides. *J.Geology* 97, 653-665.

Coates, D.R. (ed.) 1977. Landslide perspectives, *in* D.R. Coates (ed) *Reviews in Engineering Geology Vol.III., Geol. Soc. Am.,* 3-28.

Crandall, D.R. & Fahnestock, R.K. 1965. Rockfalls and avalanches from Little Tahoma Peak on Mount Rainier, Washington. *USGS Bull.* 1221A, 30pp.

Davies, T.R.H. 1982. Spreading of rock avalanche debris by mechanical fluidization. *Rock Mechanics* 15, 9-24.

Dawson, A.G., Mathews, J.A. & Shakesby, R.A. 1986. A catastrophic landslide (sturtzstrom) in Verkisladen, Rondane National Park, Southern Norway. *Geografiska Annaler* 68A, 77-87.

Dyke, A.S. 1990. A lichenometric study of Holocene rock glaciers and neoglacial moraines, Frances map area, southeastern Yukon Territory and Northwest Territories. *Geol. Surv. Canada Bull.* 394, 33pp.

Eisbacher, G.H. 1979. Cliff collapse and rock avalanches (sturtzstroms) in the MacKenzie Mountains, northwestern Canada. *Can. Geotech. J.* 16, 309-334.

Erismann, T.H. 1979. Mechanics of large landslides. *Rock Mechanics* 12, 15-46.

Evans, S.G. 1989. Rock avalanche run-up record. *Nature* 340, 271.

Evans, S.G., Aitken, J.D., Wetmiller, R.J. & Horner, R.B. 1987. A rock avalanche triggered by the October 1985 North Nahanni earthquake, District of Mackenzie, N.W.T. *Can. J. Earth Sci.* 24, 176-184.

Fenton, C.H. 1991. Neotectonics and Palaeoseismicity in North West Scotland. Unpubl. Ph.D. Thesis, University of Glasgow.

Goguel, J. 1978. Scale dependent rockslide mechanisms, with emphasis on the role of pore fluid vaporization, *in* B.Voight (ed.) *Rockslides and Avalanches 1, Natural Phenomena*, Elsevier, 693-705.

Habib, P. 1975. Production of gaseous pore pressure during rockslides. *Rock Mechanics* 7, 193-197.

Hadley, J.B. 1978. Madison Canyon rockslide, Montana, USA., *in* B.Voight (ed.) *Rockslides and Avalanches 1, Natural Phenomena*, Elsevier, 167-180.

Heim, A. 1932. *Bergsturtz und Menschenleben*. Fretz & Wasmuth Verlag, Zurich, 218pp.

Hewitt, K. 1988. Catastrophic landslide deposits in the Karakoram Himalaya. *Science* 242, 64-67.

- Holmes, G. 1984.** Rock-slope failures in parts of the Scottish Highlands. Unpubl. Ph. D. Thesis, University of Edinburgh.
- Howard, K.A. 1973.** Avalanche mode of motion: implications from Lunar examples. *Science* 180, 1052-1055.
- Hsü, K.J. 1975.** Catastrophic debris streams (Sturzstroms) generated by rockfalls. *Geol. Soc. Am. Bull.* 86, 129-140.
- Hsü, K.J. 1978.** Albert Heim: observations on landslides. *in* B. Voight (ed.) *Rockslides and Avalanches 1. Natural phenomena.* Elsevier, Amsterdam, 71-93.
- Jaeger, J.C. & Cook, N.G.W. 1979.** *Fundamentals of rock mechanics.* Chapman & Hall, London, 593pp.
- Jibson, R.W. 1987.** Summary of research on the effects of topographic amplification of earthquake shaking on slope stability. USGS Open File Report 87-268.
- Johnston, B. 1978.** Blackhawk Landslide, California, U.S.A. *in* B. Voight (ed.) *Rockslides and Avalanches 1. Natural phenomena.* Elsevier, Amsterdam, 481-504.
- Jones, B.L., Chinn, S.S.W. & Brice, J.C. 1984.** Olokele rock avalanche, island of Kauai, Hawaii. *Geology* 12, 209-211.
- Keefer, D.K. 1984a.** Landslides caused by earthquakes. *Geol. Soc. Am. Bull.* 95, 406-421.
- Keefer, D.K. 1984b.** Rock avalanches caused by earthquakes: source characteristics. *Science* 233, 1288-1289.
- Kent, P.E. 1966.** The transport mechanism in catastrophic rock falls. *J. Geol.*, 74, 79-83.
- Kobayashi, Y. 1985.** A catastrophic debris avalanche induced by the 1923 Great Kanto Earthquake. *J. Nat. Disaster Sci.* 7, 1-9.

- Lucchitta, B.K. 1978.** A large landslide on Mars. *Bull. Geol. Soc. Am.* 89, 1601-1609.
- McEwen, A.S. 1989.** Mobility of large rock avalanches: Evidence from Valles Marineris, Mars. *Geology* 17, 1111-1114.
- McSaveney, M.J. 1978.** Sherman Glacier rock avalanche, Alaska, USA., *in* B.Voight (ed) *Rockslides and Avalanches 1, Natural Phenomena*, Elsevier, 197-258.
- Melosh, H.J. 1979.** Acoustic fluidization: a new geologic process? *J. Geophys. Res.* 84B, 8097-8113.
- Melosh, H.J. 1990.** Giant rock avalanches. *Nature* 348, 483-484.
- Ringrose, P.S. 1989.** Palaeoseismic (?) liquefaction event in late Quaternary lake sediment at Glen Roy, Scotland. *Terra Nova* 1, 57-62.
- Scheidegger, A.E. 1973.** On the reach and velocity of catastrophic landslides. *Rock Mechanics* 9, 231-236.
- Shreve, R.L. 1968.** Leakage and fluidisation in air-layer lubricated avalanches. *Geol. Soc. Am. Bull.* 79, 653-658.
- Sissons, J.B. 1975.** A fossil rock glacier in Wester Ross. *Scott. J. Geol.* 11, 83-86.
- Sissons, J.B. 1976.** A fossil rock glacier in Wester Ross. *Scott. J. Geol.* 12, 175-179.
- Skermer, N.A. 1985.** Nature and mechanics of the Mount St. Helens rockslide-avalanche of 18 May 1980. *Geotechnique* 35, 357-368.
- Voight, B. & Pariseau, W.G. 1978.** Rockslides and avalanches: an introduction. *in* B.Voight (ed.), *Rockslides and Avalanches 1, Natural Phenomena*, Elsevier, 1-67.
- Voight, B. & Faust, C. 1982.** Frictional heat and strength loss in some rapid landslides. *Geotechnique* 32, 43-54.

Whalley, W.B. 1976. A fossil rock glacier in Wester Ross. *Scott. J. Geol.* 12, 175-179.

Whitehouse, I.E. 1981. A large rock avalanche in the Craigieburn Range, Canterbury. *New Zealand J. Geology and Geophysics* 24, 415-421.

Whitehouse, I.E. 1983. Distribution of large rock avalanche deposits in the central Southern Alps, New Zealand. *New Zealand J. geology and Geophysics* 26, 271-279.

Whitehouse, I.E. & Griffith, G.A. 1983. Frequency and hazard of large rock avalanches in the central Southern Alps, New Zealand. *Geology* 11, 331-334.

Yarnold, J.C. & Lombard, J.P. 1989. A facies model for large rock-avalanche deposits formed in dry climates. *in* I.P. Colburn, P.L. Abbott & J. Minch (eds.), *Conglomerates in basin analysis: a symposium dedicated to A.O. Woodford*. Pacific Section SEPM. Vol. 62, 9-31.

7.9 Figure Captions

- Figure 7.1** Location of the Beinn Alligin rock glacier. A-B-C is the line of the section in Figure 7.11.
- Figure 7.2** Debris lobe beneath Sgurr Mhor, Beinn Alligin. (Looking E from Tom na Gruagaich) Lobe is c. 1200 m long.
- Figure 7.3** Source slope (500 m high) for the Beinn Alligin rock avalanche. Note the lack of stepped topography in the triangular failure area. F marks the post-glacial fault trace.
- Figure 7.4** Plot of source slope height against source slope inclination (θ) for rock avalanches worldwide [after Keefer 1984]. Dashed lines represent the lower bounds for avalanche-prone slopes. Additional data from Dawson *et al.* (1986); Eisbacher (1979); Evans *et al.* (1987); Fenton (1991); Jones *et al.* (1984); Whitehouse (1981, 1983); Whitehouse & Griffith (1983). Beinn Alligin failure is marked by arrows. Definitions of the parameters given in Figure 7.11.
- Figure 7.5** Plots of H/L ratio against log(volume) [normalised to 10^6 m^3] for terrestrial (dots), Martian and Lunar (open circles) rock avalanches. Beinn Alligin is marked by a triangle. Note the marked decrease in H/L (equivalent coefficient of friction) with increasing avalanche volume. Definition of the parameters given in Figure 7.11)
- Figure 7.6** Headscarp at the top of the failure area beneath the peak of Sgurr Mhor (Looking W).
- Figure 7.7** Rock avalanche source slope with the basal failure plane showing the slope parallel, large wavelength corrugations (Looking NE from Toll a' Mhadaidh Mor).
- Figure 7.8** Boulders in the debris lobe at the front of the ridge separating the upper and lower sections of the lobe. Notebook is 15 cm long (Looking N).

- Figure 7.9** Run-up of at least 25 m of boulder debris against the lower slopes of Tom na Gruagaich (Looking NW).
- Figure 7.10** The rock avalanche debris lobe from the ridge crest. Note the run-up and deflection of the debris from the slopes of the opposite wall of the corrie. Debris lobe reaches 430 m in width (Looking SE).
- Figure 7.11** Section along the source slope and debris lobe of the Beinn Alligin rock avalanche (as marked in Figure 7.1). x marks the expected reach assuming a 'standard' coefficient of friction (c. 0.6). Diagrammatic representation of the parameters used in Figures 7.4 and 7.5.
- Figure 7.12(a)** Expected flow paths from debris released from point sources: 1- from the mid-point of the source slope (solid lines), and 2- from the base of the source slope (dashed lines). Arrows represent movement vectors of the upper and lower sections of the debris lobe.
- Figure 7.12(b)** Schematic representation of the flow paths of the rock avalanche as constructed from the orientation of the ridges and hollows and the idealised Figure 7.12(a).

7.10 Figures

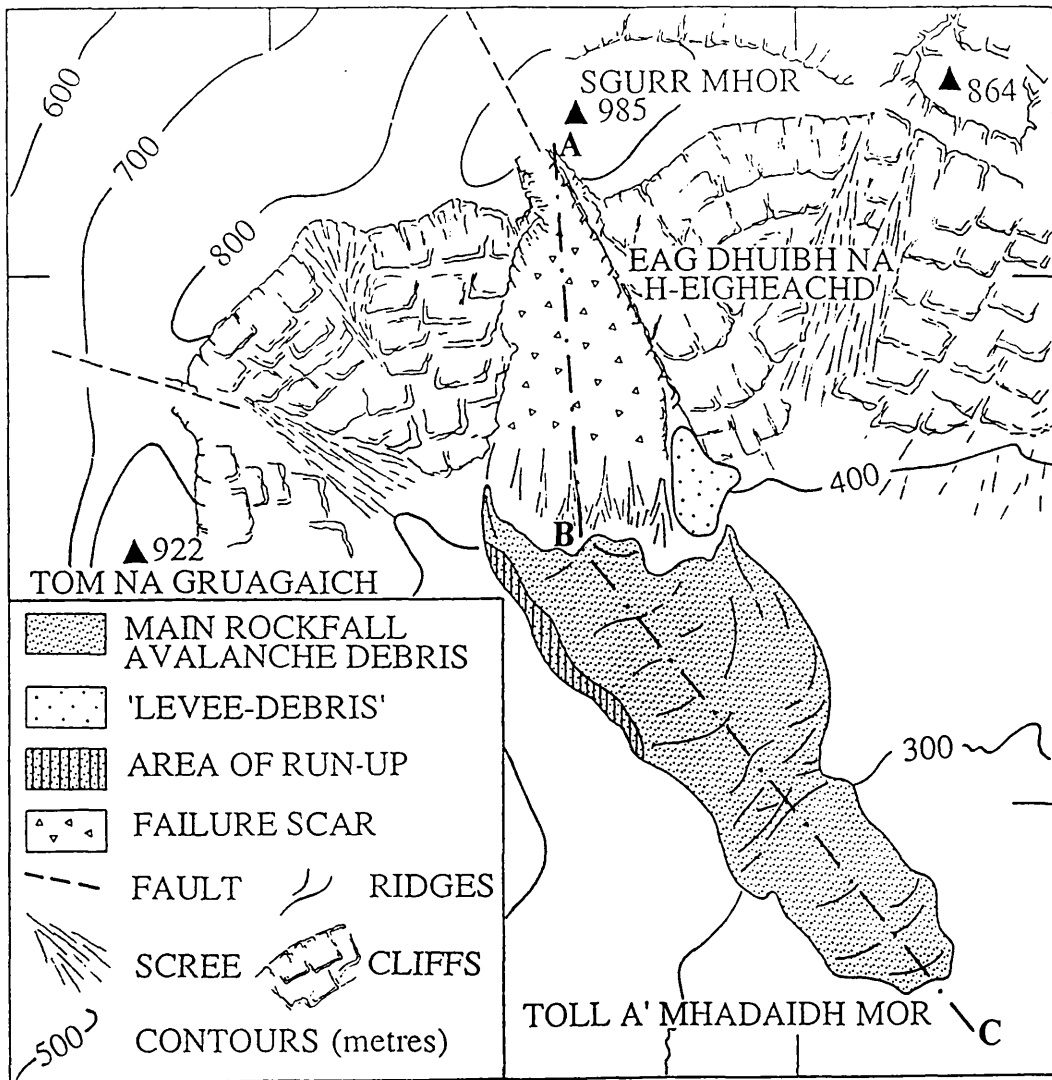


Figure 7.1



Figure 7.2



Figure 7.3

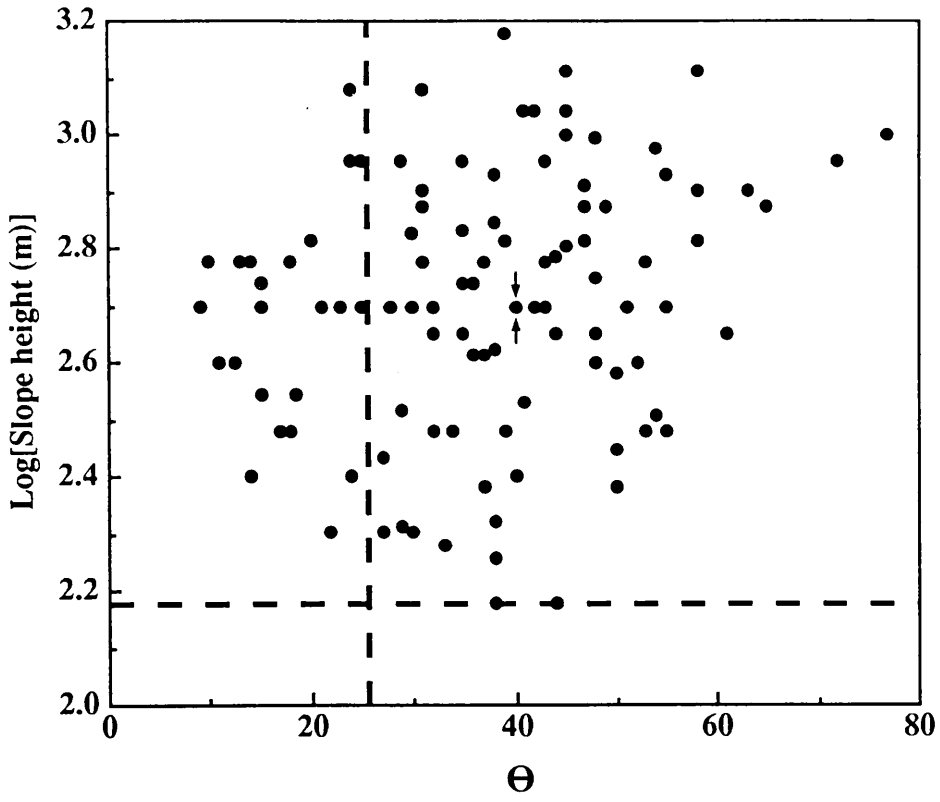


Figure 7.4

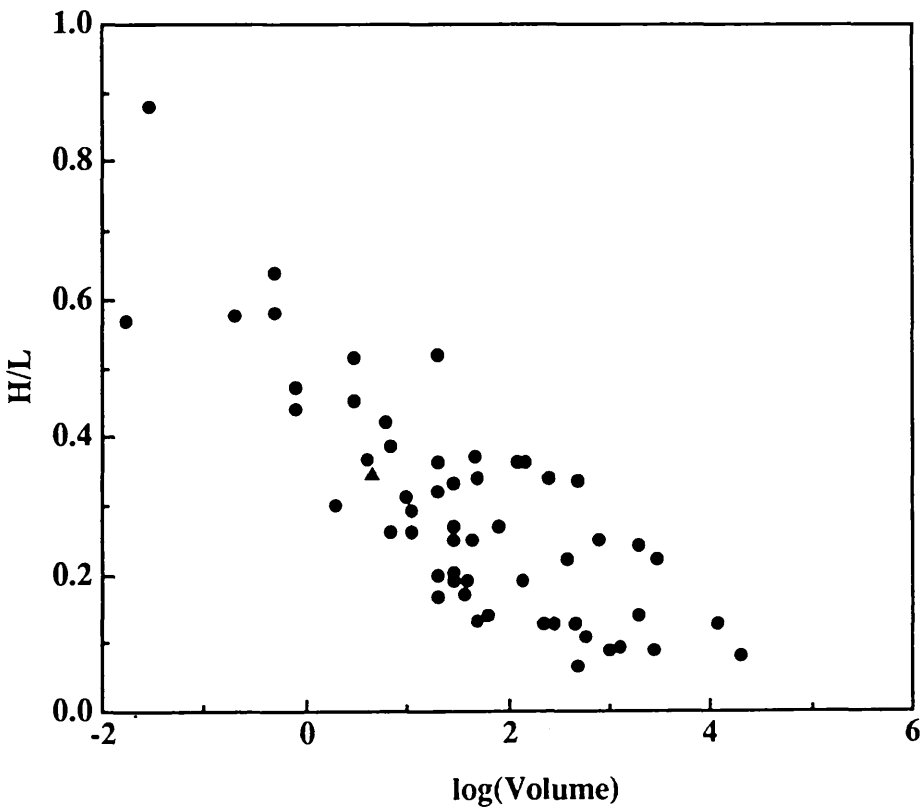
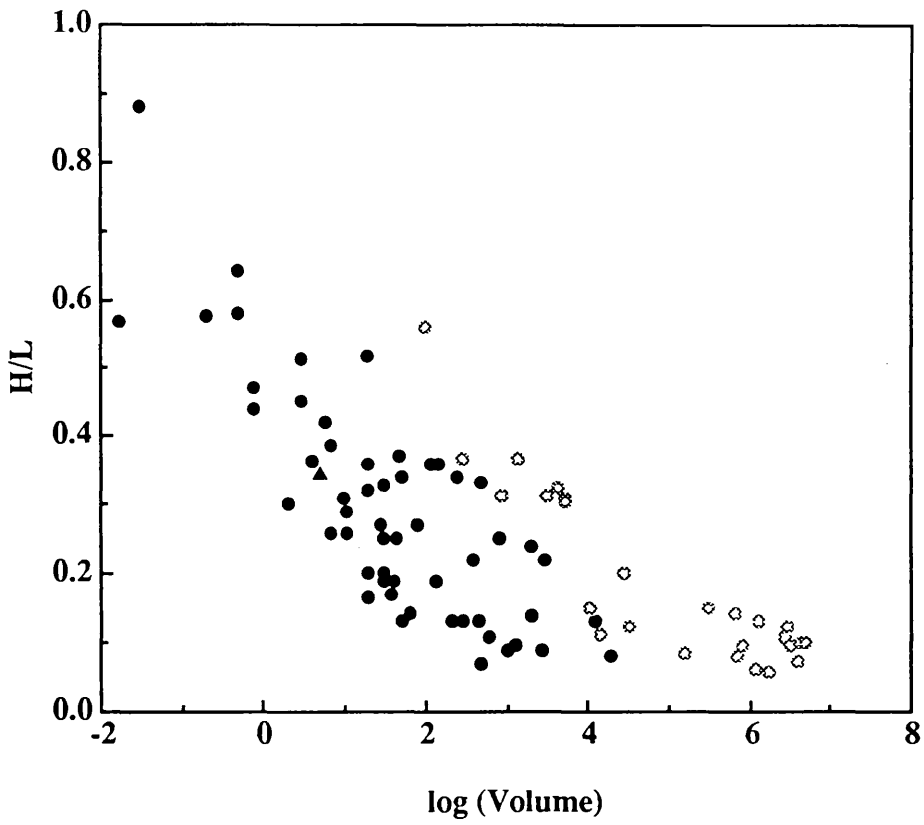


Figure 7.5



Figure 7.6



Figure 7.7



Figure 7.8



Figure 7.9



Figure 7.10

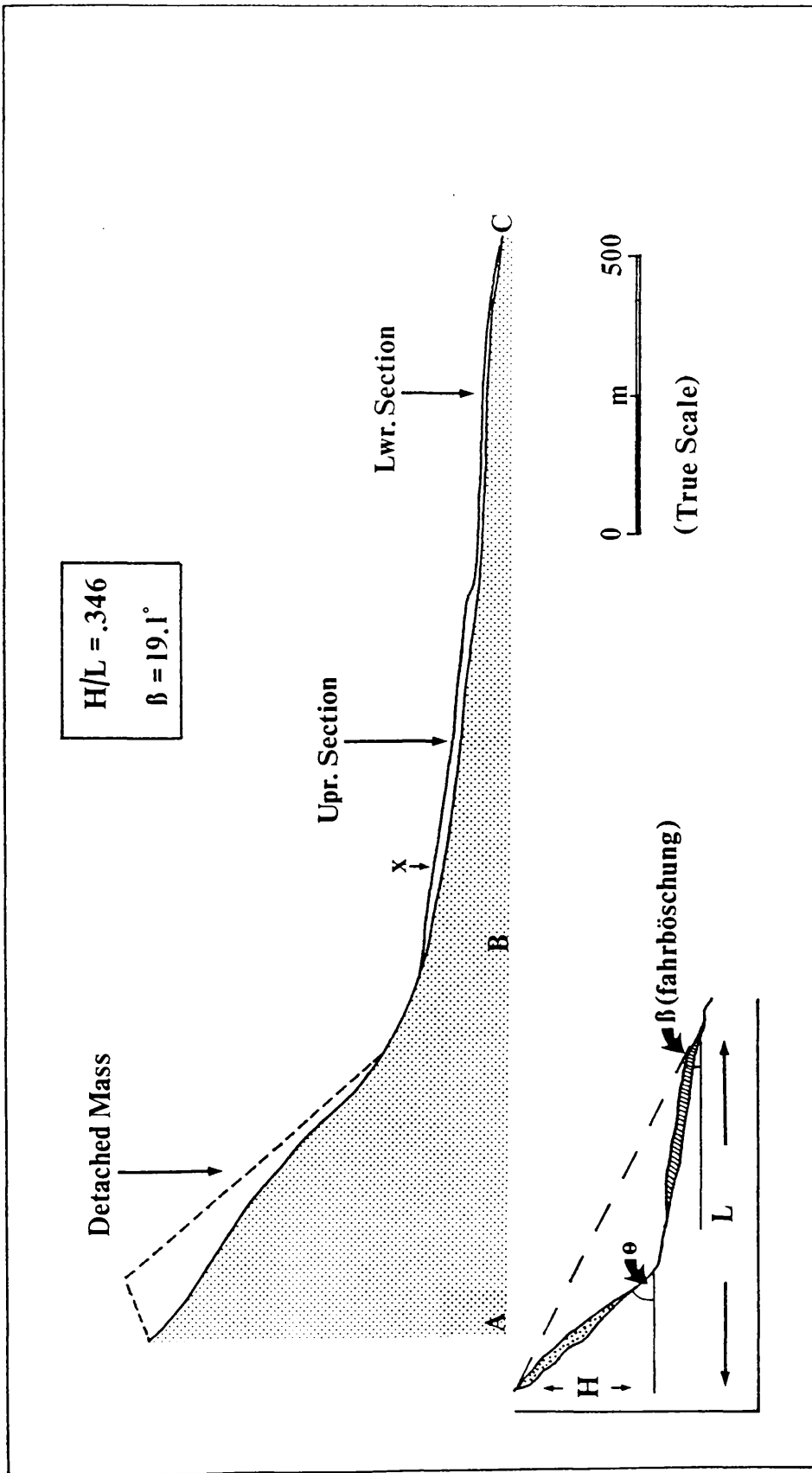


Figure 7.11

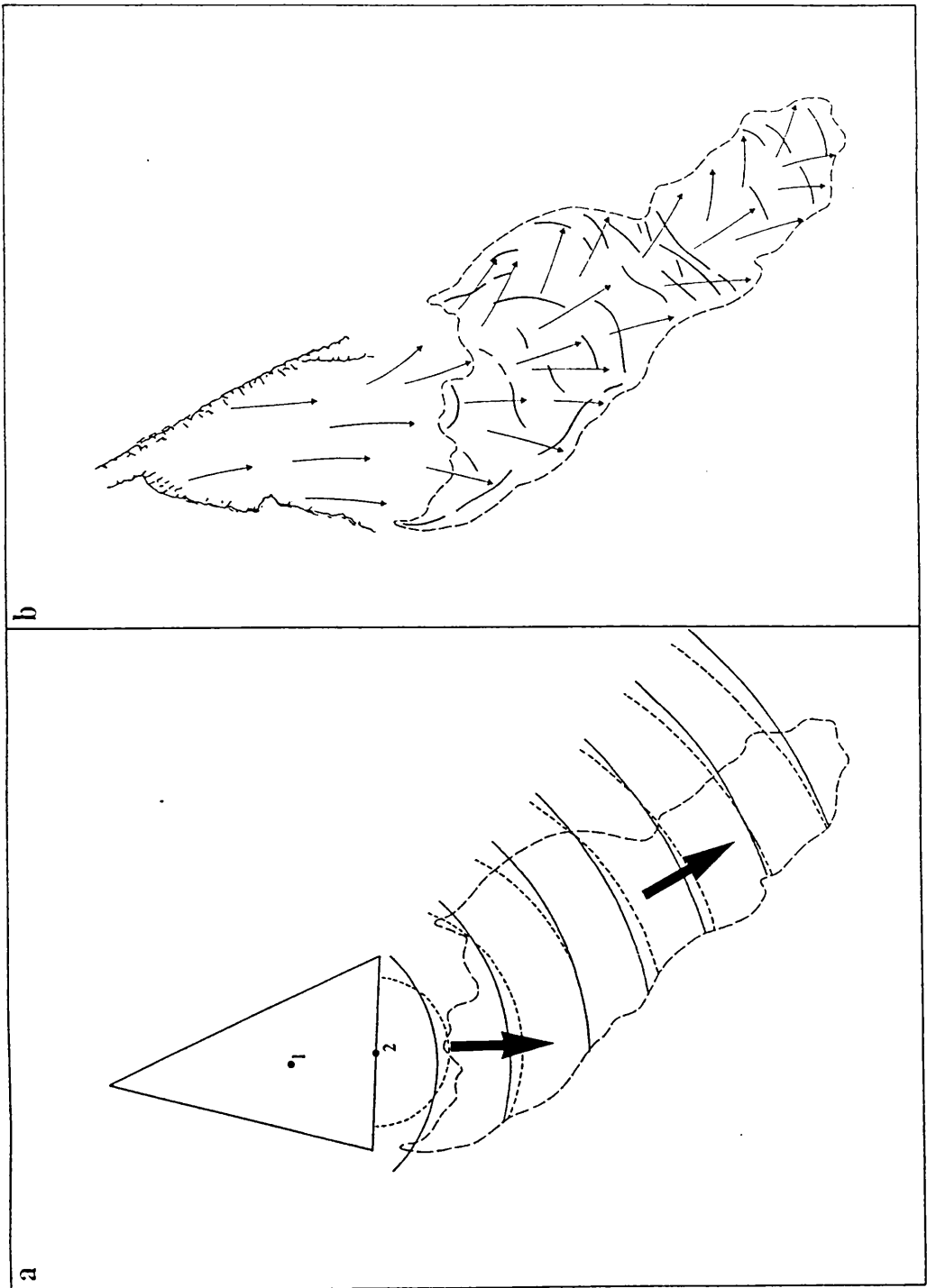


Figure 7.12

Chapter 8

Conclusions and Recommendations for Further Research

8.1 Introduction

Although each of the previous chapters [§ 2-7] has its own conclusions, it is useful to combine these in order to clarify how the understanding of post-glacial fault movement and seismotectonics in Scotland during the late Quaternary has progressed as a result of this study. In addition this allows an assessment of how well the original aims of the project have been addressed and also serves the purpose of identifying avenues for further research. The conclusions of each chapter are not repeated *verbatim*, but the essential points are assimilated to give a summary of what is known about post-glacial fault activity in Scotland.

8.2 General Comments

This thesis documents the results of three years research into the seismotectonic regime of Scotland during the late Quaternary. The topics addressed include the evidence for late Quaternary fault activity, seismicity during the Holocene, the mechanisms of glacio-isostatic faulting and glacial loading and stress system evolution during the late Quaternary.

In general the project has successfully addressed the initial aims, defined in Chapter One, concerning late Quaternary seismotectonics and has increased the understanding of tectonic movements in areas undergoing glacio-isostatic rebound. The results have been rewarding in this respect and also in the fact that they vindicate the validity of such investigations in areas of presently low seismotectonic activity.

This project has been based on extensive field study and the adoption of a multi-disciplinary approach to the understanding of post-glacial fault activity. This study has crossed the bounds of 'traditional' geological investigations merging the fields of seismology, stratigraphy, geomorphology, glaciology, geochemistry, rock mechanics and structural geology resulting in a true tectonogeophysical investigation. The wide ranging nature of this study has resulted in the creation of a new set of criteria (Figure 4.4) with which to structure an investigation of 'recent' seismotectonic activity. Criteria for the recognition of post-glacial faulting have been amended from those of previous workers (Lagerbäck 1979; Mohr 1986).

It is hoped that the success of this and similar studies will encourage further research elsewhere in order that we may better understand the nature of post-glacial faulting in areas of (presently) low level seismicity (Ringrose 1987; Bäckblom & Stanfors 1989).

8.3 Quaternary Seismotectonics

The tectonic activity described in this thesis [§ 2, p15] is seen to be the result of perturbations to the regional stress system created by the effects of crustal loading during the repeated glacial events of the latter part of the Quaternary [§ 6, p260]. The last major tectonic reorganisation on the NW margin of Europe occurred c. 6 Ma, in the late Miocene, when the combined effects of of Mid-Atlantic ridge spreading and Africa-Eurasia collision created a NW-SE orientated compressive stress regime. The magnitude and orientation of this stress regime is uniform over most of NW Europe with the exception of areas peripheral to large rift structures, e. g. the Central Graben in the North Sea which causes rotation of S_H to an E-W direction in Western Norway. Shallow stress measurements and earthquake focal plane mechanisms also show that the direction of S_H in Scotland is more WNW-ESE than the NW-SE direction measured for the remainder of the UK (Davenport *et al.* 1989). It is on this regional stress field that the effects of late Quaternary glacial loading have been superimposed and have resulted in the spectacular ground ruptures observed in Scotland [§ 2, p15].

In the UK Late Tertiary fault movement rates were up to 1 mm yr^{-1} , while at present, evidence from the study of earthquake aftershocks, suggests movement rates of 0.15 mm yr^{-1} (Main & Burton 1984; Muir Wood 1990). There is no evidence to suggest that there was a uniform decay in the tectonic deformation occurring in the UK over the duration of the Quaternary period. Indeed the evidence from offsets on Quaternary faults seems to suggest that, as a whole, the Quaternary was a time of minor tectonic activity, with fault movement rates as low as 0.01 mm yr^{-1} [§ 2, p15], punctuated by periods of violent seismotectonic activity in response to crustal unloading during deglaciation [§ 2, p15]. As the Quaternary history of onshore Scotland is poorly constrained, due to a poorly developed stratigraphy, only the last 26 kyr of the Quaternary, comprising part of the Pleistocene and the Holocene, has been studied in detail with respect to seismotectonic activity.

In a compressive tectonic regime crustal loading during the residence of an ice sheet acts to remove the crust from failure by increasing σ_3 relative to σ_1 , thus reducing the deviatoric stress [§ 6, p260]. The effects of increased crustal fluid

pressure from the action of sub-glacial meltwater, driven by the full weight of the ice sheet, further act to reduce the deviatoric stress [§ 6, p260]. This reduction in the deviatoric stress also allows the build up of tectonic stress during the period of ice sheet residence without the crust approaching the failure threshold. Upon deglaciation, with the removal of the vertical load, there is a massive decrease in σ_3 relative to σ_1 such that the deviatoric stress exceeds the strength of the crust thereby promoting failure. The stress ratio σ_1/σ_3 may also be sufficiently large to allow the triggering of less favourably orientated faults. With such high stress ratios, fluid overpressuring and the sudden relaxation of the imposed load, the immediate post-glacial time is a period of extensive fault activity, as shown by the surface rupture of this age [§ 2, p15]. The stress drop from seismic activity accompanying this fault movement will remove the crust from such critical stress levels to the point where only ideally orientated faults will be subject to reactivation [§ 6, p260].

All post-glacial fault movement in Scotland has occurred along pre-existing basement faults with NW-orientated sinistral strike-slip faults, NNW-orientated dextral strike-slip faults and NE-orientated reverse faults. There is no evidence for normal fault movement onshore, however some examples of normal fault movement have been reported from offshore localities (G. Eaton, pers. comm. 1989). The fault orientations and the sense of movement is consistent with that expected from a WNW- to NW-orientated compressive stress direction. As all the post-glacial fault ruptures observed are within the former area of glaciation their sense of movement is inconsistent with the theory that they are the result of crustal warping and up-doming due to post-glacial isostatic rebound. Thus, the controlling factor on faulting must have been the regional compressive stress regime with the effects of glacio-isostatic rebound and ice sheet loading stresses merely acting to trigger fault movement. This is seen in strike-slip faults such as the Kinloch Hourn Fault [§ 2.6.20, p47] where the 160m cumulative movement must have occurred over a greater period of time greater than the late- and post-glacial period and as such was not merely due to the actions of post-glacial rebound but is a result of the regional stress field.

The amount of offset that has occurred on individual post-glacial faults gives movement rates that are at least an order of magnitude greater than those experienced in the present day [§ 2, p15]. It is thought that the majority of post-glacial fault movements occurred as single events, similar to the style of faulting that has been described from Fennoscandia (Bäckblom & Stanfors 1989). However, as stated above, it seems that movement along NW-orientated faults was continuous throughout much of the Quaternary period as shown by the large cumulative offsets observed. In

addition this movement is seen to have continued until comparatively recently (Ringrose 1987) [§ 2.6.8, p34 & § 2.6.20, p47]. Accompanying this fault movement are a number of deformation features, such as seismically-triggered slope failures and seismite soft sediment deformation, that point to the immediate post-glacial period being one of enhanced seismic activity with events as large as $7.0M_S$, and numerous events in the range $5.5 - 6.5M_S$ [§ 4.16, p208] This is much greater than the levels of seismic activity experienced in the UK during the present day [§ 4, p149]. Comparing the seismicity during the Holocene from palaeoseismic, historical and instrumental records shows that there has been a marked decrease in the moment release rate from 8.0×10^{23} dyne cm yr⁻¹ to 1.5×10^{23} dyne cm yr⁻¹ in the last 10 kyr. This corresponds to a decrease in the tectonic moment from 1.7×10^{24} dyne cm yr⁻¹ to 1.5×10^{24} dyne cm yr⁻¹, calculated from crustal uplift rates, which show a decrease from c. 10 mm yr⁻¹ 10 kyr BP to 2.5 mm yr⁻¹ at present [§ 4.10, p174] (Maximum uplift rates in the Southern Alps of New Zealand are c. 22 mm yr⁻¹ (Adams 1980)). Throughout the entire Holocene only c. 10% of the tectonic moment has been released seismically. This is in agreement with the theory that the uplift experienced by the UK is due to the effects of glacio-isostasy where there is a passive flow of ductile sub-crustal material into the former centre of ice sheet loading. With the decrease in both tectonic and seismic moment for the last 10 kyr there is a corresponding decrease in the maximum magnitude of seismic event experienced from $7.0M_S$ for the immediate post-glacial period to $5.6M_L$ and $5.4M_L$ for the historical and instrumental periods respectively [§ 4, p149]. In addition the depth of seismic activity has also changed as, unlike the immediate post-glacial period, there have been no corroborated incidences of ground rupture in historical time. Focal plane mechanisms for palaeoseismic events seem to suggest that there has been a rotation of the regional stress field of c. 45° from a WSW-ENE direction 10 kyr BP to the WNW-ESE direction of the present day stress field [§ 4.10, p174]. However the quality of the data used in assigning these palaeoseismic focal plane mechanisms is not beyond reproach and the significance of this observation remains in doubt, except to say that there is no independent geological evidence to say that there has been such a dramatic rotation in the stress field.

In summary the stress field that has controlled the seismotectonics of Scotland for the duration of the Quaternary period has undergone significant changes in magnitude and one possible, although not proven, rotational event due to the effects of glacial episodes, resulting in periods of spectacular fault activity. From a background rate of tectonic movement of c. 0.01 mm yr⁻¹ the effects of late Devensian glaciation allowed the build up of tectonic stress over a 13 kyr period. This was then released

suddenly during ice decay and the immediate post-glacial period resulting in spectacular surface faulting and seismic activity. Partial crustal redepression during the Loch Lomond Stadial temporarily put a halt to this tectonic activity and allowed the further build up of tectonic stress. Final deglaciation at the beginning of the Holocene again resulted in a period of spectacular surface faulting and associated seismic activity. The style of faulting and orientation of the faults reactivated during these episodes was controlled by the regional stress field, with the effects of glacial unloading merely acting to trigger fault movement and in some cases prolong fault activity where crustal fluid overpressuring, resulting from sub-glacial fluid recharge, was trapped under a layer of impermeable permafrost.

8.4 Results of this Study

This study has increased the data base for post-glacial fault activity in Scotland from seven to twenty six incidences of movement along faults that have a variety of orientations.

It is seen that the majority of fault movement observed has occurred in the immediate post-glacial period. However there is evidence to suggest that movement has persisted along favourably orientated faults such as the Kinloch Hourn Fault (Ringrose 1987, 1989) [§ 2.6.20, p47] and the Beinn Tharsuinn fault [§ 2.6.8, p34] as recently as 2.4 kyr BP.

Deformation features identified as being the result of seismic activity associated with fault movement during the post-glacial period show that fault movement was associated with seismic events as large as 7.0 M_S , with a significant number of events $\geq 6.0 M_S$.

Comparison of palaeoseismic, historical and instrumental seismic data has shown that there was a marked decrease in the seismic strain release during the duration of the Holocene period from $3.6-7.6 \times 10^{23}$ dyne cm yr⁻¹ to 1.5×10^{23} dyne cm yr⁻¹.

Modelling of the stresses created by the loading of the crust by the presence of late Quaternary ice-sheets has shown that these stresses acting in conjunction with the tectonic stress field give rise to brittle failure in the immediate post-glacial period. The presence of hydraulic overpressuring due to fluid recharge at the base of the ice-sheets can give rise to the situation where fault movement occurs on unfavourably orientated

faults and movement on more favourably orientated faults persists outwith the immediate post-glacial period.

8.5 Present and Future Crustal Movements

The risk of further movement along the faults identified and the creation of new fractures has not been fully discussed in the main body of the thesis. It is true that the stress levels that are thought to have been operative in the immediate post-glacial period could not arise under the present regional stress regime and as a consequence the levels of present day seismic activity and the probability of surface fault rupture are much reduced. The annual probability of surface rupture in the UK is calculated to be 10^{-2} (Muir Wood 1990). This figure seems rather high in light of the lack of ground rupture in both the historical and instrumental seismicity records. However the evidence of geodetically recorded block movements in Finland and the incidence of surface faulting in the Ungava of eastern Canada highlights the fallacy of thinking of such shield areas as being inherently stable (Adams *et al.* 1991; P. Vuorela pers. comm. 1991). The lack of geodetic data for the UK hampers a full understanding of the large scale tectonics that are occurring at present. In addition the lack of good quality stress measurements for the UK, especially in Scotland, precludes any estimate being made of the likelihood of there being further movement along the faults investigated. Stress measurements adjacent to the Lansjärv fault in northern Sweden are anomalously low, testimony to the recency of movement along the fault (Stephansson *et al.* 1991). It is expected that the stress levels along the late Quaternary faults in N.W. Scotland would show similar low values. The spatial distribution of earthquakes around the area of Ben Nevis in Lochaber (Figure 4.6) could point to a degree of block tectonic uplift still occurring in Scotland at present. The possibility that this could be due to stress accumulation around a gravity anomaly is thought unlikely as there are no similar clusters of seismic activity noted around any other igneous centres in the area of N.W. Scotland. Recorded seismicity indicates that present tectonic movement is occurring on fault planes of only a few tens of km^2 at rates of 0.1 mm yr^{-1} (Main & Burton 1984). This would account for the absence of catastrophic events in the UK and the rather diffuse nature of the distribution of seismicity. With movement occurring along fault planes of these dimensions the risk of ground rupture is very slight indeed. Why the immediate post-glacial fault movement should have involved such large fault planes in a highly fractured crust remains a problem to be solved. A similar situation is observed in Sweden where there is no historical record of ground rupture.

The risk of the creation of new fractures is also thought to be small but not negligible. In all examples of post-glacial faulting described from both Scotland and Sweden there has been no creation of new faults. Movement has occurred along pre-existing lines of weakness. Some new fractures may have been created but these are of local importance. However it may be that such 'new' faults are yet to be discovered.

The importance of ice-cap loading in the generation of the stress system responsible for the initiation of post-glacial fault activity in both Scotland and Sweden seems to suggest that in the present climate stress levels will not reach the levels required to trigger significant fault movement. However the recent Ungava earthquake and associated surface rupture in eastern Canada suggests that the effects of glacial loading may not have been fully relieved from areas of continental crust.

8.6 Understanding Post-Glacial Fault Movements

Research into the phenomena of post-glacial fault activity is still very much in its infancy. The understanding of the behaviour of the brittle crust subject to ice-cap loading is still at an elementary stage compared to that of the mantle and the whole lithosphere. This study has confirmed the findings of previous workers in showing that the post-glacial period is one of violent seismic activity and that the isostatic response of the crust to deglaciation is not a uniform period of uplift, but is punctuated by periods of tectonic activity (Ringrose 1987; Lagerbäck 1979). The importance of sub-glacial fluid recharge has been highlighted in this work as being responsible for allowing the reactivation of less favourably orientated faults and for prolonging fault movement outwith the immediate post-glacial period. Despite a number of wide ranging studies into post-glacial fault activity (e.g. Bäckblom & Stanfors 1989) there is still much to be understood with regard to post-glacial fault timing in relation to ice decay and the exact cause of why certain faults are reactivated during this period and not others.

8.7 Recommendations for Further Work

With regard to better understanding post-glacial faulting the need for further work in a number of specific fields has come to light during the course of this research. The avenues for further work include:

- Effective age-dating of intrafault materials. This could be accomplished by improved sample collection methods, namely the use of plastic sheath coring to

recover fault gouge from depths where the ESR signal will have been fully reset. This would allow a better chronology of fault movements to be constructed, hence giving a greater understanding of the mechanisms of fault triggering.

- Better location of seismic events and the calculation of more fault plane solutions. In conjunction with a number of carefully sited stress measurements, this would allow an insight into the present day tectonics showing which faults are accommodating present movement and which have moved in the 'recent' geological past.

- Profiling across known post-glacial faults, using GPR (ground probing radar) or reflection seismology. This would give a comprehensive three dimensional picture of these faults thereby allowing a clearer understanding of the mechanics of fault reactivation.

- Further increasing the geographical extent of the data base. This will allow judgements to be made as to the uniqueness of these faults to areas that were formerly glaciated. (Do post-glacial faults exist outwith the area of ice cover ?) The discovery of faults outwith a area of former ice cover would have fundamental implications for the mechanics of fault triggering.

- An in-depth comparison of post-glacial faults from Sweden, Canada and Scotland. This has the potential to shed much light on many of the aspects of post-glacial fault activity.

- Improved modelling of the crustal response to ice-cap loading. A better understanding of the behaviour of the brittle crust when subject to the effects of glacial loading and sub-glacial fluid recharge is necessary to fully understand the stress system that was responsible for the fault movements observed.

- An on-going geodetic survey of the UK similar to that carried out in Finland to quantify present crustal movements.

- The creation of an accurate magnitude relationship to fully describe the seismic activity recorded within the UK and surrounding continental shelf. This will allow for more accurate comparisons between the various seismicity data sources.

8.8 References

- Adams, J. 1980.** Contemporary uplift and erosion of the Southern Alps, New Zealand. *Geol. Soc. Am. Bull.* 91(Part II), 1-114.
- Adams, J., Wetmiller, R.J., Drysdale, J. & Hasegawa, H. 1991.** The first surface rupture from an earthquake in eastern North America. *in* Current Research, Part C, Geological Survey of Canada, Paper 91-1C, 9-15.
- Bäckblom, G. & Stanfors, R. (eds.) 1989.** Interdisciplinary study of post-glacial faulting in the Lansjärv area northern Sweden 1986-1988. SKB Technical Report 89-31.
- Davenport, C.A., Ringrose, P.S., Becker, A., Hancock, P. & Fenton, C. 1989.** Geological investigation of late and post glacial earthquake activity in Scotland. *in* S. Gregerson & P.W. Basham (eds.). 1989. Earthquakes at North Atlantic Passive Margins: Neotectonics and postglacial rebound. 175-194. Kluwer Academic Publishers, Amsterdam.
- Lagerbäck, R. 1979.** Neotectonic structures in northern Sweden. *Geologiska Föreningens i Stockholm Förhandlingar* 100, 263-269.
- Main, I.G. & Burton, P.W. 1984.** Physical links between crustal deformation, seismic moment and seismic hazard for regions of varying seismicity. *Geophys. J. R. Astr. Soc.* 79, 469-488.
- Mohr, P. 1986.** Possible late Pleistocene faulting in Iar (west) Connacht, Ireland. *Geol. Mag.* 123, 545-552.
- Muir Wood, R. 1990.** The current tectonic regime in the United Kingdom and its NW European context (its bearing on the performance assessment of radioactive waste disposal sites). *in* Report of a meeting on "Fractures and fracture development". DOE Report No. DOE/RW/90.014. Dames & Moore International Technical Report TR-D&M-17.
- Ringrose, P.S. 1987.** Fault activity and palaeoseismicity during Quaternary time in Scotland. Unpubl. Ph.D. Thesis (2 Volumes), University of Strathclyde.

Stephansson, O., Ljunngren, C. & Jing, L. 1991. Stress measurements and tectonic implications for Fennoscandia. *Tectonophysics* 189, 317-322.

Vuorela, P. 1991. Geological Survey of Finland, Espoo, Finland.

Appendix A

LOCATION	Coire Mor.	NH2987
FAILURE SCAR/SOURCE SLOPE		
HEIGHT	180-275 m.	
INCLINATION	42°	
CONCAVITY	Convex slope.	
LENGTH	200-350 m.	
WIDTH	150 m.	
DEPTH	>50 m.	
NATURE OF SLIP SURFACES	Schistosity planes.	
LINEATIONS/SLICKENFIBRES	None.	
GOUGE/INFILL	None.	
SCARP MORPHOLOGY	Headscarp up to 30 m high above which are several open fissures marking an area of incipient failure.	
GEOMETRY OF FAILURE	Slumping along irregular schistosity planes with a small degree of rockfall at the base of the slope.	
ASPECT	ENE	
RELATION TO LLR	Within the LLR limits.	
GEOLOGICAL STRUCTURE	Complexly folded Moine psammites, moderate to steep dip to SE.	
FAILURE POTENTIAL	Possible slope creep and further rockfall also possible.	
UNDERCUTTING	Glacially steepened slopes.	
MECHANICAL WEAKENING	Extensively fractured rock due to the proximity of several fault lineaments.	
DEBRIS LOBE CHARACTERISTICS		
HEIGHT	180-275 m.	
INCLINATION	42°	
LENGTH	200-350 m.	
WIDTH	150 m.	
DEPTH	>50 m.	
CLAST SIZE	N/A	
CLAST ANGULARITY	N/A	
ABRASION/CRUSHING	N/A	
CLAST ALIGNMENT/ORIENTATION	N/A	
INTEGRITY OF 'SLIDE DEBRIS	Slumped mass disrupted by open fissures and a small degree of rockfall activity.	
RIDGE/TROUGH ORIENTATIONS	Transverse ridge and hollow features are developed just below the headscarp area.	
MARGIN MORPHOLOGY	Well defined headscarp area and fault bounded eastern margin. Western margin and toe of the failure area tend to merge with the surrounding hillside.	
SPRAY FAN	None.	
OVERALL GEOMETRY	Slump failure of a wedge bounded area of slope.	
TRAVEL DISTANCE	Maximum slumping of 30 m vertically.	
TRAJECTORY	ENE	

GENERAL NOTES

Small scale slump in close proximity to the Coire Mor fault.

LOCATION	Carn Alladale, Alladale, Easter Ross.	NH3990
FAILURE SCAR/SOURCE SLOPE		
HEIGHT	300 m.	
INCLINATION	31°	
CONCAVITY	Planar slope.	
LENGTH	500 m.	
WIDTH	250-300 m.	
DEPTH	Unknown.	
NATURE OF SLIP SURFACES	Bedding/banding planes.	
LINEATIONS/SLICKENFIBRES	None.	
GOUGE/INFILL	None.	
SCARP MORPHOLOGY	Obsequent scarp formed by down slope movement using backing joints. Lower scarps formed in boulder debris.	
GEOMETRY OF FAILURE	Sliding failure with a degree of rotation and subsequent outcrop disruption giving rise to rockfall activity.	
ASPECT	WSW	
RELATION TO LLR	Within the limits of LLR ice.	
GEOLOGICAL STRUCTURE	Moine schists and psammities dip to the W, open undulating fold surfaces.	
FAILURE POTENTIAL	Lower slope subject to slope creep as shown by the fissures in peat cover. Extensive scree cover on slopes >30° liable to movement as debris flows.	
UNDERCUTTING	Glaciated glen giving over steepened slopes.	
MECHANICAL WEAKENING	Movement-induced shattering of the rock mass along pre-existing fracture orientations.	
DEBRIS LOBE CHARACTERISTICS		
HEIGHT	300 m.	
INCLINATION	31°	
LENGTH	500 m.	
WIDTH	300 m.	
DEPTH	Unknown.	
CLAST SIZE	c. 1 m.	
CLAST ANGULARITY	Angular.	
ABRASION/CRUSHING	None.	
CLAST ALIGNMENT/ORIENTATION	None.	
INTEGRITY OF 'SLIDE DEBRIS	Slump-slide with disruption by obsequent scarps and extensive fracturing of the rock mass.	
RIDGE/TROUGH ORIENTATIONS	Obsequent scarps traverse the slope trending 130-310°, parallel to the headscarp orientation.	
MARGIN MORPHOLOGY	Well developed headscarp and lateral margins.	
SPRAY FAN	None.	
OVERALL GEOMETRY	Pear-shaped sliding-slump failure.	
TRAVEL DISTANCE	Down slope movement of at least 30 m.	
TRAJECTORY	WSW	

GENERAL NOTES

Previously reported by Holmes (1984) as a rock avalanche for reasons that are not clear. Classical slump failure morphology.

LOCATION	Bodach Beag, Alladale, Easter Ross.	NH3587
FAILURE SCAR/SOURCE SLOPE		
HEIGHT	290 m.	
INCLINATION	37°	
CONCAVITY	Concave slope.	
LENGTH	375 m.	
WIDTH	500 m.	
DEPTH	>30 m.	
NATURE OF SLIP SURFACES	Bedding/banding planes within the Moine psammites.	
LINEATIONS/SLICKENFIBRES	None.	
GOUGE/INFILL	None.	
SCARP MORPHOLOGY	Headscarp paralleling the slope formed due to detachment of sliding blocks from composite array of fracture orientations.	
GEOMETRY OF FAILURE	Block sliding failure.	
ASPECT	E	
RELATION TO LLR	Within limits of LLR.	
GEOLOGICAL STRUCTURE	Moine psammites dipping out of the slope (E) at c. 28°.	
FAILURE POTENTIAL	Rockfall from the overhanging sections of the headscarp.	
UNDERCUTTING	None.	
MECHANICAL WEAKENING	Inherited tectonic fracturing.	
DEBRIS LOBE CHARACTERISTICS		
HEIGHT	290 m.	
INCLINATION	37°	
LENGTH	375 m.	
WIDTH	4-500 m.	
DEPTH	At least 30 m.	
CLAST SIZE	Up to 4 m across.	
CLAST ANGULARITY	Angular.	
ABRASION/CRUSHING	None.	
CLAST ALIGNMENT/ORIENTATION	Rockfall terminates in finger-like lobes, behaviour exhibited by highly mobile flow-like rockfalls triggered due to seismic activity.	
INTEGRITY OF 'SLIDE DEBRIS	Block sliding failure that has broken up to form a disrupted block slide with associated rockfall.	
RIDGE/TROUGH ORIENTATIONS	Small obsequent scarps parallel to the headscarp/slope crest.	
MARGIN MORPHOLOGY	Headscarp and side walls are marked by distinct fracture controlled crags.	
SPRAY FAN	None	
OVERALL GEOMETRY	Sliding failure and associated mobile rockfall activity of a slope area of 0.25 km ² .	
TRAVEL DISTANCE	Movement of individual blocks varies from 10 to over 100 m.	
TRAJECTORY	E.	

GENERAL NOTES

Block sliding failure similar to that described from the Canadian Rockies by Eisbacher (1979) and attributed to seismic activity.

LOCATION	Cail Mhor, Gleann Beag.	NH3484
FAILURE SCAR/SOURCE SLOPE		
HEIGHT	275 m.	
INCLINATION	29°	
CONCAVITY	Convex upper and concave lower slope.	
LENGTH	500 m.	
WIDTH	125 m.	
DEPTH	>10 m.	
NATURE OF SLIP SURFACES	Schistosity/banding surfaces.	
LINEATIONS/SLICKENFIBRES	None.	
GOUGE/INFILL	None.	
SCARP MORPHOLOGY	10 m high slump scarp.	
GEOMETRY OF FAILURE	Sliding failure down schistosity planes.	
ASPECT	S	
RELATION TO LLR	?Within LLR limits.	
GEOLOGICAL STRUCTURE	SE dipping Moine psammites and quartzites.	
FAILURE POTENTIAL	?None.	
UNDERCUTTING	Glacially steepened slopes.	
MECHANICAL WEAKENING	Extensive shattering due to the proximity of the Strath Vaich fault segment.	
DEBRIS LOBE CHARACTERISTICS		
HEIGHT	275 m.	
INCLINATION	29°	
LENGTH	500 m.	
WIDTH	100-125 m.	
DEPTH	>10 m.	
CLAST SIZE	N/A	
CLAST ANGULARITY	N/A	
ABRASION/CRUSHING	N/A	
CLAST ALIGNMENT/ORIENTATION	N/A	
INTEGRITY OF 'SLIDE DEBRIS	'Slide is intact except for minor rockfall activity from the sidewall scarps.	
RIDGE/TROUGH ORIENTATIONS	Some low relief transverse ridges.	
MARGIN MORPHOLOGY	Well defined slumped head and bulging toe. Lateral margins are marked by troughs (eastern margin is bounded by the Strath Vaich fault).	
SPRAY FAN	None.	
OVERALL GEOMETRY	Tongue-shaped slump failure affecting an area of 0.0625 km ² .	
TRAVEL DISTANCE	Down slope movement of c. 10 m.	
TRAJECTORY	S	

GENERAL NOTES

Slump failure immediately adjacent to the Strath Vaich fault segment. Limited down slope movement.

LOCATION	Deanich, Gleann Mor.	NH3784
FAILURE SCAR/SOURCE SLOPE/SOURCE SLOPE		
HEIGHT	340 m.	
INCLINATION	34°	
CONCAVITY	Convex slope.	
LENGTH	625 m.	
WIDTH	875 m.	
DEPTH	>100 m.	
NATURE OF SLIP SURFACES	Banding planes dipping steeply out of the slope.	
LINEATIONS/SLICKENFIBRES	None	
GOUGE/INFILL	None.	
SCARP MORPHOLOGY	Headscarp composed of several banding/schistosity planes.	
GEOMETRY OF FAILURE	Sliding failure along steeply dipping banding planes progressing to toppling failure and rockfall.	
ASPECT	ESE	
RELATION TO LLR	?Within the LLR limits.	
GEOLOGICAL STRUCTURE	SE dipping Moine psammites.	
FAILURE POTENTIAL	Rockfall from unstable, shattered outcrops.	
UNDERCUTTING	Glacially steepened slopes.	
MECHANICAL WEAKENING	Extensive movement enhanced shattering of the rock mass.	
DEBRIS LOBE CHARACTERISTICS		
HEIGHT	340 m.	
INCLINATION	28°	
LENGTH	625 m.	
WIDTH	500-875 m.	
DEPTH	>100 m.	
CLAST SIZE	Up to 3 m across.	
CLAST ANGULARITY	Highly angular.	
ABRASION/CRUSHING	Impact crushing and 'jig-saw-fit' boulders.	
CLAST ALIGNMENT/ORIENTATION	None.	
INTEGRITY OF 'SLIDE DEBRIS	Extensively shattered slumped mass that has progressed to disruptive rockfall.	
RIDGE/TROUGH ORIENTATIONS	Obsequent scarps up to 3 m high and fissures up to 15 m deep trend 130-310° and 070-250°.	
MARGIN MORPHOLOGY	Deformation although intense dies out in all directions.	
SPRAY FAN	None.	
OVERALL GEOMETRY	0.4 km ² area that has undergone disruptive sliding and toppling failure.	
TRAVEL DISTANCE	c. 100 m of down slope movement.	
TRAJECTORY	SE	

GENERAL NOTES

An adjacent failure in Glas Choire Beag shows c. 30-40 m down slope movement also along banding/schistosity planes. Area affected by failure 500 x 200 m on a slope of 34°.

LOCATION	Creag nam Uamha, Gleann Beag.	NH3283
FAILURE SCAR/SOURCE SLOPE		
HEIGHT	50-150 m.	
INCLINATION	80-90°+	
CONCAVITY	Planar faces.	
LENGTH	50-150 m.	
WIDTH	125-200 m.	
DEPTH	c. 150 m.	
NATURE OF SLIP SURFACES	Several backing joints and composite basal sliding joints.	
LINEATIONS/SLICKENFIBRES	None.	
GOUGE/INFILL	None.	
SCARP MORPHOLOGY	Overhanging c. 150 m high cliff face.	
GEOMETRY OF FAILURE	Catastrophic rockfall.	
ASPECT	S	
RELATION TO LLR	Within LLR limits.	
GEOLOGICAL STRUCTURE	Moine psammites and schists with variable dip to the SE.	
FAILURE POTENTIAL	Rockfall from the overhanging headwall.	
UNDERCUTTING	Glacially steepened glen.	
MECHANICAL WEAKENING	Extensive fracturing of the country rock.	
DEBRIS LOBE CHARACTERISTICS		
HEIGHT	180 m.	
INCLINATION	20°	
LENGTH	500 m.	
WIDTH	125 m.	
DEPTH	At least 10-15 m thick.	
CLAST SIZE	Very large: 30 boulders $>10^3\text{m}^3$ of which 10 $> 1.2 \times 10^4\text{m}^3$.	
CLAST ANGULARITY	Highly angular.	
ABRASION/CRUSHING	Smaller clasts at the base of the debris show some mechanical crushing due to impact of larger blocks.	
CLAST ALIGNMENT/ORIENTATION	None.	
INTEGRITY OF 'SLIDE DEBRIS	Totally disrupted catastrophic rockfalls.	
RIDGE/TROUGH ORIENTATIONS	None.	
MARGIN MORPHOLOGY	Upper Bastion failure is topographically controlled on its eastern side.	
SPRAY FAN	Several large boulders have reached as far as the Banks of the river at the base of the slope.	
OVERALL GEOMETRY	Lobe shaped mass of boulder debris that has originated as a catastrophic rockfall.	
TRAVEL DISTANCE	Up to c. 500 m maximum. Mid-point to mid-point distance is c. 250 m.	
TRAJECTORY	S-SSW	

GENERAL NOTES

Large scale catastrophic rockfall due to cliff collapse from the base of the cliff upwards as shown by the fact that larger later boulders resting on top of earlier debris contain pegmatite veins only found in the upper area of the failure scar area. Pre- or glacial rockfall activity is shown by the large scars of the "Deanich Slabs" and a similar scar further to the east with no corresponding debris on the slopes below.

LOCATION	Beinn a' Chaisteil, Strath Vaich	NH3579
FAILURE SCAR/SOURCE SLOPE		
HEIGHT	350 m.	
INCLINATION	29°	
CONCAVITY	Concave slope.	
LENGTH	650 m.	
WIDTH	650 m.	
DEPTH	>10 m.	
NATURE OF SLIP SURFACES	Foliation surfaces act as out of slope slip planes.	
LINEATIONS/SLICKENFIBRES	None	
GOUGE/INFILL	None	
SCARP MORPHOLOGY	Headscarp up to 10 m high composed of a number of intersecting joint planes.	
GEOMETRY OF FAILURE ASPECT	(Rotational) slump. W	
RELATION TO LLR	Within LLR limits.	
GEOLOGICAL STRUCTURE	Moine psammities dip moderately to the SW.	
FAILURE POTENTIAL	Rockfall of minor degree from some of the disaggregated outcrops.	
UNDERCUTTING	Strath Vaich has had its Devonian land surface exhumed by glaciation i.e. no appreciable oversteepening.	
MECHANICAL WEAKENING	Extensive shattering of the rock related to movement of the rock mass during failure.	
DEBRIS LOBE CHARACTERISTICS		
HEIGHT	350 m.	
INCLINATION	29°	
LENGTH	625 m.	
WIDTH	600 m.	
DEPTH	>50 m.	
CLAST SIZE	N/A	
CLAST ANGULARITY	N/A	
ABRASION/CRUSHING	N/A	
CLAST ALIGNMENT/ORIENTATION	N/A	
INTEGRITY OF 'SLIDE DEBRIS	Shattered outcrops, but generally intact except for minor rockfall activity.	
RIDGE/TROUGH ORIENTATIONS	Small obsequent scarps up to 2 m in height trending 046-226°	
MARGIN MORPHOLOGY	Well defined slumped head and bulging toe. Lateral margins are more diffuse and merge with the surrounding hillside.	
SPRAY FAN	None.	
OVERALL GEOMETRY	Teardrop-shaped rotational slump.	
TRAVEL DISTANCE	Vertical movement of c. 10 m.	
TRAJECTORY	W	

GENERAL NOTES

Typical rotational slump failure. However excessive disruption of outcrops for the amount of displacement possibly implies a degree of seismic shaking to cause disaggregation of the rock mass.

LOCATION	Strath Vaich.	NH3475
FAILURE SCAR/SOURCE SLOPE		
HEIGHT	215 m.	
INCLINATION	23°	
CONCAVITY	Convex.	
LENGTH	500 m.	
WIDTH	1250 m.	
DEPTH	Unknown.	
NATURE OF SLIP SURFACES	Sliding along low angle fracture surfaces.	
LINEATIONS/SLICKENFIBRES	None.	
GOUGE/INFILL	None.	
SCARP MORPHOLOGY	Obsequent scarps trend 169-349°, up to 2 m high.	
GEOMETRY OF FAILURE	Outward toppling using foliation planes.	
ASPECT	ENE	
RELATION TO LLR	Within LLR limits.	
GEOLOGICAL STRUCTURE	Moine psammites and quartzites dipping >60° to the E.	
FAILURE POTENTIAL	Present day toppling and some associated rockfall.	
UNDERCUTTING	Glacially modified Devonian palaeosurface.	
MECHANICAL WEAKENING	Extensive fracturing of psammites associated with the proximity of the Strath Vaich fault.	
DEBRIS LOBE CHARACTERISTICS		
HEIGHT	215 m.	
INCLINATION	23°	
LENGTH	500 m.	
WIDTH	1250 m.	
DEPTH	Unknown, at least 50 m.	
CLAST SIZE	N/A	
CLAST ANGULARITY	N/A	
ABRASION/CRUSHING	N/A	
CLAST ALIGNMENT/		
ORIENTATION	N/A	
INTEGRITY OF 'SLIDE DEBRIS	Disrupted by obsequent scarps, fissures and clefts. Outcrops show 'dry stane dyke' textures - disaggregation along E-W and NNW-SSE fractures and the SSW dipping foliation.	
RIDGE/TROUGH ORIENTATIONS	Obsequent scarps trend NNW-SSE. Fissures in peat up to 2 m wide and 1 m deep trending N-NNW.	
MARGIN MORPHOLOGY	Diffuse margins merge with the surrounding hillside.	
SPRAY FAN	None.	
OVERALL GEOMETRY	Toppling failure of an area of 0.5 km ² .	
TRAVEL DISTANCE	Down slope movement of c. 50 m.	
TRAJECTORY	E	

GENERAL NOTES

Toppling failure that shows evidence for substantial present day movement threatening the stability of the adjacent Hydro-electric dam.

LOCATION	Sgurr Bhreac, Fannich Mountains.	NH1371
FAILURE SCAR/SOURCE SLOPE		
HEIGHT	400 m.	
INCLINATION	28°	
CONCAVITY	Convex lower slope and concave upper slope.	
LENGTH	750 m.	
WIDTH	1000 m.	
DEPTH	Unknown.	
NATURE OF SLIP SURFACES	Schistosity/banding surfaces.	
LINEATIONS/SLICKENFIBRES	None.	
GOUGE/INFILL	None.	
SCARP MORPHOLOGY	Transverse obsequent scarps parallel the small exposed area of headscarp.	
GEOMETRY OF FAILURE	Large scale slump failure.	
ASPECT	S	
RELATION TO LLR	Within LLR limits.	
GEOLOGICAL STRUCTURE	Complex area of Moine rocks with intercalated Lewisian rocks.	
FAILURE POTENTIAL	Possible slope creep?	
UNDERCUTTING	None.	
MECHANICAL WEAKENING	Pervasive regional fracturing.	
DEBRIS LOBE CHARACTERISTICS		
HEIGHT	400 m.	
INCLINATION	28°	
LENGTH	800 m.	
WIDTH	1000 m.	
DEPTH	Unknown.	
CLAST SIZE	N/A	
CLAST ANGULARITY	N/A	
ABRASION/CRUSHING	N/A	
CLAST ALIGNMENT/ORIENTATION	N/A	
INTEGRITY OF 'SLIDE DEBRIS RIDGE/TROUGH ORIENTATIONS	Slumped mass disrupted only by small obsequent scarps.	
MARGIN MORPHOLOGY	Scarps traverse across the slope. Open fissures trending 110-290° and 050-230°.	
SPRAY FAN	Diffuse margins that merge with the surrounding hillside.	
OVERALL GEOMETRY	None.	
TRAVEL DISTANCE	Large are of sliding slump failure.	
TRAJECTORY	Down slope movement of c. 50 m.	
	SW	

GENERAL NOTES

Large area of slope failure with unknown depth dimensions and relation to possible trigger mechanisms. Remarkable only for the area of slope affected.

LOCATION	A' Chailleach, Fannich Mountains.	NH1371
FAILURE SCAR/SOURCE SLOPE		
HEIGHT	250 m.	
INCLINATION	18°	
CONCAVITY	Planar slope with a convex toe area.	
LENGTH	700 m.	
WIDTH	560 m.	
DEPTH	Unknown.	
NATURE OF SLIP SURFACES	Schistosity surfaces.	
LINEATIONS/SLICKENFIBRES	None.	
GOUGE/INFILL	None.	
SCARP MORPHOLOGY	Small obsequent scarps trending across the slope for up to 400 m and up to 1.5 m high.	
GEOMETRY OF FAILURE	Large area of sliding slump failure.	
ASPECT	SE	
RELATION TO LLR	Within the LLR limits.	
GEOLOGICAL STRUCTURE	Complex area of Moine schists with Lewisian intercalations along a slide zone.	
FAILURE POTENTIAL	Slope creep?	
UNDERCUTTING	None.	
MECHANICAL WEAKENING	Pervasive regional fracturing.	
DEBRIS LOBE CHARACTERISTICS		
HEIGHT	250 m.	
INCLINATION	18°	
LENGTH	750 m.	
WIDTH	560 m.	
DEPTH	Unknown.	
CLAST SIZE	N/A	
CLAST ANGULARITY	N/A	
ABRASION/CRUSHING	N/A	
CLAST ALIGNMENT/ORIENTATION	N/A	
INTEGRITY OF 'SLIDE DEBRIS	Slumped mass cut by small obsequent scarps.	
RIDGE/TROUGH		
ORIENTATIONS	Scarps traverse slope sub-parallel to the ridge crest.	
MARGIN MORPHOLOGY	Diffuse margins that merge with the surrounding hillside.	
SPRAY FAN	None.	
OVERALL GEOMETRY	Large area of sliding slump failure.	
TRAVEL DISTANCE	Down slope movement of 20-50 m.	
TRAJECTORY	SE	
GENERAL NOTES		
Unremarkable slump failure.		

LOCATION	Garbh Choire Mor, Fannich Mountains.	NH2567
FAILURE SCAR/SOURCE SLOPE		
HEIGHT	c. 200 m.	
INCLINATION	25-35° (steepens to 55°)	
CONCAVITY	Planar, slightly undulating surface.	
LENGTH	150 m.	
WIDTH	100 m.	
DEPTH	40 m.	
NATURE OF SLIP SURFACES/ LINEATIONS/ SLICKENFIBRES/ GOUGE/INFILL	Fracture plane dipping out of the slope at 26°/053°.	
SCARP MORPHOLOGY	None	
GEOMETRY OF FAILURE ASPECT	None	
RELATION TO LLR	No head scarp - failure plane intersects the ridge crest. Very marked side wall scarp up to 40 m in height.	
GEOLOGICAL STRUCTURE	Large scale catastrophic slab failure.	
FAILURE POTENTIAL	SE	
UNDERCUTTING	Within limits of LLR.	
MECHANICAL WEAKENING	Moine schists and psammites dip in to the slope (almost perpendicular to the basal failure plane).	
	Some intermittent rockfall from the side wall area.	
	None evident - lower slope has been destroyed by the slope failure.	
	Talus slopes around the corrie show extensive freeze-thaw activity.	
DEBRIS LOBE CHARACTERISTICS		
HEIGHT	70-110 m	
INCLINATION	14°	
LENGTH	400 m.	
WIDTH	150 m.	
DEPTH	5-35 m+	
CLAST SIZE	Largest boulder is 20 m across. Average size is in the region of 3 m across.	
CLAST ANGULARITY	Most blocks are rectangular. These larger more angular blocks are found to rest on smaller, more rounded 'roller-bearing' blocks.	
ABRASION/CRUSHING	Larger blocks are sometimes shattered giving 'jig-saw-fit' morphologies. Smaller clasts at the base of the deposit have been subject to extensive crushing and rounding.	
CLAST ALIGNMENT/ ORIENTATION		
INTEGRITY OF 'SLIDE DEBRIS	Most larger blocks are aligned across the direction of travel.	
RIDGE/TROUGH ORIENTATIONS	Single teardrop-shaped lobe with poorly developed margins that merge in places with the glacial debris onto which it has fallen.	
MARGIN MORPHOLOGY	Faint ridges occur perpendicular to the travel direction.	
SPRAY FAN	Margins generally merge with	
OVERALL GEOMETRY	Boulders up to 30 m in front of the main debris mass.	
TRAVEL DISTANCE	Roughly teardrop-shaped rock avalanche deposit.	
TRAJECTORY	Frontal margin has moved 450-500 m from the area of failure (Mid-point to mid-point distance c. 220 m).	
GENERAL NOTES	ESE	

Several dozen boulders exceed 10 m across. Volume of debris is small in relation to the size of the failure scar - must have been some previous slope failure activity, most probably of LLR age as shown by the amount of large angular boulders in the terminal moraines below the corrie. Several faults in the area show evidence for recent movement and could probably have been responsible for the triggering of the rockfall avalanche.

LOCATION	Beinn Alligin, Torridon	NG8661
FAILURE SCAR/SOURCE SLOPE		
HEIGHT	500 m.	
INCLINATION	45-60° in lower section, 80-90° side and head walls.	
CONCAVITY	Planar surface with large wavelength corrugations.	
LENGTH	c. 500 m.	
WIDTH	c. 300 m.	
DEPTH	50-200 m below original ground surface.	
NATURE OF SLIP SURFACES	Fracture planes define basal failure which intersect slope to W. E margin defined by fault.	
LINEATIONS/SLICKENFIBRES	Failure scar marked by longitudinal corrugations. Lower debris slopes show linear ridges parallel to the direction of debris transport.	
GOUGE/INFILL	Fault gouge present at two localities along the fault defining the E wall of the failure scar.	
SCARP MORPHOLOGY	No obsequent scarp present; complete slope failure.	
GEOMETRY OF FAILURE ASPECT	Triangular wedge-shaped area of failure. SSE.	
RELATION TO LLR	Within limits of LLR.	
GEOLOGICAL STRUCTURE	Gently dipping Torridonian sandstone, well bedded units up to 2 m thick.	
FAILURE POTENTIAL	Present day rockfall from the steep side and head walls.	
UNDERCUTTING	No evidence, slope failure has destroyed lower slopes.	
MECHANICAL WEAKENING	Frost and fault related shattering of the sandstone.	
DEBRIS LOBE CHARACTERISTICS		
HEIGHT	130 m.	
INCLINATION	6°	
LENGTH	1200 m.	
WIDTH	100-400 m.	
DEPTH	12-20 m+	
CLAST SIZE	Blocks up to 10 m across, average size c. 3 m.	
CLAST ANGULARITY	Rectangular blocks and smaller more rounded clasts.	
ABRASION/CRUSHING	Smaller "roller-bearing" clasts are extensively rounded.	
CLAST ALIGNMENT	Orientated both longitudinally and transverse with respect to travel direction. Larger blocks on top of more rounded clasts	
INTEGRITY OF 'SLIDE DEBRIS	Well defined margins with steep margins to the W due to topographic control (some degree of run up), margins to the E and SE are less well defined.	
RIDGE/TROUGH ORIENTATIONS	Both transverse and longitudinal ridges are present.	
MARGIN MORPHOLOGY	Steep scarp face margins to the W and more diffuse lobate margins to the E and SE	
SPRAY FAN	Frontal portion of the debris lobe consists of a layer of boulder debris only a few metres deep (one boulder thick in places) that has travelled ahead of the main debris mass.	
OVERALL GEOMETRY	Elongate tongue-shaped debris lobe showing degree of run-up to the W.	
TRAVEL DISTANCE	Front margin is 1300 m from the failure scar (Mid-point to mid-point distance c. 920 m)	
TRAJECTORY	Initially to SW then topographically deflected to SE	
GENERAL NOTES		
Large amount of void space within the debris lobe. Debris consists of distinct upper and lower sections. An additional 'swash' or 'levee' deposit has remained on the slope above and was not incorporated in the main failure movement. Upper section of the debris is >20 m thick but is composed of smaller debris than the lower section where large boulders rest on smaller more rounded debris.		

LOCATION	Glenuaig, Upper Strathconon.	NH0847-1148
FAILURE SCAR/SOURCE SLOPE		
HEIGHT	245-395 m.	
INCLINATION	20-28°	
CONCAVITY	Convex slopes.	
LENGTH	500-750 m.	
WIDTH	300-625 m.	
DEPTH	Unknown.	
NATURE OF SLIP SURFACES/ LINEATIONS/ SLICKENFIBRES	Schistosity planes dipping out of the slope.	
GOUGE/INFILL	None.	
SCARP MORPHOLOGY	Curved headscarps formed from a composite of joint orientations.	
GEOMETRY OF FAILURE	Rotational sliding slump failures detaching along schistosity planes.	
ASPECT	S-SE	
RELATION TO LLR	Within LLR limits.	
GEOLOGICAL STRUCTURE	Moine pelites and psammites dip gently (10-15° occasional steepening to c. 45°) to SE.	
FAILURE POTENTIAL	Possible rockfall activity from some of the more unstable outcrops.	
UNDERCUTTING	Glaciated slopes but no obvious undercutting.	
MECHANICAL WEAKENING	Extensive pervasive tectonic shattering enhance by slope movement.	
DEBRIS LOBE CHARACTERISTICS		
HEIGHT	245-395 m.	
INCLINATION	20-28°	
LENGTH	500-750 m.	
WIDTH	300-6625 m.	
DEPTH	Unknown.	
CLAST SIZE	N/A	
CLAST ANGULARITY	N/A	
ABRASION/CRUSHING	N/A	
CLAST ALIGNMENT/ ORIENTATION	N/A	
INTEGRITY OF 'SLIDE DEBRIS	Slides are generally intact, 'though some rockfall toppling has taken place along backing joints in the failure headscarps.	
RIDGE/TROUGH ORIENTATIONS	Minor 'ripples' and fissures transverse to the slope. Some 150-330° trending lateral fissures.	
MARGIN MORPHOLOGY	Generally diffuse but with marked toe bulges. Headscarp area tends to die out into areas of incipient fissuring.	
SPRAY FAN	None.	
OVERALL GEOMETRY	Teardrop-shaped areas of sliding slump failure.	
TRAVEL DISTANCE	Down slope movement is only of the order of a few tens of metres.	
TRAJECTORY	S-SW	

LOCATION	Sgurr na Conbhaire West, West Monar.	NH0842
FAILURE SCAR/SOURCE SLOPE		
HEIGHT	550 m.	
INCLINATION	27°	
CONCAVITY	Concave upper and convex lower slopes.	
LENGTH	1075 m.	
WIDTH	375 m.	
DEPTH	150 m.	
NATURE OF SLIP SURFACES	Schistosity planes.	
LINEATIONS/SLICKENFIBRES	None.	
GOUGE/INFILL	None.	
SCARP MORPHOLOGY	Headscarp in schistosity planes bounded NW-SE by sidewall fractures.	
GEOMETRY OF FAILURE	Sliding slump failure using schistosity as sliding planes.	
ASPECT	S	
RELATION TO LLR	Within LLR limits.	
GEOLOGICAL STRUCTURE	Moine psammities dipping c. 40° to the south.	
FAILURE POTENTIAL	Slight risk of rockfall activity.	
UNDERCUTTING	None.	
MECHANICAL WEAKENING	Tectonic shattering enhanced by slope movement.	
DEBRIS LOBE CHARACTERISTICS		
HEIGHT	500 m.	
INCLINATION	26°	
LENGTH	1000 m.	
WIDTH	250-375 m.	
DEPTH	150 m.	
CLAST SIZE	N/A	
CLAST ANGULARITY	N/A	
ABRASION/CRUSHING	N/A	
CLAST ALIGNMENT/ORIENTATION	N/A	
INTEGRITY OF 'SLIDE DEBRIS	Small amount of rockfall activity from the toe of the failure area. Greatest degree of disruption in the area just below the headscarp.	
RIDGE/TROUGH ORIENTATIONS	Lateral 'channels' trending 130-310° are up to 15 m wide and 5 m deep. Small obsequent scarps trend 080-260° across the slope and are up to 2 m high.	
MARGIN MORPHOLOGY	Well defined headscarp area and corresponding bulging toe area. Lateral margins are defined by 'channels'.	
SPRAY FAN	None.	
OVERALL GEOMETRY	Translational sliding slump failure of an area of c. 0.3 km ² .	
TRAVEL DISTANCE	Down slope movement of at least 150 m.	
TRAJECTORY	S	

GENERAL NOTES

Very large slump-type slope failure with a large degree of down slope movement but showing remarkably little internal disruption. Failure extends from almost the base of the slope to the summit of the hill.

LOCATION	Sgurr na Conbhaire East, West Monar.	NH0842
FAILURE SCAR/SOURCE SLOPE		
HEIGHT	210 m.	
INCLINATION	29°	
CONCAVITY	Convex slope.	
LENGTH	375 m.	
WIDTH	75 m.	
DEPTH	50-70 m.	
NATURE OF SLIP SURFACES	Schistosity planes.	
LINEATIONS/SLICKENFIBRES	None.	
GOUGE/INFILL	None.	
SCARP MORPHOLOGY	Headscarp composed of schistosity planes and bounded by sidewall fracture planes.	
GEOMETRY OF FAILURE	Sliding slump failure detached along schistosity sliding planes.	
ASPECT	S	
RELATION TO LLR	Within LLR limits.	
GEOLOGICAL STRUCTURE	Moine psammities dipping c. 40° to the south.	
FAILURE POTENTIAL	None of any consequence.	
UNDERCUTTING	None.	
MECHANICAL WEAKENING	Pervasive tectonic fracturing enhanced by slope movement.	
DEBRIS LOBE CHARACTERISTICS		
HEIGHT	165 m.	
INCLINATION	29°	
LENGTH	300 m.	
WIDTH	75 m.	
DEPTH	70 m.	
CLAST SIZE	N/A	
CLAST ANGULARITY	N/A	
ABRASION/CRUSHING	N/A	
CLAST ALIGNMENT/ORIENTATION	N/A	
INTEGRITY OF 'SLIDE DEBRIS	Small transverse obsequent scarps (<2.0 m high) traverse the failed area.	
RIDGE/TROUGH ORIENTATIONS	Transverse scarps trending 080-260°.	
MARGIN MORPHOLOGY	Well defined headscarp area and corresponding toe bulge. Lateral margins tend to be a bit more diffuse, merging with the surrounding hillside except in the lower reaches of the failure where there has been some lateral spreading of the debris.	
SPRAY FAN	None.	
OVERALL GEOMETRY	Translational slide with a small degree of lateral spreading. Affects an area of c. 0.05 km ² .	
TRAVEL DISTANCE	Down slope movement of at least 70 m.	
TRAJECTORY	S	

GENERAL NOTES

Smaller relation of the western failure.

LOCATION	Sgurr na Feartaig 1, Achnashellach.	NH0444
FAILURE SCAR/SOURCE SLOPE		
HEIGHT	137 m.	
INCLINATION	46°	
CONCAVITY	Convex slope.	
LENGTH	130 m.	
WIDTH	125 m.	
DEPTH	5-137 m.	
NATURE OF SLIP SURFACES	Schistosity planes.	
LINEATIONS/SLICKENFIBRES	None.	
GOUGE/INFILL	None.	
SCARP MORPHOLOGY	Headscarp of up to 5 m in height composed of a composite of joint sets.	
GEOMETRY OF FAILURE	Sliding of a rock 'buttress' (nose of a ridge) down schistosity planes.	
ASPECT	N	
RELATION TO LLR	Within LLR limits.	
GEOLOGICAL STRUCTURE	Moine psammities dipping to the SE and cut by a number of NW-SE faults.	
FAILURE POTENTIAL	Small degree of rockfall and possibly some slope creep possible.	
UNDERCUTTING	Glacially steepened corrie headwall.	
MECHANICAL WEAKENING	Extensive shattering of the country rock due to the proximity of several fault lineaments.	
DEBRIS LOBE CHARACTERISTICS		
HEIGHT	137 m.	
INCLINATION	46°	
LENGTH	130 m.	
WIDTH	125 m.	
DEPTH	5-137 m.	
CLAST SIZE	N/A	
CLAST ANGULARITY	N/A	
ABRASION/CRUSHING	N/A	
CLAST ALIGNMENT/ORIENTATION	N/A	
INTEGRITY OF 'SLIDE DEBRIS	Slump failure showing progression to a rock topple.	
RIDGE/TROUGH ORIENTATIONS	None.	
MARGIN MORPHOLOGY	Well defined headscarp but lateral margins are more diffuse, merging with the surrounding hillside.	
SPRAY FAN	None.	
OVERALL GEOMETRY	Oval-shaped failure area of sliding failure progressing to toppling failure	
TRAVEL DISTANCE	Down slope movement of c. 5 m.	
TRAJECTORY	N	

LOCATION	Sgurr na Feartaig 2, Achnashellach.	NH0444
FAILURE SCAR/SOURCE SLOPE		
HEIGHT	152 m.	
INCLINATION	31°	
CONCAVITY	Convex slope.	
LENGTH	250 m.	
WIDTH	200 m.	
DEPTH	Unknown.	
NATURE OF SLIP SURFACES	Schistosity planes.	
LINEATIONS/SLICKENFIBRES	None.	
GOUGE/INFILL	None.	
SCARP MORPHOLOGY	Low, arcuate headscarp.	
GEOMETRY OF FAILURE	Coire headwall failure.	
ASPECT	N	
RELATION TO LLR	Within LLR limits.	
GEOLOGICAL STRUCTURE	Moine psammites dipping to the SE cut by a number of NW-SE faults.	
FAILURE POTENTIAL	Slope creep possible due to the steep nature of the upper area of the failure.	
UNDERCUTTING	Glacially steepened corrie heawall.	
MECHANICAL WEAKENING	Extensive shattering of the rock mass due to the proximity of several fault lineaments.	
DEBRIS LOBE CHARACTERISTICS		
HEIGHT	152 m.	
INCLINATION	31°	
LENGTH	250 m.	
WIDTH	200 m.	
DEPTH	Unknown.	
CLAST SIZE	N/A	
CLAST ANGULARITY	N/A	
ABRASION/CRUSHING	N/A	
CLAST ALIGNMENT/ORIENTATION	N/A	
INTEGRITY OF 'SLIDE DEBRIS	Large area of failure that has undergone movement without major disruption of the rock mass.	
RIDGE/TROUGH ORIENTATIONS	None.	
MARGIN MORPHOLOGY	Well defined headscarp, but other margins are diffuse and merge with the surrounding undeformed slopes.	
SPRAY FAN	None.	
OVERALL GEOMETRY	Circular slump area.	
TRAVEL DISTANCE	Down slope movement of 1-2 m.	
TRAJECTORY	N	

LOCATION	Sgurr na Feartaig 3, Achnashellach.	NH0444
FAILURE SCAR/SOURCE SLOPE		
HEIGHT	180 m.	
INCLINATION	36°	
CONCAVITY	Convex slope.	
LENGTH	250 m.	
WIDTH	250 m.	
DEPTH	>10 m.	
NATURE OF SLIP SURFACES	Schistosity planes.	
LINEATIONS/SLICKENFIBRES	None.	
GOUGE/INFILL	None.	
SCARP MORPHOLOGY	Open fissures and small obsequent scarps	
GEOMETRY OF FAILURE	Block sliding.	
ASPECT	N	
RELATION TO LLR	Within LLR limits.	
GEOLOGICAL STRUCTURE	Moine psammities dipping to SE and cut by NW-SE trending fault lineaments.	
FAILURE POTENTIAL	Some slope creep possible.	
UNDERCUTTING	Glacially steepened corrie headwall.	
MECHANICAL WEAKENING	Extensive movement-induced shattering of the rock mass. Frost-shattering of the surrounding hillside.	
DEBRIS LOBE CHARACTERISTICS		
HEIGHT	180 m.	
INCLINATION	36°	
LENGTH	250 m.	
WIDTH	250 m.	
DEPTH	10-180 m.	
CLAST SIZE	N/A	
CLAST ANGULARITY	N/A	
ABRASION/CRUSHING	N/A	
CLAST ALIGNMENT/ORIENTATION	N/A	
INTEGRITY OF 'SLIDE DEBRIS	Disrupted by open fissures and transverse obsequent scarps.	
RIDGE/TROUGH ORIENTATIONS	Scarps and fissures trend 140-320°.	
MARGIN MORPHOLOGY	Poorly defined, deformation dies out into the surrounding hillside.	
SPRAY FAN	None.	
OVERALL GEOMETRY	Block sliding failure of a topographic buttress.	
TRAVEL DISTANCE	c 10 m downslope movement.	
TRAJECTORY	N	

LOCATION	Sgurr na Feartaig 4, Achnashellach.	NH0444
FAILURE SCAR/SOURCE SLOPE		
HEIGHT	365 m.	
INCLINATION	26°	
CONCAVITY	Convex slope.	
LENGTH	750 m.	
WIDTH	1250 m.	
DEPTH	c. 100 m.	
NATURE OF SLIP SURFACES LINEATIONS/ SLICKENFIBRES	Schistosity planes.	
GOUGE/INFILL	None.	
SCARP MORPHOLOGY	Headscarp up to 2 m high composed of 044-224° and 140-320° fractures.	
GEOMETRY OF FAILURE ASPECT	Block sliding failure. S	
RELATION TO LLR	Within LLR limits.	
GEOLOGICAL STRUCTURE	Moine psammites dipping to SE cut by numerous fault lineaments trending NW-SE.	
FAILURE POTENTIAL	Slope creep in the steeper sections of the slope possible.	
UNDERCUTTING	None.	
MECHANICAL WEAKENING	Extensive shattering of the rock mass due to the proximity of several fault lineaments.	
DEBRIS LOBE CHARACTERISTICS		
HEIGHT	365 m.	
INCLINATION	26°	
LENGTH	750 m.	
WIDTH	1250 m.	
DEPTH	c. 100 m.	
CLAST SIZE	N/A	
CLAST ANGULARITY	N/A	
ABRASION/CRUSHING	N/A	
CLAST ALIGNMENT/ ORIENTATION	N/A	
INTEGRITY OF 'SLIDE DEBRIS RIDGE/TROUGH ORIENTATIONS	Disrupted by development of extensive obsequent scarps. Scarps trend 082-262° across the slope.	
MARGIN MORPHOLOGY	Well defined headscarp but all other margins are diffuse and merge with the surrounding hillside.	
SPRAY FAN	None.	
OVERALL GEOMETRY	Block sliding of 0.9 km ² area of slope.	
TRAVEL DISTANCE	Down slope movement of at least 20 m.	
TRAJECTORY	S	

LOCATION	Beinn Tharsuinn, West Monar.	NH0543
FAILURE SCAR/SOURCE SLOPE		
HEIGHT	230 m.	
INCLINATION	29°	
CONCAVITY	Convex slope.	
LENGTH	400-450 m.	
WIDTH	600 m.	
DEPTH	>15 m.	
NATURE OF SLIP SURFACES	Basal slip along foliation planes dipping out of the slope.	
LINEATIONS/SLICKENFIBRES	None	
GOUGE/INFILL	Blue-grey fault gouge in a 020-200° fault zone adjacent to the base of the failure.	
SCARP MORPHOLOGY	Sub-vertical head scarp up to 3 m in height (partly debris obscured) below which is an area of forward rotated obsequent scarps.	
GEOMETRY OF FAILURE	Planar sliding failure with a small degree of forward rotation.	
ASPECT	E	
RELATION TO LLR	Within the LLR limits.	
GEOLOGICAL STRUCTURE	Locally moderately dipping Moine schists and psammities.	
FAILURE POTENTIAL	Movement of peripheral blocks of ≤ 40 cm noted in Spring 1989 due to freeze-thaw action.	
UNDERCUTTING	None.	
MECHANICAL WEAKENING	Extensive fault related fracturing.	
DEBRIS LOBE CHARACTERISTICS		
HEIGHT	230 m.	
INCLINATION	24°	
LENGTH	500 m.	
WIDTH	400-625 m.	
DEPTH	>15 m.	
CLAST SIZE	Fractured blocks up to 2 m across.	
CLAST ANGULARITY	Highly angular.	
ABRASION/CRUSHING	None.	
CLAST ALIGNMENT/ORIENTATION	None	
INTEGRITY OF 'SLIDE DEBRIS	Failure mass extensively fractured but has moved en-mass.	
RIDGE/TROUGH ORIENTATIONS	Several obsequent scarps parallel to the head scarp.	
MARGIN MORPHOLOGY	Well defined head, base and western lateral margins. That to the east merges with the surrounding hillside.	
SPRAY FAN	None.	
OVERALL GEOMETRY	Area of sliding failure with slumped head and bulging toe.	
TRAVEL DISTANCE	>30 m down slope.	
TRAJECTORY	E	

GENERAL NOTES

Area of typical sliding failure, adjacent to a fault showing evidence for recent movement.

LOCATION	Sgurr na Ruadhe, Strathfarrar.	NH2942
FAILURE SCAR/SOURCE SLOPE		
HEIGHT	245 m.	
INCLINATION	29°	
CONCAVITY	Convex slope.	
LENGTH	1000 m.	
WIDTH	300 m.	
DEPTH	>20 m.	
NATURE OF SLIP SURFACES	Schistosity and fracture surfaces.	
LINEATIONS/SLICKENFIBRES	None.	
GOUGE/INFILL	None.	
SCARP MORPHOLOGY	Shattered headscarp up to 10 m high, truncates frost shattered debris cover. Toppling has also occurred where the failed mass has moved away from the scarp area.	
GEOMETRY OF FAILURE	Slumping with zones of compression (scarps) and tension (gashes).	
ASPECT	S	
RELATION TO LLR	Within LLR limits.	
GEOLOGICAL STRUCTURE	Moine pelites and psammites dip steeply to the SW.	
FAILURE POTENTIAL	Rockfall from the headscarp area and possible slope creep from then steeper sections of the failed area.	
UNDERCUTTING	Glacially steepened slopes.	
MECHANICAL WEAKENING	Movement-enhanced shattering of the rock mass. Extensive frost shattering produces over 2 m thickness of cover.	
DEBRIS LOBE CHARACTERISTICS		
HEIGHT	200 m.	
INCLINATION	30°+	
LENGTH	900 m.	
WIDTH	300 m.	
DEPTH	>20 m.	
CLAST SIZE	N/A	
CLAST ANGULARITY	N/A	
ABRASION/CRUSHING	N/A	
CLAST ALIGNMENT/ORIENTATION	N/A	
INTEGRITY OF 'SLIDE DEBRIS	Extensively disrupted sliding slump failure showing progression to toppling failure.	
RIDGE/TROUGH ORIENTATIONS	Transverse, lateral and oblique scarps occur within the failure area. Tension gashes are orientated en-echelon to the scarps.	
MARGIN MORPHOLOGY	All margins are well defined due to the presence of lateral spreading allowing the formation of steep debris margins as it escapes the confines of the area of the scar.	
SPRAY FAN	None.	
OVERALL GEOMETRY	Lobe-shaped sliding slump with a degree of lateral spreading the further the failure progresses down slope.	
TRAVEL DISTANCE	Down slope movement of at least 50 m.	
TRAJECTORY	S	

GENERAL NOTES

Similar failures are found in Coire Gorm [NH2942], Sgurr a' Choire Ghlais [NH2541] and Sgurr Fhuar-thuil [NH2343].

LOCATION	An Socach, Loch Mullardoch.	NH0933
FAILURE SCAR/SOURCE SLOPE		
HEIGHT	650 m.	
INCLINATION	22°	
CONCAVITY	Convex upper slope and concave lower slope.	
LENGTH	Unknown; deformation gradually dies out down slope.	
WIDTH	Unknown; deformation gradually dies out across slope.	
DEPTH	20 m minimum.	
NATURE OF SLIP SURFACES	Schistosity planes.	
LINEATIONS/SLICKENFIBRES	None.	
GOUGE/INFILL	None.	
SCARP MORPHOLOGY	Scarps are remarkably planar and are of constant height over distances of up to 500 m. Scarp faces themselves are vertical or nearly so.	
GEOMETRY OF FAILURE	Translational sliding down schistosity planes over a slope area of >1 km ² .	
ASPECT	WNW	
RELATION TO LLR	Within LLR limits.	
GEOLOGICAL STRUCTURE	Complex folding within Moine psammities and pelites, general dip to the SW.	
FAILURE POTENTIAL	None.	
UNDERCUTTING	None.	
MECHANICAL WEAKENING	Fracturing accentuated by down slope movement.	
DEBRIS LOBE CHARACTERISTICS		
HEIGHT	650 m.	
INCLINATION	22°	
LENGTH	Unknown.	
WIDTH	Unknown.	
DEPTH	At least 20 m.	
CLAST SIZE	N/A	
CLAST ANGULARITY	N/A	
ABRASION/CRUSHING	N/A	
CLAST ALIGNMENT/ORIENTATION	N/A	
INTEGRITY OF 'SLIDE DEBRIS	Large slope area cut by low relief obsequent scarps. Little or no internal deformation.	
RIDGE/TROUGH	Transverse scarps with remarkably straight trajectories across the hillside.	
ORIENTATIONS	NNE-SSW	
MARGIN MORPHOLOGY	Extremely diffuse margins. The limit of the area of failure has not been discerned.	
SPRAY FAN	None.	
OVERALL GEOMETRY	Translational slide or lateral spreading of entire hillside.	
TRAVEL DISTANCE	Few metres down slope.	
TRAJECTORY	WNW	

GENERAL NOTES

Large area of slope that has undergone limited failure with the development of extremely long and planar scarp ridges that traverse the hillside for distances of up to 500 m. May be surface manifestation of rebound faulting.

LOCATION	An Riabhachan, Loch Mullardoch.	NH1133
FAILURE SCAR/SOURCE SLOPE		
HEIGHT	240 m.	
INCLINATION	28°	
CONCAVITY	Concave slope.	
LENGTH	450 m.	
WIDTH	250 m.	
DEPTH	c. 20 m.	
NATURE OF SLIP SURFACES	Schistosity planes.	
LINEATIONS/SLICKENFIBRES	None.	
GOUGE/INFILL	None.	
SCARP MORPHOLOGY	Headscarp formed by the intersection of schistosity planes with the ridge crest on one side and NW-SE fractures on the other.	
GEOMETRY OF FAILURE	Translational sliding down schistosity planes with sidewall release along NW-SE trending fractures.	
ASPECT	S	
RELATION TO LLR	Within LLR limits.	
GEOLOGICAL STRUCTURES	SW dipping Moine schists.	
FAILURE POTENTIAL	None.	
UNDERCUTTING	Glacially steepened corrie headwall.	
MECHANICAL WEAKENING	Extensive fracturing trending both NW-SE and NE-SW, the latter orientation being sub-parallel to the trend of the nearby Strathconon fault zone.	
DEBRIS LOBE CHARACTERISTICS		
HEIGHT	240 m.	
INCLINATION	28°	
LENGTH	450 m.	
WIDTH	100-250 m.	
DEPTH	c. 20 m.	
CLAST SIZE	N/A	
CLAST ANGULARITY	N/A	
ABRASION/CRUSHING	N/A	
CLAST ALIGNMENT/ORIENTATION	N/A	
INTEGRITY OF 'SLIDE DEBRIS	Very little internal disruption of the failure area, only small obsequent and fracture parallel scarps generally less than 1 m high.	
RIDGE/TROUGH ORIENTATIONS	Scarps parallel the main fracture orientations i.e. NNW-NW and NE.	
MARGIN MORPHOLOGY	Well defined headscarp area but all other margins merge with the surrounding hillside.	
SPRAY FAN	None.	
OVERALL GEOMETRY	Translational block sliding along schistosity planes	
TRAJECTORY	S	

GENERAL NOTES

One of several slope failures in the area adjacent to the surface trace of the Strathconon fault.

LOCATION	An Riabhachan, Loch Mullardoch.	NH1233
FAILURE SCAR/SOURCE SLOPE		
HEIGHT	390 m.	
INCLINATION	32°	
CONCAVITY	Concave slope.	
LENGTH	625 m.	
WIDTH	250 m.	
DEPTH	>50 m.	
NATURE OF SLIP SURFACES	Schistosity planes.	
LINEATIONS/SLICKENFIBRES	None.	
GOUGE/INFILL	None.	
SCARP MORPHOLOGY	30 m high headscarp formed by 020-200° trending vertical or sub-vertical fracture planes.	
GEOMETRY OF FAILURE	Translational block slide progressing with increasing disruption to rock toppling.	
ASPECT	SSW	
RELATION TO LLR	Within LLR limits.	
GEOLOGICAL STRUCTURE	Moine schists dip to SWW at 60-70°.	
FAILURE POTENTIAL	Rockfall possible from the more unstable scarps and headscarp areas.	
UNDERCUTTING	Glacially steepened slopes.	
MECHANICAL WEAKENING	Extensive fracturing due to the proximity to the Strathconon fault zone.	
DEBRIS LOBE CHARACTERISTICS		
HEIGHT	340 m.	
INCLINATION	35°	
LENGTH	600 m.	
WIDTH	250 m.	
DEPTH	>50 m.	
CLAST SIZE	Blocks up to 2 m across.	
CLAST ANGULARITY	Highly angular.	
ABRASION/CRUSHING	Impact fracturing of the larger blocks.	
CLAST ALIGNMENT/ ORIENTATION	None.	
INTEGRITY OF 'SLIDE DEBRIS	Highly disrupted area near the head of the failure area where scarps have degraded into rockfalls and topples of limited transport distance. Scarps parallel and sub-parallel to the main fracture orientations occur throughout the failure area.	
RIDGE/TROUGH ORIENTATIONS	Scarps trend parallel to the main fracture orientations i.e. NNW and WNW.	
MARGIN MORPHOLOGY	Headscarp is well defined by an area of cliffs up to 30 m in height. Lateral margins and toe of the failure are marked by prominent ridges or hollows where the debris has been subject to lateral spreading.	
SPRAY FAN	None.	
OVERALL GEOMETRY	Deep-seated translational block slide that shows progression to toppling and rockfall activity.	
TRAVEL DISTANCE	Down slope movement of at least 50 m.	
TRAJECTORY	S.	

GENERAL NOTES

Large, disruptive translational block sliding failure detaching along schistosity planes.

LOCATION	An Riabhachan, Loch Mullardoch.	NH1433
FAILURE SCAR/SOURCE SLOPE		
HEIGHT	275 m.	
INCLINATION	23°	
CONCAVITY	Concave slope.	
LENGTH	625 m.	
WIDTH	300 m.	
DEPTH	>10 m.	
NATURE OF SLIP SURFACES/ LINEATIONS/ SLICKENFIBRES	Schistosity surfaces.	
GOUGE/INFILL	None.	
SCARP MORPHOLOGY	6 m high scarp formed in 060-240° and 160-340° fractures.	
GEOMETRY OF FAILURE	Translational block sliding along schistosity planes with little internal deformation.	
ASPECT	S	
RELATION TO LLR	Within LLR limits.	
GEOLOGICAL STRUCTURE	Moine pelites and psammites dip moderately steeply to the S and SSW.	
FAILURE POTENTIAL	Some slope creep possible?	
UNDERCUTTING	Glacially steepened slope.	
MECHANICAL WEAKENING	Pervasive tectonic fracturing due to the proximity to the Strathconon fault zone.	
DEBRIS LOBE CHARACTERISTICS		
HEIGHT	260 m.	
INCLINATION	23°	
LENGTH	620 m.	
WIDTH	125-300 m.	
DEPTH	>10 m.	
CLAST SIZE	N/A	
CLAST ANGULARITY	N/A	
ABRASION/CRUSHING	N/A	
CLAST ALIGNMENT/ ORIENTATION	N/A	
INTEGRITY OF 'SLIDE DEBRIS	Basically 'intact' block sliding failure with limited down slope movement and therefore limited degree of scarp development.	
RIDGE/TROUGH ORIENTATIONS	Small scarps less than 1 m in height and tension gashes that parallel the trend of the backing joints that form the headscarp	
MARGIN MORPHOLOGY	Well defined headscarp and lateral margins where the area of failure is joint controlled. Toe of the failure area is marked by a steep frontal scarp.	
SPRAY FAN	None.	
OVERALL GEOMETRY	Sliding slump failure with little or no rotation involved during down slope movement.	
TRAVEL DISTANCE	At least 6 m vertical movement.	
TRAJECTORY	S	

LOCATION	Sgurr na Lapaich, Glen Cannich.	NH1634
FAILURE SCAR/SOURCE SLOPE		
HEIGHT	380 m.	
INCLINATION	18°	
CONCAVITY	Convex upper and concave lower slope.	
LENGTH	1000 m.	
WIDTH	500 m.	
DEPTH	>100 m.	
NATURE OF SLIP SURFACES/ LINEATIONS/ SLICKENFIBRES	Sliding along schistosity planes.	
GOUGE/INFILL	None.	
SCARP MORPHOLOGY	Obsequent scarps formed parallel to the headscarp, which in turn is sub-parallel to schistosity.	
GEOMETRY OF FAILURE	Ridge-crest foundering leading to sliding slump failure with associated rockfall due to degradation of the scarp outcrops.	
ASPECT	S	
RELATION TO LLR	Within LLR limits. Top of Sgurr na Lapaich was a nunatak at this time.	
GEOLOGICAL STRUCTURE	Steeply dipping Moine Psammities and pelites tightly folded into N-S trending folds.	
FAILURE POTENTIAL	Some rockfall from shattered scarps.	
UNDERCUTTING	Glaciated corrie.	
MECHANICAL WEAKENING	Extensively shattered rock.	
DEBRIS LOBE CHARACTERISTICS		
HEIGHT	380 m.	
INCLINATION	18-32°	
LENGTH	500 m.	
WIDTH	500-1000 m.	
DEPTH	>100 m.	
CLAST SIZE	N/A	
CLAST ANGULARITY	N/A	
ABRASION/CRUSHING	N/A	
CLAST ALIGNMENT/ ORIENTATION	N/A	
INTEGRITY OF 'SLIDE DEBRIS	Ridge-crest foundering has led to extensive fracturing of the rock mass. Also cut by obsequent scarps up to 4 m high that have been disrupted to form rockfalls.	
RIDGE/TROUGH ORIENTATIONS	Obsequent scarps are parallel to sub-parallel to the ridge crest. Between scarps are en-echelon tension hollows.	
MARGIN MORPHOLOGY	Limit of failure area is controlled by topography.	
SPRAY FAN	None.	
OVERALL GEOMETRY	Ridge-crest foundering of an area of c. 0.5 km ² .	
TRAVEL DISTANCE	>20 m of down slope movement.	
TRAJECTORY	S	

GENERAL NOTES

Large scale slope failure exhibiting all the features of ridge-crest foundering as described by Jibson (1987) and attributed to topographically amplified seismic shaking. Low angle fractures with irregular spacing (1.5-2.0 m) cut 'intact' outcrops - possible neotectonic fractures or stress release joints.

LOCATION	Beinn Fhionnlaidh, Glen Affric.	NH 1128
FAILURE SCAR/SOURCE SLOPE		
HEIGHT	120 m.	
INCLINATION	25°	
CONCAVITY	Concave slope.	
LENGTH	250 m.	
WIDTH	200 m.	
DEPTH	>20 m.	
NATURE OF SLIP SURFACES/ LINEATIONS/ SLICKENFIBRES	Fracture planes dipping out of the slope at c. 40°.	
GOUGE/INFILL	None.	
SCARP MORPHOLOGY	Prominent, planar headscarp up to 20 m in height.	
GEOMETRY OF FAILURE ASPECT	Simple block sliding failure.	
RELATION TO LLR	W	
GEOLOGICAL STRUCTURE	Within LLR limits.	
FAILURE POTENTIAL	Complex folding of Moine psammities and pelites.	
UNDERCUTTING	None.	
MECHANICAL WEAKENING	Glacially steepened slopes.	
	None present except for the regionally pervasive fracture orientations.	
DEBRIS LOBE CHARACTERISTICS		
HEIGHT	120 m.	
INCLINATION	25°	
LENGTH	250 m.	
WIDTH	125-200 m.	
DEPTH	>20 m.	
CLAST SIZE	N/A	
CLAST ANGULARITY	N/A	
ABRASION/CRUSHING	N/A	
CLAST ALIGNMENT/ ORIENTATION	N/A	
INTEGRITY OF 'SLIDE DEBRIS	Large block subject to sliding without any internal disruption.	
RIDGE/TROUGH ORIENTATIONS	None.	
MARGIN MORPHOLOGY	Well defined headscarp area above an area of slope bulging.	
SPRAY FAN	None.	
OVERALL GEOMETRY	Simple block sliding failure.	
TRAVEL DISTANCE	At least 20 m of vertical movement.	
TRAJECTORY	W	

GENERAL NOTES

Block sliding failure of a remarkably large intact block.

LOCATION	Beinn Fhionnlaidh, Glen Affric.	NH 1128
FAILURE SCAR/SOURCE SLOPE		
HEIGHT	210 m.	
INCLINATION	23°	
CONCAVITY	Concave slope	
LENGTH	500 m.	
WIDTH	325 m.	
DEPTH	Unknown.	
NATURE OF SLIP SURFACES/ LINEATIONS/ SLICKENFIBRES/ GOUGE/INFILL	Out of slope dipping low angle fractures.	
SCARP MORPHOLOGY	None.	
GEOMETRY OF FAILURE	None.	
ASPECT	No headscarp visible.	
RELATION TO LLR	Surficial (block) sliding failure with a small degree of toppling failure	
GEOLOGICAL STRUCTURE	W	
FAILURE POTENTIAL	Within the LLR limits.	
UNDERCUTTING	Complexly folded Moine psammities and pelites.	
MECHANICAL WEAKENING	None.	
	Glacially steepened slopes.	
	None, except for the regionally pervasive fracture orientations.	
DEBRIS LOBE CHARACTERISTICS		
HEIGHT	210 m.	
INCLINATION	23°	
LENGTH	500 m.	
WIDTH	250-325 m.	
DEPTH	Unknown.	
CLAST SIZE	N/A	
CLAST ANGULARITY	N/A	
ABRASION/CRUSHING	N/A	
CLAST ALIGNMENT/ ORIENTATION	N/A	
INTEGRITY OF 'SLIDE DEBRIS	Down slope movement has induced some disruption of the failure area and produced limited development of toppling failure.	
RIDGE/TROUGH ORIENTATIONS	Low transverse ridges cut across the area of failure.	
MARGIN MORPHOLOGY	Obscure margins, only observable from a distance.	
SPRAY FAN	None.	
OVERALL GEOMETRY	Simple block sliding failure with some development of toppling failure.	
TRAVEL DISTANCE	Few tens of metres of downslope movement.	
TRAJECTORY	W	

LOCATION	Beinn Fhionnlaidh, Glen Affric.	NH 1128
FAILURE SCAR/SOURCE SLOPE		
HEIGHT	335 m.	
INCLINATION	28°	
CONCAVITY	Convex slope area.	
LENGTH	625 m.	
WIDTH	125 m.	
DEPTH	>50 m.	
NATURE OF SLIP SURFACES	Schistosity and low angle fracture planes dipping out of the slope.	
LINEATIONS/SLICKENFIBRES	None.	
GOUGE/INFILL	None.	
SCARP MORPHOLOGY	Large area of shattered outcrops up to 50 m high formed by a number of fracture orientations. Individual fracture planes can be up to 20 m high.	
GEOMETRY OF FAILURE	Block sliding failure that in some instances shows progression to toppling and rockfall activity.	
ASPECT	W	
RELATION TO LLR	Within the limits of the LLR.	
GEOLOGICAL STRUCTURE	Moine psammities and pelites show complex folding but in the area of failure schistosity dips out of the slope.	
FAILURE POTENTIAL	Rockfall from the headscarp area.	
UNDERCUTTING	Glacially steepened slopes.	
MECHANICAL WEAKENING	None other than regional fracture sets.	
DEBRIS LOBE CHARACTERISTICS		
HEIGHT	335 m.	
INCLINATION	28°	
LENGTH	500 m.	
WIDTH	125-250 m.	
DEPTH	>50 m.	
CLAST SIZE	Blocks of up to 10 m across.	
CLAST ANGULARITY	Highly angular.	
ABRASION/CRUSHING	Some impact fracturing.	
CLAST ALIGNMENT/ORIENTATION	No alignment, although rockfall activity has occurred as as 'mobile' streams that extend down the full length of the area of failure.	
INTEGRITY OF 'SLIDE DEBRIS	Block sliding failure that has been subject to extensive disruption by toppling failure and rockfall activity.	
RIDGE/TROUGH ORIENTATIONS	Obsequent scarps and tension hollows parallel the fracture orientations of the headscarp area.	
MARGIN MORPHOLOGY	Well defined headscarp area and debris margins.	
SPRAY FAN	None.	
OVERALL GEOMETRY	Block sliding failure showing extensive internal disruption.	
TRAVEL DISTANCE	>50 m, rockfall debris has moved up to 200 m downslope.	
TRAJECTORY	W	
GENERAL NOTES		
Extensive internal disruption and the 'mobile' nature of the rockfall debris streams strongly suggests a seismic trigger for slope failure initiation.		

LOCATION	Carn na Con Dhu West, Glen Affric.	NH0724
FAILURE SCAR/SOURCE SLOPE		
HEIGHT	300-425 m.	
INCLINATION	38°	
CONCAVITY	Convex slope.	
LENGTH	c. 400 m.	
WIDTH	500 m.	
DEPTH	>50 m.	
NATURE OF SLIP SURFACES	Toppling failure using low angle joints and detachment along NE-SW and E-W trending schistosity planes.	
LINEATIONS/SLICKENFIBRES	None.	
GOUGE/INFILL	None.	
SCARP MORPHOLOGY	Extreme disruption of the ridge crest using ridge-parallel fracture planes.	
GEOMETRY OF FAILURE ASPECT	Block flexural topple. W	
RELATION TO LLR	Within LLR limits.	
GEOLOGICAL STRUCTURE	Complex folding of Moine psammities and pelites forming a SW plunging synform.	
FAILURE POTENTIAL	Extremely unstable areas of rock on steep slopes with high risk of rockfall activity.	
UNDERCUTTING	Glacially oversteepened slope.	
MECHANICAL WEAKENING	Extensive shattering of the surrounding rock as a consequence of slope failure.	

DEBRIS LOBE CHARACTERISTICS

HEIGHT	300-425 m.
INCLINATION	38°
LENGTH	c. 400 m.
WIDTH	500 m.
DEPTH	>50 m.
CLAST SIZE	Blocks are generally greater than 20 m across.
CLAST ANGULARITY	Highly angular.
ABRASION/CRUSHING	None evident.
CLAST ALIGNMENT/ORIENTATION	None.
INTEGRITY OF 'SLIDE DEBRIS	Disrupted block flexural toppling has left a highly disaggregated rock mass.
RIDGE/TROUGH ORIENTATIONS	Ridge crest parallel scarps and fissures in the upper area that has only undergone partial failure.
MARGIN MORPHOLOGY	Deformation of the slope dies out in all directions except along the ridge crest where it merges with a slump failure that affects the eastern slopes of the hill.
SPRAY FAN	None.
OVERALL GEOMETRY	Large area of toppling failure that forms part of an area of ridge crest foundering affecting the whole hill.
TRAVEL DISTANCE	Down slope movement of at least 50 m.
TRAJECTORY	W

GENERAL NOTES

Part of an area of ridge crest foundering affecting the whole hillside. This type of failure is considered to be diagnostic of seismic activity (Jibson 1987). Best example of its type in Scotland known to the author.

LOCATION	Carn na Con Dhu East, Glen Affric.	NH0724
FAILURE SCAR/SOURCE SLOPE		
HEIGHT	450 m.	
INCLINATION	22°	
CONCAVITY	Concave slope.	
LENGTH	1125 m.	
WIDTH	1375 m.	
DEPTH	>100 m.	
NATURE OF SLIP SURFACES/ LINEATIONS/ SLICKENFIBRES	Out of slope sliding failure fractures.	
GOUGE/INFILL	None.	
SCARP MORPHOLOGY	Shattered ridge crest area, common with the failure on the western slopes of the ridge, composed of numerous obsequent scarps.	
GEOMETRY OF FAILURE	Large scale sliding slump with extensive development of obsequent scarps.	
ASPECT	E	
RELATION TO LLR	Within LLR limits.	
GEOLOGICAL STRUCTURE	Complex folding of Moine psammites and pelites to form a SW plunging synform.	
FAILURE POTENTIAL	Possible rockfall from the more shattered scarp faces.	
UNDERCUTTING	Glaciated slopes, but no evidence for any great deal of undercutting.	
MECHANICAL WEAKENING	Rock mass extensively shattered by slope movement disaggregating the rock along pre-existing fractures.	
DEBRIS LOBE CHARACTERISTICS		
HEIGHT	450 m.	
INCLINATION	22°	
LENGTH	1125 m.	
WIDTH	1375 m.	
DEPTH	>100 m.	
CLAST SIZE	N/A	
CLAST ANGULARITY	N/A	
ABRASION/CRUSHING	N/A	
CLAST ALIGNMENT/ ORIENTATION	N/A	
INTEGRITY OF 'SLIDE DEBRIS	Large area of slump failure that is traversed by numerous cross slope obsequent scarps. Some of the larger scarps, especially toward the shattered ridge crest, have been the source for rockfall activity.	
RIDGE/TROUGH ORIENTATIONS	Numerous obsequent scarps traverse the slope parallel or sub-parallel to the ridge crest.	
MARGIN MORPHOLOGY	Well defined headscarp area and toe bulge, but lateral margins merge with the surrounding hillside.	
SPRAY FAN	None.	
OVERALL GEOMETRY	Large area of slump failure, with local areas of outward toppling.	
TRAVEL DISTANCE	Downslope movement of at least 50 m.	
TRAJECTORY	E	

GENERAL NOTES

Eastern section of an area of failure affecting the entire ridge crest of Carn na Con Dhu. Morphology is that of 'Ridge-crest foundering', typically associated with seismic activity.

LOCATION	Mam Sodhail, Glen Affric.	NH1125
FAILURE SCAR/SOURCE SLOPE		
HEIGHT	?325 m.	
INCLINATION	24°	
CONCAVITY	Slightly convex slope.	
LENGTH	Unknown.	
WIDTH	Unknown.	
DEPTH	Unknown.	
NATURE OF SLIP SURFACES	Schistosity planes.	
LINEATIONS/SLICKENFIBRES	None.	
GOUGE/INFILL	None.	
SCARP MORPHOLOGY	No headscarp area.	
GEOMETRY OF FAILURE	?Shallow translational slide with little displacement.	
ASPECT	WNW	
RELATION TO LLR	Within LLR limits.	
GEOLOGICAL STRUCTURE	Complex folding within Moine psammities and pelites.	
FAILURE POTENTIAL	None.	
UNDERCUTTING	None.	
MECHANICAL WEAKENING	Pervasive tectonic joint and fracture patterns.	
DEBRIS LOBE CHARACTERISTICS		
HEIGHT	?325 m.	
INCLINATION	24°	
LENGTH	Unknown.	
WIDTH	≥100 m.	
DEPTH	Unknown.	
CLAST SIZE	N/A.	
CLAST ANGULARITY	N/A.	
ABRASION/CRUSHING	N/A.	
CLAST ALIGNMENT/		
ORIENTATION	N/A.	
INTEGRITY OF 'SLIDE DEBRIS	Slump failure with the development of small obsequent scarps.	
RIDGE/TROUGH ORIENTATIONS	Transverse across the slope for distances of up to 100 m. Scarps are generally <1 m high.	
MARGIN MORPHOLOGY	Margins of the failed area are not discernible.	
SPRAY FAN	None.	
OVERALL GEOMETRY	Shallow translational slide.	
TRAVEL DISTANCE	Few tens of metres downslope movement.	
TRAJECTORY	WNW	

LOCATION	Mam Sodhail, Glen Affric.	NH1125
FAILURE SCAR/SOURCE SLOPE		
HEIGHT	c. 280 m.	
INCLINATION	31°	
CONCAVITY	Convex slope.	
LENGTH	c. 330 m.	
WIDTH	c. 500 m.	
DEPTH	Unknown, at least 50 m.	
NATURE OF SLIP SURFACES	Low angle fractures dipping to the SE.	
LINEATIONS/SLICKENFIBRES	None.	
GOUGE/INFILL	None.	
SCARP MORPHOLOGY	Headscarp marked by a 010-190° trending hollow to the east of the summit.	
GEOMETRY OF FAILURE	Block sliding failure with little or no internal deformation of the rock mass.	
ASPECT	W	
RELATION TO LLR	Within the LLR limits.	
GEOLOGICAL STRUCTURE	Complex folding within the Moine psammites and pelites.	
FAILURE POTENTIAL	None.	
UNDERCUTTING	None.	
MECHANICAL WEAKENING	Frost-shattering of the scarps and pervasive regional tectonic shattering of the country rock.	
DEBRIS LOBE CHARACTERISTICS		
HEIGHT	c. 280 m.	
INCLINATION	31°	
LENGTH	c. 330 m.	
WIDTH	c. 500 m.	
DEPTH	Unknown, at least 50 m.	
CLAST SIZE	N/A	
CLAST ANGULARITY	N/A	
ABRASION/CRUSHING	N/A	
CLAST ALIGNMENT/ORIENTATION	N/A	
INTEGRITY OF 'SLIDE DEBRIS	Downslope slumped block slide disturbed by a few obsequent scarps of <1 m in height.	
RIDGE/TROUGH ORIENTATIONS	Transverse across the slope.	
MARGIN MORPHOLOGY	Extremely diffuse margins, only the hollow possibly defining the head of the failure area gives any indication of the extent of the area of the failure.	
SPRAY FAN	None.	
OVERALL GEOMETRY	Block sliding failure with little downslope movement or internal disruption.	
TRAVEL DISTANCE	Few tens of metres.	
TRAJECTORY	W	

GENERAL NOTES

Seemingly large area of slope failure but with little downslope movement and little internal deformation.

LOCATION	Coire Coulavie, Glen Affric	NH1124
FAILURE SCAR/SOURCE SLOPE		
HEIGHT	210 m.	
INCLINATION	31°	
CONCAVITY	Convex upper slope and concave lower slope.	
LENGTH	500 m.	
WIDTH	750 m.	
DEPTH	>50 m.	
NATURE OF SLIP SURFACES	Low angle fractures dipping to the SE.	
LINEATIONS/SLICKENFIBRES	None.	
GOUGE/INFILL	None.	
SCARP MORPHOLOGY	10 m. high headscarp composed of a composite set of backing joint sets. Extensive shattering of the rock and toppling of the more intact blocks.	
GEOMETRY OF FAILURE	Block sliding failure with toppling failure in the area of the headscarp. More shattered scarp faces have given rise to extensive rockfall activity.	
ASPECT	SE	
RELATION TO LLR	Within LLR limits.	
GEOLOGICAL STRUCTURE	Area of complex folding of Moine psammities and pelites.	
FAILURE POTENTIAL	Rockfall from the more unstable scarp areas.	
UNDERCUTTING	Glacially steepened corrie headwall.	
MECHANICAL WEAKENING	Extensive shattering of the rock mass enhanced by movement-induced disruption.	
DEBRIS LOBE CHARACTERISTICS		
HEIGHT	210 m.	
INCLINATION	31°	
LENGTH	500 m.	
WIDTH	500-750 m.	
DEPTH	>50 m.	
CLAST SIZE	Some large boulders up to 10 m across.	
CLAST ANGULARITY	Highly angular.	
ABRASION/CRUSHING	Impact crushing.	
CLAST ALIGNMENT/ORIENTATION	None.	
INTEGRITY OF 'SLIDE DEBRIS	Block sliding failure with disruption of the upper area by toppling and rockfall activity.	
RIDGE/TROUGH	Ridges and open clefts parallel the headscarp fracture orientations.	
ORIENTATIONS	Scarps parallel to the headscarp and up to 5 m in height.	
MARGIN MORPHOLOGY	Well defined headscarp area but all other margins tend to be diffuse, merging with the surrounding undeformed hillside.	
SPRAY FAN	None.	
OVERALL GEOMETRY	Block sliding failure with secondary toppling leading to rockfall activity.	
TRAVEL DISTANCE	Downslope movement of at least 50 m.	
TRAJECTORY	SE	

GENERAL NOTES

Complex area of slope failure that extends from the ridge crest area almost to the floor of the corrie below. Extreme disruption and ridge crest position of the failure suggest a seismic trigger for slope failure.

LOCATION	Sgurr na Lapaich, Glen Affric.	NH1524
FAILURE SCAR/SOURCE SLOPE		
HEIGHT	290 m.	
INCLINATION	38°	
CONCAVITY	Convex slope.	
LENGTH	375 m.	
WIDTH	1125 m.	
DEPTH	Unknown: dimensions of the failure area suggest >100 m.	
NATURE OF SLIP SURFACES	Low angle joint surfaces dipping out of the slope.	
LINEATIONS/SLICKENFIBRES	None.	
GOUGE/INFILL	None.	
SCARP MORPHOLOGY	Long continuous headscarp up to 10 m in height with numerous splay fractures creating an en-echelon array of scarps all downthrowing away from the headscarp.	
GEOMETRY OF FAILURE	Large volume slope collapse caused by sliding on low angle fractures and schistosity surfaces.	
ASPECT	N	
RELATION TO LLR	Within the LLR limits.	
GEOLOGICAL STRUCTURE	Complex folding within Moine psammites and pelites. Regional strike to the NW.	
FAILURE POTENTIAL	Slope creep possible from the steeper areas.	
UNDERCUTTING	Glaciated slopes.	
MECHANICAL WEAKENING	Extensive shattering of the rock mass enhanced by slope movement.	
DEBRIS LOBE CHARACTERISTICS		
HEIGHT	290 m.	
INCLINATION	38°	
LENGTH	375 m.	
WIDTH	1000-1125 m.	
DEPTH	Unknown, >100 m.	
CLAST SIZE	N/A	
CLAST ANGULARITY	N/A	
ABRASION/CRUSHING	N/A	
CLAST ALIGNMENT/ORIENTATION	N/A	
INTEGRITY OF 'SLIDE DEBRIS	Extremely large sliding slump failure that shows remarkably little disruption for the size of the failure. The only disruption being several sets of scarps in the upper section of the failed area adjacent to the headscarp. Majority of the slope is unaffected by surface disruption except for shattering of outcrops.	
RIDGE/TROUGH ORIENTATIONS	Several scarps parallel to an en-echelon to the headscarp in the immediate vicinity of the ridge crest.	
MARGIN MORPHOLOGY	Well defined headscarp but all other margins tend to be more diffuse, merging with the surrounding hillside.	
SPRAY FAN	None.	
OVERALL GEOMETRY	Ridge crest failure of large slope area by way of (block) sliding slump failure.	
TRAVEL DISTANCE	At least 10 m downslope movement. Most displacement internally accommodated?	
TRAJECTORY	N	
GENERAL NOTES		
Large scale slope failure that corresponds with the ridge crest failures of Jibson (1987) attributed to seismically-induced slope failure. Backing scarp probably the surface expression of rebound faulting.		

LOCATION	Sgurr na Lapaich, Glen Affric.	NH1424
FAILURE SCAR/SOURCE SLOPE		
HEIGHT	140 m.	
INCLINATION	40°	
CONCAVITY	Convex slope.	
LENGTH	250 m.	
WIDTH	500 m.	
DEPTH	Unknown, at least 50 m.	
NATURE OF SLIP SURFACES	Low angle joint surfaces and schistosity planes.	
LINEATIONS/SLICKENFIBRES	None.	
GOUGE/INFILL	None.	
SCARP MORPHOLOGY	Prominent headscarp area composed of multiple scarp orientations. Several obsequent scarps parallel to the headscarp.	
GEOMETRY OF FAILURE	Block sliding failure with a small degree of rotational slumping.	
ASPECT	N	
RELATION TO LLR	Within the LLR limits.	
GEOLOGICAL STRUCTURE	Complex folding within Moine psammites and pelites, regional strike to the NW.	
FAILURE POTENTIAL	Rockfall from the steeper more disrupted sections of the slope along with the possibility of slope creep.	
UNDERCUTTING	Glacially oversteepened slope.	
MECHANICAL WEAKENING	Extensive regional development of joint patterns enhanced by slope movement.	
DEBRIS LOBE CHARACTERISTICS		
HEIGHT	210 m.	
INCLINATION	40°	
LENGTH	250 m.	
WIDTH	500 m.	
DEPTH	At least 50 m.	
CLAST SIZE	N/A	
CLAST ANGULARITY	N/A	
ABRASION/CRUSHING	N/A	
CLAST ALIGNMENT/ORIENTATION	N/A	
INTEGRITY OF 'SLIDE DEBRIS	Extensively fractured rock mass with some progression to rockfall activity where the scarps are most disrupted. More disruption than the main Sgurr na Lapaich slope failure.	
RIDGE/TROUGH ORIENTATIONS	Small transverse ridges up to 1 m in height are developed in the area immediately below the headscarp.	
MARGIN MORPHOLOGY	Margins are diffuse, all merging with the surrounding undeformed hillside. Even the headscarp is a poorly developed feature developed in several fracture planes that extend for almost the whole width of the ridge.	
SPRAY FAN	None.	
OVERALL GEOMETRY	Large area of block sliding with progression to minor rockfall activity.	
TRAVEL DISTANCE	c. 10 m down slope movement.	
TRAJECTORY	N	
GENERAL NOTES		
Ridge crest failure in the ridge mid-point area that would be subject to the greatest seismic amplification (Jibson 1987).		

LOCATION	Sgurr na Lapaich, Glen Affric.	NH1324
FAILURE SCAR/SOURCE SLOPE		
HEIGHT	30 m.	
INCLINATION	40°	
CONCAVITY	Concave slope.	
LENGTH	250 m.	
WIDTH	90 m.	
DEPTH	At least 30 m.	
NATURE OF SLIP SURFACES	NW and NE trending sub-vertical fractures act as backing joints.	
LINEATIONS/SLICKENFIBRES	None.	
GOUGE/INFILL	None.	
SCARP MORPHOLOGY	Shattered headscarp area.	
GEOMETRY OF FAILURE	Rockfall detached along steep NW and NE trending joint.	
ASPECT	S	
RELATION TO LLR	Within LLR limits.	
GEOLOGICAL STRUCTURE	Complex folding within Moine psammites and pelites, regional strike to the NE.	
FAILURE POTENTIAL	Further rockfall likely from the unstable headscarp area.	
UNDERCUTTING	Glacially oversteepened slopes.	
MECHANICAL WEAKENING	Extensive regional fracturing of the rock mass.	
DEBRIS LOBE CHARACTERISTICS		
HEIGHT	210 m.	
INCLINATION	40°	
LENGTH	250 m.	
WIDTH	50-90 m.	
DEPTH	At least 30 m.	
CLAST SIZE	Up to 5 m across.	
CLAST ANGULARITY	Highly angular.	
ABRASION/CRUSHING	Impact crushing of the blocks.	
CLAST ALIGNMENT/ORIENTATION	None.	
INTEGRITY OF 'SLIDE DEBRIS RIDGE/TROUGH	Highly disrupted rockfall.	
ORIENTATIONS	None.	
MARGIN MORPHOLOGY	Diffuse due to lateral spreading of the debris stream on an unconfined slope.	
SPRAY FAN	None.	
OVERALL GEOMETRY	Catastrophic rockfall.	
TRAVEL DISTANCE	c. 180 m.	
TRAJECTORY	S	

GENERAL NOTES

Post-glacial catastrophic rockfall in close proximity to two ridge crest disruptive failures, generally thought to be the result of seismic activity (Keefer 1984).

LOCATION	An Sornach, Glen Affric.	NH0921
FAILURE SCAR/SOURCE SLOPE		
HEIGHT	400 m.	
INCLINATION	38°	
CONCAVITY	Convex slope.	
LENGTH	500 m.	
WIDTH	875 m.	
DEPTH	>70 m.	
NATURE OF SLIP SURFACES	Fractures dipping out of the slope.	
LINEATIONS/SLICKENFIBRES	None.	
GOUGE/INFILL	None.	
SCARP MORPHOLOGY	Headscarp formed from the intersection of a number of fracture sets. Sidewall fractures parallel to 'fault lineament' of Holmes (1984).	
GEOMETRY OF FAILURE	Major slump failure associated with differential block movement due to isostatic rebound.	
ASPECT	S	
RELATION TO LLR	Within LLR limits.	
GEOLOGICAL STRUCTURE	Moine psammites and pelites folded to give variable dips to SE and NW.	
FAILURE POTENTIAL	Rockfall from unstable, shattered scarp faces.	
UNDERCUTTING	Glaciated glen, but no obvious oversteepening.	
MECHANICAL WEAKENING	Pervasive regional fracture patterns.	

DEBRIS LOBE CHARACTERISTICS

HEIGHT	400 m.
INCLINATION	38°
LENGTH	500 m.
WIDTH	800-875 m.
DEPTH	>70 m.
CLAST SIZE	N/A
CLAST ANGULARITY	N/A
ABRASION/CRUSHING	N/A
CLAST ALIGNMENT/ ORIENTATION	N/A
INTEGRITY OF 'SLIDE DEBRIS	Failed area is cut by obsequent scarps trending across the slope. These have acted as latter release points for rockfall and toppling activity.
RIDGE/TROUGH ORIENTATIONS	Major obsequent scarps trend across the slope, while smaller scarps in between show more random orientation, generally en-echelon to the larger scarps.
MARGIN MORPHOLOGY	Margins are well marked by well developed scarps or hollows fronting the bulging areas of the failure.
SPRAY FAN	None.
OVERALL GEOMETRY	Elliptical slope area that has under gone slump failure in response to underlying differential block movement.
TRAVEL DISTANCE	At least 50 m down slope movement.
TRAJECTORY	S

GENERAL NOTES

The slumped mass is cut by a 123-303° trending 'fault' scarp that extends outwith the area of failure. Above the area of failure it alters trajectory to 330-340°. Where it crosses the headscarp there is a preponderance of 60-80°/130° fractures. This doesn't seem to be a true fault scarp, but the surface expression of differential block movement in response to isostatic rebound, that in turn was probably the trigger for slope failure initiation.

LOCATION	Fraoch-choire, Glen Affric.	NH1019
FAILURE SCAR/SOURCE SLOPE		
HEIGHT	370 m.	
INCLINATION	23°	
CONCAVITY	Slightly concave.	
LENGTH	875 m.	
WIDTH	250 m.	
DEPTH	>30 m.	
NATURE OF SLIP SURFACES	Out of slope dipping fracture planes.	
LINEATIONS/SLICKENFIBRES	Basal sliding surfaces show groove lineations parallel to the direction of failure movement.	
GOUGE/INFILL	None	
SCARP MORPHOLOGY	Basal sliding fractures intersect the slope and form a headscarp with headwall release fractures on the ridge crest.	
GEOMETRY OF FAILURE	Basal sliding failure with a small degree of slumping and backward rotation.	
ASPECT	NW	
RELATION TO LLR	Within LLR limits.	
GEOLOGICAL STRUCTURE	Moine psammities dip into the slope.	
FAILURE POTENTIAL	Possible rockfall from shattered sidewall scarps.	
UNDERCUTTING	Fluvial undercutting at the base of the slope.	
MECHANICAL WEAKENING	Pervasive regional fracturing.	
DEBRIS LOBE CHARACTERISTICS		
HEIGHT	300 m.	
INCLINATION	26°	
LENGTH	625 m.	
WIDTH	250 m.	
DEPTH	>30 m.	
CLAST SIZE	Boulders up to 5 m across.	
CLAST ANGULARITY	Highly angular.	
ABRASION/CRUSHING	Impact crushing of underlying blocks.	
CLAST ALIGNMENT/ORIENTATION	Some 'jig-saw-fit' boulders.	
INTEGRITY OF 'SLIDE DEBRIS RIDGE/TROUGH	Disrupted rockslide.	
ORIENTATIONS	Transverse ridges and lateral 'levee' ridges.	
MARGIN MORPHOLOGY	Well defined steep margins (up to 37°).	
SPRAY FAN	None.	
OVERALL GEOMETRY	Rock mass of $6.8-7.5 \times 10^5 \text{ m}^3$ has failed as a disrupted block slide.	
TRAVEL DISTANCE	Down slope movement of 300 m+	
TRAJECTORY	NW	

GENERAL NOTES

Holmes (1984) states that this is a wedge failure - no mention of the 43°/273° basal sliding planes or the extensively disrupted nature of the failed mass. This is similar to example described by Eisbacher (1979) from the Canadian Rockies attributed to seismic activity.

LOCATION	Bcinn Fhada, Gleann Lichd	NH0018
FAILURE SCAR/SOURCE SLOPE		
HEIGHT	840 m.	
INCLINATION	31°	
CONCAVITY	Convex slope.	
LENGTH	1300 m.	
WIDTH	2000 m.	
DEPTH	>100 m.	
NATURE OF SLIP SURFACES	Joint surfaces dipping sub-parallel to the slope.	
LINEATIONS/SLICKENFIBRES	Scarp face rugosities imply dip-slip movement.	
GOUGE/INFILL	None.	
SCARP MORPHOLOGY	Obsequent scarps trend across the hillside. Uphill faces are c. 80° and up to 7 m high. Head scarp is formed from a number of intersecting fracture orientations. This is up to 90 m in height.	
GEOMETRY OF FAILURE	Sliding failure with compressional scarps- thrusting despite the implied dip-slip movement on the scarp faces.	
ASPECT	SW	
RELATION TO LLR	Within the limits of the LLR.	
GEOLOGICAL STRUCTURE	Moine schists dipping steeply to SE.	
FAILURE POTENTIAL	Possible slope creep and rockfall from areas of unstable scarps.	
UNDERCUTTING	Ice erosion at the base of the slope. Little or no present day fluvial undercutting.	
MECHANICAL WEAKENING	Some fracturing due to the proximity of the Allt Ruighe nam Freumh fault.	
DEBRIS LOBE CHARACTERISTICS		
HEIGHT	840 m.	
INCLINATION	31°	
LENGTH	1250 m.	
WIDTH	1500-2000 m.	
DEPTH	>100 m.	
CLAST SIZE	Up to 5 m in diameter below the larger scarps. Generally c. 1 m.	
CLAST ANGULARITY	Angular, blocky debris.	
ABRASION/CRUSHING	None.	
CLAST ALIGNMENT/ORIENTATION	None.	
INTEGRITY OF 'SLIDE DEBRIS	Except for minor rockfall activity slope failure is only disrupted by transverse obsequent scarps.	
RIDGE/TROUGH ORIENTATIONS	Scarps trend across the slope in an arcuate manner (concave upslope).	
MARGIN MORPHOLOGY	Margins merge with the surrounding hillside. Even above the well marked head scarp is an area of incipient failure shown by the abundance of open fissures.	
SPRAY FAN	None	
OVERALL GEOMETRY	Large scale slump failure.	
TRAVEL DISTANCE	Downslope movement of at least 200 m.	
TRAJECTORY	S-SW	

GENERAL NOTES

Large sliding failure with exceptionally large obsequent scarps. These scarps impound the local drainage. The headscarp is up to 90 m high and merely marks the end of major slope disturbance, as above this is an area of incipient failure. Obsequent scarps are up to 700 m long and generally 5-7 m in height, spaced at about 50 m apart.

LOCATION	Sgurr na Carnach, Glen Shiel.	NG9715
FAILURE SCAR/SOURCE SLOPE		
HEIGHT	200 m.	
INCLINATION	45°	
CONCAVITY	Convex slope.	
LENGTH	200 m.	
WIDTH	200 m.	
DEPTH	>100 m.	
NATURE OF SLIP SURFACES	Toppling from 110-290° backing fractures.	
LINEATIONS/SLICKENFIBRES	Backing fractures show concentric plumose tension patterns on fracture faces.	
GOUGE/INFILL	None.	
SCARP MORPHOLOGY	Single headscarp up to 60 m high steeply dipping into the hillside.	
GEOMETRY OF FAILURE	Block topple progressing into confined rockfall.	
ASPECT	SSW	
RELATION TO LLR	Within LLR limits.	
GEOLOGICAL STRUCTURE	Moine psammites dip steeply (>60°) to the E	
FAILURE POTENTIAL	Further rockfall from the Headscarp area.	
UNDERCUTTING	Extensive gullying at the base of the failure area.	
MECHANICAL WEAKENING	Rock mass is extensively shattered due to the proximity of the 'Five Sisters' fault swarm.	
DEBRIS LOBE CHARACTERISTICS		
HEIGHT	150 m.	
INCLINATION	40-45°	
LENGTH	200 m.	
WIDTH	150-200 m.	
DEPTH	>100 m.	
CLAST SIZE	Up to 10 m across. Average c. 2 m.	
CLAST ANGULARITY	Highly angular.	
ABRASION/CRUSHING	Impact crushing of larger blocks.	
CLAST ALIGNMENT/ORIENTATION	None.	
INTEGRITY OF 'SLIDE DEBRIS	Highly disrupted to form a confined rockfall.	
RIDGE/TROUGH ORIENTATIONS	Tension gashes in the slope above the headscarp.	
MARGIN MORPHOLOGY	Well defined margins - rockfall debris!	
SPRAY FAN	None.	
OVERALL GEOMETRY	Rock block topple progressing into a confined rockfall.	
TRAVEL DISTANCE	Down slope movement of c. 100 m.	
TRAJECTORY	SSW	

GENERAL NOTES

Rockfall showing excess travel distance due to the confined nature of its travel path. Probable sturzstrom-type activity if it did not have to follow such a confined trajectory.

LOCATION	Sgurr na Ciste Duibhe, Glen Shiel	NG9814
FAILURE SCAR/SOURCE SLOPE		
HEIGHT	760 m.	
INCLINATION	c. 23°	
CONCAVITY	Convex base and concave upper slope.	
LENGTH	1750 m.	
WIDTH	750 m.	
DEPTH	>50 m.	
NATURE OF SLIP SURFACES	Slip surfaces are fractures dipping c. 20° more than the slope angle.	
LINEATIONS/SLICKENFIBRES	Present on fault surfaces and suggest downthrow to the SSW.	
GOUGE/INFILL	Some fractures have epidote covered faces.	
SCARP MORPHOLOGY	Transverse obsequent scarps with steep faces (c. 40°), generally 1-4 m in height.	
GEOMETRY OF FAILURE	Complex sliding failure also involving toppling, rockfall, slumping and backward rotation.	
ASPECT	S	
RELATION TO LLR	Within the limits of LLR.	
GEOLOGICAL STRUCTURE	Moine schists dipping steeply to the E.	
FAILURE POTENTIAL	Possible rockfall from the larger scarps and cliff faces created by toppling failure.	
UNDERCUTTING	Incision by the River Shiel and glacial oversteepening.	
MECHANICAL WEAKENING	Extensive fracturing due to the 'Five Sisters fault swarm'.	
DEBRIS LOBE CHARACTERISTICS		
HEIGHT	760 m.	
INCLINATION	23°	
LENGTH	1750 m.	
WIDTH	500-750 m.	
DEPTH	>50 m.	
CLAST SIZE	Generally c. 1 m, but toppled blocks are up to 5 m across.	
CLAST ANGULARITY	Highly angular blocky debris.	
ABRASION/CRUSHING	None	
CLAST ALIGNMENT/ORIENTATION	None.	
INTEGRITY OF 'SLIDE DEBRIS	Disrupted block sliding failure that has degenerated into rockfalls and rock topples.	
RIDGE/TROUGH ORIENTATIONS	Obsequent scarps are transverse to the slope (120-300°). Tension gashes are oblique to the scarp orientations.	
MARGIN MORPHOLOGY	Diffuse, area of failure merges with the surrounding hillside.	
SPRAY FAN	None.	
OVERALL GEOMETRY	Teardrop-shaped area of block sliding failure.	
TRAVEL DISTANCE	Downslope displacement of at least 50 m.	
TRAJECTORY	S	

GENERAL NOTES

The area of failure seems to exhibit the classic features of rotational failure with a slumped head and a bulging toe. However this is complicated by areas of compression (obsequent scarps) and extension (en-echelon fissures, toppling and slumping) occurring at random across the area of failure. Obsequent scarp faces steepen up hill showing an additional degree of toppling acting after the initial slump failure.

LOCATION	Sgurr a' Bhealaich Dheirg	NH0213
FAILURE SCAR/SOURCE SLOPE		
HEIGHT	485 m.	
INCLINATION	26°	
CONCAVITY	Convex lower and slightly concave upper slope.	
LENGTH	1000 m.	
WIDTH	600 m.	
DEPTH	>100 m.	
NATURE OF SLIP SURFACES	Fractures dipping c. 60° to SE i.e. sub-parallel to the slope	
LINEATIONS/SLICKENFIBRES	None	
GOUGE/INFILL	None	
SCARP MORPHOLOGY	Large obsequent scarps up to 6 m in height trending 300-340° cut across the middle section of the failure area.	
GEOMETRY OF FAILURE ASPECT	Slump failure. SW	
RELATION TO LLR	Within the LLR limits.	
GEOLOGICAL STRUCTURE	Moine schists and psammites dip c. 80° to E.	
FAILURE POTENTIAL	Some slope creep and rockfall on oversteepened slopes.	
UNDERCUTTING	Glacial steepening of the slopes.	
MECHANICAL WEAKENING	Extensive fracturing due to the proximity of the 'Five Sisters' and Cluanie fault swarms.	
DEBRIS LOBE CHARACTERISTICS		
HEIGHT	485 m.	
INCLINATION	26° (Steepens c. 40° in area of scarps)	
LENGTH	1000 m.	
WIDTH	250-600 m.	
DEPTH	Unknown, at least 100 m.	
CLAST SIZE	None	
CLAST ANGULARITY	None	
ABRASION/CRUSHING	None	
CLAST ALIGNMENT/ ORIENTATION	None	
INTEGRITY OF 'SLIDE DEBRIS	Large block sliding mass disrupted by the presence of an area of intense obsequent scarp development.	
RIDGE/TROUGH ORIENTATIONS	Obsequent scarps, up to 5 m in height, traverse the slope as continuous features up to 200 m in length, dying out as they bifurcate and decrease in size.	
MARGIN MORPHOLOGY	Well defined slumped head on the ridge crest. All other margins are diffuse, merging with the surrounding hillside.	
SPRAY FAN	None	
OVERALL GEOMETRY	Pear-shaped area of sliding-slump failure.	
TRAVEL DISTANCE	c. 20 m vertical movement at the head scarp, but unknown amount of downslope movement.	
TRAJECTORY	S-SW	

GENERAL NOTES

Large scale sliding-slump failure related to vertical rebound movement of the Cluanie-'Five Sisters' fault swarm. Hollows created by scarps are now filled with peat and silted-up lochans created by scarp impoundment of local drainage courses. Similar failure occurs on the adjacent hillside of Saileag.

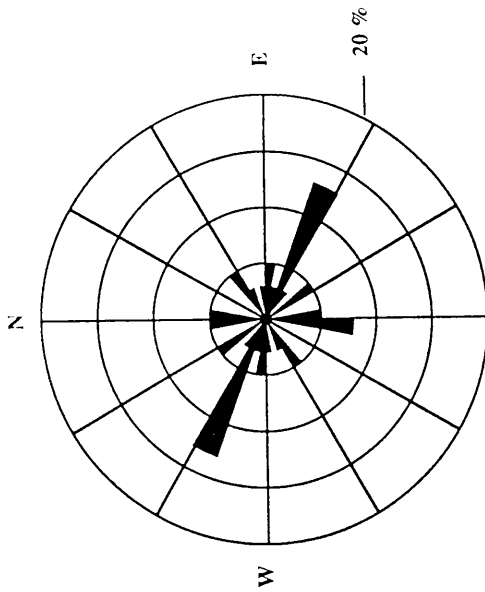
LOCATION	Sgurr Fhuaran, Glen Shiel.	NG9716
FAILURE SCAR/SOURCE SLOPE		
HEIGHT	300 m.	
INCLINATION	40-45°	
CONCAVITY	Slightly convex slope.	
LENGTH	300 m.	
WIDTH	150 m.	
DEPTH	>50 m.	
NATURE OF SLIP SURFACES	Toppling out from 114-294° and 72°/274° fracture planes.	
LINEATIONS/SLICKENFIBRES	None, only plumose tension release fracture faces.	
GOUGE/INFILL	None	
SCARP MORPHOLOGY	Headscarp up to 30 m high dipping into the hillside.	
GEOMETRY OF FAILURE	Toppling failure with progression to complete failure by rockfall.	
ASPECT	SSW	
RELATION TO LLR	Within LLR limits.	
GEOLOGICAL STRUCTURE	Moine schists and psammites dip steeply to the E.	
FAILURE POTENTIAL	Rockfall from shattered headscarp.	
UNDERCUTTING	Extreme gullying at the base of the failure area.	
MECHANICAL WEAKENING	Extensive fracture development and associated shattering due to the proximity to the 'Five Sisters' fault swarm.	
DEBRIS LOBE CHARACTERISTICS		
HEIGHT	400 m.	
INCLINATION	35-40°	
LENGTH	350-400 m.	
WIDTH	50-80 m.	
DEPTH	10-50 m.	
CLAST SIZE	Up to 5 m, average 1.5 m.	
CLAST ANGULARITY	Highly angular.	
ABRASION/CRUSHING	Smaller underlying blocks have been shattered due to the impact of larger blocks.	
CLAST ALIGNMENT/ ORIENTATION	None.	
INTEGRITY OF 'SLIDE DEBRIS	Toppled upper section has degraded into a catastrophic rockfall.	
RIDGE/TROUGH ORIENTATIONS	None.	
MARGIN MORPHOLOGY	Confined by topography of the gully. Upper toppled area dies out as an area of tension gashes and obsequent scarps.	
SPRAY FAN	None.	
OVERALL GEOMETRY	Rock topple progressing to a catastrophic rockfall	
TRAVEL DISTANCE	c. 200 m downslope for rockfall debris.	
TRAJECTORY	S-SW	

GENERAL NOTES

Simple topple and incipient failure that has progressed to complete failure in its lower portion to give a confined rockfall into a narrow gully that has enhanced the transport distance of the debris.

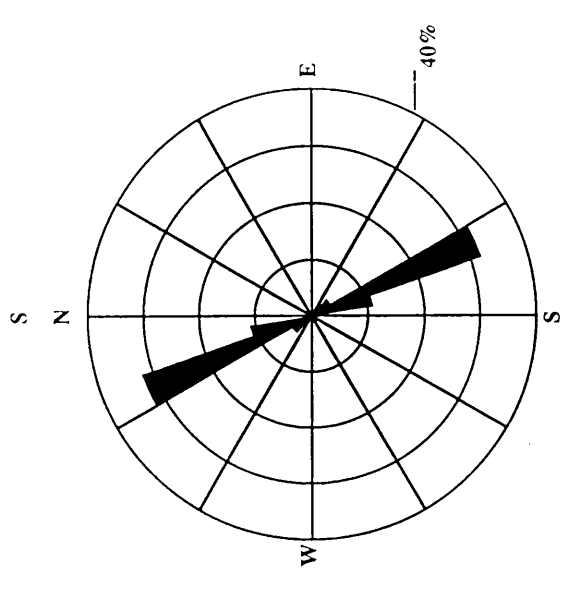
Appendix B

Rose diagrams of neotectonic faults and fractures described in *Chapter 2*. All fractures measured show evidence for recent movement, either offsetting glacial surfaces and late-glacial or post-glacial deposits. All fractures are of 'fresh' appearance i.e. they are open fractures containing loose unconsolidated breccia or soft fault gouge material.



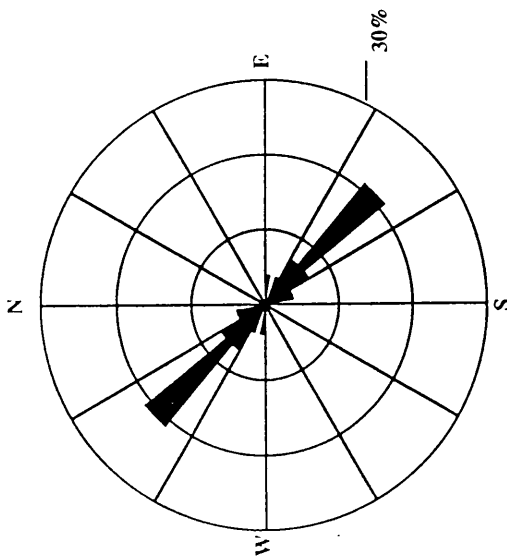
Garbh Chuire Mor
n = 40

Major Trend = 295°
Percentage = 13%



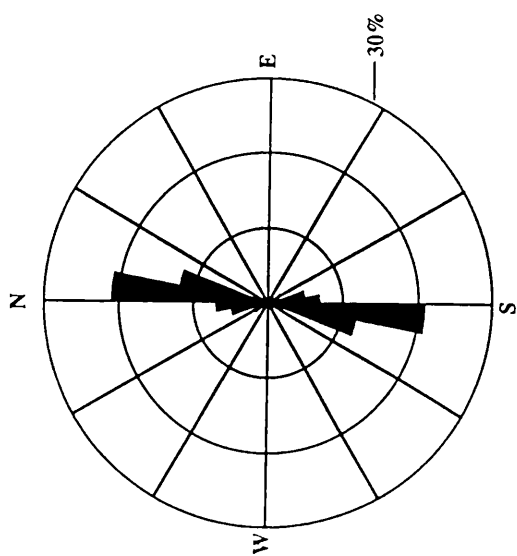
Beinn Alligin
n = 28

Major Trend = 155°
Percentage = 32%



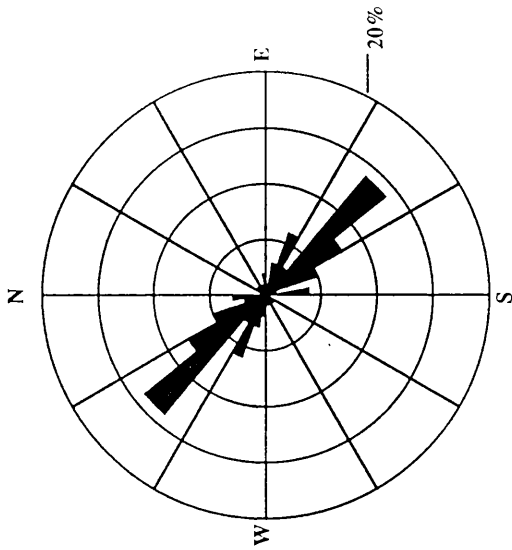
Coire Mor
n = 28

Major Trend = 135°
Percentage = 21%

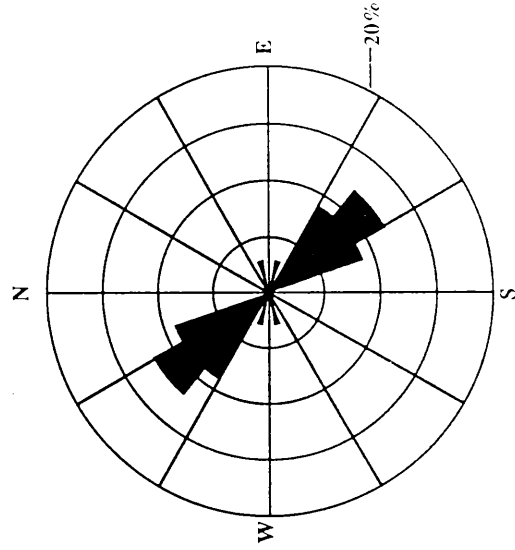


Strath Vaich
n = 42

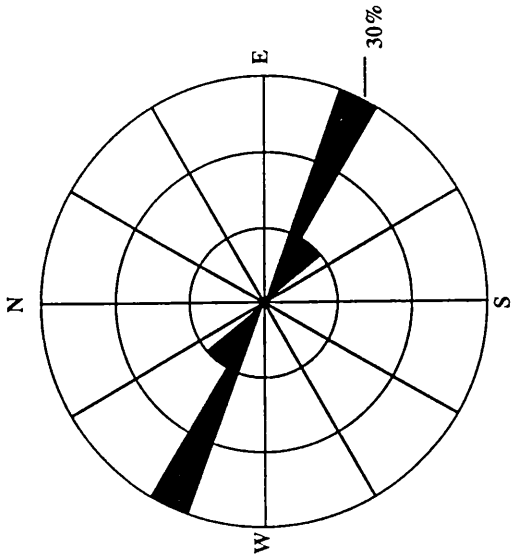
Major Trend = 185°
Percentage = 21%



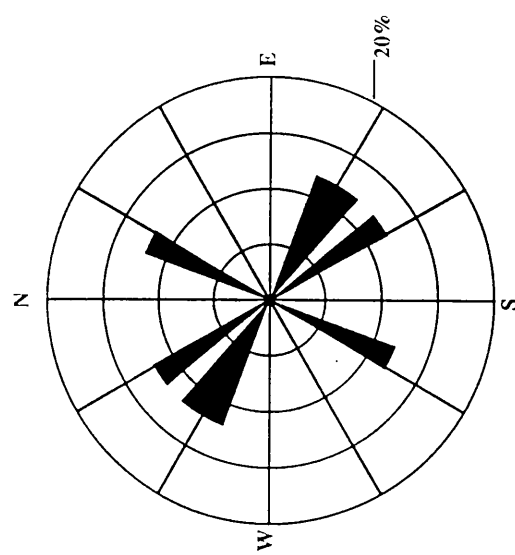
Scardroy
 n = 150
 Major Trend = 315°
 Percentage = 14%



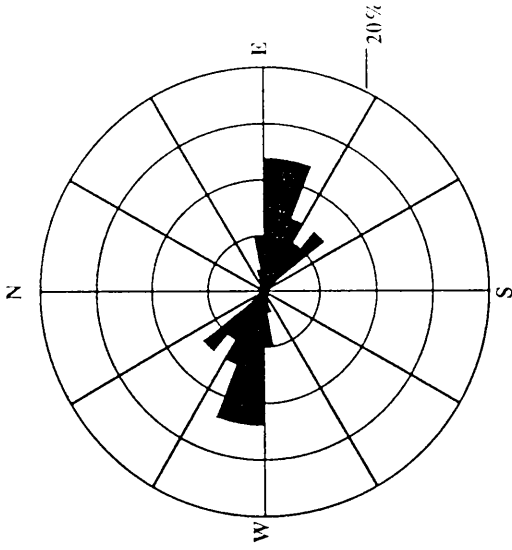
Bac nan Eich
 n = 32
 Major Trend = 135°
 Percentage = 12%



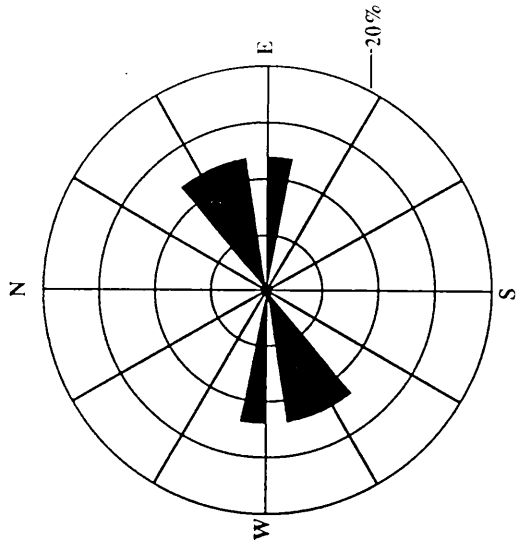
Cuaig
 n = 10
 Major Trend = 295°
 Percentage = 30%



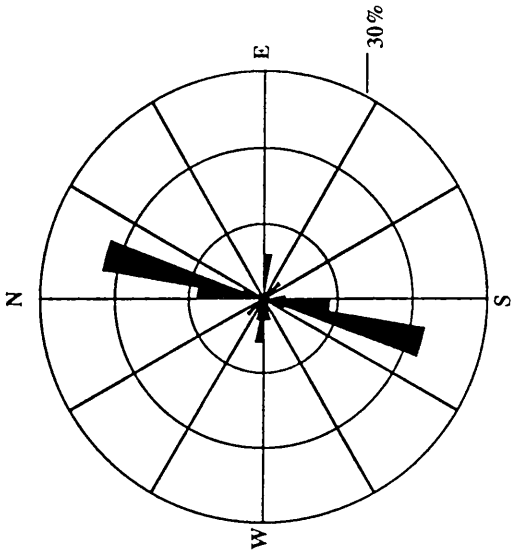
Loch Marce (L. Crann)
 n = 8
 Major Trend = 115°
 Percentage = 12%



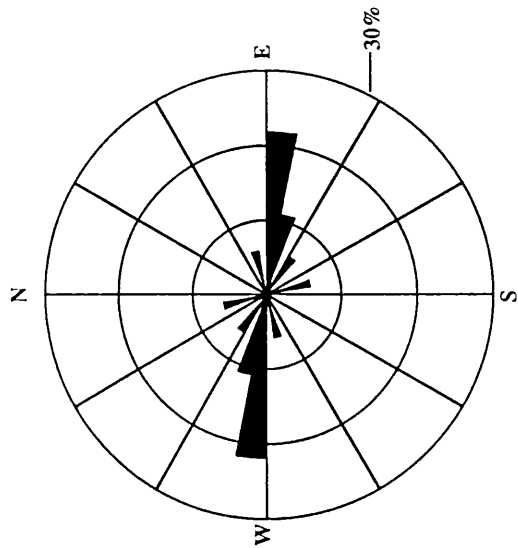
Coire Eoghainn
 n = 42
 Major Trend = 285°
 Percentage = 12%



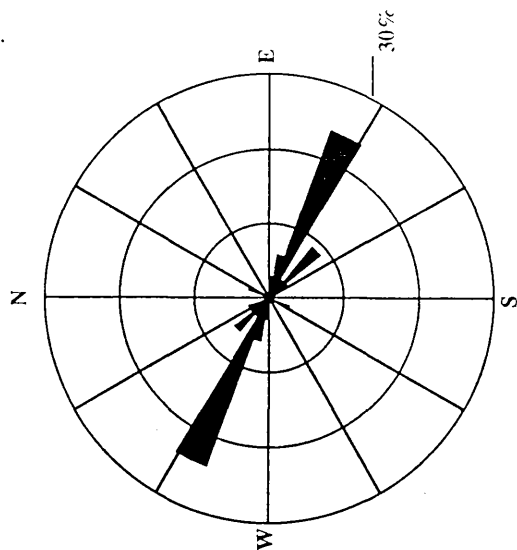
Glen Elchaig
 (Strathconon Fault)
 n = 8
 Major Trend = 095°
 Percentage = 12%



Beinn Tharsuinn
 n = 32
 Major Trend = 015°
 Percentage = 22%

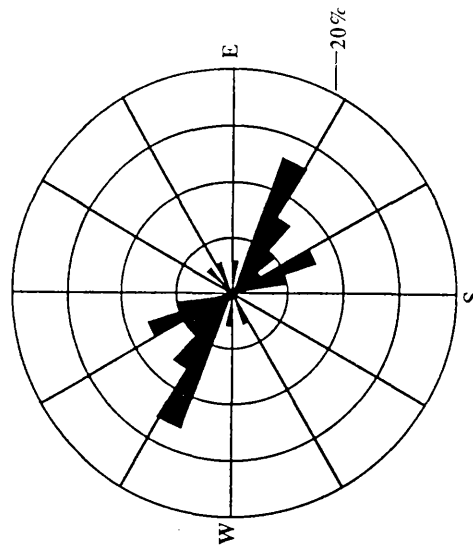


Loch Monar
 n = 18
 Major Trend = 095°
 Percentage = 22%



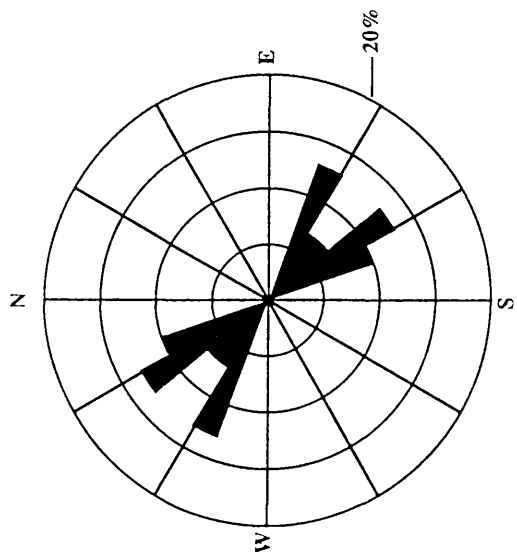
Gleann Lichd
n = 34

Major Trend = 29S°
Percentage = 24%



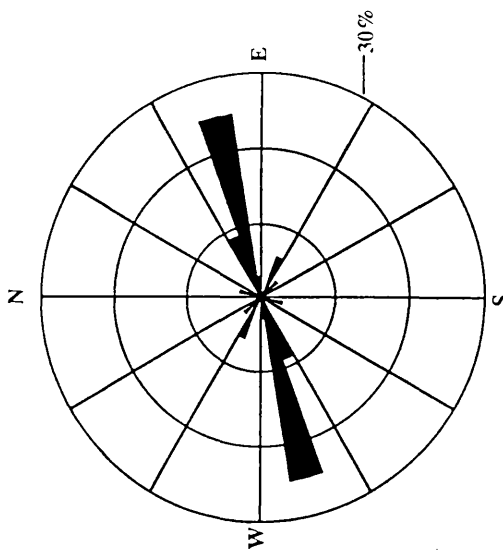
Creag nam Damh
n = 38

Major Trend = 115°
Percentage = 13%



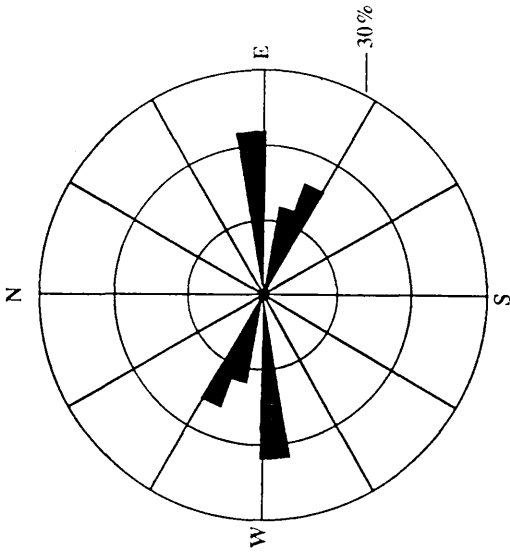
An Sornach
n = 30

Major Trend = 115°
Percentage = 13%



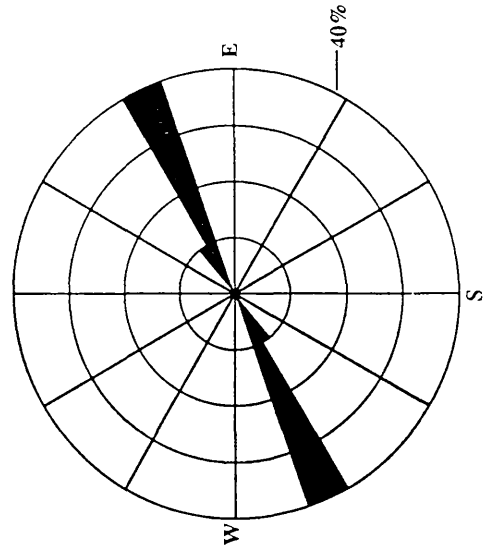
Sruir na Lapaich
n = 32

Major Trend = 075°
Percentage = 25%



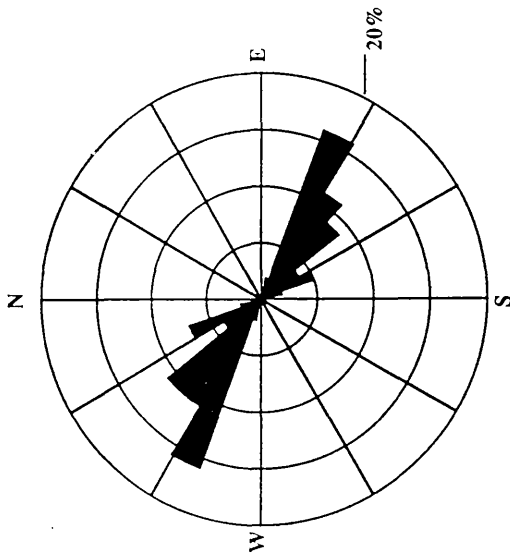
Arnisdale
n = 32

Major Trend = 85°
Percentage = 22%



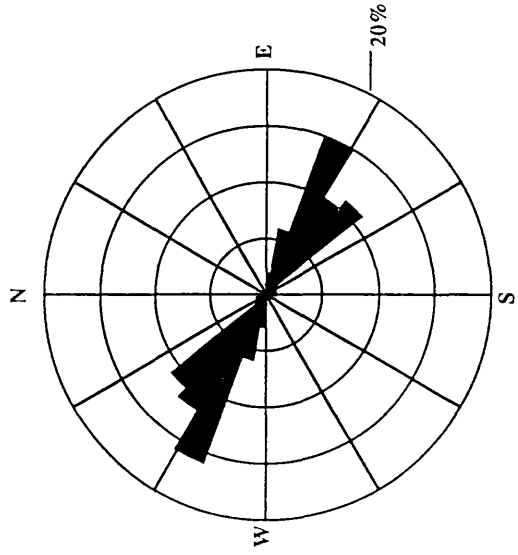
Coire Dhu
n = 10

Major Trend = 065°
Percentage = 40%



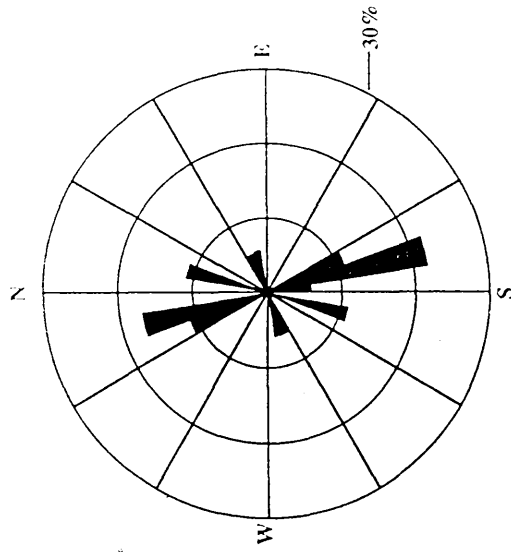
Sgurr a' Bhealaitich Dhearg
n = 56

Major Trend = 115°
Percentage = 16%



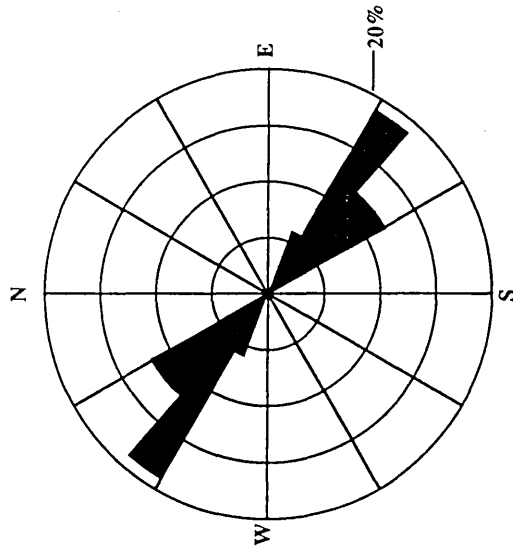
Sgurr na Ciste Duibhe
n = 146

Major Trend = 295°
Percentage = 16%



GLEN GLOX
n = 18

Major Trend = 165°
Percentage = 22%



KINLOCH HOUSEN
n = 16

Major Trend = 305°
Percentage = 19%

UNIVERSITY OF
GLASGOW
LIBRARY